

METHODS IN MOLECULAR MEDICINE™

# Alzheimer's Disease

*Methods and Protocols*

Edited by

**Nigel M. Hooper**



Humana Press

## Introduction to Alzheimer's Disease

David Allsop

### 1. Introduction

In 1907, Alois Alzheimer published an account (*1*) of a 51-year-old female patient, Auguste D., who suffered from strong feelings of jealousy towards her husband, increased memory impairment, disorientation, hallucinations, and often loud and aggressive behavior. After four and a half years of rapidly deteriorating mental illness, Auguste D died in a completely demented state. Post-mortem histological analysis of her brain using the Bielschowsky silver technique revealed dense bundles of unusual fibrils within nerve cells (neurofibrillary tangles or NFTs) and numerous focal lesions within the cerebral cortex, subsequently named “senile plaques” by Simchowicz (*2*) (**Fig. 1**). This combination of progressive presenile dementia with senile plaques and neurofibrillary tangles came to be known as Alzheimer's disease (AD), a term that was later broadened to include senile forms of dementia with similar neuropathological findings. It was Divry (*3*) who first demonstrated the presence of amyloid at the center of the senile plaque, by means of Congo red staining. All amyloid deposits were originally thought to be starch-like in nature (hence the name), but it is now apparent that they are formed from a variety of different peptides and proteins (the latest count being 18). All amyloid share the property of a characteristic birefringence under polarized light after staining with Congo red dye, which is due to the presence of well-ordered 10 nm fibrils. The underlying protein component of these fibrils invariably adopts predominantly an antiparallel  $\beta$ -pleated sheet configuration. Ultrastructural observations have confirmed that the core of the senile plaque consists of large numbers of closely-packed, radiating fibrils, similar in appearance to those seen in other forms of amyloidosis (*4,5*), and have also revealed the presence of paired helical filaments (PHFs) within the NFTs (*6*). However, it took more than 50 yr

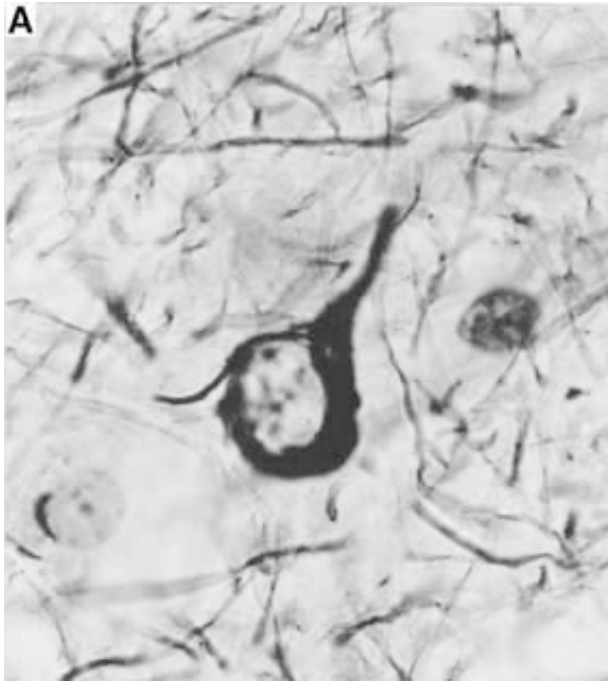


Fig. 1. (A) Neurofibrillary tangle (Palmgren silver technique).

from Divry's original observation to determine the precise chemical nature of the senile plaque amyloid. Many neuropathologists have regarded this amyloid as a "tombstone" (an inert bystander) of AD. However, the advent of molecular genetics has finally and firmly established the central role of amyloid in the pathogenesis of the disease, although this is still disputed by some workers in the field. This introductory chapter is written in support of what has become known as the "amyloid cascade" hypothesis.

## 2. Chemical Nature of Cerebral Amyloid and PHFs

The first attempts to determine the chemical nature of senile plaque amyloid were based on immunohistochemical methods, which, not surprisingly, gave unequivocal results. A method for the isolation of senile plaque amyloid "cores" from frozen post-mortem brain was first reported in 1983 (7), and around the same time methods were also developed for the isolation of PHFs (8). The unusual amino acid composition of the senile plaque core protein clearly excluded forms of amyloid known at the time (e.g., AA, AL types) as major components of the plaque core (7). In 1984, a 4-kDa protein, termed " $\beta$ -protein," now commonly referred to as  $A\beta$ , was isolated from amyloid-laden meningeal

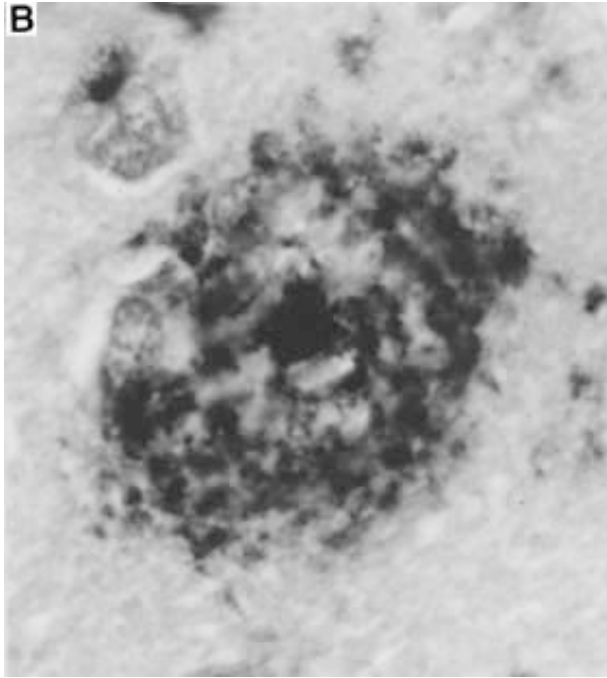


Fig. 1. **(B)** Senile plaque (Anti-A $\beta$  immunohistochemistry, monoclonal antibody 1G10/2/3, **ref. 11**). Magnification for both x1100.

blood vessels (a frequent concomitant of AD), and its N-terminal amino acid sequence was determined to be unique (**9**). Antibodies raised to synthetic peptides corresponding to various fragments of A $\beta$  were found to react with both senile plaque (**Fig. 1B**) and cerebrovascular amyloid in brains from patients with AD (**10,11**), and immunogold labeling studies showed that the amyloid fibrils were decorated with gold particles (**12**). It was soon recognized that synthetic A $\beta$  peptides will assemble spontaneously into fibrils closely resembling those seen in AD (**13**). These observations clearly demonstrated that A $\beta$  is an essential and integral component of the Alzheimer amyloid fibril.

The chemical nature of PHFs remained in dispute for some time after the discovery of A $\beta$ , until evidence for the microtubule-associated protein tau as the principal constituent of PHFs became overwhelming (**14–17**). The demonstration that structures closely resembling PHFs could be assembled in vitro from tau established beyond reasonable doubt that tau is an integral component of the PHF (**18**). There are six major isoforms of human tau (*see Fig. 2*) derived by alternative mRNA splicing from a single gene on human chromosome 17. Alternative splicing of exon 10 gives rise to 3-repeat and 4-repeat forms, which

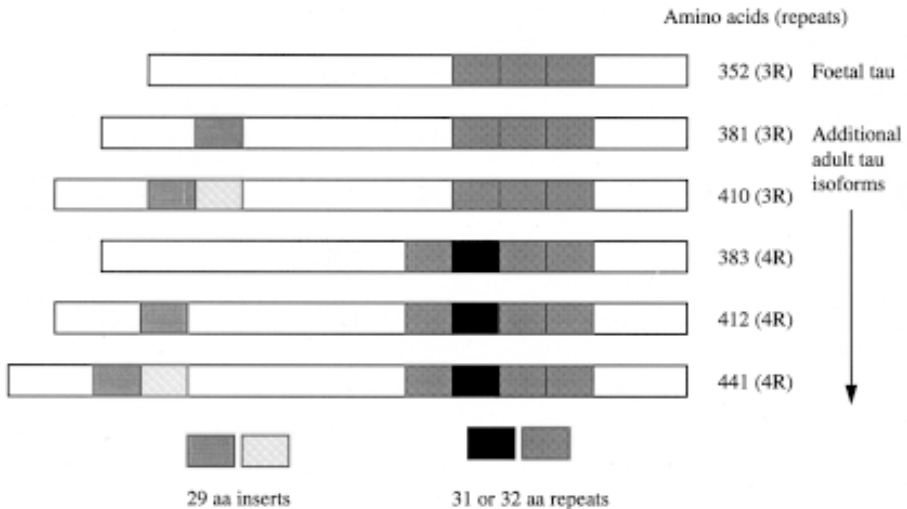


Fig. 2. Diagrammatic representation of the major isoforms of human tau.

refers to the number of microtubule-binding units. All six of these tau isoforms are expressed in the adult brain, but only the shortest isoform (tau-352) is expressed in the fetal brain. Tau can be phosphorylated at multiple sites, and tau from the fetal brain is more heavily phosphorylated than tau from the adult brain. Tau protein extracted from PHFs (PHF-tau) was found to contain all of the six major isoforms (19). NFTs in AD are composed predominantly of tau in the form of PHFs, but a minority of pathological tau can also exist in the form of so-called “straight” filaments. Intraneuronal filamentous inclusions in other neurodegenerative diseases (e.g., progressive supranuclear palsy) can be composed almost entirely of straight filaments. The studies of Goedert and coworkers (18) on the *in vitro* assembly of filamentous structures from different tau isoforms suggest that PHFs and straight filaments are formed from 3-repeat and 4-repeat forms of tau, respectively.

Numerous studies (reviewed in ref. 20) using antibodies specific for particular phosphorylation-dependent epitopes demonstrated that PHF-tau appears to be abnormally hyperphosphorylated (i.e., more heavily phosphorylated than fetal tau, and at additional unique sites in the molecule). It later became apparent that the abnormal hyperphosphorylation of tau in AD may have been overemphasized in these studies. Some of the supposed AD-specific phosphorylation sites on tau have now been seen in living neurons. In particular, analysis of human biopsy tissue has suggested that tau protein is more highly phosphorylated than previously thought in living brain, due to a rapid (1–2 h) postmortem dephosphorylation (21). This has led to the conclusion that there may be a



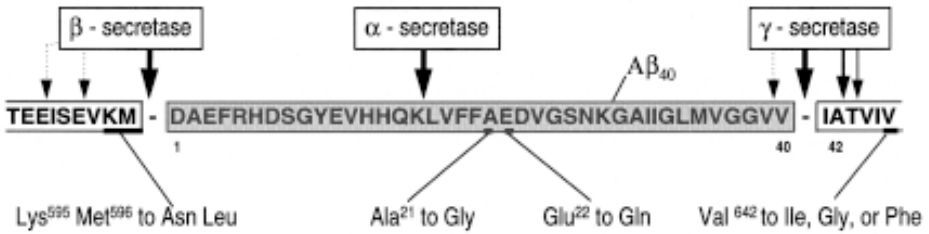


Fig. 4. A $\beta$  region of APP, showing the pathogenic APP mutations and the  $\alpha$ -,  $\beta$ -, and  $\gamma$ -secretase cleavage sites.

rise to amyloid in the brain. DeSavage and Octave (27) have also found a smaller APP mRNA variant (APP-593) lacking the A $\beta$  coding region.

#### 4. Proteolytic Processing of APP

Following discovery of the full-length APP cDNA clone, numerous studies were undertaken to detect the APP protein in cells and tissues. Full-length, membrane-bound forms of APP were readily detected by Western blotting, and it soon became apparent that a large, soluble, N-terminal fragment of APP (sAPP $\alpha$ ) is released by the action of a putative “ $\alpha$ -secretase” into conditioned tissue culture medium, cerebrospinal fluid, serum, and tissues such as brain (see Fig. 4). Esch et al. (28) and Anderson et al. (29) showed that this was due to cleavage of APP at the Lys<sup>16</sup>-Leu<sup>17</sup> bond in the middle of the A $\beta$  sequence, which would preclude formation of the intact A $\beta$  peptide. This led to speculation that the production of A $\beta$  from APP must be a purely pathological event (30). However, it soon became apparent that C-terminally truncated forms of secreted APP completely lacking A $\beta$  immunoreactivity could also be detected (31,32), along with C-terminal membrane-associated fragments of APP apparently containing the entire A $\beta$  sequence (33). Seubert et al. (32) demonstrated the existence of a form of secreted APP (sAPP $\beta$ ) that terminates at the Met<sup>596</sup> residue immediately prior to the N terminus of the A $\beta$  sequence. This was demonstrated by means of a specific monoclonal antibody (termed “92”) to residues 591–596 of APP<sub>695</sub>, the reaction of which depended on the presence of the free carboxyl-terminal Met<sup>596</sup>. These observations suggested the presence of an alternative “ $\beta$ -secretase” activity that cleaves APP to release the N terminus of the A $\beta$  peptide. The detection of A $\beta$  itself in culture medium from cells, and in body fluids (cerebrospinal fluid, blood, urine) from normal individuals (34–37), showed that this peptide is, in fact, a product of the normal metabolism of APP. These findings also inferred the action of a third “ $\gamma$ -secretase” activity that acts within the membrane-spanning domain of APP to produce the C-terminus of A $\beta$ . The detection of “short” (predominantly A $\beta$ 40) and “long” (predominantly

A $\beta$ 42) forms of A $\beta$  (*see, e.g., ref. 38*) was also important, given later data on the effects of familial AD mutations on APP processing. The A $\beta$  peptide may be physiologically active in brain, as in its soluble form it has weak neurotrophic properties (*see below*).

The identity of the  $\alpha$ -,  $\beta$ -, and  $\gamma$ -secretases is unknown, although it is likely that  $\alpha$ -secretase is a zinc metalloproteinase (**39**). There are numerous reports claiming identification of  $\beta$ -secretase and fewer reports claiming the identification of  $\gamma$ -secretase, but in no case for the various candidates in the literature is there strong evidence that they are actually  $\beta$ - or  $\gamma$ -secretase. As far as  $\beta$ -secretase is concerned, the multicatalytic proteinase or "proteasome" has been implicated (**40**), as have several chymotrypsin-like serine proteinases (**41–43**). The metallopeptidase thimet has been proposed (**44**), but has always been an unlikely candidate, as it seems not to tolerate large substrates such as APP, and can now be discounted (**45**). Cathepsin D (an aspartyl proteinase) has received considerable attention as a potential  $\beta$ -secretase due to its ability to cleave peptide substrates containing the APP Swedish mutant sequence at a much faster rate than the normal sequence (**46**). However, the fact that cathepsin D knockout mice still produce A $\beta$  (**47**) indicates that this enzyme cannot be  $\beta$ -secretase.

A number of small peptide aldehydes of the type known to inhibit both cysteine and serine proteinases have been shown to inhibit A $\beta$  formation from cultured cells, probably through inhibition of the  $\gamma$ -secretase pathway (**48–51**). The activity of these compounds as inhibitors of  $\gamma$ -secretase cleavage has been shown to correlate with their potency as inhibitors of the chymotrypsin-like activity of the proteasome, suggesting that the latter may be involved, either directly or indirectly, in the  $\gamma$ -secretase cleavage event (**52**). Further candidates for  $\gamma$ -secretase include prolyl endopeptidase (**53**), and cathepsin D (**54**).

In the case of  $\gamma$ -secretase, there is the additional complication that there may be separate enzymes responsible for the generation of A $\beta$ 40 and A $\beta$ 42 (**50,51**). APP is synthesized in the rough endoplasmic reticulum, and follows the conventional secretory pathway through the Golgi apparatus where it is tyrosyl sulfated and sialylated (**55**), and then to secretory vesicles and the cell surface. Studies on the subcellular compartments where the  $\alpha$ -,  $\beta$ -, and  $\gamma$ -secretase cleavages take place are complicated by the fact that the sites of processing may well be different in neuronal and nonneuronal cells, and also the fact that many published data were obtained using APP-transfected cells where the overexpressed APP could be forced into a nonphysiological compartment. Current evidence suggests that in differentiated neuronal cells the formation of A $\beta$ 40 occurs in the trans-Golgi network, whereas A $\beta$ 42 is synthesized at an earlier point en route to the cell surface within the endoplasmic reticulum (**56**). This finding that A $\beta$ 40 and A $\beta$ 42 appear to be formed in different subcellular

compartments has strengthened the possibility that they may be derived by different  $\gamma$ -secretases. However, an alternative possibility is that the intracellular membranes at the sites of production of A $\beta$ 40 and A $\beta$ 42 by the same  $\gamma$ -secretase are slightly different thicknesses (56).

## 5. Aggregated Forms of A $\beta$ Show Neurotoxic Properties

Whitson et al. (57,58) first reported that A $\beta$  has mild neurotrophic effects in vitro, and Yankner et al. (59) showed that A $\beta$  can also have neurotoxic properties. Initial difficulties in reproducing these findings in other laboratories were largely resolved when it was realized that the physiological properties of A $\beta$  are critically dependent on its state of aggregation. Freshly dissolved, soluble peptide appeared to promote neuronal survival, whereas peptide that had been “aged” for >24 h (and was therefore in an aggregated, fibrillar form) showed neurotoxic properties (60). The precise mechanism by which aggregated A $\beta$  causes neuronal degeneration in vitro is unclear, but the effect is likely to be due to disruption of Ca<sup>2+</sup> homeostasis and induction of oxidative free radical damage. Also, A $\beta$  can induce apoptosis or necrosis, depending on the concentration of A $\beta$  and the cell type under investigation. There is still no clear evidence that this toxicity is mediated via an initial binding between A $\beta$  and a membrane-bound receptor, although the “RAGE” (receptor for advanced glycation end products) has been suggested to be involved (61). The identity of the precise molecular form of A $\beta$  responsible for its cytotoxic effects is unclear, with both mature fibrils (62) and dimers (63) being implicated. The identification of a protofibrillar intermediate in  $\beta$ -amyloid fibril formation may shed light on this matter (62,64). There is also considerable debate concerning the relevance of these observations to the actual process of neurodegeneration in the brains of patients with AD. Yankner has recently provided compelling evidence that A $\beta$  also shows neurotoxic properties in vivo when injected into the brains of aged primates (65). This effect was not found with younger animals, suggesting that the aged brain may be particularly vulnerable to A $\beta$ -mediated neurotoxicity. This very important finding also casts doubt on the relevance of many of the in vitro A $\beta$ -induced models of toxicity.

It has also become increasingly apparent that the in vivo aggregation of A $\beta$  probably precipitates a chronic and destructive inflammatory process in the brain (66). Activation of both microglia and astrocytes occurs in the immediate vicinity of senile plaques in the brains of AD patients. These two cell types are the primary mediators of inflammation in the CNS, through the production of a wide range of proinflammatory molecules such as complement, cytokines, and acute-phase proteins. Because APP synthesis is upregulated by interleukins such as IL-1, this is likely to lead to a vicious cycle whereby amyloid deposits stimulate microglial activation and cytokine production, leading to

even higher expression of APP (66), with the whole process culminating in the degeneration of neuronal cells, possibly via the production of free radicals by activated microglia, or by complement lysis of neuronal membranes. The initiating event in this process may be the A $\beta$ -mediated activation of complement (67,68), or the binding of A $\beta$  peptide to microglia via scavenger (69,70) or RAGE receptors (61).

## 6. The Normal Functions of APP

Many potential functions have been ascribed to either full-length or secreted APP, including protease inhibition, membrane receptor (possibly G<sub>0</sub> coupled), cell adhesion molecule, regulation of neurite outgrowth, promotion of cell survival, protection against a variety of neurotoxic insults, stimulation of synaptogenesis, and modulation of synaptic plasticity (*see ref. 71* for a recent review).

Kang et al. (23) originally pointed out similarities between full-length APP and cell-surface receptors. This idea has received some support from the finding that the cytoplasmic domain of APP can catalyze guanosine triphosphate (GTP) exchange with G<sub>0</sub> suggesting that APP might function as a G<sub>0</sub>-coupled receptor (72). However, this finding remains to be confirmed by others. If this finding is true, the activating ligand is unknown, but APP is clearly not a conventional 7-transmembrane G protein-coupled receptor.

The secreted form of APP containing the (KPI) insert was found some time ago to be identical to protease nexin II, a growth regulatory molecule produced by fibroblasts (73). Protease nexin II is an inhibitor of serine proteinases, including factor XIa of the blood clotting cascade (74). APP has also been found to inhibit the matrix metalloproteinase gelatinase A (75), possibly through a small homologous motif between residues 407–417 of APP-695 and Cys<sup>3</sup>–Cys<sup>13</sup> of tissue inhibitor of matrix metalloproteinases (TIMP) (76).

Several studies have suggested that APP functions as an adhesion molecule, promoting cell–cell or cell–extracellular matrix interactions (71). APP has at least one high-affinity heparin-binding site (77), a collagen-binding site (78), and an integrin-binding motif (amino acid sequence RHDS at residues 5–8 of A $\beta$  (79) and has been shown to bind to laminin, collagen, and heparan sulfate proteoglycans (80).

A growth-promoting effect of soluble APP has been shown for fibroblasts and cultured neurons, and this activity has been claimed to reside in the amino acid sequence RERMS at residues 328–332 of APP<sub>695</sub> (81,82). Synthetic RERMS peptide and a 17-mer peptide containing this sequence were reported to retain the neurotrophic properties of soluble APP. In addition, the bioactivity of these peptides was reversed by the antagonist peptide RMSQ, which overlaps the active RERMS pentapeptide at the C-terminal end. Specific and satu-

rable binding for soluble APP and the 17-mer has been detected on a rat neuronal cell line (B103) after heparinase treatment ( $K_d = 20 \text{ nM}$ ) (83). Thus, the beneficial trophic effects of soluble APP would appear to be mediated via an unknown membrane receptor.

Soluble APP has also been reported to be neuroprotective (71), which might explain its rapid upregulation in response to heat shock, ischemia, and neuronal injury. Soluble APP can protect against  $A\beta$ - or glutamate-mediated neuronal damage (84,85), and the 17-mer peptide mentioned previously has been claimed to retain these properties. Soluble APP or the 17-mer peptide have also been reported to protect against neurological damage in vivo (86,87). However, not all of the neurotrophic and neuroprotective activities of soluble APP can be attributed to the RERMS pentapeptide region (88). Soluble APP released by cleavage at the  $\alpha$ -secretase site (sAPP $\alpha$ ) seems to be ~100-fold more potent than sAPP $\beta$  in protecting hippocampal neurons against excitotoxicity or  $A\beta$ -mediated toxicity (89). This may be due to the VHHQK heparin-binding domain (residues 12–16 of  $A\beta$ ) which is present on sAPP $\alpha$  but not sAPP $\beta$ .

## 7. The “Amyloid Cascade” Hypothesis

The relative importance of senile plaques and neurofibrillary tangles in AD has been the subject of debate ever since they were first discovered. Molecular genetic analysis of early onset familial AD has provided powerful evidence that the formation and aggregation of  $A\beta$  in the brain are central events in the pathogenesis of AD and some forms of inherited cerebrovascular amyloidosis (CVA). This was set out clearly in a review by Hardy and Allsop in 1991 (90). The first mutation to be discovered in the APP gene on chromosome 21 was the Glu<sup>22</sup> Gln (Dutch) mutation within the  $A\beta$  sequence (91). Synthetic  $A\beta$  peptides containing this mutation were shown to have an increased propensity to aggregate (92,93). This is a common theme in inherited forms of amyloidosis, where a mutant protein or peptide is particularly “amyloidogenic,” i.e., it has an increased tendency to form antiparallel  $\beta$ -pleated sheet fibrillar structures. Subsequently, some families with early onset AD were found to have pathogenic mutations at position 642 of APP (numbered according to APP<sub>695</sub>), resulting in a change from Val to Ile, Gly, or Phe (94–96). These mutations were all shown to result in an increase in the relative amounts of long  $A\beta_{42}$  compared to short  $A\beta_{40}$  (see ref. 97 for key references). Because synthetic  $A\beta_{42}$  aggregates more readily in vitro than  $A\beta_{40}$  (98), this suggests that these mutations directly influence amyloid deposition, in this case by diverting the proteolytic processing of APP towards the production of the longer, more amyloidogenic forms of  $A\beta$ . The development of specific monoclonal antibodies for determination of these different length forms of  $A\beta$  has been crucial in providing experimental support for these effects. The Swedish double mutation (Lys<sup>595</sup>,

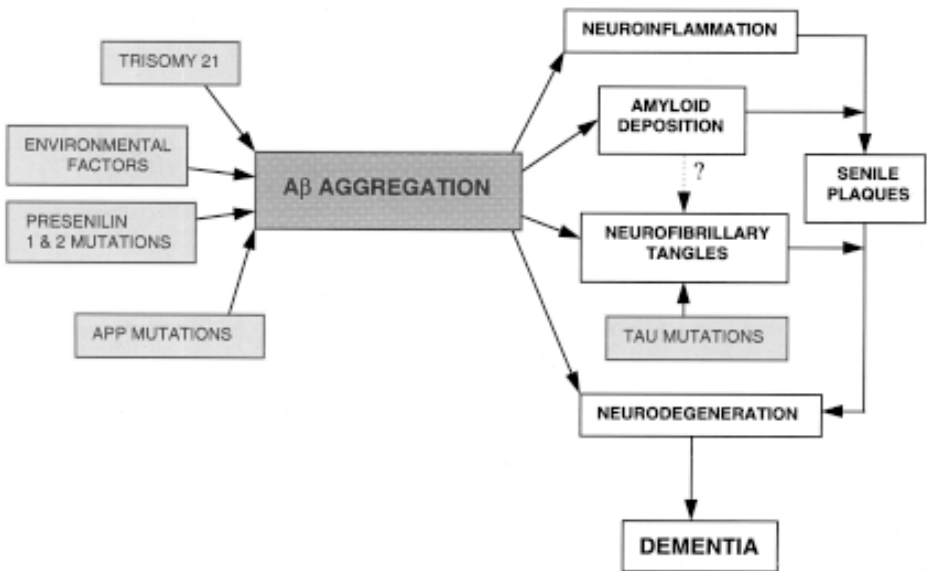


Fig. 5. Version of the “amyloid cascade” stressing the central role of A $\beta$  aggregation in the pathogenesis of AD. Note that neurotoxic A $\beta$  can precipitate NFT formation, but in FTDP-17 intracellular aggregates of tau can also be induced by mutations in the tau gene.

Met<sup>596</sup>→Asn, Leu on the immediate N-terminal side of A $\beta$ ) results in secretion of larger amounts of A $\beta$  in total, presumably through enhanced cleavage at the  $\beta$ -secretase site (99,100). Thus, all of these APP mutations seem to influence either the production or properties of A $\beta$ , and because some of these APP mutations give rise to familial AD with large numbers of NFTs, this suggests that amyloid deposition precedes and precipitates the formation of NFTs in these patients (i.e., a cascade of events including NFT formation and culminating in neurodegeneration and dementia is initiated by the formation/aggregation of A $\beta$  — see Fig. 5). The effects of the Ala<sup>21</sup> Gly mutation (found in a Dutch family with a history of both CVA and AD) are less clear, as A $\beta$  peptides incorporating this mutation seem to have a reduced propensity to aggregate (101), but cells transfected with this mutant form of APP produce more A $\beta$  than cells transfected with wild-type APP (102).

The amyloid cascade hypothesis predicted that all of the other undiscovered familial AD gene mutations would also have effects on APP processing and A $\beta$  formation/aggregation. Shortly after this hypothesis was clearly formulated, the genes responsible for the majority of cases of familial AD were found to be presenilin-1 (PS1) on chromosome 14 (103) and presenilin-2 (PS2) on chro-

mosome 1 (**104**). These PS mutations were also shown to divert APP processing towards production of long A $\beta$ 42 compared to short A $\beta$ 40 (**105,106**).

The reasons for the deposition of aggregated forms of A $\beta$  in the brain in late-onset sporadic AD are less clear, but may be due to a variety of factors including increased production of A $\beta$ , reduced clearance of A $\beta$  by proteolytic or other mechanisms, or induction of “pathological chaperones” such as apolipoprotein E that induce the aggregation of A $\beta$  into insoluble fibrils.

In considering the amyloid cascade hypothesis, it is important to realise that the amyloid fibrils themselves do not necessarily initiate the cascade of events that ultimately leads to neurodegeneration and dementia. The real culprit in AD may be an intermediate aggregate en route to fibril formation, as this is more likely to show neurotoxic properties (A $\beta$  that has been “aged” for several days eventually loses its neurotoxicity). In this respect, mature amyloid fibrils could turn out to be an “inert tombstone.” What is clear is that the A $\beta$ -peptide in some form plays a seminal role in the pathogenesis of AD. Indeed, the culpable form of A $\beta$  need not be extracellular. Given recent data on the intracellular formation of A $\beta$ 42 (**56**), it is possible that A $\beta$  aggregation begins in an intracellular environment, and that this initiates NFT formation and neurodegeneration. Whether intracellular aggregates of A $\beta$  can be regarded as “amyloid” is a matter of semantics, and is not a helpful argument. It should also be borne in mind that alterations in APP processing can affect not only the synthesis and aggregation of A $\beta$ , but also production of the potentially beneficial and protective soluble APP. Thus, lack of soluble APP could also contribute to disease pathology.

## 8. Mutations in Tau Cause Inherited Frontotemporal Dementia

An increased interest in tau and neurodegeneration has arisen through the recent identification of certain families with a mutation in the tau gene leading to an inherited form of dementia called “frontotemporal dementia and Parkinsonism linked to chromosome 17” or FTDP-17 (**107–109**). This condition occurs between the ages of 45–65 yr, and is characterized clinically by behavioral, cognitive, and motor disturbances. At postmortem, patients with FTDP-17 display a pronounced frontotemporal atrophy, with neuronal loss, gray and white matter gliosis, and spongiform changes. Many cases also have inclusions within neurons that react with antibodies to tau, but are not typical NFTs.

The human tau gene contains 11 exons. As noted previously, the alternative splicing of exon 10 generates the 3-repeat and 4-repeat isoforms. Hutton et al. (**107**) identified three missense mutations in the tau gene, namely, Gly<sup>272</sup>Val (within exon 9), Pro<sup>301</sup>Leu (within exon 10), and Arg<sup>406</sup>Trp (within exon 13). Poorkaj et al. (**108**) identified an additional Val<sup>339</sup> Met mutation (within

exon 12). The Pro<sup>301</sup>Leu mutation within exon 10 can affect 4-repeat tau only, whereas the other mutations can affect all of the tau isoforms. Those mutations within the 3/4-repeat region of tau (exons 9–12) are likely to influence tau-microtubule binding, and give rise to tau-immunoreactive inclusions within neurons that are not typical NFTs. On the other hand, the Arg<sup>406</sup>Trp mutation in exon 13 was found in a family diagnosed with progressive supranuclear palsy, including the presence of typical Alzheimer's-like PHFs.

Families with FTDP-17 have also been identified with mutations in a small cluster of nucleotides 13–16bp 3' of the exon 10 splice donor site, which is postulated to be part of a stem–loop structure involved in the alternative splicing of exon 10 (*107*). The latter mutations were shown to result in an increase in the proportion of tau mRNA encoding the 4-repeat forms. These mutations suggest that an alteration in the ratio of 3/4-repeat tau can lead to tau dysfunction and neurodegeneration.

What is clear from these studies is that tau mutations can result in neurodegenerative disease, but they do not give rise to typical AD, unlike the APP and PS1/PS2 mutations. The amyloid cascade hypothesis would predict that A $\beta$  aggregation can lead to tau pathology, but not vice versa. So far, this does appear to be the case, as tau mutations do not produce a pathological picture that includes the presence of substantial deposits of A $\beta$ . The presence of NFTs or tau-derived inclusions in a wide range of neurodegenerative conditions (e.g., postencephalitic Parkinsonism, progressive supranuclear palsy, amyotrophic lateral sclerosis) suggests that NFT formation is a relatively non-specific neuronal response to a variety of neurotoxic insults, one of which is the accumulation of A $\beta$  in the brain. Mutations in the tau gene can lead directly to the formation of pathological tau inclusions.

## **9. Relation Between Amyloid Deposition and Tau Phosphorylation**

A number of studies have now shown that exposure of cells, including human primary neuronal cultures, to fibrillised forms of  $\beta$ -amyloid leads to tau phosphorylation (*110–111*). More recently, these studies have been expanded to include whole animal studies. Geula et al. (*65*) have reported that microinjection of fibrillar A $\beta$  into aged rhesus monkey cerebral cortex leads to tau phosphorylation at sites Ser<sup>262</sup> and Ser<sup>396</sup>/Ser<sup>404</sup>, as detected by antibodies A $\beta$ 31 and PHF-1. Although APP transgenic mice are reported not to show full-blown NFTs, they do show evidence of tau phosphorylation in the vicinity of senile plaques (*112*). All of these observations support the idea of a direct link between amyloid deposition and NFT formation in AD. If NFTs or PHFs could be induced in an APP transgenic mouse (or APP/PS double transgenic) then this would provide strong confirmatory evidence for the amyloid cascade

hypothesis. So far, true PHFs have not been observed in such transgenic mice, but this may only be possible in mice containing the human tau gene.

Clearly, as explained briefly in this chapter, our understanding of the molecular neuropathology and genetics of AD has advanced enormously over the last 20 years. In particular, the central role played by amyloid A $\beta$  in the pathogenesis of the disease has been highlighted. This book details many of the biochemical, cell biological, and molecular biological techniques and approaches that have made this possible. Hopefully, the next 20 years will see even more rapid progress, given the huge amount of both academic and pharmaceutical company research in this area worldwide, and eventually culminate in the successful treatment of the disorder.

## References

1. Alzheimer, A. (1907) Uber eine eigenartige Erkrankung der Hirnrinde. *Allg. Zschr. f. Psychiatr. Psychisch-Gerichtl. Mediz.* **64**, 146–148.
2. Simchowicz, T. (1911) Histologische Studien uber der senile Demenz. *Nissl-Alzheimer Histologische histopathologische. Arbeiten* **4/2**, 267–444.
3. Divry, P. (1927) Etude histochemique des plaques seniles. *J. Neurol. Psychiatry* **27**, 643–657.
4. Kidd, M. (1964) Alzheimer's disease: an electron microscopical study. *Brain* **87**, 307–320.
5. Terry, R. D., Gonatas, H. K., and Weiss, M. (1964) Ultrastructural studies in Alzheimer's presenile dementia. *Am. J. Pathol.* **44**, 269–297.
6. Kidd, M. (1963) Paired helical filaments in electron microscopy of Alzheimer's disease. *Nature* **97**, 192–193.
7. Allsop, D., Landon, M., and Kidd, M. (1983) The isolation and amino acid composition of senile plaque core amyloid. *Brain Res.* **259**, 348–352.
8. Selkoe, D. J., Ihara, Y., and Salazar, F. J. (1982) Alzheimer's disease: insolubility of partially purified paired helical filaments in sodium dodecyl sulphate and urea. *Science* **215**, 1243–1245.
9. Glenner, G. G. and Wong, C. W. (1984) Alzheimer's disease: initial report of the purification and characterisation of a novel cerebrovascular amyloid protein. *Biochem. Biophys. Res. Commun.* **120**, 885–890.
10. Wong, C. W., Quaranta, V., and Glenner, G. G. (1985) Neuritic plaques and cerebrovascular amyloid in Alzheimer's disease are antigenically related. *Proc. Natl. Acad. Sci. USA* **82**, 8729–8732.
11. Allsop, D., Landon, M., Kidd, M., Lowe, J. S., Reynolds G. P., and Gardner, A. (1986) Monoclonal antibodies raised against a subsequence of senile plaque core protein react with plaque cores, plaque periphery and cerebrovascular amyloid in Alzheimer's disease. *Neurosci. Lett.* **68**, 252–256.
12. Ikeda, S. I., Wong, C. W., Allsop, D., Landon, M., Kidd, M., and Glenner, G. G. (1987) Immunogold labeling of cerebrovascular and neuritic plaque amyloid fibrils in Alzheimer's disease with an anti- $\beta$  protein monoclonal antibody. *Lab. Invest.* **57**, 446–449.

13. Kirschner, D. A., Inouye, H., Duffy, L. K., Sinclair, A., Lind, M., and Selkoe, D. J. (1987) Synthetic peptide homologous to  $\beta$  protein from Alzheimer disease forms amyloid-like fibrils in vitro. *Proc. Natl. Acad. Sci. USA* **84**, 6953–6957.
14. Grundke-Iqbal, I., Iqbal, K., Tung, Y. C., Quinlan, M., Wisniewski, H. M., and Binder, L. I. (1986) Abnormal phosphorylation of the microtubule-associated protein tau in Alzheimer cytoskeletal pathology. *Proc. Natl. Acad. Sci. USA* **83**, 4913–4917.
15. Kosik, K. S., Joachim, C. L., and Selkoe, D. J. (1986) Microtubule-associated protein tau is a major antigenic component of paired helical filaments in Alzheimer's disease. *Proc. Natl. Acad. Sci. USA* **83**, 4044–4048.
16. Lee, V. M.-Y., Balin, B. J., Otvos, L., and Trojanowski, J. Q. (1991) A68, a major subunit of paired helical filaments and derivatized forms of normal tau. *Science* **251**, 675–678.
17. Wischik, C. M., Novak, M., Thogersen, H. C., Edwards, P. C., Runswick, M. J., Jakes, R., et al. (1988) Isolation of a fragment of tau derived from the core of the paired helical filament of Alzheimer disease. *Proc. Natl. Acad. Sci. USA* **85**, 4506–4510.
18. Goedert, M., Jakes, R., Spillantini, M. G., Hasegawa, M., Smith, M. J., and Crowther, R. A. (1996) Assembly of microtubule-associated protein tau into Alzheimer-like filaments induced by sulphated glycosaminoglycans. *Nature* **383**, 550–553.
19. Goedert, M., Spillantini, M. G., Cairns, N. J., and Crowther, R. A. (1992) Tau proteins of Alzheimer paired helical filaments: abnormal phosphorylation of all six brain isoforms. *Neuron* **8**, 159–168.
20. Goedert, M. (1996) Tau protein and the neurofibrillary pathology of Alzheimer's disease. *Ann. NY Acad. Sci.* **777**, 121–131
21. Matsuo, E. S., Shin, R.-W., Billingsley, M. L., Van deVoorde, A., O'Connor, M., Trojanowski, J. Q., et al. (1994) Biopsy-derived adult human brain tau is phosphorylated at many of the same sites as Alzheimer's disease paired helical filament tau. *Neuron* **13**, 989–1002.
22. Consensus report of the Working Group on: "Molecular and Biochemical Markers of Alzheimer's Disease" (1998) *Neurobiol. Aging* **19**.
23. Kang, J., Lemaire, H. G., Unterbeck, A., Salbaum, J. M., Masters, C. L., Grzeschik, K. H., et al. (1987) The precursor of Alzheimer's disease amyloid A4 protein resembles a cell-surface receptor. *Nature* **325**, 733–736.
24. Ponte, P., Gonzalez-DeWhitt, P., Schilling, J., Miller, J., Hsu, D., Greenberg B., et al. (1988) A new A4 amyloid mRNA contains a domain homologous to serine proteinase inhibitors. *Nature* **331**, 525–527.
25. Kitaguchi, N., Takahashi, Y., Tokushima, Y., Shiojiri, S., and Ito, H. (1988) Novel precursor of Alzheimer's disease amyloid protein shows protease inhibitory activity. *Nature* **331**, 530–532.
26. Sandbrink, R., Masters, C. L., and Beyreuther, K. (1994)  $\beta$ A4-amyloid protein precursor mRNA isoforms without exon 15 are ubiquitously expressed in rat tissues including brain, but not in neurons. *J. Biol. Chem.* **269**, 1510–1517.
27. deSauvage, F. and Octave, J. N. (1989) A novel mRNA of the A4 amyloid precursor gene coding for a possibly secreted protein. *Science* **245**, 651–653.

28. Esch, F. S., Keim, P. S., Beattie, E. C., Blacher, R. W., Culwell, A. R., Olersdorf, T., et al. (1990) Cleavage of amyloid  $\beta$  peptide during constitutive processing of its precursor. *Science* **248**, 1122–1124.
29. Anderson, J. P., Esch, F. S., Keim, P. S., Sambamurti, K., Lieberberg, I., and Robakis, N. K. (1991) Exact cleavage site of Alzheimer amyloid precursor in neuronal PC-12 cells. *Neurosci. Lett.* **128**, 126–128.
30. Palmert, M. R., Siedlak, S. L., Podlisny, M. B., Greenberg, B., Shelton, E. R., Chan, H. W., et al. (1989) Soluble derivatives of the  $\beta$  amyloid protein precursor of Alzheimer's disease are labeled by antisera to the  $\beta$  amyloid protein. *Biochem. Biophys. Res. Commun.* **165**, 182–188.
31. Kennedy, H. E., Kametani, F., and Allsop, D. (1992) Only kunitz-inhibitor-containing isoforms of secreted Alzheimer amyloid precursor protein show amyloid immunoreactivity in normal cerebrospinal fluid. *Neurodegeneration.* **1**, 59–64.
32. Seubert, P., Oltersdorf, T., Lee, M. G., Barbour, R., Blomquist, C., Davis, D. L., et al. (1993) Secretion of beta-amyloid precursor protein cleaved at the amino terminus of the  $\beta$ -amyloid peptide. *Nature* **361**, 260–263.
33. Estus, S., Golde, T. E., Kunishita, T., Blades, D., Lowery, D., Eisen, M., et al. (1992) Potentially amyloidogenic, carboxyl-terminal derivatives of the amyloid protein precursor. *Science* **255**, 726–728.
34. Haass, C., Schlossmacher, M. G., Hung, A. Y., Vigo-Pelfrey, C., Mellon, A., Ostaszewski, B. L., et al. (1992) Amyloid  $\beta$ -peptide is produced by cultured cells during normal metabolism. *Nature* **359**, 322–325.
35. Shoji, M., Golde, T. E., Ghiso, J., Cheung, T. T., Estus, S., Shaffer, L. M., et al. (1992) Production of the Alzheimer amyloid  $\beta$  protein by normal proteolytic processing. *Science* 1992 **258**, 126–129.
36. Seubert, P., Vigo-Pelfrey, C., Esch, F., Lee, M., Dovey, H., Davis, D., et al. (1992) Isolation and quantification of soluble Alzheimer's  $\beta$ -peptide from biological fluids. *Nature* **359**, 325–327.
37. Ghiso, J., Calero, M., Matsubara, E., Governale, S., Chuba, J., Beavis, R., et al. (1997) Alzheimer's soluble amyloid  $\beta$  is a normal component of human urine. *FEBS Lett.* **408**, 105–108.
38. Asami-Odaka, A., Ishibashi, Y., Kikuchi, T., Kitada, C., and Suzuki, N. (1995) Long amyloid  $\beta$ -protein secreted from wild-type human neuroblastoma IMR-32 cells. *Biochemistry* **34**, 10,272–10,278.
39. Parvathy, S., Hussain, I., Karran, E. H., Turner, A. J., and Hooper, N. M. (1998) Alzheimer's amyloid precursor protein  $\alpha$ -secretase is inhibited by hydroxamic acid-based zinc metalloprotease inhibitors: similarities to the angiotensin converting enzyme secretase. *Biochemistry* **37**, 1680–1685.
40. Ishiura, S., Tsukahara, T., Tabira, T., and Sugita, H. (1989) Putative N-terminal splitting enzyme of amyloid A4 peptides is the multicatalytic proteinase, ingensin, which is widely distributed in mammalian cells. *FEBS Lett.* **257**, 388–392.
41. Nelson, R. B., Siman, R., Iqbal, M. A., and Potter, H. (1993) Identification of a chymotrypsin-like mast cell protease in rat brain capable of generating the N-terminus of the Alzheimer amyloid  $\beta$ -protein. *J. Neurochem.* **61**, 567–577.
42. Sahasrabudhe, S. R., Brown, A. M., Hulmes, J. D., Jacobsen, J. S., Vitek, M. P., Blume, A. J., and Sonnenberg, J. L. (1993) Enzymatic generation of the amino terminus of the  $\beta$ -amyloid peptide. *J. Biol. Chem.* **268**, 16699–16705.

43. Savage, M. J., Iqbal, M., Loh, T., Trusko, S. P., Scott, R., and Siman, R. (1994) Cathepsin G: localization in human cerebral cortex and generation of amyloidogenic fragments from the  $\beta$ -amyloid precursor protein. *Neuroscience* **60**, 607–619.
44. McDermott, J. R., Biggins, J. A. and Gibson, A. M. (1992) Human brain peptidase activity with the specificity to generate the N-terminus of the Alzheimer  $\beta$ -amyloid protein from its precursor. *Biochem. Biophys. Res. Commun.* **185**, 746–752.
45. Chevallier, N., Jiracek, J., Vincent, B., Baur, C. P., Spillantini, M. G., Goedert, M., et al. (1997) Examination of the role of endopeptidase 3.4.24. 15 in A $\beta$  secretion by human transfected cells. *Br. J. Pharmacol.* **121**, 556–562.
46. Lador, U. S., Snyder, S. W., Wang, G. T., Holzman, T. F., and Krafft, G. A. (1994) Cleavage at the amino and carboxyl termini of Alzheimer's amyloid- $\beta$  by cathepsin D. *J. Biol. Chem.* **269**, 18,422–18,428.
47. Saftig, P., Peters, C., Von Figura, K., Craessaerts, K., Van Leuven, F., and De Strooper, B. (1996) Amyloidogenic processing of human amyloid precursor protein in hippocampal neurons devoid of cathepsin D. *J. Biol. Chem.* **271**, 27,241–27,244.
48. Higaki, H., Quon, D., Zhong, Z., and Cordell, B. (1995) Inhibition of  $\beta$ -amyloid formation identifies proteolytic precursors and subcellular site of catabolism. *Neuron* **14**, 651–659.
49. Allsop, D., Christie, G., Gray, C., Holmes, S., Markwell, R., Owen, D., et al. (1997) Studies on inhibition of  $\beta$ -amyloid formation in APP751-transfected IMR-32 cells and SPA4CT-transfected SHSY5Y cells, in *Alzheimer's Disease: Biology, Diagnostics and Therapeutics* (Iqbal, K., Winblad, B., Nishimura, T., Takeda, M. and Wisniewski, H. M., eds.), Wiley, New York, pp. 717–727.
50. Citron, M., Diehl, T. S., Gordon, G., Biere, A. L., Seubert, P., and Selkoe, D. J. (1996) Evidence that the 42- and 40-amino acid forms of amyloid  $\beta$  protein are generated from the  $\beta$ -amyloid precursor protein by different protease activities. *Proc. Natl. Acad. Sci. USA* **93**, 13,170–13,175.
51. Klafki, H., Abramowski, D., Swoboda, R., Paganetti, P. A., and Staufenbiel, M. (1996) The carboxyl termini of  $\beta$ -amyloid peptides 1-40 and 1-42 are generated by distinct  $\gamma$ -secretase activities. *J. Biol. Chem.* **271**, 28655–28659.
52. Christie, G., Markwell, R. E., Gray, C. W., Smith, L., Godfrey, F., Mansfield, F., et al. (1999) Alzheimers disease: correlation of the suppression of  $\beta$ -amyloid peptide secretion from cultured cells with inhibition of the chymotrypsin-like activity of the proteasome. *J. Neurochem.* in press.
53. Ishiura, S. (1991) Proteolytic cleavage of the Alzheimer's disease amyloid A4 precursor protein. *J. Neurochem.* **56**, 363–369
54. Evin, G., Cappai, R., Li, Q. X., Culvenor, J. G., Small, D. H., Beyreuther, K., and Masters, C. L. (1995) Candidate  $\gamma$ -secretases in the generation of the carboxyl terminus of the Alzheimer's disease  $\beta$ A4 amyloid: possible involvement of cathepsin D. *Biochemistry* **34**, 14185–14192
55. Weidemann, A., Konig, G., Bunke, D., Fischer, P., Salbaum, J. M., Masters, C. L. and Beyreuther, K. (1989) Identification, biogenesis, and localization of precursors of Alzheimer's disease A4 amyloid protein. *Cell* **57**, 115–126.
56. Hartmann, T., Bieger, S. C., Bruhl, B., Tienari, P. J., Ida, N., Allsop, D., et al. (1997) Distinct sites of intracellular production for Alzheimer's disease A $\beta$  40/42 amyloid peptides. *Nature (Med.)* **3**, 1016–1020

57. Whitson, J. S., Selkoe, D. J., and Cotman, C. W. (1989) Amyloid  $\beta$ -protein enhances the survival of hippocampal neurons *in vitro*. *Science* **243**, 1488–1490.
58. Whitson, J. S., Glabe, C. G., Shintani, E., Abcar, A., and Cotman, C. W. (1990)  $\beta$ -amyloid protein promotes neuritic branching in hippocampal cultures. *Neurosci. Lett.* **110**, 319–324.
59. Yankner, B. A., Duffey, L. K., and Kirschner, D. A. (1990) Neurotrophic and neurotoxic effects of amyloid  $\beta$  protein. Reversal by tachykinin neuropeptides. *Science* **250**, 279–281.
60. Pike, C. J., Walencewicz, A. J., Glabe, C. G., and Cotman, C. W. (1991) *In vitro* aging of  $\beta$ -amyloid protein causes peptide aggregation and neurotoxicity. *Brain Res.* **563**, 311–314.
61. Yan, S. D., Chen, X. Fu-J., Chen, M., Zhu, H., Roher, A., Slattery, T., et al. (1996) RAGE and amyloid- $\beta$  peptide neurotoxicity in Alzheimer's disease. *Nature* **382**, 685–691.
62. Harper, J. D., Wong, S. S., Lieber, C. M., and Lansbury, P. T. (1997) Observation of metastable A $\beta$  amyloid protofibrils by atomic force microscopy. *Chem. Biol.* **4**, 119–125.
63. Roher, A. E., Chaney, M. O., Kuo, Y. M., Webster, S. D., Stine, W. B., Haverkamp, L. J., et al. (1996) Morphology and toxicity of A $\beta$  (1-42) dimer derived from neuritic and vascular amyloid deposits of Alzheimer's disease. *J. Biol. Chem.* **271**, 20631–20635.
64. Walsh, D. M., Lomakin, A., Benedek, G. B., Condron, M. M., and Teplow, D. B. (1997) Amyloid  $\beta$ -protein fibrillogenesis. Detection of a protofibrillar intermediate. *J. Biol. Chem.* **272**, 22364–22372.
65. Geula, C., Wu, C.-K., Saroff, D., Lorenzo, A., Yuan, M., and Yankner, B. A. (1998) Aging renders the brain vulnerable to amyloid  $\beta$ -protein neurotoxicity. *Nature Med.* **4**, 827–831.
66. Eikelenboom, P., Zhan, S. S., van-Gool, W. A., and Allsop, D. (1994) Inflammatory mechanisms in Alzheimer's disease. *Trends Pharmacol. Sci.* **15**, 447–450.
67. Webster, S., Bonnell, B., and Rogers, J. (1997) Charge-based binding of complement component C 1 q to the Alzheimer amyloid  $\beta$ -peptide. *Am. J. Pathol.* **150**, 1531–1536.
68. Webster, S., Bradt, B., Rogers, J., and Cooper, N. (1997) Aggregation state-dependent activation of the classical complement pathway by the amyloid  $\beta$  peptide. *J. Neurochem.* **69**, 388–398.
69. El-Khoury, J., Hickman, S. E., Thomas, C. A., Cao, L., Silverstein, S. C., and Loike, J. D. (1996) Scavenger receptor-mediated adhesion of microglia to  $\beta$ -amyloid fibrils. *Nature* **382**, 716–719.
70. Paresce, D. M., Ghosh, R. N., and Maxfield F. R. (1996) Microglial cells internalize aggregates of the Alzheimer's disease amyloid  $\beta$ -protein via a scavenger receptor. *Neuron* **17**, 553–565.
71. Mattson, M. (1997) Cellular actions of  $\beta$ -amyloid precursor protein and its soluble and fibrillogenic derivatives. *Physiol. Rev.* **77**, 1081–1132.
72. Nishimoto, I., Okamoto, T., Matsuura, Y., Takahashi, S., Okamoto, T., Murayama, Y., and Ogata, E. (1993) Alzheimer amyloid protein precursor complexes with brain GTP-binding protein G(0). *Nature* **362**, 75–79.

73. Van Nostrand, W. E., Wagner, S. L., Suzuki, M., Choi, B. H., Farrow, J. S., Geddes, J. W., Cotman, C. W., and Cunningham, D. D. (1989) Protease nexin-II, a potent antichymotrypsin, shows identity to amyloid  $\beta$ -protein precursor. *Nature* **341**, 546–549.
74. Smith, R. P., Higuchi, D. A., and Broze, G. J. J. (1990) Platelet coagulation factor Xia-inhibitor, a form of Alzheimer amyloid precursor protein. *Science* **248**, 1126–1128.
75. Miyazaki, K., Hasegawa, M., Funahashi, K., and Umeda, M. (1993) A metalloproteinase inhibitor domain in Alzheimer amyloid protein precursor. *Nature* **362**, 839–841.
76. Allsop, D., Clements, A., Kennedy, H., Walsh, D., and Williams, C. (1994) Mechanism of cerebral amyloidosis in Alzheimer's disease, in *Amyloid Protein Precursor in Development, Aging and Alzheimer's Disease* (Masters, C. L., Beyreuther, K., Trillet, M., and Christen, Y., eds.), Springer-Verlag, Berlin, pp. 47–59.
77. Multhaup, G., Mechler, H., and Masters, C. L. (1995) Characterization of the high affinity heparin binding site of the Alzheimer's disease  $\beta$ A4 amyloid precursor protein (APP) and its enhancement by zinc(II). *J. Mol. Recognit.* **8**, 247–57.
78. Behr, D., Hesse, L., Masters, C. L., and Multhaup, G. (1996) Regulation of amyloid protein precursor (APP) binding to collagen and mapping of the binding sites on APP and collagen type I. *J. Biol. Chem.* **271**, 1613–1620.
79. Ghiso, J. A., Rostagno, J. E., Gardella, L., Liem, P. D., Gorevic, P. D., and Frangione, B. (1992) A 109-amino-acid C-terminal fragment of Alzheimer's-disease amyloid precursor protein contains a sequence, -RHDS-, that promotes cell adhesion. *Biochem. J.* **288**, 1053–1059.
80. Breen, K. C., Bruce, M., and Anderton, B. H. (1991) Beta amyloid precursor protein mediates neuronal cell-cell and cell-surface adhesion. *J. Neurosci. Res.* **28**, 90–100.
81. Ninomiya, H., Roch, J. M., Sundsmo, M. P., Otero, D. A., and Saitoh, T. (1993) Amino acid sequence RERMS represents the active domain of amyloid  $\beta$ A4 protein precursor that promotes fibroblast growth. *J. Cell Biol.* **121**, 879–886.
82. Jin, L. W., Ninomiya, H., Roch, J. M., Schubert, D., Masliah, E., Otero, D. A., and Saitoh, T. (1994) Peptides containing the RERMS sequence of amyloid  $\beta$ A4 protein precursor bind cell surface and promote neurite extension. *J. Neurosci.* **14**, 5461–5470.
83. Ninomiya, H., Roch, J. M., Jin, L. W. and Saitoh, T. (1994) Secreted form of amyloid  $\beta$ A4 protein precursor (APP) binds to two distinct APP binding sites on rat B103 neuron-like cells through two different domains, but only one site is involved in neurotropic activity. *J. Neurochem.* **63**, 495–500.
84. Goodman, Y. and Mattson, M. P. (1994) Secreted forms of  $\beta$ -amyloid precursor protein protect hippocampal neurons against amyloid  $\beta$ -peptide-induced oxidative injury. *Exp. Neurol.* **128**, 1–12.
85. Mattson, M. P., Cheng, B., Culwell, A. R., Esch, F. S., Lieberburg, I., and Rydel, R. E. (1993) Evidence for excitoprotective and intraneuronal calcium-regulating roles for secreted forms of the  $\beta$ -amyloid precursor protein. *Neuron* (1993) **10**, 243–254.
86. Smith-Swintosky, V. L., Pettigrew, L. C., Craddock, S. D., Culwell, A. R., Rydel, R. E., and Mattson, M. P. (1994) Secreted forms of  $\beta$ -amyloid precursor protein protect against ischemic brain injury. *J. Neurochem.* **63**, 781–784.

87. Masliah, E., Westland, C. E., Rockenstein, E. M., Abraham, C. R., Mallory, M., Veinberg, I., et al. (1997) Amyloid precursor proteins protect neurons of transgenic mice against acute and chronic excitotoxic injuries in vivo. *Neuroscience* **78**, 135–146.
88. Ohsawa, I., Takamura, C., and Kohsaka, S. (1997) The amino-terminal region of amyloid precursor protein is responsible for neurite outgrowth in rat neocortical explant culture. *Biochem. Biophys. Res. Commun.* **236**, 59–65.
89. Furukawa, K., Sopher, B. L., Rydel, R. E., Begley, J. G., Pham, D. G., Martin, G. M., et al. (1996) Increased activity-regulating and neuroprotective efficacy of  $\alpha$ -secretase-derived secreted amyloid precursor protein conferred by a C-terminal heparin-binding domain. *J. Neurochem.* **67**, 1882–1894.
90. Hardy, J. and Allsop, D. (1991) Amyloid deposition as the central event in the aetiology of Alzheimer's disease. *Trends Pharmacol. Sci.* **12**, 383–388.
91. Levy, E., Carman, M. D., Fernandez-Madrid, I. J., Power, M. D., Lieberburg, I., van-Duinen, S. G., et al. (1990) Mutation of the Alzheimer's disease amyloid gene in hereditary cerebral hemorrhage, Dutch type. *Science* **248(4959)**, 1124–1126.
92. Wisniewski, T., Ghiso, J., and Frangione, B. (1991) Peptides homologous to the amyloid protein of Alzheimer's disease containing a glutamine for glutamic acid substitution have accelerated amyloid fibril formation. *Biochem. Biophys. Res. Commun.* **179**, 1247–1254.
93. Clements, A., Walsh, D. M., Williams, C. H., and Allsop, D. (1993) Effects of the mutations Glu22 to Gln and Ala21 to Gly on the aggregation of a synthetic fragment of the Alzheimer's amyloid  $\beta$ /A4 peptide. *Neurosci. Lett.* **161**, 17–20.
94. Goate, A., Chartier-Harlin, M. C., Mullan, M., Brown, J., Crawford, F., Fidani, L., et al. (1991) Segregation of a missense mutation in the amyloid precursor protein gene with familial Alzheimer's disease. *Nature* **349**, 704–706.
95. Chartier-Harlin, M. C., Crawford, F., Houlden, H., Warren, A., Hughes, D., Fidani, L., et al. (1991) Early-onset Alzheimer's disease caused by mutations at codon 717 of the  $\beta$ -amyloid precursor protein gene. *Nature* **353**, 844–846.
96. Murrell, J., Farlow, M., Ghetti, B., and Benson, M. D. (1991) A mutation in the amyloid precursor protein associated with hereditary Alzheimer's disease. *Science* **254**, 97–99.
97. Younkin, S. G. (1995) Evidence that A $\beta$  42 is the real culprit in Alzheimer's disease. *Ann. Neurol.* **37**, 287–288.
98. Burdick, D., Soreghan, B., Kwon, M., Kosmoski, J., Knauer, M., Henschen, A., et al. (1992) Assembly and aggregation properties of synthetic Alzheimer's A4/ $\beta$  amyloid peptide analogs. *J. Biol. Chem.* **267**, 546–554.
99. Citron, M., Oltersdorf, T., Haass, C., McConlogue, L., Hung, A. Y., Seubert, P., et al. (1992) Mutation of the  $\beta$ -amyloid precursor protein in familial Alzheimer's disease increases  $\beta$ -protein production. *Nature* **360**, 672–674.
100. Cai, X. D., Golde, T. E., and Younkin, S. G. (1993) Release of excess amyloid  $\beta$  protein from a mutant amyloid  $\beta$  protein precursor. *Science* **259**, 514–516.
101. Clements, A., Allsop, D., Walsh, D. M., and Williams, C. H. (1996) Aggregation and metal-binding properties of mutant forms of the amyloid A $\beta$  peptide of Alzheimer's disease. *J. Neurochem.* **66**, 740–747.

102. Haass, C., Hung, A. Y., Selkoe, D. J., and Teplow, D. B. (1994) Mutations associated with a locus for familial Alzheimer's disease result in alternative processing of amyloid  $\beta$ -protein precursor. *J. Biol. Chem.* **269**, 17741–17748.
103. Sherrington, R., Rogaev, E. I., Liang, Y., Rogaeva, E. A., Levesque, G., Ikeda, M., et al. (1995) Cloning of a gene bearing missense mutations in early-onset familial Alzheimer's disease. *Nature* **375**, 754–760.
104. Levy-Lahad, E., Wasco, W., Poorkaj, P., Romano, D. M., Oshima, J., Pettingell, W. H., et al. (1995) Candidate gene for the chromosome 1 familial Alzheimer's disease locus. *Science* **269**, 973–977.
105. Borchelt, D. R., Thinakaran, G., Eckman, C. B., Lee, M. K., Davenport, F., Ratovitsky, T., et al. (1996) Familial Alzheimer's disease-linked presenilin 1 variants elevate A $\beta$  1–42/1–40 ratio in vitro and in vivo. *Neuron* **17**, 1005–1013.
106. Mehta, N. D., Refolo, L. M., Eckman, C., Sanders, S., Yager, D., Perez-Tur, J., et al. (1998) Increased A $\beta$ 42(43) from cell lines expressing presenilin 1 mutations. *Ann. Neurol.* **43**, 256–258.
107. Hutton, M., Lendon, C. L., Rizzu, P., Baker, M., Froelich, S., Houlden, H., et al. (1998) Association of missense and 5'-splice-site mutations in tau with the inherited dementia FTDP-17. *Nature* **393**, 702–705.
108. Poorkaj, P., Bird, T. D., Wijsman, E., Nemens, E., Garruto, R. M., Anderson, L., et al. (1998) Tau is a candidate gene for chromosome 17 frontotemporal dementia. *Ann. Neurol.* **43**, 815–825.
109. Spillantini, M. G., Bird, T. D., and Ghetti, B. (1998) Frontotemporal dementia and Parkinsonism linked to chromosome 17: a new group of tauopathies. *Brain Pathol.* **8**, 387–402.
110. Busciglio, J., Lorenzo, A., Yeh, J., and Yankner, B. A. (1995)  $\beta$ -amyloid fibrils induce tau phosphorylation and loss of microtubule binding. *Neuron* **14**, 879–888.
111. Takashima, A., Noguchi, K., Michel, G., Mercken, M., Hoshi, M., Ishiguro, K., and Imahori, K. (1996) Exposure of rat hippocampal neurons to amyloid  $\beta$  peptide (25–35) induces the inactivation of phosphatidylinositol-3 kinase and the activation of tau protein kinase I/glycogen synthase kinase-3  $\beta$ . *Neurosci. Lett.* **203**, 33–36.
112. Sturchler-Pierrat, C., Abramowski, D., Duke, M., Wiederhold, K.-H., Mistl, C., Rothacher, S., et al. (1997) Two amyloid precursor protein transgenic mouse models with Alzheimer disease-like pathology. *Proc. Natl. Acad. Sci. USA* **94**, 13,287–13,292.

## The Genetics of Alzheimer's Disease

Nick Brindle and Peter St. George-Hyslop

### 1. Introduction

Since the first description of Alzheimer's disease (AD) at the beginning of the century until relatively recently, it was customary to define Alzheimer's disease as occurring in the presenium. The same neuropathological changes occurring in brains over the age of 65 were called "senile dementia." Because there have been no clinical or pathological features to separate the two groups, this somewhat arbitrary distinction has been abandoned. Although AD is currently considered to be a heterogeneous disease, the most consistent risk factor to be implicated other than advancing age is the presence of a positive family history. This potential genetic vulnerability to AD has been recognized for some time. Some of the earliest evidence suggestive of a genetic contribution to AD came from Kallmann's 1956 study (1) demonstrating a higher concordance rate in monozygotic twins for "parenchymatous senile dementia" compared with dizygotic twins and siblings. This monozygotic excess has been confirmed in studies applying more rigorous diagnostic criteria although there may be widely disparate ages of onset between twins (2). The most convincing evidence for a genetic contribution to AD has come from the study of pedigrees in which the pattern of disease segregation can be clearly defined. Thus, the abandonment of the early and late-onset dichotomy has occurred at a time when, at the genetic level, important differences have been identified through the discovery of specific gene defects in early onset cases

### 2. Genetic Epidemiology

A number of case control studies have reported a severalfold increase in AD in first degree relatives of affected probands and often demonstrating a more pronounced effect in early onset cases (3-10). Although the reported risk var-

ies between studies van Duijn et al. (10) calculated a threefold increase in the disease in first-degree relatives and that genetic factors could play a part in at least a quarter of cases. Familial aggregation of both AD and Down's syndrome has been postulated because of the higher frequency of presenile AD observed in relatives of Down's syndrome (11). Four other studies have observed a significant association between family history of Down's syndrome and AD (7,10,12,13), although the relationship remains controversial (14). A variety of patterns of inheritance of AD have been implicated. Some have suggested that all cases are inherited in an autosomal dominant fashion with age-dependent penetrance (8,15), whereas others have proposed a more complex interaction between genetic and environmental processes (16). What has become apparent is that there are a minority of pedigrees, principally with early onset disease, that clearly segregate AD as an autosomal dominant trait.

Despite epidemiological and genetic studies suggesting familial aggregation for AD (FAD), genetic studies of AD and other late-onset dementias have a number of inherent problems. There is an innate inaccuracy of clinical diagnosis to contend with and although definite diagnosis requires autopsy confirmation this may also be subject to interpretation. In addition, there are a number of factors that tend to underestimate the familiarity of AD. As the disease is generally one of later life, individuals who are genetically predisposed may die of other causes prior to disease development. Individuals may be examined before an age at which they would be likely to express the disease and affected relatives of AD patients will usually be dead, limiting the number of individuals in whom marker genotyping is possible for linkage analysis.

### 3. Molecular Cloning and Alzheimer's Disease

The evidence that has unequivocally defined the importance of genetic factors in at least a proportion of cases has come from the application of molecular cloning techniques. Stratification of these affected families into early-onset AD (EOAD) and late-onset AD (LOAD) depending on age of onset before 60–65 yr has simplified genetic analyzes considerably. This dichotomy has led to the identification of three genes that when mutated cause a particularly aggressive form of AD that may present as early as the third decade. In addition possession of the  $\epsilon 4$  allele of the apolipoprotein E gene (ApoE) is a risk factor for both the sporadic and late-onset familial forms of AD (see Table 1).

Although extremely important, the group of patients with EOAD and a specific gene defect is small. The much larger group of late-onset cases is likely to be etiologically and genetically more heterogeneous. This group may consist of a mixture of dominantly inherited single-gene effects, polygenetic effects and other environmental influences. As a result of this etiological complexity, there are a number of methodological issues in specifying the pattern of trans-

**Table 1**  
**Chromosomal Localization of AD Loci**

Locus	Localization	Gene	Early/late-onset
FAD 1	21q21	APP	EOAD
FAD 2	19q13.2	ApoE	LOAD/sporadic
FAD 3	14q24.3	Presenilin 1	EOAD
FAD 4	1q31–42	Presenilin 2	EOAD

APP = amyloid precursor protein, Apo E = apolipoprotein E; FAD = familial AD; EOAD = early onset AD; LOAD = late-onset AD.

mission and the precise genetic effects in families with apparent late-onset disease. For instance, the incidence of AD in late life may mean that the clustering of AD that occurs in late-onset families may be due to nongenetic factors. However, in a genomewide search, Pericak-Vance et al. (17) established linkage to markers on chromosomes 4, 6, 12, and 20 in late-onset familial AD. The best evidence was demonstrated to a 30-centimorgan region on chromosome 12p11–12. Replication of linkage to this region of chromosome 12 was confirmed in approximately half of the 53 late-onset families analyzed by Rogaevea et al. (18), although the genetic complexity of late-onset disease was illustrated by the failure of Wu et al. (19) to demonstrate chromosome 12 linkage in their data set.

## 4. Apolipoprotein E

### 4.1. Genetic Epidemiology of Apolipoprotein E

Apolipoprotein E (ApoE) is encoded by a gene on chromosome 19q within a region previously associated with familial late-onset AD (20). Common ApoE alleles are designated by  $\epsilon 2$ ,  $\epsilon 3$ , and  $\epsilon 4$ . The three isoforms differ in the presence of cysteine/arginine residues in the receptor-binding domain: ApoE2, Cys112 Cys 158; ApoE3, Cys 112 Arg158; and ApoE4, Arg 112 Arg 158.

An association of the ApoE  $\epsilon 4$  allele with late-onset FAD was first reported by Strittmater et al. (21). In a series of 243 people from 42 FAD families, an eightfold increase in risk of AD was associated with inheritance of two  $\epsilon 4$  alleles. Late-onset FAD patients inherited a single  $\epsilon 4$  allele at a rate three times that of the normal population. In a postmortem series of sporadic AD, the allele frequency of the  $\epsilon 4$  allele in autopsy confirmed AD patients was 0.4 compared with 0.16 in the normal control population (22) (see Table 2 for genotype frequencies reported by Saunders et al.). This relationship between ApoE  $\epsilon 4$  and AD has been confirmed in more than 50 studies conducted worldwide. Corder et al. (23) demonstrated a dose effect of the inheritance of ApoE  $\epsilon 4$  on the age

**Table 2**  
**Genotype Frequencies in Sporadic AD and Controls Reported**  
**by A. M. Saunders, et al. (22).**

	Sporadic Alzheimer's	%	Control subjects	%
Apo E genotype				
4/4	29/176	17	2/91	2
3/4	76/176	43	19/91	21
3/3	58/176	33	52/91	57
2/4	7/176	4	7/91	8
2/3	6/176	3	10/91	11
2/2	0/176	0	1/91	1
% with 1 or 2 ε4 alleles		64		31
% with no ε4 allele		36		69
Allele frequency				
Apo E ε4		0.40		0.16
Apo E ε3		0.56		0.74
Apo E ε2		0.04		0.10
	352		182	
	chromosomes		chromosomes	

of onset in FAD. Each ApoE ε4 allele inherited increases the risk and decreases the age of onset of the disease. The inheritance of an ε2 allele is associated with a lower relative risk and later age of onset (24). Thus the mean age of onset of disease for those who inherit the ε4/ε4 genotype is under 70 yr and for those with the ε2/ε3 genotype the mean age of onset is over 90.

In contrast to these case/control studies, in a large population-based study, Evans et al. (25) confirmed an increased risk associated with the ε4 allele, although it accounted for only a small fraction of the disease incidence in their population. Therefore, because approximately half of AD cases do not possess any ε4 alleles the utility of ApoE typing as a predictive test is unreliable, although it can be argued that it has a role in the differential diagnosis of dementia.

In studies of the effect of the ApoE type in different ethnic groups, Osuntokun et al. (26) did not find an association between Apo $\epsilon$ 4 and AD in Nigerians, although Hendrie et al. (27) reported an association in African-Americans. Another large study by Tang and colleagues (28) reported a higher relative risk of AD in African-Americans and Hispanics living in Manhattan, New York City, although this risk was not modified by the ApoE genotype. However, meta-analysis of over 14,000 AD sufferers by Farrer et al. (29) confirmed that the  $\epsilon$ 4 allele represents a major risk factor in a large number of ethnic groups of both sexes.

#### **4.2. Apolipoprotein E and the Pathogenesis of AD**

In the periphery ApoE is found complexed to lipid particles involved in lipid delivery and uptake. Much less is known about the biochemistry of ApoE in the central nervous system, but it is thought to be involved in the movement of cholesterol during membrane remodeling. Although controversial, a number of isoform-specific functions of ApoE have already been characterized that may contribute to the pathogenesis of the disease. Variation in isoform specific interactions include binding with the low-density lipoprotein receptor and with A $\beta$  peptide (21). In vitro studies have demonstrated that ApoE3 containing lipoproteins were more efficient at binding and clearance of A $\beta$  than those containing ApoE4 (21,30–32). There are variations in the ability of the ApoE isoforms to associate with the microtubule-associated proteins tau (33) and MAP-2 (34). In vitro, ApoE2 and ApoE3 but not E4 bind to the microtubule binding domains of tau and MAP2c. Binding of ApoE2 and E3 to tau may also inhibit the ability of tau to self-associate in the formation of PHFs. In culture experiments the ApoE isoforms differentially determine neurite extension in neurons (35), ApoE3 containing lipoproteins stimulate neurite outgrowth while ApoE4 containing lipoproteins fail to do so.

ApoE4 is associated with the earlier presence and greater density of the two major deposits in AD, amyloid plaques and neurofibrillary tangles (NFTs), along with greater loss of synaptic density and cerebral atrophy in patients meeting clinicopathological criteria for AD. In addition, the presence of the  $\epsilon$ 4 allele may significantly enhance the severity of magnetic resonance imaging (MRI) defined hippocampal atrophy (36) and be associated with more severe memory impairment in AD. The ApoE genotype influences the levels of amyloid deposited in the brains of individuals with AD and coexistent Down's syndrome (37). There are, however, no effects on the expression of other neurodegenerative diseases such as Parkinson's disease or Lewy body dementia (38). The  $\epsilon$ 4 genotype has disparate effects on the expression of mutant phenotypes, lowering the age of onset in the APP kindreds and having no effect on presenilin mutants.

Further studies have illuminated the effect of the ApoE isoforms on brain function. Recovery from severe head trauma, concussion, boxing stroke, and intracerebral haemorrhage are impaired in an ApoE isoform-specific manner comparing  $\epsilon 4$ -carrying and non- $\epsilon 4$ -carrying groups. Functional differences in brain metabolism have been demonstrated by positron emission tomography (PET) in cognitively normal  $\epsilon 4/\epsilon 4$ -carrying subjects aged between 40 and 60 yr compared with controls (39).

ApoE is therefore the single most common genetic susceptibility locus to AD and it has been estimated that ApoE genotype may account for 50% of the risk for AD (23). It is evident that many individuals who inherit the  $\epsilon 4$  allele do not develop disease, and therefore it is not invariably associated with AD. Thus, ApoE should not be considered to be a disease locus but a genetic association conferring a different relative risk for the development of the disease. Inheritance of particular isoforms may modify this risk by demonstrable differences in brain function in asymptomatic individuals and differential effects on the pathogenic processes of the disease.

## **5. The Amyloid Precursor Protein and AD**

### **5.1. The Amyloid Cascade Hypothesis**

The amyloid cascade hypothesis invokes a central role for the deposition of  $\beta$ -amyloid ( $A\beta$ ) in the pathogenesis of AD. The amyloid precursor protein (APP) is the transmembrane glycoprotein precursor of  $A\beta$  mapping to chromosome 21. APP exists in more than 10 different forms generated by alternative mRNA splicing.  $A\beta$  is mainly a 40–42 amino acid peptide that forms one of the major constituents of neuritic plaques and vascular deposits of amyloid in AD. It is postulated that the accumulation of  $A\beta$  is the primary abnormality in AD and that its deposition finally leads to neuronal cell death and the secondary features of the disease such as NFTs. The evidence in favor of the amyloid cascade hypothesis arises from a number of observations but is broadly derived from three strands: the association of AD with Down's syndrome, the association of mutations in the APP gene and AD, and data derived from experimental neurotoxicity of  $A\beta$ .

### **5.2. Alzheimer's Disease and Down's Syndrome**

It has long been recognized that individuals with Down's syndrome inevitably develop the pathological hallmarks of AD by their fourth decade (40). Down's syndrome can result from partial or complete trisomy of chromosome 21 leading to three copies of the APP gene. Overexpression of APP mRNA has been confirmed in Down's syndrome and preamyloid deposits can occur as early as the age of 12 yr. Therefore, APP overexpression in Down's syndrome may be partially or wholly responsible for the early development of AD type pathology.

### 5.3. APP Mutations

There were initial unsuccessful attempts to demonstrate linkage of sporadic and familial AD to APP. However, Goate et al. (41) subsequently demonstrated linkage to chromosome 21 in one family. Segregation of disease in this family was then demonstrated to be a result of a Val-Ile substitution at codon 717 of APP. There have now been a total of five mutations discovered in the APP gene that lead to AD (see Fig 4., Chapter 1). Two mutations result from the substitution of Gly or Phe at the 717 codon (42–45). Disease in two large Swedish kindreds was demonstrated to cosegregate with a double amino acid substitution at codons 690/671 (46).

Other APP mutations have been described that lead to hereditary cerebral hemorrhage with amyloidosis (HCHWA). The first family of this type was found to have a mutation within exon 17 resulting in a Gln-Glu change at codon 693 (HCHWA-Dutch) (47). The affected individuals presented with recurrent cerebral hemorrhages in the fourth decade. A second family exhibiting a similar phenotype has been described with an Ala-Gly substitution at position 692, which causes AD in some cases and cerebral hemorrhages and angiopathy in others. All APP mutations are 100% penetrant and lie near or within the A $\beta$  domain close to the sites of processing by the putative secretases. APP mutations are, however, responsible for a vanishingly small proportion (approx 2%) of FAD cases. Less than 20 APP mutant pedigrees have been identified worldwide and mutations have not been identified in a large number of FAD or sporadic cases (48).

### 5.4. APP and Amyloidogenesis

In vitro studies using synthetic A $\beta$  peptides have demonstrated that toxicity depends on the presence of a fibrillar, predominantly  $\beta$  pleated, sheet conformation. This form is more easily adopted by the A $\beta$  species that is 42 amino acid residues in length (A $\beta$ <sub>42</sub>). It is suggested that A $\beta$ <sub>42</sub> production is accelerated in AD and is first deposited in preamyloid (diffuse) lesions. These become compacted over a period of many years and gradually acquire the properties of amyloid leading to neuronal damage and NFTs. All the APP mutations described to date have demonstrable effects on the production of this longer species of A $\beta$ . Cells transfected with the Swedish double mutation at codons 670/671 of APP secrete higher levels of total A $\beta$  (49). However cells expressing the codon 717 mutation produce more of the putatively more toxic A $\beta$ <sub>42</sub>. It has been suggested that APP mutations not only alter changes in A $\beta$  secretion but may also influence the intracellular processing and subsequent trafficking of APP. Further in vivo evidence has been generated in transgenic experiments. Mice expressing high levels of mutant human APP show the development of diffuse amyloid plaques (50), and although there have been no clear neurofibrillary changes demonstrated in the animal models memory deficits have been reported in mice expressing mutant APP and amyloid fragments.

Although there is compelling evidence in support of the amyloid hypothesis there remains a number of inconsistencies. APP expression levels have been closely examined in AD and there is no convincing evidence that local overexpression of APP contributes to the neuropathology of AD. There is considerable discrepancy in the mechanism and conformation of the A $\beta$  species leading to neurotoxicity, and there is a poor anatomical and temporal correlation between the deposition of neuritic plaques and the appearance of NFTs. Indeed, both amyloid deposition and neuritic plaque formation may occur independently of each in other disease states as well as in normal, nondemented individuals. Therefore, it remains uncertain as to whether A $\beta$  deposition is causally related to the disease process or represents a surrogate marker for some other more fundamental disturbance in neuronal metabolism.

## 6. The Presenilins

### 6.1. Molecular Genetics of the Presenilins

Following the discovery of mutations in APP and the fact that they were a rare cause of FAD, several groups undertook a survey of the remaining nonsex chromosomes excluding chromosomes 19 and 21. Robust evidence of linkage ( $z = 23$ ) was demonstrated between an early onset form of FAD and a number of polymorphic genetic markers on chromosome 14q24.3 (51–53). Subsequent genetic mapping studies narrowed the region down and employing a positional cloning strategy the disease gene was cloned (presenilin-1/PS-1) (54). The gene was found to be highly conserved in evolution encoding what appears to be an integral membrane protein (*see following*).

To date, more than 40 different mutations have been discovered in PS-1. The majority are missense mutations giving rise to the substitution of a single amino acid and were therefore considered to be “gain in function” mutations. A single splicing defect has been identified in a British pedigree that is caused by a point mutation in the splice acceptor site at the 5' end of exon 10. This leads to an in-frame deletion of the exon and an amino acid substitution (55). More recently, however, a G deletion in intron 4 was recognized in two cases of early onset AD, resulting in a frame shift and a premature termination codon (56). Mutations have been identified throughout the coding sequence although there are areas of regional concentration. They are predominantly located in highly conserved transmembrane domains (TM, *see following*) at or near putative membrane interfaces and in the N-terminal hydrophobic or C-terminal hydrophobic residues of the putative TM6–TM7 loop domain. Two main clusters of mutations within exon 5 and exon 8 are observed in PS-1 and contain approx 60% of mutations and seem to be associated with an earlier mean age of onset. It is likely that mutations in PS-1 account for around 50% of early onset FAD.

Although it was clear that many early onset families were linked to the FAD 3 locus on chromosome 14, a further locus on chromosome 1 at 1q31–q42 was identified in FAD pedigrees of Volga-German ancestry (57). Subsequent to the cloning of PS-1, a very similar sequence mapping to the chromosome 1 locus was identified in expressed sequence tagged (EST) databases (58). After the full-length cDNA (STM-2 or E5–1) was cloned, it was evident that this sequence was derived from a gene encoding a polypeptide with substantial amino acid homology to PS-1 (approx 60%). Mutational analyzes discovered two different missense mutations in this gene. The first mutation (Asn141Ile) was detected in a proportion of the Volga-German families (58,59). The second mutation (Met239Val) was identified in an Italian pedigree (58) and affects a residue that is also mutated in PS-1. Screening of large data sets revealed that mutations in this gene, now named presenilin-2 (PS-2), are likely to be rare (60). Mutations in PS-1 appear to be fully penetrant with PS-1 kindreds exhibiting a narrower range and earlier mean age of onset than families possessing either of the two PS-2 mutations.

The open reading frame of both genes are encoded by 10 exons with highly conserved intron/exon boundaries and the 5' untranslated regions are encoded by a further two exons (54,61). Northern blot analysis demonstrates two mRNA species for PS-1 at approx 2.7 and 7.5kb (54) and two for PS-2 at 2.3 and 2.6 kb (59) and that both messages are present in most tissues. In situ hybridization studies show transcripts for PS-1 and PS-2 in neuronal cells of the hippocampus, cerebral cortex, and cerebellum with particularly prominent staining in the choroid plexus in both human and mouse brain.

Alternatively spliced forms have been identified for both PS-1 and PS-2. A splice variant common to both PS-1 and PS-2 leading to loss of transcript encoding part of the sixth transmembrane domain and the beginning of the hydrophilic loop domain results in deletion of exon 8 (54,58). An additional PS-1 transcript lacking four amino acids (VRSQ) at the 3' end of exon 3 has also been reported (54,61). When present, this sequence constitutes a potential phosphorylation site for protein kinase C. In addition Anwar et al. (62) identified a number of truncated transcripts of PS-1 using splice sites different from the previously defined intron/exon boundaries, although the functional significance of this is unclear. Other splice variants of PS-2 have been identified lacking exons 3 and 4 resulting in loss of transcript for TM1 and alternate use of splice acceptor sites in intron 9 and intron 10.

Examination of the hydropathy plots for both proteins reveals a number of sequences that are sufficiently hydrophobic to be candidates for TM spanning stretches. The original interpretation was that the presenilins were likely to be seven transmembrane-spanning proteins with a large hydrophilic loop that colocalize with proteins from the Golgi apparatus (63). Subsequent studies

provided evidence for a six or eight transmembrane structure with both N-terminus and loop domains facing toward the cytoplasm (63,64). However, the exact membrane topology remains controversial, Dewji and Singer (65) provided evidence for a seven-transmembrane structure with an exoplasmic orientation of N-terminal and loop domains. Endoproteolysis of both presenilins has been demonstrated in vivo and in vitro. For example, the PS-1 holoprotein migrates at 43–47 kDa, with proteolysis generating two fragments of 25–28 kDa (amino terminal) and 16–18 kDa (carboxy terminal).

## **6.2. Functions and Pathogenesis of the Presenilins and Their Mutated Isoforms**

A potential clue to the function of the presenilins comes from the recognition of strong homology of PS1 to *Caenorhabditis elegans* proteins sel-12 and spe-4. PS-1 shares 60% homology with sel-12 (66), which has been demonstrated to facilitate Lin-12-mediated signaling. In mammals, lin-12 homologues are members of the Notch family of receptors known as Notch1, Notch2, and Notch3. The molecular homology of both presenilins to sel-12 implies a role in the signal transduction mechanisms mediated by lin-12/Notch, thus they may play a direct role in the cell fate decisions mediated by these same genes. Reducing or eliminating sel-12 in *C. elegans* causes an egg-laying defective (Egl) phenotype. Normal human presenilins can substitute for the *C. elegans* sel-12 and rescue the Egl phenotype (67). Mutant presenilins were found to incompletely rescue the sel-12 mutant phenotype suggesting they have lower presenilin activity. PS-1 homology to spe-4 in *C. elegans*, a protein involved in sperm morphogenesis, suggests a role in protein transport and storage.

PS-1 knockout mice die during early embryogenesis due to defects in somite segmentation. This suggests that the presenilins play an important part in directing the development of the axial skeleton (68). The importance of Notch signaling in the development of the central nervous system raises the possibility that presenilins may be directly involved in neuronal differentiation. To this end, presenilin expression and proteolytic processing has been shown to be developmentally regulated during neuronal differentiation (69,70). In mouse and rat brains the developmental expression of presenilin mRNA parallels Notch expression (71).

Presenilins are also substrates for a caspase-3 family of proteases and were cleaved at alternative sites during apoptosis (72). Cells expressing mutant PS-2 showed an increased ratio of alternatively cleaved PS-2 relative to normal. These findings suggest that neuronal cell death in AD could be contributed to by alternate caspase-3 cleavage in sensitive cells, although Brockhaus et al. (73) demonstrated that caspase-mediated processing of PS-1 and PS-2 is not required for A $\beta$ <sub>42</sub> production or the effect of mutant PS proteins on abnormal A $\beta$  generation.

All PS-1 and PS-2 mutations analyzed have demonstrable effects on the generation of the more toxic  $A\beta_{42}$  fragment.  $A\beta$  production in fibroblasts and plasma levels of  $A\beta$  in carriers of PS mutations indicate altered APP processing in favor of  $A\beta_{42}$  generation (74,75). Similar increases in  $A\beta_{42}$  production results were obtained in transgenic mice overexpressing PS mutations (76). Double transgenic mice expressing mutant human PS-1 with a 670/671 APP mutant cDNA demonstrated earlier deposition of fibrillar  $A\beta$  with a selective increase in  $A\beta_{42}$ , compared with singly mutant APP littermates (77). The mechanism of amyloidogenesis as a result of PS mutations remains more obscure although De Strooper et al. (78) demonstrated that PS mutants increase  $\gamma$ -secretase activity.

In conclusion, the presenilins are highly conserved proteins that may play important roles in the trafficking of proteins through the Golgi apparatus and the endoplasmic reticulum, and in cell fate determination via the Notch pathway. Mutations are clustered in regions encoding putative transmembrane domains and could be directed toward a hydrophilic core formed by the predicted transmembrane-spanning regions. How mutations in the presenilins lead to the pathology of the disease is not entirely clear. It may be through an effect on APP metabolism as evidenced by the increase in the plasma concentration of  $A\beta_{42}$  in subjects with presenilin mutations. Increased  $A\beta_{42}$  secretion has also been demonstrated in culture and transgenic models of AD. Mutations in the presenilins may also render cells more vulnerable to apoptotic cell death, or neuronal death in AD may result from altered interaction of the presenilins with other proteins such as the catenins (79).

## **7. Association Studies in Alzheimer's Disease**

Association studies typically compare a marker frequency in patients with that in control subjects. The studies implicate either the gene from which the polymorphic marker was derived or a nearby susceptibility gene in linkage disequilibrium with the marker. Although association studies are simpler to conduct and may be capable of detecting minor susceptibility loci, they are less robust than linkage analysis and positive results are often less conclusive. Discrepancies arise through difficulties associated with deriving appropriately matched controls, lack of power, or through population specific effects. A selection of reported associations is outlined as follows, and illustrates some of the inconsistencies encountered in such studies.

In view of the association of ApoE with sporadic AD, polymorphic variants of genes encoding proteins involved in lipid metabolism have been examined. Apolipoprotein CII maps to the same region of chromosome 19 as apolipoprotein E. Schellenberg et al. (80,81) reported an association between apolipoprotein C2 in affected family members. Homozygosity of a common

variant in the ApoE transcription regulatory region was demonstrated in AD (82) independent of the Apo $\epsilon$ 4 status and it was suggested that there may be effects on the level of ApoE protein expression, although Song et al. (83) were unable to replicate these findings.

Okuizumi et al. (84) reported an association between a 5-repeat allele in the very-low-density lipoprotein receptor in a cohort of Japanese AD patients. However in other population- and clinic-based studies, the association was not confirmed (85–87). Another candidate gene is the low-density lipoprotein receptor-related protein (LRP1), which maps close to the region demonstrating linkage to late-onset FAD. The encoded protein acts as a receptor for ApoE and as a putative receptor for clearance of extracellular APP. At least three studies have suggested associations between AD and different alleles of LRP1 (88–90), although others have failed to confirm this association (17,91).

Other genetic associations have demonstrated similarly contradictory results. Wragg et al. (92) reported an association between an intronic polymorphism in PS-1 downstream from exon 8 and late-onset AD without family history. The more common allele (allele 1) was associated with an approximate doubling of risk in AD cases compared with the 1,2 and 2,2 genotypes combined. It was suggested that the polymorphism could affect splicing of exon 8 or that it was in linkage disequilibrium with a pathological variation somewhere else in the gene. Kehoe et al. (93) subsequently confirmed this association. However other large studies have been unable to replicate these findings (94–97).

The  $\alpha$ -1-antichymotrypsin (ACT) gene was invoked as a candidate gene to explain part of the remaining genetic component of AD. This was prompted by the observation that ACT expression is enhanced in AD brains and thus may be important in the pathogenesis of the disease. Kamboh et al. (98) reported that a common polymorphism in ACT conferred a significant risk for AD. Furthermore, they reported a gene dosage effect between homozygosity of the A/A variant and ApoE  $\epsilon$ 4/4 genotypes. Although this study has met with some published support (99–101) analyzes on larger cohorts have failed to confirm this result (102–105).

The K variant of the butyrylcholinesterase (BCHE) gene was reported by Lehmann and colleagues (106) to be associated with AD in carriers of the Apo  $\epsilon$ 4 allele. The excess of K-variant carriers in LOAD was replicated by Sandbrink et al. (107), but they found no major interaction between BCHE-K and ApoE. At least two other studies (108,109) have been unable to confirm this association of BCHE-K with sporadic disease, and analysis of the segregation of microsatellite markers flanking the gene on chromosome 3 in AD kindreds suggested that there is no gene in linkage disequilibrium with BCHE-K contributing to familial disease (108).

An association has been reported between homozygosity of a polymorphism in bleomycin hydrolase and sporadic AD (*110*). The protein encoded by this gene belongs to the papain family of cysteine proteases, which have been implicated in APP processing. The gene exists in two forms, depending on the presence of a G or A nucleotide at position 1450 resulting in a Ile/Ile, Ile/Val, or Val/Val genotype at residue 443. Val/Val homozygosity was significantly increased in cases compared with controls, although in a larger cohort Premkumar et al. (*111*) were unable to confirm this association in Caucasian patients.

More recently, an association with a variant of  $\alpha$ -2-macroglobulin was reported (*112*) although again this has not been confirmed in other patient populations (St. George-Hyslop, unpublished data). Although by no means an exhaustive list of associations, the lack of consistency between studies argues for caution in over-interpreting the role of these loci in AD and should not be used to provide information about individual risk of AD. Novel approaches employing variations of allelic association such as transmission disequilibrium testing (TDT) and genome searches by association using single nucleotide polymorphisms (SNPs) may hold future prospects for identifying further susceptibility loci.

## **8. Summary and Conclusions**

There has been remarkable progress in molecular genetic and biological research into AD over the past decade. Mutations and polymorphisms in four different genes have now been shown to be either causative or associated with the onset of AD. Mutations in PS-1, PS-2, and APP directly cause the disease with very close to 100% penetrance. Inheritance of the  $\epsilon$ 4 allele of the ApoE gene is associated with an increased risk of developing AD but is not sufficient to cause the disease.

It is evident that the neurodegeneration associated with AD involves a complex system of cellular and molecular interactions, including components of the inflammatory response, the complement system, excitotoxic and oxidative damage etc. leading to metabolic derangements, abnormal protein deposition, cytoskeletal abnormalities, and cell death. It is also apparent that genetic factors lead to quantitatively worse brain disease but not to a qualitatively different pattern of brain involvement. Despite some of the pitfalls of the amyloid cascade hypothesis, the deposition of A $\beta$  seems to be the neuropathological factor most strongly influenced by genetic factors, and any hypothesis of the pathogenesis of AD must address the mechanisms of proteinacious deposition of A $\beta$  and tau. Thus, AD is probably similar to other complex trait diseases in that there may be a common pathophysiological process to which various genetic and environmental influences might

contribute, possibly by causing increased A $\beta$  deposition, resulting in a similar clinical and neuropathological phenotype.

Despite the considerable advances made in delineating genetic determinants of AD, the precise biochemical events leading to the disease phenotype remain to be fully elucidated. Following the identification of mutant genes, the ultimate goal is to characterize the normal and pathophysiological mechanisms involved through the generation of animal and cellular models. Genetic mapping of further genes, particularly those involved in late-onset disease, is currently underway. This holds the promise of generating further insights into the pathogenesis of the disease and the possibility of in vivo testing of potential therapeutic compounds.

It is to be hoped that these important discoveries will fuel advances into the development of more useful diagnostic markers for the disease. Currently available markers such as ApoE genotype lack positive predictive value limiting utility in diagnosis and prediction. There is insufficient confidence in minor genetic susceptibility loci for them to be employed as meaningful genetic markers. However, in the future it may be possible to stratify individuals according to their genetic risk factors such that they may be more effectively targeted for preventative strategies.

## References

1. Kallmann, F. J. (1956) Genetic aspects of mental disorders in late life, in *Mental Disorders In Late Life* (Kaplan, O. J., ed.), Stanford University Press, Palo Alto, CA.
2. Brietner, J. C. S., Gatz, M., and Gergem, A. C. M. (1993) Use of twin cohorts for research in Alzheimer's disease. *Neurology* **43**, 261–267.
3. Heston, L. L., Mastri, A. R., Anderson, E., and White, J. (1981) Dementia of the Alzheimer type. Clinical genetics, natural history and associated conditions. *Arch. Gen. Psych.* **112**, 227–239.
4. Thal, L. J., Grundman, M., and Klauber, M. R. (1988) Dementia: characteristics of a referral population and factors associated with progression. *Neurology* **38**, 1083–1090.
5. Hofman, A., Schulte, W., Tanja, T. A., et al. (1989) History of dementia and Parkinson's disease in first degree relatives of patients with Alzheimer's disease. *Neurology* **39**, 1589–1592.
6. Hoininen, H. and Heinonen, O. P. (1982) Clinical and etiological aspects of senile dementia. *Eur. Neurol.* **21**, 401–410.
7. Heyman, A., Wilkinson, W. E., Stafford, J. A., Helms, M. J., Sigmon, A. H., and Weinberg, T. (1984) Alzheimer's disease: a study of epidemiological aspects. *Ann. Neurol.* **15**, 335–341.
8. Huff, J., Auerbach, J., Chackravarti, A., and Boller, F. (1988) Risk of dementia in relatives of patients with Alzheimer's disease. *Neurology* **38**, 786–790.
9. Breitner, J. C., Silverman, J. M., Mohs, R. C., and Davis, K. L. (1988) Familial aggregation in Alzheimer's disease: comparison of risk among relatives of early-

- and late-onset cases, and among male and female relatives in successive generations. *Neurology* **38**, 207–212.
10. van Duijn, C. M., Clayton, D., Chandra, C. M., Fratiglioni, L., Graves, A. B., Heyman, A., et al. (1991) Familial aggregation of Alzheimer's disease and related disorders: a collaborative re-analysis of case control. studies. *Int. J. Epidemiol.* **20(suppl. 2)**, S13–S20.
  11. Yatham, L. N., McHale, P. A., and Kinsella, A. (1988) Down's syndrome and its association with Alzheimer's disease. *Acta. Psychiatr. Scand.* **77**, 38–41.
  12. H. Broe, G. A., Henderson, A. S., Creasey, H., McCusker, E., Korten, A. E., Jorm, A. F., et al. (1990) A case control. study of Alzheimer's disease in Australia. *Neurology* **40**, 1698–1707.
  13. Zubenko, G. S., Huff, H. J., Beyer, J., Auerbach, J., and Teply, I. (1988) Familial risk of dementia associated with a biologic subtype of Alzheimer's disease. *Arch. Gen. Psych.* **45**, 889–893.
  14. Berr, C., Borghi, E., Rethore, M. O., Lejeune, J., and Alperovitch, A. (1989) Absence of familial association between dementia of the Alzheimer type and Down's syndrome. *Am. J. Med. Genet.* **33**, 545–550.
  15. Breitner, J. C. S. and Folstein, M. F. (1984) Familial Alzheimer dementia: a prevalent disorder with specific clinical features. *Psychol. Med.* **14**, 63–80.
  16. Farrer, L. A., Meyers, R. H., Cupples, L. A., et al. (1990) Transmission and age at onset patterns in familial Alzheimer's disease: evidence of heterogeneity. *Neurology* **40**, 395–403.
  17. Pericak-Vance, M. A., Bass, M. P., Yamaoka, L. H., Gaskell P. C., Scott, W. K., Terwedow, H. A., et al. (1997) Complete genomic screen in late onset familial Alzheimer's disease. Evidence for a new locus on chromosome 12. *JAMA* **278**, 1237–1241.
  18. Rogaeva, E., Premkumar, S., Song, Y. Q., Sorbi, S., Brindle, N., Paterson, A., et al. (1998) Evidence for an Alzheimer disease susceptibility locus on chromosome 12 and for further locus heterogeneity. *JAMA* **280**, 614–618
  19. Wu, W. S., Holmans, P., Wavrant-Devrieze, F., Shears, S., Kehoe, P., Crook, R., et al. (1998) Genetic studies on chromosome 12 in late-onset Alzheimer disease. *JAMA* **280**, 619–622.
  20. Pericak-Vance, M. A., Bass, M. P., Yamaoka, L. H., Gaskell P. C., Scott, W. K., Terwedow, H. A., et al. (1991) Linkage studies in familial Alzheimer's disease—evidence for chromosome 19 linkage. *Am. J. Hum. Genet.* **48**, 1034–1050.
  21. Strittmatter, W. J., Saunders, A. M., Schmechel, D., Pericak-Vance, M., Enghild, J., Salvesen, G. S., and Roses, A. D. (1993) Apolipoprotein E — high-avidity binding to beta-amyloid and increased frequency of type-4 allele in late-onset familial Alzheimer-disease. *Proc. Natl. Acad. Sci. USA* **90**, 1977–1981.
  22. Saunders, A. M., Strittmatter, W. J., Schmechel, D., St. George-Hyslop, P. H., Pericak-Vance, M. A., Joo, S. H., et al. (1993) Association of Apolipoprotein E allele  $\epsilon$ 4 with the late onset familial and sporadic Alzheimer's disease. *Neurology* **43**, 1467–1472.
  23. Corder, E. H., Saunders, A. M., Strittmatter, W. J., et al. (1993) Gene dosage of apolipoprotein E type 4 allele and the risk for Alzheimer's disease in late onset families. *Science* **261**, 921–923.

24. Corder, E. H., Saunders, A. M., Strittmatter, W. J., Schmechel, D. E., Gaskell, P. C., Small, G. W., et al. (1994) Protective effect of apolipoprotein E type 2 allele for late onset Alzheimer's disease. *Nature Genet.* **7**, 180–184.
25. Evans, D. A., Beckett, L. A., Field, T. S., Feng, L., Albert, M. S., Bennett, D. A., et al. (1997) Apolipoprotein E  $\epsilon$ 4 and incidence of Alzheimer's disease in a community population of older persons. *JAMA* **277**, 822–824.
26. Osuntokun, B. O., Sahota, A., Ogunniyi, A. O., Gureje, O., Baiyewu, O., Adeyinka, A., et al. (1995) Lack of association between Apolipoprotein E $\epsilon$ 4 and Alzheimer's disease in elderly Nigerians. *Ann. Neurol.* **38**, 463–465.
27. Hendrie, H. C., Hall, K. S., Hui, S., Unverzagt, F. W., Yu, C. E., Lahiri, D. K., et al. (1995) Apolipoprotein E genotypes and Alzheimer's disease in a community study of elderly African Americans. *Ann. Neurol.* **37**, 118–120.
28. Tang, M. X., Stern, Y., Marder, K., Bell, K., Gurland, B., Lantigua, R., et al. (1998) The ApoE- $\epsilon$ 4 allele and the risk of Alzheimer's disease among African-Americans, whites and Hispanics. *JAMA* **279**, 751–755.
29. Farrer, L. A., Cupples, L. A., Myers, R. H., van Duijn, C. M., Mayeux, R., Haines, J. L., et al. (1998) Effects of age and ethnicity on the link between Apolipoprotein E genotype and Alzheimer disease: a meta-analysis. *JAMA* **278**, 1349–1356.
30. Strittmatter, W. J., Saunders, A. M., Goedert, M., Weisgraber, K. H., Dong, L. M., Jakes, R., et al. (1995) Purification of apolipoprotein E attenuates isoform specific binding to  $\beta$ -amyloid. *J. Biol. Chem.* **270**, 9039–9042.
31. LaDu, M. J., Falduto, M. T., Manelli, A. M., Reardon, C. A., Getz, G. S., Frail, D. E. (1994) Isoform specific binding of apolipoprotein E to  $\beta$  amyloid. *J. Biol. Chem.* **269**, 23,403–23,406.
32. Zhou, Z., Smith, J. D., Greengard, P. and Gandy, S. (1996) Alzheimer amyloid  $\beta$  peptide forms denaturant resistant complex with type E3 but not type E4 isoform of apolipoprotein E. *Mol. Med.* **2**, 175–180.
33. Strittmatter, W. J., Saunders, A. M., Goedert, M., Weisgraber, K. H., Dong, L. M., Jakes, R., et al. (1994) Isoform specific interactions of Apolipoprotein E with microtubule associated protein tau: implications for Alzheimer's disease. *Proc. Natl. Acad. Sci. USA* **91**, 11183–11186.
34. Huang, D. Y., Goedert, M., Jakes, R., Weisgraber, K. H., Garner, C. C., Saunders, A. M., et al. (1994) Isoform-specific interactions of Apolipoprotein-E with the microtubule-associated protein MAP2c — implications for Alzheimer's-disease. *Neurosci. Lett.* **182**(1), 55–58.
35. Nathan, B. P., Bellosta, S., Sanan, D. A., Weisgraber, K. H., Mahley, R. W., and Pitas, R. E. (1994) Differential effects of apolipoproteins E3 and E4 on neuronal growth in vitro. *Science* **264**, 850–852.
36. Lehtovirta, M., Soininen, H., Laakso, M. P., Partanen, K., Helisalmi, S., Mannermaa, A., et al. (1996) SPECT and MRI analysis in Alzheimer's disease: relation to apolipoprotein E epsilon-4 allele. *J. Neurol. Neurosurg. Psychiat.* **60**, 644–649.
37. Gomez-Isla, T., West, H. L., Rebeck, G. W., Harr, S. D., Growdon, J. H., Locascio, J. J., et al. (1996) Clinical and pathological correlates of apolipoprotein E  $\epsilon$ 4 in Alzheimer's disease. *Ann. Neurol.* **39**, 62–70.

38. Benjamin, R., Leake, A., Edwardson, J. A., McKeith, J. G., Ince, P. G., Perry, R. H., and Morris, C. M. (1994) Apolipoprotein E genes in Lewy body and Parkinson's disease. *Lancet* **343**, 1565.
39. Reiman, E. M., Caselli, R. J., Yun, L. S., Chen, K. W., Bandy, D., Minoshima, S., et al. (1996) Preclinical evidence of Alzheimer's disease in persons homozygous for epsilon 4 allele for apolipoprotein E. *N. Engl. J. Med.* **334**, 752–758.
40. Jervis, G. A. (1948) Early senile dementia in Mongoloid idiocy. *Am. J. Psychiatry* **105**, 102–106.
41. Goate, A., Chartier-Harlin, M. C., Mullan, M., Brown, J., Crawford, F., Fidani, L., et al. (1991) Segregation of a missense mutation in the amyloid precursor protein gene with familial Alzheimer's disease. *Nature* **349**, 704–706.
42. Chartier-Harlin, M. C., Crawford, F., Houlden, H., Warren, A., Hughes, D., Fidani, L., et al. (1991) Early onset Alzheimer's disease caused by mutation at codon 717 of the  $\beta$ -amyloid precursor protein gene. *Nature* **353**, 844–846.
43. Murrel, J., Farlow, M., Ghetti, B., and Benon, M. D. (1991) A mutation in the amyloid precursor protein associated with hereditary Alzheimer's disease. *Science* **254**, 97–99.
44. Kennedy, A. M., Newman, S., McCaddon, A., Ball, J., Roques, P., Mullan, M., et al. (1993) Familial Alzheimer's disease: a pedigree with a missense mutation in the amyloid precursor protein (amyloid precursor protein 717 valine-glycine). *Brain* **116**, 309–324.
45. Farlow, M., Murrell, J., Ghetti, B., Unverzagt, F., Zeldenrust, S., and Benson, M. (1994) Clinical characteristics in a kindred with early onset Alzheimer's disease and their linkage to a G-T change at position 2149 of the amyloid precursor protein gene. *Neurology* **44**, 105–111.
46. Mullen, M., Crawford, F., Axelman, K., et al. (1992) A new mutation in APP demonstrates that the pathogenic mutations for probable Alzheimer's disease frame the  $\beta$ -amyloid sequence. *Nature Genet.* **1**, 345–347.
47. Levy, E., Carman, M. D., Fernandez-Madrid, I. J., Levy, E., Carman, M. D., Fernandez-Madrid, I. J., et al. (1990) Mutation of the Alzheimer's disease amyloid gene in hereditary cerebral haemorrhage, Dutch Type. *Science* **248**, 1124–1126.
48. Tanzi, R. E., Vaula, G., Romano, D. M., Mortilla, M., Huang, T. L., Tupler, R. G., et al. (1992) Assessment of amyloid beta protein gene mutations in a large set of familial and sporadic Alzheimer's disease cases. *Am. J. Hum. Genet.* **51**, 273–282.
49. Citron, M., Oltersdorf, T., Haass, C., McConlogue, L., Hung, A., Seubert, P., et al. (1992) Mutation of the  $\beta$ -amyloid precursor protein in familial Alzheimer's disease increases  $\beta$ -protein production. *Nature* **360**, 672–674.
50. Games, D., Adams, D., Alessandrini, R., Barbour, R., Berthelette, P., Blackwell, C., et al. (1995) Alzheimer type neuropathology in transgenic mice overexpressing V717F  $\beta$ -amyloid precursor protein. *Nature* **373**, 523–527.
51. Schellenberg, G. D., Bird, T. D., Wijsman, E. M., Orr, H. T., Anderson, L., Nemens, E., et al. (1992) Genetic linkage evidence for a Familial Alzheimer's disease locus on chr 14. *Science* **258**, 668–671.
52. St George-Hyslop, P., Haines, J., Rogaev, E., Mortilla, M., Vaula, G., Pericak-Vance, M., et al. (1992) Genetic evidence for a novel familial Alzheimer's disease gene on chromosome 14. *Nature Genet.* **2**, 330–334.

53. Van Broeckhoven, C., Backhovens, H., Cruts, M., DeWinter, G., Bruyland, M., Cras, P., and Martin, J. J. (1992) Mapping of a gene predisposing to early-onset Alzheimer's disease to chromosome 14q24.3. *Nature Genet.* **2**, 335–339.
54. Sherrington, R., Rogaev, E. I., Liang, Y., Rogaeva, E. A., Levesque, G., Ikeda, M., et al. (1995) Cloning of a gene bearing missense mutations in early-onset familial Alzheimer's disease. *Nature* **375**, 754–760.
55. Perez-Tur, J., Froelich, S., Prihar, G., Crook, R., Baker, M., Duff, K., et al. (1996) A mutation in the splice acceptor site in the presenilin-1 gene. *Neuroreport* **7**, 297–301.
56. Tysoe, C., Whittaker, J., Xuereb, J., Cairns, N. J., Cruts, M., Van Broeckhoven, C., et al. (1998) A presenilin-1 truncating mutation is present in two cases with autopsy confirmed early-onset Alzheimer's disease. *Am. J. Hum. Genet.* **62**, 70–76.
57. Levy-Lehad, E., Wasco, W., Poorkaj, P., Romano, D. M., Oshima, J., Pettingell, W. H., et al. (1995) A familial Alzheimer's disease locus on chromosome 1. *Science* **269**, 973–977.
58. Rogaev, E., Sherrington, R., Rogaeva, E. A., Levesque, G., Ikeda, M., Liang, Y., et al. (1995) Familial Alzheimer's disease in kindred with missense mutations in a gene on chromosome 1 related to the Alzheimer's disease type 3 gene. *Nature* **376**, 775–778.
59. Levy-Lehad, E., Wasco, W., and Poorkaj, P. (1995) Candidate gene for the chromosome 1 familial Alzheimer's disease locus. *Science* **269**, 973–977.
60. Sherrington, R., Froelich, S., Sorbi, S., Campion, D., Chi, H., Rogaeva, E. A., et al. (1996) Alzheimer's disease associated with mutations in PS-2 is rare and variably penetrant. *Hum. Molec. Genet.* **5**, 985–988.
61. Clark, R. F., Hutton, M., Fuldner, R. A., Froelich, S., Karran, E., Talbot, C., et al. (1995) The structure of the Presenilin 1(S182) gene and identification of six novel mutations in early onset AD families. *Nature Genet.* **11**, 219–222.
62. Anwar, R., Moynihan, T. P., Ardley, H., Brindle, N., Coletta, P. L., Cairns, N., et al. (1996) Molecular analysis of the Presenilin-1 (S-182) gene in sporadic cases of Alzheimer's disease: identification and characterisation of unusual splice variants. *J. Neurochem.* **66**, 1774–1777.
63. De Strooper, B., Beullens, M., Contreras, B., Levesque, L., Craessaerts, K., Cordell, B., et al. (1997) Phosphorylation, subcellular localisation and membrane orientation of the Alzheimer's disease associated presenilins. *J. Biol. Chem.* **272**, 3590–3598.
64. Doan, A., Thinakara, G., Borchelt, D. R., Slunt, H. H., Ratovitsky, T., Podlisny, M., et al. (1996) Protein topology of presenilin-1. *Neuron* **17**, 1023–1030.
65. Dewji, N. and Singer, S. J. (1997) The seven-transmembrane spanning topology of the Alzheimer's disease related presenilin protein in the plasma membrane of cultured cells. *Proc. Natl. Acad. Sci. USA* **94**, 14,025–14,030.
66. Levitan, D. and Greenwald, I. (1995) Facilitation of lin-12 mediated signalling by sel-12, a *Caenorhabditis elegans* S182 Alzheimer's disease gene. *Nature* **377**, 351–354.
67. Levitan, D., Doyle, T. G., Brousseau, D., Lee, M. K., Thinakaran, G., Slunt, H. H., et al. (1996) Assessment of normal and mutant presenilin function in *Caenorhabditis elegans*. *Proc. Natl. Acad. Sci. USA* **93**, 14,940–14,944.

68. Shen, J., Bronson, R. T., Chen, D. F., Xia, W., Selkoe, O., J., and Tonegawa, S. (1997) Skeletal and CNS deficits in presenilin-1 deficient mice. *Cell* **89**, 629–639.
69. Hartmann, H., Busciglio, J., Baumann, K. H., Staufenbiel, M., and Yankner, B. A. (1997) Developmental regulation of presenilin-1 processing in the brain suggests a role in neuronal differentiation. *J. Biol. Chem.* **272**, 14505–14508.
70. Capell, A., Saffrich, R., Olivo, J. C., Meyn, L., Walter, J., Grunberg, J., et al. (1997) Cellular expression and proteolytic processing of presenilin proteins is developmentally regulated during neuronal differentiation. *J. Neurochem.* **69**, 2432–2440.
71. Berezovska, O., Xia, M. Q., Page, K., Wasco, W., Tanzi, R. E., and Hyman, B. T. (1997) Developmental regulation of presenilin mRNA expression parallels notch expression. *J. Neuropath. Exp. Neurol.* **56**, 40–44.
72. Kim, T. W., Pettingell, W. H., Jung, Y. K., Kovacs, D. M., and Tanzi, R. E. (1997) Alternative cleavage of Alzheimer's associated presenilins during apoptosis by caspase-3 family proteases. *Science* **277**, 373–376.
73. Brockhaus, M., Grunberg, J., Rohrig, S., Loetscher, H., Wittenburg, N., Baumeister, R., et al. (1998) Caspase-mediated cleavage is not required for the activity of presenilins in amyloidogenesis and NOTCH signaling. *Neuroreport* **9**, 1481–1486.
74. Scheuner, D., Eckman, C., Jensen, M., Song, X., Citron, M., Suzuki, N., et al. (1996) Secreted amyloid beta-protein similar to that in the senile plaques of Alzheimer's disease is increased in vivo by the presenilin 1 and 2 and APP mutations linked to familial Alzheimer's disease. *Nat. Med.* **2**, 864–870.
75. Borchelt, D. R., Thinakaran, M. G., Eckman, C. B., Lee, M. K., Davenport, F., Ratovitsky, T., et al. (1996) Familial Alzheimer's disease linked presenilin-1 variants elevate A beta 1–42/1–40 ratio *in vitro* and *in vivo*. *Neuron* **17**, 1005–1013.
76. Citron, M., Westaway, D., Xia, W. M., Carlson, G., Diehl, T., Levesque, G., et al. (1997) Mutant presenilins of Alzheimer's disease increase production of 42 residue amyloid beta protein on both transfected cells and transgenic mice. *Nature Med.* **3**, 67–72.
77. Holcomb, L., Gordon, M. N., McGowan, E., Yu, X., Benkovic, S., Jantzen, P., et al. (1998) Accelerated Alzheimer-type phenotype in transgenic mice carrying both mutant amyloid precursor protein and presenilin 1 transgenes. *Nature Med.* **4**, 97–100.
78. De Strooper, B., Saftig, P., Craessaerts, K., Vanderstichele, H., Guhde, G., Annaert, W., et al. (1998) Deficiency of presenilin-1 inhibits the normal cleavage of amyloid precursor protein. *Nature* **391**, 387–390.
79. Yu, G., Chen, F. S., Levesque, G., Nishimura, M., Zhang, D. M., Levesque, L., et al. (1998) The presenilin 1 protein is a component of a high molecular weight intracellular complex that contains beta-catenin. *J. Biol. Chem.* **273**, 16,470–16,475.
80. Schellenberg, G. D., Deeb, S. S., Boehnke, M., Bryant, E. M., Martin, G. M., Lampe, T. H., and Bird, T. D. (1987) Association of apolipoprotein CII with familial dementia of the Alzheimer type. *J. Neurogenet.* **4**, 97–108.
81. Schellenberg, G. D., Boehnke, M., Wijsman, E. M., Moore, D. K., Martin, G. M., and Bird, T. D. (1992) Genetic association and linkage analysis of the Ap<sup>o</sup>CII locus and familial Alzheimer's disease. *Ann. Neurol.* **31**, 223–227.
82. Bullido, M. J., Artiga, M. J., Recuero, M., Sastre, I., Garcia, M. A., Aldudo, J., et al. (1998). A polymorphism in the regulator region of Apolipoprotein E associated with risk for Alzheimer's dementia. *Nature Genet.* **18**, 69–71.

83. Song, Y.-Q., Rogaeva, E., Premkumar, S., Brindle, N., Kawarai, T., Orlacchio, A., et al. (1998) Absence of association between Alzheimer disease and the -491 regulatory region polymorphism of APOE. *Neurosci. Letts.* **250**, 189–192.
84. Okuizumi, K., Onodera, O., Namba, Y., Ikeda, K., Yamamoto, T., Seki, K., et al. (1996) Genetic association of very low density lipoprotein (VLDL) receptor gene with sporadic Alzheimer's disease. *Nature Genet.* **11**, 207–209.
85. Fallin, D., Gauntlett, A. C., Scibelli, P., Cai, X. G., Duara, R., Gold M., et al. (1997) No association between the very-low density lipoprotein receptor gene and late-onset Alzheimer's disease, nor interaction with apolipoprotein E gene in population based and clinic samples. *Genet. Epidemiol.* **14**, 299–205.
86. Chen, L., Baum, L., Ng, H. K., Chan, Y. S., Mak, Y. T., Woo, J., et al. (1998) No association detected between the very low density lipoprotein receptor (VLDL-R) and late onset Alzheimer's disease in Hong Kong Chinese. *Neurosci. Lett.* **241**, 33–36.
87. Okuizumi, K., Onodera, O., Seki, T., Tanaka, H., Namba, Y., Ikeda, K., et al. (1997) Lack of association of the very-low density lipoprotein receptor gene polymorphism with Caucasian Alzheimer's disease. *Am. J. Hum. Genet.* **61**, 1686.
88. Lendon, C. L., Talbot, C. J., Craddock, N. J., Han, S. W., Wragg, M., Morris, J. C., and Goate, A. M. (1997) Genetic association studies between dementia of the Alzheimer's type and three receptors for apolipoprotein E in a Caucasian population. *Neurosci. Lett.* **222**, 187–190.
89. Wavrant DeVrieze, F., Perez-Tur, J., Lambert, J. C., Frigard, B., Pasquier, F., Delacourte, A., et al. (1997) Association between the low density lipoprotein receptor-related protein (LRP) and Alzheimer's disease. *Neurosci. Lett.* **227**, 68–70.
90. Kang, D. E., Saitoh, T., Chen, X., Xia, Y., Masliah, E., Hansen, L. A., et al. (1997) Genetic association of the low density lipoprotein receptor-related protein gene (LRP), an apolipoprotein E receptor with late onset Alzheimer's disease. *Neurology* **49**, 56–61.
91. Fallin, D., Kundz, A., Town, T., Fallin, D., Kundtz, A., Town, T., Gauntlett, A. C., Duara, R., Barker, W., Crawford, and F., Mullan, M. (1997) No association between the low density lipoprotein receptor related protein and late onset Alzheimer's disease. *Am. J. Hum. Genet.* **61**, 1143.
92. Wragg, M., Hutton, M., Talbot, C., Busfield, F., Han, S. W., Lendon, C., Clark, R. F., et al. (1996) Genetic association between intronic polymorphism in presenilin-1 gene and late-onset Alzheimer's disease. *Lancet* **347**, 509–512.
93. Kehoe, P., Williams, J., Lovestone, S., Wilcock, G., and Owen, M. J. (1996) Presenilin polymorphism and Alzheimer's disease. *Lancet* **347**, 1185.
94. Perez-Tur, J., Wavrant-De Vrieze, F., Lambert, J. C., et al. (1996) Presenilin polymorphism and Alzheimer's disease. *Lancet* **347**, 1560–1561.
95. Scott, W. K., Growdon, J. H., Roses, A. D., Haines, J. L., Pericak-Vance, M. A. (1996) Presenilin polymorphism and Alzheimer's disease. *Lancet* **347**, 1186–1187.
96. Scott, W. K., Yamaoka, L. H., Locke, P. A., Rosi, B. L., Gaskell, P. C., Saunders, A. M., et al. (1997) No association or linkage between an intronic polymorphism of presenilin-1 and sporadic or late onset familial Alzheimer's disease. *Genet. Epidemiol.* **14**, 307–315.
97. Cai, X. G., Stanton, J., Fallin, D., Hoyne, J., Duara, R., Gold, M., et al. (1997) No association between the intronic presenilin-1 polymorphism and Alzheimer's disease in clinic based and population based samples. *Am. J. Hum. Genet.* **74**, 202–203.

98. Kamboh, M. I., Sanghera, D. K., Ferrell, R. E., and DeKosky, S. T. (1995) APOE 4 associated Alzheimer's disease risk is modified by alpha-1-antichymotrypsin polymorphism. *Nature Genet.* **10**, 486–488.
99. Muramatsu, T., Matsushita, S., Arai, H., Sasaki, H., and Higuchi, S. (1996) Alpha-1-antichymotrypsin gene polymorphism and risk for Alzheimer's disease. *J. Neurol. Trans.* **103**, 1205–1210.
100. Yoshiiwa, A., Kamino, K., Yamamoto, H., Kobayashi, T., Imagawa, M., Nonomura, Y., et al. (1997) Alpha-1-antichymotrypsin as a risk modifier for late onset Alzheimer's disease in Japanese apolipoprotein  $\epsilon$ 4 allele carriers. *Ann. Neurol.* **42**, 115–117.
101. Wischik, C., Harrington, C., and Kalsheker, N. A. (1997) Microsatellite polymorphism of the alpha-1-antichymotrypsin gene locus associated with sporadic Alzheimer's disease. *Hum. Genet.* **99**, 27–31.
102. Muller, U., Bodeker, R. H., Gerundt, I., and Kurz, A. (1996) Lack of association between alpha-1-antichymotrypsin polymorphism, Alzheimer's disease and allele  $\epsilon$ 4 of apolipoprotein E. *Neurology* **47**, 1575–1577.
103. Haines, J. L., Pritchard, M. L., Saunders, A. M., Schilckraut, J. M., Growdon, J. H., Gaskell, P. C., et al. (1996) No association between alpha-1-antichymotrypsin and familial Alzheimer's disease. *Ann. NY Acad. Sci.* **802**, 35–41.
104. Murphy G. M., Sullivan, E. V., Gallagher Thompson, D., Thompson, L. W., van Duijn, C. M., Forno, L. S., et al. (1997) No association between the alpha-1-antichymotrypsin A allele and Alzheimer's disease. *Neurology* **48**, 1313–1316.
105. Fallin, D., Reading, S., Schinka, et al. (1997) No interaction between the ApoE and the alpha-1-antichymotrypsin genes on risk for Alzheimer's disease. *Am. J. Med. Genet.* **74**, 192–194.
106. Lehmann, D. J., Johnson, C., and Smith, A. D. (1997) Synergy between the genes for butyrylcholinesterase K variant and apolipoprotein E4 in late onset confirmed Alzheimer's Disease. *Hum. Mol. Genet.* **6**, 1933–1936.
107. Sandbrink, R., Gasperina, A., Zarfass, R., Weber, B., Masters, C. L., Beyreuther, K., and Heuser, I. (1998) Butyrylcholinesterase K variant (BCHE-K): association with late-onset Alzheimer's disease. *Neurobiol. Aging* **19**, S69.
108. Brindle, N., Song, Y., Rogaeva, E., Premkumar, S., Levesque, G., Yu, G., et al. (1998) Analysis of the butyrylcholinesterase gene and nearby chromosome 3 markers in Alzheimer's disease and aging. *Hum. Mol. Genet.* **7**, 933–935.
109. Singleton, A. B., Smith, G., Gibson, A. M., Woodward, R., Perry, R., Ince, P., et al. (1998) No association between the K variant of the butyrylcholinesterase gene and pathologically confirmed Alzheimer's disease. *Hum. Mol. Genet.* **7**, 937–939.
110. Montoya, S. E., Aston, C. E., DeKosky, S. T., Kamboh, M. I., Lazo, J. S., and Ferrell, R. E. (1998) Bleomycin hydrolase is associated with risk of sporadic Alzheimer's disease. *Nature Genet.* **18**, 211–212.
111. Premkumar, S., Song, Y., Pericak-Vance, M., Haines, J. L., Rogaeva, E., Scott, W. K., et al. (1998) Analysis of the association between bleomycin hydrolase and Alzheimer's disease in Caucasians. *Neurobiol. Aging* **19**, S68.
112. Blacker, D., Wilcox, M. A., Laird, N. M., Rodes, L., Horvath, S. M., Go, P. C. P., et al. (1998) Alpha-2-macroglobulin is genetically associated with Alzheimer's disease. *Nature Genet.* **19**, 357–360.

## **Advances in Methodology and Current Prospects for Primary Drug Therapies for Alzheimer's Disease**

**David S. Knopman**

### **1. Introduction**

There has been gratifying progress in the development of drugs for Alzheimer's disease (AD). Even though the current generation of medications, the cholinesterase inhibitors (CEIs), has produced only modest benefits, our concept of an "effective" therapy has matured considerably over this time. A less visible but equally important advance has been a quantum leap in expertise in clinical trial methodology. This chapter reviews the methodological underpinnings of clinical trials in AD: patient selection issues, key design issues, and an overview of currently available agents and the prospects for drugs of the future.

### **2. Patient Selection**

#### ***2.1. Definition of Alzheimer's Disease***

The development of the NINCDS-ADRDA criteria (*1*) has proved to be a major advance for the identification of potential AD drug trial participants. The criteria define probable AD and also provide an operational definition of exclusionary criteria. The key features for probable AD involve documented cognitive impairment involving recent memory disturbance as well as one other cognitive deficit, decline from a previously higher level and evidence for progressive worsening of memory and other cognitive functions. Clinical pathological studies of derivatives of the NINCDS-ADRDA criteria have shown that 87% of patients who are diagnosed with probable AD proved to have the neuropathological diagnosis of AD when they eventually died (*2*).

As our understanding of the pathology of AD has increased, so has our understanding of the diagnostic limits of AD. The presence of coexistent

cerebrovascular pathology probably does not eliminate a diagnosis of AD (3,4). Similarly, the presence of extrapyramidal signs does not rule out AD (5). Instead, AD and cerebrovascular pathology, and AD and Parkinsonian pathology coexist, probably more frequently than we realize. Regardless of the overlap of these disorders, from the perspective of defining which patients should participate in clinical trials, maintenance of diagnostic purity is still necessary. Clinical trials are most reliable when the enrolled patients are homogeneous. Although exclusion of patients with AD plus cerebrovascular or Parkinsonian pathology may limit enrollment somewhat and may reduce generalizability of results, the benefits of diagnostic homogeneity to the investigation of new anti-AD agents is almost certainly to increase the probability of detecting drug effects.

## **2.2. Dementia Severity**

In addition to diagnosis, patient severity is an important point to consider in AD clinical trials. The standard approach in most studies to date has been to define a range on a mental status examination, the Mini-Mental State examination (MMSE), of 10–26 points correct (out of a possible 30) (6). This range was chosen to select a patient cohort that was not so mild as to lead to the inclusion of nondemented patients. The range also ensured that the symptoms of enrolled patients were not so severe that cognitive testing became impossible.

Recently, there has been considerable interest in including milder patients in clinical trials. The spectrum of preAD known as mild cognitive impairment (MCI) could become an area of major focus for new agents for AD. Petersen and colleagues have defined mild cognitive impairment as a disorder of recent memory, with other cognitive functions preserved and with functional status preserved (7). Approximately 15% of MCI patients per year decline to the point of being diagnosed with probable AD. Thus, MCI could either be viewed as an at-risk state or as the earliest manifestation of AD. At the moment the criteria for MCI have not been used in a clinical trial, so that their operational success remains to be proved.

At the other end of the spectrum of severity are patients with more severe impairment at enrollment. The only current example of a trial that used a patient cohort more impaired than the standard defined by the MMSE range of 10–26 was the Sano et al. study (8). The entry criteria for that study required that patients were to be rated as a Clinical Dementia Rating (CDR) (9) stage of 2. A CDR rating of 2 is consistent with a moderate stage of dementia severity, with substantially impaired memory, substantially impaired daily living skills, and some decline in ability to carry out tasks such as dressing and toileting independently. The rationale for employing this range of severity was to be able to utilize nursing home placement and a decline to the next lower rating,

that of a CDR of 3, as outcome measures. Patients who were milder than CDR 2 at entry into the study have been shown to have too low a rate of passage to one of these outcomes to conduct the study within the 2-yr time frame. The Sano et al. study (8) showed that enrolling patients of this severity was feasible and did result in the predicted number of endpoints.

### **2.3. Concomitant Medical Problems**

One additional issue in patient selection has to do with how many other medical problems, what severity of other medical problems, and what concomitant medications are allowable to participate in a clinical trial. Part of the decision process may be driven by the pharmacology, tolerability, and safety profile of the agent to be tested. A new drug with suspected influences on cardiac function might prompt rather restrictive exclusion criteria for heart diseases. Assuming that the decision is not driven by toxicity considerations, the use of relatively broad versus relatively restrictive entry criteria may reflect the goals of the study sponsor. Lax exclusion criteria may allow a sponsor to claim greater generalizability of their results, while more restrictive exclusion criteria may allow a sponsor to seek higher study completion rate. In one study of a cholinesterase inhibitor, lax exclusion criteria are thought to have resulted in a rate of decline in the placebo group that exceeded most other comparable studies (with more stringent entry criteria). However, it is not clear whether these speculations actually are causally related to entry criteria.

## **3. Clinical Trial Methods**

### **3.1. Choice of Study Design**

Prior to the development of cholinesterase inhibitors that were easy to tolerate, there was no question that placebo-controlled trials were the only viable design. There is growing controversy over whether placebo controls are either ethically appropriate or methodologically efficient to advance the field beyond the current generation of CEIs. Those in favor of continuing the use of placebos assert that the placebo-controlled design is the least biased and the least prone to misinterpretation. Those in favor of moving beyond placebo-controlled trials point to the feasibility of using a CEI either as an active control or as a treatment for all participants in a design referred to as an "add-on." The question of whether to use placebo controls depends on the specific question being asked. Under certain circumstances, placebo-controlled trials are most appropriate. In other circumstances especially with agents with mechanisms of action other than CEI, active control designs or add-on designs would be preferred.

The active control design would be one where a new drug would be tested against an existing efficacious agent, at the present a CEI. One key point in this

design is that superiority to the CEI would be the only acceptable result. This is to contrast with the use of active controls where only equivalence to the active agent is sought. CEIs have modest benefits (*see Subheading 4.1.*), and developing new drugs that merely match their benefits seems pointless. This is particularly true because several of the current CEIs have such favorable safety and tolerability that there is little motivation to find safer drugs. Thus, equivalence designs do not seem appropriate for AD at this time.

The add-on design would be used when a new agent was being tested that had a completely different mechanism of action from the standard agent, currently a CEI. In one arm of the study, the new agent would be used in conjunction with a CEI, while in the other arm, only the CEI would be given. The advantages of add-on designs include the replication of actual clinical use of medications (i.e., in combination) but more importantly, there is sound theoretical grounds for combining agents of different mechanisms in order to produce greater efficacy.

One of the major issues in AD drug therapy, and hence in trial design, is whether an agent is strictly palliative or whether it has disease-modifying effects. In other words, is the drug merely affecting symptoms or is it actually affecting the underlying biology of the disease? Although investigators can speculate based on presumed mechanisms of action, empirical proof of disease modification is a formidable challenge. Several ways of establishing this property have been proposed.

One method of determining whether a drug has disease-modifying properties begins with a parallel-group, placebo-controlled trial of at least 6 mo duration and then adds a single-blind washout phase at the end of the trial. If the patients receiving active treatment do not decline back to the level of the placebo-treated patients, then that lack of deterioration would be the basis for a claim of disease-modifying properties of the agent. The problem, however, with such a design is to specify how long the washout should be before a claim of disease modification can be supported over merely a delay in washout of the symptomatic effect. Is a 6-wk washout period sufficient or is a longer duration needed to prove that a drug has disease-modifying properties? It seems as if no duration would be criticism proof. If patients initially treated with the active agent were performing better 6 mo after being washed out compared to the placebo-treated patients, some could still claim that outcome at 1 yr might not be different between initial treatment groups. The other problem with this design is that it is probably not feasible to withhold treatment from the placebo group for periods beyond 6 mo.

Another design intended to answer the question of disease modification was proposed by Leber (*10*) and is known as the randomized start design. In this model, patients participate in a 6-mo placebo-controlled trial and then are all

placed on active medication. If patients initially treated with placebo do not achieve the same levels of performance by 1–2 mo after starting active treatment as do the patients initially treated with active drug, then that would support the claim of disease modification. This design appears less prone to interpretive errors in principle, but only one study has so far utilized it (*11*). A full length report of this study has not yet appeared.

### **3.2. Outcome Measures**

#### **3.2.1. Cognitive Assessment Instruments**

At the present time, guidelines developed by an expert panel convened by the FDA in the late 1980s called for the use of an objective cognitive assessment and a clinician's global assessment. The Alzheimer's Disease Assessment Scale — cognitive portion (ADAS-cog) (*12*) rapidly became the standard tool for cognitive assessment of AD patients in clinical trials. The MMSE (*6*) is used as a secondary measure of outcome because it serves in another capacity, namely as the basis for one of the inclusion criteria. The advantages of cognitive outcome measures are many. They include reliability, validity and precision. A test such as the ADAS-cog has test-retest reliability that exceeds values of  $r = .8$  (*13*). Mental status examinations, in general, have been shown to correlate with neuropathology (*14*), and functional assessments (*15*) and to be predictive of nursing home placement (*16*). On the other hand, as patients become too impaired, patients become untestable on tests such as the ADAS-cog or the MMSE. Cognitive measures have also been criticized for lacking a close enough correlation to the daily affairs of dementia patients. Of the many stakeholders in the outcome of AD drug trials, some regulatory agencies and health care providers have asserted that benefits on mental status instruments are insufficient by themselves to prove that a drug is active. Hence, there is interest in other types of assessment instruments.

#### **3.2.2. The Clinician's Global Impression-of-Change Instruments**

The clinician's global impressions of change (CGIC) were introduced to provide the trials with the expert opinions of the treating physicians. For a long time a fixture in trials of antidepressants, CGICs were unknown in the field of dementia until the last decade. Subsequently, progress has been made in defining the methodology of the CGIC (*17,18*). Usually, an interview of the patient and caregiver is carried out at the baseline visit prior to initiation of treatment. Then, at the end of the study, the clinician who conducted the baseline interview again assesses the patient and interviews the family. On the basis of these interviews, but without regard to other test results, the clinician will rate the patient on a 7-point scale. A rating of "4" would indicate no change compared to baseline assessment, ratings of "1," "2," or "3" would indicate degrees of

improvement from marked to minimal, and ratings of “5,” “6,” or “7” indicate declines of minimal to marked amounts. CGICs are not as reliable as cognitive assessments (17), but they appear to be valid. Their relative lack of responsiveness (i.e., they change only small amounts) is a useful feature, because they can be assumed to not be detecting trivial changes with therapy.

### 3.2.3. Functional Assessments

Assessments of function are increasingly being sought in order to gauge whether the anti-AD agent has any effects on daily functioning of the patient. The main impediment in this effort is that functional assessments were not available that were specific for AD, suitable for serial assessments, and modifiable for the mild- to moderate-stage disease that was being studied. Older instruments had either prominent floor effects, where moderately impaired AD patients were too impaired on functions such as driving or dealing with financial affairs, or ceiling effects where mild patients had no trouble (yet) with such functions as bathing or toileting. Newer instruments have been developed such as the Alzheimer’s Disease Cooperative Study (ADCS) ADL scale (19) that have a broad range of sampled activities.

### 3.2.4. Global Severity Ratings

Global severity ratings are another method of assessing change. The CDR scale (9) includes both cognitive (orientation, memory, and judgment) and functional (performance in community affairs, hobbies, and self-cares) components. The Global Deterioration Scale (GDS) (20) is another global composite measure of disease severity. As composite scores, GDS or CDR ratings have unique merits for summarizing a patient’s overall status. However, the GDS’s measurement error, precisely because it attempts to classify patients into only one of a few categories, makes it somewhat unreliable. Nonetheless, just like the CGIC, the insensitivity of a scale such as the CDR implies that when changes in ratings are observed that they are “bigger” effects.

### 3.2.5. Milestones of Dementia

Use of milestones of dementia such as decline to a rating of 3 on the CDR or entry into a nursing home is a different approach to measuring outcomes compared to the quantitative ones such as cognitive or functional instruments (21). The use of endpoints is a powerful methodology that has advantages over the quantitative methods. Survival analyses are more efficient in accounting for patients who drop out due to disease progression. So far, this methodology has been used only in the setting of severe dementia, but it would work in mild dementia. Milestones associated with mild disease could be those such as a diagnosis of AD or CDR of 1.

### 3.2.6. Behavioral Observations

Assessment of behaviors such as apathy, agitation, depression, or hallucinations has also been receiving more attention for two reasons. First, it was recognized that the CEIs and muscarinic agonists (*see Subheadings 4.1. and 4.2.*) had beneficial effects on these behaviors. Equally important is the recognition that these behaviors are important in AD. They are not secondary and inconsequential but rather are major burdens of the AD itself. Although there were several assessment tools in existence that measured some of the behaviors subsumed under the general topic of behavioral disturbances in AD, there was no instrument specifically designed for AD clinical trials of mild to moderately severe patients until Cummings and colleagues developed the Neuropsychiatric Inventory (NPI) scale (22). It has recently been used successfully in a clinical trial (23).

### 3.3. Duration of Clinical Trials

Duration of definitive (or pivotal) clinical trials in AD are tending to become longer as our experience with more drugs increases. Public and professional expectations of new drugs have increased as well. It is remarkable to consider that the initial trial design for the drug tacrine was essentially only 6 wk long (24). After that study was completed, it became clear that there were many compelling reasons to utilize a longer period of study. First, effects of the drugs might be amplified over time. Second, there was a noticeable placebo effect in the context of initial exposure to a treatment in a double-blind placebo-controlled trial. Third, public reaction to results from a 6-wk duration study were understandably muted, given that patients, caregivers, physicians, health care executives, and government officials rejected the idea of extrapolating from short duration studies, to a long duration of treatment. Consequently, studies of 12 wk, and more recently, 24 wk became standard for the development of CEIs. No sooner had these studies of 6 mo duration appeared, than many of the stakeholders were calling for studies of 1 yr duration or longer. Part of the motivation for longer studies was to replicate better the manner in which the drugs would be used in routine clinical practice. Another reason had to do with the observation that participants in clinical trials tended to decline slower than patients in uncontrolled natural history studies. As a consequence, deterioration in placebo-treated patients was so modest that it became difficult to document differences between experimental agents and placebo over just 6 mo. Because functional decline is viewed as more ecologically valid than cognitive decline, longer trials may be needed for meaningful interpretation of functional measures as well. For the future, as agents with mechanisms of action thought to be disease modifying rather than palliative come to be studied, 1–2 yr will be the standard length for investigations.

### **3.4. Analytic Methods**

Approaches that use the intent-to-treat principle are the most conservative for analyzing data from AD clinical trials. Most trials up to the present have employed quantitative outcome measures such as the ADAS-cog that are given to patients at baseline and then at the end of the study. Collecting data on patients on their assigned treatment at the end of the study becomes crucial because anything less (i.e., halfway through the study, or at the end of the study but after patients had ceased taking study medication) will tend to attenuate a true drug effect. Unfortunately, the long duration of future AD clinical trials and the relationship between probability of dropout and rate of disease progression raises the possibility that quantitative analytic methods, such as analysis of variance, will be biased by differential dropout. In contrast, survival methods might be more efficient and give more reliable answers.

## **4. Current Approaches to AD Therapy: A Measure of Progress**

### **4.1. Cholinesterase Inhibitors**

As of this writing (May 1998), there are said to be over a dozen CEIs in various stages of clinical development, but only six of them have clinical trial data that has been presented in public. This chapter summarizes the findings with tacrine (TAC) (25), donepezil (DON) (26a), rivastigmine (RIV) (27a), and metrifonate (MET) (23).

#### **4.1.1. General Comments**

All of these agents have a narrow therapeutic window. Efficacy is strongly dose dependent, however. Peripheral tolerance to the gastrointestinal side effects develops slowly; hence, all of the agents must be titrated slowly.

#### **4.1.2. Pharmacology**

There are many differences between the four drugs. TAC has a short plasma half-life and is a reversible inhibitor of cholinesterase (28). DON has a long plasma half-life and is also a reversible CEI (29). MET is a prodrug that is nonenzymatically converted to dichlorvos, an irreversible CEI (23). RIV is a pseudo-irreversible CEI, meaning that it dissociates from the enzyme, but very slowly (30). Both DON and RIV are selective for brain CEI, whereas TAC and MET are nonselective. There was intense speculation that these differences would result in differences in efficacy, but so far no evidence in support of the superiority of one pharmacologic profile has emerged.

#### **4.1.3. Efficacy**

The effect size for the ADAS-cog for all four drugs falls in the 3- to 5-point range (23,25–27a). This value reflects the difference between baseline score

and end-of-study score for the drug-treated patient group minus the placebo-treated group. For the clinical global assessments in intent to treat analyzes, the effect sizes have ranged between 0.2 and 0.5 points (23,25–27a).

In addition to effects on cognition and clinician's global assessments, these four agents have also had effects on a broader array of characteristics of dementia. Unfortunately, in the areas of functional assessments and behavior, there has been a lack of consistency in the instruments used. As a consequence, it is harder to generalize across the agents. Most students of these drugs suspect that the effects on functional assessment and behavior do, in fact, apply to all of the agents, but the data are more limited. In intent to treat analyses, DON (26a) and RIV (27) produced effects on functional measures superior to placebo. The data on behavioral changes is more limited. MET is the only agent for which a behavioral assessment, the NPI (22), was included in the clinical trial (23). MET showed beneficial effects on hallucinations, apathy, and aberrant motor behavior.

#### 4.1.4. Dosing, Safety, and Tolerability

TAC was dosed at four times per day. RIV is a twice-a-day-dosed medication, whereas DON and MET are dosed once a day. The four times daily dosing of TAC proved to be an impediment to treatment. In the AD population, caregivers are often not available throughout the day.

TAC proved to have two problems that limited its use (28). A number of patients developed transaminase elevations within the first 12–18 wk of therapy. This effect led to the requirement for frequent laboratory monitoring. In addition, the highest doses of tacrine were associated with a high (35%) rate of nausea or vomiting. None of the other agents produce transaminase elevations. DON (26a) and MET (23) have a particularly low rate of gastrointestinal side effects with most of the adverse events occurring during the titration phase of the therapy. RIV (27,30) has a level of gastrointestinal side effects that appears higher during titration than DON or MET. One wonders whether the gastrointestinal side effect profile is a function of effective dose or actually reflects differences in the pharmacology of comparably potent agents.

#### 4.1.5. Conclusions Regarding CEIs

There is considerable evidence that the CEIs have effects on AD, although their effects are modest. As the first generation of anti-AD agents, their development occurred simultaneously with creation of trial methodology. There is scant data to suggest that CEIs have anything other than palliative effects. The one exception comes from a set of tissue culture studies by Lahiri and Farlow (31) that have suggested that TAC has effects on amyloid processing. Besides physostigmine, other CEIs have not been tested in this assay.

As subsequent generations of anti-AD agents come along, it is likely that some of the inefficiencies and confusion that arose during CEI development can be avoided.

## **4.2. Muscarinic Agonists**

Muscarinic agonists should be the logical successors to CEIs. CEIs theoretically lead to activation of both presynaptic and postsynaptic muscarinic receptors. Only the latter should be enabled, because presynaptic receptor activation should decrease synaptic function. A further rationale for the use of muscarinic agonists is based on evidence that stimulation of the M1 muscarinic receptor alters amyloid precursor protein processing and reduces amyloid  $\beta$  protein ( $A\beta$ ) secretion (32) (see Chapter 13).

The results from the muscarinic agonists have been disappointing. Although some changes have been observed on cognitive assessments with two of the drugs, xanomeline (33) and SB202026 (34), the effects were no larger than those seen with the CEIs. Moreover, the peripheral side effects have been prominent. Syncope was a troublesome adverse event, occurring in 12.6% of patients treated with high-dose xanomeline (33). On the positive side, there was a notable behavioral effect of xanomeline in the form of reductions in several troublesome behaviors such as agitation, delusions, and hallucinations.

## **4.3. Estrogen**

There is evidence supporting a biological role for estrogen in the pathogenesis of AD. Estrogen receptors are present on hippocampal and cholinergic neurons (35,36). Estrogen might function as an antioxidant or act to stimulate nerve growth factor release (37). Prospective observational studies suggest a protective effect of estrogen on the subsequent development of AD (38,39). Epidemiological studies do not establish causation, however.

Clinical trial data are beginning to emerge. A small pilot study of estrogen in AD has been reported (40) in which verbal memory improvements were seen in the estrogen-treated group. A larger double-blind clinical trial of estrogen in hysterectomized women with AD is underway under the auspices of the ADCS funded by the National Institute on Aging. A placebo-controlled prevention trial using estrogen (and progesterone) in nondemented women, sponsored by the Women's Health Initiative (41) has completed in recruiting subjects at present. The latter study will require several years before results are available. These studies may help to resolve whether there are actual benefits of estrogen therapy for AD patients. At present, the data are insufficient to recommend estrogen replacement for the primary therapy of AD or as a prevention for AD. The development of estrogen receptor analogs with activity restricted to the brain is being vigorously pursued.

## **4.4. Anti-inflammatory Agents**

Analogous to estrogen, clinical studies provide evidence that individuals using anti-inflammatory (AI) agents have a lower probability of developing

AD (42–46). The rationale for AI therapy is supported by immunohistochemical findings in the AD brain (47). These include demonstrations of excess quantities of proteins known to be associated with an inflammatory response (such as  $\alpha$ -1-antichymotrypsin, cytokines, and complement) as well as activated microglia. These observations provide strong support for anti-inflammatory interventions aimed at slowing the AD pathological process. As knowledge of the mechanism of  $\beta$ -amyloid peptide ( $A\beta$ ) action has accumulated,  $A\beta$  itself appears to be an inducer of the inflammatory response (48).

Only a single placebo-controlled trial with an AI, indomethacin, has been reported to date (49). Interpretation of the effects of the drug was hampered by a high attrition rate due to gastrointestinal toxicity. The ADCS is completing a trial of prednisone in AD; results should be available in late 1999. Currently available nonsteroidal AI agents have substantial gastrointestinal toxicity, especially in the elderly (50). At present, AI agents cannot be recommended for treatment of AD because evidence for benefit is only indirect and the toxicity of current drugs is considerable.

The mechanism of gastrointestinal and renal toxicity is their inhibition of cyclooxygenase-1 (COX-1). Cyclooxygenase-2 (COX-2) inhibitors have been developed that are selective for the inducible enzyme associated with inflammation while sparing the constitutively expressed COX-1 enzyme (51,52). COX-2 inhibitor drugs with far less gastrointestinal toxicity than presently available agents are in the final stages of clinical trials in arthritic conditions. They are also in phase III trials in AD. Inhibition of COX-2 reduces ischemic injury in an acute stroke model (53), but it is yet to be clarified whether COX-2 is involved in the pathogenesis of AD. Other agents with anti-inflammatory properties are plausible to use in AD patients (46), but all have some drawbacks.

#### 4.5. Antioxidants

The evidence for oxidative stress in the brains of patients dying with AD is strong. Excess lipid peroxidation (54) and evidence for oxidative injury to neuronal DNA (55) and proteins (56) have been observed. There are several ways in which oxidant molecules could accumulate in the AD brain.  $A\beta$  itself might induce free radical production (48). Elevated brain iron that has been observed in AD may also contribute to free radical generation (57). A consequence of the just-discussed inflammatory response that occurs in the AD brain (see **Subheading 4.4.**) may induce the production of nitric oxide molecules, which are potent oxidants (58).

The clinical trial using the antioxidants selegiline and  $\alpha$ -tocopherol (vitamin E) (1000 IU twice daily) was the first to report convincing benefits of antioxidants (8). Tocopherol is a fat-soluble substance that blocks lipid peroxidation. There is an extensive literature on tocopherol supporting its role

as an antioxidant, including in vitro evidence of improved cell survival in the presence of toxins, including A $\beta$  (59). On the other hand, there is no evidence of tocopherol deficiency in AD brain. Tocopherol is inexpensive and nontoxic. Selegiline will not be further discussed, as its effects were no greater than tocopherol.

The median delay in appearance of one of the study endpoints of severe dementia in the tocopherol and selegiline-treated groups was about 8 mo, compared to the placebo group, after adjustment for baseline MMSE group differences (which appeared despite random assignment) (8). In examining nursing home placement specifically, only tocopherol alone showed statistically significant delays compared to placebo. There were no differences in cognitive scores between groups at the end of the study. There was no indication of improvement in patients in the active treatment arms. Rather, the drugs appeared to delay the appearance of manifestations of severe dementia. Adverse events were negligible in all but the combination therapy group.

These preliminary findings (8), coupled with the very favorable safety and cost profile of  $\alpha$ -tocopherol, suggest that it can be recommended to most patients with AD. Note that  $\alpha$ -tocopherol may exacerbate coagulopathies in some individuals.

The modest success of  $\alpha$ -tocopherol provides support for the hypothesis that oxidative stress plays a role in AD. Several future approaches are suggested by this study. One would be to develop more potent antioxidant compounds. A report that  $\gamma$ -tocopherol (58) is more effective in blocking lipid peroxidation in vitro than  $\alpha$ -tocopherol should be pursued.

#### **4.6. Neurotrophic Factors**

Because the survival of cholinergic neurons in the basal forebrain is dependent on nerve growth factor (NGF), therapy with this and other growth factors has been conceptualized for some time. However, these proteins do not cross the blood-brain barrier, and thus, intrathecal delivery is required. One case report has appeared on a patient who received intrathecal NGF (60). Few conclusions can be drawn from one patient, other than to note that the results were not dramatic. There also have been reports of unanticipated side effects of NGF in experimental models.

An alternative to NGF itself is to use an orally administered agent that stimulates NGF activity. Several drugs currently under study may have this property. Estrogen is one. Propentofylline is another agent that appears to have NGF-enhancing properties (61) among its several actions. Some of the other effects of propentofylline are in influencing microglia proliferation and possibly modulating inflammatory mechanisms in AD (62).

Idebenone increases brain NGF levels (63) in aged rodents. In addition, idebenone has antioxidant properties and appears to be related to coenzyme Q

(64,65). Two trials of idebenone have been reported from Germany (66,67) in which positive results have been seen. A trial of this agent in AD in progress in the United States was recently suspended because of the lack of efficacy.

## 5. Conclusions

The prospects for more potent anti-AD therapies are slowly but steadily rising. Therapies of several different mechanisms are under investigation. One can only hope that medications that are more potent than the CEIs can be developed. Among the approaches likely to be studied intensively over the next decade are combination therapy regimens and attempts at either presymptomatic or very early symptomatic treatment.

## Acknowledgments

Dr. Knopman has served as a paid consultant to Parke-Davis, Athena Neuroscience, Eisai/Pfizer, Novartis, Janssen and Wyeth-Ayerst. He is currently participating or will participate in clinical trials with Pfizer and Eisai. Dr. Knopman and his family do not own stock or have equity interests in any pharmaceutical or biotechnology company whose agents were mentioned in this article.

## References

1. McKhann, G., Drachman, D., Folstein, M., Katzman, R., Price, D., and Stadlan, A. (1984) Clinical diagnosis of Alzheimer's disease: report of the NINCDS-ADRDA Work Group under the auspices of Department of Health and Human Services Task Force on Alzheimer's Disease. *Neurology* **34**, 939–944.
2. Gearing, M., Mirra, S. S., Hedreen, J. C., Sumi, S. M., Hansen, L. A., and Heyman, A. (1995) The consortium to establish a registry for Alzheimer's Disease (CERAD). Part X. Neuropathology confirmation of the clinical diagnosis of Alzheimer's disease. *Neurology* **45**, 461–466.
3. Hulette, C., Nochlin, D., McKeel, D., Morris, J. C., Mirra, S. S., Sumi, S. M., and Heyman, A. (1997) Clinical-neuropathological findings in multi-infarct dementia: a report of six autopsied cases. *Neurology* **48**, 668–672.
4. Wade, J. P. H., Mirsen, T. R., Hachinski, V. C., Fisman, M., Lau, C., and Merskey, H. (1987) The clinical diagnosis of Alzheimer's disease. *Arch. Neurol.* **44**, 24–29.
5. Hansen, L. and Samuel, W. (1997) Criteria for Alzheimer Disease and the nosology of dementia with Lewy bodies. *Neurology* **48**, 126–132.
6. Folstein, M. F., Folstein, S. E., and McHugh, P. R. (1975) "Mini-mental state": a practical method for grading the cognitive status of patients for the clinician. *J. Psychiatr. Res.* **12**, 189–198.
7. Petersen, R. C., Smith, G. E., Ivnik, R. J., Tangalos, E. G., Schaid, D. J., Thibodeau, S. N., et al. (1995) Apolipoprotein E status as a predictor of the development of Alzheimer's disease in memory-impaired individuals. *JAMA* **273**, 1274–1278.

8. Sano, M., Ernesto, C., Thomas, R. G., Klauber, M. R., Schafer, K., Grundman, M., et al. (1997) A controlled trial of selegiline, alpha-tocopherol, or both as treatment for Alzheimer's disease. *N. Engl. J. Med.* **336**, 1216–1222.
9. Morris, J. C. (1993) The Clinical Dementia Rating (CDR): Current version and scoring rules. *Neurology* **43**, 2412–2414.
10. Leber, P. (1997) Slowing the progression of Alzheimer disease: methodological issues. *Alzheimer Dis Assoc Disord* **11(Suppl. 5)**, S10–S21.
11. Rother, M. (1998) Long term efficacy and safety of propentofyllene in patients with Alzheimer's disease — results of an 18 month placebo controlled trial. *Neurobiol. Aging* **19(Suppl. 4)**, S176.
12. Rosen W. G., Mohs R. C., and Davis, K. L. (1984) A new rating scale for Alzheimer's disease. *Am. J. Psychiatry* **141**, 1356–1364.
13. Knopman, D. and Gracon, S. (1994) Observations on the short-term “natural history” of probable Alzheimer's disease in a controlled clinical trial. *Neurology* **44**, 260–265.
14. DeKosky, S. T. and Scheff, S. W. (1990) Synapse loss in frontal cortex biopsies in Alzheimer's disease: correlation with cognitive severity. *Ann. Neurol.* **27**, 457–464.
15. Reed, B. R., Jagust, W. J., and Seab, J. P. (1989) Mental status as a predictor of daily function in progressive dementia. *Gerontologist* **29**, 804–807.
16. Heyman, A., Peterson, B., Fillenbaum, G., and Pieper, C. (1997) Predictors of time to institutionalization of patients with Alzheimer's disease: the CERAD experience, part XVII. *Neurology* **48**, 1304–1309.
17. Knopman, D. S., Knapp, M. J., Gracon, S. I., and Davis, C. S. (1994) The clinician interview-based impression (CIBI): a clinician's global change rating scale in Alzheimer's disease. *Neurology* **44**, 2315–2321.
18. Schneider, L. S., Olin, J. T., Doody, R. S., Clark, C. M., Morris, J. C., Reisberg, B., et al. (1997) Validity and reliability of the Alzheimer's Disease Cooperative Study-Clinical global impression of change (ADCS-CGIC). *Alzheimer Dis. Assoc. Disord.* **11(Suppl. 2)**, S22–S32.
19. Galasko, D., Bennett, D., Sano, M., Ernesto, C., Thomas, R., Grundman, M., and Ferris, S. (1997) An inventory to assess activities of daily living for clinical trials in Alzheimer's disease. *Alzheimer Dis. Assoc. Disord.* **11(Suppl. 2)**, S33–S39.
20. Reisberg, B., Ferris, S. H., deLeon, M. J., and Crook, T. (1982) The Global Deterioration Scale for assessment of primary degenerative dementia. *Am. J. Psychiatry* **139**, 1136–1139.
21. Galasko, D., Edland, S. D., Morris, J. C., Clark, C., Mohs, R., and Koss, E. (1995) The consortium to establish a registry for Alzheimer's disease (CERAD). Part XI. Clinical milestones in patients with Alzheimer's disease followed over 3 years. *Neurology* **45**, 1451–1455.
22. Cummings, J. L., Mega, M., Gray, K., Rosenberg-Thompson, S., Carusi, D. A., and Gornbein, J. (1994) The neuropsychiatric inventory: comprehensive assessment of psychopathology in dementia. *Neurology* **44**, 2308–2314.
23. Morris, J. C., Cyrus, P. A., Orazem, J., et al. (1998) Effects of metrifonate on the cognitive, global and behavioral function of Alzheimer's disease patients: results of a randomized, double-blind, placebo-controlled study. *Neurology* **50**, 1222–1230.

24. Davis, K., Thal, L. J., Gamzu, E. R., Davis, C. S., Woolson, R. F., Gracon, S. I., et al. (1992) A double-blind, placebo-controlled multicenter study of tacrine for Alzheimer's disease. *N. Engl. J. Med.* **327**, 1253–1259.
25. Knapp, M. J., Knopman, D. S., Solomon, P. R., Pendlebury, W. W., Davis, C. S., and Gracon, S. I. (1994) A 30-wk randomized controlled trial of high-dose tacrine in patients with Alzheimer's disease. *JAMA* **271**, 985–991.
26. Rogers, S. L., Farlow, M. R., Doody, R. S., Mohs, R., Friedhoff, L. T., and the Donepezil Study Group. (1998) A 24 week double-blind, placebo-controlled trial of donepezil in patients with Alzheimer's disease. *Neurology* **50**, 136–145.
- 26a. Rosler, M., Anand, R., Cicin-Sain, A., Gauthier, S., Agid, Y., Dal-Bianco, P., Stahelin, H. B., et al. (1999) Efficacy and safety of rivastigmine in patients with Alzheimer's disease: international randomised controlled trial. *BMJ* **318**, 633–649.
27. Corey-Brown, J., Anand, R., and Veach, J. (1998) ENA 713 (rivastigmine tartrate), a new acetylcholinesterase inhibitor, in patients with mild to moderately severe Alzheimer's disease. *Int. J. Geriatric Psychopharmacol.* **1**, 55–65.
- 27a. Burns, A., Rossor, M., Hecker, J., Gauthier, S., Petit, H., Miller, H., Roger, S. L., et al. (1999) The effects of Donepezil in Alzheimer's disease—results from a multinational trial. *Dement. Geriatr. Cogn. Disord.* **10**, 237–244.
28. Davis, K. L. and Powchik, P. (1995) Tacrine. *Lancet* **345**, 625–630.
29. Bryson, H. M. and Benfield, P. (1997) Donepezil. *Drugs Aging* **10**, 234–239.
30. Anand, R., Gharabawi, G., and Enz, A. (1996) Efficacy and safety result of the early phase studies with exelon (ENA-713) in Alzheimer's disease: an overview. *J. Drug Dev. Clin. Pract.* **8**, 1–8.
31. Lahiri, D. K. and Farlow, M. R. (1996) Differential effect of tacrine and physostigmine on the secretion of the beta-amyloid precursor protein in cell lines. *J. Mol. Neurosci.* **7**, 41–49.
32. Growdon, J. (1997) Muscarinic agonists in Alzheimer's disease. *Life Sci.* **60**, 993–998.
33. Bodick, N., Offen, W., Levey, A. I., Cutler, N. R., Gauthier, S. G., Satlin, A., et al. (1997) Effects of xanomeline, a selective muscarinic receptor agonist, on cognitive function and behavioral symptoms in Alzheimer disease. *Arch. Neurol.* **54**, 465–473.
34. Kumar, R., on behalf of the SmithKline Beecham Alzheimer's Disease Study Group. (1996) Efficacy and safety of SB202026 as a symptomatic treatment for Alzheimer's disease. *Ann. Neurol.* **40**, 504 (abstr.).
35. Luine, V. N. (1985) Estradiol increases choline acetyltransferase activity in specific basal forebrain nuclei and projection areas of female rats. *Exp. Neurol.* **89**, 484–490.
36. Gould, E., Woolley, C. S., Frankfurt, M., and McEwen, B. S. (1990) Gonadal steroids regulate dendritic spine density in hippocampal pyramidal cells in adulthood. *J. Neurosci.* **10**, 1286–1291.
37. Toran-Allerand, C. D., Miranda, R. C., Bentham, W. D., Sohrabji, F., Brown, T. J., Hochberg, R. B., and MacLusky, N. J. (1992) Estrogen receptors colocalize with low-affinity nerve growth factor receptors in cholinergic neurons of the basal forebrain. *Proc. Natl. Acad. Sci. USA* **89**, 4668–4672.

38. Tang, M. X., Jacobs, D., Stern, Y., Marder, K., Schofield, P., Gurland, B., et al. (1996) Effect of estrogen during menopause on risk and age at onset of Alzheimers disease. *Lancet* **348**, 429–432.
39. Kawas, C., Resnick, S., Morrison, A., Brookmeyer, R., Corrada, M., Zonderman, A., et al. (1997) A prospective study of estrogen replacement therapy and the risk of developing Alzheimers disease. *Neurology* **48**, 1517–1521.
40. Asthana, S., Craft, S., Baker, L. D., et al. (1996) Transdermal estrogen improves memory in women with Alzheimer's disease. *Soc. Neurosci. Abstr.* **22**, 200.
41. Shumaker, S. and Rapp, S. (1996) Hormone therapy in dementia prevention: the Womens Health Initiative memory study. *Neurobiol. Aging* **17(Suppl. 4s)**, S9.
42. Breitner, J. C. S., Gau, B. A., Welsh, K. A., Plassman, B. L., McDonald, W. M., Helms, M. J., and Anthony, J. C. (1994) Inverse association of anti-inflammatory treatments and Alzheimer's disease: initial results of a co-twin control. study. *Neurology* **44**, 227–232.
43. Andersen, K., Launer, L. J., Ott, A., Hoes, A. W., Breteler, M. M., and Hofman, A. (1995) Do nonsteroidal anti-inflammatory drugs decrease the risk for Alzheimer's disease. *Neurology* **45**, 1441–1445.
44. McGeer, P. L., Schulzer, M., and McGeer, E. G. (1996) Arthritis and anti-inflammatory agents as possible protective factors for Alzheimer's disease: a review of 17 epidemiologic studies. *Neurology* **47**, 425–432.
45. Stewart, W. F., Kawas, C., Corrada, M., and Metter, E. J. (1997) Risk of Alzheimer's disease and duration of NSAID use. *Neurology* **48**, 626–632.
46. Aisen, P. S., and Davis, K. L. (1997) The search for disease-modifying treatment for Alzheimers disease. *Neurology* **48(Suppl. 6)**, S35–S41.
47. Lue, L. F., Brachova, L., Civin, W. H., and Rogers, J. (1996) Inflammation, A $\beta$  deposition and neurofibrillary tangle formation as correlates of Alzheimer's disease neurodegeneration. *J. Neuropathol. Exp. Neurol.* **55**, 1083–1088.
48. Yan, S. D., Chen, X., Fu, J., Chen, M., Zhu, H., Roher, A., et al. (1996) RAGE and amyloid-peptide neurotoxicity in Alzheimer's disease. *Nature* **382**, 685–691.
49. Rogers, J., Kirby, L. C., Hempelman, S. R., Berry, D. L., McGeer, P. L., Kaszniak, A. W., et al. (1993) Clinical trial of indomethacin in Alzheimer's disease. *Neurology* **43**, 1609–1611.
50. Zeidler, H. (1991) Epidemiology of NSAID induced gastropathy. *J. Rheumatol.* **18(Suppl. 28)**, S2–S5.
51. Smith, W. L. and DeWitt, D. L. (1995) Biochemistry of prostaglandin endoperoxide H synthase-1 and synthase-2 and their differential susceptibility to nonsteroidal anti-inflammatory drugs. *Semin. Nephrol.* **15**, 179–194.
52. Seibert, K., Masferrer, J., Zhang, Y., Gregory, S., Olson, G., Hauser, S., et al. (1995) Mediation of inflammation by cyclo-oxygenase-2. *Agents Actions Suppl.* **46**, 41–50.
53. Nogawa, S., Zhang, F., Ross, M. E., and Iadecola, C. (1997) Cyclo-oxygenase-2 gene expression in neurons contributes to ischemic brain damage. *J. Neurosci.* **17**, 2746–2755.
54. Palmer, A. M. and Burns, M. A. (1994) Selective increase in lipid peroxidation in the inferior temporal cortex in Alzheimers disease. *Brain Res.* **645**, 338–342.

55. Mecocci, P., MacGarvey, U., and Beal, M. F. (1994) Oxidative damage to mitochondrial DNA is increased in Alzheimers disease. *Ann. Neurol.* **36**, 747–751.
56. Hensley, K., and Hall, N., Subramaniam, R., Cole, P., Harris, M., Aksenov, M., et al. (1995) Brain regional correspondence between Alzheimer's disease histopathology and biomarkers of protein oxidation. *J. Neurochem.* **65**, 2146–2156.
57. Smith, M. A. and Perry, G. (1995) Free radical damage, iron and Alzheimer's disease. *J. Neurol. Sci.* **134(Suppl.)**, 92–94.
58. Christen, S., Woodall, A. A., Shigenaga, M. K., Southwell-Keely, P. T., Duncan, M. W., and Ames, B. N. (1997) Gamma-tocopherol. traps mutagenic electrophiles such as NO(X) and complements  $\alpha$ -tocopherol: physiological implications. *Proc. Natl. Acad. Sci. USA* **94**, 3217–3222.
59. Behl, C., Davis, J., Cole, G. M., and Schubert, D. (1992) Vitamin E protects nerve cells from amyloid-protein toxicity. *Biochem. Biophys. Res. Commun.* **186**, 944–950.
60. Olson, L., Nordberg, A., von Holst, H., Backman, L., Ebendal, T., Alafuzoff, I., et al. (1992) Nerve growth factor affects 11C-nicotine binding, blood flow, EEG, and verbal episodic memory in an Alzheimer patient (case report). *J. Neural. Transm. Park Dis. Dement. Sect.* **4**, 79–95.
61. Yamada, K., Nitta, A., Hasegawa, T., Fuji, K., Hiramatsu, M., Kameyama, T., et al. (1997) Orally active NGF stimulators: potential therapeutic agents in Alzheimers disease. *Behav. Brain Res.* **83**, 117–122.
62. McRae, A., Rudolphi, K. A., and Schubert, P. (1994) Propentopylline depresses amyloid and Alzheimer's CSF microglial antigens after ischaemia. *NeuroReport* **5**, 1193–1196.
63. Nitta, A., Hasegawa, T., and Nabeshima, T. (1993) Oral administration of idebenone, a stimulator of NGF synthesis recovers reduced NGF content in aged rat brain. *Neurosci. Lett.* **163**, 219–222.
64. Bruno, V., Battaglia, G., Copani, A., Sortino, M. A., Canonico, P. L., and Nicoletti, F. (1994) Protective action of idebenone against excitotoxic degeneration in cultured cortical neurons. *Neurosci. Lett.* **178**, 193–196.
65. Wieland, E., Schutz, E., Armstrong, V. W., Kuthe, F., Heller, C., and Oellerich, M. (1995) Idebenone protects hepatic microsomes against oxygen radical-mediated damage in organ preservation solutions. *Transplantation* **60**, 444–51.
66. Weyer, G., Erzigkeit, H., Hadler, D., and Kubicki, S. (1996) Efficacy and safety of idebenone in the long-term treatment of Alzheimer's disease — a double-blind, placebo controlled multicentre study. *Hum. Psychopharmacol.* **11**, 53–65.
67. Weyer, G., Babejdolle, R. M., Hadler, D., Hofmann, S., and Herrmann, W. M. (1997) A controlled study of 2 doses of idebenone in the treatment of Alzheimer's disease. *Neuropsychobiology* **36**, 73–82.

## Production and Functional Assays of Recombinant Secreted Amyloid Precursor Protein (APP) (sAPP $\alpha$ )

Steven W. Barger

### 1. Introduction

The  $\beta$ -amyloid precursor protein (APP) is connected to Alzheimer's disease by both biochemistry and genetics. As the source of the major constituent of amyloid plaques, APP has been the subject of many studies of its expression and metabolism. The accumulation of amyloid  $\beta$ -peptide (A $\beta$ ) in these plaques was the first evidence that APP might be processed abnormally in Alzheimer's, and this idea was strengthened by the discovery of mutations in APP that segregate with the disease with high penetrance. Aberrant processing of APP was incorporated into the Amyloid Hypothesis, which supposes that the clinical symptoms, neuropathology, and ultimate fatality of Alzheimer's result from the actions of A $\beta$ . But to the extent that the Amyloid Hypothesis remains hypothetical, it would be irresponsible to ignore other theories that might explain the links between APP and Alzheimer's. APP can be proteolytically processed in a way that does not produce (and, in fact, precludes) A $\beta$ . This " $\alpha$ -secretase" event cleaves within the A $\beta$  sequence and liberates most of the extracellular portion (sAPP $\alpha$ ) of APP from the cell surface (**Fig. 1**). Because the " $\beta$ -secretase" event required for the generation of A $\beta$  creates a different soluble derivative (sAPP $\beta$ ), disease-related increases in  $\beta$ -secretase processing — such as demonstrated with the "Swedish" mutation of APP — have the potential to affect events dependent on the normal function(s) of sAPP $\alpha$ . Furthermore, the increases in APP expression that occur as a result of injury or trisomy 21 may elevate the total levels of all sAPP species. To understand the implications of these events, it is critical to elucidate the biological activities of sAPP $\alpha$  and related moieties.

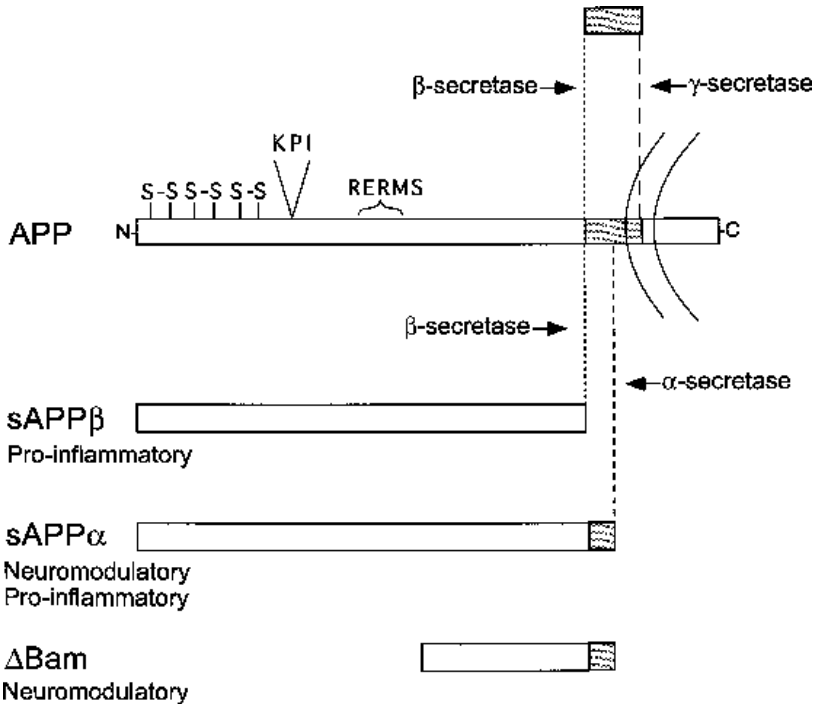


Fig. 1. Schematic of APP soluble derivatives. APP is depicted as a transmembrane protein containing the A $\beta$  sequence (striped), a cysteine-rich region near the N-terminus, the differentially spliced KPI region, and a region containing the sequence R-E-R-M-S (a.k.a., heparin-binding domain 2) connected to some bioactivities of sAPP. The  $\alpha$ -secretase cleavage generates sAPP $\alpha$ , whereas  $\beta$ -secretase releases sAPP $\beta$  and, in combination with  $\gamma$ -secretase, A $\beta$ .  $\Delta$ Bam is not a naturally occurring fragment but a deletion mutant that retains residues 444–612 (APP<sub>695</sub> numbering) and neuro-modulatory activity (10).

APP and its soluble derivatives are structurally complex proteins, a characteristic that allows a diverse array of biological activities: protease inhibition, enhancement of cellular proliferation, neuromodulation of electrophysiological activity, enhancement of cellular attachment, and proinflammatory activation of microglia. APP is synthesized as at least four variants that arise from differential splicing of a single gene, and these differences all reside in exons included in the secreted portion of the protein. APP<sub>751</sub> and APP<sub>770</sub> contain Kunitz protease inhibitor (KPI) domains; indeed, the sAPP arising from APP<sub>751</sub> was first isolated by virtue of this activity and termed protease nexin-2 (1–3). An additional protease-inhibitor domain has been described in a region shared by all splice variants (4). Decreases in proliferation rates were documented in

fibroblasts subjected to down-regulation of APP, and this effect was overcome by the addition of sAPP $\alpha$  (5). A role for sAPP $\alpha$  in neuromodulation was first suggested by Mattson et al. (6), who found that sAPP $\alpha_{695}$  and sAPP $\alpha_{751}$  could rapidly depress intraneuronal calcium concentration ( $[Ca^{2+}]_i$ ). This effect was subsequently attributed to a cyclic guanosine 3':5'-monophosphate ( $c$ GMP)-dependent activation of potassium currents (7); it appears to be responsible for actions of sAPP $\alpha$  on long-term depression of synaptic efficacy (8) and, at least partially, for an ability of sAPP $\alpha$  to protect neurons against excitotoxic and oxidative insults (9,10). Three heparin-binding sites can be found in sAPP $\alpha$ . Two of these have been implicated in the ability of sAPP $\alpha$  to facilitate cellular attachment and neuritic growth (11,12). Most recently, sAPPs were shown to elevate markers of inflammatory activation in microglia (13). Of these bioactivities of sAPPs, the neuromodulatory activity and the neurite trophism have been demonstrated to vary between the products of  $\alpha$ - and  $\beta$ -secretase processing (10,13,14). Neuromodulation and microglial activation are both modified by interactions of sAPP $\alpha$  with apolipoprotein E (13,15).

This chapter describes detailed methods for production and purification of sAPPs. Several bioassays useful in testing the functions of sAPPs are included, as well. Unfortunately, space does not allow an exhaustive description of all the assays used to date. It is hoped that these techniques may be useful toward further elucidation of the roles of sAPPs in both normal neurobiology and Alzheimer's disease.

## 2. Materials

### 2.1. Production/Purification of sAPP $\alpha$ from Mammalian Cells

1. APPcDNA stably transfected into HEK293 (human embryonic kidney) or similar cell line.
2. Serum-free medium: Dulbecco's minimal essential medium/F12 (1:1) supplemented with 0.5 mM L-glutamine, 10 nM sodium selenite, and 50  $\mu$ M ethanolamine.
3. Roller bottles (1400 cm<sup>2</sup>) and roller apparatus (or equivalent high-capacity culture arrangement).
4. Poly-L-lysine (mol wt 150,000–300,000).
5. Borate buffer, pH 8.4: 50 mM borate, 10 mM sodium tetraborate (Borax).
6. High-speed centrifuge and 250- to 500-mL bottles.
7. Diethylaminoethyl (DEAE)-Sephacrose column, 20-mL, low pressure.
8. Heparin-Sepharose column, 5-mL, low pressure (e.g., HighTop™ heparin-sepharose, Amersham, Pharmacia [Piscataway, NJ]).
9. MonoQ or equivalent fast preparative liquid chromatography (FPLC) (moderate pressure) anion-exchange column, 1-mL.
10. Dialysis tubing, 12,000–14,000 mol wt cut-off, 25 mm wide.

11. Chromatography buffer A: phosphate-buffered saline, pH 7.4 (PBS), containing 0.5 mM EDTA and 1 mM phenylmethylsulfonyl fluoride (PMSF) (protease inhibitors).
12. Chromatography buffer B: PBS containing 0.75 M NaCl and protease inhibitors.
13. Chromatography buffer C: PBS containing 1 M NaCl and protease inhibitors.
14. Chromatography buffer D: 20 mM triethanolamine-HCl (pH 7.4), 100 mM NaCl.
15. Chromatography buffer E: 20 mM triethanolamine-HCl (pH 7.4), 1 M NaCl.
16. Antibody specific for sAPP.

## **2.2. Production/Purification of sAPP from Bacterial Cultures**

1. sAPP coding sequence in a bacterial polyhistidine-tagging expression vector.
2. Suitable strain of *E. coli*.
3. Luria broth.
4. Isopropyl- $\beta$ -D-thiogalactopyranoside (IPTG).
5. One-liter growth flasks and shaker apparatus (or equivalent high-capacity culture arrangement).
6. Spectrophotometer, visible wavelength.
7. Low-speed centrifuge and tubes.
8. Nickel-chelating column, 5 mL (e.g., ProBond™, Invitrogen, San Diego, CA).
9. Lysis buffer: 6 M guanidine hydrochloride, 20 mM sodium phosphate, 500 mM sodium chloride, pH 7.8.
10. Chromatography loading buffer: 8 M Urea, 20 mM sodium phosphate, 500 mM sodium chloride, pH 7.8.
11. Wash buffer A: 8 M Urea, 20 mM sodium phosphate, 500 mM sodium chloride, pH 6.0.
12. Wash buffer B: 8 M Urea, 20 mM sodium phosphate, 500 mM sodium chloride, pH 5.3.
13. Elution buffer: 8 M Urea, 20 mM sodium phosphate, 500 mM sodium chloride, pH 4.0.
14. Dialysis tubing, 12,000–14,000 mol wt cut-off.
15. Dialysis buffer: 10 mM Tris-HCl (pH 7.4).

## **2.3. Bioassays**

### **2.3.1. Cyclic GMP Assay**

1. Guanosine monophosphate (cGMP), 3:5-cyclic.
2. Anti-cGMP antibody (Calbiochem, San Diego, CA).
3. [<sup>125</sup>I]cGMP, >2500 mCi/mg (Biomedical Technologies, Inc., Stoughton MA).
4. Triethylamine (TEA), 4°C.
5. Acetic anhydride (AA), 4°C.
6.  $\gamma$ -Globulin, 1% solution.
7. Isopropanol, 4°C.
8. Sodium acetate buffer (10 $\times$ ): 500 mM Sodium acetate, pH 6.2.
9. Bovine serum albumin (BSA), 0.1 mg/mL solution in 1 $\times$  sodium acetate buffer.
10. High-precision pH indicator strips.
11. HCl, 0.1 M.
12. (Membrane assay only): Homogenization buffer: 250 mM sucrose, 50 mM Tris-HCl (pH 8.0), 1 mM  $\beta$ -mercaptoethanol, 1 mM EDTA.

13. Membrane suspension buffer: 50 mM Tris-HCl (pH 7.0), 1 mM  $\beta$ -mercaptoethanol.
14. 2 $\times$  Membrane assay buffer: 40 mM Tris-HCl (pH 7.0), 8 mM MgCl<sub>2</sub>, 2 mM isobutylmethylxanthine, 11  $\mu$ g/mL phosphocreatine, 1  $\mu$ g/mL creatine kinase.
15. Guanosine triphosphate.

### 2.3.2. Electrophoretic Mobility Shift Assay (EMSA)

1. Lysis buffer: 10 mM HEPES (pH 7.9), 10 mM KCl, 3 mM MgCl<sub>2</sub>, 0.5 mM  $\beta$ -mercaptoethanol, 10  $\mu$ g/mL leupeptin, 10  $\mu$ g/mL aprotinin, 0.5 mM PMSF.
2. Nonidet P-40.
3. Extraction buffer: 10 mM HEPES (pH 7.9), 420 mM NaCl, 1.5 mM MgCl<sub>2</sub>, 0.2 mM EDTA, 25% glycerol, 0.5 mM  $\beta$ -mercaptoethanol, 10  $\mu$ g/mL leupeptin, 10  $\mu$ g/mL aprotinin, 0.5 mM PMSF.
4. Dilution buffer: 10 mM HEPES (pH 7.9), 50 mM KCl, 0.2 mM EDTA, 20% glycerol, 0.5 mM  $\beta$ -mercaptoethanol, 10  $\mu$ g/mL leupeptin, 10  $\mu$ g/mL aprotinin, 0.2 mM PMSF.
5. Double-stranded oligonucleotide containing the  $\kappa$ B enhancer sequence: GGGGACTTTC.
6. [ $\gamma$ -<sup>32</sup>P]ATP, 3000 Ci/mmol, 10 mCi/mL.
7. T<sub>4</sub> polynucleotide kinase (and commercial buffer).
8. Spun-columns (16).
9. 5 $\times$  TBE: 500 mM Tris-HCl (pH 8.0), 450 mM borate, 5 mM EDTA.
10. Acrylamide and bis-acrylamide (37.5 : 1).
11. 5 $\times$  Binding Buffer: 50 mM Tris-HCl (pH 7.4), 20% glycerol, 5 mM MgCl<sub>2</sub>, 2.5 mM EDTA, 0.5% Nonidet P-40, 5 mM  $\beta$ -mercaptoethanol, 0.25 mg/mL poly dI-dC.
12. Bromophenol blue, 0.1%.

## 3. Methods

### 3.1 Production/Purification of sAPP $\alpha$ in Mammalian Cultures

The primary advantage of mammalian expression is structural veracity. Certainly, posttranslational modifications like glycosylation cannot even take place in prokaryotic systems, and some nonmammalian eukaryotic expression systems (yeast, baculovirus) may perform glycosylations that differ from mammals. In addition, cotranslational folding of a secretory protein can create an irreversibly distinct structure, including a defined set of disulfide bridges that occur only in the more oxidizing environment in the lumen of the endoplasmic reticulum (ER).

The primary disadvantage of mammalian expression is low yield. Nevertheless, sufficient sAPP $\alpha$  for 3–6 mo of cell biology experiments (~3 mg) can be generated from the HEK293 cell line (American Type Culture Collection, Rockville, MD) with the protocol below. The stable transfectants were made with either the pCMV695 or pOCK<sub>751</sub> expression plasmids (coding for APP<sub>695</sub>

and APP<sub>751</sub>, respectively), both of which contain the neomycin resistance gene for selection. Transfection and selection procedures are not within the scope of this chapter and can be found elsewhere (17). The stable cell lines are maintained in minimal essential medium (MEM) supplemented to 10% with fetal bovine serum (FBS) and 0.2 mg/mL Geneticin (G418). From a T75 maintenance flask, the cells can be expanded into 12 flasks in two passages.

Once confluent, the 12 T75 flasks will provide cells for seeding four roller bottles. On the day of seeding, the roller bottles are coated for  $\geq 2$  h with 100 mL of 100  $\mu\text{g/mL}$  poly-L-lysine (*see Note 1*) in borate buffer (while rotating on the roller apparatus), then washed three times with PBS. The cells are seeded and grown in the coated bottles with 200 mL of MEM/FBS (G418 can be omitted) while rotating at  $\sim 3$  rpm in a humidified 37°C incubator containing 5% CO<sub>2</sub>. Alternatively, the bottles can be gassed with sterile-filtered 5% CO<sub>2</sub>, and the lids can be closed tightly for culturing in a less-regulated “warm room.” Over the course of 7–10 d, the cells should expand in a monolayer on the walls of the bottles to near 70% confluence (*see Note 2*). Then the medium is removed, and the walls of the bottles are washed gently with 100 mL PBS. Serum-free medium (200 mL) is added, and the bottles are returned to the above culture conditions for 5 d.

### 3.1.1. Protein Purification, Day 1

Steps 3–6 are performed at 4°C.

1. Pour the conditioned medium from the roller bottles into a beaker; put fresh serum-free medium back on the roller bottles (as three to four cycles can be collected; *see Note 3*).
2. Add EDTA and PMSF to the collected medium at final concentrations of 5 mM and 1 mM, respectively. Adjust the pH to 7.4 with careful addition of 10 N NaOH.
3. Centrifuge the medium in large centrifuge bottles at 11,000g for 30 min. This step usually chills the medium sufficiently for loading onto the column (next step).
4. Transfer the supernatant to a clean container and load by gravity feed onto a 10-mL DEAE column equilibrated with chromatography buffer A.
5. Wash the column with 100 mL of chromatography buffer A.
6. Elute with 20 mL chromatography buffer B; collect 1-mL fractions.
7. Spot 1  $\mu\text{L}$  of each fraction onto nitrocellulose marked with a grid to allow fraction identification; store the remainder of the fractions at  $-80^\circ\text{C}$ .
8. Develop the fraction spot blot by immunodetection using anti-APP antibody (e.g., as per a Western blot; *see Chapter 13*).

### 3.1.2. Day 2 (Not Necessarily Consecutive)

All steps except **step 14** are performed at 4°C (*see Note 4*).

9. Pool the APP-positive fractions and dialyze for  $\sim 1$  h against 1 L of chromatography buffer A.

10. Clear the dialysate by filtration through a 0.45- $\mu$ , low protein-binding syringe filter.
11. Load onto a heparin-Sepharose column. This column can be run by gravity feed with a two-cylinder gradient maker such as used for pouring gradient gels. However, the gradient (*see step 13*) can be generated with better control using a moderate-pressure FPLC system (*see Note 5*).
12. Wash with 50 mL of chromatography buffer A.
13. Elute with gradient from chromatography buffer A to chromatography buffer C (~0.5 mL/min, traversing the gradient within 60 min), collecting 0.5-mL fractions.
14. Again, generate and develop a spot blot for each fraction and store the remainder at  $-80^{\circ}\text{C}$ .

### 3.1.3. Day 3 (Not Necessarily Consecutive)

Steps through 19 are performed at  $4^{\circ}\text{C}$

15. Pool the APP-positive fractions and dialyze for ~1 h against 1 L of chromatography buffer D (*see Note 6*).
16. Clear the dialysate by syringe filtration.
17. Load onto a MonoQ HR 5/5 column (Pharmacia Biotech, Piscataway, NJ) using a moderate-pressure FPLC system and a flow rate of ~0.5 mL/min. Other anion exchange columns have been used successfully, as well.
18. Wash with 10 mL of chromatography buffer D.
19. Run a gradient from chromatography buffer D to 70% chromatography buffer E (0.5 mL/min), traversing the gradient within 30 min (*see Note 7*); collect 0.5-mL fractions. Strip the column with 100% chromatography buffer E.
20. Again create a spot blot for each fraction, save a 10- $\mu$ L aliquot of each, and store the remainder in separate tubes at  $-80^{\circ}\text{C}$ .
21. Use the 10- $\mu$ L aliquots to analyze the APP-immunopositive fractions on a 5–15% polyacrylamide gradient sodium dodecyl sulfate (SDS) gel with silver-stain development to identify fractions containing the best yield and purity.
22. Pool and sterile filter the desired fractions; store in convenient aliquots at  $-80^{\circ}\text{C}$ .

## 3.2. Production/Purification of sAPP in Bacterial Cultures

*Observe U.S. Centers for Disease Control/National Institute of Health Biosafety Level 2 containment/decontamination procedures (or equivalent)*

Bacterial cultures offer the benefit of very high protein yields. Despite their deficiencies in modification, etc., sAPPs produced in bacteria retain some of their important bioactivities (**10,13,14**). Indeed, the currently used purification protocol involves denaturation of the proteins during chromatography, suggesting that at least some of the biologically active structures of sAPP can renature sufficiently in physiological solutions. The production has been made more facile by expressing the proteins in a vector that fuses a polyhistidine sequence to the N-terminus. This modification allows one-step purification on a nickel-affinity column. In addition to the time this cuts from the purification time, the polyhistidine tag standardizes purification of APP structural variants

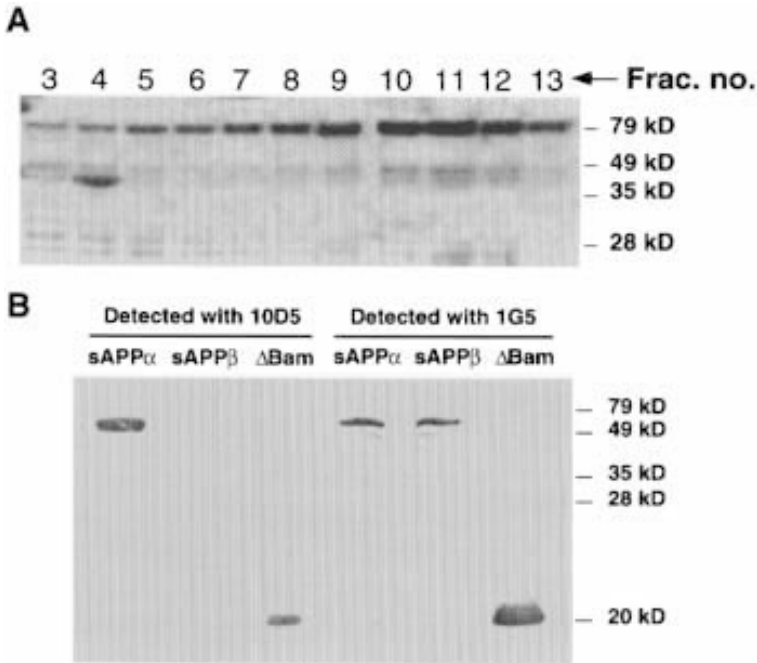


Fig. 2. Purification of bacterially produced sAPP protein constructs. **(A)** Elution profile of sAPP $\alpha$  from nickel-chelate column; silver stained. The apparent minor contaminants in fraction 11 react with anti-APP antibodies, suggesting that they may be incomplete translation products or proteolytic fragments. **(B)** Differential antigenicity of sAPP $\alpha$ , sAPP $\beta$ , and  $\Delta$ Bam. Aliquots of each protein were subjected to Western blot analyzes using alternatively 10D5, a monoclonal antibody generated against A $\beta$ <sub>1-16</sub>, or 1G5, a monoclonal antibody generated against  $\Delta$ Bam (both generous gifts from Athena Neurosciences, Inc., South San Francisco, CA).

(e.g., sAPP $\beta$  or deletion mutants) (**Fig. 2**). Therefore, bioassays intended for structure-function analysis do not suffer from differences arising from artifacts of purification.

The bacterial expression system applied to sAPP production utilizes the pTrcHis vector system (Invitrogen); the purification protocol has been based on commercial documentation (**18**), with modifications for a somewhat larger scale. The *KpnI-EcoRI* fragment of APP<sub>695</sub> cDNA was subcloned into the *KpnI-EcoRI*-cut pTrcHisC. A double-stranded oligonucleotide cassette was synthesized, annealed, and spliced into the *EcoRI* site of the resulting plasmid to complete the coding sequence of sAPP $\alpha$ ; a “stop” codon was engineered in place of amino acid 613 of APP<sub>695</sub> (amino acid 17 of the A $\beta$  sequence). Transcription from pTrcHis is regulated by the *lac* operon and thus is inducible

with IPTG. The vector was transformed into TOP10™ *E. coli* (Invitrogen), an optimal expression strain. A 0.5-L culture in Luria broth is grown (from a 20-mL overnight starter culture) to an A<sub>600</sub> of 0.6. At this point, IPTG is added to a final concentration of 1 mM for 3–5 h.

Protein purification:

1. The cells are collected by centrifugation at 8000g for 20 min at 4°C. The supernatant is discarded.
2. Twenty milliliters of lysis buffer is added to the cell pellet, and the sample is rocked gently for 5–10 min at room temperature until the pellet is dispersed (repeated aspiration and expulsion through a large-bore pipet may facilitate dispersion).
3. The lysate is sonicated with three 5-s pulses at ~0.425 relative output (Fisher Sonic Dismembrator 300, Fisher Scientific, Pittsburgh, PA).
4. Centrifuge the lysate at 11,000g for 20 min at 20°C; transfer the supernatant to a clean container.
5. Load the sonicated, cleared lysate onto a 5-mL nickel-chelating (e.g., ProBond™; Invitrogen) column preequilibrated with loading buffer (*see Note 8*).
6. Wash the column with 50 mL of loading buffer.
7. Wash the column with 30 mL wash buffer A.
8. Wash the column with 30 mL wash buffer B.
9. Elute the column with 12 mL of elution buffer, collecting 0.5-ml fractions.
10. Run 10  $\mu$ L of each fraction on a 5–15% polyacrylamide gradient sodium dodecyl sulfate (SDS) gel; during this time, the fractions may be stored at 4°C.
11. Pool the desired fractions (usually four to five) and dialyze against 10 mM Tris-HCl, pH 7.4: Dialyze against 2 L for 10 min at room temperature, then place the dialysis chamber at 4°C; after 4 h, refresh the dialysis with prechilled (4°C) buffer, and continue with dialysis for an additional 16 h (*see Note 9*).
12. Sterile filter the dialysate, and store aliquots at –80°C.

### 3.3. Bioassays

#### 3.3.1. Cyclic GMP Assay

Elevations of cGMP levels by sAPP $\alpha$  can be detected in cultures of primary central nervous system neurons (**9**) or in membranes prepared from neonatal rat brain (**19**). The cGMP can be quantified by radioimmunoassay (RIA), described as follows.

##### 3.3.1.1. DAY 1

1. Rat primary hippocampal or neocortical neurons are cultured as described (**20**) in 60-mm plates.
2. After treatment for  $\leq 5$  min with 0.01–1 nM sAPP $\alpha$ , the medium is removed from the cultures, 400  $\mu$ L of 0.1 M HCl is added, and the plates are frozen on a slab of dry ice. (Plates can be stored at –20°C for several weeks.)

3. Thaw the plates and scrape with cell harvesters; transfer the lysates to microfuge tubes.
4. Clear the lysates by centrifugation at 12–14,000g for 5 min at 4°C.
5. Transfer 360  $\mu\text{L}$  of each lysate to a new tube and place on ice; save the pellets for **step 16**.
6. Correct the pH of the samples (*see Note 10*):
  - a. Add approx 43  $\mu\text{L}$  of a 10:1 mixture of 10 $\times$  sodium acetate buffer/10 *N* NaOH to one sample (the precise amount must be determined empirically).
  - b. After thorough mixing with the buffer/NaOH mixture, spot  $\sim$ 1  $\mu\text{L}$  of the sample onto a high-resolution pH indicator strip.
  - c. If the pH approximates 6, proceed with the remaining tubes.
  - d. If the pH differs from  $6 \pm 0.5$ , correct with the addition of 0.5–2  $\mu\text{L}$  increments of 1 *N* NaOH or HCl. Adjust the volume of buffer/NaOH added to the next sample, then proceed from **step 6b**.
  - e. Once all the samples have been adjusted with buffer/NaOH, check the pH of each by spotting as in **step 6b**. Adjust as necessary.
7. Transfer 100  $\mu\text{L}$  of each sample to a 12  $\times$  75 mm glass tube containing 400  $\mu\text{L}$  1 $\times$  sodium acetate buffer on ice.
8. By serial dilution, set up standards containing 0.01–3.0 nM cGMP; transfer 100  $\mu\text{L}$  of each standard to 400  $\mu\text{L}$  sodium acetate buffer, as for the samples.
9. Set up a 0-cGMP standard tube and a “nonspecific” (NS) tube, each containing only 500  $\mu\text{L}$  sodium acetate buffer.
10. Move the tubes to a fume hood for acetylation (*see Note 11*):
  - a. Add 20  $\mu\text{L}$  ice-cold TEA to one tube and immediately mix by vortexing.
  - b. Add 10  $\mu\text{L}$  ice-cold AA to the tube, immediately mix and place back on ice.
  - c. Proceed with each remaining tube, one by one (including standards and NS tubes).
11. Transfer 100  $\mu\text{L}$  from each tube to new tubes, in duplicate.
12. Add 100  $\mu\text{L}$  of 100 nCi/mL [ $^{125}\text{I}$ ]cGMP to each tube; also add to two empty tubes (“total input”; TI). Mix thoroughly by vortexing.
13. Add to each tube (except the NS and TI tubes) 100  $\mu\text{L}$  anti-cGMP antibody prepared at the optimal concentration (*see Note 12*) in sodium acetate buffer containing 0.1 mg/mL BSA.
14. Add 100  $\mu\text{L}$  0.1 mg/mL BSA to the NS tubes.
15. Mix each tube, cover with parafilm, and place at 4°C overnight.
16. Hydrolyze the pellets from **step 5** in 25  $\mu\text{L}$  of 0.2 *N* NaOH (30 min, room temperature); quantify protein in a 10-fold dilution with bicinchronic acid (BCA) (Pierce Chemical Co., Rockford, IL).

### 3.3.1.2. DAY 2

17. Add 50  $\mu\text{L}$  of 1%  $\gamma$ -globulin to all tubes except TI and mix by vortexing.
18. Add 2 mL of ice-cold isopropanol to each tube except TI; mix.
19. Centrifuge all tubes except TI at 1200g for 40 min at 4°C.
20. Aspirate the supernatant to a radioisotope-compatible collection chamber.

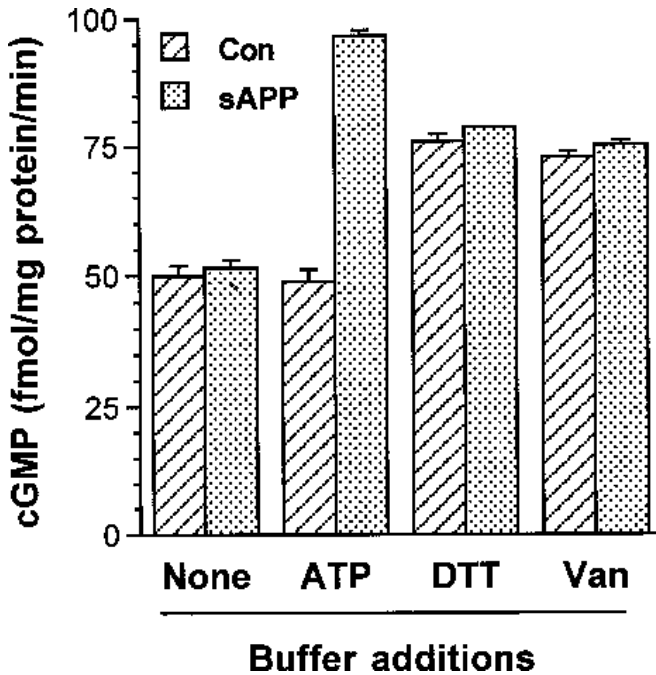


Fig. 3. Dependence of sAPP $\alpha$ -stimulated cGMP generation on ATP. Rat cortical membranes were assayed for responses to 5 nM sAPP $\alpha$  in the absence (“None”) or presence of various modulators of other particulate guanylate cyclase activities: 1 mM ATP, 1 mM dithiothreitol (“DTT”), or 0.1 mM sodium orthovanadate (“Van”).

21. Quantify the pellets on a  $\gamma$ -counter (2 min/tube).
22. Subtract NS from each value. Generate a standard curve and interpolate unknowns (most accurate in the log-linear portion of the curve).

### 3.3.1.3. MEMBRANE ASSAY

Cyclic GMP generation in membranes can be measured with the following modifications to the above protocol. The impact of agents reported to affect other particulate guanylate cyclases were surveyed; only adenosine triphosphate (ATP) made a significant impact on sAPP $\alpha$  responses (**Fig. 3**).

**Steps 1–4** are performed at 0–4°C

1. Perform Dounce homogenization of cortical tissue from neonatal rats (postnatal day  $\leq 3$ ) in homogenization buffer (~3 mL/cerebrum; 6–8 strokes).
2. Centrifuge the homogenate at 700g for 10 min to remove large contaminants.
3. Transfer the supernatant to a suitable tube and centrifuge at 100,000g for 60 min.
4. Discard the supernatant, wash the pellet briefly in membrane suspension buffer, then suspend in same (~100  $\mu$ L/cerebrum); store on ice until **step 6**.

5. Hydrolyze 5- $\mu$ L aliquots in 15  $\mu$ L 0.2 *N* NaOH for 15 min at room temperature; perform BCA (Pierce Chemical) protein determination on a fivefold dilution of the hydrolysate.
6. Dilute membrane in membrane assay buffer to a final concentration of 0.6–1.2  $\mu$ g protein/ $\mu$ L and dispense 50  $\mu$ L to 12  $\times$  75 glass tubes at 37°C.
7. After 45 s, add 50  $\mu$ L of a mixture of 2 *mM* GTP and sAPP $\alpha$  (0.2–20 *nM*) or the appropriate dilution of vehicle; react 2–6 min at 37°C.
8. Stop the reaction by the addition of 900  $\mu$ L ice-cold sodium acetate buffer.
9. Transfer the stopped reaction mixture to microfuge tubes and centrifuge at 12,000–14,000*g* for 5 min.
10. Start cGMP RIA at **step 7** (above).

### 3.3.2. Electrophoretic Mobility Shift Assay

In the two cell types which we have assayed sAPP $\alpha$  biological activity, the protein activates  $\kappa$ B-binding transcription factors. In microglia, *bona fide* NF $\kappa$ B is the target of sAPP-activated cellular signals (**13**). However, considerable evidence suggests that sAPP $\alpha$  activates a novel  $\kappa$ B-binding factor in primary neurons; efforts are underway to isolate and sequence this factor. Either factor can be detected by EMSA using a  $\kappa$ B sequence as the DNA probe. In either case, this assay requires at least  $2 \times 10^6$  cells.

#### 3.3.2.1. NUCLEAR EXTRACTION

All steps performed at 0–4°C

1. Put plates on ice and wash in PBS, then once in lysis buffer.
2. Scrape each plate in 150–200  $\mu$ L lysis buffer containing 0.5% Nonidet P-40 and transfer this lysate to a prechilled microfuge tube (*see Note 13*); incubate for 5 min, then vortex vigorously.
3. Centrifuge in a microfuge (12,000–14,000*g*) at 4°C for 5 min.
4. Discard the supernatant and wash the pellet (nuclei) with 1 mL lysis buffer (without Nonidet P-40); centrifuge in a microfuge as in **step 3**.
5. Discard the supernatant and resuspend the pellet in 20  $\mu$ L extraction buffer; incubate for 10 min at 4°C.
6. Vortex the tube vigorously; centrifuge in a microfuge as in **step 3**.
7. Transfer 20  $\mu$ L of the supernatant to a new, prechilled tube; centrifuge in a microfuge as in **step 3**.
8. Transfer the supernatant to a new, prechilled tube and add 30  $\mu$ L dilution buffer; mix gently.
9. Take two 5- $\mu$ L aliquots for protein determination; freeze the remainder at –80°C.

#### 3.3.2.2. ELECTROPHORETIC MOBILITY SHIFT ASSAY GEL

1. Start a labeling reaction using 3.5 pmol  $\kappa$ B oligonucleotide, 10  $\mu$ Ci [ $\gamma$ -<sup>32</sup>P]ATP, and 5 U T<sub>4</sub> polynucleotide kinase; incubate at 37°C for 1–3 h.
2. Pour a large (20  $\times$  20 cm) 6% polyacrylamide (37.5:1, acrylamide/bis-acrylamide) gel with 0.75-mm spacers (buffer is 0.25 $\times$  Tris-borate-EDTA).

3. Stop the probe reaction (**step 1**) by adding 1  $\mu$ L 500 mM EDTA; add 40  $\mu$ L Tris-EDTA (TE) and separate the probe from unincorporated ATP in a spun-column preequilibrated with TE; count a 1- $\mu$ L aliquot in a liquid scintillation counter.
4. Dilute the nuclear extract sample (**Subheading 3.3.2.2., step 9**) to 1–5  $\mu$ g protein/28  $\mu$ L; add 7  $\mu$ L 5 $\times$  binding buffer.
5. Set up nonspecific tubes containing the same protein content and 1–3  $\mu$ L cold oligonucleotide in 28  $\mu$ L; add 7  $\mu$ L 5 $\times$  binding buffer.
6. Incubate the sample and nonspecific tubes on ice for 15 min.
7. Add 10–50,000 cpm  $^{32}$ P-labeled oligonucleotide to each tube; incubate at room temperature for 20 min.
8. Add 2  $\mu$ L 0.1% bromophenol blue (*see Note 14*) to each tube and load on the 6% polyacrylamide gel; run at 150 V for approx 2 h.
9. Dry the gel on a gel dryer (1–2 h) (*see Note 15*), then expose to X-ray film (overnight is usually sufficient) (*see Note 16*).

#### 4. Notes

1. Poly-L-lysine can be made as a 10 mg/mL stock and autoclaved.
2. Monitoring roller-bottle growth on a conventional inverted microscope can be difficult. Removal of the condenser from a Nikon TMS works handily.
3. Cells slough from the walls of the roller bottles if they become too dense. If sloughing occurs relatively late in the culture cycle, the conditioned medium is still useful, but additional cycles will be futile.
4. The heparin-Sepharose and MonoQ columns can be run at room temperature with a yield of active protein, but sAPP has an inherent lability that may be suppressed partially at 4°C.
5. “FPLC” is an acronym coined by Pharmacia Biotech for “fast preparative liquid chromatography.” Several chromatography systems can satisfy the requirements for pumping large volumes of corrosive aqueous buffers through chemically inert (e.g., polyetheretherketon [PEEK]) pumps. The Waters 650 workstation (Millipore, Bedford, MA) has been used for the work presented here.
6. Tris-HCl can be substituted for TEA-HCl in the MonoQ chromatography, but it is a poorer buffer at pH 7.4 and thus should be used at no lower than pH 7.6.
7. Depending on the column and conditions, greater resolution on the MonoQ column may be achieved by replacing the linear gradient with a parabolic gradient, such that the gradient becomes more gradual near the elution point of sAPP.
8. The bacterial lysate can be stored at –20°C for several days prior to running the nickel-chelate column.
9. Large yields may result in precipitation of bacterially expressed sAPP during dialysis. This can be prevented by adding 0.1% Triton X-100 to the dialysis buffer.
10. Cyclic GMP is sensitive to nonenzymatic hydrolysis under alkaline conditions. Adjustment of the pH should be performed with care to avoid prolonged incubation of the samples at a high pH. Haste is also helpful in the acetylation step, as TEA dramatically raises the pH before it is corrected again by the AA.
11. Acetylation of cGMP is performed in the RIA because most commercial anti-cGMP antibodies are generated against conjugated cGMP; it can be omitted with a loss of sensitivity and specificity.

12. Determination of the optimal anti-cGMP concentration in the RIA must be made empirically. An RIA relies on having a limiting amount of antibody so that proper competition will occur between the [<sup>125</sup>I]cGMP and the cold cGMP. Initially, test a 1:100 dilution. Run the cGMP RIA with only standards' NS and TI. As a rule of thumb, total precipitated cpm (0-cGMP standard) should be approximately half of the TI cpm. If the antibody concentration is too high, the standard curve will flatten out at the low standard concentrations; if the antibody concentration is too low, resolution will be lost at the high end of the curve. Thus, the antibody input should be tailored to the range of cGMP amounts expected in a typical experiment.
13. Nuclear extraction for electrophoretic mobility shift assay may be most conveniently done in a 2-mL, screw-cap microfuge tube, as the tip has a more shallow slope that allows the pellets to be spread more broadly across the tube wall. This makes more convenient both the aspirations of supernatants and resuspensions of pellets.
14. Bromophenol blue and borate buffers inhibit the DNA-binding activity of some transcription factors, but they do not affect  $\kappa$ B-binding factors appreciably.
15. The electrophoretic mobility shift assay requires rapid drying in a heated, vacuum-driven gel dryer to prevent diffusion of the labeled products in an unfixed gel.
16. Interpretation of EMSA results is based on the appearance of a retarded band at 2–3 cm from the top of the gel. Specificity of the binding is apparent from suppression with unlabeled oligonucleotide. In the case of NF $\kappa$ B, identity of the band can be confirmed by "supershift": further retardation by an antibody to a subunit of the factor (e.g., **ref. 13**).

## Acknowledgments

This work was sponsored by funds from National Institute of Neurological Disorders and Stroke (NINDS), Bethesda, MD (NS35872), Alzheimer's Association, Chicago, IL (RG1-96-076), and the Inglewood Foundation, Little Rock, AR. Dr. Russell Rydel (Elan Pharmaceuticals, San Francisco, CA) offered advice on the productin and purification of sAPP $\alpha$  from mammalian cells.

## References

1. Knauer, D. J., Thompson, J. A., and Cunningham, D. D. (1983) Protease nexins: cell-secreted proteins that mediate the binding, internalization, and degradation of regulatory serine proteases. *J. Cell. Physiol.* **117**, 385–396.
2. Oltersdorf, T., Fritz, L. C., Schenk, D. B., Lieberburg, I., Johnson-Wood, K. L., Beattie, E. C., et al. (1989) The secreted form of the Alzheimer's amyloid precursor protein with the Kunitz domain is protease nexin-II. *Nature* **341**, 144–147.
3. Van Nostrand, W. E., Wagner, S. L., Suzuki, M., Choi, B. H., Farrow, J. S., Geddes, J. W., et al. (1989) Protease nexin-II, a potent antichymotrypsin, shows identity to amyloid  $\beta$ -protein precursor. *Nature* **341**, 546–549.
4. Miyazaki, K., Hasegawa, M., Funahashi, K., and Umeda, M. (1993) A metalloproteinase inhibitor domain in Alzheimer amyloid protein precursor. *Nature* **362**, 839–841.

5. Saitoh, T., Sundsmo, M., Roch, J.-M., Ximura, M., Cole, G., Schubert, D., et al. (1989) Secreted form of amyloid  $\beta$  protein precursor is involved in the growth regulation of fibroblasts. *Cell* **58**, 615–622.
6. Mattson, M. P., Cheng, B., Culwell, A. R., Esch, F. S., Lieberburg, I., and Rydel, R. E. (1993) Evidence for excitoprotective and intraneuronal calcium-regulating roles for secreted forms of the  $\beta$ -amyloid precursor protein. *Neuron* **10**, 243–254.
7. Furukawa, K., Barger, S. W., Blalock, E. M., and Mattson, M. P. (1996) Activation of potassium channels and suppression of neuronal activity by secreted  $\beta$ -amyloid precursor protein. *Nature* **379**, 74–78.
8. Ishida, A., Furukawa, K., Keller, J. N., and Mattson, M. P. (1997) Secreted form of  $\beta$ -amyloid precursor protein shifts the frequency dependency for induction of LTD, and enhances LTP in hippocampal slices. *Neuroreport* **8**, 2133–2137.
9. Barger, S. W., Fiscus, R. R., Ruth, P., Hofmann, F., and Mattson, M. P. (1995) The role of cyclic GMP in the regulation of neuronal calcium and survival by secreted forms of  $\beta$ -amyloid precursor. *J. Neurochem.* **64**, 2087–2096.
10. Furukawa, K., Sopher, B. L., Rydel, R. E., Begley, J. G., Pham, D. G., Martin, G. M., et al. (1996) Increased activity-regulating and neuroprotective efficacy of  $\alpha$ -secretase-derived secreted amyloid precursor protein conferred by a c-terminal heparin-binding domain. *J. Neurochem.* **67**, 1882–1896.
11. Small, D. H., Nurcombe, V., Reed, G., Clarris, H., Moir, R., Beyreuther, K., and Masters, C. L. (1994) A heparin-binding domain in the amyloid protein precursor of Alzheimer's disease is involved in the regulation of neurite outgrowth. *J. Neurosci.* **14**, 2117–2127.
12. Jin, L. W., Ninomiya, H., Roch, J. M., Schubert, D., Masliah, E., Otero, D. A., and Saitoh, T. (1994) Peptides containing the RERMS sequence of amyloid  $\beta$ /A4 protein precursor bind cell surface and promote neurite extension. *J. Neurosci.* **14**, 5461–5470.
13. Barger, S. W. and Harmon, A. D. (1997) Microglial activation by secreted Alzheimer amyloid precursor protein and modulation by apolipoprotein E. *Nature* **388**, 878–881.
14. Li, H. L., Roch, J. M., Sundsmo, M., Otero, D., Sisodia, S., Thomas, R., and Saitoh, T. (1997) Defective neurite extension is caused by a mutation in amyloid  $\beta$ /A4 ( $A\beta$ ) protein precursor found in familial Alzheimer's disease. *Neurobiology* **32**, 469–480.
15. Barger, S. W. and Mattson, M. P. (1997) Isoform-specific modulation by apolipoprotein E of the activities of secreted  $\beta$ -amyloid precursor protein. *J. Neurochem.* **69**, 60–67.
16. Sambrook, J., Fritsch E. F., and Maniatis, T. (eds.) (1989) *Molecular Cloning, A Laboratory Manual*, 2nd ed. Cold Spring Harbor Laboratory Press, Plainview NY, pp. E37–E38.
17. Kaufman, R. J. (1997) Expression of proteins in mammalian cells, in *Current Protocols in Molecular Biology* (Ausubel, F. M. et al., eds.), Wiley, New York, pp. 16.12.1–16.14.13.
18. *Xpress System Protein Purification*, Version B; Invitrogen, San Diego CA.

19. Barger, S. W. and Mattson, M. P. (1995) Secreted form of the Alzheimer's  $\beta$ -amyloid precursor protein stimulates a membrane-associated guanylate cyclase. *Biochem. J.* **311**, 45–47.
20. Mattson, M. P., Barger, S. W., Begley, J., and Mark, R. J. (1995) Calcium, free radicals, and excitotoxic neuronal death in primary cell culture. *Methods Cell. Biol.* **46**, 187–216.

## Quantifying $A\beta_{1-40}$ and $A\beta_{1-42}$ Using Sandwich-ELISA

Daniel M. Skovronsky, Jun Wang, Virginia M.-Y. Lee,  
and Robert W. Doms

### 1. Introduction

The role of  $A\beta$  accumulation in the pathogenesis of Alzheimer's disease (AD) is supported by genetic studies showing that mutations in the amyloid- $\beta$  precursor protein (APP) that alter  $A\beta$  production are linked to a subset of familial AD (FAD) cases with autosomal penetrance (reviewed in **ref. 1**). Several of these FAD-associated APP mutations, as well as FAD-associated mutations in the presenilin 1 (PS1) and presenilin 2 (PS2) genes, lead to an increase in the production of  $A\beta_{1-42}$  relative to  $A\beta_{1-40}$ . This, combined with the observation that these peptides are differentially deposited in senile plaques (SPs) *in vivo*, suggests that differential production of  $A\beta_{1-40}$  and  $A\beta_{1-42}$  may be crucially important in the pathogenesis of AD. Thus, it is important to use techniques that not only quantitate  $A\beta$  production, but also specifically differentiate between these two peptides in a variety of experimental paradigms. Here we describe the use of a highly sensitive sandwich-ELISA (enzyme-linked immunosorbent assay) to quantitate both  $A\beta_{1-40}$  and  $A\beta_{1-42}$  in soluble pools, after secretion by cultured cells into the medium or in human cerebrospinal fluid (CSF) samples, as well as in insoluble pools, as found intracellularly in cultured cells, or deposited in the brain parenchyma.

#### **1.1. $A\beta_{1-40}$ and $A\beta_{1-42}$ are Differentially Deposited in AD Plaques**

Immunocytochemical studies of senile plaques using antibodies specific to the carboxyl termini of  $A\beta_{1-40}$  and  $A\beta_{1-42}$  demonstrate that almost all diffuse and immature plaques stain for  $A\beta$  ending at residue 42 ( $A\beta_{42}$ ), whereas very

few contain A $\beta$  ending at residue 40 (A $\beta$ 40). In contrast, mature core senile plaques contain both A $\beta$ 40 and A $\beta$ 42, with A $\beta$ 40 mainly in the core and A $\beta$ 42 present in the core and the periphery, accounting for most of the volume of the plaque (2,3). Interestingly, it is these A $\beta$ 40 containing SPs rather than diffuse plaques that seem to be directly involved in AD, since compared to control patients, cortices from AD patients have significantly higher levels of A $\beta$ 40 containing SPs, the presence of which are correlated with regions of neuronal loss (4). In addition to these correlative findings, the observation that microglial cells are associated with virtually all A $\beta$ 40-containing cored plaques but with very few of the A $\beta$ 40-negative uncored plaques further suggests that these cored plaques may be critically important in the pathogenesis of AD (5).

Although very little is known about the mechanisms by which these different types of senile plaques are generated, the presence of A $\beta$ <sub>1-40</sub> and A $\beta$ <sub>1-42</sub> in the CSF of normal and AD patients suggests that A $\beta$  is constitutively produced and secreted in vivo. Furthermore, several studies suggest that CSF from AD patients contains less A $\beta$ <sub>1-42</sub> than that of controls, perhaps due to increased deposition of this species in SPs of affected individuals (6,7). In contrast to the paucity of A $\beta$ 40 (relative to A $\beta$ 42) found in the brain, A $\beta$ 40 is the major species found in CSF. Interestingly, the ratio A $\beta$ <sub>1-40</sub> and A $\beta$ <sub>1-42</sub> found in the CSF (approx 10:1) mirrors the ratio of A $\beta$ <sub>1-40</sub> and A $\beta$ <sub>1-42</sub> secreted by cultured neurons (8).

### **1.2. Production of A $\beta$ <sub>1-40</sub> and A $\beta$ <sub>1-42</sub> by Cultured Cells**

Numerous studies have documented that cells that express APP (either endogenously or as a result of engineered overexpression) secrete both A $\beta$ <sub>1-40</sub> and A $\beta$ <sub>1-42</sub>. In such cell lines, A $\beta$  secretion is modulated by FAD associated mutations, with expression of APP<sub>717</sub> mutants or coexpression of FAD associated PS1 and PS2 mutations increasing the A $\beta$ <sub>1-42</sub> to A $\beta$ <sub>1-40</sub> ratio (9-12). These experiments form the basis for the hypothesis that overproduction of A $\beta$ <sub>1-42</sub> is a key step in the pathogenesis of AD and illustrate the necessity for careful quantitation of A $\beta$ <sub>1-40</sub> and A $\beta$ <sub>1-42</sub>.

Interestingly, secretion of A $\beta$ <sub>1-40</sub> and A $\beta$ <sub>1-42</sub> by neurons (NT2N) derived from a human embryonal carcinoma cell line (NT2) increases with time spent in culture (8). This result suggests that an age-dependent increase in A $\beta$  secretion by neurons in vivo may play a role in the deposition of A $\beta$  into senile plaques during AD, as well as in the cortex and hippocampus of transgenic mice that over-express mutant forms of APP (13,14).

Although the study of secreted A $\beta$ <sub>1-40</sub> and A $\beta$ <sub>1-42</sub> has elucidated factors which affect A $\beta$  production, intracellular A $\beta$  must be examined in order to clarify the sites and mechanisms of A $\beta$  production. A recent study has shown that A $\beta$ <sub>1-40</sub> may be generated in the trans-Golgi network (TGN), enroute to

secretion (15). In contrast, several studies have demonstrated that intracellular  $A\beta_{1-42}$  is generated in the endoplasmic reticulum/intermediate compartment (ER/IC), a site from which  $A\beta$  is not secreted (16,17). Interestingly, the ER/IC is a site where presenilins have been localized (18,19). Because mutations in the presenilin gene have been implicated in the upregulation of  $A\beta_{1-42}$  production, the colocalization of the presenilins with a major site of  $A\beta_{1-42}$  production raises the possibility that alterations in  $A\beta$  production by the ER/IC pathway may play an important role in AD pathogenesis. Additionally,  $A\beta_{1-42}$  generated in the ER remains within the cell in a relatively insoluble pool, which cannot be extracted using detergent-containing buffers (20). This insoluble  $A\beta_{1-42}$  accumulates intracellularly over time in culture, possibly as a result of the very slow turnover of this pool. If a similar phenomena occurs in neurons in vivo, a gradual accumulation of insoluble intracellular  $A\beta_{1-42}$  may be involved in the genesis of senile plaques.

Thus, when studying  $A\beta$  production by cultured cells, it is important not only to quantitate  $A\beta_{1-40}$  and  $A\beta_{1-42}$  secreted by cells but also  $A\beta_{1-40}$  and  $A\beta_{1-42}$  in the soluble and insoluble intracellular pools.

### 1.3. *In Vitro* Fibrillogenesis of $A\beta_{1-40}$ and $A\beta_{1-42}$

$A\beta_{1-40}$  and  $A\beta_{1-42}$  have very different properties in vivo, whereas  $A\beta_{1-42}$  makes up the bulk of insoluble  $A\beta$ , both in the brain and intracellularly in cultured cells,  $A\beta_{1-40}$  is more abundant in soluble pools, such as the CSF and in material secreted by cultured cells. These differences may be accounted for by the basic chemical properties of these peptides. Studies by Jarrett and Lansbury (21) have demonstrated that although  $A\beta_{1-40}$  and  $A\beta_{1-42}$  have similar thermodynamic solubilities, they have very different kinetic solubilities, with  $A\beta_{1-42}$  forming insoluble fibrils at a much faster rate than  $A\beta_{1-40}$ . Thus, solutions of kinetically soluble  $A\beta_{1-40}$  could undergo amyloid formation after seeding by  $A\beta_{1-42}$ -containing nuclei (22). Although such a situation does not completely explain the paucity of  $A\beta_{1-40}$  in senile plaques in vivo, it may help explain how slight changes in levels of  $A\beta_{1-42}$  relative to  $A\beta_{1-40}$  could initiate disease.

## 2. Materials

### 2.1. Sandwich-ELISA

1. Synthetic  $A\beta_{1-40}$  and  $A\beta_{1-42}$  peptides (Bachem Biosciences, King of Prussia, PA).
2. BlockAce solution: 1% BlockAce (Snow Brand Milk Products, Sapporo, Japan) in phosphate-buffered saline (PBS), 0.05%  $NaN_3$ .
3. Buffer C: 0.1 M  $NaH_2PO_4$ , 0.1 M  $Na_2HPO_4$ , 2 mM ethylene diaminetetraacetic acid (EDTA), 0.4 M NaCl, 0.2% BSA, 0.05% CHAPS, 0.4% BlockAce, 0.05%  $NaN_3$ , pH 7.0.

4. Buffer EC: 0.1 M NaH<sub>2</sub>PO<sub>4</sub>, 0.1 M Na<sub>2</sub>HPO<sub>4</sub>, 2 mM EDTA, 0.4 M NaCl, 1% bovine serum albumin (BSA), 0.005% Thimerosal (Sigma, St. Louis, MO), pH 7.0.
5. 1× Dulbecco's PBS (Life Technologies, Inc., Rockville, MD).
6. Tween-20.
7. Ban50, BA-27, BC-05 monoclonal antibodies (provided by and courtesy of Dr. N. Suzuki and Takeda Pharmaceutical, Japan).
8. Coating buffer: 0.1 M NaHCO<sub>3</sub>, 0.1 M Na<sub>2</sub>CO<sub>3</sub>, pH 9.6.
9. Maxisorp Immuno-assay plates (Nunc, Roskilde, Denmark).
10. Tris-maleate buffer (TMB) peroxidase solutions (Kirkegaard and Perry Laboratories, Gaithersburg, MD).
11. Spectrophotometric plate reader (i.e., Dynatech MR4000, Dynatech, Chantilly, VA).

## 2.2. Extraction of Cells/Tissue

1. Radioimmunoprecipitation assay (RIPA) buffer: 0.5% sodium deoxycholate, 0.1% sodium dodecyl sulfate (SDS), 1% NP40, 5 mM EDTA in TBS, pH 8.0, with a cocktail of protease inhibitors added before use (1 μg/mL each of pepstatin A, leupeptin, TPCK, TLCK, and soybean trypsin inhibitor in 5 mM ethyleneglycoltetraacetic acid [EGTA] and 0.5 mM phenylmethylsulfonyl fluoride [PMSF]).
2. 70% Formic acid.
3. 1 M Tris base (pH should be ~10 ; do not adjust).
4. 1× Dulbecco's PBS (Life Technologies).
5. 1× Tris-buffered saline (TBS): 50 mM Tris-HCl, 150 mM NaCl, pH 7.6.

## 3. Methods

### 3.1. Aβ Sandwich-ELISA

The Aβ sandwich-ELISA relies on the use of three monoclonal antibodies: BAN-50 (anti-Aβ<sub>1-16</sub>) is used as a capturing antibody, whereas HRP-conjugated BA-27 (which is specific for Aβ ending at residue 40) and BC-05 (which is specific for Aβ ending at residue 42) are used as reporter antibodies (9). Using the previously described conditions, the ELISA distinguishes Aβ<sub>1-40</sub> and Aβ<sub>1-42</sub> with very low crossreactivity and a sensitivity of approx 0.1–0.5 femtomoles (fmol) of Aβ per sample (9,23). The sandwich-ELISA saturates at approx 50–100 fmol of Aβ per sample (23). The protocol detailed below (adapted from ref. 9) forms the basis for the Aβ sandwich-ELISA.

#### 3.1.1. Day 1

1. Dilute Ban50 antibody in sodium bicarbonate coating buffer at 5 μg/mL (see Note 1).
2. Add 100 μL of Ban50 antibody to each well, allow to coat for 24 h at 4°C (see Note 2).

#### 3.1.2. Day 2

3. Remove the Ban50 antibody solution and wash the plate twice with 300 μL PBS per well (see Note 3).

4. Add 300  $\mu$ L BlockAce solution per well and allow the plates to block for at least 24 h at 4°C (see **Note 4**).

### 3.1.3. Day 3

5. Remove the BlockAce solution and wash the plate twice with 300  $\mu$ L PBS per well.
6. Add 50  $\mu$ L EC buffer to each well to prevent the wells from drying while loading the samples.
7. Prepare serial dilutions of A $\beta_{1-40}$  and A $\beta_{1-42}$  standards (see **Note 5**).
8. Add 100  $\mu$ L of the samples and standards and allow the samples to bind for 24 h at 4°C (see **Note 6**).

### 3.1.4. Day 4

9. Remove the samples from the wells and wash the plate twice with 300  $\mu$ L PBS per well.
10. Dilute BA-27 or BC-05 antibodies 1:2000 in buffer C (see **Note 7**). Add 100  $\mu$ L per well to the appropriate plates.

### 3.1.5. Day 5

11. Remove the antibodies and wash the plate twice with 300  $\mu$ L PBS per well.
12. Wash the plate twice with 300  $\mu$ L PBS + 0.05% Tween-20.
13. Add 100  $\mu$ L of a 1:1 mix of TMB peroxidase substrates (allow peroxidase substrates to warm to room temperature before use).
14. Allow the ELISA to develop for up to 1 h (see **Note 8**).
15. Stop the reaction by adding 100  $\mu$ L 1 M H<sub>3</sub>PO<sub>4</sub> per well, and measure the absorbance of the wells at 450 nm (see **Note 9**).

## 3.2. Quantitation of A $\beta$ Secreted by Cultured Cells

As the sandwich-ELISA allows for the direct analysis of conditioned media, it provides a simple and rapid method to quantitate the secretion of A $\beta_{1-40}$  and A $\beta_{1-42}$  from cultured cells. It has been utilized to examine A $\beta$  secretion in a variety of paradigms, including expression of APP and presenilin FAD mutants (9–12), as well as treatment of cells with various drugs meant to alter A $\beta$  production (24).

Because, in addition to A $\beta$ , most nonneuronal cell lines secrete large amounts of p3 (the secreted product of  $\alpha$ - and  $\gamma$ -secretase cleavage of APP) it is important to note that using Ban50 antibody excludes p3 and other amino-truncated A $\beta$  species from analysis. Although in many situations it may be useful to quantitate p3 production as well as A $\beta$  production (and thus compare activities of  $\alpha$ - and  $\beta$ -secretase pathways), p3 specific antibodies are not available and thus the exclusive analysis of p3 by ELISA is not currently possible. Instead, investigators have utilized HRP-coupled 4G8 antibody (anti-A $\beta_{17-24}$ ) to detect A $\beta$  and p3 after capturing with BC-O5 or BA-27 antibodies (2). Data

from such an experiment can then be compared to that obtained after analysis with the A $\beta$  specific (Ban50/BC-05 and Ban50/BA-27) sandwich-ELISA in order to assess p3 secretion.

### **3.3. Extraction of Intracellular A $\beta$ for Quantitation by Sandwich-ELISA**

Although several studies have demonstrated the presence of detergent soluble pools of intracellular A $\beta$  in a variety of cell lines (8,15–17,25,26), we have recently discovered the presence of an additional pool of relatively insoluble intracellular A $\beta$ . We found that in many cell lines, this insoluble pool of A $\beta$  represents the majority of the total intracellular A $\beta$ , and can be quantitatively extracted using 70% formic acid (20). Although direct extraction of cells into formic acid yields both the soluble and insoluble pools of A $\beta$ , it is also possible to simultaneously monitor A $\beta$  in each intracellular pool by sequential extraction of cells with RIPA buffer followed by formic acid. In **Subheading 3.3.1.** we detail the protocols for each of these extraction methods (adapted from **ref. 20**).

#### **3.3.1. Lysis of Cells Directly Into Formic Acid (see Note 10)**

1. Remove the media, and wash the cells twice in ice-cold PBS.
2. Scrape the cells in 1 mL cold PBS.
3. Centrifuge at 3000g for 2 min to pellet the cells.
4. Remove the PBS, and resuspend the cells in 100  $\mu$ L 70% formic acid (*see Note 11*).
5. Sonicate for 10 s with a probe sonicator.
6. Centrifuge at 100,000g for 20 min at 4°C to remove remaining insoluble material.
7. Transfer the supernatant to a fresh tube, and neutralize with 1.9 mL of 1 M Tris-base (*see Notes 12 and 13*).
8. Dilute the sample 1:3 in H<sub>2</sub>O, and load 100  $\mu$ L into the microtiter plate well for sandwich-ELISA (**Subheading 3.1.**) (*see Note 14*).

#### **3.3.2. Sequential Extraction of Cells with RIPA Buffer and Formic Acid (see Note 15)**

1. Remove the media and wash the cells twice in ice-cold PBS.
2. Scrape the cells in 600  $\mu$ L RIPA buffer containing protease inhibitors.
3. Sonicate for 10 s with a probe sonicator.
4. Pellet insoluble material by centrifugation at 40,000g for 30 min at 4°C.
5. Remove the supernatant and save for direct loading of 100  $\mu$ L into microtiter well for sandwich-ELISA (**Subheading 3.1.**).
6. Resuspend the pellet in 100  $\mu$ L 70% formic acid with sonication until pellet is resuspended (*see Note 16*).
7. Neutralize the formic acid with 1.9 mL of 1 M Tris-base.

8. Dilute the sample 1:3 in H<sub>2</sub>O, and load 100  $\mu$ L into microtiter well for sandwich-ELISA (**Subheading 3.1.**) (*see Note 17*).

### **3.4. Extraction of A $\beta$ from Brain Samples for Quantitation by Sandwich-ELISA**

The analysis of A $\beta$  deposited in the AD brain was one of the first quantitative applications of the A $\beta$  sandwich-ELISA (27), and continues to prove useful in clarifying the mechanisms of plaque formation, both in postmortem human brain samples and in transgenic mouse models of AD. Serial extraction of brain samples with TBS, detergent-containing buffer (RIPA or 10% SDS), and formic acid demonstrates that only a small fraction of A $\beta_{1-40}$  and A $\beta_{1-42}$  is soluble in TBS or detergent containing buffer, whereas a far larger pool of A $\beta$  is recovered by formic acid extraction (2,27,28). After formic acid extraction of brain samples, the formic acid must be removed by drying or by neutralization in order to quantitate A $\beta$  using the sandwich-ELISA (2,28). Using either of these methods, greater than 95% of A $\beta$  can be recovered and detected by sandwich-ELISA, as assessed by A $\beta$  spiking experiments (2). Furthermore, elution of formic acid solubilized samples from a Superose 12 column shows that the sandwich-ELISA recognizes only low molecular weight containing fractions, and thus does not detect full-length APP or large APP fragments (2). Recently we have developed a protocol for the sequential extraction of brain samples (adapted from J. Wang et al., manuscript submitted) and this protocol is summarized as follows.

1. Remove the meninges from brain samples (0.15 g wet brain weight) and Dounce-homogenize, on ice, in 4 mL of TBS containing protease inhibitors.
2. Pellet the homogenate by centrifugation at 100,000g for 1 h at 4°C.
3. Remove the supernatant and save for direct loading of 100  $\mu$ L into a microtiter well for sandwich-ELISA.
4. Resuspend the pellet in 4 mL of RIPA buffer containing protease inhibitors by Dounce-homogenization.
5. Pellet the homogenate by centrifugation at 100,000g for 1 h at 4°C.
6. Remove the supernatant and save for direct loading of 100  $\mu$ L into a microtiter well for sandwich-ELISA (**Subheading 3.1.**).
7. Resuspend the pellet in 1 mL of 70% formic acid by dounce-homogenization.
8. Pellet the homogenate by centrifugation at 100,000g for 1 h at 4°C.
9. Remove the supernatant, and neutralize with 19 vol Tris-base.
10. Dilute 1:5, 1:25, and 1:125 in EC buffer for loading onto sandwich-ELISA (**Subheading 3.1.**) (*see Note 18*).

## **4. Notes**

1. BNT77 (anti-A $\beta_{11-28}$ ) antibody can also be used as a capturing antibody. Because its epitope is located in A $\beta_{11-16}$ , it will not recognize p3, but it will

recognize A $\beta$  with a truncated or modified amino terminus (23,26). However, using BNT77 decreases the sensitivity of the sandwich-ELISA by approx 10-fold (23).

2. Overnight incubations are required after each step of the sandwich-ELISA to ensure efficient coating, blocking, and A $\beta$ /antibody binding. Shortened incubations will decrease the sensitivity of the ELISA.
3. We find that Ban50 antibody can be reused at least once after coating plates if supplemented with an additional 0.5  $\mu$ g/mL freshly diluted Ban50 antibody, although doing so results in a slight (less than 10%) loss of sensitivity.
4. At this point in the sandwich-ELISA protocol, the plates can be stored for as long as several months at 4°C if tightly sealed to prevent evaporation.
5. A $\beta$  standards should range in concentration from 400 fmol/mL to 3.125 fmol/mL and should be freshly diluted from frozen, concentrated dimethyl sulfoxide stocks of synthetic A $\beta$ <sub>1-40</sub> and A $\beta$ <sub>1-42</sub> peptides. Standards should be diluted in the same buffer as the samples being quantitated.
6. Samples are loaded in duplicate wells in order to ensure the accuracy of the quantitation. Sandwich-ELISA plates should be set up in duplicate, with one plate for detection of A $\beta$ <sub>1-40</sub> with horseradish peroxidase (HRP)-conjugated BA-27 antibody and another for detection of A $\beta$ <sub>1-42</sub> with HRP-conjugated BC-05 antibody.
7. The dilution factor for the HRP-conjugated antibodies may need to be adjusted to compensate for lot-to-lot variability.
8. Longer incubations with TMB peroxidase substrates increase the sensitivity of the sandwich-ELISA but may lead to saturation of more concentrated samples. Thus incubation times must be tailored to the specific application.
9. Plates should be read immediately after stopping the reaction.
10. Other methods of extraction, such as lysis in 10% SDS or 6 M GuHCl, will also extract at least a fraction of the insoluble pool of A $\beta$ .
11. A volume of 100  $\mu$ L formic acid was found to extract A $\beta$  optimally from cell lysates containing approx 1 mg of total protein.
12. After neutralization, the pH should be about 7–7.5.
13. Although we were also able to recover a fraction of the formic acid-solubilized A $\beta$  by lyophilization followed by resuspension (with sonication) of the pellet in 60% acetonitrile followed by 1:20 dilution in RIPA buffer, we found that this technique was not quantitative for the extraction of intracellular A $\beta$ .
14. We found that samples neutralized with 1 M Tris-base greatly decreased the sensitivity of the sandwich-ELISA. For this reason, we always diluted such samples at least 1:3 in H<sub>2</sub>O before application on the sandwich-ELISA. Standard curves for quantitation of such samples should be generated in a similar method.
15. Volumes of RIPA and formic acid are appropriate for approx 2–7 million cells, or up to 1 mg of total protein. Sequential extraction is not recommended for smaller amounts of cellular protein.
16. Vigorous sonication (with a probe sonicator) was found to be necessary for efficient A $\beta$  extraction from the RIPA-insoluble pellet. Longer incubation times in formic acid (up to 24 h) or high incubation temperatures (up to 37°C) did not increase A $\beta$  recovery.

17. We find it useful to normalize ELISA results to total protein extracted or to steady-state levels of APP. If protein determination is desired, RIPA samples can be assayed by the bicinchoninic acid assay (BCA, Pierce Chemical Co., Rockford, IL). However, neutralized formic acid samples are not compatible with the BCA assay and must be assayed by Coomassie protein determination. Alternatively, steady-state levels of APP can be determined by quantitative Western blotting using [ $^{125}$ I] labeled secondary antibody (29).
18. Because of the high concentration of A $\beta$  extracted from AD brains by formic acid, it is sometimes necessary to dilute samples by up to 125-fold in order to remain within the linear range of the sandwich-ELISA.

## References

1. Selkoe, D. J. (1997) Cellular and molecular biology of the  $\beta$ -amyloid precursor protein and Alzheimer's disease, in *The Molecular and Genetic Basis of Neurological Disease* (Rosenberg, R. N., Prusiner, S. B., DiMauro, S., and Barchi, R. L., eds.), Butterworth-Heinemann, Boston, MA, pp. 601–612.
2. Gravina, S. A., Ho, L., Eckman, C. B., Long, K. E., Otvos, L. J., Younkin, L. H., et al. (1995) Amyloid  $\beta$  protein (A $\beta$ ) in Alzheimer's disease brain. Biochemical and immunocytochemical analysis with antibodies specific for forms ending at A $\beta$ 40 or A $\beta$ 42(43). *J. Biol. Chem.* **270**, 7013–7016.
3. Iwatsubo, T., Odaka, A., Suzuki, N., Mizusawa, H., Nukina, N., and Ihara, Y. (1994) Visualization of A $\beta$ 42(43) and A $\beta$ 40 in senile plaques with end-specific A $\beta$  monoclonals: evidence that an initially deposited species is A $\beta$ 42(43). *Neuron* **13**, 45–53.
4. Fukumoto, H., Asami-Odaka, A., Suzuki, N., Shimada, H., Ihara, Y., and Iwatsubo, T. (1996) Amyloid  $\beta$  protein deposition in normal aging has the same characteristics as that in Alzheimer's disease. Predominance of A $\beta$ 42(43) and association of A $\beta$ 40 with cored plaques. *Am. J. Pathol.* **148**, 259–265.
5. Fukumoto, H., Asami-Odaka, A., Suzuki, N., and Iwatsubo, T. (1996) Association of A $\beta$ 40-positive senile plaques with microglial cells in the brains of patients with Alzheimer's disease and in non-demented aged individuals. *Neurodegeneration*. **5**, 13–17.
6. Ida, N., Hartmann, T., Pantel, J., Schroder, J., Zerfass, R., Forstl, H., et al. (1996) Analysis of heterogeneous A4 peptides in human cerebrospinal fluid and blood by a newly developed sensitive Western blot assay. *J. Biol. Chem.* **271**, 22,908–22,914.
7. Tamaoka, A., Sawamura, N., Fukushima, T., Shoji, S., Matsubara, E., Shoji, M., et al. (1997) Amyloid  $\beta$  protein 42(43) in cerebrospinal fluid of patients with Alzheimer's disease. *J. Neurol. Sci.* **148**, 41–45.
8. Turner, R. S., Suzuki, N., Chyung, A. S., Younkin, S. G., and Lee, V. M.-Y. (1996) Amyloids  $\beta$ 40 and  $\beta$ 42 are generated intracellularly in cultured human neurons and their secretion increases with maturation. *J. Biol. Chem.* **271**, 8966–8970.
9. Suzuki, N., Cheung, T. T., Cai, X. D., Odaka, A., Otvos, L. J., Eckman, C., et al. (1994) An increased percentage of long amyloid  $\beta$  protein secreted by familial amyloid  $\beta$  protein precursor ( $\beta$ APP717) mutants. *Science* **264**, 1336–1340.
10. Borchelt, D. R., Thinakaran, G., Eckman, C. B., Lee, M. K., Davenport, F., Ratovitsky, T., et al. (1996) Familial Alzheimer's disease-linked presenilin 1 variants elevate A $\beta$ 1–42/1–40 ratio in vitro and in vivo. *Neuron* **17**, 1005–1013.

11. Duff, K., Eckman, C., Zehr, C., Yu, X., Prada, C. M., Perez-tur, J., Hutton, M., et al. (1996) Increased amyloid- $\beta$ 42(43) in brains of mice expressing mutant presenilin 1. *Nature* **383**, 710–713.
12. Scheuner, D., Eckman, C., Jensen, M., Song, X., Citron, M., Suzuki, N., et al. (1996) Secreted amyloid  $\beta$ -protein similar to that in the senile plaques of Alzheimer's disease is increased in vivo by the presenilin 1 and 2 and APP mutations linked to familial Alzheimer's disease. *Nat. Med.* **2**, 864–870.
13. Games, D., Adams, D., Alessandrini, R., Barbour, R., Berthelette, P., Blackwell, C., et al. (1995) Alzheimer-type neuropathology in transgenic mice overexpressing V717F  $\beta$ -amyloid precursor protein. *Nature* **373**, 523–527.
14. Hsiao, K., Chapman, P., Nilsen, S., Eckman, C., Harigaya, Y., Younkin, S., et al. (1996) Correlative memory deficits, A $\beta$  elevation, and amyloid plaques in transgenic mice. *Science* **274**, 99–102.
15. Xu, H., Sweeney, D., Wang, R., Thinakaran, G., Lo, A. C., Sisodia, S. S., et al. (1997) Generation of Alzheimer  $\beta$ -amyloid protein in the trans-Golgi network in the apparent absence of vesicle formation. *Proc. Natl. Acad. Sci. USA* **94**, 3748–3752.
16. Cook, D. G., Forman, M. S., Sung, J. C., Leight, S., Kolson, D. L., Iwatsubo, T., et al. (1997) Alzheimer's A $\beta$ (1–42) is generated in the endoplasmic reticulum/intermediate compartment of NT2N cells. *Nat. Med.* **3**, 1021–1023.
17. Hartmann, T., Bieger, S. C., Bruhl, B., Tienari, P. J., Ida, N., Allsop, D., et al. (1997) Distinct sites of intracellular production for Alzheimer's disease A $\beta$ 40/42 amyloid peptides. *Nat. Med.* **3**, 1016–1020.
18. De, S. B., Beullens, M., Contreras, B., Levesque, L., Craessaerts, K., Cordell, B., et al. (1997) Phosphorylation, subcellular localization, and membrane orientation of the Alzheimer's disease-associated presenilins. *J. Biol. Chem.* **272**, 3590–3598.
19. Cook, D. G., Sung, J. C., Golde, T. E., Felsenstein, K. M., Wojczyk, B. S., Tanzi, R. E., et al. (1996) Expression and analysis of presenilin 1 in a human neuronal system: localization in cell bodies and dendrites. *Proc. Natl. Acad. Sci. USA* **93**, 9223–9228.
20. Skovronsky, D. M., Doms, R. W., and Lee, V. M.-Y. (1998) Detection of a novel intraneuronal pool of insoluble amyloid b protein that accumulates with time in culture. *J. Cell Biol.* **141**, 1031–1039.
21. Jarrett, J. T. and Lansbury, P. T. J. (1993) Seeding “one-dimensional crystallization” of amyloid: a pathogenic mechanism in Alzheimer's disease and scrapie? *Cell* **73**, 1055–1058.
22. Jarrett, J. T., Berger, E. P., and Lansbury, P. T. J. (1993) The carboxy terminus of the b amyloid protein is critical for the seeding of amyloid formation: implications for the pathogenesis of Alzheimer's disease. *Biochemistry* **32**, 4693–4697.
23. Asami-Odaka, A., Ishibashi, Y., Kikuchi, T., Kitada, C., and Suzuki, N. (1995) Long amyloid  $\beta$ -protein secreted from wild-type human neuroblastoma IMR-32 cells. *Biochemistry* **34**, 10272–10278.
24. Yamazaki, T., Haass, C., Saido, T. C., Omura, S., and Ihara, Y. (1997) Specific increase in amyloid  $\beta$ -protein 42 secretion ratio by calpain inhibition. *Biochemistry* **36**, 8377–8383.

25. Wertkin, A. M., Turner, R. S., Pleasure, S. J., Golde, T. E., Younkin, S. G., Trojanowski, J. Q., and Lee, V. M.-Y. (1993) Human neurons derived from a teratocarcinoma cell line express solely the 695-amino acid amyloid precursor protein and produce intracellular  $\beta$ -amyloid or A4 peptides. *Proc. Natl. Acad. Sci. USA* **90**, 9513–9517.
26. Wild-Bode, C., Yamazaki, T., Capell, A., Leimer, U., Steiner, H., Ihara, Y., and Haass, C. (1997) Intracellular generation and accumulation of amyloid  $\beta$ -peptide terminating at amino acid 42. *Biol. J. Chem.* **272**, 16085–16088.
27. Suzuki, N., Iwatsubo, T., Odaka, A., Ishibashi, Y., Kitada, C., and Ihara, Y. (1994) High tissue content of soluble  $\beta$  1–40 is linked to cerebral amyloid angiopathy. *Am. J. Pathol.* **145**, 452–460.
28. Tamaoka, A., Odaka, A., Ishibashi, Y., Usami, M., Sahara, N., Suzuki, N., et al. (1994) APP717 missense mutation affects the ratio of amyloid  $\beta$  protein species (A $\beta$  1–42/43 and A $\beta$  1–40) in familial Alzheimer's disease brain. *J. Biol. Chem.* **269**, 32,721–32,724.
29. Forman, M. S., Cook, D. G., Leight, S., Doms, R. W., and Lee, V. M.-Y. (1997) Differential effects of the swedish mutant amyloid precursor protein on  $\beta$ -amyloid accumulation and secretion in neurons and nonneuronal cells. *J. Biol. Chem.* **272**, 32,247–32,253.

## Electrophoretic Separation and Immunoblotting of A $\beta$ <sub>1-40</sub> and A $\beta$ <sub>1-42</sub>

Matthias Staufenbiel and Paolo A. Paganetti

### 1. Introduction

The main protein component of the plaques found in the brains of Alzheimer's disease patients is A $\beta$ , a peptide of 39 to 43 amino acids (reviewed in refs. **1** and **2**). Two major A $\beta$  isoforms have been identified in the brains of affected individuals ending at amino acids 40 and 42, respectively (**3**). The longer form, A $\beta$ <sub>42</sub>, aggregates more rapidly in vitro (**4**) and is preferentially deposited in vivo (**3,5,6**). Normally, A $\beta$  is secreted as an apparently soluble molecule (**7-9**). It is generated by all cultured cells expressing its precursor protein, APP, and can be detected in vivo in the cerebrospinal fluid (**10**) and in plasma (**11**). Mutations linked to familial forms of Alzheimer's disease have been found in the APP gene as well as two other genes encoding presenilin 1 and presenilin 2. They were shown to alter APP metabolism and, in particular, to either increase total A $\beta$  or the relative abundance of the longer A $\beta$ <sub>42</sub> isoform (**12-17**). These observations have led to the hypothesis that A $\beta$ <sub>42</sub> may play a critical role in amyloid plaque formation and the development of Alzheimer's disease. Obviously methods discriminating between the two major A $\beta$  species are important in order to study this notion.

Currently, the use of end-specific antibodies or electrophoretic separation are the two main alternatives to distinguish between A $\beta$ <sub>40</sub> and A $\beta$ <sub>42</sub>. Reverse phase liquid chromatography after CNBr cleavage of A $\beta$  has also been described but is very complex and time consuming (**14**). Conventional reverse phase liquid chromatography (**18**), capillary zone electrophoresis (**19**), acid-urea PAGE (**19**) or different SDS-PAGE methods (**18,20**) have been tested without success to separate A $\beta$ <sub>1-40</sub> and A $\beta$ <sub>1-42</sub>. End-specific antibodies have been used in enzyme-linked immunosorbent assay (ELISA) or immunoblotting

methods (**14,21**). Although the ELISA offers the advantage of a high sample throughput, both methods require antibodies that do not crossreact between  $A\beta_{1-40}$  and  $A\beta_{1-42}$ . Furthermore, the small amount of  $A\beta_{42}$  present in most samples requires high-affinity antibodies for detection. Such tools become available only slowly. Electrophoretic separation of  $A\beta_{1-40}$  and  $A\beta_{1-42}$  allows processing of fewer samples in parallel. To increase the sensitivity,  $A\beta$  peptides can be analyzed after prior immunoprecipitation using a general  $A\beta$  antibody. On the other hand, the peptides are directly visualized and end-specific antibodies are not required.

We have optimized both the electrophoretic separation of  $A\beta_{1-40}$  from  $A\beta_{1-42}$  and the immunoblotting of  $A\beta$  to obtain high sensitivity even in the absence of radioactive labeling. To start with, two electrophoresis systems designed to separate low molecular weight proteins or peptides were used: the bicine/Tris (glycerol) or the tricine/Tris SDS-polyacrylamide gels according to Wiltfang (**22**) or Schägger and von Jagow (**23**), respectively. Close inspection of the gels indicated a slightly different mobility of  $A\beta_{1-40}$  and  $A\beta_{1-42}$ ; however, mixing of the peptides showed with both systems that this effect was not sufficient for a separation. Based on this notion we searched for conditions enhancing the separation of  $A\beta_{1-40}$  and  $A\beta_{1-42}$ . For the 15% T/5% C bicine/Tris gels (*see Note 2*), a clear separation of  $A\beta_{1-40}$  and  $A\beta_{1-42}$  is obtained with 8 M urea in the separation gel combined with 0.25% SDS in the cathode buffer (**22,24**). Unexpectedly the longer  $A\beta_{1-42}$  peptide migrated faster than the smaller  $A\beta_{1-40}$ . We assume that such a migration behavior is due to differences in secondary structure and SDS binding induced by the two terminal amino acids, whereas the increased peptide length is less important. Other gel systems may require different urea and SDS concentrations for a successful separation of  $A\beta_{1-40}$  and  $A\beta_{1-42}$ . As an example, both  $A\beta$  peptides comigrated on 16.5% T/3% C tricine/Tris gels with 0.25% SDS in the cathode buffer, whereas they were clearly separated using the original buffer with 0.1% SDS (**24**).

The separation distance between  $A\beta_{1-40}$  and  $A\beta_{1-42}$  can be further increased when lower percentage acrylamide gels (10% T) are used (**25**). These gels also allow to resolve the  $A\beta_{1-42}$  and  $A\beta_{1-43}$  peptides, which are not well separated on the smaller pore size gels previously described. It should be noted that the structural basis that enables the separation of molecules differing only by two amino acids is not well understood. In addition to SDS binding and secondary structure, the aggregation properties of  $A\beta$  may also differ. Aggregation of the peptides may influence their migration on 10% T gels as postulated based on the considerably reduced mobility compared to marker proteins (**25**). Yet we observed a continuous mobility shift with an increasing urea concentration in both 10% and 15% T gels.

For immunodetection, the separated  $A\beta$  peptides can be electrophoretically transferred to polyvinylidene fluoride (PVDF) membranes. We achieved best

results by semidry blotting using a multibuffer system with 0.025% SDS in the cathode buffer, 30% methanol in the anode buffers and a high ionic strength buffer next to the anode (25). The sensitivity also depends on the PVDF membrane used. It can be increased considerably by boiling the blot in phosphate-buffered saline (PBS) right after the transfer (21,25). The detection limits are in the low nanogram range for silver staining and about 5–10 pg (1–2 fmol) for immunostaining using a good A $\beta$  antibody.

We have also used both separation of A $\beta$  peptides and immunoblotting to analyze biological material. These studies demonstrated the separation of A $\beta$ <sub>1–40</sub> and A $\beta$ <sub>1–42</sub> generated from cultured cells after metabolic radiolabeling and immunoprecipitation (24,26,27). They also showed that SDS-PAGE can be used to obtain quantitative data and to determine the ratio of A $\beta$ <sub>1–42</sub> and A $\beta$ <sub>1–40</sub>. Similar studies have been done with nonradioactive A $\beta$  peptides that were detected by immunoblotting and quantified. In addition to A $\beta$  derived from cultured cells, we have also successfully analyzed A $\beta$ <sub>1–40</sub> and A $\beta$ <sub>1–42</sub> peptides isolated from the brains of Alzheimer's disease patients as well as from the brains of APP transgenic mice.

## 2. Materials

### 2.1. Gel Electrophoresis (SDS-PAGE)

1. Minigel apparatus (e.g., Bio-Rad Mini-Protean II [Bio-Rad Laboratories, Hercules, CA], 7 cm gels, 0.75 mm spacers).
2. Bicine/Tris gels.
  - a. Anode buffer: 0.2 M Tris, 50 mM H<sub>2</sub>SO<sub>4</sub>, pH 8.1.
  - b. Cathode buffer: 0.2 M Bicine, 0.1 M NaOH, pH 8.2, 0.25% SDS.
  - c. 4 $\times$  Gel buffer: 1.6 M Tris, 0.4 M H<sub>2</sub>SO<sub>4</sub>, pH 8.4.
  - d. 2 $\times$  Stacking buffer: 0.8 M *bis*-Tris, 0.2 M H<sub>2</sub>SO<sub>4</sub>, pH 6.7.
  - e. 2 $\times$  Comb buffer: 0.718 M *bis*-Tris, 0.318 M bicine, pH 7.7.
  - f. Acrylamide/*bis*: 57% Acrylamide, 3% *bis*-acrylamide.
  - g. 2 $\times$  sample buffer: 2% SDS, 30% sucrose, 0.718 M *bis*-Tris, 0.318 M bicine, 5%  $\beta$ -mercaptoethanol, 0.01% bromphenol blue.
  - h. APS: 10% Ammoniumpersulfate.
  - i. TEMED (N,N,N,'N'-tetramethylethylenediamine, Sigma T9281) (Sigma Chemical Co., St. Louis, MO).
3. Tricine/Tris gels.
  - a. Anode buffer: 0.2 M Tris/ $\mu$ Cl, pH 8.9.
  - b. Cathode buffer: 0.1 M Tris, 0.1 M tricine, pH 8.25, 0.1% SDS.
  - c. 3 $\times$  Gel buffer: 3 M Tris/ $\mu$ Cl, pH 8.45, 0.3% SDS.
  - d. Acrylamide/*bis*: 30% Acrylamide, 0.8% *bis*-acrylamide.
  - e. 2 $\times$  Sample buffer: 4% SDS, 12% glycerol, 50 mM Tris/ $\mu$ Cl, pH 6.8, 50 mM dithiothreitol (DTT), 0.01% Coomassie brilliant blue.

### 2.2. Western Blotting

1. Semidry blotting cell (e.g., Bio-Rad Trans-Blot SD) (Bio-Rad Laboratories).
2. PVDF membrane: Immobilon P transfer membrane (Millipore IPVH 000 10) (Millipore, Bedford, MA).

**Table 1**  
**Compositions of Bicine/Tris Separating Gels (8M Urea)**

Stock solution	Separating gel (5 mL) 10% acrylamide	Separating gel (5mL) 15% acrylamide
Urea	2.4 g	2.4 g
Acrylamide/ <i>bis</i>	0.833 mL	1.25 mL
4× Gel buffer	1.25 mL	1.25 mL
10% SDS	50 $\mu$ L	50 $\mu$ L
H <sub>2</sub> O	Up to 5 mL	Up to 5 mL
APS	20 $\mu$ L	20 $\mu$ L
TEMED	2.5 $\mu$ L	2.5 $\mu$ L

3. Chromatography paper: 3MM Whatman (Whatman, Clifton, NJ).
4. Buffer A: 0.3 M Tris, 30% methanol; do not adjust the pH.
5. Buffer B: 25 mM Tris, 30% methanol; do not adjust the pH.
6. Buffer C: 25 mM Tris (adjusted to pH 9.40 with boric acid), 0.025% SDS.
7. PBS: 10 mM NaHPO<sub>4</sub>, pH 7.4, 2.7 mM KCl, 0.137 M NaCl (Sigma P4417) (Sigma Chemical).

### 2.3. Immunodetection

1. Nonfat milk powder, low phosphate.
2. Biomax-MR films (Kodak 873 6936) (Eastman Kodak, Rochester, NY) or Amersham Hyperfilm (RPN3103N) (Amersham, UK).
3. ECL+Plus detection reagent (Amersham, RPN2132).
4. Whatman 3MM chromatographic paper.
5. Mouse monoclonal antibody 6E10, ascite fluid (Senetec plc, Maryland Heights, MD, 1:1 in glycerol, -20°C).
6. Goat  $\alpha$ -mouse immunoglobulin G (IgG) coupled to horseradish peroxidase ( $\alpha$ -mIgG-HRP, Chemicon/Milan (Temecula, CA), AP127P, 1:1 with glycerol, -20°C).
7. 10× TBS-T: 0.2 M Tris/HCl, pH 7.4, 1.5 M NaCl, 0.5% Tween-20.
8. Blocking solution: 5% milk powder in Tris-buffered saline containing Tween-20 (TBS-T).

### 2.4. Synthetic Peptides

All A $\beta$  peptides were purchased from Bachem (Switzerland) (A $\beta$ <sub>1-40</sub>: H1194, A $\beta$ <sub>1-42</sub>: H1368, A $\beta$ <sub>1-43</sub>: H1586).

## 3. Methods

### 3.1. Gel Electrophoresis

#### 3.1.1. Bicine/Tris SDS-PAGE Containing 8 M Urea

1. Follow the recipes given in **Table 1** to prepare 10% or 15% polyacrylamide separating gel solutions (see **Notes 1** and **2**).

**Table 2**  
**Compositions of Bicine/Tris Stacking and Comb Gels**

Stock solution	Stacking gel (1 mL)	Comb gel (3 mL)
Acrylamide/bis	0.1 mL	0.375 mL
2× Stacking buffer	0.5 mL	—
2× Comb buffer	—	1.5 mL
10% SDS	10 $\mu$ L	30 $\mu$ L
H <sub>2</sub> O	0.385 mL	1.07 mL
APS	4 $\mu$ L	24 $\mu$ L
TEMED	1 $\mu$ L	3 $\mu$ L

- Pipet the separating gel solution into the assembled gel chamber (gel length approx 54 mm), overlay with water-saturated 2-butanol, wait until the gel is polymerized, remove the 2-butanol, rinse with deionized water, tilt, and remove the remaining water with a piece of filter paper.
- Prepare the stacking gel solution as indicated in **Table 2**, pour on top of the separating gel (gel length 5 mm), let it polymerize, and wash as in **step 2**.
- Add the comb gel solution (**Table 2**) on top of the polymerized stacking gel to fill the chamber completely. Rapidly insert a comb for 10 or 15 samples. The bottom of the comb should be placed about 5 mm above the stacking gel.
- After complete polymerization, place the gel into the running chamber, add the cathode and anode buffers, remove the comb, and rinse the sample pockets with cathode buffer using a syringe (*see Note 3*).
- To prepare the samples, dilute with an equal volume of 2× sample buffer (for bicine/Tris gels), heat for 3–5 min at 95°C and centrifuge for 5 min at 12,000g (*see Notes 4 and 5*).
- Load the samples, including the molecular weight markers, carefully in the comb gel pockets.
- Run the gel at 40 V until the samples have reached the separating gel, thereafter run the separation at maximal 120 V.
- Stop the electrophoretic separation when the blue dye reaches the end of the gel (*see Notes 6 and 7*).

### 3.1.2. Tricine/Tris SDS-PAGE Containing 8 M Urea

- Prepare the samples as described previously using the 2× sample buffer for tricine/Tris gel electrophoresis.
- Prepare the gel according to the recipe in **Table 3** and the description for bicine/Tris gels but omit the comb gel. In other words, the comb is inserted directly into the stacking gel of this biphasic gel system.
- Load the samples on the gel and electrophorese as detailed in **Subheading 3.1.1**.

## 3.2. Western Blotting

### 3.2.1. Assembly of Blotting Sandwich

Prewet the chromatography filter papers as follows: two sheets each in buffer A and buffer B, three sheets in buffer C. Prewet the PVDF membrane with

**Table 3**  
**Compositions of Tricine/Tris Separating**  
**and Stacking Gels (8M Urea)**

Stock solution	Separating gel (5 mL)	
	15% acrylamide	Stacking gel (2 mL)
Urea	2.4 g	—
Acrylamide/ <i>bis</i>	2.5 mL	256 $\mu$ L
3 $\times$ Gel buffer	1.67 mL	500 $\mu$ L
10% SDS	50 $\mu$ L	50 $\mu$ L
H <sub>2</sub> O	Up to 5 mL	1.24 mL
APS	25 $\mu$ L	16 $\mu$ L
TEMED	2.5 $\mu$ L	1.6 $\mu$ L

methanol, briefly rinse with H<sub>2</sub>O, and equilibrate in buffer B. Equilibrate the gel immediately after electrophoresis in buffer C for 1–3 min (not longer). Assemble the blotting sandwich, avoiding any air bubbles, in the following order: anode (+), 2 $\times$  filter papers equilibrated in buffer A, 2 $\times$  filter papers in buffer B, PVDF membrane, gel, 3 $\times$  filter papers in buffer C, cathode (–). Remove any remaining air bubbles by gently pressing a roller over the sandwich before closing the unit.

### 3.2.2. Blotting and Fixation

1. Run the blot at 0.12 A per gel (the actual voltage will be about 10–12 V) for 40 min.
2. Remove the PVDF membrane with the blotted protein from the sandwich and place into boiling PBS for 3–5 min to fix the low molecular weight peptides on the membrane (*see Note 8*).

### 3.3. Immunodetection

1. Before immunoblotting, block excess binding sites on the PVDF membrane by incubation for 1–2 h in blocking solution.
2. Add the first antibody, e.g., the 6E10 monoclonal antibody diluted 1:2500 in TBS-T, and incubate for 1 h at room temperature or overnight at 4°C.
3. Wash the blot three times for 10 min with TBS-T.
4. Add the second antibody (e.g., goat  $\alpha$ -mIgG-HRP, 1:2000 in TBS-T) and incubate for 1 h at room temperature.
5. Wash the blot three times for 10 min with TBS-T.
6. For detection, mix ECL+Plus reagents A and B in a ratio of 1:40 and apply to the membrane. After an incubation for 5 min, gently adsorb excess reagent with some 3MM filter paper. Avoiding air bubbles, wrap the PVDF membrane in cellophane and expose to an autoradiography film in a dark room. Several exposures can be taken.

#### 4. Notes

1. The solutions containing urea should always be prepared fresh and should not be heated to improve solubility, as urea is not very stable in solution.
2. To define the pore size of the polyacrylamide gels, the total concentration of acrylamide plus cross-linker (*bis*-acrylamide) in the gels is given (T). The ratio of acrylamide and cross-linker is kept constant in gels of different percentage, therefore, the amount of cross-linker as percentage of T is indicated (C). As an example, a solution containing 57% acrylamide and 3% *bis*-acrylamide is referred to as 60% T/5% C.
3. When using the bicine/Tris gel system, it is important to raise the SDS concentration in the cathode buffer to 0.25% . The standard concentration of 0.1% will not allow for a reproducible separation of A $\beta$ <sub>1-40</sub> and A $\beta$ <sub>1-42</sub>. Both A $\beta$  peptides can also be separated on tricine/Tris gels. However, the SDS concentration in the cathode buffer has to be kept at 0.1%. In general, we obtained similar results with both systems although in our hands the gel quality appeared somewhat better with the bicine/Tris gels.
4. SDS often is not sufficient for complete extraction of A $\beta$  peptides from the Alzheimer's disease brain and formic acid is required (*see* Chapter 5) (3). A $\beta$  secreted from cells, intracellular A $\beta$ , or immunoprecipitated A $\beta$  appear to be soluble in SDS sample buffer. Predissolving in another buffer is often done to facilitate protein determination.
5. A $\beta$  peptides readily aggregate in a concentration-dependent manner even in denaturing buffers as used for SDS-PAGE. Aggregates can be observed on SDS gels. This might be misleading if samples with a large difference in A $\beta$  concentration are compared, e.g., radioactive material and synthetic A $\beta$  marker peptides.
6. Synthetic A $\beta$  peptides can be visualized in the gel after separation using various stains like Coomassie brilliant blue or silver staining (25). Following metabolic radiolabeling, immunoprecipitation, and electrophoresis, separated A $\beta$  peptides may be visualized by fluorography. To avoid losing small peptides that may diffuse from the gel during these procedures, fix the gel with glutaraldehyde (0.25% in 0.4 M boric acid, pH 6.2, adjusted with 1 M Na<sub>2</sub>HPO<sub>4</sub>).
7. Deletion of amino-terminal amino acids can lead to faster migration of A $\beta$ . Hence the amino-terminal heterogeneity of natural A $\beta$  may render electrophoretic separation of the carboxy-terminal isoforms difficult. In other words, a set of heterogeneous A $\beta$  peptides may result in an increased number of bands on the gels. Their identification may be difficult and may be misleading if truncated A $\beta$ <sub>40</sub> molecules comigrate with the faster migrating A $\beta$ <sub>1-42</sub>. This possibility should be considered although we have been able to separate and identify natural A $\beta$ <sub>1-40</sub> and A $\beta$ <sub>1-42</sub> peptides generated by different cell lines as well as *in vivo* in mouse and human brain. Few major A $\beta$  species were detected even in material from the brains of Alzheimer's disease patients. Nonetheless, in cases of uncertainty identification of the peptides using end-specific antibodies may be helpful. On the other hand, the gel system can be used with synthetic peptides to assess the specificity of antisera directed against the different carboxy-termini of A $\beta$ .

8. After electrophoretic transfer of the peptides, the blot membrane can also be fixed with 1% glutaraldehyde to improve sensitivity. However, reactivity with some antibodies may be lost. In contrast, we never observed a reduced immunoreactivity after boiling the blot in PBS.

## References

1. Selkoe, D. J. (1997) Alzheimer's disease: genotypes, phenotypes, and treatments. *Science* **275**, 630–631.
2. Yankner, B. A. (1996) Mechanisms of neuronal degeneration in Alzheimer's disease. *Neuron* **16**, 921–932.
3. Roher, A. E., Lowenson, J. D., Clarke, S., Wolkow, C., Wang, R., Cotter, R. J., et al. (1993) Structural alterations in the peptide backbone of  $\beta$ -amyloid core protein may account for its deposition and stability in Alzheimer's disease. *J. Biol. Chem.* **268**, 3072–3083.
4. Jarrett, J. T., Berger, E. P., and Lansbury, P. T., Jr. (1993) The carboxy-terminus of the  $\beta$ -amyloid protein is critical for the seeding of amyloid formation: implication for the pathogenesis of Alzheimer's disease. *Biochemistry* **32**, 4693–4697.
5. Gravina, S. A., Ho, L., Eckman, C. B., Long, K. E., Otvos, L., Jr., Younkin, L. H., Suzuki, N., and Younkin, S. G. (1995) Amyloid  $\beta$  (A $\beta$ ) in Alzheimer's disease brain. Biochemical and immunocytochemical analysis with antibodies specific for forms ending at A $\beta$  40 or A $\beta$  42(43). *J. Biol. Chem.* **270**, 7013–7016.
6. Iwatsubo, T., Odaka, A., Suzuki, N., Mizusawa, H., Nukina, N., and Ihara, Y. (1994) Visualization of A $\beta$ 42(43) and A $\beta$ 40 in senile plaques with end-specific monoclonals: evidence that an initially deposited species is A $\beta$ 42(43). *Neuron* **13**, 45–53.
7. Haass, C., Schlossmacher, M. G., Hung, A. Y., Vigo-Pelfrey, C., Mellon, A., Ostaszewski, B. L., et al. (1992) Amyloid  $\beta$ -peptide is produced by cultured cells during normal metabolism. *Nature* **359**, 322–325.
8. Shoji, M., Golde, T. E., Ghiso, J., Cheung, T. T., Estus, S., Shaffer, L. M., et al. (1992) Production of the Alzheimer amyloid  $\beta$ -protein by normal proteolytic processing. *Science* **258**, 126–129.
9. Busciglio, J., Gabuzda, D. H., Matsudaira, P., and Yankner, B. A. (1993) Generation of  $\beta$ -amyloid in the secretory pathway in neuronal and nonneuronal cells. *Proc. Natl. Acad. Sci. USA* **90**, 2092–2096.
10. Seubert, P., Vigo-Pelfrey, C., Esch, F., Lee, M., Dovey, H., Davis, D., et al. (1992) Isolation and quantification of soluble Alzheimer's  $\beta$ -peptide from biological fluids. *Nature* **359**, 325–327.
11. Scheuner, D., Eckman, C., Jensen, M., Song, X., Citron, M., Suzuki, N., et al. (1996) Secreted amyloid  $\beta$ -protein similar to that in senile plaques of Alzheimer's disease is increased in vivo by the presenilin 1 and 2 and APP mutations linked to Alzheimer's disease. *Nat. Med.* **2**, 864–870.
12. Citron, M., Olterdorf, T., Haass, C., McConlogue, L., Hung, A. Y., Seubert, P., et al. (1992) Mutation of the  $\beta$ -amyloid precursor protein in familial Alzheimer's disease increases  $\beta$ -protein production. *Nature* **360**, 672–674.

13. Cai, X.-D., Golde, T. E., and Younkin, S. G. (1993) Release of excess amyloid  $\beta$  protein from a mutant amyloid  $\beta$  protein precursor. *Science* **259**, 514–516.
14. Suzuki, N., Cheung, T. T., Cai, X. D., Odaka, A., Otvos, L., Eckman, C., et al. (1994) An increased percentage of long amyloid  $\beta$ -protein secreted by familial amyloid  $\beta$ -protein precursor ( $\beta$ APP<sub>717</sub>) mutants. *Science* **264**, 1336–1340.
15. Tamaoka, A., Odaka, A., Ishibashi, Y., Usami, M., Sahara, N., Suzuki, N., et al. (1994) APP717 missense mutation affects the ratio of amyloid  $\beta$  protein species. *J. Biol. Chem.* **269**, 32,721–32,724.
16. Citron, M., Westaway, D., Xia, W., Carlson, G., Diehl, T., Levesque, G., et al. (1997) Mutant presenilins of Alzheimer's disease increase production of 42-residue amyloid  $\beta$ -protein in both transfected cells and transgenic mice. *Nat. Med.* **3**, 67–72.
17. Mehta, N. D., Refolo, L. M., Eckman, C., Sanders, S., Yager, D., Perez-Tur, J., et al. (1998) Increased A $\beta$ 42(43) from cell lines expressing presenilin 1 mutations. *Ann. Neurol.* **43**, 256–258.
18. Burdick, D., Soreghan, B., Kwon, M., Kosmoski, J., Knauer, M., Henschen, A., et al. (1992) Assembly and aggregation properties of synthetic Alzheimer's A4/ $\beta$  amyloid peptide analogs. *J. Biol. Chem.* **267**, 546–554.
19. Sweeney, P. J., Darker, J. G., Neville, W. A., Humphries, J., and Camilleri, P. (1993) Electrophoretic techniques for the analysis of synthetic amyloid  $\beta$ A4-related peptides. *Anal. Biochem.* **212**, 179–184.
20. Hilbich, C., Kisters-Woike, B., Reed, J., Masters, C. L., and Beyreuther, K. (1991) Aggregation and secondary structure of synthetic amyloid  $\beta$ A4 peptides of Alzheimer's disease. *J. Mol. Biol.* **218**, 149–163.
21. Ida, N., Hartmann, T., Pantel, J., Schroder, J., Zerfass, R., Forstl, H., et al. (1996) Analysis of heterogeneous A4 peptides in human cerebrospinal fluid and blood by a newly developed sensitive Western blot assay. *J. Biol. Chem.* **271**, 22,908–22,914.
22. Wiltfang, J., Arold, N., and Neuhoff V. (1991) A new multiphasic buffer system for sodium dodecyl sulfate-polyacrylamide gel electrophoresis of proteins and peptides with molecular masses 100,000–1,000, and their detection with picomolar sensitivity. *Electrophoresis* **12**, 352–366.
23. Schagger, H. and von Jagow, G. (1987) Tricine-sodium dodecyl sulfate-polyacrylamide gel electrophoresis for the separation of proteins in the range from 1 to 100 kDa. *Anal. Biochem.* **166**, 368–379.
24. Klafki, H.-W., Wiltfang, J., and Staufenbiel, M. (1996) Electrophoretic separation of  $\beta$ A4 peptides (1–40) and (1–42). *Anal. Biochem.* **237**, 24–29.
25. Wiltfang, J., Smirnov, A., Schnierstein, B., Kelemen, G., Matthies, U., Klafki, H.-W., et al. (1997) Improved electrophoretic separation and immunoblotting of beta-amyloid (A $\beta$ ) peptides 1–40, 1–42, and 1–43. *Electrophoresis* **18**, 527–532.
26. Klafki, H.-W., Abramowski, D., Swoboda, R., Paganetti, P. A., and Staufenbiel, M. (1996) The carboxyl termini of  $\beta$ -amyloid peptides 1–40 and 1–42 are generated by distinct  $\gamma$ -secretase activities. *J. Biol. Chem.* **271**, 28,655–28,659.
27. Manni, M., Cescato, R., and Paganetti, P. A. (1998) Lack of  $\beta$ -amyloid production in M19 cells deficient in site 2 processing of the sterol regulatory element binding proteins. *FEBS Lett.* **427**, 367–370.

## **A $\beta$ -Induced Proinflammatory Cytokine Release from Differentiated Human THP-1 Monocytes**

**Kurt R. Brunden, June Kocsis-Angle, Paula Embury,  
and Stephen L. Yates**

### **1. Introduction**

As noted in the introductory chapters of this book, neuritic plaques composed of accumulated amyloid  $\beta$  (A $\beta$ ) peptide are a hallmark pathological feature of the Alzheimer's disease (AD) brain. Compelling genetic data now implicate these plaques as key causative agents in AD onset, as all known mutations that lead to early onset familial AD (**1–6**) result in an increased production of the amyloidogenic A $\beta_{1-42}$  isoform (**7–11**). Although it appears likely that the deposition of multimeric A $\beta$  fibrils into plaques is a necessary step in AD onset, there is still uncertainty as to how A $\beta$  and neuritic plaques might cause the neuropathology that leads to the dementia that is characteristic of this disease.

A growing body of experimental data suggest that senile plaques may initiate a glial-mediated inflammatory reaction within the AD brain that contributes to neuronal damage and death. Activated microglial cells, which are phenotypically similar to macrophages, are found to be intimately associated with neuritic plaques (**12,13**). These microglia express elevated major histocompatibility complex surface markers (**14**) and proinflammatory cytokines such as interleukin-1 (IL-1) (**15**). Reactive astrocytes generally surround the perimeter of neuritic plaques (**16**), and these cells have been shown to have increased expression of IL-6,  $\alpha$ -antichymotrypsin, and nitric oxide after exposure to IL-1 (**17,18**). It is thus conceivable that microglial activation at the site of plaques results in IL-1 release that subsequently triggers astrocyte reactivity and the production of additional bioactive molecules. This hypothetical course of

events is consistent with the observed increases of IL-1 (19) and IL-6 (20) seen in the AD brain.

The premise that inflammatory proteins contribute to AD pathology is strengthened by a number of epidemiological studies. As reviewed by McGeer et al. (21), there have been many retrospective analyses that suggest that a course of steroidal or nonsteroidal anti-inflammatory drug treatment reduces the odds of AD onset. Moreover, a recent prospective study (22) indicated that the use of a nonsteroidal anti-inflammatory drug (ibuprofen) for >2 yr significantly reduced the risk of AD.

Based on the evidence of glial-mediated inflammation in AD, there is reason to believe that agents that would suppress this cellular response might prove beneficial in slowing disease progression. Unfortunately, the present repertoire of steroidal and nonsteroidal anti-inflammatory drugs are generally not well tolerated in the elderly population that comprises the vast majority of AD patients. Accordingly, there is an interest in developing novel compounds that can be used to treat these individuals. The identification of new molecular entities that attenuate inflammation in the AD brain would be greatly aided by a better understanding of the mechanism of glial activation at senile plaques.

Towards this aim, there have been several studies showing that A $\beta$  causes increased release of cytokines from cultures of microglia or related cell types, such as macrophage and monocytes. Araujo and Cotman (23) demonstrated that A $\beta_{1-42}$  caused a modest proliferative response in rat microglia and astrocyte cultures. An elevation of IL-1 release was also observed in these amyloid-treated cells, although the increase in cytokine production may have resulted from the increase in cell number. Meda and colleagues (24) showed that the addition of the truncated A $\beta_{25-35}$  peptide to mouse microglia cultures caused an increased release of tumor necrosis factor  $\alpha$  (TNF $\alpha$ ) into the culture medium, and this amyloid-induced response was augmented when the peptide was coincubated with interferon- $\gamma$ . Similarly, the naturally occurring A $\beta_{1-40}$  peptide elicits TNF $\alpha$  production in the mouse microglial cell line, BV-2 (25).

Our laboratory (26 and unpublished) has found that lipopolysaccharide (LPS)-treated human THP-1 monocytes, which resemble macrophages, release increased amounts of IL-1 $\beta$  and TNF- $\alpha$  after the addition of the fibrillar forms of A $\beta_{1-40}$  or A $\beta_{1-42}$  (see Fig. 1). Interestingly, we have found that the nonfibrillar form of A $\beta_{1-40}$  has no effect on cytokine release from the cells, which is consistent with the colocalization of IL-1-positive microglia with fibrillar A $\beta$ -containing senile plaques in the AD brain. These data thus provide a rational explanation for the elevated levels of proinflammatory cytokines reported in the AD brain. This chapter describes the *in vitro* cellular assay system that is typically used in our laboratory to evaluate cytokine release following the addition of A $\beta$  peptide.

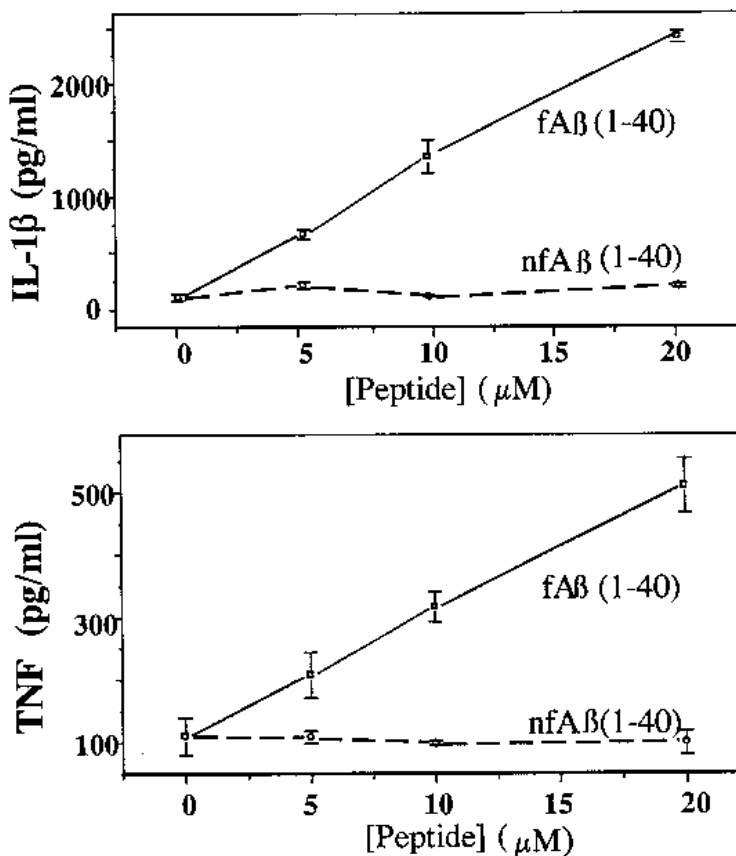


Fig. 1. Fibrillar A $\beta$ (1-40) induces cytokine release from THP-1 cells. The cells were treated with 0.5  $\mu$ g/mL of lipopolysaccharide and increasing concentrations of either fibrillar or nonfibrillar A $\beta$ (1-40) for 48 h, followed by analysis of the amount of IL-1 $\beta$  and TNF $\alpha$  in the culture medium.

## 2. Materials

### 2.1. Characterization of A $\beta$ Peptides

#### 2.1.1. Equipment

1. Variable wavelength fluorimeter.
2. Cuvets.
3. Adjustable pipets.
4. Pipet tips.

#### 2.1.2. Reagents and Materials

1. A $\beta$ <sub>1-40</sub> and/or A $\beta$ <sub>1-42</sub> (Bachem Inc., Torrance, CA, or equivalent source; 1 mg or more).
2. Thioflavine T (Sigma #T 3516 or equivalent, Sigma Chemical Co., St. Louis, MO).

### 2.1.3. Solutions

1. A $\beta$ <sub>1-40</sub> or A $\beta$ <sub>1-42</sub> stock.

- a. Fibrillar A $\beta$ .

To prepare fibrillar stocks of either A $\beta$ <sub>1-40</sub> or A $\beta$ <sub>1-42</sub>, lyophilized peptide is resuspended in deionized water to a final concentration of 2 mM. It is recommended that this solution be immediately split into ~25  $\mu$ L aliquots and re-lyophilized for storage until needed. A single aliquot of the relyophilized peptide should be dissolved in deionized water to a concentration of 2 mM and stored at 4°C. The fibril content of this sample should be determined as a function of storage time, as described in Methods **Subheading 3.1**.

- b. Nonfibrillar A $\beta$ <sub>1-40</sub> (see **Note 1**).

Nonfibrillar A $\beta$ <sub>1-40</sub> is prepared by dissolving lyophilized peptide in hexafluoroisopropanol (HFIP) (see **Note 2**) to a concentration of 2 mM. After a 30-min incubation period, it is recommended that this solution be split into ~25  $\mu$ L aliquots and relyophilized for storage until needed. A single aliquot of relyophilized peptide should be dissolved in deionized water to a final concentration of 2 mM and stored at 4°C. If the preparation is to be stored in water for more than 2 d, it is recommended that the fibril content of this sample be determined as a function of storage time, as described in Methods, **Subheading 3.1**.

2. Thioflavine T stock: Thioflavine T is dissolved in deionized water to a concentration of 3 mM. This solution should be stored in the dark at 4°C, and can be used for up to 1 wk.

## 2.2. THP-1 Monocyte Cell Culture

### 2.2.1. Equipment

1. Humidified incubator (37°C, 5% CO<sub>2</sub>).
2. Biohazard laminar flow hood.
3. Inverted microscope.
4. Pipet aid.
5. Vacuum trap to collect biohazard waste.
6. Hemocytometer with coverslip.
7. Adjustable pipets (covering volumes of 2–1000  $\mu$ L).
8. Multichannel pipet (20–200  $\mu$ L).
9. Multichannel pipet (5–50  $\mu$ L).
10. Pipet tips.
11. Biohazard waste receptacle.
12. Centrifuge.
13. Vortex.
14. Water bath (37°C).
15. Refrigerator (2–6°C).
16. Freezer (–20°C).

### 2.2.2. Reagents and Materials (see **Note 3**)

1. THP-1 human monocyte cell line (American Tissue Type Collection #TIB202, Rockville, MD).

2. RPMI-1640 media (Gibco #11875 or equivalent, Gibco-BRL, Gaithersburg, MD).
3. Penicillin/streptomycin solution (Gibco #15070–063 or equivalent; 5000 U/mL penicillin G and 5 mg/mL streptomycin).
4.  $\beta$ -Mercaptoethanol.
5. Fetal bovine serum (FBS), heat inactivated (HyClone #SH30070.03 or equivalent, HyClone, Logan, UT).
6. Lipopolysaccharide (LPS) (Sigma #L2654 or equivalent; *E. coli* serotype O26:B6).
7. Phosphate-buffered saline (PBS) (Sigma #1000-3 or equivalent).
8. Trypan Blue (Sigma #T8154 or equivalent; 0.4% solution).
9. A $\beta$ <sub>1–40</sub> or A $\beta$ <sub>1–42</sub> peptide solutions (*see* **Subheading 2.1.3.**).
10. Tissue culture flasks (162 cm<sup>2</sup>).
11. 96-Well tissue culture-treated microtiter plates, flat-bottom (Costar #3595 or equivalent, Costar, Cambridge, MA).
12. Disposable pipets (1, 5, 10, 25 mL).
13. Pasteur pipets, sterile.
14. Pasteur pipets, sterile and cotton plugged.
15. 0.2  $\mu$ m Syringe and disk filters.
16. Centrifuge tubes (sterile; 15 mL and 50 mL).
17. Microcentrifuge tubes (sterile; 2.0 mL and 0.7 mL).
18. Sterile bottles for culture media (200 mL and 500 mL).
19. Chlorine bleach (undiluted).

### 2.2.3. Solutions

1.  $\beta$ -Mercaptoethanol supplement for growth medium:

RPMI-1640 medium	17.8 mL
Penicillin/streptomycin	0.2 mL
FBS	2.0 mL
$\beta$ -Mercaptoethanol	7.0 $\mu$ L

Sterilize solution with 0.2  $\mu$ m filter. This solution can be stored for several months at 2–6°C.

2.  $\beta$ -Mercaptoethanol supplement for assay medium:

RPMI-1640 medium	19.4 mL
Penicillin/streptomycin	0.2 mL
FBS	0.4 mL
$\beta$ -Mercaptoethanol	7.0 $\mu$ L

Sterilize solution with 0.2  $\mu$ m filter. This solution can be stored for several months at 2–6°C.

3. THP-1 growth medium (for stock cultures):

RPMI-1640 medium	440.5 mL
Penicillin/streptomycin	4.5 mL
FBS	50.0 mL
$\beta$ -Mercaptoethanol supplement	5.0 mL

Store at 2–6°C.

4. THP-1 assay medium (for cytokine release assay):
 

RPMI-1640 medium	96.0 mL
Penicillin/streptomycin	0.98 mL
FBS	2.0 mL
$\beta$ -Mercaptoethanol supplement	1.0 mL

 Store at 2–6°C
5. LPS stock: Solubilize lyophilized LPS in sterile water to a concentration of 1 mg/mL. Aliquots (1 mL) can be stored indefinitely at –20°C. The solution is stable for 1 mo at 2–6°C.

### 2.3. Cytokine Assays

#### 2.3.1. Equipment

1. Spectrophotometric plate reader.
2. Adjustable pipets (2  $\mu$ L–1000  $\mu$ L).
3. Multichannel pipet (50–1000  $\mu$ L).
4. Pipet tips (covering volumes of 2  $\mu$ L–1000  $\mu$ L).
5. Refrigerator (2–4°C).

#### 2.3.2. Reagents and Materials

1. 96-Well medium-binding plates (Costar #2589 or equivalent).
2. Mouse antihuman IL-1 $\beta$  monoclonal antibody (R and D Systems, Minneapolis, MN, #MAB201 or equivalent).
3. Goat antihuman IL-1 $\beta$  polyclonal antibody (R and D Systems #AB-201–NA or equivalent).
4. IL-1 $\beta$  (R and D Systems #201–LB-005 or equivalent).
5. Peroxidase-labeled antigoat IgG (Vector Laboratories [Burlingame, CA] #PI-9500 or equivalent; typically 1 mg/mL).
6. Tetramethylbenzidine (TMB) peroxidase substrate and solution (Kirkegard and Perry Laboratories [Gaithersburg, MD] #50-76-00 or equivalent).
7. PBS (Sigma #1000-3 or equivalent).
8. Tween-20.
9. Dry nonfat milk.
10. 1 M Phosphoric acid.

#### 2.3.3. Solutions

1. Wash buffer:
 

PBS	1000 mL
Tween-20	0.5 mL

 Store the buffer at 4°C for up to 1 wk.
2. Blocking solution:
 

PBS	995 mL
Dry nonfat milk	50 g

 Prepare this solution the day it is used.
3. IL-1 $\beta$  Standards: Prepare a stock solution containing 1 ng/mL of IL-1 $\beta$  in THP-1 assay medium (*see Subheading 2.2.3., step 4*). This should be divided into 1 mL aliquots and each aliquot should be stored frozen at –80°C until needed.

4. Monoclonal antibody solution: Dissolve a 0.5-mg vial of IL-1 $\beta$  monoclonal antibody in 1.0 mL of PBS. This stock solution is typically divided into 0.2 mL aliquots that can be stored at  $-80^{\circ}\text{C}$  for up to 6 mo or at  $4^{\circ}\text{C}$  for up to 1 mo. Prior to use in an ELISA, the stock solution is diluted to 1.5  $\mu\text{g}/\text{mL}$  in PBS (10 mL/plate).
5. Polyclonal antibody solution: Dissolve a 1.0 mg vial of IL-1 $\beta$  polyclonal antibody in 1.0 mL of PBS. This stock solution is typically divided into 0.2 mL aliquots that can be stored at  $-80^{\circ}\text{C}$  for up to 6 mo or at  $4^{\circ}\text{C}$  for up to 1 mo. Prior to use in an ELISA, the stock solution is diluted to 1.5  $\mu\text{g}/\text{mL}$  in a 1:1 mixture of PBS and PBS + 5% nonfat milk (*see Subheading 2.3.3., step 2*; 10 mL/plate).
6. Peroxidase-labeled antibody solution: For each plate, mix 5  $\mu\text{L}$  of peroxidase-conjugated anti-goat IgG (1 mg/mL) with 5 mL of PBS. Add 5 mL of blocking solution to yield a final 1:2000 dilution of antibody in PBS + 2.5% nonfat milk.
7. TMB peroxidase substrate: For each plate, mix 5 mL of TMB substrate solution and 5 mL of hydrogen peroxide solution. Note: prepare this solution immediately before use.

### 3. Methods

#### 3.1. Characterization of A $\beta$ Peptides

1. Aliquots of the A $\beta$  stocks are subjected to analysis in a thioflavine T fluorescence assay (27) to determine the extent of fibril content in the preparations.
2. At daily intervals, A $\beta$  stock solutions are mixed with thioflavine T as follows:
 

A $\beta$ stock solution	2 $\mu\text{L}$	(2 $\mu\text{M}$ final concentration)
Thioflavine T stock solution	2 $\mu\text{L}$	(30 $\mu\text{M}$ final concentration)
Deionized water	2.0 mL	
3. Analyze the samples in a fluorimeter, with an excitation wavelength of 450 nm and an emission wavelength of 482 nm.
4. Plot the thioflavine T fluorescence signal that results from the dye binding to amyloid fibrils against the number of days that the peptide stocks have been stored at  $37^{\circ}\text{C}$  (*see Note 4*).
5. When used for the treatment of THP-1 cells, nonfibrillar A $\beta$  is typically defined as a peptide that elicits minimal thioflavine T fluorescence (i.e.,  $<10\%$  of maximal signal). Fibrillar A $\beta$  is typically defined as peptide that has reached  $>80\%$  of the maximal thioflavine T fluorescence signal (i.e., 80% of the fluorescence signal plateau that is typically seen after  $>2$  wk of aging).

#### 3.2. THP-1 Cell Culture Maintenance and Plating for Cytokine Assays

1. THP-1 cells obtained from the vendor should be thawed and diluted according to the vendor's recommendations. Maintain the THP-1 culture stocks in tissue culture flasks in THP-1 growth medium within a humidified  $\text{CO}_2$  incubator at  $37^{\circ}\text{C}$ . The cultures should be maintained at a cell density of  $0.15\text{--}1.0 \times 10^6$  cells/mL. Typical growth rates result in a requirement for passaging the cells every 3–4 d.

2. For a single 96-well plate, a volume of culture stock containing  $2.0 \times 10^6$  cells should be centrifuged at 450g for 5.5 min in a sterile centrifuge tube. After removing the supernatant (being careful not to dislodge the cell pellet), the cells are rinsed with an equal volume of RPMI-1640 medium (without additives). The resulting solution is centrifuged again at 450g for 5.5 min, and the rinse step is repeated.
3. After the second rinse, the supernatant is carefully removed and the cell pellet is resuspended in a volume of assay medium that results in a density of at least  $1.5 \times 10^5$  cells/mL (typical volume of 8–9 mL).
4. Perform a viable cell count with a hemocytometer and trypan blue, using standard cell culture protocols.
5. Using the results from the cell count, dilute the cells with assay medium to a final concentration of  $1.5 \times 10^5$  cells/mL. A total of  $1.5 \times 10^6$  cells (10 mL volume) will be needed for each 96-well plate.
6. Add LPS stock solution to the cell suspension to yield a final LPS concentration of 0.1–10.0  $\mu\text{g/mL}$  (see **Note 5**).
7. Determine the number of wells in which A $\beta$  is to be added. It is recommended that each experimental condition be performed in triplicate (i.e., three wells). Multiply the number of wells times 0.11 mL to determine the volume of LPS-treated cell suspension to transfer to a separate sterile conical tube. Add 0.5  $\mu\text{L}$  of stock A $\beta$  solution per 0.1 mL of cell suspension (final A $\beta$  concentration of 10  $\mu\text{M}$ ). For example, if 30 wells are to be prepared in which cells are treated with A $\beta$ , remove 3.3 mL of LPS-treated cell suspension and add 16.5  $\mu\text{L}$  of A $\beta$  stock.
8. To each well of a 96-well plate, add 0.1 mL of either LPS-treated or LPS + A $\beta$ -treated cell suspensions ( $1.5 \times 10^4$  cells), making sure to keep the cells fully mixed during the dispensing step.
9. Incubate the plates (undisturbed) for 48 h at 37°C in a 5% CO<sub>2</sub> incubator.
10. At the end of the incubation period, remove 50  $\mu\text{L}$  of medium from each well for subsequent measurement of cytokine (see **Note 6**).

### **3.3. Analysis of Cytokine Levels in Culture Supernatants**

#### **3.3.1. Commercial ELISA Kits**

Several commercial ELISA kits for both human and mouse TNF $\alpha$  and IL-1 $\beta$  are available. These kits are generally in a 96-well format, and come with all required reagents (e.g., cytokine standards, antibodies, colorimetric dyes). A typical detection range for such kits is 5–500 pg/mL of cytokine. It is recommended that the culture medium samples be diluted over a range of 1:4–1:20 during the initial testing to determine a dilution that will fall within the linear detection range of the assay.

#### **3.3.2. Standard Human IL-1 $\beta$ ELISA**

1. The day before culture medium samples are to be collected for measurement of cytokine levels, treat 96-well medium-binding plates with 0.1 mL per well of monoclonal antibody solution. Cover the plates and incubate with the antibody overnight at 4°C.

2. Aspirate each well and wash with 0.4 mL of wash buffer. Repeat the washes five times. After the last wash, invert the plate and blot briskly onto paper towels (*see Note 7*).
3. Treat each well with 0.2 mL of blocking solution for 1 h at room temperature.
4. Remove the blocking solution and add, in triplicate, 0.2 mL of either standards or media samples to each well. Standards are prepared by making a twofold dilution series of the 1 ng/mL IL-1 $\beta$  stock in THP-1 assay medium. Typically, a standard curve consists of IL-1 $\beta$  ranging from 500–1.95 pg/mL. Incubate at room temperature for 2 h. It is recommended that the culture medium samples be diluted over a range of 1:4–1:20 during the initial testing to determine a dilution that will fall within the linear detection range of the assay.
5. Repeat the washes in **Subheading 3.3.2., step 2** a minimum of three times, blotting the plate after the last wash.
6. Add 0.1 mL of the polyclonal antibody solution to each well and incubate for 1 h at room temperature.
7. Repeat the washes in **Subheading 3.3.2., step 2** a minimum of three times, blotting the plate after the last wash.
8. Add 0.1 mL of peroxidase-conjugated antigoat IgG solution to each well and incubate for 1 h.
9. Repeat the washes in **Subheading 3.3.2., step 2** five times, blotting the plate after the last wash.
10. TMB color substrate (0.1 mL) is added to each well and incubated for 20 min at room temperature.
11. The color reaction is stopped by the addition of 0.1 mL of 1 M phosphoric acid per well.
12. The plates are analyzed at 450 nm in a plate reader, using a reference (background) wavelength of 570 nm. The absorbance reading should be performed within 30 min after the addition of the phosphoric acid stopping solution.

### 3.3.3. Data Analysis

1. The mean absorbance values for the triplicate analyses of each concentration of IL-1 $\beta$  standard are determined. These values are plotted against the log of IL-1 $\beta$  concentration to generate a linear standard curve. Typically, the correlation coefficient of this curve should be >0.95.
2. The mean absorbance values for the triplicate analyzes of each media sample are determined. The concentration of IL-1 $\beta$  in each media sample is determined by extrapolation from the standard curve.
3. The actual IL-1 $\beta$  concentration in the media samples is obtained by multiplying the value obtained in the ELISA assay by the sample dilution used in the assay.

## 4. Notes

1. Commercial preparations of lyophilized A $\beta$  show considerable variation in the degree of fibril content on solubilization. To ensure that nonfibrillar peptide is used, we recommend the methodology described in **Subheading 2.1.3., item 1.b.**

2. Although A $\beta$ <sub>1-40</sub> dissolves readily in HFIP, we have found that some commercial preparations of A $\beta$ <sub>1-42</sub> do not fully dissolve in this solvent.
3. Materials that are not sterile should be sterilized by filtration through a 0.2- $\mu$ m filter. An exception to this rule are A $\beta$  solutions, which **should not** be filtered, as the peptide can be retained on the filter.
4. Typically, A $\beta$ <sub>1-40</sub> that has been dissolved directly into deionized water reaches maximal fluorescence after 1–7 d of storage, with the rate varying with different peptide lots. The HFIP-treated A $\beta$ <sub>1-40</sub> forms fibrils at a much slower rate, and typically will not elicit a significant fluorescence signal until it has been stored for >7 d (for examples, *see ref. 28*). Aliquots of A $\beta$  stocks from the same peptide lot that are stored lyophilized show similar fibril formation kinetics on solubilization.
5. Each lot of LPS must be tested to determine the optimal concentration to use for the cytokine assays. Several small aliquots of THP-1 cells (e.g., 1 mL of a  $1 \times 10^5$  cell/mL) are treated with LPS such that the final concentration ranges from 0.1–10.0  $\mu$ g/mL. Cells from each of the different LPS concentrations are plated, in triplicate, as described in **Subheading 3.2., step 8**. An aliquot (0.4 mL) of each of the LPS-treated cell preparations should be treated with fibrillar A $\beta$  as described in **Subheading 3.2., step 7.**, and plated in triplicate as described in **Subheading 3.2., step 8**. Upon collection of culture medium (*see Subheading 3.2., step 10*) and completion of the ELISA assay (**Subheading 3.3.**), the cytokine values obtained in the presence and absence of A $\beta$  for each LPS concentration should be compared. The ideal LPS concentration is that which results in (1) cells that received both A $\beta$  and LPS releasing >200 pg/mL of IL-1 $\beta$  into the culture medium and (2) cells that received both A $\beta$  and LPS releasing > fivefold more IL-1 $\beta$  into the culture medium than cells that received only LPS.
6. The culture medium can be frozen once prior to ELISA analysis.
7. It is important to remove as much liquid as possible from the ELISA wells after the washings before proceeding to the next step.

## References

1. Chartier-Harlin, M.-C., Crawford, F., Houlden, H., Warren, A., Hughes, D., Fidani, L., et al. (1991) Early-onset Alzheimer's disease caused by mutations at codon 717 of the  $\beta$ -amyloid precursor protein gene. *Nature* **353**, 844–845.
2. Goate, A., Chartier-Harlin, M.-C., Mullan, M., Brown, J., Crawford, F., Fidani, L., et al. (1991) Segregation of a missense mutation in the amyloid precursor protein gene with familial Alzheimer's disease. *Nature* **349**, 704–706.
3. Mullan, M., Crawford, F., Axelman, K., Houlden, H., Lilius, L., Winblad, B., and Lannfelt, L. (1992) A pathogenic mutation for probable Alzheimer's disease in the APP gene at the N-terminus of  $\beta$ -amyloid. *Nat. Genet.* **1**, 345–347.
4. Murrell, J., Farlow, M., Ghetti, B., and Benson, M. D. (1991) A mutation in the amyloid precursor protein associated with hereditary Alzheimer's disease. *Science* **254**, 97–99.
5. Levy-Lahad, E., Wasco, W., Poorkaj, P., Romano, D. M., Oshima, J., Pettingell, W. H., et al. (1995) Candidate gene for the chromosome 1 familial Alzheimer's disease locus. *Science* **269**, 973–977.

6. Sherrington, R., Rogaev, E. I., Liang, Y., Rogaeva, E. A., Levesque, G., Ikeda, M., et al. (1995) Cloning of a gene bearing missense mutations in early-onset familial Alzheimer's disease. *Nature* **375**, 754–760.
7. Cai, X.-D., Golde, T. E., and Younkin, S. G. (1993) Release of excess amyloid  $\beta$  protein from a mutant amyloid  $\beta$  protein precursor. *Science* **259**, 514–516.
8. Citron, M., Oltersdorf, T., Haass, C., McConlogue, L., Hung, A. Y., Seubert, P., et al. (1992) Mutation of the  $\beta$ -amyloid precursor protein in familial Alzheimer's disease increases  $\beta$ -protein production. *Nature* **360**, 672–674.
9. Suzuki, N., Cheung, T. T., Cai, X.-D., Odaka, A., Otvos, L., Eckman, C., et al. (1994) An increased percentage of long amyloid  $\beta$  protein secreted by familial amyloid  $\beta$  protein precursor ( $\beta$ APP717) mutants. *Science* **264**, 1336–1340.
10. Duff, K., Eckman, C., Zehr, C., Yu, X., Prada, C.-M., Perez-tur, J., et al. (1996) Increased amyloid- $\beta$ 42(43) in brains of mice expressing mutant presenilin 1. *Nature* **383**, 710–713.
11. Scheuner, D., Eckman, C., Jensen, M., Song, X., Citron, M., Suzuki, N., et al. (1996) Secreted amyloid  $\beta$ -protein similar to that in the senile plaques of Alzheimer's disease is increased in vivo by the presenilin 1 and 2 and APP mutations in familial Alzheimer's disease. *Nat. Med.* **2**, 864–870.
12. Haga, S., Adai, K., and Ishii, T. (1989) Demonstration of microglial cells in and around senile (neuritic) plaques in the Alzheimer brain: an immunohistochemical study using a novel monoclonal antibody. *Acta Neuropathol.* **77**, 569–575.
13. McGeer, P. L., Itagaki, S., Tago, H., and McGeer, E. G. (1987) Reactive microglia in patients with senile dementia of the Alzheimer type are positive for the histocompatibility glycoprotein HLA-DR. *Neurosci. Lett.* **9**, 195–200.
14. Rogers, J., Luber-Narod, J., Styren, S. D., and Civin, W. H. (1988) Expression of immune system-associated antigens by cells of the human central nervous system: relationship to the pathology of Alzheimer's disease. *Neurobiol. Aging* **9**, 339–349.
15. Griffin, W. S. T., Stanley, L. C., Ling, C., White, I., Macleod, V., Perrot, L., et al. (1989) Brain interleukin-1 and S-100 immunoreactivity are elevated in Down syndrome and Alzheimer disease. *Proc. Natl. Acad. Sci. USA* **86**, 7611–7615.
16. Itagaki, S., McGeer, P. L., Akiyama, H., Zhu, S., and Selkoe, D. J. (1989) Relationship of microglia and astrocytes to amyloid deposits of Alzheimer's disease. *J. Neuroimmunol.* **24**, 173–182.
17. Das, S. and Potter, H. (1995) Expression of the Alzheimer amyloid-promoting factor antichymotrypsin is induced in human astrocytes by IL-1. *Neuron* **14**, 447–456.
18. Lee, S. C., Dickson, D. W., and Brosnan, C. F. (1995) Interleukin-1, nitric oxide and reactive astrocytes. *Brain Behav. Immun.* **9**, 345–354.
19. Cacabelos, R., Alvarez, X. A., Fernandez-Novoa, L., Franco, A., Mangués, R., Pellicer, A., and Nishimura, T. (1993) Brain interleukin-1 $\beta$  in Alzheimer's disease and vascular dementia. *Methods Find. Exp. Clin. Pharmacol.* **16**, 141–151.
20. Blum-Degen, D., Muller, T., Kuhn, W., Gerlach, M., Przuntek, H., and Riederer, P. (1995) Interleukin-1 $\beta$  and interleukin-6 are elevated in the cerebrospinal fluid of Alzheimer's and de novo Parkinson's disease patients. *Neurosci. Lett.* **202**, 17–20.
21. McGeer, P. L., Schulzer, M., and McGeer, E. G. (1996) Arthritis and anti-inflammatory agents as possible protective factors for Alzheimer's disease: a review of 17 epidemiologic studies. *Neurology* **47**, 425–432.

22. Stewart, W. F., Kawas, C., Corrada, S. M., and Metter, E. J. (1997) Risk of Alzheimer's disease and duration of NSAID use. *Neurology* **48**, 626–632.
23. Araujo, D. M. and Cotman, C. W. (1992)  $\beta$ -Amyloid stimulates glial cells in vitro to produce growth factors that accumulate in senile plaques in Alzheimer's disease. *Brain Res.* **569**, 141–145.
24. Meda, L., Cassatella, M. A., Szendrel, G. I., Otvos, L., Baron, P., Villalba, M., et al. (1995) Activation of microglial cells by  $\beta$ -amyloid protein and interferon- $\gamma$ . *Nature* **374**, 647–650.
25. Yan, S. D., Chen, X., Fu, J., Chen, M., Zhu, H., Roher, A., et al. (1996) RAGE and amyloid- $\beta$  peptide neurotoxicity in Alzheimer's disease. *Nature* **382**, 685–691.
26. Lorton, D., Kocsis, J., King, L., Madden, K., and Brunden, K. R. (1996)  $\beta$ -Amyloid induces increased release of interleukin-1 $\beta$  from lipopolysaccharide-activated human monocytes. *J. Neuroimmunol.* **67**, 21–29.
27. LeVine, H. (1993) Thioflavine T interaction with synthetic Alzheimer's disease  $\beta$ -amyloid peptides: detection of amyloid aggregation in solution. *Protein Sci.* **2**, 404–410.
28. Gupta-Bansal, R. and Brunden, K. R. (1998) Congo red inhibits proteoglycan and serum amyloid P binding to amyloid  $\beta$  fibrils. *J. Neurochem.* **70**, 292–298.

## Effects of the $\beta$ -Amyloid Peptide on Membrane Ion Permeability

Hugh A. Pearson

### 1. Introduction

Several lines of evidence suggest a role for membrane ion channels in the neurotoxic effects of the  $\beta$ -amyloid peptide ( $A\beta$ ). This chapter describes the electrophysiological techniques that can be employed to isolate and record specific membrane conductances that may be altered by  $A\beta$ . In general, an increase in conductances that cause depolarization of the cell membrane may be considered excitotoxic since they will: (1) increase  $Ca^{2+}$  influx through voltage-gated  $Ca^{2+}$  channels and (2) reduce  $Mg^{2+}$ -dependent block of ionotropic glutamate receptors, thereby increasing  $Ca^{2+}$  influx through *N*-methyl-D-aspartate (NMDA) receptor channels. Conversely, an increase in conductances that cause membrane hyperpolarization might be considered to have a protective effect. This is a simplistic view, as it has been shown that for certain forms of apoptosis an increase in hyperpolarizing  $K^+$  currents may be involved (*1*). It is, therefore, important to consider the functional effects of any changes in membrane conductances or ion channel currents induced by  $A\beta$  in the light of neurotoxic effects of the peptide.

#### **1.1. Effects of $A\beta$ on Voltage-Gated Ion Channels**

$A\beta$  has been shown to alter the activity of a range of voltage-gated ion channels in both primary cultures of neurons and in neuronal cell lines. Several groups have demonstrated that  $A\beta$  can induce an increase in the  $Ca^{2+}$  channel current of neurons using the whole-cell patch-clamp technique. In the N1E-115 cell line, 24-h preincubation of cells with  $20 \mu M A\beta_{1-40}$  resulted in an increase in  $Ca^{2+}$  channel activity (*2*). A similar increase has been observed in cultured rat cerebellar granule neurons (*3*) and cortical neurons (*4*,  $A\beta_{25-35}$ ).

Both L- and N-type  $\text{Ca}^{2+}$  channels have been suggested to be involved in this effect.

Two lines of evidence point to an involvement of  $\text{K}^+$  channels in the effects of  $\text{A}\beta$ . Using human fibroblasts isolated from Alzheimer's disease (AD) patients, Etcheberrigaray and coworkers (5) have shown the absence of a tetraethylammonium-sensitive  $\text{K}^+$  channel with a unitary conductance of 113 pS. This channel is always present in fibroblasts from age-matched control subjects. Furthermore, incubation of cells with soluble  $\text{A}\beta_{1-40}$  (10 nM) for 48 h leads to a selective loss of this  $\text{K}^+$  conductance from the control fibroblasts. In rat hippocampal neurons Good et al. (6) observed that 100  $\mu\text{M}$   $\text{A}\beta_{1-40}$  applied acutely to cells inhibited a 4-aminopyridine-sensitive, inactivating  $\text{K}^+$  channel current. No effects of  $\text{A}\beta$  have been observed on  $\text{Na}^+$  channel currents (6) and, as far as I am aware, no studies of the effects of  $\text{A}\beta$  on inward rectifier,  $\text{Ca}^{2+}$ -( $\text{I}_{\text{KCa}}$ ), ATP-sensitive  $\text{K}^+$  channels ( $\text{I}_{\text{KATP}}$ ), or of  $\text{Cl}^-$  channels have been published.

### **1.2. Effects of $\text{A}\beta$ on Ligand-Gated Ion Channels**

Evidence for an interaction of  $\text{A}\beta$  with NMDA receptors has been found. Acutely applied  $\text{A}\beta_{1-40}$  enhances NMDA receptor-mediated excitatory postsynaptic currents in rat hippocampal slices with no effect on  $\alpha$ -amino-3-hydroxy-5-methyl-4-isoxazole (AMPA) receptor mediated events (7) and experiments where  $\text{A}\beta_{1-40}$  is applied to the inside of the cell suggested that this is a postsynaptic effect. This enhancement appears to give rise to a later reduction in glutaminergic transmission that can be blocked by NMDA receptor antagonists (8). In *Aplysia* neurons gamma-aminobutyric acid<sub>A</sub> ( $\text{GABA}_A$ ) receptor mediated currents were inhibited by both  $\text{A}\beta_{1-40}$  and  $\text{A}\beta_{25-35}$  (9). In contrast to these effects there is little evidence in the literature that  $\text{A}\beta$  alters nicotinic receptor mediated electrophysiological events, despite the fact that reductions in nicotinic receptor binding occur early in AD.

### **1.3. Formation of Conductances by $\text{A}\beta$ Peptides**

In addition to possible effects on voltage- and ligand-gated  $\text{Ca}^{2+}$  channels,  $\text{A}\beta$  may be able to induce  $\text{Ca}^{2+}$  flux across cell membranes in its own right. Aripse and colleagues have observed that incorporation of liposomes containing partially aggregated  $\text{A}\beta_{1-40}$  into lipid bilayers gives rise to nonselective cation channels that conduct  $\text{K}^+$ ,  $\text{Na}^+$ , and  $\text{Ca}^{2+}$  ions (10). In cultured cortical neurons  $\text{A}\beta_{25-35}$  has been found to induce an irreversible, nonspecific cation current, and a similar current has been induced in frog sympathetic neurons by  $\text{A}\beta_{25-35}$  (11,12). By contrast, other workers, including ourselves, have been unable to detect such conductance changes using  $\text{A}\beta_{1-40}$  (3,6).

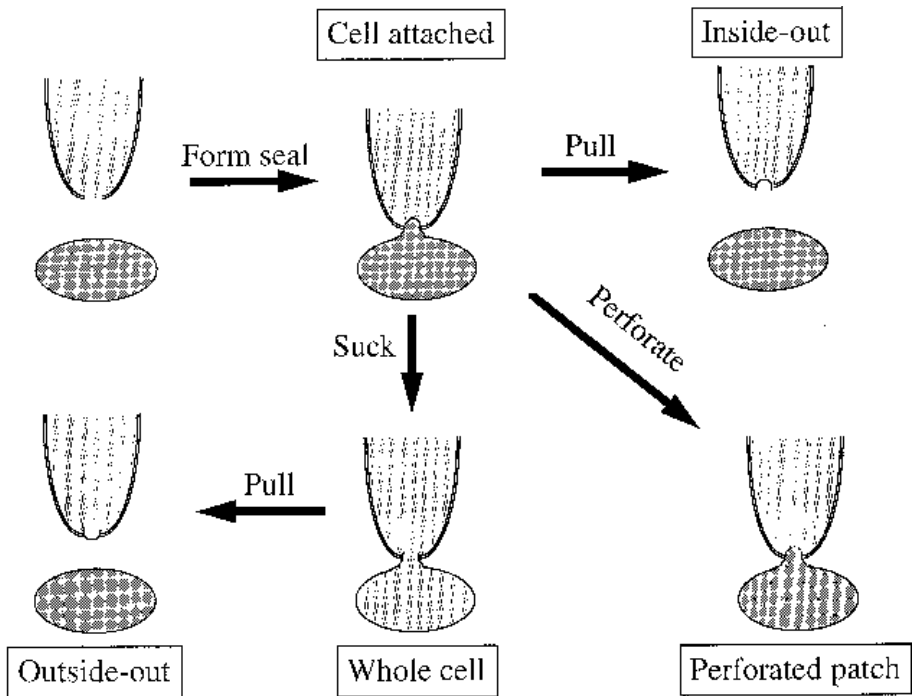


Fig. 1. The different configurations of the patch-clamp technique. Formation of a high resistance seal with the cell membrane allows recording of current flow through individual channels present in the patch of membrane under the lumen of the patch pipet (cell attached). Moving the pipet away from the cell rips off the patch of membrane exposing the intracellular surface of the channels to the bath solution (inside out). Suction gives access to the cell interior and allows measurement of currents across the entire cell membrane (whole cell). From the whole cell the outside-out configuration can be attained by moving the pipet away from the cell. An alternative to the whole-cell configuration makes use of ionophores to give access to the cell interior, which prevents loss of intracellular proteins important for modulation of channel activity.

#### 1.4. The Patch-Clamp Technique

One of the most powerful electrophysiological techniques available today is the patch-clamp technique (13). The basic principle of the patch-clamp technique is that a saline filled, blunt-ended glass capillary (micropipet) with a tip diameter of approx  $1 \mu\text{m}$  is placed on the membrane of a cell. Gentle suction applied to the micropipet leads to the formation of a mechanically and electrically tight seal between the glass and the cell membrane (Fig. 1). The patch of membrane under the opening of the micropipet can be voltage clamped and currents flowing across the membrane patch measured. In this configuration,

known as cell-attached or on-cell, currents flowing through individual ion channels can be observed. Other patch-clamp configurations can be attained from this starting point. By gently moving the micropipet away from the cell, the patch of membrane will be pulled off but remains attached to the micropipet. This gives rise to the “ripped off” or inside-out configuration, so called because the internal surface of the cell membrane is exposed to the bath. This allows the application of channel modulators or drugs to the intracellular side of the channel protein. It also allows the saline on both sides of the membrane to be manipulated to allow more effective isolation of specific conductances. This is not possible in the case of the cell-attached configuration, as the cell membrane is intact and the internal surface of the cell is therefore in contact with the cell cytoplasm. As with the cell-attached configuration, single-channel currents can be measured in inside-out patches. The third configuration that allows recording of single-channel events is the outside-out patch. To attain this configuration, the patch of membrane under the micropipet tip is ruptured by suction or by application of a strong (1–5 V) but brief (0.1–1 ms) voltage pulse. This gives rise to the whole-cell configuration (*see below*) where the rim of the pipet tip is still sealed onto the membrane, but the inside of the cell is in direct physical contact with the lumen of the micropipet. Gently moving the micropipet away from the cell pulls a long neck of membrane with it. When this parts, a region of the membrane reforms across the pipet tip with the outer surface of the ion channel facing the bath and the inner surface in contact with the saline in the pipet. This configuration is particularly necessary for recording single ligand-gated ion channel currents, as agonists need to be applied to the outer surface of the ion channel for their activation.

With the whole-cell configuration of the patch-clamp technique, currents flowing through all of the channels in the cell membrane are measured. The inside of the cell is both physically and electrically in contact with the lumen of the pipet. This allows control of the intracellular potential of the cell and the dialysis and replacement of the cell cytoplasm with the saline used to fill the micropipet. A disadvantage of this technique is that, in the case of some channels, loss of intracellular constituents required for channel activation and modulation (e.g., phosphorylating enzymes) leads to a gradual loss of channel activity with time. To overcome this sort of problem, the perforated patch technique can be used. Using this technique the membrane patch under the micropipet is not ruptured, but instead is perforated using pore-forming compounds such as amphotericin B, nystatin, or gramicidin. Ions and small molecules can pass through these channels to dialyze the cytoplasm and electrical contact between the cell interior and the micropipet is maintained; however, large molecules are unable to pass through the pores and remain within the cell.

## **2. Materials**

The advent of the patch-clamp technique has allowed the possibility of isolating and measuring specific membrane conductances in practically any cell type. Experiments can be performed on primary cultures, cell lines, and in slice preparations.

### **2.1. Patch-Clamp Amplifiers**

Several patch-clamp amplifiers are available commercially. The most widely used are the Axopatch amplifiers (Axon Instruments, Foster City, CA) and the EPC-9 (Heka Elektronik, Lambrecht, Germany). The principle behind these amplifiers is the same in each case. The amplifier sets the voltage of the cell or membrane patch to a user-determined potential and measures current flow at this potential. The opening of ion channels in response to changes in voltage or application of agonist compounds results in changes in current flow, which can be quantified and related to agonist concentration and/or potential across the cell membrane. Axon Instruments produces two amplifiers specifically designed for use in patch-clamp experiments, the Axopatch-1D and the Axopatch-200B. Both can be used for whole-cell or single-channel recording of ion channel currents, but the Axopatch-200B is particularly suited for recording of single-channel events. Heka Elektronik produces the EPC-9, which does not have the ultralow noise characteristics of the Axopatch-200B, but it does have the advantage for first-time patch clampers that capacitance neutralization and series resistance compensation (electronic removal of artefacts) can be fully automated using built-in software.

### **2.2. Data Acquisition/Analysis Hardware and Software**

Currents measured in cells are converted to an equivalent voltage by the amplifier and are seen as voltage outputs whose amplitude is directly proportional to the current. The voltage across the cell membrane is also output, usually at 10 times the voltage seen at the cell. In order to record these signals on computer, they need to be converted from analog (voltage) signals to a digital form that can be processed by the computer. Similarly, the computer can be used to initiate complex changes in the voltage that the amplifier applies to the cell membrane, such as stepwise voltage changes and “ramped” changes in voltage. This is achieved using an analog/digital converter (ADC), which will convert digital information from the computer to analog waveforms and analog signals to a digital form. The EPC-9 amplifier comes complete with an ADC that can be specified to be compatible with either Windows or Macintosh operating systems. Voltage protocols and data analyses are performed using Pulse/Pulsefit software. For Axopatch amplifiers the ADC is supplied separately; the acquisition and analysis software (pClamp v6 or v7) is written to be run on PCs only.

### **2.3. Microscopes**

For primary cell cultures and cell lines an inverted microscope is usually used. With brain slices, an upright microscope is the most common choice. Optics differ according to the preparation. For slice work differential interference contrast optics are popular, whereas phase contrast is effective when working with cultures and cell lines. High magnification is necessary for accurate placement of the patch pipet, typically objectives of 10×, 20×, and 40× magnification are used in conjunction with 10× eyepieces.

### **2.4. Manipulators**

Accurate placement of micropipets on the cell requires the use of manipulators with a minimum movement of 0.1–0.2  $\mu\text{m}$ . Several types are marketed, the most popular being hydraulic manipulators (Narishige, Tokyo, Japan) and piezoelectric manipulators (Burleigh Instruments, Fishers NY). Hydraulic manipulators can be prone to drift, particularly when room temperature fluctuates throughout the day and when heavy headstages are attached to them. These problems can be overcome by the use of piezo-electric micromanipulators. In addition to the fine movement provided by the micromanipulators, coarse movement is also required, together with a system for mounting the entire assembly on the microscope. Integrated systems are provided by the manufacturers.

### **2.5. Antivibration Tables**

Relatively small movements of the patch pipet can disrupt the seal between cell membrane and pipet tip, resulting in loss of the seal and death of the cell. To isolate the recording equipment from vibration, air tables that damp out small movements are usually employed (Newport, Irvine CA). These can be free standing or benchtop. The microscope and manipulators are mounted on the vibration isolation system and all electrical equipment is mounted separately in a rack.

### **2.6. Micropipet Fabrication**

Micropipets are fabricated from glass capillaries with external diameters of 1.2–1.6 mm. The glass itself can be either soda, borosilicate, or quartz glass. The noise characteristics (important for single-channel recording) vary according to the type of glass used, with soda glass having the highest noise and quartz glass the lowest. Quartz glass has the disadvantage of having a high melting point and may require a laser-based puller to provide a high enough temperature. A good compromise is to use borosilicate glass for both single-channel and whole-cell recording. We have found that 1.5 mm outside diameter, 0.86 mm internal diameter borosilicate glass

such as GC150F-15 from Clark's Electromedical (Reading, UK) produces patch pipets that can be used to record a wide range of whole-cell and single-channel currents.

Microelectrode pullers take at least two pulls to form patch pipets. During the first pull, the glass is melted by a platinum filament and a narrow tapering neck is formed. On the second pull, this is extended further until the glass parts, leaving two micropipets each with a tip of approx 1  $\mu\text{m}$  in diameter. The two main types of micropipet pullers available are horizontal pullers and vertical pullers. The main difference between the two types is the source of tension used to pull the glass into a tip. For vertical pullers a weight is attached to the bottom end of the glass, whereas for horizontal pullers springs are usually used to provide tension. Models such as the PP-830 (Narishige Co., Tokyo, Japan) and P-97 (Sutter Instrument Co., Novato, CA) can be used to form pipets suitable for both single-channel and whole-cell patch-clamp recordings. Pipet resistances of 2–5  $\text{M}\Omega$  are usual for whole-cell recording and 8–10  $\text{M}\Omega$  for single-channel recording.

After pulling the patch-clamp pipets it is usual (but not always necessary) to fire polish them. This involves bringing the pipet tip close (20–40  $\mu\text{m}$ ) to a heated platinum or nichrome filament. The tip of the pipet is smoothed by this heating process, aiding formation of a seal between pipet tip and cell membrane. Microforges to fire polish patch pipets are available commercially (e.g., MF-830, Narishige Co.). Pipets should always be made on the day of the experiment and discarded after use. We usually make up pipets in batches of 10 to 20 and replace these once they have run out.

Following fabrication, pipets are filled with a suitable saline immediately prior to forming a seal. Before placing the pipet in its holder, we dip the tip of the pipet (approx 5 mm) into Sigmacote<sup>®</sup> solution (Sigma Chemical Co., Poole, Dorset, UK). This is a silicone solution dissolved in heptane, which forms a water-repellent coating on the outside of the pipet. The coated pipet has a lower capacitance, which helps to reduce noise, and produces less optical distortion when in the bath containing the cells.

## **2.7. Suction at the Pipet Tip**

Electrode holders for pipet tips are provided with a sidearm through which suction can be applied. A length of tubing (approx 1 mm internal diameter) is attached to the side arm and run outside the Faraday cage. At the end of this tubing a three-way tap is attached. The second port of the tap is open to the atmosphere and to the third port is attached to a 1-mL disposable syringe. The syringe can then be used to provide suction (negative pressure) or positive pressure to the pipet when required. The inclusion of the three-way tap allows this pressure to be held or to be released by opening the second port.

## **2.8. Perfusion/Drug Application**

A variety of drug application systems can be used in patch clamping and choice of method often depends on the quantity of compound available and the speed with which it needs to be applied. The simplest method of drug application is by perfusing the recording chamber. Reservoirs suspended above the microscope allow gravity flow of saline into the recording chamber. Fluid is removed by suction from the opposite end of the chamber. The disadvantages of this method are that relatively large quantities of drug are required and application times are relatively slow — in the order of tens of seconds. To apply small quantities of a drug, an alternative method is low-pressure ejection from a blunt micropipet. This allows use of small quantities (10–20  $\mu\text{L}$ ) of a drug-containing saline to be rapidly applied directly to cells in a static bath; however, washing the cells relies on the slow diffusion of the compound away from the cell. A variation on this method that allows washing of the cell by use of multibore pipets is described by Carbone and Lux (**14**). Others prefer to use the U-tube technique, which also allows rapid solution changes and is therefore useful for activation of desensitizing ligand-gated ion channels (**15**).

## **2.9. Solutions Suitable for Isolating Specific Membrane Conductances**

One of the main advantages of the patch-clamp technique is the ability to control the constituents of the cytoplasm. In the case of  $\text{Ca}^{2+}$  channels, where the  $\text{Ca}^{2+}$  conductance can be an order of magnitude smaller than the  $\text{K}^{+}$  conductance, this is particularly important, as it allows a more complete block of contaminating  $\text{K}^{+}$  channels. The formulation of both the bath solution and solutions used to fill the micropipet in whole-cell patch-clamp experiments is therefore significant in terms of which currents are to be recorded. Recipes for solutions suitable for recording of the main types of voltage- and ligand-gated ion channels are given in **Tables 1–9**. Pipet solutions should be filtered through a 0.2- $\mu\text{m}$  filter prior to use to prevent blockage of the pipet tip by particulate matter.

For experiments using the perforated-patch technique, a stock solution of amphotericin B (60 mg/mL) is made from the powdered compound dissolved in dimethylsulphoxide. Amphotericin is light sensitive and should be kept wrapped in aluminium foil to protect it from light. This stock solution will retain its activity for up to 3 h after which time fresh stock solution should be made. Stock amphotericin solution can then be added to an appropriate pipet solution to perforate membranes during experiments (*see Subheading 3.5*).

### 3. Methods

#### 3.1. Forming a Seal/Cell-Attached Patch

1. Fill the pipet with the appropriate solution; e.g., solution B for the recording of  $K^+$  channel currents. Dip the pipet into Sigmacote (Sigma Chemical) and attach it to the pipet holder.
2. Set data acquisition software to provide a 40-ms, 1-mV voltage step once every second to the electrode. The amplifier should be in voltage-clamp mode.
3. Select an appropriate cell to patch. Under phase contrast optics, the best cells are usually smooth looking and phase bright.
3. Move the plane of focus to just above the surface of the solution. Bring the pipet tip into the field of view. Apply positive pressure to the pipet (approx 0.3–0.5 mL on the 1-mL syringe) and hold this pressure.
4. Gently lower the pipet into the solution using the coarse controls of the manipulator.
5. Adjust the pipet offset current to zero. This removes any offset potentials from the system. You should now *see* a square current step in response to the imposed voltage change (*see* **Fig. 2**). The size of this step is inversely proportional to the pipet resistance (Ohm's Law,  $R = V/I$ ) and the pipet resistance (in  $M\Omega$ ) can be calculated from the voltage step (in mV) and the resultant current flow (in nA).
6. Bring the pipet tip down towards the cell using the coarse controls. The distance of the pipet tip from the cell can be estimated by changing the plane of focus between the cell surface and the pipet tip.
7. Once close enough, very gently touch the pipet tip onto the cell using the fine manipulator controls. Touching the cell surface will produce a slight dimpling of the cell at the pipet tip or slight movement of the cell. Alternatively, this can be detected by the observation of a slight decrease in the size of the current flowing across the pipet in response to the voltage step.
8. Once the pipet has touched the cell, suction needs to be applied. Gradually increase the suction using the syringe until the current step begins to decrease (**Fig. 2A**), then hold the suction at this level.
9. Change to a 40-ms, 10-mV voltage step every second. This will allow better observation of the change in resistance as the seal forms. Seal formation can be relatively slow and steady or can occur abruptly. Ideally the seal should have a resistance of greater than 1  $G\Omega$  (>10  $G\Omega$  is ideal for single-channel recording), this results in a current trace that appears almost flat apart from capacitance spikes at the beginning and end of the voltage step (**Fig. 2B**, top trace). If a high-resistance seal does not form within 5 min, discard the pipet and begin again, selecting a new cell (*see also* **Note 1**).
10. As soon as a high resistance seal has formed, release the pressure from the pipet. Using the controls on the amplifier, minimize the pipet capacity transients on the current trace. You are now in the cell-attached configuration. Noise levels should be less than 1 pA peak to peak if filtering at 2–5 kHz and the trace should be flat. If not, this may be due to excessive noise or interference (*see* **Note 2**).
11. Set the holding potential of the pipet to the required voltage (NB: bear in mind that the polarity of current and voltage is reversed in this configuration).

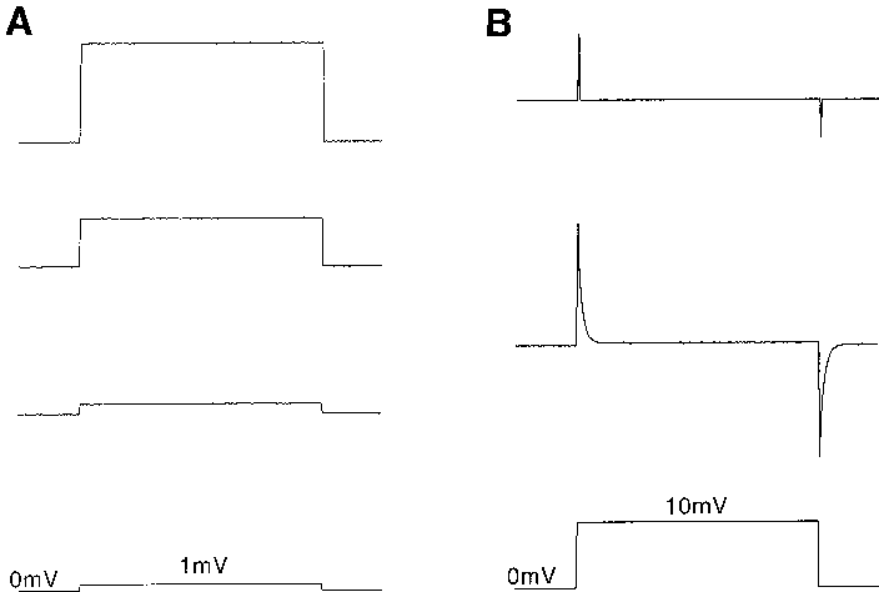


Fig. 2. Forming a seal and going whole-cell. Current and voltage traces recorded during seal formation and after rupture of the patch to attain the whole-cell configuration. **(A)** Current flow (top three traces) through a patch pipet in response to a 40-ms, 1-mV voltage step (bottom trace). With the pipet in the bath the amplitude of the voltage step is 0.25 nA, hence the pipet resistance is 4 M $\Omega$  ( $R = V/I$ ). After gently touching the cell and applying gentle suction the size of the current step reduces as the apparent resistance of the pipet increases. **(B)** As a higher resistance is reached, the voltage step is increased to 10 mV (bottom trace) to allow better resolution of resistance and capacity transients. The top trace shows the current resulting from the voltage step after formation of a G $\Omega$  seal. Spikes at the beginning and end of the step are a result of the pipet capacitance. Apart from the spikes, the current trace should appear to be almost flat if a good seal has been formed. This is the cell-attached configuration. These artefacts can now be removed electronically using controls on the amplifier. To attain a whole cell, the patch of membrane is ruptured by suction or “zapping.” Successful rupture results in the appearance of large transients that reflect the cell capacitance (middle trace).

To apply  $-50$  mV holding potential to the membrane patch, set the pipet potential to  $+50$  mV). Switch to the appropriate voltage protocol for recording single-channel currents.

### 3.2. Forming an Inside-Out Patch

1. Form a cell-attached patch (**Subheading 3.1.**). Continue to use the 10-mV, 40-ms, 1-Hz voltage step.

2. Once a seal has been formed, gently move the pipet away from the cell using the fine manipulator. Check visually to ensure that the cell is not still attached to the pipet. Check that a good seal ( $>10\text{ G}\Omega$ ) is still present.
3. Set the holding potential of the pipet to the required voltage (as with the cell-attached configuration in **Subheading 3.1.** the polarity of current and voltage is reversed). Switch to the appropriate voltage protocol for recording single-channel currents.

### **3.3. Forming the Whole-Cell Configuration**

1. Form a cell-attached patch (**Subheading 3.1.**).
2. Set the required holding potential for the whole-cell experiment.
3. Apply a small amount of suction (0.2–0.3 mL on the syringe).
4. Either (a) Set the zap control to its shortest setting and press the zap button. Increase the zap duration until the patch is ruptured (*see step 5*) or (b) gradually increase suction until the patch ruptures.
5. Successful rupture of the patch is seen as a sudden increase in the capacitance transients at the beginning and end of the voltage step (**Fig. 2B**, middle trace).
6. Reduce the transients using the series resistance and whole-cell capacitance compensation controls. Advance percent series-resistance compensation as far as possible without causing oscillation of the current trace.
7. Switch to the appropriate voltage protocol for the recording of whole-cell currents.

### **3.4. Forming the Outside-Out Configuration**

1. Form the whole-cell configuration (**Subheading 3.3.**) but do not neutralize the whole-cell capacity transients.
2. Once the whole-cell configuration has been formed, gently move the pipet away from the cell using the fine manipulator. The whole-cell capacity transients should disappear when the pipet is detached from the cell. Check visually to ensure that the cell is not still attached to the pipet. Check that a good seal ( $>10\text{ G}\Omega$ ) is still present.
3. Set the holding potential of the pipet to the required voltage. Switch to an appropriate voltage protocol for recording single-channel currents.

### **3.5. Whole-Cell Recording Using the Perforated Patch Configuration**

1. Add 2  $\mu\text{L}$  of amphotericin stock solution (60 mg/mL in dimethylsulphoxide, *see above*) to 0.5 mL of pipet solution immediately prior to starting the experiment. This will be usable for a maximum of 2 h, after which its pore-forming ability is lost.
2. Dip the pipet tip into the pipet solution containing no amphotericin for approx 1 s. Backfill the pipet with amphotericin-containing solution and insert the pipet into the electrode holder. Pipets should have as low a resistance as possible. We use pipets with resistances of 1–2  $\text{M}\Omega$  for perforated patch experiments compared to 3–5  $\text{M}\Omega$  for whole-cell experiments.
3. Form a cell-attached patch (**Subheading 3.1.**). No positive pressure should be applied to the pipet when placing the pipet on the cell, as this will cause ejection

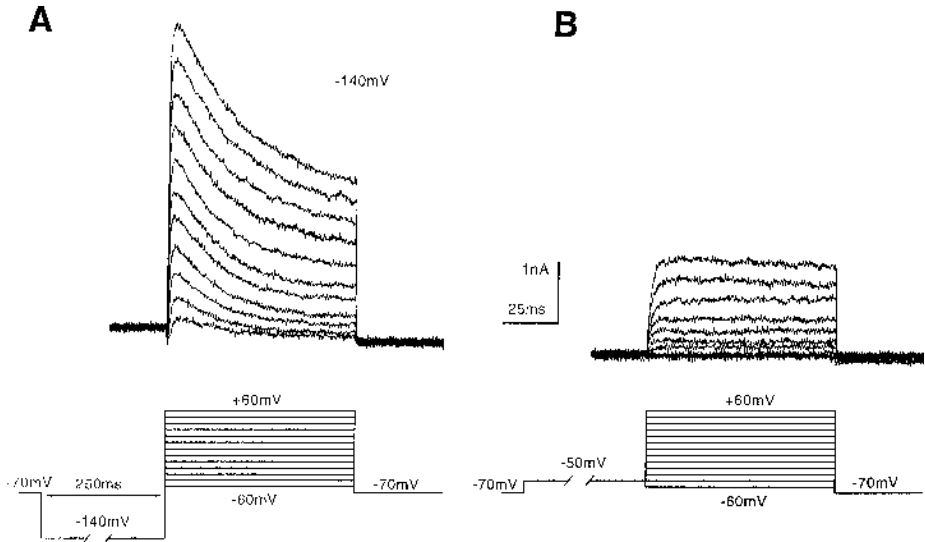


Fig. 3. Voltage protocols for recording of voltage-gated  $K^+$  channel currents. **(A)** To record both the A-type and delayed rectifier currents, cells are held at  $-70$  mV (bottom trace). A 250-ms prepulse to  $-140$  mV primes both current types for opening. The cell is the depolarized to a range of potentials to activate the currents (top traces). Increasing depolarization results in larger current amplitudes. Both inactivating and noninactivating components of the current are seen. **(B)** To activate the delayed rectifier alone, the prepulse voltage is set to  $-50$  mV (bottom trace). This results in inactivation of the A-type current and only the delayed rectifier is seen. All currents are shown after subtraction of leak and capacity transients by a P/5 leak subtraction protocol (*see Note 3*).

of amphotericin resulting in pore formation outside the patch. The time taken from filling the pipet with amphotericin-containing solution to forming the seal should be kept as short as possible for the same reason.

4. Set the required holding potential. Continue to apply 40-ms, 10-mV steps to monitor the progress of pore formation.
5. Complete perforation of the patch typically takes 5–10 min. The progress of pore formation will be seen as a gradual development of large-capacity transients with time. These have a small amplitude and slow decay at first, but by the end of the process the capacity transients should resemble those seen when using the ruptured patch method.
6. Once large, rapidly decaying transients have stabilized (**Fig. 3B**, middle trace), reduce the transients using the series-resistance and whole-cell capacitance compensation controls. Advance percent series-resistance compensation as far as possible without causing oscillation of the current trace.
7. Switch to the appropriate voltage protocol for recording whole-cell currents.

### 3.6. Whole-Cell Recording

#### 3.6.1. Voltage-Gated Ion Channels

##### 3.6.1.1. $K^+$ CHANNELS

A wide range of channels allowing passage of  $K^+$  ions through neuronal membranes exist, each with their own particular functional characteristics. This is reflected by the large number of genes encoding  $K^+$  channel subunits that have now been identified. The most commonly observed channels are those giving rise to the inactivating “A”-type current and the noninactivating delayed rectifier current (see **Fig. 3**). In addition, inward rectifier (so called because they only allow  $K^+$  to pass into the cell with relatively little efflux of  $K^+$  occurring through them)  $Ca^{2+}$ - and ATP-sensitive  $K^+$  channels have also been observed.

Solutions suitable for recording whole-cell  $K^+$  channel currents are given in **Table 1**. Cells are bathed in solution A and pipets filled with solution B.  $CdCl_2$  can also be included in solution A to block  $Ca^{2+}$  channel currents and hence any contribution from  $Ca^{2+}$ -sensitive  $K^+$  channels. To activate the  $K^+$  channels, cells are held at a potential of  $-70$  mV. A prepulse to  $-120$  mV followed immediately by depolarization to potentials ranging from  $-70$  to  $+70$  mV will result in the activation of an outward current that gets larger with increasing depolarization (**Fig. 3A**). In most central neurons this current contains both A-type and delayed rectifier currents. The two currents can be separated by setting a prepulse of potential  $-50$  mV instead of  $-120$  mV. This results in the inactivation of the A current so that only the delayed rectifier is seen during the depolarizing step (**Fig. 3B**).

Defining the  $K^+$  channel subtypes present pharmacologically can be difficult, as many compounds will block several  $K^+$  channel subtypes. Tetraethylammonium and 4-aminopyridine will both block delayed rectifier-, inward rectifier- and A-type currents, although in some cell types they can be selective for one over the other.  $Ca^{2+}$ - and ATP-sensitive  $K^+$  channels are more readily defined pharmacologically, as they can be blocked selectively by apamin (large conductance  $Ca^{2+}$  sensitive), charybdotoxin (small conductance  $Ca^{2+}$  sensitive), and glibenclamide and tolbutamide (ATP sensitive). In addition, ATP-sensitive  $K^+$  channels can be activated by  $K^+$  channel openers such as cromokalim and diazoxide.

##### 3.6.1.2. $Ca^{2+}$ CHANNELS

$Ca^{2+}$  channel currents have been defined functionally as T, L, N, P/Q, and R. These definitions are based on the electrophysiological characteristics and pharmacology of the channels. T-type channels are activated by small depolarizations (low-voltage activated, LVA) and are rapidly inactivating. L-, N-, P/Q-, and R-type channels require stronger depolarization for their activation than

**Table 1**  
**Solutions for Recording Whole-Cell K<sup>+</sup> Channel Currents**

Compound	Concentration (mM)	Comments
<b>Bath solution (A)</b>		
NaCl	120	—
KCl	1.3	—
CaCl <sub>2</sub>	2	—
MgCl <sub>2</sub>	1.2	—
Glucose	5	
Tetrodotoxin	0.001	(TTX) blocks Na channel
HEPES	10	—
pH 7.4	(NaOH)	—
Osmolarity	320 mosmol (sucrose)	—
<b>Pipet solution (B)</b>		
KCl	140	—
CaCl <sub>2</sub>	0.5	—
EGTA	5	—
HEPES	10	—
pH 7.2 (KOH)	—	—
Osmolarity	320 mosmol (sucrose)	—

T-type channels (high-voltage activating, HVA). Solutions suitable for recording Ca<sup>2+</sup> channel currents are given in **Table 2**. Ba<sup>2+</sup> is used as the charge carrying ion in solution C rather than Ca<sup>2+</sup> because it will pass more readily through some Ca<sup>2+</sup> channels than Ca<sup>2+</sup>, is less likely to cause Ca<sup>2+</sup>-dependent inactivation, and because it blocks K<sup>+</sup> channels. Further block of K<sup>+</sup> conductances is provided by using Cs<sup>+</sup> in the pipet solution (D) rather than K<sup>+</sup>. Ca<sup>2+</sup> channel currents can be activated by holding cells at a potential of -80 to -100 mV and depolarizing the cell for 100 ms every 10 s. More depolarized holding potentials (e.g., -40 mV), result in the steady-state inactivation of several channel types, most particularly the T-type current. If the cell is depolarized from a -40 mV holding potential, the current is mainly composed of L-type channel openings.

Pharmacological dissection of the contribution of the various Ca<sup>2+</sup> channel subtypes to the whole-cell current is possible using a variety of subtype selective compounds. L-type channels are sensitive to the dihydropyridines such as nifedipine and nimodipine. Channel block is largely complete at concentrations around 1 μM. At concentrations higher than 10 μM, other channel subtypes can be inhibited. N-type channels are selectively blocked by ω-conotoxin

**Table 2**  
**Solutions for Recording Whole-Cell Ca<sup>2+</sup> Channel Currents**

Compound	Concentration (mM)	Comments
<b>Bath solution (C)</b>		
Tetraethylammonium acetate	70	(TEA-Ac) blocks K channels
<i>N</i> -methyl-D-glucamine	70	(NMDG) impermeant
BaCl <sub>2</sub>	10	Charge carrier
Mg acetate	0.6	—
Glucose	5	—
KOH	3	—
HEPES	10	—
TTX	0.001	Blocks Na channels
pH	7.4 (acetic acid)	—
Osmolarity	320 mosmol (sucrose)	—
<b>Pipet solution (D)</b>		
MgCl <sub>2</sub>	2.5	—
CaCl <sub>2</sub>	1	—
K <sub>2</sub> ATP	3.3	—
EGTA	30	—
HEPES	100	Free acid
pH	7.2 (CsOH)	Cs blocks K channels
Osmolarity	320 mosmol (sucrose)	—

GVIA (1  $\mu$ M) and P-type channels by  $\omega$ -agatoxin IVA (100 nM).  $\omega$ -conotoxin MVIIC (1  $\mu$ M) has been used to define the Q-type component of whole-cell currents, although it is still not clear whether the P- and Q-type channels are distinct and separate entities.  $\omega$ -conotoxin MVIIC at this concentration will also block P- and N-type channels and should therefore only be used to measure the possible contribution of Q-type channels after block of N- and P-type components by  $\omega$ -conotoxin GVIA and  $\omega$ -agatoxin IVA respectively.

### 3.6.1.3. Na<sup>+</sup> CHANNELS

Na<sup>+</sup> channels show less diversity than K<sup>+</sup> channels; nevertheless several subtypes exist. Functionally Na<sup>+</sup> channels can be broadly divided into tetrodotoxin-sensitive and -insensitive subtypes based on the blocking ability of tetrodotoxin. Na<sup>+</sup> channels are rapidly activating and inactivating and can present problems for recording in terms of adequate spatial control of

**Table 3**  
**Solutions Recording of Whole-Cell Na<sup>+</sup> Channel Currents**

Compound	Concentration (mM)	Comments
<b>Bath solution (E)</b>		
NaCl	140	—
KCl	1.3	—
CdCl <sub>2</sub>	1	Blocks Ca channels
MgCl <sub>2</sub>	1.2	—
Glucose	5	—
TEA-Cl	30	Blocks K channels
HEPES	10	—
pH	7.4 (NaOH)	—
Osmolarity	320 mosmol (sucrose)	—
<b>Pipet solution (F)</b>		
CsCl	100	Blocks K channels
MgCl <sub>2</sub>	2.5	—
CaCl <sub>2</sub>	1 —	—
K <sub>2</sub> ATP	3.3	—
TEA-Cl	25 —	—
EGTA	5 —	—
HEPES	10 —	—
pH	7.2 (CsOH)	—
Osmolarity	320 mosmol (sucrose)	—

membrane potential (*see Note 4*). Several other blockers of Na<sup>+</sup> channels exist, many of them derived from venoms, including therapeutically important local anesthetics such as lignocaine. In terms of defining a membrane conductance as a Na<sup>+</sup> channel, however, tetrodotoxin is probably the most widely used, completely blocking Na<sup>+</sup> channel currents in central neurons at concentrations of around 100 nM.

Solutions suitable for the recording of Na<sup>+</sup> channels are given in **Table 3**. Because Na<sup>+</sup> channels have rapid kinetics and inactivate at relatively negative potentials, cells are held at more hyperpolarized potentials (−90 to −100 mV) and depolarizing steps are much shorter. Step depolarizations of 20–30 ms are sufficient in most cases for substantial inactivation of Na<sup>+</sup> currents in neurons. Thus a simple protocol for obtaining a Na<sup>+</sup> current I-V relationship would be to hold cells at −90 mV and repetitively depolarize the cell in 10 mV increments for 25 ms every 10 s.

### 3.6.2. Ligand-Gated Ion Channels

Because ligand-gated ion channels do not require voltage changes for activation to occur, complex voltage protocols are not always necessary. To obtain an I-V relationship, cells are held at a range of potentials and agonists are applied. The current obtained at each potential can be plotted against the holding potential to obtain the I-V relationship. Alternatively, a voltage ramp protocol can be used. With this protocol agonist is applied to activate the current and the voltage of the cell is then changed continuously between, for instance,  $-80$  mV and  $+80$  mV (see example in **Fig. 4**). The resultant current trace is plotted against the voltage to produce an I-V relationship. The voltage ramp protocol can only be used for currents that do not show rapid desensitization. Typical rates for the voltage change during the ramp are  $1-2$  mV/ms. Solutions G-L, suitable for recording the different whole-cell ligand gated ion channel currents are given in **Tables 4-6**.

Separation of glutamate receptor responses into their AMPA, kainate, and NMDA components requires the use of the eponymous agonists. Further certainty in the identification of these components can be confirmed by blocking unwanted components with appropriate antagonists such as 6-cyano-7-nitroquinoxaline (CNQX, AMPA, and kainate antagonist), MK-801, and 2-amino-5-phosphonovaleric acid (APV, NMDA receptor antagonists). Kainate responses can be further identified by the fact that following exposure to concanavalin A they change from rapidly desensitizing to nondesensitizing. GABA<sub>A</sub> receptor responses can be competitively inhibited by bicuculline and noncompetitively by picrotoxin.

### 3.6.3 A $\beta$ Channels

Channels formed by A $\beta$  are permeable to a wide range of ions. For measurement of possible conductance changes in neurons as a result of A $\beta$  channel insertion, currents can be measured using the solutions given in **Table 1**, which mimic the physiological ionic concentration (solutions A and B). To monitor changes in conductance as a result of A $\beta$  channel formation, the resting current can be monitored using a continuous data acquisition protocol. Repetitive steps to  $+10$  mV and  $-10$  mV from the holding potential every  $1-2$  s will allow an estimation of the resting conductance of the cell.

## 3.7. Single Channel Recording

### 3.7.1 Voltage-Gated Ion Channels

#### 3.7.1.1. K<sup>+</sup> CHANNELS

K<sup>+</sup> channel subtypes that show little or no inactivation do not require changes in membrane potential for their activation. In these cases, the patch can be held

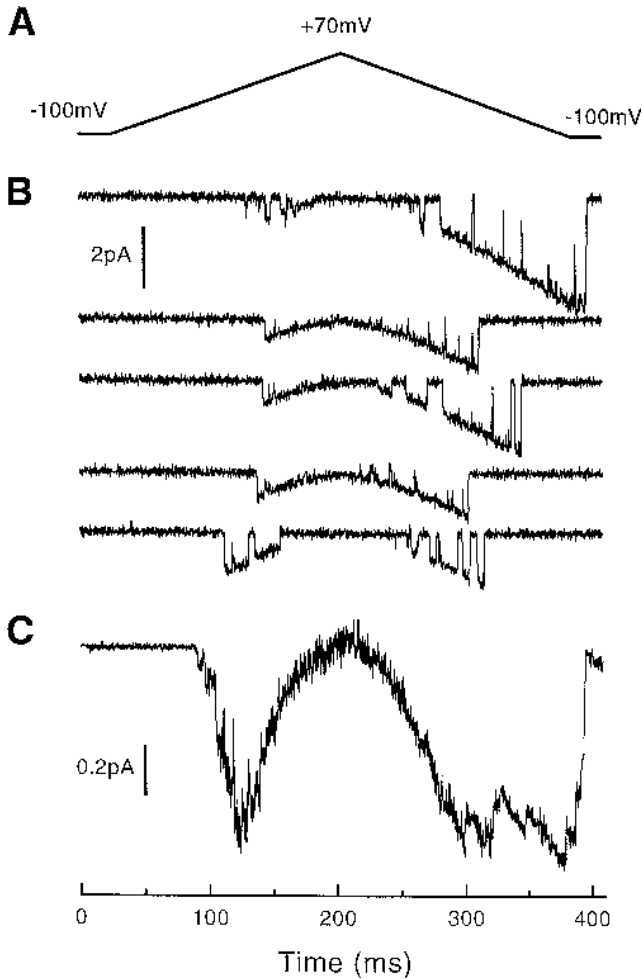


Fig. 4. Activation of L-type  $\text{Ca}^{2+}$  channel currents by voltage ramps. Currents can be activated by voltage ramps. In this example, a cell-attached patch is held at  $-100$  mV and the voltage is then changed at a rate of  $1$  mV/ms until it reaches  $+70$  mV (A). The potential across the patch is then returned to  $-100$  mV at the same rate, although in some cases it may be more appropriate to return the potential to  $-100$  mV by a step change. The depolarization results in the activation of an L-type  $\text{Ca}^{2+}$  channel in the patch as seen by the downward current deflections in the current trace (B). The current flowing through the channel decreases with depolarization as the reversal potential for  $\text{Ca}^{2+}$  is approached. From the traces in (B) an I-V relationship can be constructed (C) by averaging together the individual current traces. In the case of a whole-cell recording each trace will give an I-V relationship. (-)-BayK 8644 ( $1 \mu\text{M}$ ) was present in the bath solution during recording to prolong L-type  $\text{Ca}^{2+}$  channel openings.

**Table 4**  
**Solutions for Recording Whole-Cell Glutamate Receptor Currents**

Compound	Concentration (mM)	Comments
<b>Bath solution (G)</b>		
NaCl	140	—
KCl	2.8	—
CaCl <sub>2</sub>	1	Mg removed to reduce block of NMDA channels
Glucose	15	—
Glycine	0.005	—
HEPES	10	—
pH	7.4 (NaOH)	—
Osmolarity	320 mosmol (sucrose)	—
<b>Pipet solution (H)</b>		
CsF	110	Blocks K channels
CsCl	30	Blocks K channels
CaCl <sub>2</sub>	0.5	—
EGTA	5	—
HEPES	5	—
pH	7.2 (KOH)	—
Osmolarity	320 mosmol (sucrose)	—

at different potentials and currents are recorded in continuous mode. Those that do inactivate (e.g., A-type channels) can be opened by depolarizing the cells from a holding potential of  $-100$  mV every 5 s. Many channel subtypes show little or no run-down throughout a recording in which case the outside-out and inside-out recording variants can be used.

### 3.7.1.2. Ca<sup>2+</sup> CHANNELS

Most Ca<sup>2+</sup> channels undergo rapid run-down in cell-free conditions (i.e., inside-out and outside out recording) and therefore unitary currents are recorded using the cell attached technique (**Table 7**). To ensure that the voltage across the cell membrane is constant, it is usual to bathe cells in a high K<sup>+</sup>-containing medium that sets the membrane potential to approx 0 mV (solution M). All pipet voltages are therefore assumed to be relative to this potential. Cells are held at a potential of  $-80$  to  $-100$  mV and step depolarized to activate channels. Length of depolarization depends on the inactivation characteristics of the channels, slowly inactivating channels such as the L-type will show

**Table 5**  
**Solutions for Recording Whole-Cell Nicotinic Receptor Currents**

Compound	Concentration (mM)	Comments
<b>Bath solution (I)</b>		
NaCl	140	—
KCl	2.8	—
MgCl <sub>2</sub>	2	—
CaCl <sub>2</sub>	1	—
Glucose	10	—
HEPES	10	—
pH	7.4 (NaOH)	—
Osmolarity	320 mosmol (sucrose)	—
<b>Pipet solution (J)</b>		
CsCl	140	Blocks K channels
CaCl <sub>2</sub>	0.5	—
EGTA	5	—
HEPES	10	—
pH 7.2 (CsOH)		
Osmolarity	320 mosmol (sucrose)	—

activity at the end of 800 ms, whereas rapidly inactivating channels such as the T-type show few openings at the end of a 200-ms depolarization. I-V relationships can be obtained by recording channel activity at a range of depolarizing potentials or, alternatively, by applying ramp depolarizations (**Fig. 4**). Because many of the compounds that inhibit Ca<sup>2+</sup> channel activity are membrane impermeant, it is necessary to include them in the solution used to fill the patch pipet and compare records with those where the compound has been omitted. The exceptions to this are the dihydropyridines (e.g., nifedipine and the agonist (-)-BayK 8644), which are highly lipid soluble and can be applied to the bath.

### 3.7.1.3. Na<sup>+</sup> CHANNELS

Single Na<sup>+</sup> channel currents are usually recorded using the cell-attached configuration. A similar high K<sup>+</sup> solution to that used for unitary Ca<sup>2+</sup> channel currents zeroes the membrane potential (**Table 8**). Tetraethylammonium (TEA) and Ba are included in the patch pipet to block K<sup>+</sup> channel currents and Ca<sup>2+</sup> channel currents are blocked using Cd<sup>2+</sup> at low concentrations. Because of the inactivating nature of the Na<sup>+</sup> current, channel openings tend to cluster at the beginning of the voltage step. A similar voltage protocol to that used for whole-cell currents can therefore be used.

**Table 6**  
**Solutions for Recording Whole-Cell GABAA Receptor Currents**

Compound	Concentration (mM)	Comments
<b>Bath solution (K)</b>		
NaCl	140	—
KCl	2.5	—
CaCl <sub>2</sub>	1.5	—
MgCl <sub>2</sub>	1.2	—
Glucose	19	—
HEPES	10	—
pH	7.4 (NaOH)	—
Osmolarity	320 mosmol (sucrose)	—
<b>Pipet solution (L)</b>		
CsCl	140	Blocks K channels
CaCl <sub>2</sub>	0.5	—
MgCl <sub>2</sub>	2	—
EGTA	5	—
HEPES	10	—
pH	7.2 (CsOH)	—
Osmolarity	320 mosmol (sucrose)	—

#### 3.7.1.4. LIGAND-GATED ION CHANNELS

Most recordings of ligand-gated ion channels are carried out using outside-out patches to allow application of agonists to open the channels. In this case, solutions similar to those used in whole-cell experiments can be used. In some instances it may be necessary to carry out cell-attached experiments in which case low, nondensensitizing concentrations of agonist are included in the patch pipet. Ligand-gated ion channels can be recorded using continuous modes of data acquisition that overcome the need for leak subtraction during analysis (*see Note 3*).

#### 3.7.1.5. A $\beta$ CHANNELS

Channels formed in cell membranes by A $\beta$  have been recorded using the cell-free variants of the patch-clamp technique (inside-out and outside-out, **ref. 16**). The main concern in these experiments is to ensure that no native channels are active in the cell membrane. By using cell-free techniques Ca<sup>2+</sup> channel activity is prevented, whereas K<sup>+</sup> channel activity can be prevented by use of Cs as the main ion in both pipet (solution R) and bath solutions (solution Q,

**Table 7**  
**Solutions Used to Record Unitary Ca<sup>2+</sup> Channel Currents**

Compound	Concentration (mM)	Comments
<b>Bath solution (M)</b>		
K aspartate	140	zeroes membrane potential
MgCl <sub>2</sub>	1	—
EGTA	10	Prevents excessive Ca influx
HEPES	10	—
pH	7.2 (KOH)	—
Osmolarity	320 mosmol (sucrose)	—
<b>Pipet solution (N)</b>		
Ba-Ac	90	Charge carrier
TEA-Ac	30	Blocks K channels
TTX	0.001	Blocks Na channels
HEPES	10	—
pH	7.4 (BaOH)	—
Osmolarity	320 mosmol (sucrose)	—

see **Table 9**). Zn<sup>2+</sup> at a concentration of 250 μM reportedly blocks channels formed when Aβ is applied to patches (**16**).

#### 4. Notes

1. High-resistance seals: There are several common reasons for an inability to form high-resistance seals and some approaches that can sometimes aid good seal formation.
  - a. Vibration caused by resting elbows or arms on the air table. Once the pipet is close to the cell and the fine manipulators are in use, only gentle contact with the microscope-focusing knobs and micromanipulator controls should occur.
  - b. Too much suction. A very gradual increase in suction should be used until the resistance begins to go up. At this point the suction should be held at this level until no further increases in resistance are observed. Suction may then be increased slightly again. Often, releasing the suction pressure can cause an increase in seal formation. The suction pressure required for good seal formation can vary considerably between cell types and between different batches of cells. Ideal suction pressures therefore need to be determined empirically.
  - c. Pipet movement during suction. Pipets are clamped in their holders by means of a rubber gasket. If the pipet is not secured properly, suction and positive pressure can result in movement of the pipet tip. This can be checked by observing the pipet tip through the microscope while applying pressure. If the pipet tip moves, then the gasket should be replaced or tightened further.

**Table 8**  
**Solutions Used to Record Unitary Na<sup>+</sup> Channel Currents**

Compound	Concentration (mM)	Comments
<b>Bath solution (O)</b>		
K aspartate	140	Zeroes membrane potential
MgCl <sub>2</sub>	2	—
EGTA	10	Prevents excessive Ca influx
HEPES	10	—
pH	7.2 (KOH)	—
Osmolarity	320 mosmol (sucrose)	—
<b>Pipet solution (P)</b>		
NaCl	140	Charge carrier
TEA-Cl	20	Blocks K channels
BaCl <sub>2</sub>	2	Blocks K channels
CdCl <sub>2</sub>	0.5	Blocks Ca channels
HEPES	10	—
pH	7.4 (NaOH)	—
Osmolarity	320 mosmol (sucrose)	—

- d. The time taken from filling the pipet to touching the pipet tip onto the cell should be kept to a minimum. This is difficult at first, but familiarity with the movement of micromanipulators comes with practice and it should be possible to get this time down to approx 60 s.
- e. Cells have been kept too long in the recording bath. Some of the solutions used for recording currents, particularly those for recording whole-cell Ca<sup>2+</sup> channel currents, result in degeneration of cells, which prevents good seal formation. For cultured neurons we routinely use a new batch of cells every 60–90 min. Well-oxygenated slice preparations usually last longer.
- f. Seal formation can sometimes be aided by the application of holding potential to the pipet after the seal has started to form. Once the seal has a resistance of several hundred M $\Omega$ , gradually increase the holding potential. With negative holding potential, the current trace will move down the oscilloscope screen. As the seal resistance increases, the current trace will move back up the screen towards the zero current level.
- g. Keep the pipet holder clean. Silver, silver chloride, and glass fragments build up inside the pipet holder. These should be washed out with water daily and the holder thoroughly dried.
- h. No suction at the pipet tip. Check the integrity of pressure application by applying strong positive pressure to the pipet. By looking down the microscope it should be possible to observe that solution is being ejected.

**Table 9**  
**Solutions Used to Record Channel Activity Resulting**  
**from A $\beta$  Insertion into Membranes**

Compound	Concentration (mM)	Comments
<b>Bath solution (Q)</b>		
CsCl	140	Blocks K channels
CaCl <sub>2</sub>	0.5	—
MgCl <sub>2</sub>	0.5	—
EGTA	1	—
NaHEPES	5	—
pH	7.4 (CsOH)	—
Osmolarity	320 mosmol (sucrose)	—
<b>Pipet solution (R)</b>		
Cs Cl	140	Blocks K channels
CaCl <sub>2</sub>	0.5	—
MgCl <sub>2</sub>	0.5	—
EGTA	1	—
NaHEPES	5	—
pH	7.4 (CsOH)	—
Osmolarity	320 mosmol (sucrose)	—

- i. Vibration of wires, suction lines, perfusion lines, and micromanipulator control lines. All trailing wires within the Faraday cage should be firmly clipped or taped down to prevent their movement during the course of an experiment. Vibration in the pipet tip can also be minimized by keeping the distance between the pipet and the headstage connection to the manipulator to a minimum.
2. Noise and interference: A good signal-to-noise ratio is particularly important with single-channel recording, and electrical interference from the mains supply, lighting, and machinery can cause problems with whole-cell recording. To keep noise and interference to a minimum the following points can be important:
  - a. Keep solution levels in the recording chamber as low as possible to reduce noise levels.
  - b. Noise can be reduced by coating pipet tips in Sigmacote<sup>®</sup> or Sylgard<sup>®</sup> (Sigma).
  - c. Ground all equipment casings, the equipment rack and the Faraday cage and its contents.
  - d. All grounding should be to a common point; this is usually the oscilloscope earth socket. Equipment within the Faraday cage is usually grounded to a common point on the cage which is connected to the oscilloscope earth.

- e. For microscopes without an external DC stabilized power supply, power cables and the lamp housing should be covered in aluminium foil, which is then connected to the Faraday cage earthing point.
  - f. To test for noise sources in the recording setup it is usual to start with a minimum of equipment and gradually build in the connections. Begin with the headstage mounted on the microscope, amplifier, and oscilloscope with the pipet holder (no pipet) attached to the headstage. The Faraday cage should be connected to the oscilloscope earth, as should the rack and amplifier casing. Ground the air table to the Faraday cage earthing point. Check noise levels on the oscilloscope. Increasing the amplifier gain should enable the detection of even the lowest levels of interference. Ground components within the Faraday cage to reduce noise levels. Bear in mind that connection to one part of a piece of equipment (e.g., the micromanipulator) does not mean that the whole assembly is grounded. Several connections may be necessary. It should be possible to completely abolish the AC waveform (50–60 Hz) that occurs by grounding within the Faraday cage. Next, try switching on the microscope light source and ground cables and lamp housing if interference returns. Following this the DAC connections can be made from amplifier to oscilloscope, again checking for noise. Finally, connect the computer to the DAC and then switch on. The computer can be a major source of noise, as can the monitor. If grounding does not work, try wrapping aluminium foil around the computer casing and connecting to ground. Alternatively, try moving the position of the computer.
3. Leak subtraction: Because the cell membrane acts as an ohmic resistor, an artefact is introduced into the measurement of voltage-gated ion channels when cells are depolarized or hyperpolarized to activate currents. This is known as the “leak” current. To remove this artefact, together with any uncompensated capacity artefact from traces, it is common to perform what is known as a leak subtraction. The easiest way to do this is in the form of a P/5 subtraction protocol. Prior to the voltage step, which activates currents, five voltage steps one-fifth the size of the channel-activating voltage step are made. The currents from these steps are summed and subtracted from the current activated by the large depolarization. Most data-capture software has the ability to perform this automatically. Care must be taken to ensure that currents are not activated by the leak subtraction steps. If this is the case then leak steps can be made in the hyperpolarizing direction.
- For single-channel recordings, capacity and leak artefacts are removed by averaging together sections of data that contain no channel activity. This average is then subtracted from the raw data.
4. Space and voltage clamp: For whole-cell experiments it can be difficult to voltage clamp the more distal regions of cells effectively. Furthermore, there can be problems with the speed with which the membrane voltage can be changed and voltage drops across the pipet. These problems can be overcome in part by:
    - a. Choosing cells with fewer or smaller processes.
    - b. Using pipets with as low a resistance as possible.
    - c. Increasing the speed of voltage clamp by using the series resistance compensation controls.

Poor spatial control of voltage can often be seen in voltage-gated current recordings as a secondary notch on the current trace during the voltage step or as an overlong decay of current when the cell is returned to the holding potential.

## References

1. Yu, S. P., Yeh, C.-H., Sensi, S. L., Gwag, B. J., Canzoniero, L. M. T., Farhangrazi, Z. S., Ying, H. S., Tian, M., Dugan, L. L., and Choi, D. W. (1997) Mediation of neuronal apoptosis by enhancement of outward potassium current. *Science* **278**, 114–117.
2. Davidson, R. M., Shajenko, L., and Donta, T. S. (1994) Amyloid  $\beta$  peptide (A $\beta$ P) potentiates a nimodipine-sensitive L-type barium conductance in N1E-115 neuroblastoma cells. *Brain Res.* **643**, 324–327.
3. Price, S. A., Held, B., and Pearson, H. A. (1998) Amyloid  $\beta$  protein increases  $\text{Ca}^{2+}$  currents in rat cerebellar granule neurones. *Neuroreport* **9**, 539–545.
4. Ueda, K., Shinohara, S., Yagami, T., Asakura, K., and Kawasaki, K. (1997) Amyloid  $\beta$  protein potentiates  $\text{Ca}^{2+}$  influx through L-type voltage-sensitive  $\text{Ca}^{2+}$  channels: a possible involvement of free radicals. *J. Neurochem.* **68**, 265–271.
5. Etcheberrigaray, R., Ito, E., Kim, C. S., and Alkon, D. L. (1994) Soluble  $\beta$ -amyloid induction of Alzheimer's phenotype for human fibroblast  $\text{K}^+$  channels. *Science* **264**, 276–279.
6. Good, T. A., Smith, D. O., and Murphy, R. M. (1996)  $\beta$ -Amyloid peptide blocks the fast-inactivating  $\text{K}^+$  current in rat hippocampal neurones. *Biophys. J.* **70**, 296–304.
7. Wu, J., Anwyl, R., and Rowan, M. J. (1995)  $\beta$ -amyloid selectively augments NMDA receptor-mediated synaptic transmission in rat hippocampus. *Neuroreport* **6**, 2409–2413.
8. Cullen, W. K., Wu, J., Anwyl, R., and Rowan, M. J. (1996)  $\beta$ -Amyloid produces a delayed NMDA receptor-dependent reduction in synaptic transmission in rat hippocampus. *Neuroreport* **8**, 87–92.
9. Sawada, M. and Ichinose, M. (1996) Amyloid  $\beta$  proteins reduce the GABA-induced  $\text{Cl}^-$  current in identified Aplysia neurons. *Neurosci. Lett.* **213**, 213–215.
10. Aripse, N., Pollard, H. B., and Rojas, E. (1994)  $\beta$ -Amyloid  $\text{Ca}^{2+}$ -channel hypothesis for neuronal death in Alzheimer disease. *Mol. Cell. Biochem.* **140**, 119–125.
11. Furukawa, K., Abe, Y., and Akaike, N. (1994) Amyloid  $\beta$  protein-induced irreversible current in rat cortical neurones. *Neuroreport* **5**, 2016–2018.
12. Simmons, M. A. and Schneider, C. R. (1993) Amyloid  $\beta$ -peptides act directly on single neurons. *Neurosci. Lett.* **150**, 133–136.
13. Hamill, M., Marty, A., Neher, E., Sakmann, B., and Sigworth, F. J. (1981) Improved patch-clamp techniques for high-resolution current recording from cells and cell-free membrane patches. *Pflügers Archiv.* **391**, 85–100.
14. Carbone, E. and Lux, H. D. (1987) Kinetics and selectivity of a low-voltage-activated calcium current in chick and rat sensory neurones. *J. Physiol.* **386**, 547–570.
15. Fenwick, E. M., Marty, A., and Neher, E. (1982) A patch-clamp study of bovine chromaffin cells and of their sensitivity to acetylcholine. *J. Physiol.* **331**, 577–597.
16. Kawahara, M., Arispe, N., Kuroda, Y., and Rojas, E. (1997) Alzheimer's disease amyloid beta-protein forms  $\text{Zn}(2+)$ -sensitive, cation-selective channels across excised membrane patches from hypothalamic neurons. *Biophys. J.* **73**, 67–75.

## Analysis of $\beta$ -Amyloid Peptide Degradation In Vitro

Barbara Cordell and Asha Naidu

### 1. Introduction

The accumulation of insoluble A $\beta$  peptide aggregates in the brain is the diagnostic feature of Alzheimer's disease. Identical deposits are seen in the elderly who are at risk for this disease. The formation of the approx 4 kDa A $\beta$  peptide is implicated as a key component in the development of Alzheimer's disease pathology. Genetic evidence strongly supports this contention (1,2), as well as a number of demonstrated relevant biological activities of the A $\beta$  peptide such as its neurotoxicity (3) and proinflammatory properties (4). A great deal of attention has been focused on the processes involved in the generation of A $\beta$  peptide. In contrast, the fate of this peptide once it has been released from the cell is less well understood. Recently, this situation has been changing as studies on the clearance of A $\beta$  peptide are being published. The identification of A $\beta$ -degrading enzymes produced in the brain, their class, and selectivity, as well as their cellular origin, are important unresolved questions. One key issue of A $\beta$  peptide clearance is whether the brain may be limited in its capacity to degrade this protein, as all cells produce A $\beta$ , yet it is seen to accumulate only in brain tissue. Because alterations in A $\beta$  peptide clearance may potentially contribute to increased levels and to the development of insoluble A $\beta$  deposits in the brains of afflicted individuals, this chapter focuses on specific approaches to clarifying A $\beta$  peptide-clearance mechanisms.

The topic of A $\beta$  peptide degradation in vivo has obvious important implications in the context of Alzheimer's disease. It may be therapeutically feasible to offset basal and increased synthetic levels of A $\beta$  favoring plaque formation by enhancing conditions amenable to A $\beta$  degradation. This notion is supported by the observations suggesting that the A $\beta$  plaque is not a static but, rather, a dynamic structure. Contrary to expectations, plaques do not appear to continue

to grow in size and number as Alzheimer's disease progresses. Instead, both of these parameters have been shown to remain constant for many years over the duration of the disease (5,6). These data imply that deposits of A $\beta$  may be continuously resorbing and forming. Additional relevant *in vivo* evidence for the role of A $\beta$  clearance in a pathological setting is seen in transgenic mice genetically engineered to overexpress the A $\beta$  peptide. Such transgenic mice have been demonstrated to produce large quantities of A $\beta$  peptide compared to endogenous levels and, consequently, they develop numerous plaques of A $\beta$  peptide over their life span (7). When these transgenic mice were crossed to mice deleted for the apolipoprotein E protein, a protein proposed to be involved in physically assisting the formation of amyloid deposits, plaques were not observed (8). Furthermore, the A $\beta$  plaque level in the brains of mice from this cross was reduced by approx 60% as compared with the levels measured in the original plaque-forming mouse (8). This result suggests that clearance of increased levels of A $\beta$  can occur if the A $\beta$  peptide remains in a soluble state.

The turnover rate for A $\beta$  peptide in mouse brain has recently been measured and found to be between 1 and 2.5 h (9). This first report on the *in vivo* clearance of A $\beta$  used transgenic mice engineered to express the human form of A $\beta$  peptide and the turnover was exclusively determined for the recombinant protein. The turnover rate was measured by *in vivo* radiolabeling of the protein. Its synthesis and catabolism was followed over time using immunoprecipitation of A $\beta$  peptide from labeled brain extracts. In a very different *in vivo* experiment that was designed to examine clearance from a compartment in contrast to turnover, the A $\beta$  peptide was seen to be cleared very rapidly (10). Radiolabeled synthetic A $\beta$  peptide was infused directly into the lateral ventricle of the rat brain, after which the radiolabeled protein was followed into blood and cerebrospinal fluid. The clearance time for the bulk of the labeled protein was 6.5 min. Unfortunately, the turnover rate was not measured for the peptide once present in serum or cerebrospinal fluid. The very rapid removal of A $\beta$  peptide is qualified given that this peptide is frequently found complexed with other proteins, which would undoubtedly influence its clearance rate.

Identification of the enzyme(s) responsible for A $\beta$  peptide degradation and turnover has been pursued using several different approaches. A collection of diverse candidate enzymes have been identified that may reflect the diverse strategies employed to investigate this topic. One approach has been to use synthetic A $\beta$  peptide and to evaluate known and biologically relevant enzymes for the ability to degrade this protein. For example, matrix metalloproteinase 2 was tested, as this enzyme was previously shown to cleave the  $\beta$ -amyloid precursor protein within the A $\beta$  domain (11) and was found to hydrolyze synthetic A $\beta$  peptide (12). Peptide cleavage was determined using high-performance liquid chromatography (HPLC) and matrix-assisted laser

desorption ionization mass spectrometry. Similarly, synthetic A $\beta$  peptide was shown to be hydrolyzed by insulin-degrading enzyme (13). In another study, trypsin-activated  $\alpha$ 2-macroglobulin degraded synthetic A $\beta$  peptide (14). The rationale for this experiment was that  $\alpha$ 2-macroglobulin is synthesized by neurons of the brain and is associated with A $\beta$  plaques in Alzheimer's disease. In addition,  $\alpha$ 2-macroglobulin is an abundant secreted protein capable of binding serine proteinases that remain active toward small, but not large, proteins. A different report confirmed this observation using conditioned medium containing native A $\beta$  peptide secreted by cultured cells (15). Furthermore, the serine proteinase present in the conditioned medium, which formed a complex with  $\alpha$ 2-macroglobulin, was characterized by N-terminal amino acid analysis and was found to be previously unidentified. The fetal bovine serum (FBS) used to propagate the cells for these experiments was the source of the unknown serine proteinase. Yet a different study found that synthetic A $\beta$  peptide was degraded by an unidentified serine proteinase activity associated with rat and human brain microvessels (16). Whether this degradation was due to an  $\alpha$ 2-macroglobulin:enzyme complex is not known. Inhibitors selective for each enzymatic class were applied to determine that the degrading activity was from the serine proteinase family and reversed-phase HPLC was the method to assay A $\beta$  peptide cleavage.

Our laboratory pursued a somewhat different approach to study this subject. We employed an entirely native cell-based system to characterize A $\beta$  peptide degradation in vitro and to identify the types of enzymes mediating the turnover of this protein (17). Subsequently, others have successfully used an identical approach to characterize A $\beta$  peptide-degrading enzymes from a variety of cell types (18). This chapter describes the method we developed. Basically, native A $\beta$  peptide produced by culture cells is the substrate and the enzymes secreted by these same or different cells is the degrading activity. The A $\beta$  peptide clearance is measured by two different immunoassays, immunoprecipitation and sandwich-ELISA (see Note 1). Known inhibitors from commercial sources are tested in this system to characterize the class of proteinase(s) responsible for A $\beta$  peptide hydrolysis.

## 2. Materials

### 2.1. Immunoprecipitation

1. Wash buffers:
  - a. NET-NON: 50 mM Tris-HCl, pH 7.5, 500 mM NaCl, 5 mM EDTA, 0.5% Nonidet P-40.
  - b. NET-N: 50 mM Tris-HCl, pH 7.5, 150 mM NaCl, 5 mM EDTA, 0.5% Nonidet P-40.
  - c. 10 mM Tris-HCl, pH 7.5.

2. Radioimmunoprecipitation assay (RIPA) buffer: 10 mM Tris-HCl, pH 8.0, 150 mM NaCl, 1% deoxycholate, 0.1% sodium dodecyl sulfate (SDS), 1% Triton-X-100.
3. Protein-A-Sepharose (PAS) (available from Pharmacia, Kalamazoo, MI): 10% solution (weight to volume) in RIPA buffer.
4. <sup>35</sup>S-Methionine/cysteine (Trans<sup>35</sup>S-label) can be purchased from ICN Biomedicals, Costa Mesa, CA.

## 2.2. Polyacrylamide Gel Electrophoresis Buffers and Matrices

1. Buffer G: 3 M Tris-HCl, pH 8.45, 0.3% SDS.
2. 50% Glycerol.
3. Water.
4. Acrylamide: *Bis* (48:1.5) (48% acrylamide, 3% *Bis*) (Sigma Chemical, St. Louis, MO).
5. Tetramethylethylenediamine (TEMED) (Sigma).
6. 10% Ammonium persulfate.
7. Sample buffer (2×): 4% SDS, 125 mM Tris-HCl pH 6.8, 0.01% bromophenol blue, 20% glycerol, 10% mercaptoethanol.
8. Anode buffer (A): 0.2 M Tris-HCl, pH 8.9.
9. Cathode buffer (B): 0.1 M Tris-HCl, pH 8.25, 0.1 M Tricine, 0.1% SDS.
10. Fixing solution: Water:methanol:acetic acid (60:20:20).

## 2.3. ELISA

1. Buffers.
  - a. PBS/Tween: phosphate-buffered saline (PBS), 0.05% Tween-20.
  - b. PBS/bovine serum albumin (BSA)/Tween: PBS, 0.1% BSA, 0.05% Tween-20.
  - c. 1% BSA in PBS.
2. 96-Well flat bottom microtiter plate (Corning Glassworks, Corning, NY; Falcon, Los Angeles, CA, etc.).
3. Synthetic A $\beta$  peptide 1–40 (Bachem, Torrance, CA; QCB).
4. Horseradish peroxidase (HRP)-conjugated streptavidin (Sigma).
5. 3,3',5,5'-tetramethylbenzidine (TMB) substrate solution (Sigma, Pierce Chemical CO., Rockford, IL, etc.).
6. 0.5 N Sulfuric acid (Sigma, Pierce, etc.).

## 2.4. Sources of Inhibitors and Antibodies

*N*-*p*-tosyl-L-lysine chloromethyl ketone (TLCK) and *p*-amino benzamidine can be purchased from Sigma. Phenylmethylsulfonyl fluoride (PMSF) can be bought from Dade (Cambridge, MA) and aprotinin, leupeptin, antipain, pepstatin, E64, and phosphoramidon from Boehringer Mannheim (Mannheim, Germany).

For ELISA, any one of the two antibodies (monoclonal or polyclonal) raised to A $\beta$  peptide that recognize two separate binding epitopes of the molecule should be biotinylated. Antibodies to A $\beta$  peptide are available commercially (e.g., 4G8 and 6E10 from Senetek, Maryland Heights, MO). For immunopre-

**Table 1**  
**Proteinase Inhibitors and Concentrations for Use**

Inhibitor	Class	Concentration range to use
EDTA	Metallo	5–10 mM
Phosphoramidon	Metallo	1–20 $\mu$ M
Benzamidine	Serine	2.5 mM
Phenylmethylsulfonyl fluoride <sup>a</sup>	Serine	0.05–2 mM
Aprotinin	Serine	1.5–3 $\mu$ M
Antipain <sup>b</sup>	Serine	0.01–0.2 mM
TLCK <sup>c</sup>	Serine	0.01–0.2 mM
Pepstatin	Aspartyl	1–20 $\mu$ M
Leupeptin <sup>d</sup>	Thiol	0.01–0.2 mM
E64	Thiol	1–20 $\mu$ M

<sup>a</sup>Phenylmethylsulfonyl fluoride should be dissolved in propan-2-ol and stored at 4°C. Its half-life in aqueous solution is 1 h at pH 7.5.

<sup>b</sup>Antipain can also inhibit some thiol proteinases.

<sup>c</sup>TLCK should be dissolved in methanol and should be made fresh before each use.

<sup>d</sup>Leupeptin can also inhibit some trypsin-like serine proteinases.

precipitation, any antibody (monoclonal or polyclonal) that recognizes A $\beta$  peptide. Antibodies to A $\beta$  are commercially available from Senetek; Calbiochem, San Diego, CA; or Boehringer Mannheim.

### 3. Methods

The general experimental design to enable an assessment of A $\beta$  peptide turnover, to determine the class of enzyme(s) responsible for this degradation, and to compare degradative activities from different cell types, is as follows. For turnover studies, cultured cells are briefly radiolabeled with an amino acid, usually methionine, (referred to as a “pulse”) after which the cells are placed in medium lacking radioactivity (referred to as a “chase”). Radiolabeled A $\beta$  production and degradation is monitored over time, usually hours (*see Note 2*). Over time the labeled A $\beta$  peptide diminishes due to clearance by cell-associated or -secreted proteinases. Adding proteinase inhibitors from each of the known classes (**Table 1**) can be assessed, individually or in combination, for the ability to block the degradation of radiolabeled A $\beta$  peptide (*see Note 3*). Alternatively, unlabeled A $\beta$  peptide present in conditioned medium can be incubated with conditioned medium from the same cell source or from a different cell source, and the proteolysis of A $\beta$  peptide can be measured by ELISA. In this scenario, the peak period of production and secretion of A $\beta$  peptide needs to be predetermined and conditioned medium from this optimal time should be used. The conditioned medium containing potential degrading proteinases is generally conditioned for a longer period of time to permit accu-

mulation of secreted proteinases and to reduce the endogenous A $\beta$  peptide levels from the test sample (17). Similarly, known enzymes can be evaluated for A $\beta$  peptide-degrading activity by adding a physiologically relevant concentration of the enzyme to the A $\beta$  peptide-containing medium followed by incubation. Both the immunoprecipitation and ELISA methods for scoring A $\beta$  peptide in these experiments rely on the physical integrity of the approx 4 kDa peptide.

### 3.1. Assaying A $\beta$ Peptide by Immunoprecipitation

1. Culture cells in multiple 10 cm or 6 cm dishes at 70% confluence. Incubate overnight at 37°C.
2. Remove the medium from the cells and wash the cells three times with saline. Add 2.0 mL (for 10 cm dish) or 1.0 mL (for 6 cm dish) of serum-free medium or serum-free and methionine/cysteine-free medium containing 150  $\mu$ Ci/mL 35S-methionine/cysteine.
3. Incubate the cells for 8–16 h after which time harvest the medium and clarify of debris by low-speed centrifugation (2000g for 10 min).
4. PAS (10%, weight to volume) is prepared by swelling the resin in an appropriate volume of 10 mM Tris-HCl, pH 7.5, for 1 h with rocking. The resin is centrifuged at 2000g for 10 min and the supernatant is discarded. The pellet is taken up in an appropriate volume of RIPA buffer to give a 10% solution.
5. At the end of the incubation period (**step 3**), add the appropriate volume of anti-A $\beta$  antibody (optimal amount predetermined) and 100  $\mu$ L of PAS to the harvested medium and incubate at 4°C overnight with rocking.
6. Centrifuge the sample at 2000g for 5 min at room temperature to pellet the PAS. The supernatant is discarded to radioactive waste and the PAS pellet is taken up in 1 mL NET-NON wash buffer and transferred to Eppendorf tubes.
7. Wash the pellet as follows, centrifuging in an Eppendorf microfuge briefly between washes to pellet the PAS:
  - a. Three times with 1 mL NET-NON.
  - b. Three times with 1 mL NET-N.
  - c. Two times with 1 mL 10 mM Tris-HCl, pH 7.5.
8. After the washes are complete, the sample is centrifuged for 10 min at 2000g and the supernatant is removed as completely as possible.

### 3.2. Preparation and Electrophoresis of 16.5% Tris/Tricine Gels

1. The gel is prepared by pouring the separating gel first (10 cm high) followed by the spacer gel (2 cm high) and the stacking gel (3–4 cm high), allowing the gels to set between each step (*see Table 2* for gel composition).
2. To the pelleted PAS (**Subheading 3.1., step 8**) add 55  $\mu$ L of 2 $\times$  sample buffer. Vortex and boil for 5 min. Then pellet the PAS by centrifugation for 5 min at 2000g or a brief pulse in an Eppendorf centrifuge.
3. Load a 50- $\mu$ L aliquot of the supernatant onto the 16.5% Tris/tricine gel. Electrophorese overnight at 90 V.

**Table 2**  
**Ingredients to Prepare Polyacrylamide Gels**

Solutions	Separation gel (16.5%)	Spacer(10%)	Stack (5%)
Buffer G (3 $\times$ )	6.0 mL	2.0 mL	2.0 mL
50% Glycerol	4.5 mL	—	—
Water	1.5 mL	2.8 mL	3.4 mL
Acrylamide: <i>bis</i>	6.0 mL	1.2 mL	0.6 mL
10% Ammonium persulfate	75 $\mu$ L	25 $\mu$ L	50 $\mu$ L
TEMED	7.5 $\mu$ L	2.5 $\mu$ L	5.0 $\mu$ L

- The resulting gel is fixed in fixing solution for 30 min and dried onto filter paper.
- Visualize the dried gel by autoradiography or by phosphorimaging.

### 3.3. Assaying A $\beta$ Peptide by ELISA

- Culture cells in multiple 10 cm or 6 cm dishes at 70% confluence. Incubate overnight at 37°C.
- Remove the medium from the cells, wash cells three times with saline, and add serum-free medium.
- Incubate the cells for 8–16 h after which time harvest the medium and clarify of debris by centrifugation at 2000g for 10 min.
- Coat 96-well microtiter plates with 100  $\mu$ L of primary antibody (capture) in PBS overnight at 4°C. (See **Subheading 2.4.** regarding antibody. Also see **Note 4.**)
- Wash the wells four times with 200  $\mu$ L of PBS/Tween.
- Block the wells by incubating with 100  $\mu$ L of 1% BSA in PBS for 1 h at 37°C.
- Wash the wells three times with 200  $\mu$ L PBS/Tween.
- Add 100  $\mu$ L of synthetic A $\beta$  peptide standards (obtained from Bachem or QCB) or test samples (**step 3**) diluted in medium. Incubate overnight at 4°C (see **Note 5**).
- Wash the wells four times with 200  $\mu$ L PBS/Tween.
- Add 100  $\mu$ L of biotinylated secondary antibody (detector), e.g., goat antirabbit immunoglobulin G (IgG). Incubate for 2 h at 37°C (see **Note 6**).
- Wash the wells four times with 200  $\mu$ L PBS/Tween.
- Add 100  $\mu$ L of HRP-conjugated streptavidin. Incubate for 15 min at room temperature (see **Note 7**).
- Wash the wells four times with PBS/Tween.
- Add 100  $\mu$ L of TMB substrate and incubate at room temperature (see **Note 8**).
- Add 100  $\mu$ L of 0.5 N sulfuric acid to stop the reaction. The color will turn yellow.
- Measure the absorbance in the wells in a microtiter plate reader at 450 nm.

### 3.4. Determining the Kinetics of A $\beta$ Peptide Turnover

- Culture cells in multiple 10 cm or 6 cm dishes at 70% confluence. Incubate overnight at 37°C.

2. Remove the medium from the cells and wash three times with saline. Add 2.0 mL (for 10 cm dish) or 1.0 mL (for 6 cm dish) serum-free, methionine/cysteine-free medium containing approx 150  $\mu\text{Ci/mL}$   $^{35}\text{S}$ -methionine/cysteine.
3. Label the cells for 1 h at 37°C, then remove the radioactive medium, wash the cells with saline, and replace with serum-free growth medium lacking an isotope.
4. Continue to incubate the cells for varying lengths of time up to approx 24 h (one or two dishes per time point). Harvest the medium and clarify the cell debris by centrifugation at 2000g for 10 min. Store media samples at 4°C until all samples are harvested.
5. Assay media by immunoprecipitation (**Subheading 3.1.**) and polyacrylamide gel electrophoresis (**Subheading 3.2.**) to determine relative levels of A $\beta$  peptide at each time point (*see Note 9*).

### **3.5. Identifying the Class of A $\beta$ Peptide-Degrading Enzyme Using Inhibitors**

Either the immunoprecipitation (*see Subheading 3.1.*) or ELISA (*see Subheading 3.3.*) method can be applied to classifying the type of enzyme(s) responsible for the turnover of native A $\beta$  peptide observed in vitro with cultured cells. Briefly, conditioned medium is prepared with optimal levels of A $\beta$  peptide. In addition, extensively conditioned medium is prepared (>24 h) that contains proteolyzing activity. The media are mixed, incubated, then assayed for a change in A $\beta$  peptide level. Medium that has not been conditioned serves as a control. Repeating this experiment with the inclusion of selective proteinase inhibitors (**Table 1**), individually or in combination, should prevent the degradation of A $\beta$  peptide and identify the enzyme class mediating the turnover of the peptide.

### **4. Notes**

1. Variable amounts of A $\beta$  peptide are secreted from cultured cells and different cell types may have more or less A $\beta$ . If levels are very low for immunoprecipitation or ELISA, A $\beta$  peptide in the conditioned medium can be concentrated by Sepak 18 chromatography and batch elution with 50% CH<sub>3</sub>CN.
2. The kinetics of A $\beta$  peptide synthesis and turnover is likely to vary, therefore, a wide time range may need to be examined to capture both the synthesis and degradation phases of A $\beta$  peptide.
3. Because cultured mammalian cells secrete a large number of diverse proteinases, many of which could potentially hydrolyze A $\beta$ , a mix of proteinase inhibitors spanning all known classes should be tested initially. Selective and progressive elimination of inhibitor(s) from each class should enable a profile to be determined if there are multiple A $\beta$  peptide degrading enzymes produced by the cell type of interest.
4. The concentration of the antibody to use should be determined by the user by testing a wide range of dilutions. For purified monoclonal antibody, the concentration range is typically 1–4 mg/mL.

5. Concentration range to test is typically between 100–0.1 ng/mL. The concentration range could be higher or lower depending on the sensitivity of the antibody used.
6. The concentration of the antibody to use should be determined by the user by testing a wide range of dilutions.
7. The dilution to use should be determined by the user or follow vendor directions.
8. Incubation time will vary depending on the speed of color development (blue color, typically 3 min or longer).
9. Turnover measurements can also be made with nonradioactive medium and A $\beta$  peptide ELISA method using the same experimental format.

## References

1. Hendriks, L. and Van Broeckhoven, C. (1996) The  $\beta$ A4 amyloid precursor protein gene and Alzheimer's disease. *Eur. J. Biochem.* **237**, 6–15.
2. Hardy, J. (1997) The Alzheimer family of diseases: many etiologies, one pathogenesis? *Proc. Natl. Acad. Sci. USA* **94**, 2095–2097.
3. Yankner, B. A. (1996) Mechanisms of neuronal degeneration in Alzheimer's disease. *Neuron* **16**, 921–932.
4. Pachter, J. S. (1997) Inflammatory mechanisms in Alzheimer's disease: the role of  $\beta$ -amyloid/glial interactions. *Mol. Psychiatry* **2**, 91–95.
5. Hyman, B. T., Marzloff, K., and Arriagada, P. V. (1993) The lack of accumulation of senile plaques or amyloid burden in Alzheimer's disease suggests a dynamic balance between amyloid deposition and resolution. *J. Neuropathol. Exp. Neurol.* **52**, 594–600.
6. Cruz, L., Urbanc, B., Buldyrev, S. V., Christie, R., Gomez-Isla, T., Havlin, S., et al. (1997) Aggregation and disaggregation of senile plaques in Alzheimer's disease. *Proc. Natl. Acad. Sci. USA* **94**, 7612–7616.
7. Games, D., Adams, D., Alessandrini, R., Barbour, R., Berthelette, P., Blackwell, C., et al. (1995) Alzheimer's-type neuropathology in transgenic mice overexpressing V717F  $\beta$ -amyloid precursor protein. *Nature* **373**, 523–527.
8. Bales, K. R., Verina, T., Dodel, R. C., Du, Y., Alstiel, L., Bender, M. et al. (1997) Lack of apolipoprotein E dramatically reduces amyloid  $\beta$ -peptide deposition. *Nat. Genet.* **17**, 263–264.
9. Savage, M. J., Trusko, S. P., Howland, P. S., Pinsky, L. R., Mistretta, S., Reasume, A. G., et al. (1998) Turnover of amyloid  $\beta$ -protein in mouse brain and acute reduction of its level by phorbol ester. *J. Neurosci.* **18**, 743–1752.
10. Ghersu-Eghea, J. E., Gorevic, P. D., Ghiso, J., Frangione, B., Patlak, C. S., and Fenstermacher, J. D. (1996) Fate of cerebrospinal fluid-borne amyloid  $\beta$ -peptide: rapid clearance into blood and appreciable accumulation by cerebral arteries. *J. Neurochem.* **67**, 880–883.
11. Miyazaki, K., Hasegawa, M., Funhashi, K., and Umdea, M. (1993) A metalloproteinase inhibitor domain in Alzheimer amyloid protein precursor. *Nature* **362**, 839–841.
12. Roher, A. E., Kasunic, T. C., Woods, A. S., Cotter, R. J., Ball, M. J., and Fridman, R. (1994) Proteolysis of A $\beta$  peptide from Alzheimer's disease brain by gelatinase A. *Biochem. Biophys. Res. Commun.* **205**, 1755–1761.

13. Kurochkin, I. V. and Goto, S. (1994) Alzheimer's  $\beta$ -amyloid peptide specifically interacts with and is degraded by insulin degrading enzyme. *FEBS Lett.* **345**, 33–37.
14. Zhang, Z., Drzewiecki, G. J., May, P. C., Rydel, R. E., Paul, S. M., and Hyslop, P. A. (1996) Inhibition of  $\alpha$ 2-macroglobulin/proteinase-mediated degradation of amyloid  $\beta$ -peptide by apolipoprotein E and  $\alpha$ 1-antichymotrypsin. *Int. J. Exp. Clin. Invest.* **3**, 156–161.
15. Qiu, W. Q., Borth, W., Ye, Z., Haass, C., Teplow, D. R., and Selkoe, D. J. (1996) Degradation of amyloid  $\beta$ -protein by a serine protease- $\alpha$ 2-macroglobulin complex. *J. Biol. Chem.* **271**, 8443–8451.
16. McDermott, J. R. and Gibson, A. M. (1997) Degradation of Alzheimer's  $\beta$ -amyloid protein by serine protease activity in brain microvessels. *Neurosci. Res. Commun.* **20**, 93–102.
17. Naidu, A., Quon, D., and Cordell, B. (1995)  $\beta$ -Amyloid peptide produced in vitro is degraded by proteinases released by cultured cells. *J. Biol. Chem.* **270**, 1369–1374.
18. Qiu, W. Q., Ye, Z., Kholodenko, D., Seubert, P., and Selkoe, D. J. (1997) Degradation of amyloid  $\beta$ -protein by a metalloprotease secreted by microglia and other neural and non-neural cells. *J. Biol. Chem.* **272**, 6641–6646.

## Posttranslational Modifications of Amyloid Precursor Protein

### *Ectodomain Phosphorylation and Sulfation*

**Jochen Walter and Christian Haass**

#### **1. Introduction**

The amyloid precursor protein (APP) is a type I transmembrane protein with a large ectodomain, a single transmembrane domain and a small cytoplasmic tail (**1**). Translation of APP occurs at the endoplasmic reticulum (ER) and the protein is translocated into the ER lumen. The N-terminal domain of APP is directed towards the luminal compartment of the ER, whereas the C-terminal domain faces the cytoplasm. After synthesis, APP passes from the ER to the Golgi compartment. APP can then be transported in secretory vesicles to the cell surface, where the large ectodomain faces the extracellular milieu. Cell surface APP can be reinternalized into endosomes and lysosomes (for review *see refs. 2 and 3*). During its passage through the secretory pathway, APP is subjected to a variety of posttranslational modifications, including proteolytic processing, glycosylation, sulfation, and phosphorylation. Immediately on translocation into the ER, the signal peptide of APP is removed from the N-terminus by signal peptidase. APP is then modified cotranslationally by N-glycosylation on NH<sub>2</sub>-groups of asparagine residues. After passage into the Golgi compartment, the ectodomain of APP is subjected to O-glycosylation. In late Golgi compartments, e.g., the trans Golgi network, APP is subjected to sulfation on tyrosine residues within its ectodomain (**4**).

Proteolytic processing of APP is complex and involves at least three different proteases, which are called  $\alpha$ -,  $\beta$ -, and  $\gamma$ -secretases (for review *see [2,3,5]*). Cleavage by  $\alpha$ -secretase results in the liberation of the large soluble N-terminal ectodomain. The  $\alpha$ -secretase cleavage occurs within

From: *Methods in Molecular Medicine Biology, Vol. 32: Alzheimer's Disease: Methods and Protocols*  
Edited by: N. M. Hooper © Humana Press Inc., Totowa, NJ

the  $\beta$ -amyloid peptide ( $A\beta$ ) domain, thus precluding generation of  $A\beta$ . In contrast,  $\beta$ -secretase cleaves APP at the N-terminus of the  $A\beta$ -domain generating a potentially amyloidogenic C-terminal peptide. Subsequently,  $\gamma$ -secretase can generate  $A\beta$ . Interestingly, proteolytic processing of APP is regulated by protein phosphorylation (6,7). Activation of protein kinase A (PKA) or protein kinase C (PKC) result in an increased  $\alpha$ -secretase cleavage of APP, and therefore in increased secretion of soluble forms of APP into the extracellular environment of the cell. In turn, production of  $A\beta$  is reduced on activation of PKA and PKC (8,9). Similar effects were observed on activation of muscarinic acetylcholine receptors of type m1 and m3 (10), indicating that proteolytic processing can be regulated by extracellular stimuli. It has been demonstrated that PKC-regulated proteolytic processing of APP involves the MAP kinase signaling pathway (11). Interestingly, secreted forms of APP were shown to activate the MAP kinase pathway (12), which indicates a positive feedback regulation of  $\alpha$ -secretory processing of APP (11).

### **1.1. Ectodomain Phosphorylation of APP**

It was suggested that phosphorylation of APP itself alters proteolytic processing and it was shown that a synthetic peptide representing the C-terminal cytoplasmic sequence of APP can be phosphorylated by PKC in vitro (13). In addition, exogenous PKC was able to phosphorylate APP in permeabilized cells (14). However, in vivo phosphorylation of APP in the cytoplasmic domain was shown to be independent of PKC activities (15,16), and appears to be dependent on cell cycle phases (16,17). A mutated form of APP, in which potential phosphorylation sites in the cytoplasmic tail were substituted by alanine residues (S655A, S675A) still showed regulated  $\alpha$ -secretory proteolytic processing, which increases on activation of PKC (15). Therefore, phosphorylation of APP within the cytoplasmic domain does not seem to be necessary for PKA- and PKC-regulated cleavage. PKA and PKC might phosphorylate either  $\alpha$ -secretase directly or another protein component that is involved in the regulation of proteolytic processing or protein trafficking (18).

Beside phosphorylation within the cytoplasmic domain (16,17), APP was shown to be phosphorylated within its luminal N-terminal ectodomain (15,19). Ectodomain phosphorylation seems to be a common feature of members of the APP superfamily, as the APP-like proteins (APLP), which are highly homologous, are also phosphorylated within this domain (20) (see Chapter 18).

In initial studies using APP constructs in which large portions of the ectodomain were deleted, phosphorylation was first mapped to the N-terminal half of the ectodomain (15). By site directed mutagenesis it was then shown that APP is phosphorylated on serine residues 198 and 206. Substitution of the serine residues 198 and 206 by alanine residues significantly reduced ectodomain

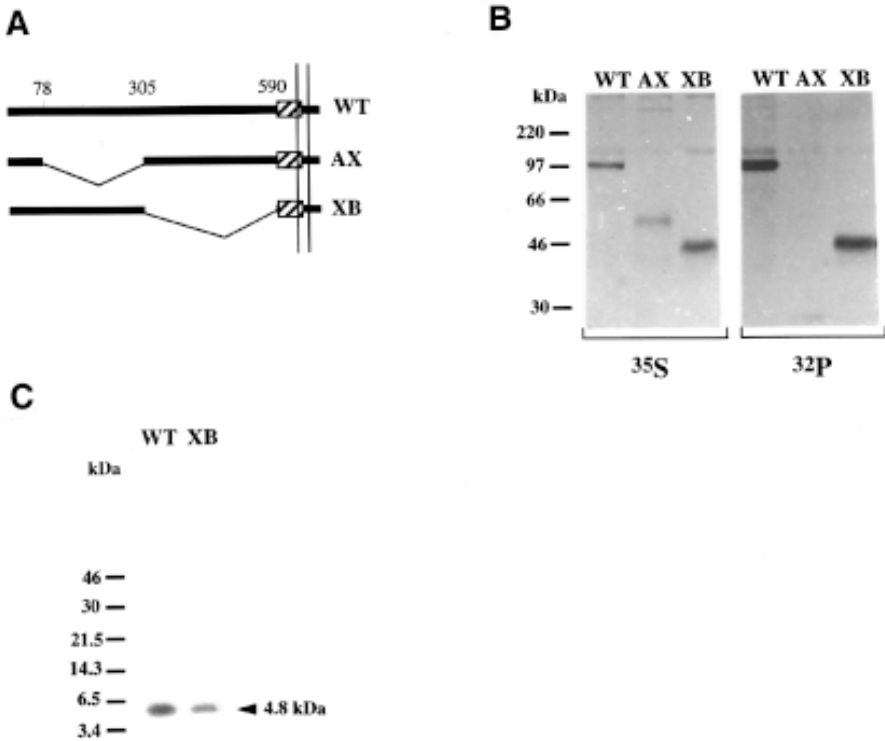


Fig. 1. Identification of phosphorylation sites the APP ectodomain. **(A)** Schematic of wild-type APP (WT) and the AX and XB constructs, missing large portions of the N-terminal and the C-terminal half of the APP ectodomain (15). The A $\beta$ -domain is represented by a striped bar, vertical lines represent cellular membranes. The numbers above denote amino acid residues with the restriction sites used to generate the constructs indicated (15). **(B)** Kidney 293 cells stably transfected with WT APP695, AX, or XB were labeled with [<sup>35</sup>S]-methionine (<sup>35</sup>S) and [<sup>32</sup>P]-orthophosphate (<sup>32</sup>P), respectively and conditioned media were immunoprecipitated with antibody 1736, recognizing APP<sub>5</sub> cleaved by  $\alpha$ -secretase (48). Radiolabeled proteins were visualized by autoradiography after separation by SDS-PAGE. **(C)** Phosphopeptide map of radiolabeled, secreted forms of wild-type (WT) APP or XB. After SDS-PAGE proteins were transferred to nitrocellulose membrane and digested with trypsin as described in **Subheading 3.4.**, the resulting tryptic peptides were separated on a 10–20% Tris/tricine gel and analyzed by autoradiography. The position of the phosphorylated 4.8 kDa peptide is marked by an arrowhead.

phosphorylation of APP to approx 20% and 80% , respectively (**Fig. 1; 20**). The corresponding double mutation (Ser 198/206 Ala) completely abolished phosphorylation (21), indicating that ectodomain phosphorylation of APP



**Table 1**  
**Characteristics of Ectoprotein Kinases**

Ecto-protein kinase type	Cosubstrates	Substrate-induced release	Sequence recognition motifs ( <i>see ref. 43</i> ) <sup>a</sup>	Inhibitors (IC <sub>50</sub> and/or K <sub>i</sub> values) (refs.)
PKA ( <b>24</b> )	ATP	No	K/R-X-S*/T*	H-89 (48.0 nM) ( <b>44</b> ) KT5720 (56.0 nM) ( <b>45</b> )
CK-1 ( <b>29</b> )	ATP	Yes	D/E-X-X-S*/T*	CK I-7 (9.5 mM) ( <b>46</b> )
CK-2 ( <b>25–29</b> )	ATP, GTP	Yes	S*/T*-X-X-D/E	DRB (6.0 mM) ( <b>47</b> ) Heparin (0.1 mg/mL) ( <b>28,35</b> )

<sup>a</sup>The amino acid sequences of protein kinase recognition motifs are given in the single letter code (X is any amino acid). Phosphorylatable serine (S) or threonine (T) residues are marked by (\*).

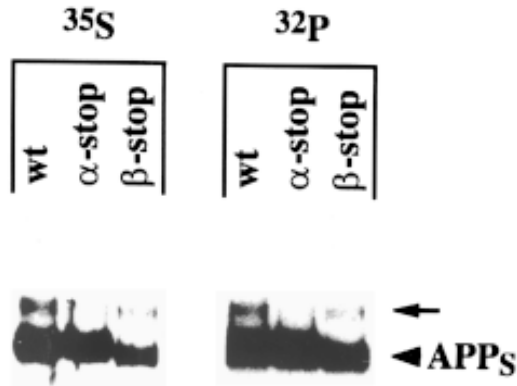


Fig. 2. Phosphorylation of truncated, soluble forms of APP. Stop codons were introduced into the wildtype APP cDNA corresponding to the cleavage sites of  $\alpha$ -secretase ( $\alpha$ -stop), and  $\beta$ -secretase ( $\beta$ -stop), respectively. Kidney 293 cells stably expressing these constructs were metabolically labeled with [ $^{35}\text{S}$ ]-methionine (**left panel**) or [ $^{32}\text{P}$ ]-orthophosphate (**right panel**) and precipitated from conditioned media with antibody B5, which was raised against amino acids 444–595 in the ectodomain of APP (49). The arrowhead marked with APP<sub>S</sub> indicates APP<sub>S</sub> derived from the transfected cDNA constructs. The unmarked arrow indicates APP<sub>S</sub> from endogenous APP<sub>751</sub>. Differences in the amounts of APP<sub>S</sub> in these cell lines are due to different expression levels of APP.

### 1.2. Cellular Sites of APP Ectodomain Phosphorylation

For APP two different subcellular locations were identified where ectodomain phosphorylation can occur. First, APP can be phosphorylated by protein kinase(s), which act in the lumen of post-Golgi secretory compartments. This has been demonstrated by *in vivo* phosphorylation experiments in which forward protein transport was inhibited either with Brefeldin A or by incubation of cells at 20°C (20). Brefeldin A inhibits forward protein transport in the *cis* Golgi compartment (22), whereas 20°C treatment leads to accumulation of secretory proteins in the *trans* Golgi network (23). Both Brefeldin A and 20°C treatment of cells completely inhibit phosphorylation of APP, indicating that ectodomain phosphorylation occurs later during the secretory pathway, most likely within post-Golgi secretory vesicles (20).

In addition to phosphorylation within the secretory pathway, APP can also be phosphorylated at the cell surface by ectoprotein kinases. It was demonstrated that incubation of intact monolayer cell cultures with [ $\gamma$ - $^{32}\text{P}$ ]ATP leads to phosphorylation of APP within its ectodomain (Fig. 3A; 20). Similar to the luminal protein kinase, the cell surface-located protein kinase also phosphorylates soluble APP, which is not inserted into the plasma membrane (Fig. 3B). Thus, secreted forms of APP derived from proteolytic processing

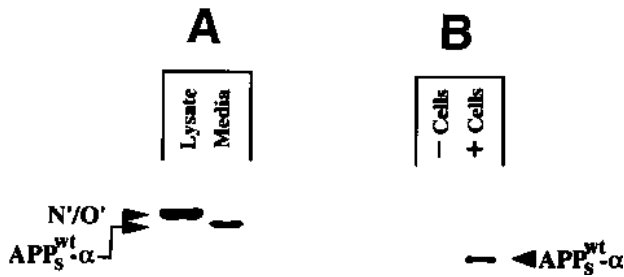


Fig. 3. Cell surface phosphorylation of APP by ecto-protein kinase activity. **(A)** Cell surface proteins of kidney 293 cells stably transfected with APP cDNA were phosphorylated in presence of 1  $\mu$ M [ $\gamma^{32}$ -P]ATP for 20 min at 37°C. Full-length mature APP (arrow marked with N/O) was immunoprecipitated from cell lysates with antibody C7 (lysate), which recognizes the cytoplasmic tail of APP (50). Secreted APP<sub>S</sub> was precipitated from cell supernatants (Media) with antibody 1736, which specifically recognizes APP<sub>S</sub> generated by  $\alpha$ -secretase cleavage. **(B)** Phosphorylation of soluble APP<sub>S</sub> by ectoprotein kinase on the surface of kidney 293 cells. APP<sub>S</sub> was collected for 1 h from supernatants of kidney 293 cells stably transfected with a cDNA construct containing a stop codon corresponding to the  $\alpha$ -secretase site. The supernatant was taken off and split into two halves. One-half was incubated with untransfected kidney 293 cells (+ cells) and the other half in a Petrie dish without cells (- cells) for 15 min at 37°C in the presence of 1  $\mu$ M [ $\gamma^{32}$ -P]ATP. APP<sub>S</sub> was immunoprecipitated with antibody 1736 and separated by SDS-PAGE. Note that both cell surface bound and soluble APP (APP<sub>S</sub>) can be phosphorylated by ectoprotein kinase activity.

by  $\alpha$ -secretase or  $\beta$ -secretase can be substrates of cell surface located protein kinase(s).

Different types of ectoprotein kinases have been characterized (Table 1). A cAMP-dependent protein kinase activity was identified to be located at the extracellular face of the plasma membrane. This protein kinase is activated by cAMP and phosphorylates kemptide, a specific peptide substrate of PKA (24). In addition, two different cell surface-located CK like protein kinases have been identified (25–27). One ecto-CK shares characteristics of CK-1, the other is homologous to CK-2 (28,29). Interestingly, both CK-type ectoprotein kinases can be released from the cell surface on interaction with specific protein substrates (Table 1; 25,26,29). Evidence for PKC like (30) and tyrosine kinase activities (31) located at the cell surface has also been published. Ectoprotein kinases use extracellular ATP as a cosubstrate, which is present in micromolar levels in extracellular fluids (32,33). It has been shown that the local extracellular ATP concentration increases up to the millimolar range on activation of platelets (34). The availability of the cosubstrate ATP might represent a regulatory principle for extracellular phosphorylation reactions.

In order to characterize ectoprotein kinases that phosphorylate APP at the cell surface, the cosubstrate usage for APP phosphorylation was analyzed. CK-1 and CK-2 can be distinguished by their usage of ATP and GTP as cosubstrates. CK-1 is dependent on ATP, whereas CK-2 uses ATP and GTP to an approximately similar extent (**Table 1; 35**). In fact, CK-2 is the only kinase that uses GTP as a cosubstrate efficiently. Because cell surface-located APP is phosphorylated on cell incubation with [ $\gamma$ - $^{32}$ P]GTP (**21**), it is evident that an ectoprotein kinase of the CK-2 type is involved in APP phosphorylation. This is supported by the fact that heparin, a potent inhibitor of CK-2, decreases the ectodomain phosphorylation of APP. In addition, both authentic CKs can phosphorylate APP *in vitro* (**21**). Taken together, these data indicate that APP is phosphorylated within the ectodomain by CK-type protein kinase(s) *in vivo*. The functional role of ectodomain phosphorylation of APP is not known. Notably, A $\beta$  has been demonstrated to activate both CK-1 and CK-2 *in vitro* (**36**). Because CK-type protein kinases were identified to phosphorylate APP it is therefore possible that A $\beta$  influences the ectodomain phosphorylation of its precursor at the cell surface. It has been shown that ecto-phosphorylation of special cell surface proteins is implicated in physiological processes, like homeostasis, synaptogenesis, myogenesis and long-term potentiation. It would now be interesting to investigate the biological role of APP ectodomain phosphorylation.

### **1.3. Sulfation of APP**

Many secretory and cell surface proteins, like blood coagulation factors, immunoglobulins, and extracellular matrix proteins undergo sulfation on tyrosine residues (for review *see refs. 37 and 38*). This posttranslational modification occurs in late Golgi compartments, e.g., the trans Golgi network and is catalysed by tyrosylprotein sulfotransferase. This protein appears to have broad substrate specificity enabling the enzyme to sulfate many different protein substrates. Tyrosine sulfation of proteins occurs exclusively within the luminal domains of secretory and cell surface proteins (**37,38**). APP had been also shown to be sulfated on tyrosine residues (**4**). However, the respective tyrosine residue(s) that are modified by sulfation remain to be determined. There are two tyrosine residues, Tyr 217 and Tyr 262, that are localized within a putative recognition motif for tyrosylprotein sulfotransferase (**4,37**). This enzyme appears to be dependent on acidic residues at the N-terminal side of the respective tyrosine residue (**37,38**). Tyrosine sulfation was demonstrated to affect protein transport and proteolytic processing of secretory proteins, and to modulate protein-protein interaction (for review *see refs. 37 and 38*). However, the role of tyrosine sulfation of APP remains to be determined. In this chapter we describe methods used to study phosphorylation and sulfation of APP.

## 2. Materials

### 2.1. *In Vivo* Phosphorylation of Intracellular APP

1.  $\beta$ -Radiation safety equipment (plastic boxes to incubate cell culture Petri dishes, benchtop plastic protection shields).
2. Dulbecco's minimal essential medium without sodium phosphate (Gibco Lifesciences).
3. [ $^{32}\text{P}$ ]-Orthophosphate in aqueous solution (carrier free: 10 mCi/mL [Amersham, Amersham, UK]).
4. Specific antibodies for immunoprecipitation (*see Figs. 1–3*).
5. Buffer A: 50 mM Tris-HCl, pH 7.6, 150 mM NaCl, 2 mM EDTA, 0.2% (w/v) NP-40, 1 mM phenylmethylsulfonyl fluoride (PMSF), 5 mg/mL leupeptin.
6. Protein A Sepharose (Sigma Chemical Co., St. Louis, MO): 100 mg/mL in buffer A.

### 2.2. *In Vivo* Phosphorylation of Cell Surface Located APP by Ectoprotein Kinases

1.  $\beta$ -Radiation safety equipment (*see Subheading 2.1.*).
2. Buffer B: 30 mM Tris-HCl, pH 7.3, 70 mM NaCl, 5 mM magnesium acetate, 83 mM D(+) glucose, 0.5 mM EDTA, 5 mM  $\text{KH}_2\text{PO}_4/\text{K}_2\text{HPO}_4$ , 290  $\pm$  10 milliosmolar (*see Note 1*).
3. [ $\gamma$ - $^{32}\text{P}$ ]ATP or [ $\gamma$ - $^{32}\text{P}$ ]GTP (spec. act. 3000 Ci/mmol [Amersham]); dilute with unlabeled ATP or GTP to a final concentration of 100  $\mu\text{M}$  ATP.
4. Specific antibodies for immunoprecipitation (*see Figs. 1–3*).
5. Buffer A: 50 mM Tris-HCl, pH 7.6, 150 mM NaCl, 2 mM EDTA, 0.2% (w/v) NP-40, 1 mM PMSF, 5  $\mu\text{g}/\text{mL}$  leupeptin.
6. Protein A Sepharose (Sigma): 100 mg/mL in buffer A.

### 2.3. Phosphoamino Acid Analysis (One Dimensional)

1. 20  $\times$  20 cm thin-layer chromatography (TLC) cellulose plates (Merck, Rahway, NJ; *see Note 2*).
2. High-voltage electrophoresis apparatus (we use the multiphor II system from Pharmacia, Piscataway, NJ).
3. pH 2.5 Electrophoresis buffer: 5.9% (v/v) glacial acetic acid, 0.8% (v/v) formic acid, 0.3% (v/v) pyridine, 0.3 mM EDTA.
4. 6 M HCl.
5. Incubation oven.
6. Speed Vac concentrator (Savant Bioblock Scientific, Illkirch, France).
7. Phosphoamino acid standards (P-Ser, P-Thr, P-Tyr, 1  $\mu\text{g}/\mu\text{L}$  in pH 2.5 electrophoresis buffer).
8. Ninhydrin solution: 0.25% (w/v) in acetone.
9. Whatman 3MM filter paper (Whatman, Clifton, NJ).

### 2.4. Phosphopeptide Mapping with Trypsin (One Dimensional)

In addition to the material needed for *in vivo* phosphorylation (*see Subheading 2.1.*), the following material is required:

1. Digestion buffer: 50 mM  $\text{NH}_4\text{HCO}_3$ , pH 8.0, 10% (v/v) acetonitrile.
2. Polyvinylpyrrolidone (PVP-40) 0.5% (w/v) in 100 mM acetic acid.
3. Trypsin solution, sequencing grade (1  $\mu\text{g}/\mu\text{L}$  (Boehringer)).
4. Speed Vac concentrator (Savant Bioblock).

### **2.5. In Vivo Sulfation (see Note 3)**

1.  $\beta$ -Radiation safety equipment (*see Subheading 2.1.*).
2. Sulfate free minimal essential medium (Gibco Lifesciences).
3. [ $^{35}\text{S}$ ]-Sulfate in aqueous solution (carrier free, 10 mCi/mL [Amersham]).
4. Specific antibodies for immunoprecipitation (*see Figs. 1–3*).
5. Buffer A: 50 mM Tris-HCl, pH 7.6, 150 mM NaCl, 2 mM EDTA, 0.2% (w/v) NP-40, 1 mM PMSF, 5  $\mu\text{g}/\text{mL}$  leupeptin.
6. Protein A Sepharose (Sigma): 100 mg/mL in buffer A.
7. 1 M Sodium salicylate.

### **2.6. Detection of Tyrosine Sulfate in APP (One-Dimensional)**

1. Digestion buffer: 50 mM  $\text{NH}_4\text{HCO}_3$ , pH 8.0.
2. Pronase, mixture of endo- and exoproteases (Boehringer Mannheim) 1  $\mu\text{g}/\mu\text{L}$  in digestion buffer.
3. Polyvinylpyrrolidone (PVP-40) 0.5% (w/v) in 100 mM acetic acid.
4. 20  $\times$  20 cm TLC cellulose plates (Merck, *see Note 2*).
5. High-voltage electrophoresis apparatus (we use the multiphor II system from Pharmacia).
6. pH 3.5 Electrophoresis buffer: 5% (v/v) acetic acid, 0.5% (v/v) pyridine.
7. Unlabeled tyrosine sulfate as marker: 1  $\mu\text{g}/\mu\text{L}$  in pH 3.5 electrophoresis buffer.
8. Acetone.

## **3. Methods**

### **3.1. In Vivo Phosphorylation of Intracellular APP**

1. Wash the cell cultures once with prewarmed (37°C) phosphate-free medium and incubate with phosphate-free medium for 45 min.
2. Aspirate the medium and add fresh phosphate-free medium together with an appropriate amount of [ $^{32}\text{P}$ ]-orthophosphate (approx 0.5 mCi/mL medium). Incubate the cell cultures at 37°C (5%  $\text{CO}_2$ ) for 2–5 h (*see Notes 4 and 5*).
3. When phosphorylation of secreted APP is to be analyzed, transfer the conditioned medium after incubation to microcentrifuge tubes (screw capped), and keep on ice. Proceed to **step 5**.
4. For analysis of membrane-bound APP, wash the remaining cells once with PBS and lyse in buffer A containing 1% NP-40 for 10 min on ice. Cell lysis can be carried out within the cell culture dish. Transfer the cell lysates into microcentrifuge tubes.
5. Both the conditioned media (*see step 3*) and cell lysates (*see step 4*) are clarified by centrifugation at 14,000g for 10 min in a microcentrifuge. Transfer the supernatants after centrifugation of conditioned media and/or cell lysates, respectively,

to new microcentrifuge tubes and incubate for 2–16 h, together with appropriate antisera and 25  $\mu$ L of the protein A Sepharose slurry at 4°C with constant shaking (see **Notes 6** and **7**).

7. Collect immunoprecipitates by centrifugation at 2000g for 5 min and wash the precipitates by three subsequent washes (for 20 min each) with buffer A containing 500 mM NaCl, buffer 2 $\times$  A containing 0.1% SDS and finally with buffer A alone. Collect immunoprecipitates by centrifugation (5 min at 2000g), add 15  $\mu$ L of SDS sample buffer to the pellets and heat the samples for 5 min at 100°C.
8. Eluted proteins are separated by sodium dodecyl sulfate-polyacrylamide gel electrophoresis (SDS-PAGE). For subsequent phosphoamino acid analysis the proteins should be transferred to polyvinylidene fluoride (PVDF) membrane after SDS-PAGE. Otherwise, the gels can be fixed and dried. Radiolabeled proteins can be visualised on both dried gels or dried PVDF membranes by autoradiography or by phosphor imaging (see **Note 8**).

### **3.2. In Vivo Phosphorylation of Cell Surface Located APP by Ectoprotein Kinases (see Notes 9 and 10)**

1. Wash the cell monolayer culture twice with buffer B prewarmed to 37°C.
2. Incubate the cells for 5 min at 37°C (5% CO<sub>2</sub>) in buffer B and start the phosphorylation reaction by adding [ $\gamma$ -<sup>32</sup>P]ATP or [ $\gamma$ -<sup>32</sup>P]GTP (to a final concentration of 1  $\mu$ M) and incubate for 15–30 min at 37°C (see **Notes 9–14**).
3. For analysis of cell surface phosphorylated APP, which was secreted into the medium during the phosphorylation reaction (by  $\alpha$ -secretase cleavage), transfer the supernatant to microcentrifuge tubes (screw capped, see **Note 7**), add unlabeled ATP to a final concentration of 1 mM, and keep on ice. To analyze cell-surface-bound phosphorylated APP, wash the remaining cell monolayer culture three times with ice cold buffer B containing 1 mM unlabeled ATP.
4. Lyse the cells as described in **Subheading 3.1., step 4**, and process both the cell supernatants and the cell lysates as described in **Subheading 3.1., steps 5–8**.

### **3.3. Phosphoamino Acid Analysis (One-Dimensional)**

1. Localize the radiolabeled protein by autoradiography (see **Subheading 3.1.**). Mark the PVDF membrane with radioactive ink and expose to X-ray film (see **Notes 15** and **16**). After exposure, align the membrane with the autoradiogram and mark the position of the radiolabeled protein by sticking a needle through the autoradiogram and the membrane on both ends of the radiolabeled band. Cut out the piece of membrane containing the phosphorylated protein and cut it into smaller pieces (approx 2  $\times$  2 mm). The correct excision of the band can be controlled by subsequent exposure of the membrane to X-ray film.
2. Transfer the small membrane pieces to a microcentrifuge tube (screw capped), rewet the membrane with isopropanol, and wash three times with 1 mL H<sub>2</sub>O and once with 6 M HCl. Add 50–100 mL of 6 M HCl to fully cover the membrane pieces, seal the tube (screw capped), and incubate for 60 min at 110°C in an oven (acidic hydrolysis).

3. After acidic hydrolysis briefly vortex, centrifuge for 5 min at 14,000g, and transfer the supernatant to a new tube. Evaporate the HCl in a Speed Vac (Savant Bioblock) (equipped with a NaOH trap to collect acid) and resuspend the remaining pellet in 10  $\mu$ L of pH 2.5 electrophoresis buffer.
4. Centrifuge at 14,000g for 5 min and spot the supernatant onto TLC cellulose plates (*see Note 2*). Spots should be applied in aliquots of 1  $\mu$ L and be immediately dried with a cold air blower to keep the spots as small as possible. The spots should be applied at a distance of 3 cm from the cathodic edge of the TLC cellulose plate (*see Fig. 4*). In addition, apply a mixture of P-Ser, P-Thr, and P-Tyr (1  $\mu$ g of each) on the spot of the radiolabeled phosphoamino acid sample. On one 20  $\times$  20 cm TLC cellulose plate 8–10 samples can be applied (*see Fig. 4; see Note 16*).
5. Wet the TLC cellulose plate with pH 2.5 electrophoresis buffer either by spraying or by using a “mask” of Whatman 3MM filter paper prewetted in pH 2.5 electrophoresis buffer. The usage of a filter paper mask is recommended when the spots are large and need to be concentrated by concentric diffusion. To prepare a mask, Whatman 3MM filter paper is cut to the size of the TLC cellulose plate (20  $\times$  20 cm) and holes (approx 1.5–2.0 cm diameter) are cut with a cork borer at positions corresponding to the sample spots. The prewetted mask, drained to remove excess buffer, is carefully placed on the TLC plate and the buffer is pressed with gloved hands around the edges of the holes. The liquid should converge in the center of the circle. Remove the filter paper from the TLC plate. Before applying the plate to the electrophoresis apparatus, drain excess buffer from the plate carefully with filter paper. There should be no “lakes” of buffer on the plate and it should look dull gray.
6. Fill both buffer tanks of the high voltage electrophoresis apparatus with pH 2.5 electrophoresis buffer and place the TLC cellulose plate in the correct orientation (the edge with the sample spots at the cathode). The platform for holding the TLC plates should be precooled to 4–7°C before applying the plate. Connect the buffer tanks with the TLC plate by three prewetted (pH 2.5 electrophoresis buffer) layers of Whatman 3MM filter paper and electrophorese at 20 mA for 45 min.
7. After electrophoresis, air dry the TLC cellulose plate and visualize the unlabeled standard phosphoamino acids by staining with ninhydrin. For this purpose, spray the TLC cellulose plate with 0.25% (w/v) ninhydrin in acetone and place the plate into an oven. Incubate at 100°C for a few minutes until the phosphoamino acid standards appear as purple spots.
8. Visualize the radiolabeled phosphoamino acids by autoradiography and identify the phosphorylated amino acids by alignment of the ninhydrin stained standards on the TLC cellulose plate and the autoradiogram (*see Note 8*).

### 3.4. Phosphopeptide Mapping with Trypsin (One-Dimensional)

1. In vivo [<sup>32</sup>P]-phosphorylated APP isolated by immunoprecipitation from conditioned media or cell lysates is subjected to SDS-PAGE and transferred to nitrocellulose or PVDF membrane (*see Subheading 3.1.; see Note 17*).

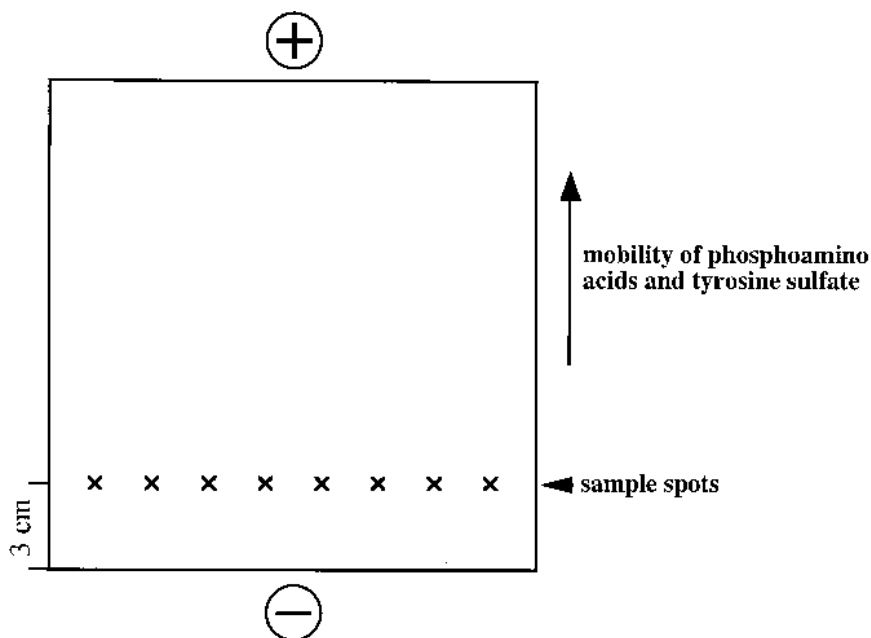


Fig. 4. Schematic showing a  $20 \times 20$  cm TLC cellulose plate for one-dimensional analysis of phosphoamino acids and tyrosine sulfate, respectively. Sample spots (x) are applied at a distance of 3 cm from the cathodic edge (-), and the plate is placed in a horizontal electrophoresis apparatus as described in **Subheadings 3.3.** and **3.6.** The migration direction of phosphoamino acids and tyrosine sulfate is indicated by an arrow.

2. The radioactive band is localized by autoradiography as described previously, excised from the membrane and cut into small pieces (approx  $2 \times 2$  mm).
3. Rewet the membrane pieces with isopropanol and wash three times with 1 mL  $H_2O$  and once with 0.5% (v/v) PVP-40. Incubate the membranes in PVP-40 for 30 min at  $37^\circ C$ . Collect the membrane pieces by centrifugation and wash three times with digestion buffer (see **Subheading 2.4.**). Add an appropriate amount of digestion buffer 2  $\mu L$ , so that the membrane pieces are totally covered and add 5  $\mu L$  trypsin solution (1  $\mu g/\mu L$ ).
4. Incubate for 12–16 h at  $37^\circ C$ . Vortex briefly and centrifuge for 5 min at 14,000g. Transfer the supernatant to a new microcentrifuge tube and measure the release of radioactivity from the membrane into the supernatant in a scintillation counter by Cerenkov counting. Usually, 70–90% of radioactivity is released into the supernatant.
5. Evaporate the supernatant in a Speed Vac concentrator (Savant Bioblock) and add 20  $\mu L$  of SDS sample buffer to the remaining pellet. Vortex briefly, heat the sample for 5 min at  $100^\circ C$  and carry out SDS-PAGE using 10–20% polyacrylamide gradient Tris/tricine gels.

6. After fixing and drying the gel, radiolabeled peptides are detected by autoradiography.

The radiolabeled peptide migrates at about 4.8 kDa and is the only detected peptide when the tryptic digestion is complete (*see Fig. 1*). This peptide was identified by MALDI mass spectrometry to represent the amino acid sequence from glycine 181 to lysine 224 (*see ref. 20 and Fig. 1*).

### 3.5. *In Vivo Sulfation*

The protocol for *in vivo* labeling of proteins with [<sup>35</sup>S] sulfate is similar to that for *in vivo* phosphorylation with [<sup>32</sup>P] orthophosphate (*see Subheading 3.1*).

1. Wash cells once with prewarmed sulfate-free medium and preincubate in the same medium for 45 min at 37°C in a cell incubator.
2. Aspirate the medium and add fresh prewarmed medium together with [<sup>35</sup>S]sulfate (1 mCi/mL). Incubate for time periods from 15 min up to 5 h (depending on experimental needs) at 37°C in a cell incubator. For longer labeling time periods, it may be necessary to add 2–5% of dialyzed serum, as cell viability might be affected on longer incubation periods without serum. In this case it may also help to add fresh [<sup>35</sup>S]sulfate to the conditioned medium to yield higher rates of labeling.
4. Isolate APP from conditioned media and/or from cell lysates by immunoprecipitation as described in **Subheading 3.1**.
5. After separation by SDS-PAGE, fix the gel and incubate in 1 M sodium salicylate for 20 min at room temperature to enhance the signals during autoradiography. The gel is then dried and exposed to X-ray film at –80°C. Alternatively, proteins can be transferred to PVDF membrane by Western blot techniques. Transfer of proteins to PVDF membrane is recommended, when the sulfated protein should be further analyzed, e.g., detection of tyrosine sulfate (*see Subheading 3.6*).

### 3.6. *Detection of Tyrosine Sulfate in APP (One-Dimensional)*

1. After localizing the [<sup>35</sup>S]-labeled protein by autoradiography as described in **Subheading 3.5**, the protein is excised from the membrane and cut into small pieces of approx 2 × 2 mm.
2. Rewet the membrane pieces briefly in isopropanol, wash two times with 1 mL H<sub>2</sub>O and once with 0.5% PVP-40, and incubate with 0.5% PVP-40 as described in **Subheading 3.4**. (*see Note 3*). Wash three times with digestion buffer. Then add digestion buffer containing 1 µg/µL Pronase (Boehringer Mannheim) and incubate for 12–24 h at 37°C. During this time the protein should be digested to single amino acids, which are released from the membrane into the supernatant. Digestion can be controlled by measuring the release of radioactivity from the membrane into the digestion buffer by scintillation counting.
3. After digestion, transfer the supernatant to a new microcentrifuge tube and add 5 vol of acetone to precipitate excess Pronase. Collect the precipitate by

centrifugation and transfer the supernatant to a new tube. Evaporate the supernatant in a Speed Vac concentrator (Savant Bioblock) and dissolve the pellet in 10  $\mu$ L of pH 3.5 electrophoresis buffer.

4. Spot the sample onto a 20  $\times$  20 cm TLC cellulose plate 3 cm from the cathodic edge as described in **Subheading 3.4.** (see **Fig. 4**). After drying the sample spot, apply 3  $\mu$ L of tyrosine sulfate standard solution to the spot and dry.
5. Wet the TLC cellulose plate as described in **Subheading 3.4.** and carry out high-voltage electrophoresis at 1.5 kV for 30 min.
6. Air dry the TLC cellulose plate and visualize the standard tyrosine sulfate by ninhydrin staining (see **Subheading 3.4.**) and detect the [ $^{35}$ S]tyrosine sulfate by autoradiography.

#### 4. Notes

1. The osmolarity of this buffer is determined by the glucose, which is added as an energy source for longer cell incubations.
2. Take care that TLC cellulose plates used for phosphoamino acid and tyrosine sulfate analysis are smooth and have an even surface. For this purpose the TLC plates can be illuminated from beneath in a light box. Scratches and nicks in the cellulose layer may influence the mobility of the samples and lead to smears.
3. An alternative method for the detection of tyrosine sulfate in proteins is described by Huttner (42), using alkaline hydrolysis with Ba(OH)<sub>2</sub>. This method might be used when quantitative detection of tyrosine sulfate is required.
4. The amounts of radioactivity used in the respective experiments may vary depending on the experimental needs. Generally, for short periods of labeling (e.g., pulse labeling) up to 15 min relatively high amounts of carrier-free [ $^{32}$ P]orthophosphate or [ $^{35}$ S]sulfate, respectively, should be used ( $\geq 0.5$  mCi/mL). To analyze phosphorylation and sulfation of membrane-bound APP, labeling periods significantly longer than 2 h may not necessarily increase the levels of phosphorylated and sulfated APP. Because APP is secreted from cells into the conditioned medium or degraded by cellular proteolytic systems, labeling of intracellular APP reaches a steady-state level. In turn, secreted APP accumulates in the conditioned media and longer periods of incubation yields higher levels of labeled soluble APP.
5. For in vivo labeling of cells with [ $^{32}$ P]-orthophosphate or [ $^{35}$ S]-sulfate, use proliferating cell cultures depending on personal interests. We prefer to use monolayer cell cultures, because they are easier to handle during working steps with radioactivity as compared with suspension cell cultures.
6. Immunoprecipitations should be carried out at 4°C to inhibit proteolysis and dephosphorylation of APP. When immunoprecipitates, especially those derived from cell lysates, appear to be “dirty,” it may help to decrease the time periods of incubation. We usually precipitate APP from cell lysates for 2–3 h.
7. It is recommended to use screwcapped tubes for working steps handling radioactivity, as this reduces the potential for contamination while closing and opening the tubes. Always centrifuge the tubes briefly before opening.

8. X-ray films should be exposed to dried gels, PVDF membranes, or TLC cellulose plates carrying  $^{32}\text{P}$ -labeled samples at  $-80^\circ\text{C}$  using an intensifying screen. When signals are weak and can hardly be detected, more sensitive X-ray films (e.g., BioMax films, Kodak, Rochester, NY) can be used. These sensitive films are often helpful for analyzing cell surface phosphorylation of APP by ectoprotein kinases.
9. For cell surface phosphorylation of APP by ectoprotein kinases, the final concentration of extracellularly added ATP should not exceed  $1\ \mu\text{M}$ , because higher concentrations of ATP may cause pharmacological side effects (39).
10. Use subconfluent cell monolayer cultures for phosphorylation of cell surface proteins, because ectoprotein kinase activity decreases with increasing cell density (25).
11. It is absolutely necessary to control cell viability, e.g., the intactness of plasma membranes, for specific detection of cell surface phosphorylation of APP, as release of intracellular compounds derived from “leaky” cells can render ectophosphorylation (40). The viability of cells can be monitored by standard cell viability tests. We prefer to measure (1) the release of lactate dehydrogenase activity, and/or (2) the cellular uptake of trypan blue under conditions used for ectophosphorylation of APP (40).
12. For analysis of cell surface phosphorylation of APP, it is necessary in most cases to use cells that stably overexpress APP, because expression of endogenous APP appears to be too low to detect cell surface phosphorylation.
13. To characterize the protein kinases involved in both cell surface phosphorylation and intracellular phosphorylation of APP, *in vivo* phosphorylations can be carried out in the presence or absence of selective protein kinase inhibitors (see Table 1).
14. Remember to include appropriate controls with the respective solvents (ethanol, dimethyl sulfoxide), when analyzing the effects of inhibitors of protein trafficking (e.g., Brefeldin A) or protein kinases (see Table 1).
15. Although there are protocols for phosphoamino acid analysis of proteins from fixed gels (41), we prefer to transfer the proteins after SDS-PAGE to PVDF membranes, as this method is faster with fewer working steps and the recovery of labeled phosphoamino acids appears to be higher. The usage of PVDF membrane is important, because nitrocellulose membrane dissolves during acidic hydrolysis in  $6\ \text{M}\ \text{HCl}$  at  $110^\circ\text{C}$ . Proteolytic digestions with trypsin or Pronase can be carried out using either membranes, PVDF, or nitrocellulose.
16. For the detection of phosphoamino acids, only about 10–100 cpm are required in the sample. To monitor migration during high-voltage electrophoresis of both phosphoamino acid and tyrosine sulfate analysis, a marker dye (phenol red) can be spotted onto the TLC cellulose plate.
17. About 100 pmol of APP should be used as the starting material, when proteolytic peptides of APP (e.g., after tryptic digestion) should be further analyzed by mass spectrometry or microsequencing (see Fig. 1).

## References

1. Kang, J., Lemaire, H., Unterbeck, A., Salbaum, J. M., Masters C. L., Grzeschik, K. H., et al. (1987) The precursor of Alzheimer's disease amyloid A4 protein resembles a cell-surface receptor. *Nature* **325**, 733–736.
2. Haass, C. and Selkoe, D. J. (1993) Cellular processing of  $\beta$ -amyloid precursor protein and the genesis of amyloid  $\beta$ -peptide. *Cell* **75**, 1039–1042.
3. Selkoe, D. J. (1994) Cell biology of the amyloid  $\beta$ -protein precursor and the mechanism of Alzheimer's disease. *Annu. Rev. Cell Biol.* **10**, 373–403.
4. Weidemann, A., König, G., Bunke, D., Fischer, P., Salbaum, J. M., Masters, C., and Bayreuther, K. (1989) Identification, biogenesis, and localization of precursors of Alzheimer's disease A4 amyloid protein. *Cell* **57**, 115–126.
5. Checler, F. (1995) Processing of the  $\beta$ -amyloid precursor protein and its regulation in Alzheimer's disease. *J. Neurochem.* **65**, 1431–1444.
6. Buxbaum, J. D., Gandy, S. E., Cicchetti, P., Ehrlich, M. E., Czernik, A. J., Fracasso, P. R., et al. (1990) Processing of Alzheimer  $\beta$ /A4 amyloid precursor protein: modulation by agents that regulate protein phosphorylation. *Proc. Natl. Acad. Sci. USA* **87**, 6003–6006.
7. Carporaso, G. L., Gandy, S. E., Buxbaum, J. D., and Greengard, P. (1992) Choroquine inhibits intracellular degradation but not secretion of Alzheimer  $\beta$ /A4 amyloid precursor protein. *Proc. Natl. Acad. Sci. USA* **89**, 2252–2256.
8. Buxbaum, J. D., Koo, E. H., and Greengard, P. (1993) Protein phosphorylation inhibits production of Alzheimer amyloid  $\beta$ /A4 peptide. *Proc. Natl. Acad. Sci. USA* **90**, 9195–9198.
9. Hung, A. Y., Haass, C., Nitsch, R. M., Qiu, W. Q., Citron, M., Wurtman, R. J., and Selkoe, D. J. (1993) Activation of protein kinase C inhibits cellular production of the amyloid  $\beta$ -protein. *J. Biol. Chem.* **268**, 22959–22962.
10. Nitsch, R. M., Slack, B. E., Wurtman, R. J., and Growdon, J. H. (1992) Release of Alzheimer amyloid precursor derivatives stimulated by activation of muscarinic acetylcholine receptors. *Science* **258**, 304–307.
11. Mills, J., Charest, D. L., Lam, F., Beyreuther, K., Pelech, S. L., and Reiner, P. B. (1997) Regulation of amyloid precursor protein catabolism involves the mitogen-activated protein kinase signal transduction pathway. *J. Neurosci.* **17**, 9415–9422.
12. Greenberg, S. M., Koo, E. H., Selkoe, D. J., Qiu, W. Q., and Kosik, K. S. (1994) Secreted  $\beta$ -amyloid precursor protein stimulates mitogen-activated protein kinase and enhances  $\tau$  phosphorylation. *Proc. Natl. Acad. Sci. USA* **91**, 7104–7108.
13. Gandy, S. E., Czernik, A. J., and Greengard, P. (1988) Phosphorylation of Alzheimer disease amyloid precursor peptide by protein kinase C and  $\text{Ca}^{2+}$ /calmodulin-dependent protein kinase II. *Proc. Natl. Acad. Sci. USA* **85**, 6218–6221.
14. Suzuki, T., Nairn, A. C., Gandy, S. E., and Greengard, P. (1992) Phosphorylation of Alzheimer amyloid precursor protein by protein kinase C. *Neuroscience* **48**, 755–761.
15. Hung, A. Y. and Selkoe, D. J. (1994) Selective ectodomain phosphorylation and regulated cleavage of  $\beta$ -amyloid precursor protein. *EMBO J.* **13**, 534–542.

16. Oishi, M., Nairn, A. C., Czernik, A. J., Lim, G. S., Isohara, T., Gandy, S. E., et al. (1997) The cytoplasmic domain of Alzheimer's amyloid precursor protein is phosphorylated at Thr654, Ser655, and Thr668 in adult rat brain and cultured cells. *Mol. Med.* **3**, 111–123.
17. Suzuki, T., Oishi, M., Marshak, D. R., Czernik, A. J., Nairn, A. C., and Greengard, P. (1994) Cell cycle-dependent regulation of the phosphorylation and metabolism of the Alzheimer amyloid precursor protein. *EMBO J.* **13**, 1114–1122.
18. Xu, H., Sweeny, D., Greengard, P., and Gandy, S. E. (1996) Metabolism of Alzheimer  $\beta$ -amyloid precursor protein: regulation by protein kinase A in intact cells and a cell-free system. *Proc. Natl. Acad. Sci. USA* **93**, 4081–4084.
19. Knops, J., Gandy, S. E., Greengard, P., Lieberburg, I., and Sinha, S. (1993) Serine phosphorylation of the secreted extracellular domain of APP. *Biochem. Biophys. Res. Comm.* **197**, 380–385.
20. Walter, J., Capell, A., Hung A. Y., Langen, H., Schnölzer, M., Thinakaran, G., et al. (1997) Ectodomain phosphorylation of  $\beta$ -amyloid precursor protein at two distinct cellular locations. *J. Biol. Chem.* **272**, 1896–1903.
21. Schindzierlorz, A., Grünberg, J., Haass, C., and Walter, J. (1999) Characterization of protein kinases phosphorylating the  $\beta$ -amyloid precursor protein within its ectodomain and identification of *in vivo* phosphorylation sites, in *Alzheimer's Disease and Related Disorders* (Igbal, K., Swaab, D. F., Winblad, B., and Wisniewski, H. M., eds.), John Wiley and Sons, LTD, Chichester, England, pp. 231–239.
22. Kelly, R. B. (1990) Microtubules, membrane traffic and cell organization. *Cell* **61**, 5–7.
23. Matlin, K. S. and Simons, K. (1983) Reduced temperature prevents transfer of a membrane glycoprotein to the cell surface but does not prevent terminal glycosylation. *Cell* **34**, 233–243.
24. Kübler, D., Pyerin, W., Bill, O., Hotz, A., Sonka, J., and Kinzel, V. (1989) Evidence for ecto-protein kinase activity that phosphorylates Kemptide in a cyclic AMP-dependent mode. *J. Biol. Chem.* **264**, 14549–14555.
25. Kübler, D., Pyerin, W., and Kinzel, V. (1983) Substrate-effected release of surface-located protein kinase from intact cells. *Proc. Natl. Acad. Sci. USA* **80**, 4021–4025.
26. Skubitz, K. M., Ehresmann, D. D., and Ducker, T. P. (1991) Characterization of human neutrophil ecto-protein kinase activity released by kinase substrates. *J. Immunol.* **147**, 638–650.
27. Walter, J., Kinzel, V., and Kübler, D. (1994) Evidence for CK1 and CK2 at the cell surface. *Cell. Mol. Biol. Res.* **40**, 473–480.
28. Pyerin, W., Burow, E., Michaely, K., Kübler, D., and Kinzel, V. (1986) Catalytic and molecular properties of highly purified phosphatase/casein kinase type II from epithelial cells in culture (HeLa) and relation to ecto-protein kinase. *Biol. Chem. Hoppe-Seyler* **368**, 215–227.
29. Walter, J., Schnölzer, M., Pyerin, W., Kinzel, V., and Kübler, D. (1996) Substrate induced release of ecto-protein kinase yields CK-1 and CK-2 in tandem. *J. Biol. Chem.* **271**, 111–119.

30. Hogan, M. V., Pawlowska, Z., Yang, H.-A., Kornecki, E., and Ehrlich Y. H. (1995) Surface phosphorylation by ecto-protein kinase C in brain neurons: a target for Alzheimer's  $\beta$ -amyloid peptides. *J. Neurochem.* **65**, 2022–2030.
31. Skubitz, K. M. and Goueli, S. A. (1994) CD31 (PECAM-1), CDw32 (Fc $\gamma$ RII), and anti-HLA class I monoclonal antibodies recognize phosphotyrosine-containing proteins on the surface of human neutrophils. *J. Immunol.* **152**, 5902–5911.
32. Dubyak, G. R. and El-Moatassim, C. (1993) Signal transduction via P2–purinergic receptors for extracellular ATP and other nucleotides. *Am. J. Physiol.* **265**, C577–C606.
33. Zimmermann, H. (1994) Signalling via ATP in the nervous system *Trends Neurosci.* **17**, 420–426.
34. Meyers, K. M., Holmsen, H., and Seachord, C. L. (1982) Comparative study of platelet dense granule constituents. *Am. J. Physiol.* **243**, R454–R461.
35. Tuazon, P. T. and Traugh, J. A. (1991) Casein kinase I and II — multipotential serine protein kinases: structure, function, and regulation. *Adv. Second Messenger Phosphoprotein Res.* **23**, 123–163.
36. Chauhan, A., Chauhan, V. P. S., Murakami, N., Brockerhof, H., and Wisniewski, H. M. (1993) Amyloid  $\beta$ -protein stimulates casein kinase I and casein kinase II activities. *Brain Res.* **629**, 47–52.
37. Huttner, W. B. (1987) Tyrosine sulfation and the secretory pathway. *Trends Biol. Sci.* **12**, 361–363
38. Niehrs, C., Beisswanger, R., and Huttner, W. B. (1994) Protein tyrosine sulfation, 1993 — an update. *Chem.-Biol. Interact.* **92**, 257–271.
39. Kübler, D., Pyerin, W., Fehst, M., and Kinzel, V. (1986) Physiological aspects of surface protein kinase activity, in *Cellular Biology of Ectoenzymes* (Kreuzberg, G. W., Redington, M., and Zimmerman, H., eds.) Springer-Verlag, Berlin, Heidelberg, Germany, pp. 191–204.
40. Kübler, D., Pyerin, W., and Kinzel, V. (1982) Assays of cell surface protein kinase: importance of selecting cytophilic substrates. *Eur. J. Biochem.* **26**, 306–309.
41. Boyle, W. J., van der Geer, P., and Hunter, T. (1991) Phosphopeptide mapping and phosphoamino acid analysis by two-dimensional separation on thin-layer cellulose plates. *Methods Enzymol.* **201**, 110–149.
42. Huttner, W. B. (1984) Determination and occurrence of tyrosine O-sulfate in proteins. *Methods Enzymol.* **107**, 200–223.
43. Pearson, R. B. and Kemp, B. E. (1991) Protein kinase phosphorylation site sequences and consensus specificity motifs: tabulations. *Methods Enzymol.* **200**, 62–81.
44. Chijiwa, T., Mishima, A., Hagiwara, M., Sano, M., Hayashi, K., Inoue, T., et al. (1990) Inhibition of forskolin induced neurite outgrowth and protein phosphorylation by a newly selective inhibitor of cyclic AMP-dependent protein kinase, N-[2-(p-bromocinnamylamino)ethyl]-5-isoquinolinesulfonamide (H-89), of PC-12D pheochromocytoma cells. *J. Biol. Chem.* **265**, 5267–5272.
45. Kase, H., Iwahashi, K., Nakanishi, S., Matsuda, Y., Yamada, K., Takahashi, M., et al. (1987) K-252 compounds, novel and potent inhibitors of protein kinase C and cyclic nucleotide-dependent protein kinases. *Biochem. Biophys. Res. Commun.* **142**, 436–440.

46. Chijiwa, T., Hagiwara, M., and Hidaka, H. (1989) A newly synthesized selective casein kinase I inhibitor, N-(2-aminoethyl)-5-chloroisoquinoline-8-sulfonamide, and affinity purification of casein kinase I from bovine testis. *J. Biol. Chem.* **264**, 4924–4927.
47. Zandomeni, R., Zandomeni, M. C., Shugar, D., and Weinmann, R. (1986) Casein kinase type II is involved in the inhibition by 5,6-dichloro-1-beta-D-ribofuranosylbenzimidazole of specific RNA polymerase II transcription. *J. Biol. Chem.* **261**, 3414–3419.
48. Haass, C., Koo, E. H., Mellon, A., Hung, A. Y., and Selkoe, D. J. (1992) Targeting of cell-surface  $\beta$ -amyloid precursor protein to lysosomes: alternative processing into amyloid-bearing fragments. *Nature* **357**, 500–503.
49. Oltersdorf, T., Ward, P. J., Henrikson, T., Beattie, E. C., Neve, R., Lieberberg, I., and Fritz, L. C. (1990) The Alzheimer amyloid precursor protein. Identification of a stable intermediate in the biosynthetic/degradative pathway. *J. Biol. Chem.* **265**, 4492–4497.
50. Podlisny, M. B., Tolan, D., and Selkoe, D. J. (1991) Homology of the amyloid  $\beta$ -protein precursor in monkey and human supports a primate model for  $\beta$ -amyloidosis in Alzheimer's disease. *Am. J. Pathol.* **138**, 1423–1435.

## Posttranslational Modifications of the Amyloid Precursor Protein

### *Glycosylation*

**Chen Liu, Tomasz Rozmyslowicz, Magda Stwora-Wojczyk,  
Boguslaw Wojczyk, and Steven L. Spitalnik**

#### **1. Introduction**

Many studies have demonstrated the importance of amyloid precursor protein (APP) in the pathogenesis of Alzheimer's disease. Nonetheless, the exact mechanism by which APP contributes to the pathogenesis of Alzheimer's disease is still not clear. Because APP is a glycoprotein, and because glycosylation can be important in the cell biology of individual glycoproteins (for review, *see refs. 1 and 2*), it is possible that changes in APP glycosylation during development and aging are important in APP biosynthesis, proteolysis, and degradation. However, few studies have addressed this issue (*3–8*). This chapter provides methods for analyzing the glycosylation of APP that is actively synthesized by living cells in tissue culture. These methods can be applied to primary cultures, continuous cell lines, and transfected cell lines expressing recombinant APP.

#### **1.1. APP Structure and Synthesis**

APP is a Type I membrane glycoprotein with three major isoforms containing 695, 751, or 770 amino acids (denoted APP<sub>695</sub>, APP<sub>751</sub>, and APP<sub>770</sub>, respectively) that are generated by alternative splicing of mRNA derived from the APP gene on chromosome 21. APP<sub>695</sub> is the predominant isoform expressed in the central nervous system (*9*). These three APP isoforms undergo multiple posttranslational modifications, including N- and O-glycosylation (*10,11*). Each isoform of APP has two potential N-glycosylation sites at Asn467 and

From: *Methods in Molecular Medicine, Vol. 32: Alzheimer's Disease: Methods and Protocols*  
Edited by: N. M. Hooper © Humana Press Inc., Totowa, NJ

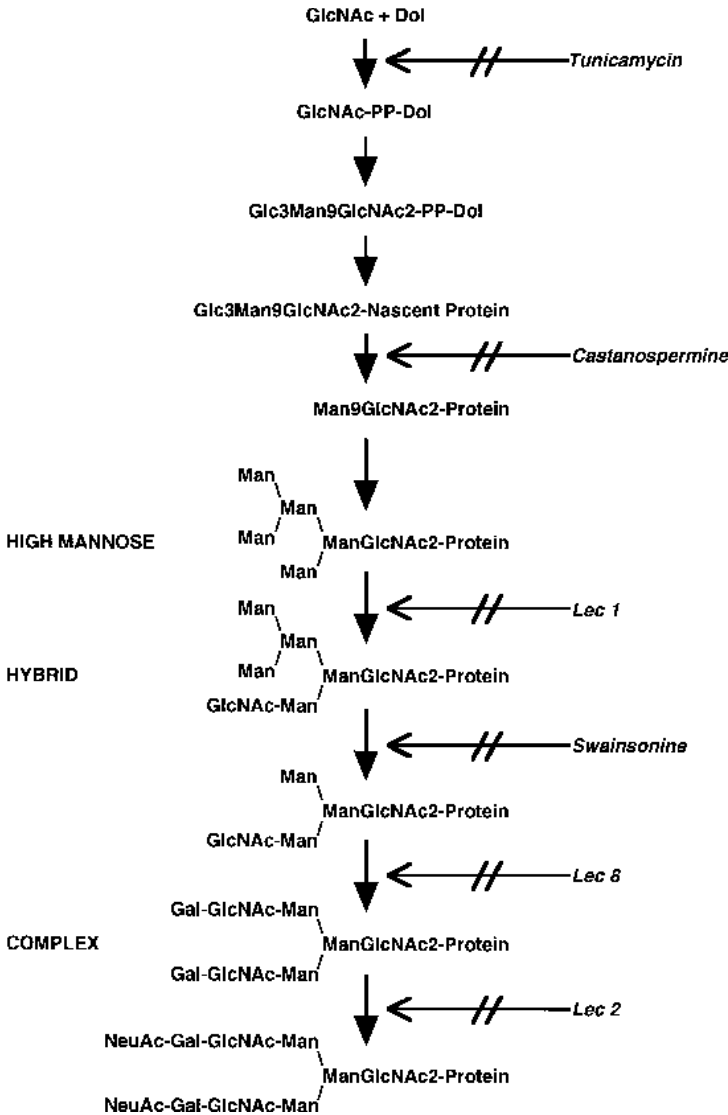


Fig. 1. N-glycan biosynthetic pathway. The positions in the pathway where biosynthesis can be blocked by soluble glycosylation inhibitors (tunicamycin, castanospermine, and swainsonine) and glycosylation-defective cell lines (Lec 1, Lec 2, and Lec 8) are indicated.

Asn496, only one of which is glycosylated on recombinant human APP<sub>695</sub> expressed by transfected Chinese hamster ovary (CHO) cells (3). In addition, cell surface and secreted forms of APP have multiple O-glycans (4,10),

although the specific locations of the O-glycosylated serine and/or threonine residues on APP have not yet been determined. Finally, several studies suggest that, in certain cell types, APP is modified on its extracellular domain by the biosynthetic addition of glycosaminoglycan chains (**12, 13**); however, this type of modification will not be discussed further in this chapter.

Although initially synthesized as a transmembrane glycoprotein, full-length APP can be cleaved in the secretory pathway by the  $\alpha$ -,  $\beta$ -, and  $\gamma$ -secretases to generate soluble, secreted forms of APP. Therefore, mature forms of APP can be either expressed on the cell surface as transmembrane proteins or secreted into the extracellular milieu as soluble proteins. There is some evidence that these cleavages may occur later in the secretory pathway following the modification of APP by O-glycans (**7**).

### **1.2. N-Linked Glycosylation**

The biosynthetic pathways involving N-glycosylation are complex (for review, *see* **ref. 14**). N-glycosylation is initiated by the synthesis of a 14-sugar oligosaccharide on the lipid carrier dolichol (**Fig. 1**). This oligosaccharide is then transferred en bloc by the enzyme oligosaccharyl transferase onto an appropriate asparagine residue on a nascent polypeptide; this process occurs in the endoplasmic reticulum, is cotranslational, and is termed “core glycosylation.” Asparagine residues in the sequence Asn-X-Ser/Thr are the only ones that may be core glycosylated, where X is any amino acid except Pro. This acceptor sequence is termed a “glycosylation sequon.” Interestingly, not all such glycosylation sequons are core glycosylated and the rules governing this process are not fully understood (**15–17**). Following core glycosylation, a spatially and sequentially ordered series of modifications involving glycosidases and glycosyltransferases takes place in the endoplasmic reticulum, Golgi apparatus, and trans-Golgi network (**Fig. 1**); this chain of events is termed “processing.” Processing of N-glycans leads to three primary classes of oligosaccharides termed “high mannose,” “hybrid,” and “complex” type depending on whether slight, moderate, or extensive processing has taken place, respectively (**Fig. 1**). The general mechanisms determining the regulation of the degree of N-glycan processing at any particular glycosylation sequon are very poorly understood; however, recent studies have provided some insights in particular cases (e.g., *see* **refs. 18–20**).

In many cell types, the mature forms of APP that are found at the cell surface or secreted into the extracellular milieu contain complex type N-glycans; in contrast, the immature, intracellular forms of APP contain high mannose type N-glycans (*see* below, **Figs. 3 and 4**, and **refs. 3 and 4**).

### **1.3. O-Linked Glycosylation**

Although various sugars, including fucose and GlcNAc, for example, can be coupled to proteins through O-glycosidic linkages, this chapter restricts its

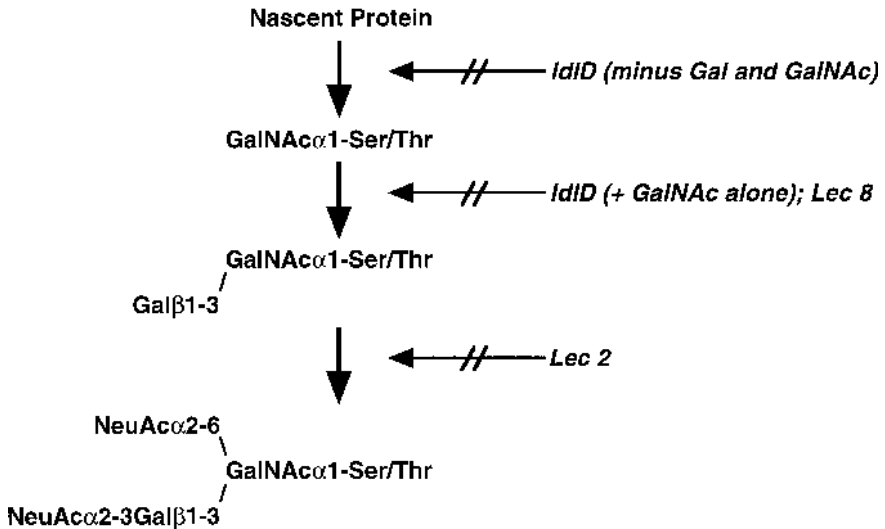


Fig. 2. O-glycan biosynthetic pathway. The positions in the pathway where biosynthesis can be blocked by glycosylation-defective cell lines (Id1D, Lec 2, and Lec 8) are indicated.

focus to the classical mucin-like oligosaccharides that are linked to serine and threonine residues (**Fig. 2**; for review, *see ref. 21*). In this case, core glycosylation results from covalent coupling of a GalNAc to a nascent soluble or membrane-bound protein in the secretory apparatus, typically in the endoplasmic reticulum or *cis*-Golgi. This modification occurs posttranslationally and is accomplished by a member of a family of enzymes termed UDP-GalNAc:polypeptide N-acetylgalactosaminyl-transferases (**22**). In contrast to N-glycosylation, relatively little is known about the sequences surrounding individual Ser/Thr residues that control core O-glycosylation at these sites (**23,24**). Processing of O-glycans occurs in a stepwise fashion by the transfer of individual sugars by glycosyltransferases to the growing oligosaccharide chain (**Fig. 2**); again, the regulation of site-specific O-glycan processing is poorly understood.

## 2. Materials

### 2.1. Cell Lines

#### 2.1.1. Chinese Hamster Ovary Cells

Wild-type CHO cells, clone Pro-5 (**25**), are purchased from the American Type Culture Collection (ATCC, Rockville, MD). These cells are proline auxotrophs. The Lec 1, Lec 2, and Lec 8 glycosylation-defective mutant CHO

cell lines were initially derived from clone Pro-5 (26) and are also purchased from the ATCC. The IdID glycosylation-defective mutant CHO cell line was derived from clone Pro-5 (27) and was kindly provided by Dr. Monty Krieger (Massachusetts Institute of Technology, Cambridge, MA). The use of these cell lines to study glycosylation of APP is described below.

A clone of wild-type Pro-5 CHO cells expressing high levels of stably transfected human APP<sub>695</sub> was described previously (3). Clone 26.1.5, a clone of wild-type Pro-5 CHO cells expressing high levels of stably transfected human glycoprotein A, a red blood cell membrane glycoprotein, was described previously (28).

All CHO cells except for the IdID cell line are cultured in complete  $\alpha$ -minimal essential medium ( $\alpha$ -MEM CM):  $\alpha$ -MEM supplemented with 10% fetal bovine serum (FBS), 2 mM glutamine, 100 IU/mL of penicillin, 100  $\mu$ g/mL of streptomycin, and 0.25  $\mu$ g/mL of amphotericin B.

The IdID cell line is grown in IdID complete medium (IdID CM), which contains 1:1 mixture of Ham's F12 and  $\alpha$ -MEM supplemented with 10% dialyzed FBS and ITS+Premix (Collaborative Research Inc., Bedford, MA). ITS + Premix is a culture supplement that contains a mixture of insulin, transferrin, and selenium. Under these conditions the cellular glycoproteins do not contain Gal and GalNAc (see below, Figs. 1 and 2, and refs. 27 and 29); therefore, in this case APP would not contain O-glycans or highly processed, complex-type N-glycans (4). In order for IdID cells to synthesize glycoproteins with complete N- and O-glycans, the cells are maintained in IdID CM supplemented with 20  $\mu$ M Gal and 200  $\mu$ M GalNAc (4).

### 2.1.2. NT2 Cells

The NT2/D1 (NT2) clonal cell line was derived from the Tera-2 human embryonal carcinoma cell line (30,31). NT2 cells synthesize APP (32). These cells are cultured in Dulbecco's modified Eagle's medium (DMEM) containing 10% FBS, 2 mM glutamine, 100 IU/mL of penicillin, 100  $\mu$ g/mL of streptomycin, and 0.25  $\mu$ g/mL of amphotericin B.

NT2 cells can be induced to differentiate into postmitotic neuronlike cells (NT2-N cells) by exposure to retinoic acid (30,31). NT2-N cells ("Replate #2"; >95% pure) are obtained following exposure of NT2 cells to 10  $\mu$ M retinoic acid, as described previously (33).

## 2.2. Antibodies

1. The KAREN anti-APP polyclonal antibody, obtained by immunizing a goat with purified, bacterially expressed recombinant secreted form of human APP, recognizes a peptide epitope in the extracellular domain of APP. The antiserum is kindly provided by Dr. Barry D. Greenberg (Cephalon, Inc., West Chester, PA).
2. The 2493 anti-APP polyclonal antibody, obtained by immunizing a rabbit with a synthetic peptide comprising the C-terminal 40 amino acids in the cytoplasmic

domain of human APP, is kindly provided by Dr. Virginia Lee (University of Pennsylvania, Philadelphia, PA).

3. The 6A7 mouse monoclonal antibody recognizes a sialic acid dependent epitope on M-type glycoporphin A (34,35), and the hybridoma cell line is purchased from the ATCC. The antibody is purified from hybridoma culture supernatant by immunoaffinity chromatography (36).

### **2.3. Metabolic Labeling**

1. Hanks' balanced salt solution (Sigma, St. Louis, MO).
2. Methionine-free DMEM (Sigma).
3. <sup>35</sup>S-Methionine (Amersham Life Science, Arlington Heights, IL).

### **2.4. Immunoprecipitation of Membrane-Bound and Soluble Forms of APP**

1. PBS-PMSF: Phosphate-buffered saline (PBS; 0.01 M Na<sub>2</sub>HPO<sub>4</sub>/NaH<sub>2</sub>PO<sub>4</sub>, 0.15 M NaCl, pH 7.4) containing 200 µg/mL phenylmethylsulfonyl fluoride (PMSF).
2. Lysis buffer: 0.05 M Tris-HCl, pH 8.0, 0.15 M NaCl, 0.005 M EDTA, containing 1% NP-40 and 200 µg/mL PMSF.
3. 5× Radioimmunoprecipitation assay (RIPA) buffer: 0.25 M Tris-HCl, pH 8.0, 0.75 M NaCl, 0.025 M EDTA, containing 5% NP-40, 2.5% sodium deoxycholate, and 0.5% sodium dodecyl sulfate (SDS).
4. Protein A agarose beads and protein G agarose beads (Gibco-BRL, Grand Island, NY).
5. Wash buffer: 0.015 M Tris-HCl, pH 7.5, 0.5 M NaCl, 0.005 M EDTA, containing 1% NP-40.
6. 1× Laemmli sample buffer: 62 mM Tris-HCl, pH 6.8 containing 2% SDS and 10% glycerol.
7. <sup>14</sup>C-Labeled molecular weight standards (Gibco-BRL).
8. Amplify (Amersham).
9. Biomax Film (Kodak, Rochester, NY).

### **2.5. Glycosidase Digestion**

1. The following glycosidases are purchased from Boehringer Mannheim GmbH, Mannheim, Germany: N-glycosidase F, endoglycosidase H, endo-β-galactosidase, O-glycosidase, and neuraminidase.
2. 1.25% SDS and 1% SDS.
3. N-Glycosidase F buffer: 30 mM Na<sub>2</sub>HPO<sub>4</sub>/NaH<sub>2</sub>PO<sub>4</sub>, pH 7.2, 20 mM EDTA.
4. Endo H buffer: 60 mM Na<sub>2</sub>HPO<sub>4</sub>/NaH<sub>2</sub>PO<sub>4</sub>, pH 5.5, containing 1% SDS and 200 µg/mL PMSF.
5. Endo-β-galactosidase buffer: 50 mM Sodium acetate, pH 5.8, containing 0.6% N-octyl-β-D-glucoside.
6. O-Glycosidase buffer: 50 mM Tris maleate, pH 7.5, containing 0.6% N-octyl-β-D-glucoside.

7. Neuraminidase buffer: 50 mM sodium acetate, pH 5.5, containing 0.6% N-octyl- $\beta$ -D-glucoside.
8. O-Glycosidase/Neuraminidase Buffer: 500 mM Tris maleate, pH 7.5, containing 0.6% N-octyl- $\beta$ -D-glucoside.

## 2.6. Soluble Glycosylation Inhibitors

The following soluble glycosylation inhibitors are purchased from Boehringer Mannheim: tunicamycin, castanospermine, and swainsonine.

## 3. Methods

### 3.1. Metabolic Labeling

1. For steady-state labeling of glycoproteins, wash 10 cm Petri dishes containing 80–95% confluent cells with HBBS.
2. Incubate the cells with 2 mL of methionine-free DMEM containing 32–48  $\mu$ Ci/mL of  $^{35}$ S-methionine for 4 h at 37°C (see **Note 1**).

### 3.2. Immunoprecipitation of Membrane-Bound APP

1. To immunoprecipitate full-length, membrane-bound forms of APP, wash the radiolabeled cell monolayers twice with PBS-PMSF.
2. Gently scrape the cells from each dish in the presence of 1 mL of PBS-PMSF.
3. Pellet the cells by brief centrifugation at 16,000g for 1 min and discard the supernatant.
4. Prepare the cell lysates by solubilizing the cells in 800  $\mu$ L of lysis buffer.
5. Clarify the lysates by centrifugation at 16,000g for 10 min.
6. Add 1/4 vol of 5X RIPA buffer.
7. Preabsorb the lysate for 30 min at 4°C with 25  $\mu$ L of protein A agarose beads and then save the supernatant.
8. Add rabbit polyclonal antibody 2493 (see **Subheading 2.2.2.**) to a final dilution of 1:100 along with 50  $\mu$ L of protein A agarose beads.
9. Incubate for 16 h at 4°C.
10. Wash the beads twice with 1X RIPA buffer, once with wash buffer, and then boil for 5 min in 25  $\mu$ L of 1X Laemmli sample buffer.
11. Analyze the immunoprecipitated proteins by electrophoresis on 6% or 10% SDS-PAGE gels (6% crosslinker) for 1.5 h at 160 V. Run 14C-labeled molecular weight standards in a separate lane as controls.
12. Fix the gels in 50% methanol/7.5% acetic acid, treat with Amplify (Amersham), rinse with water, dry, and expose to Biomax Film (Kodak) at  $-70^{\circ}$ C with an intensifying screen (see **Note 2**).

The autoradiograph in **Fig. 3** shows the results for cell-associated APP synthesized by untransfected CHO cells (lane 4) and for CHO cells transfected with human APP<sub>695</sub> (lane 5). The transfected cells synthesize significantly higher amounts of APP as compared with untransfected CHO cells (**4**). In

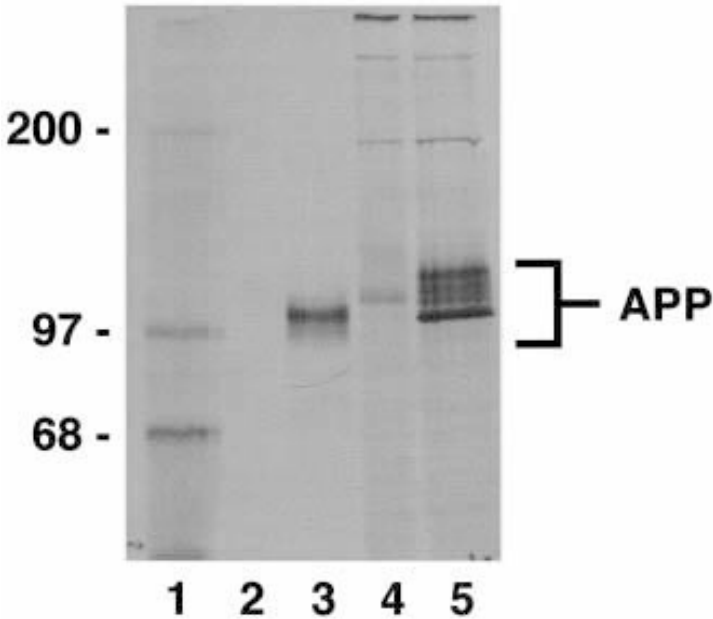


Fig. 3. Immunoprecipitation of secreted and cell-associated forms of APP. Untransfected wild-type CHO cells (lanes 2 and 4) and a clone of wild-type CHO cells expressing high amounts of stably transfected human APP<sub>695</sub> cDNA (lanes 3 and 5) were metabolically labeled with <sup>35</sup>S-methionine. Detergent cell lysates (lanes 4 and 5) and conditioned media (lanes 2 and 3) were separately immunoprecipitated with the 2493 rabbit polyclonal anti-APP antibody and the KAREN goat polyclonal anti-APP antibody, respectively. The immunoprecipitates were isolated, separated by SDS-PAGE, and visualized by autoradiography. <sup>14</sup>C-labeled electrophoretic standards (myosin: 200 kDa; phosphorylase B: 97 kDa; and bovine serum albumin: 68 kDa) were loaded in lane 1; their migration positions are indicated on the left of the gel. The position of immunoprecipitated APP is indicated on the right of the gel. The secreted APP found in the conditioned medium results from the proteolytic cleavage of the membrane-bound form and, therefore, migrates faster by SDS-PAGE. Following longer exposure of the gel, a faint band corresponding to secreted APP was seen in lane 2. The fastest migrating form of APP in lane 5 corresponds to the immature form of membrane-bound APP, which contains unprocessed, high-mannose type N-glycans and lacks O-glycans.

addition, because CHO cells primarily synthesize APP<sub>751/770</sub>, the APP immunoprecipitated from the transfected cells migrates faster by SDS-PAGE. The sharp, fastest-migrating APP band in lane 5 represents the immature form of APP; this form contains unprocessed, high-mannose type N-glycans and lacks O-glycans (3,4). The slower migrating bands represent the mature

forms of APP that contain complex type N-glycans and mature, processed O-glycans (3,4).

### 3.3. Immunoprecipitation of Soluble Forms of APP

1. To immunoprecipitate secreted forms of APP, add 300  $\mu$ L of 5X RIPA buffer to 1200  $\mu$ L of conditioned media.
2. Boil the sample for 10 min.
3. Centrifuge at 16,000g for 5 min.
4. Preabsorb the resulting supernatant with 30  $\mu$ L of protein G-agarose for 30 min at 4°C.
5. Add the KAREN goat polyclonal antibody (*see Subheading 2.2.1.*) to a final dilution of 1:500.
6. Following a 16-h incubation at 4°C, the immunoprecipitated proteins are isolated and analyzed as described in **Subheading 3.2.**, except that protein G-agarose is used for isolating the immunoprecipitates instead of protein A-agarose.

The autoradiograph in **Fig. 3** shows the results for secreted forms of APP synthesized by untransfected CHO cells (lane 2) and for CHO cells transfected with human APP<sub>695</sub> (lane 3). Again, the transfected cells synthesize significantly higher amounts of APP as compared with untransfected CHO cells (4). Because secretory APP results from proteolytic cleavage of mature, cell-associated APP, the secreted forms are smaller than the cell-associated forms and migrate faster by SDS-PAGE (**Fig. 3**, compare lanes 3 and 5). In addition, because this proteolysis is a late event in APP synthesis (7), secretory APP contains highly processed, complex type N-glycans and mature O-glycans (3,4).

### 3.4. Glycosidase Digestion

Enzyme digestion of glycoproteins with defined exo- and endo-glycosidases is a straight-forward and classical method for obtaining structural information concerning the oligosaccharides carried on the glycoprotein of interest. Many glycosidases of varying specificity have been described. Five glycosidases that are commonly used to characterize N- and O-glycans will be described here: N-glycosidase F, endoglycosidase H, endo- $\beta$ -galactosidase, O-glycosidase, and neuraminidase.

To use glycosidase digestion to analyze the oligosaccharides on cell-associated or secreted forms of metabolically labeled APP, cell lysates or conditioned media are first immunoprecipitated, as described in **Subheadings 3.2.** and **3.3.** If the glycosidase of interest successfully releases the recognized monosaccharides and/or oligosaccharides, the digested form of APP will exhibit increased migration on by sodium dodecyl sulfate polyacrylamide gel electrophoresis (SDS-PAGE) analysis. However, if the glycosidase preparation is contaminated by significant amounts of proteases, anomalous results can be obtained.

### 3.4.1. N-Glycosidase F

This enzyme, also termed PNGase F, is derived from *Flavobacterium meningosepticum*. It hydrolyzes all types of N-glycans on mammalian glycoproteins. It is an endoglycosidase that cleaves off an intact oligosaccharide from the glycoprotein by breaking the GlcNAc-Asn linkage.

1. To analyze APP for the presence of N-glycans, elute the immunoprecipitated proteins from the washed protein A- or protein G-agarose beads (for the cell lysates, [see **Subheading 3.2.**] or conditioned media [see **Subheading 3.3.**], respectively) by boiling first for 2 min in 4  $\mu$ L of 1.25% SDS and then for another 3 min in an additional 36  $\mu$ L of N-glycosidase F buffer.
2. Divide each sample into two equal parts: a test sample and a control sample.
3. Supplement each test sample with 4  $\mu$ L (0.8 U) of N-glycosidase F. As a negative control, incubate each identical control sample in the same volume of N-glycosidase F buffer alone.
4. Incubate for 16 h at 37°C.
5. Individually mix each sample with 6  $\mu$ L of 5 $\times$  Laemmli sample buffer (see **Subheading 2.4.**) and boil for 5 min.
6. Analyze the proteins by SDS-PAGE, as described in **Subheading 3.2.**

Using this approach, it is possible to confirm that the immature form of APP synthesized by NT2 cells is N-glycosylated (**Fig. 4**, lanes 2 and 4).

### 3.4.2. Endoglycosidase H (Endo H)

The enzyme is derived from *Streptomyces plicatus*. It is an endoglycosidase that removes high-mannose type N-glycans from glycoproteins. Therefore, the results of Endo H digestion are often used in comparison with those obtained with N-glycosidase F to determine whether the N-glycans on the glycoprotein of interest are either of the high-mannose type or are more highly processed. Endo H releases an oligosaccharide by breaking the bond between the two GlcNAc residues in the sequence R-Man( $\beta$ 1-4)GlcNAc( $\beta$ 1-4)GlcNAc-Asn.

1. Elute the immunoprecipitated forms of APP from the protein A- or protein G-agarose beads (see **Subheadings 3.2.** and **3.3.**) by boiling for 5 min in 40  $\mu$ L Endo H buffer.
2. Divide each sample in half and supplement with either 4  $\mu$ L (4 mU) of Endo H or Endo H buffer alone.
3. Incubate for 16 h at 37°C.
4. Mix each sample with 6  $\mu$ L of 5X Laemmli sample buffer (see **Subheading 2.4.**) and boil for 5 min.
5. Analyze the proteins by SDS-PAGE, as described in **Subheading 3.2.**

Using this approach, it is possible to confirm that the immature form of APP synthesized by NT2 cells contains only high-mannose type N-glycan(s) (**Fig. 4**, lanes 1 and 3).

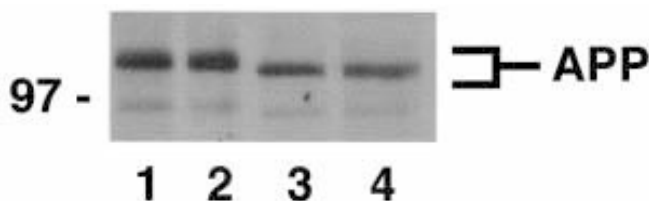


Fig. 4. Release of N-glycans from APP by digestion with Endo H and N-glycosidase F. Human NT2 cells were metabolically labeled with  $^{35}\text{S}$ -methionine. Cell-associated APP was immunoprecipitated with the 2493 rabbit polyclonal anti-APP antibody. The immunoprecipitates were then incubated overnight at  $37^\circ\text{C}$  with Endo H buffer alone (lane 1), N-glycosidase F buffer alone (lane 2), Endo H (lane 3), or N-glycosidase F (lane 4). The migration position of the immature form of cell-associated APP is indicated on the right; the migration position of the phosphorylase B standard is indicated on the left. Notice that the immature form of APP contains high-mannose type N-glycan(s).

### 3.4.3. Endo- $\beta$ -Galactosidase

Endo- $\beta$ -galactosidase from *Bacteroides fragilis* is an endoglycosidase that recognizes poly-lactosamine chains on either N- or O-glycans. It hydrolyzes internal linkages of the type Gal( $\beta$ 1-4)GlcNAc or Gal( $\beta$ 1-3)GlcNAc in the following types of sequences: R-GlcNAc( $\beta$ 1-3)Gal( $\beta$ 1-3,4)GlcNAc-R.”

1. Elute the immunoprecipitated forms of APP from protein A- or protein G-agarose beads (see **Subheadings 3.2.** and **3.3.**) by boiling for 2 min in 4  $\mu\text{L}$  of 1% SDS.
2. Add 36  $\mu\text{L}$  of Endo- $\beta$ -galactosidase buffer and boil for an additional 3 min.
3. Divide each sample in half and supplement with either 2  $\mu\text{L}$  (2 mU) endo- $\beta$ -galactosidase or 2  $\mu\text{L}$  Endo- $\beta$ -galactosidase buffer alone.
4. Incubate for 16 h at  $37^\circ\text{C}$ .
5. Mix each sample with 6  $\mu\text{L}$  of 5 $\times$  Laemmli sample buffer (**Subheading 2.4.**) and boil for 5 min.
6. Analyze the proteins by SDS-PAGE, as described in **Subheading 3.2.**

### 3.4.4. O-Glycosidase

This enzyme is an endoglycosidase derived from *Diplococcus pneumoniae* that cleaves the GalNAc( $\alpha$ 1-O)Ser/Thr linkage, releasing the O-glycosidically linked disaccharide Gal( $\beta$ 1-3)GalNAc from the sequence Gal( $\beta$ 1-3)GalNAc( $\alpha$ 1-O)Ser/Thr. Thus, this enzyme is useful for analyzing O-glycans. However, in contrast to PNGase F, which cleaves all types of N-glycans, O-glycosidase has a very limited specificity; if the Gal( $\beta$ 1-3)GalNAc( $\alpha$ 1-O)Ser/Thr sequence is substituted with any other monosaccharides, such as sialic acid, then O-glycosidase is not active. Nonetheless,

O-glycosidase is the only endoglycosidase currently available that is useful for the analysis of O-glycans.

1. Elute the immunoprecipitated proteins from the protein A- or protein G-agarose beads (*see Subheadings 3.2. and 3.3.*) by boiling for 2 min in 1% SDS.
2. Boil each sample for another 3 min in an additional 36  $\mu\text{L}$  of O-glycosidase buffer.
3. Divide each sample in half and supplement with either 2  $\mu\text{L}$  (1 mU) of O-glycosidase or O-glycosidase buffer alone.
4. Incubate for 16 h incubation at 37°C.
5. Mix each sample with 6  $\mu\text{L}$  of 5X Laemmli sample buffer (**Subheading 2.4.**) and boil for 5 min.
6. Analyze the proteins by SDS-PAGE, as described in **Subheading 3.2.**

### 3.4.5. Neuraminidase

Many neuraminidases, also termed sialidases, have been isolated from multiple organisms. The neuraminidase from *Vibrio cholerae* is an exoglycosidase with a reasonably broad specificity that will cleave sialic acid off the nonreducing terminal of glycoprotein N- or O-glycans when the sialic acid is found in an  $\alpha 2-3$ ,  $\alpha 2-6$ , or  $\alpha 2-8$  linkage.

1. Elute the immunoprecipitated proteins from the protein A- or protein G-agarose beads (*see Subheadings 3.2. and 3.3.*) by boiling for 2 min in 1% SDS.
2. Add 36  $\mu\text{L}$  of neuraminidase buffer and boil for an additional 3 min.
3. Divide each sample in half and supplement with either 4  $\mu\text{L}$  (4 mU) neuraminidase or with 4  $\mu\text{L}$  neuraminidase buffer alone.
4. Incubate for 16 h at 37°C.
5. Mix each sample with 6  $\mu\text{L}$  of 5X Laemmli sample buffer (**Subheading 2.4.**) and boil for 5 min.
6. Analyze the proteins by SDS-PAGE, as described in **Subheading 3.2.**

Using this approach, one can determine that the oligosaccharides on the mature form of cell-associated APP synthesized by NT2 cells contain sialic acid residues (**Fig. 5**, lanes 1 and 2). In contrast, as expected, this late modification of oligosaccharides is not present on the N-glycan(s) of the immature form of cell-associated APP (**Fig. 5**, lanes 1 and 2).

### 3.4.6. O-Glycosidase and Neuraminidase

Because O-glycosidase cannot cleave sialylated forms of O-glycans with the sequence Gal( $\beta 1-3$ )GalNAc( $\alpha 1-O$ )Ser/Thr, in some experiments neuraminidase and O-glycosidase are used sequentially.

1. After an initial 16 h incubation of the immunoprecipitated proteins (*see Subheadings 3.2. and 3.3.*) with neuraminidase (*see Subheading 3.4.5.*), add 1 mU of O-glycosidase in 3  $\mu\text{L}$  of O-glycosidase/neuraminidase buffer.
2. Incubate the sample for an additional 16 h at 37°C.

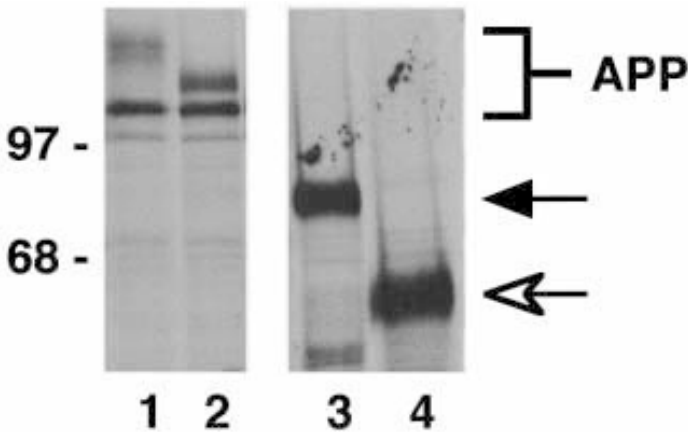


Fig. 5. Digestion of glycoproteins using neuraminidase. NT2 cells and glycoporphin A-transfected CHO cells were metabolically labeled with  $^{35}\text{S}$ -methionine. Cell-associated APP from NT2 cells (lanes 1 and 2) and glycoporphin A from transfected CHO cells (lanes 3 and 4) were immunoprecipitated from detergent cell lysates with the 2493 rabbit polyclonal anti-APP antibody and 50  $\mu\text{g}/\text{mL}$  of the 6A7 mouse monoclonal antiglycoporphin A antibody, respectively. The immunoprecipitates were then incubated overnight at  $37^\circ\text{C}$  with either neuraminidase buffer alone (lanes 1 and 3) or neuraminidase (lanes 2 and 4). The migration positions of the phosphorylase B and bovine serum albumin standards are indicated on the left. The migration positions of the various APP forms, the undigested glycoporphin A homodimer (closed arrow), and the digested glycoporphin A dimer (open arrow) are indicated on the right. Recombinant glycoporphin A was used as a positive control for neuraminidase digestion (T. Rozmyslowicz and S. L. Spitalnik, unpublished observations). Notice that sialic acid residues are only found on the mature, highly processed, slower migrating forms of APP.

3. Mix each sample with 6  $\mu\text{L}$  of  $5\times$  Laemmli sample buffer (**Subheading 2.4.**) and boil for 5 min.
4. Analyze the proteins by SDS-PAGE, as described in **Subheading 3.2.**

### 3.5. Soluble Glycosylation Inhibitors

Soluble inhibitors of protein N-glycosylation are very useful and powerful tools for understanding the biochemistry, cell biology, and function of glycoproteins. Many such inhibitors are available that typically block a single step in N-glycan biosynthesis (for general reviews, *see refs. 38 and 39*). These inhibitors are simple to use in that they are just added to tissue culture medium and the cells can then be metabolically labeled and analyzed. Because these inhibitors block new N-glycan synthesis or processing, to obtain clean results the cells must be incubated with the inhibitors for sufficient lengths of time before metabolic labeling to allow completion of synthesis of the previously nascent

glycoproteins. In addition, some glycosylation inhibitors also block generalized protein synthesis in a nonspecific fashion. Therefore, controls for general protein synthesis need to be included and results need to be interpreted with care. Finally, none of these glycosylation inhibitors are specific for APP, but instead affect the synthesis of all relevant cellular glycoproteins. Again, careful controls must be performed before a function is attributed to the glycosylation of a specific cellular glycoprotein.

Three generally useful inhibitors of N-glycosylation are discussed as follows: tunicamycin, castanospermine, and swainsonine. Although there are not yet any generally useful soluble inhibitors of O-glycosylation, the current state-of-the-art is also discussed.

### 3.5.1. Tunicamycin

Tunicamycin is an antibiotic analog of UDP-GlcNAc that blocks the formation of the lipid-linked oligosaccharide donor,  $\text{Glc}_3\text{Man}_9\text{GlcNAc}_2\text{-PP-Dol}$ , by inhibiting the first reaction in this biosynthetic pathway: the formation of  $\text{GlcNAc-PP-Dol}$  from UDP-GlcNAc and Dol-P (**Fig. 1**). Therefore, tunicamycin completely blocks core N-glycosylation by preventing the addition of the  $\text{Glc}_3\text{Man}_9\text{GlcNAc}_2$  oligosaccharide to the nascent glycoprotein.

1. To study the effect of N-glycosylation on the cell biology of APP, wash a 10-cm Petri dish containing a confluent monolayer of cells with HBBS (**Subheading 2.3.**).
2. Incubate cells for 2 h with 5  $\mu\text{g/mL}$  of tunicamycin in complete medium.
3. Metabolically label the cells, as described in **Subheading 3.1**. The labeling medium also contains 5  $\mu\text{g/mL}$  of the tunicamycin.
4. Analyze the cell-associated and secreted APP by immunoprecipitation and SDS-PAGE, as described in **Subheadings 3.2.** and **3.3.**

Results with cell-associated APP synthesized by NT2-N cells are shown in **Fig. 6**, lane 3. Because inhibition of N-glycosylation leads to significant changes in the size of APP, analysis by SDS-PAGE easily demonstrates changes in electrophoretic migration. These results are similar to those found following digestion with N-glycosidase F or Endo H (*see* **Subheadings 3.4.1.** and **3.4.2.**, and **Fig. 4**).

### 3.5.2. Castanospermine

Castanospermine is a plant alkaloid that inhibits the N-glycan processing enzymes  $\alpha$ -glucosidase I and  $\alpha$ -glucosidase II. Therefore, when cells are incubated with this inhibitor, the N-glycans on glycoproteins do not undergo processing and oligosaccharides with the structure  $\text{Glc}_3\text{Man}_{7-9}\text{GlcNAc}_2$  accumulate (**Fig. 1**).

1. To study the effect of N-glycan processing on the cell biology of APP, wash a 10-cm Petri dish containing a confluent monolayer of cells with HBBS (**Subheading 2.3.**).

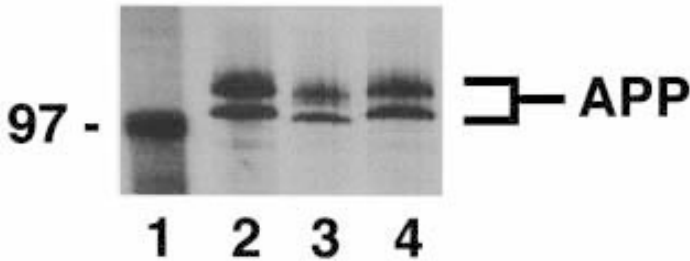


Fig. 6. The effect of soluble glycosylation inhibitors on cell-associated forms of APP. NT2-N cells were cultured in the absence of soluble glycosylation inhibitors (lane 2) or in the presence of 5  $\mu\text{g}/\text{mL}$  of tunicamycin (lane 3) or 100  $\mu\text{g}/\text{mL}$  of castanospermine (lane 4) and metabolically labeled with  $^{35}\text{S}$ -methionine. Cell-associated APP was immunoprecipitated from detergent cellular lysates using the 2493 rabbit polyclonal anti-APP antibody, and the immunoprecipitates were analyzed by SDS-PAGE and autoradiography. The migration position of the phosphorylase B standard (lane 1) is indicated on the left; the migration positions of the various APP forms is indicated on the right. Notice that both immature and mature forms of APP migrate faster by SDS-PAGE when they are synthesized in the presence of tunicamycin, which prevents N-glycosylation.

2. Incubate the cells for 2 h with 100  $\mu\text{g}/\text{mL}$  of castanospermine in complete medium.
3. Metabolically label the cells, as described in **Subheading 3.1**. The labeling medium also contains 100  $\mu\text{g}/\text{mL}$  of the inhibitor.
4. Analyze the cell-associated and secreted APP by immunoprecipitation and SDS-PAGE, as described in **Subheadings 3.2.** and **3.3**.

Results with cell-associated APP synthesized by NT2-N cells are shown in **Fig. 6**, lane 4. Because inhibition of  $\alpha$ -glucosidases does not lead to significant changes in the sizes of N-glycans, analysis by SDS-PAGE does not often demonstrate changes in electrophoretic migration. However, because castanospermine blocks N-glycan processing, if a glycoprotein normally has complex type N-glycans, then in the presence of castanospermine they will be of high-mannose type and thus will be sensitive to digestion with Endo H (*see Subheading 3.4.2.* and *refs. 40* and *41*).

### 3.5.3. Swainsonine

Swainsonine is a plant alkaloid that inhibits the N-glycan processing enzyme  $\alpha$ -mannosidase II, which is found in the Golgi apparatus. Therefore, when cells are incubated with this inhibitor, the oligosaccharides on glycoproteins cannot be processed to complex type N-glycans and, therefore, hybrid type N-glycans accumulate (**Fig. 1**).

1. To study the effect of late stages of N-glycan processing on the cell biology of APP, wash a 10-cm Petri dish containing a confluent monolayer of cells with HBBS (*see Subheading 2.3.*).
2. Incubate the cells for 2 h with 100  $\mu\text{g}/\text{mL}$  of swainsonine in complete medium.
3. Metabolically label the cells, as described in **Subheading 3.1**. The labeling medium also contains 100  $\mu\text{g}/\text{mL}$  of the inhibitor.
4. Analyze cell-associated and secreted APP by immunoprecipitation and SDS-PAGE, as described in **Subheadings 3.2.** and **3.3.**

Because inhibition of  $\alpha$ -mannosidase II does not necessarily lead to significant changes in the sizes of N-glycans, analysis by SDS-PAGE may not demonstrate changes in electrophoretic migration. However, if a glycoprotein normally has complex type N-glycans, then in the presence of swainsonine they will be of high-mannose and hybrid type and may thus be sensitive to digestion with Endo H (*see Subheading 3.4.2.* and *refs. 39–41.*).

#### 3.5.4. O-Glycosylation

In contrast to the large number of well-characterized soluble inhibitors available to study protein N-glycosylation, there are no widely used, generally applicable, soluble inhibitors of O-glycosylation. Nonetheless, over the last several years progress has begun to be made in this direction. In particular, soluble derivatives of  $\alpha\text{GalNAc}$ , such as the commercially available benzyl-, phenyl-, and *p*-nitrophenyl-N-acetyl- $\alpha$ -galactosaminides, are taken up by cells and act as competitive acceptors for the galactosyltransferase(s) that form the O-glycan structure  $\text{Gal}\beta 1-3\text{GalNAc}(\alpha 1\text{-O})\text{Ser}/\text{Thr}$  (**42**). In this way they block elongation (*i.e.*, processing) of O-glycans, thus producing glycoproteins with truncated O-glycans similar to those found with *ldld* mutant CHO cells cultured in the presence of GalNAc alone (*see Subheading 3.6.4.* and **Fig. 2**). Although these compounds have not yet been used to study the cell biology of APP, they have been successfully used to examine O-glycosylation of intestinal mucins (**42**), the insulin receptor (**43**), and galectin-1 (**44**).

Another soluble molecule, the antihuman immunodeficiency virus drug 3'-azidothymidine (*i.e.*, zidovudine or AZT), inhibits protein glycosylation in human cells by interfering with nucleotide sugar biosynthesis and subsequent transport into the Golgi apparatus (**45,46**). As such, it particularly can inhibit the incorporation of Gal and sialic acid into O-glycans. However, because these sugars are also incorporated into N-glycans and glycosphingolipids, this effect is not specific for O-glycans.

#### 3.6. Glycosylation-Deficient Cell Lines

Over the last 25 years many different glycosylation-deficient continuous cell lines have been constructed and characterized (for review, *see ref. 26*). Most of

these cell lines were derived by mutagenizing wild-type CHO cells and isolating lectin-resistant cells. The resulting cell lines have been very valuable for elucidating glycoprotein and glycolipid biosynthetic pathways, studying the function and cell biology of particular glycoproteins, and cloning and characterizing proteins important in glycoprotein biosynthesis, such as specific glycosyltransferases (47). In addition, these cell lines may be useful in biotechnology applications for constructing recombinant therapeutic proteins carrying defined oligosaccharide structures (48).

Four clonal glycosylation-deficient mutant CHO cell lines that are useful for studying glycoproteins, in general, and APP, in particular, are discussed in the following paragraphs. These include the Lec 1, Lec 2, Lec 8, and Id1D cell lines (Figs. 1 and 2). These CHO cell lines all produce low, but easily detectable, levels of endogenous, hamster APP<sub>751/770</sub> (Fig. 3 and refs. 3,4). Therefore, untransfected cells can be used to study the role of glycosylation in the cell biology of APP (4). However, because it is very easy to use standard methods to stably transfect CHO cells and clone the resulting transfectants (49), it is possible to study wild-type and mutant variants of human APP<sub>695</sub> which are expressed at high levels in the transfected cells (see Fig. 3 and refs. 3 and 4).

The cell biology of APP can be studied in these cell lines using the methods described previously: metabolic labeling (see Subheading 3.1.), immunoprecipitation (Subheadings 3.2. and 3.4.), glycosidase digestion (Subheading 3.4.), and soluble glycosylation inhibitors (Subheading 3.5.).

### 3.6.1. Lec 1

These cells have a defect in the enzyme N-acetylglucosaminyltransferase I (25). This enzyme is important in the biosynthetic pathway of N-glycans (Fig. 1). It is the key enzyme that allows the processing of high-mannose N-glycans into those of hybrid and complex type. Therefore, APP synthesized by Lec 1 cells would have only high-mannose type N-glycans and would be susceptible to cleavage by Endo H (see Subheading 3.4.2.). This enzyme defect has no effect on the biosynthesis of O-glycans.

### 3.6.2. Lec 2

These cells are defective in the transport of CMP-sialic acid into the lumen of the Golgi apparatus (50,51). Therefore, these cells are not able to incorporate sialic acid residues into O-glycans, N-glycans, or glycosphingolipids (Figs. 1 and 2). As a result, APP synthesized by these cells will be resistant to digestion with neuraminidase (Subheading 3.4.5.).

### 3.6.3. Lec 8

These cells are defective in the transport of UDP-galactose into the lumen of the Golgi apparatus (52). Therefore, these cells are not able to incorporate Gal

into O-glycans, N-glycans, or glycosphingolipids (**Figs. 1 and 2**). In addition, because most sialic acid residues are linked to Gal, the glycoproteins of these cells are substantially deficient in sialic acid and are predominantly resistant to neuraminidase digestion (**Subheading 3.4.5**).

#### 3.6.4. *Id1D*

These cells are deficient in the UDP-Gal/UDP-GalNAc 4-epimerase (**27**). As such, they are not able to transform UDP-Glc or UDP-GlcNAc into UDP-Gal or UDP-GalNAc, respectively. Thus, when they are cultured in medium containing glucose, but lacking both Gal and GalNAc (i.e., *Id1D* CM (see **Subheading 2.1**)), they are not able to synthesize any O-glycans (**Fig. 2**) and the resulting N-glycans are similar to those found with Lec 8 cells (**Fig. 1**). When *Id1D* cells are cultured in medium containing Gal alone, they are also unable to synthesize any O-glycans (**Fig. 2**), but can synthesize a normal complement of intact complex-type N-glycans (**Fig. 1**). When cultured in medium containing GalNAc alone, they can synthesize truncated O-glycans (**Fig. 2**), and their N-glycans are similar to those found with Lec 8 cells (**Fig. 2**). Finally, when cultured in the presence of both Gal and GalNAc (see **Subheading 2.1**), they synthesize a normal complement of both N- and O-glycans. In addition, because Gal and GalNAc are normal constituents of glycosphingolipids, when *Id1D* cells are cultured under restrictive conditions, the composition of their glycosphingolipids also changes.

### Notes

1. If desired, the oligosaccharides on glycoproteins can be specifically labeled using <sup>3</sup>H- or <sup>14</sup>C-labeled glucosamine or mannose (**37**). Radiolabeled mannose will be incorporated without major modifications into the N-glycans, but not the O-glycans, of mammalian glycoproteins. In contrast, following cellular uptake, glucosamine is metabolized into GlcNAc, GalNAc, and sialic acid; therefore, it will label glycosphingolipids and both the N-glycans and O-glycans of mammalian glycoproteins.
2. Alternatively, the amount of radioactivity in a given band can be quantified by a phosphorimaging technique using the IMAGEQUANT software provided with the Storm 860 phosphorimager (Molecular Dynamics, Sunnyvale, CA).

### Acknowledgments

These studies were supported in part by P01 AG11542 from the National Institutes of Health. The authors thank Drs. M. Krieger, B. Greenberg, and V. M. Y. Lee for providing valuable reagents. We also thank Drs. V. M. Y. Lee and J. Q. Trojanowski for encouraging us to study Alzheimer's disease and for their continuous advice and support.

## References

1. Opdenakker, G., Rudd, P. M., Ponting, C. P., and Dwek, R. A. (1993) Concepts and principles of glycobiology. *FASEB J.* **7**, 1330–1337.
2. Varki, A. (1993) Biological roles of oligosaccharides: all of the theories are correct. *Glycobiology* **3**, 97–130.
3. Pahlsson, P., Shakin-Eshleman, S. H., and Spitalnik, S. L. (1992) N-linked glycosylation of  $\beta$ -amyloid precursor protein. *Biochem. Biophys. Res. Commun.* **189**, 1667–1673.
4. Pahlsson, P. and Spitalnik, S. L. (1996) The role of glycosylation in synthesis and secretion of  $\beta$ -amyloid precursor protein by Chinese hamster ovary cells. *Arch. Biochem. Biophys.* **331**, 177–186.
5. Yazaki, M., Tagawa, K., Maruyama, K., Sorimachi, H., Tsuchiya, T., Ishiura, S., and Suzuki, K. (1996) Mutation of potential N-linked glycosylation sites in the Alzheimer's disease amyloid precursor protein (APP). *Neurosci. Lett.* **221**, 57–60.
6. Saito, F., Yanagisawa, K., and Miyatake, T. (1993) Soluble derivatives of beta/A4 amyloid protein precursor in human cerebrospinal fluid are both N- and O-glycosylated. *Brain Res.* **19**, 171–174.
7. Tomita, S., Kirino, Y., and Suzuki, T. (1998) Cleavage of Alzheimer's amyloid precursor protein (APP) by secretases occurs after O-glycosylation of APP in the protein secretory pathway. Identification of intracellular compartments in which APP cleavage occurs without using toxic agents that interfere with protein metabolism. *J. Biol. Chem.* **273**, 6277–6284.
8. Graebert, K. S., Popp, G. M., Kehle, T., and Herzog, V. (1995) Regulated O-glycosylation of the Alzheimer beta-A4 amyloid precursor protein in thyrocytes. *Eur. J. Cell. Biol.* **66**, 39–46.
9. Palmert, M. R., Podlisny, M. B., Witker, D. S., Oltersdorf, T., Younkin, L. H., Selkoe, D. J., and Younkin, S. G. (1989) The beta-amyloid protein precursor of Alzheimer disease has soluble derivatives found in human brain and cerebrospinal fluid. *Proc. Natl. Acad. Sci. USA* **86**, 6338–4632.
10. Weidemann, A., Konig, G., Bunke, D., Fischer, P., Salbaum, J. M., Masters, C. L., and Beyreuther, K. (1989) Identification, biogenesis, and localization of precursors of Alzheimer's disease A4 amyloid protein. *Cell* **57**, 115–126.
11. Oltersdorf, T., Ward, P. J., Kenriksson, T., Beattie, E. C., Neve, R., Lieberburg, I., and Fritz, L. C. (1990) The Alzheimer amyloid precursor protein. Identification of a stable intermediate in the biosynthetic/degradative pathway. *J. Biol. Chem.* **265**, 4492–4497.
12. Shioi, J., Anderson, J. P., Ripellino, J. A., and Robakis, N. K. (1992) Chondroitin sulfate proteoglycan form of the Alzheimer's beta-amyloid precursor. *J. Biol. Chem.* **267**, 13,819–13,822.
13. Pangalos, M. N., Shioi, J., and Robakis, N. K. (1995) Expression of the chondroitin sulfate proteoglycans of amyloid precursor (appican) and amyloid precursor-like protein 2. *J. Neurochem.* **65**, 762–769.
14. Kornfeld, R. and Kornfeld, S. (1985) Assembly of asparagine-linked oligosaccharides. *Annu. Rev. Biochem.* **54**, 631–664.

15. Shakin-Eshleman, S. H., Kasturi, L., Spitalnik, S. L., and Mellquist, J. (1998) The amino acid following an Asn-X-Ser/Thr sequon is an important determinant of N-linked core-glycosylation efficiency. *Biochemistry* **37**, 6833–6837.
16. Shakin-Eshleman, S. H. and Spitalnik, S. L. (1993) The role of glycosylation at individual sequons in the cell surface expression of glycoproteins. *Trends Glycosci. Glycotechnol.* **5**, 355–368.
17. Shakin-Eshleman, S. H., Spitalnik, S. L., and Kasturi, L. (1996) The amino acid at the X position of an Asn-X-Ser sequon is an important determinant of N-linked core glycosylation efficiency. *J. Biol. Chem.* **271**, 6363–6366.
18. Nishikawa, A., Gregory, W., Frenz, J., Cacia, J., and Kornfeld, S. (1997) The phosphorylation of bovine DNase I Asn-linked oligosaccharides is dependent on specific lysine and arginine residues. *J. Biol. Chem.* **272**, 19,408–19,412.
19. Mengeling, B. J., Manzella, S. M., and Baenziger, J. U. (1995) A cluster of basic amino acids within an alpha-helix is essential for alpha-subunit recognition by the glycoprotein hormone N-acetylgalactosaminyltransferase. *Proc. Natl. Acad. Sci. USA* **92**, 502–506.
20. Smith, P. L. and Baenziger, J. U. (1992) Molecular basis of recognition by the glycoprotein hormone-specific N-acetylgalactosamine-transferase. *Proc. Natl. Acad. Sci. USA* **89**, 329–333.
21. Carraway, K. L. and Hull, S. R. (1991) Cell surface mucin-type glycoproteins and mucin-like domains. *Glycobiology* **1**, 131–138.
22. Clausen, H. and Bennett, E. P. (1996) A family of UDP-GalNAc:polypeptide N-acetylgalactosaminyl-transferases control the initiation of mucin-type O-linked glycosylation. *Glycobiology* **6**, 635–646.
23. Nehrke, K., Ten Hagen, K. G., Hagen, F. K., and Tabak, L. A. (1997) Charge distribution of flanking amino acids inhibits O-glycosylation of several single-site acceptors in vivo. *Glycobiology* **7**, 1053–1060.
24. Wilson, I. B. H., Gavel, Y., and Von Heijne, G. (1991) Amino acid distributions around O-linked glycosylation sites. *Biochem. J.* **275**, 529–534.
25. Stanley, P., Narasimhan, S., Siminovitich, L., and Schachter, H. (1975) Chinese hamster ovary cells selected for resistance to the cytotoxicity of phytohemagglutinin are deficient in a UDP-N-acetylglucosamine-glycoprotein N-acetylglucosaminyltransferase activity. *Proc. Natl. Acad. Sci. USA* **72**, 3323–3327.
26. Stanley, P. (1984) Glycosylation mutants of animal cells. *Annu. Rev. Genet.* **18**, 525–552.
27. Kingsley, D. M., Kozarsky, K. F., Hobbie, L., and Krieger, M. (1986) Reversible defects in O-linked glycosylation and LDL receptor expression in a UDP-Gal/UDP-GalNAc 4-epimerase deficient mutant. *Cell* **44**, 749–759.
28. Remaley, A. T., Ugorski, M., Litzky, L., Wu, N., Burger, S. R., Moore, J., et al. (1991) Expression of human glycoporphin A cDNA in wild type and glycosylation deficient Chinese hamster ovary cells. *J. Biol. Chem.* **266**, 24,176–24,183.
29. Matzuk, M. M., Krieger, M., Corless, C. L., and Boime, I. (1987) Effects of preventing O-glycosylation on the secretion of human chorionic gonadotropin in Chinese hamster ovary cells. *Proc. Natl. Acad. Sci. USA* **84**, 6354–6358.

30. Andrews, P. W. (1984) Retinoic acid induces neuronal differentiation of a cloned human embryonal carcinoma cell line in vitro. *Dev. Biol.* **103**, 285–293.
31. Andrews, P. W., Damjanov, I., Simon, D., Banting, G. S., Carlin, C., Dracopoli, C., and Fogh, J. (1984) Pluripotent embryonal carcinoma clones derived from the human teratocarcinoma cell line Tera-2. *Lab. Invest.* **50**, 147–162.
32. Wertkin, A. M., Turner, R. S., Pleasure, S. J., Golde, T. E., Younkin, S. G., Trojanowski, J. Q., and Lee, V. M. Y. (1993) Human neurons derived from a teratocarcinoma cell line express solely the 695-amino acid amyloid precursor protein and produce intracellular beta-amyloid or A4 peptides. *Proc. Natl. Acad. Sci. USA* **90**, 9513–9517.
33. Pleasure, S. J., Page, C., and Lee, V. M. Y. (1992) Pure, postmitotic, polarized human neurons derived from NTera 2 cells provide a system for expressing exogenous proteins in terminally differentiated neurons. *J. Neurosci. Res.* **12**, 1802–1815.
34. Bigbee, W. L., Vanderlaan, M., Fong, S. S. N. and Jensen, R. H. (1983) Monoclonal antibodies specific for the M and N forms of human glycoporphin A. *Mol. Immunol.* **20**, 1353–1362.
35. Blackall, D. P., Ugorski, M., Pålsson, P., Shakin-Eshleman, S. H., and Spitalnik, S. L. (1994) A molecular biological approach to study the fine specificity of antibodies directed to the MN human blood group antigens. *J. Immunol.* **152**, 2241–2247.
36. Czerwinski, M., Siemaszko, D., Siegel, D. L., and Spitalnik, S. L. (1998) Only selected light chains combine with a given heavy chain to confer specificity for a model glycopeptide antigen. *J. Immunol.* **160**, 4406–4417.
37. Varki, A. (1991) Radioactive tracer techniques in the sequencing of glycoprotein oligosaccharides. *FASEB J.* **5**, 226–235.
38. Elbein, A. D. (1991) Glycosidase inhibitors: inhibitors of N-linked oligosaccharide processing. *FASEB J.* **5**, 3055–3063.
39. Fuhrmann, U., Bause, E., and Ploegh, H. (1985) Inhibitors of oligosaccharide processing. *Biochim. Biophys. Acta* **825**, 95–110.
40. Wojczyk, B., Shakin-Eshleman, S. H., Doms, R. W., Xiang, Z. Q., Ertl, H. C. J., Wunner, W. H., and Spitalnik, S. L. (1995) Influence of N-glycan processing on secretion of a secreted form of rabies virus glycoprotein. *Biochemistry* **34**, 2599–2609.
41. Wojczyk, B., Stwora-Wojczyk, M., Shakin-Eshleman, S. H., Wunner, W. H., and Spitalnik, S. L. (1997) The role of site-specific N-glycosylation in secretion of soluble forms of rabies virus glycoprotein. *Glycobiology* **8**, 121–130.
42. Kuan, S. F., Byrd, J. C., Basbaum, C., and Kim, Y. S. (1989) Inhibition of mucin glycosylation by aryl-N-acetyl-alpha-galactosaminides in human colon cancer cells. *J. Biol. Chem.* **264**, 19,271–19,277.
43. Collier, E. and Gordon, P. (1991) O-linked oligosaccharides on insulin receptor. *Diabetes* **40**, 197–203.
44. Perillo, N. L., Pace, K. E., Seilhamer, J. J., and Baum, L. G. (1995) Apoptosis of T cells mediated by galectin-1. *Nature* **378**, 736–739.

45. Yan, J. P., Ilsley, D. D., Frohlick, C., Steet, R., Hall, E. T., Kuchta, R. D., and Melancon, P. (1995) 3'-Azidothymidine (zidovudine) inhibits glycosylation and dramatically alters glycosphingolipid synthesis in whole cells at clinically relevant concentrations. *J. Biol. Chem.* **270**, 22,836–22,841.
46. Hall, E. T., Yan, J. P., Melancon, P., and Kuchta, R. D. (1994) 3'-Azido-3'-deoxythymidine potently inhibits protein glycosylation. *J. Biol. Chem.* **269**, 14,355–14,358.
47. Stanley, P. and Ioffe, E. (1995) Glycosyltransferase mutants: key to new insights in glycobiology. *FASEB J.* **9**, 1436–1444.
48. Stanley, P. (1992) Glycosylation engineering. *Glycobiology* **2**, 99–107.
49. Burger, S. R., Remaley, A. T., Danley, J. M., Moore, J., Muschel, R. J., Wunner, W. H., and Spitalnik, S. L. (1991) Stable expression of rabies virus glycoprotein in Chinese hamster ovary cells. *J. Gen. Virol.* **72**, 359–367.
50. Deutscher, S. L., Nuwayhid, H., Stanley, P., Barak Briles, E. I., and Hirschberg, C. B. (1984) Translocation across Golgi vesicle membranes: a CHO glycosylation mutant deficient in CMP-sialic acid transport. *Cell* **39**, 295–299.
51. Berninsone, P., Eckhardt, M., Gerardy-Schahn, R., and Hirschberg, C. B. (1997) Functional expression of the murine Golgi CMP-sialic acid transporter in *Saccharomyces cerevisiae*. *J. Biol. Chem.* **272**, 12,616–12,619.
52. Deutscher, S. L. and Hirschberg, C. B. (1986) Mechanism of galactosylation in the Golgi apparatus. A Chinese hamster ovary cell mutant deficient in translocation of UDP-galactose across Golgi vesicle membranes. *J. Biol. Chem.* **261**, 96–100.

## Using an Amyloid Precursor Protein (APP) Reporter to Characterize $\alpha$ -Secretase

Susan Boseman Roberts

### 1. Introduction

Human genetic studies suggest decreasing amyloid peptide ( $A\beta$ ) levels in the brain could alter the course of Alzheimer's disease (AD) (1-4). Proteolytic cleavages govern the level of  $A\beta$  generated from the amyloid precursor protein (APP).  $\beta$ - and  $\gamma$ -cleavages at the amino and carboxyl termini of  $A\beta$  produce amyloidogenic peptides; in contrast,  $\alpha$ -cleavage within the  $A\beta$  domain destroys the amyloidogenic potential of APP. The proteases responsible for these cleavages have not been identified.

A basic understanding of the cellular mechanisms that regulate APP processing and the proteases that modulate  $A\beta$  production could help us identify novel therapeutic targets for the treatment of AD. An APP reporter protein was constructed to facilitate study of the metabolic fate of APP and to develop assays to screen for inhibitors and activators of the cellular proteases that generate  $A\beta$ . Tagging a protein with an enzymatically active reporter enhances detection when the signal from a single molecule is amplified. The human placental alkaline phosphatase protein (HPLAP) offers distinct advantages as a reporter for APP processing (5):

1. The enzymatic activity of HPLAP is extremely stable, and it can be distinguished from endogenous cellular phosphatases because, unlike cellular phosphatases, HPLAP is active in the presence of homoarginine and after heat treatment.
2. The glycosylation pattern and size of the HPLAP protein are similar to APP.
3. HPLAP has a signal sequence, and the wild type protein is anchored in the membrane.
4. A truncated version of HPLAP was engineered to be enzymatically active and constitutively secreted (6).

From: *Methods in Molecular Medicine, Vol. 32: Alzheimer's Disease: Methods and Protocols*  
Edited by: N. M. Hooper © Humana Press Inc., Totowa, NJ

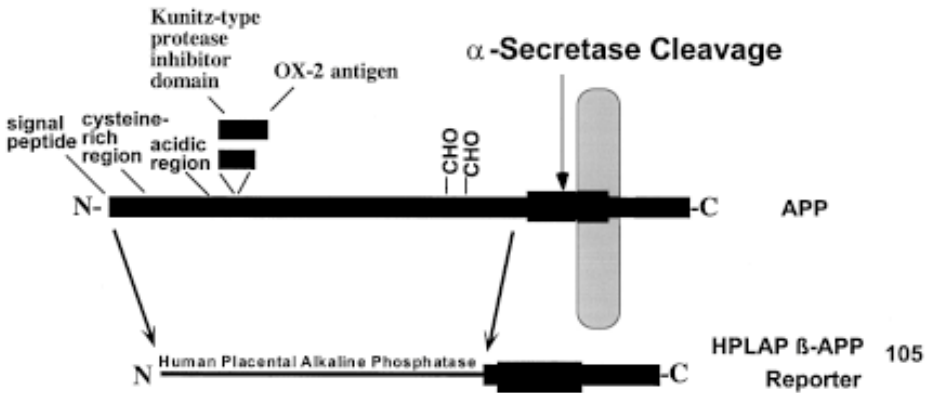


Fig. 1. HPLAP- $\beta$ -APP<sub>105</sub> reporter construct. A schematic representation of APP indicates the complexity of the gene. Splice variants generate protein products of different sizes. A gene fragment encoding the amino terminus of human placental alkaline phosphatase was substituted for the amino terminus of APP in the HPLAP- $\beta$ -APP<sub>105</sub> reporter.

5. Antibodies recognizing different epitopes of HPLAP have been developed and are commercially available.

Fusing HPLAP to the carboxyl terminal 105 amino acids of APP yielded a substrate that was cleaved by cells at the  $\alpha$ -cleavage site, but not at the  $\beta$ -cleavage site, making it a particularly good substrate to characterize  $\alpha$ -secretase activity (**Fig. 1**). The usefulness of the fusion protein as a model for APP was confirmed by pulse-chase analysis that established it followed the same processing pathway as APP (S. Roberts, unpublished data; 7). Sequence analysis established the cleavage site of the fusion protein was at the same peptide bond as native APP (8,9).

A cell-free assay that detects site-specific cleavage of the membrane-embedded APP reporter at the  $\alpha$ -secretase site was developed. To detect  $\alpha$ -secretase cleavage, crude membranes were isolated from an H4 neuroglioma cell line expressing the HPLAP- $\beta$ -APP<sub>105</sub> fusion protein. The membranes were incubated at 37°C, pH 7.2, for 90 min, and the cleaved fragments were analyzed by Western blot. Specific cleavage of the precursor in the cell-free system generated products that appeared by size and antibody binding to be the same as the products of HPLAP- $\beta$ -APP<sub>105</sub> produced by H4 cells in culture (**Fig. 2A**). The level of cleaved product increased approximately fivefold compared to the control sample incubated at 0°C. Furthermore, the fully glycosylated precursor showed a concomitant quantitative decrease in intensity, showing it is cleaved to form the product (**Fig 2A**).

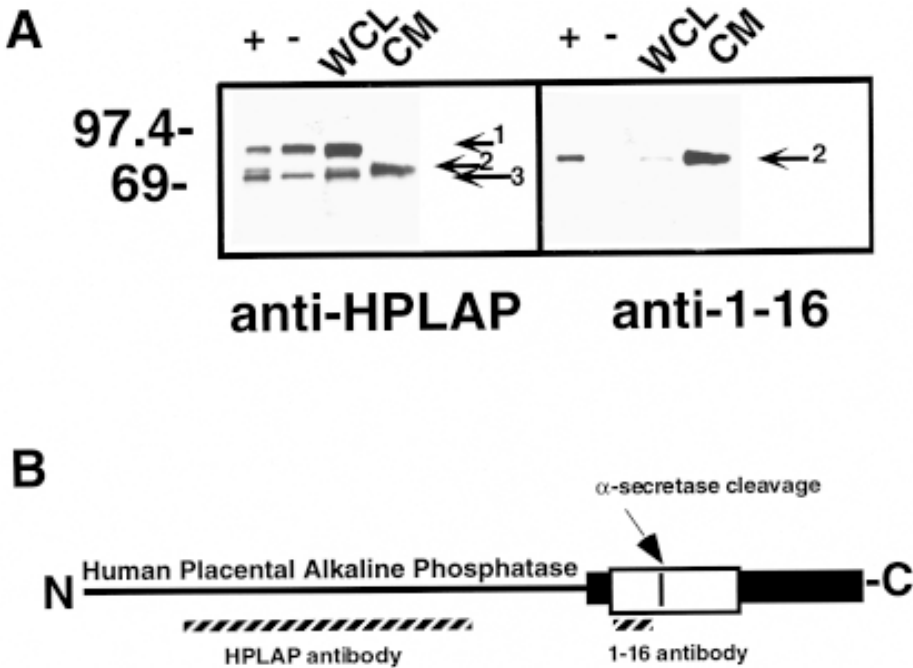


Fig. 2. Processing of HPLAP- $\beta$ -APP reporter construct. HPLAP- $\beta$ -APP fusion protein is cleaved by whole cells and in the cell-free assay into products that are similar in size and antibody reactivity. (A) The western blots are from HPLAP- $\beta$ -APP<sub>105</sub> cleaved by isolated membranes and by cells in culture: (+) membranes incubated at 37°C in the cell-free assay; (-) membranes incubated at 0°C in the cell-free assay; WCL prepared from cells expressing HPLAP- $\beta$ -APP<sub>105</sub>; CM from cells expressing HPLAP- $\beta$ -APP<sub>105</sub>. Fragment 1: N- plus O-glycosylated HPLAP- $\beta$ -APP; fragment 2, cleaved HPLAP- $\beta$ -APP; fragment 3, immature N-glycosylated HPLAP- $\beta$ -APP. (B) The epitopes within the reporter recognized by the antibodies are indicated by the dashed lines.

Antibody specific for the reporter (anti-HPLAP) detected full-length precursors (N- plus O-glycosylated as well as immature N-glycosylated; **Fig. 2A**, fragments 1 and 3) and cleaved product (**Fig. 2A**, fragment 2) similar to the pattern previously described for APP expressed in H4 cells (7). Antibody specific for the amino terminus of A $\beta$  (anti-1-16) detected the  $\alpha$ -cleaved product (**Fig. 2A**, fragment 2). Preference for the cleaved product indicates the A $\beta$ <sub>1-16</sub> epitope recognized by this antibody is unmasked by cleavage. The identity of each reporter fragment was assigned based on the size predicted from the sequence of the fusion protein, the use of multiple antibodies to detect the fragments, and the fact that the fragments are not detected in untransfected H4 cells (10).

**Table 1**  
**Inhibitor Profile**

Reagent tested	Concentration	Cleavage (%)
No addition	Positive control	100
Serine protease inhibitors		
PMSF	1.0 mM	100 ± 13
Aprotinin	5.0 µg/mL	91 ± 15
Cysteine protease inhibitors		
Leupeptin	100 µM	75 ± 13
E-64	10 µM	82 ± 9
Aspartylprotease inhibitor		
Pepstatin	50 µg/mL	70 ± 12
Metalloprotease inhibitors		
1,10 phenanthroline	5–10 mM	6 ± 9
EDTA	0.125–10 mM	56 ± 16
EGTA	0.125–10 mM	58 ± 7
DTT	2.0–5 mM	0 ± 0
2,2'-bipyridine	10 mM	30 ± 13
Imidazole	5–10 mM	66 ± 13
Phosphoramidon	0.2–3.0 mg/mL	100 ± 7
α2-macroglobulin	400 µg/mL	95 ± 35

The *maximum* effect observed is reported in column 3 of the table. Membranes were incubated with the test agent for 15 min on ice and shifted to 37°C for 90 min. The effects on cleavage were determined from Western blots. Average values are shown in the table ± standard deviations from two to four determinations.

To determine the protease class to which α-secretase belongs, a panel of protease inhibitors was tested. Cleavage was dramatically inhibited by 1,10 phenanthroline (5–10 mM), a hydrophobic compound and chelator, and by dithiothreitol (1 mM), but not by inhibitors specific for serine, cysteine, or aspartyl proteases (**Table 1**) (*10*). Other chelators (EDTA, EGTA) and another general metalloprotease inhibitor 2,2' bipyridine also inhibited cleavage approx 50%. Based on these results we concluded that α-secretase is a metalloendopeptidase. A recent report demonstrated inhibition of α-secretase in whole cells with hydroxamic acid-based zinc metalloprotease inhibitors (*11*).

To determine whether the proteolytic activity was a membrane-associated protein, membrane vesicles were washed with various concentrations of salt and detergents. Neither hypotonic nor hypertonic treatment with KCl or NaCl removed the cleavage activity (**Table 2**). Washing membranes with detergents such as Tween-80 (0.1%) solubilized approx 50% of the total protein, but did not affect cleavage. The results show that α-secretase is tightly associated with the membrane. A membrane association of α-secretase is consistent with

**Table 2**  
**Membrane Stability of the Cleavage Activity**

Wash	Concentration	Cleavage (%)
No wash	Positive control	100
Nonisotonic		
NaCl	1 M	102 $\pm$ 23
KCl	1 M	98 $\pm$ 18
HEPES or Tris-HCl	0.03 M	100 $\pm$ 0
Detergent		
Tween-80 (HLB 15.0)	1.0%	92 $\pm$ 4

Crude membranes were added to 10 vol of the ice-cold wash agent (e.g., 1 M salt or detergent in 30 mM HEPES, pH 7.2) and incubated for 15 min on ice. Membranes were collected by centrifugation at 25,000g for 15 min at 4°C. Washed membranes were reconstituted in the original volume of assay buffer and assayed as described in **Subheading 3**.

mutation data that suggest the membrane may be important in specifying the cleavage site of APP (**12–14**).

Many reports have identified proteases of various classes that cleave soluble synthetic peptides containing the amino acid sequence at the  $\alpha$ -secretase cleavage site (**9,15–19**); however, this strategy demonstrates cleavage of a protein precursor anchored in the membrane. The strength of this approach is that specific cleavage of APP at the  $\alpha$ -secretase site is accomplished by a protease colocalized with the APP precursor. Membrane fractions washed free of soluble proteins and loosely associated membrane proteins were completely competent for cleavage. The N-glycosylated form of the precursor, constant throughout the incubation, is not a substrate for the cleavage. This observation is consistent with results that show  $\alpha$ -secretase cleavage occurs after translocation through the trans-Golgi complex (after O-glycosylation and sulfation; **20**) and suggests preliminary processing of the precursor is essential.

Different APP fusion proteins containing reporters have been used to determine additional characteristics of APP processing. An HPLAP reporter containing the carboxyl terminal 164 amino acids of APP was used to characterize the effect of protein kinase C (PKC) activation on  $\alpha$ - and  $\beta$ -secretase cleavage (**21**). The study showed that  $\alpha$ -secretase cleavage increased with a concomitant decrease in  $\beta$ -secretase cleavage when PKC was stimulated using phorbol ester. The same reporter containing a specific mutation near the  $\beta$ -secretase cleavage site (**22**) was used to demonstrate a shift from  $\alpha$ -cleavage to  $\beta$ -cleavage in mutant APP (**23**). A horseradish peroxidase (HRP) fusion protein containing the carboxyl terminal 107 amino acids of APP was used to study secretion of APP in polarized cells (**24**). The results demonstrated appropriate sorting of APP to the basolateral surface requires amino acid determinants in the

extracellular and cytoplasmic domains of APP. Reporters (1) provide a sensitive and quantitative measure of expression when experimental cell lines transfected with APP recombinants are developed; (2) provide a sensitive and quantitative measure of cleavage products; and (3) permit experimental constructs to be distinguished from endogenous APP.

The method of analysis and the reagents used to characterize the  $\alpha$ -secretase cleavage activity (the anti-1–16 antibody and the HPLAP-APP<sub>105</sub> substrate) focused the analysis on cleavage at Lys<sup>16</sup> of the A $\beta$  domain. We detected a similar pattern of cleavage and inhibition in a membrane fraction prepared from H4 cells expressing APP<sub>751</sub>, a native amyloid precursor protein (25). This result further confirms the reliability of the reporter for characterizing  $\alpha$ -secretase. This system provides a basis for the isolation and identification of the protease(s).

## 2. Materials

1. The human placental alkaline phosphatase- $\beta$ -amyloid precursor protein reporter: A reporter construct was made by fusing the cDNA that encodes the carboxy terminal 105 amino acids of APP to a gene fragment encoding the amino terminal 495 amino acids of human placental alkaline phosphatase (HPLAP) (Fig. 1). The HPLAP fragment, engineered to be constitutively secreted (6), was fused to an APP fragment containing five amino acids N-terminal to the A $\beta$  domain, the entire A $\beta$  domain, and the cytoplasmic domain. The reporter encodes a fusion protein that is anchored in the membrane by the transmembrane domain of APP. Active alkaline phosphatase is produced and secreted by cells expressing the construct. We have found the reporter to be a faithful model system to study APP metabolism (10,21,23,26,27). Secreted human placental alkaline phosphatase constructs are available from Clontech (6043-1).
2. Antibodies: Commercially available (DAKO, Carpinteria, CA) polyclonal rabbit antiserum and a monoclonal antibody (8B6) specific for human placental alkaline phosphatase (anti-HPLAP) detect nothing in whole cell lysates or conditioned medium from untransfected human neuroglioma (H4) cells. The A $\beta$ <sub>1–16</sub> antiserum directed against the A $\beta$ -peptide epitope Asp<sup>1</sup> to Lys<sup>16</sup> (amino acids 597–612 of APP<sub>695</sub>) detects  $\alpha$ -secretase cleaved product and has been described previously (8).
3. Cells and cell membranes: H4 human neuroglioma cells (American Type Culture Collection HTB 148) stably transfected with pHPLAP- $\beta$ -APP<sub>105</sub> were grown in selection medium containing Dulbecco's modified Eagle's medium (DMEM), 10% fetal bovine serum, G418 (100  $\mu$ g/mL), penicillin/streptomycin (50 U/mL), and glutamine (2 mM). Membranes containing  $\alpha$ -secretase and the HPLAP- $\beta$ -APP reporter were prepared from these cells.
4. Membrane preparation and wash buffer: 0.25 M Sucrose/0.02 M HEPES, pH 7.2. Some membranes were washed with 1 M salt or detergent (see Note 1) in 30 mM HEPES, pH 7.2.
5. Membrane suspension and storage buffer: 0.02 M HEPES, pH 7.2/20% glycerol.
6. Cleavage assay buffer: 30 mM Tris-HCl, pH 7.2.

7. Whole-cell lysate (WCL) buffer: 1% Triton X-100, 0.1% sodium dodecyl sulfate, 0.5% deoxycholate, 0.02 M Tris-HCl, pH 8.3, 0.1 M NaCl.

### 3. Methods

#### 3.1. Generating a Cell Line Expressing HPLAP- $\beta$ -APP105

1. Transfect plasmid DNA encoding the HPLAP- $\beta$ -APP reporter construct into H4 cells using the calcium phosphate method (28).
2. Grow colonies from transfected cultures selected in G418.
3. Evaluate stable cell lines for expression by measuring the level of alkaline phosphatase activity in the culture medium using nitrophenylphosphate as the substrate (6).

#### 3.2. Demonstrating the Reporter Behaves Like Wild-Type APP

The site of cellular cleavage of the fusion protein was shown by immunological analysis to be near Lys<sup>16</sup> the same site as endogenous APP (see Note 2). To prove the site was the same, the amino acid sequence of the cleaved product was determined.

1. Grow cells stably expressing pHPLAP- $\beta$ -APP<sub>105</sub> in UltraCulture (Biowhitaker, Walkersville, MD), a serum-free medium, at 37°C.
2. Remove conditioned medium (CM) from the cultures and add phenylmethylsulfonyl fluoride (0.5 mM).
3. Centrifuge the CM at 10,000g to remove debris, freeze in liquid nitrogen, and store at -70°C.
4. Isolate the fusion protein in the CM by affinity chromatography using a monoclonal antibody specific for human placental alkaline phosphatase coupled to protein A Agarose (Sigma, St. Louis, MO).
5. Determine the carboxy terminal sequence of the purified protein using carboxypeptidase Y release of amino acids (10).

#### 3.3. Production and Characterization of APP Antibodies

Rabbit polyclonal antibody was made from A $\beta$ <sub>1-16</sub> peptide coupled to keyhole limpet hemocyanin and emulsified in Freund's adjuvant for immunizations (29). Specificity of the antibody was shown by competition (see Note 3). Aliquots of antiserum diluted 1:1000 were preincubated with 2, 10, 40, or 80  $\mu$ g/mL peptide (APP<sub>659-695</sub> or APP<sub>597-637</sub>) for 16 h at 4°C. The preadsorbed antiserum was used to probe Western blots (30). The protein band detected by the antibody was competed by the immunizing peptide under conditions where an unrelated peptide had no effect on the signal.

#### 3.4. Isolation of Membranes

1. Wash cells (10<sup>8</sup>) grown in T175 flasks three times with phosphate-buffered saline and twice with ice-cold sucrose/HEPES, then scrape into a minimal volume (1.0 mL/flask) of ice-cold sucrose/HEPES.

2. Homogenize a pool of scraped cells in 35 mL of buffer in a Dounce glass/glass homogenizer (B pestle, 7 strokes).
3. Centrifuge the homogenate at 700g for 7 min in a general purpose centrifuge equipped with a swinging bucket rotor.
4. Decant the supernatant and save on ice.
5. Resuspend the pellet containing nuclei and unbroken cells in 20 mL sucrose/HEPES, Dounce 7× (approx 95% lysis), and centrifuge the suspension at 700g for 7 min.
6. Discard the nuclear pellet (approx 0.3 mL; clear in appearance).
7. Combine the supernatants and recentrifuge for 7 min at 1000g.
8. Use the postnuclear supernatant (PNS) from this centrifugation to prepare membrane fractions.
9. Centrifuge the PNS at 2000g × 30 min at 4°C.
10. Centrifuge the resulting supernatant at 12,000g for 30 min at 4°C.
11. Discard the supernatant and resuspend the pellet in 1.0–2.0 mL glycerol/HEPES for a final protein concentration of 1–2 mg/mL.
12. Freeze the membrane suspensions in liquid nitrogen and store in aliquots at –80°C. All fractions from the membrane preparation were evaluated for cleavage activity. The membrane fraction from the 12,000g pellet was the most active in the cleavage assay.

### **3.5. Detergent Wash of Membranes**

1. Add crude membranes to 10 vol of an ice-cold membrane wash containing salt or detergent and incubate for 15 min on ice.
2. Collect membranes by centrifugation at 25,000g for 15 min at 4°C.
3. Reconstitute washed membranes in the original volume and assay as described in **Subheading 3.7**.

### **3.6. Analyzing the Cleavage**

1. To assay for  $\alpha$ -secretase cleavage, dilute crude membrane preparations fivefold in ice-cold assay buffer containing the protease inhibitors to be tested (*see Note 3*).
2. Transfer the reaction mixture (50  $\mu$ L) to 37°C and incubate for 90 min (*see Note 4*).
3. Stop the reaction by adding an equal quantity of 2× sodium dodecyl sulfate/polyacrylamide gel (SDS-PAGE) electrophoresis loading buffer and heating at 100°C for 5 min.
4. Fractionate aliquots (20  $\mu$ L) by SDS-PAGE under reducing conditions on 8% polyacrylamide gels containing Tris/glycine buffer.
5. Transfer fractionated protein electrophoretically to Immobilon-P (Millipore Corp. Bedford, MA), and probe the blots with antibody.
6. Detect antibody binding by chemiluminescence (*31*).

### **3.7. Demonstrating the Cleavage Generated in Cell-Free Assay is the Same Made by Cells**

1. Incubate membrane fractions containing the HPLAP- $\beta$ -APP<sub>105</sub> reporter at 37°C and 0°C for 90 min.

2. Stop the reaction by adding SDS-PAGE loading buffer.
3. Collect and prepare WCL and CM from cells grown at 37°C.
4. Fractionate the samples (WCL, CM, and cell-free cleavage assay) by SDS-PAGE and analyze by Western blot using anti-HPLAP and anti-1–16 antibodies (**Fig. 2A**).
5. Compare the size and antibody reactivity of each fragment to determine if cleavage in the isolated membranes is the same as cleavage in whole cells.

#### 4. Notes

1. A fusion protein must be extensively characterized for the intended use. For example, HPLAP- $\beta$ -APP<sub>105</sub> would not be an effective substrate for investigating  $\beta$ -secretase since cleavage at the  $\beta$ -site is ineffective.
2. Antibodies can crossreact with epitopes unrelated to the protein of interest and must be characterized thoroughly by competition studies.
3. Stock solutions of protease inhibitors should be prepared and stored according to the suppliers instructions. Since different inhibitor stocks require various solvents, include a control for each solvent.
4. It is important to use detergents at concentrations above the critical micelle concentration.
5. The optimal time, temperature, pH and buffer for cleavage must be determined empirically.

#### References

1. Selkoe, D. J. (1997) Images in neuroscience. Alzheimer's disease: from genes to pathogenesis. *Am. J. Psychiatry* **154**, 1198–1199.
2. Selkoe, D. J. (1997) Alzheimer's disease: genotypes, phenotypes, and treatments. *Science* **275**, 630–631.
3. Schenk, D. B., Rydel, R. E., May, P., Little, S., Panetta, J., Lieberburg, I., and Sinha, S. (1995) Therapeutic approaches related to amyloid- $\beta$  and Alzheimer's disease. *J. Med. Chem.* **38**, 4141–4154.
4. Scheuner, D., Eckman, C., Jensen, M., Song, X., Citron, M., Suzuki, N., et al. (1996) Secreted amyloid  $\beta$ -protein similar to that in the senile plaques of Alzheimer's disease is increased in vivo by the presenilin 1 and 2 and APP mutations linked to familial Alzheimer's disease. *Nat. Med.* **2**, 864–870.
5. Cullen, B. R. and Malim, M. H. (1992) Secreted placental alkaline phosphatase as a eukaryotic reporter. *Methods Enzymol.* **216**, 362–368.
6. Berger, J., Hauber, J., Geiger, R., and Cullen, B. R. (1988) Secreted placental alkaline phosphatase: a powerful new quantitative indicator of gene expression in eukaryotic cells. *Gene* **66**, 1–10.
7. Kuentzel, S. L., Ali, S. M., Altman, R. A., Greenberg, B. D., and Raub, T. J. (1993) The Alzheimer  $\beta$ -amyloid protein precursor/protease nexin-II is cleaved by secretase in a trans-Golgi secretory compartment in human neuroglioma cells. *Biochem. J.* **295**, 367–378.
8. Anderson, J. P., Esch, F. S., Keim, P. S., Sambamurti, K., Lieberburg, I., and Robakis, N. K. (1991) Exact cleavage site of Alzheimer amyloid precursor in neuronal PC-12 Cells. *Neurosci. Lett.* **128**, 126–128.

9. Esch, F. S., Keim, P. S., Beattie, E. C., Blacher, R. W., Culwell, A. R., Oltersdorf, T., et al. (1990) Cleavage of amyloid  $\beta$  peptide during constitutive processing of its precursor. *Science* **248**, 1122–1124.
10. Roberts, S. B., Ripellino, J. A., Ingalls, K. M., Robakis, N. K., and Felsenstein, K. M. (1994) Non-amyloidogenic cleavage of the  $\beta$ -amyloid precursor protein by an integral membrane metalloendopeptidase. *J. Biol. Chem.* **269**, 3111–3116.
11. Parvathy, S., Hussain, I., Karran, E. H., Turner, A. J., and Hooper, N. M. (1998) Alzheimer's amyloid precursor protein  $\alpha$ -secretase is inhibited by hydroxamic acid-based zinc metalloprotease inhibitors: similarities to the angiotensin converting enzyme secretase. *Biochemistry*, **37**, 1680–1685.
12. Hooper, N. M. and Turner, A. J. (1995) Specificity of the Alzheimer's amyloid precursor protein  $\alpha$ -secretase. *Trends Biochem. Sci.* **20**, 15–16.
13. Maruyama, K., Kametani, F., Usami, M., Yamao-Harigaya, W., and Tanaka, K. (1991) "Secretase," Alzheimer amyloid protein precursor secreting enzyme is not sequence specific. *Biochem. Biophys. Res. Commun.* **179**, 1670–1676.
14. Sisodia, S. S. (1992)  $\beta$ -Amyloid precursor protein cleavage by a membrane-bound protease. *Proc. Natl. Acad. Sci. USA* **89**, 6075–6079.
15. Allsop, D., Yamamoto, T., Kametani, F., Miyazaki, N., and Ishii, T. (1991) Alzheimer amyloid  $\beta$ /A4 peptide binding sites and a possible APP-secretase activity associated with rat brain cortical membranes. *Brain Res.* **551**, 1–9.
16. McDermott, J. R. and Gibson, A. M. (1991) The processing of Alzheimer A4/ $\beta$ -amyloid protein precursor: identification of a human brain metalloproteinase which cleaves -Lys-Leu- in a model peptide. *Biochem. Biophys. Res. Commun.* **179**, 1148–1154.
17. Kojima, S. and Omori, M. (1992) Two-way cleavage of  $\beta$ -amyloid protein precursor by multicatalytic proteinase. *FEBS Lett.* **304**, 57–60.
18. Miyazaki, K., Hasegawa, M., Funahashi, K., and Umeda, M. (1993) A metalloproteinase inhibitor domain in Alzheimer amyloid protein precursor. *Nature* **362**, 839–841.
19. Tagawa, K., Kunishita, T., Maruyama, K., Yoshikawa, K., Kominami, E., Tsuchiya, T., et al. (1991) Alzheimer's disease amyloid  $\beta$ -clipping enzyme (APP secretase): identification, purification, and characterization of the enzyme. *Biochem. Biophys. Res. Commun.* **177**, 377–387.
20. Sambamurti, K., Shioi, J., Anderson, J. P., Pappolla, M. A., and Robakis, N. K. (1992) Evidence for intracellular cleavage of the Alzheimer's amyloid precursor in PC12 cells. *J. Neurosci. Res.* **33**, 319–329.
21. Felsenstein, K. M., Ingalls, K. M., Hunihan, L. W., and Roberts, S. B. (1994) Reversal of the Swedish familial Alzheimer's disease phenotype in cultured cells treated with phorbol 12, 13-dibutyrate. *Neurosci. Lett.* **174**, 173–176.
22. Mullan, M., Crawford, F., Axelman, K., Houlden, H., Lilius, L., Winblad, B., and Lannfelt, L. (1992) A pathogenic mutation for probable Alzheimer's disease in the APP gene at the N-terminus of  $\beta$ -amyloid. *Nat. Gen.* **1**, 345–347.
23. Felsenstein, K. M., Hunihan, L. W., and Roberts, S. B. (1994) Altered cleavage and secretion of a recombinant  $\beta$ -amyloid precursor protein bearing the Swedish familial Alzheimer's disease mutation. *Nat. Gen.* **6**, 251–257.

24. DeStrooper, B., Craessaerts, K., Van, F., Leuven, and Van Den Berghe, H. (1995) Exchanging the extracellular domain of amyloid precursor protein for horseradish peroxidase does not interfere with  $\alpha$ -secretase cleavage of the  $\beta$ -amyloid region, but randomizes secretion in Madin-Darby canine kidney cells. *J. Biol. Chem.* **270**, 30,310–30,314.
25. Roberts, S. B., Ingalls, K. M., Ripellino, J. A., Robakis, N. K., and Felsenstein, K. M. (1995) Specific Cleavage of  $\beta$ -Amyloid Precursor Protein by an Integral Membrane Metalloendopeptidase, in *Alzheimer's and Parkinson's Diseases: Recent Advances*, vol. 44, (Hanin, I., Fisher, A., and Yoshida, M., eds.), Plenum, New York, pp. 111–118.
26. Felsenstein, K. M., Treloar, A., Roome, J. M., Hunihan, L. W., Ingalls, K. M., and Roberts, S. B. (1995) Transgenic rat and *in vitro* studies of  $\beta$ -amyloid precursor protein processing, in *Alzheimer's and Parkinson's Diseases: Recent Advances*, vol. 44, (Hanin, I., Fisher, A., and Yoshida, M., eds.), Plenum, New York, pp. 401–409.
27. Mellman, I., Matter, K., Yamamoto, E., Pollack, N., Roome, J., Felsenstein, K., and Roberts, S. (1995) Mechanisms of molecular sorting in polarized cells: relevance to Alzheimer's disease, in *Alzheimer's Disease: Lessons in Cell Biology* (Kosik, K. S., ed.), Springer-Verlag, New York.
28. Kingston, R. E. (1991) Introduction of DNA into Mammalian Cells, in *Current Protocols in Molecular Biology* (Ausubel, F. M., Brent, R., Kingston, R. E., Moore, D. D., Seidman, J. G., Smith, J. A., and Struhl, K., eds.), Greene Publishing Associates and Wiley Interscience, New York.
29. Harlow, E. and Lane, D., (eds.) (1988) Immunizations, in *Antibodies: A Laboratory Manual*. Cold Spring Harbor Laboratory Press, Cold Spring Harbor, NY, pp. 72–128.
30. Harlow, E. and Lane, D. (eds.) (1988) Immunoblotting, in *Antibodies: A Laboratory Manual*. Cold Spring Harbor Laboratory Press, Cold Spring Harbor, NY, pp. 475–502.
31. Hengen, P. N. (1997) Methods and reagents. Chemiluminescent detection methods. *Trends. Biochem. Sci.* **22**, 313–314.

## Inhibition of $\alpha$ -Secretase by Zinc Metalloproteinase Inhibitors

S. Parvathy, Anthony J. Turner, and Nigel M. Hooper

### 1. Introduction

The amyloid precursor protein (APP) is cleaved by at least three proteinases termed the  $\alpha$ -,  $\beta$ -, and  $\gamma$ -secretases. Cleavage of APP at the N-terminus of the  $\beta$ -amyloid (A $\beta$ ) peptide by  $\beta$ -secretase and at the C-terminus by one or more  $\gamma$ -secretases constitutes the amyloidogenic pathway. In the nonamyloidogenic pathway,  $\alpha$ -secretase cleaves APP within the A $\beta$  peptide between Lys16 and Leu17 (numbering from the N-terminus of the A $\beta$  peptide) (*1*), thereby preventing deposition of intact A $\beta$  peptide. The  $\alpha$ -secretase cleavage site lies some 12 amino acid residues on the extracellular side of the membrane, releasing the large ectodomain of APP (sAPP $\alpha$ ), which has neuroprotective properties (*2,3*). The identification and characterization of the APP secretases is important for the development of therapeutic strategies to control the buildup of A $\beta$  in the brain and the subsequent pathological effects of Alzheimer's disease. Regulation of the balance of APP processing by the amyloidogenic and nonamyloidogenic pathways through either selective inhibition of  $\beta$ - and  $\gamma$ -secretases or activation of  $\alpha$ -secretase can all be considered as potential therapeutic approaches. As a first step towards isolating the APP secretases, we have investigated the effect of protease inhibitors on the activities of  $\alpha$ - and  $\beta$ -secretase. From these studies we have identified low molecular weight inhibitors of  $\alpha$ -secretase.

#### 1.1. Membrane Protein Secretases

An increasing number of secreted proteins are now known to be derived from integral membrane proteins through a posttranslational proteolytic cleavage event (*4-6*). In addition to APP, other proteins existing in both membrane-

bound and soluble forms as a result of proteolysis, include the vasoregulatory enzyme angiotensin-converting enzyme (ACE; EC 3.4.15.1), tumor necrosis factor (TNF) ligand and receptor superfamily, transforming growth factor- $\alpha$ , Fas ligand, and certain cytokine receptors. The proteinases responsible for the cleavage and release of such membrane proteins have been referred to collectively as secretases, sheddases, or convertases and display many properties in common. For example, they appear to be integral membrane proteins themselves, are zinc metalloproteinases inhibited by certain hydroxamic acid-based compounds, such as batimastat, and are upregulated by phorbol esters. Whether there is a single secretase responsible for the cleavage and release of this functionally and structurally diverse range of membrane proteins or, more likely, multiple activities, is still not clear (7).

### 1.1.1. ACE Secretase

ACE is a widely distributed ectoenzyme that occurs both as the membrane-bound form on the endothelial and epithelial surfaces of tissues and as a soluble form in plasma and other body fluids (8,9). The secretase that releases ACE from the membrane is itself an integral membrane protein, localized to the plasma membrane (10). We have shown that the secretase has an absolute requirement for its substrate (ACE) to be anchored in a membrane for cleavage to occur (11), a phenomenon that appears to apply to several other secretases including the APP  $\alpha$ - and  $\beta$ -secretases (12,13). This observation may have a significant bearing on the means by which such secretases can be assayed and may rule out the use of short soluble synthetic peptides as substitute substrates (6). Like the APP  $\alpha$ -secretase, ACE secretase is a zinc metalloproteinase inhibited by 1,10-phenanthroline (10). More recently we have shown that a range of hydroxamic acid-based zinc metalloproteinase inhibitors, such as batimastat and marimastat, inhibit ACE secretase (11).

### 1.1.2. TNF- $\alpha$ Convertase

TNF- $\alpha$  is cleaved from its membrane-bound precursor by TNF- $\alpha$  convertase. The physiological importance of this inflammatory cytokine has led to intense interest in the mechanism of its generation and to the potential therapeutic benefit of inhibitors of this process (14). TNF- $\alpha$  convertase (ADAM 17) has been isolated, cloned, and sequenced (15,16). The cDNA encodes a protein of 824 amino acids, consisting of a multidomain extracellular part, a transmembrane helix, and an intracellular C-terminal tail. The extracellular part comprises an N-terminal prodomain, a 259-residue catalytic domain containing the extended HEXXH zinc-binding motif, and a Cys-rich domain that is composed of a disintegrinlike, an epidermal growth factorlike, and a crambinlike domain. This domain structure is characteristic of the adamalysin or ADAMs (*a* disintegrin

and metalloproteinase) family of zinc metalloproteinases (17,18). The similarity in properties between TNF- $\alpha$  convertase and other secretases has led to speculation that TNF- $\alpha$  convertase may be involved in shedding other cell-surface proteins, in addition to TNF- $\alpha$ .

### 1.2. Inhibition of $\alpha$ -Secretase

Although  $\alpha$ -secretase has yet to be isolated, this proteinase appears to be plasma membrane-associated (12,19). Roberts et al. (12) described the development of a cell-free assay for  $\alpha$ -secretase utilizing a construct of the C-terminal 105 amino acids of APP linked to the C-terminus of alkaline phosphatase (see Chapter 12). Expression of this construct in human H4 neuroglioma cells resulted in cleavage at the prototypic Lys16–Leu17  $\alpha$ -secretase cleavage site. Of a range of class-specific proteinase inhibitors examined, only the zinc-chelating agent, 1,10-phenanthroline, caused significant inhibition of  $\alpha$ -secretase cleavage. A comparison of the properties of  $\alpha$ -secretase and ACE secretase led us to propose that these two proteinases are either the same or closely related integral membrane zinc metalloproteinases, and caused us to examine the effect of batimastat and related hydroxamic acid-based compounds on the activity of  $\alpha$ -secretase in two neuronal cell lines (SH-SY5Y and IMR32) and in human umbilical vein endothelial cells (HUVECs) (20). Site-specific antibodies were used in immunoelectrophoretic blot analysis of conditioned medium to detect sAPP $\alpha$  (antibodies 6E10 or 1–25) and sAPP $\beta$  (Ab1A9), the initial products of  $\alpha$ - and  $\beta$ -secretase cleavage of APP, respectively (Fig. 1). Full-length APP in the cell membrane was detected with Ab54 (Fig. 1). By using this approach we found that  $\alpha$ -secretase displays a remarkably similar inhibition profile to that observed for ACE secretase (Table 1), which further highlights the similarities between these two activities. Batimastat, marimastat, and BB2116 all inhibited  $\alpha$ -secretase with  $I_{50}$  values in the low micromolar range. Structural analogs of batimastat were also assessed for their effect on the activity of  $\alpha$ -secretase. Compound 1 differs from batimastat only by the absence of the thienothiomethyl substituent adjacent to the hydroxamic acid moiety (Table 1) and yet is less potent than batimastat in inhibiting  $\alpha$ -secretase. Compound 4, which differs from compound 1 by the presence of a tertiary amine rather than a secondary amine at its C-terminus, was even less potent.

Batimastat, marimastat, and BB2116 are all hydroxamic acid-based zinc metalloproteinase inhibitors that were originally designed as inhibitors of matrix metalloproteinases (21,22). From studies with the zinc metalloproteinase thermolysin, hydroxamates were identified as the preferred zinc ligand. Studies of batimastat and other hydroxamates cocrystallized with the snake venom metalloproteinase atrolysin C (EC 3.4.24.42) (23,24) or the matrix metalloproteinase collagenase (EC 3.4.24.34) (25,26) clearly show that these compounds bind at

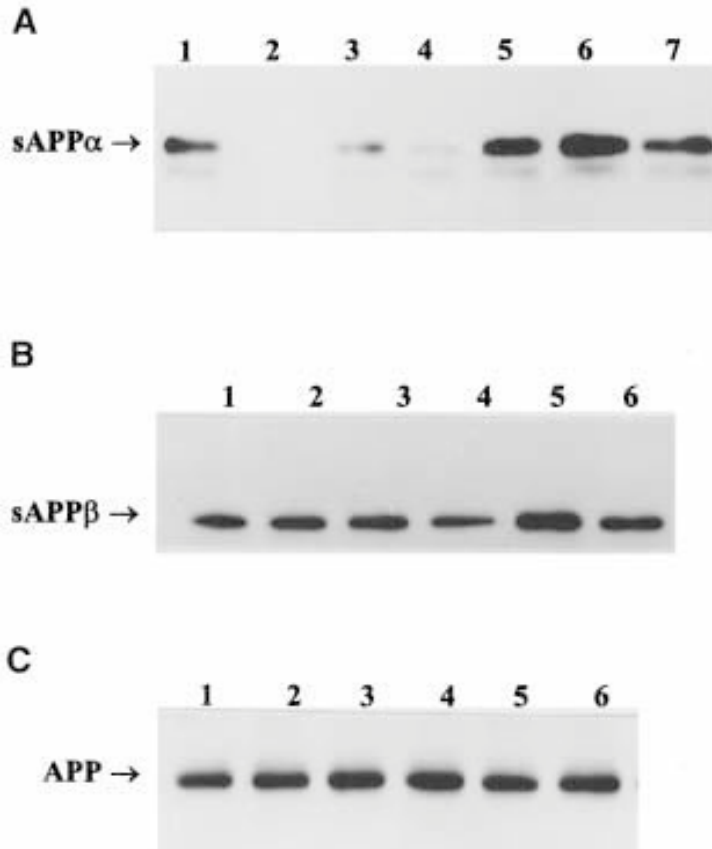
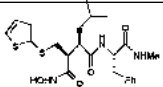
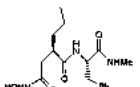
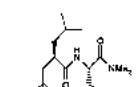
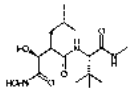
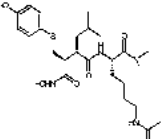


Fig. 1. Inhibition of  $\alpha$ -secretase by zinc metalloprotease inhibitors. IMR32 cells were incubated in the absence or presence of the indicated compound in the medium. After 7 h the medium was removed, concentrated, and subjected to immunoelectrophoretic blot analysis with either (A) Ab1–25 to detect sAPP $\alpha$  or (B) Ab1A9 to detect sAPP $\beta$ . The cells were harvested and the cell lysate subjected to immunoelectrophoretic blot analysis (C) with Ab54 to detect full-length APP. (A) Lane 1, control (no compound); lane 2, batimastat (20  $\mu$ M); lane 3, TAPI-2 (20  $\mu$ M); lane 4, compound 1 (20  $\mu$ M); lane 5, compound 4 (20  $\mu$ M); lane 6, phosphoramidon (20  $\mu$ M); lane 7, enalaprilat (10  $\mu$ M). (B,C) Lane 1, control (no compound); lane 2, batimastat (20  $\mu$ M); lane 3, compound 1 (20  $\mu$ M); lane 4, compound 4 (20  $\mu$ M); lane 5, phosphoramidon (20  $\mu$ M); lane 6, enalaprilat (10  $\mu$ M). Reprinted with permission from **ref. 20**. Copyright 1998 American Chemical Society.

the active site and coordinate to the essential zinc ion. As batimastat, marimastat, BB2116, compounds 1 and 4 inhibit collagenase with  $I_{50}$  values that range from 5–220 nM (**Table 1**), it would appear that marked differences

**Table 1**  
**Structures and Inhibitory Effects of Compounds**  
**on  $\alpha$ -Secretase, ACE Secretase, TNF- $\alpha$  Convertase, and Collagenase**

Compound	Structure	$\alpha$ -secretase <sup>a</sup>	I <sub>50</sub> $\mu$ M		
			ACE secretase <sup>b</sup>	TNF- $\alpha$ convertase <sup>c</sup>	Collagenase <sup>b</sup>
Batimastat		3.3	1.6	0.019	0.005
1		17.9	38.3	0.037	0.056
4		>20	>100	0.18	0.22
Marimastat		1.2	8.3	—	0.005
BB2116		7.7	3.5	—	0.004

<sup>a</sup>Data from (20).

<sup>b</sup>Data from (11).

<sup>c</sup>Data from (7).

exist between the recognition features essential for the inhibition of  $\alpha$ -secretase and the matrix metalloproteinases, suggesting that  $\alpha$ -secretase is a distinct, but possibly related, zinc metalloproteinase. This observation is consistent with the lack of cleavage of full-length APP by gelatinase A (27) and the lack of inhibition of sAPP $\alpha$  release by either tissue inhibitor of metalloproteinases (TIMP-1) (28) or  $\alpha_2$ -macroglobulin (12).

Although batimastat, compound 1, and compound 4 have very similar effects on  $\alpha$ -secretase and ACE secretase, marked differences were observed in the inhibition of TNF- $\alpha$  convertase (Table 1) (7). All of the hydroxamic acid-based compounds examined were significantly (100–500-fold) more potent against TNF- $\alpha$  convertase than against  $\alpha$ -secretase, and at a concentration (20  $\mu$ M) at which compound 4 failed to inhibit  $\alpha$ -secretase, complete inhibition of TNF- $\alpha$  convertase was observed. The recently determined crystal structure of the catalytic domain of TNF- $\alpha$  convertase with a hydroxamic acid-based compound

bound at the active site (29), revealed that the C-terminus of the inhibitor extends away from the active site cleft and adopts different conformations. It is possible that the active site cleft in  $\alpha$ -secretase makes closer contact with the C-terminus of the inhibitor such that an amide H (as in batimastat and compound 1) is critical for efficient binding, whereas replacement of this group with a bulkier methyl group (as in compound 4) disrupts the interaction. Thus TNF- $\alpha$  convertase is distinct from, but possibly related to,  $\alpha$ -secretase. Whether  $\alpha$ -secretase is another member of the adamalysin family of zinc metalloproteinases awaits its isolation and sequencing.

### 1.3. Activation of $\alpha$ -Secretase

The secretion of sAPP $\alpha$  is known to be enhanced by phorbol esters and other activators of protein kinase C (30). This effect is probably through activation of  $\alpha$ -secretase either directly or indirectly via phosphorylation (31,32). The muscarinic agonist carbachol activates protein kinase C through the generation of diacylglycerol and inositol 1,4,5-trisphosphate leading to an increase in sAPP $\alpha$  release (33,34). In SH-SY5Y cells, carbachol dramatically increases the release of sAPP $\alpha$ , and batimastat completely blocked this enhanced release of APP (Fig. 2), indicating that a single activity is probably involved in both the basal and protein kinase C-stimulated release of APP (20).

In this chapter we describe the protocols used to investigate the effect of hydroxamic acid-based inhibitors and other compounds (such as carbachol) on  $\alpha$ -secretase activity using site-specific antibodies in immunoelectrophoretic blot analysis of cell medium and lysate samples.

## 2. Materials

### 2.1. Cell Culture

1. Cells that express and process APP (e.g., IMR32 and SH-SY5Y, see Note 1).
2. Growth medium for IMR32 and SH-SY5Y cells: Dulbecco's modified Eagle's medium/Ham's F12 with glutamax (Gibco-BRL, Paisley, UK) supplemented with 10% fetal bovine serum, penicillin (50 U/mL) and streptomycin (50  $\mu$ g/mL).
3. Trypsin/EDTA (Gibco-BRL).
4. Sterile phosphate-buffered saline without Ca<sup>2+</sup> and Mg<sup>2+</sup> (Gibco-BRL).

### 2.2. Incubation of Cells with Inhibitors or Carbachol

1. Hydroxamic acid-based inhibitors, e.g., batimastat (BB94) and marimastat (BB2516) are available from British Biotechnology Pharmaceuticals (Oxford, UK), or TAPI-2 available from Dr. R. Black (Immunex, Seattle, WA) (see Note 2) are dissolved in dimethyl sulphoxide (DMSO) to give a stock solution of 10 mM concentration. This should be stored at -20°C and diluted with tissue culture medium before use.
2. Carbachol (carbamylcholine chloride; Sigma, St. Louis, MO).

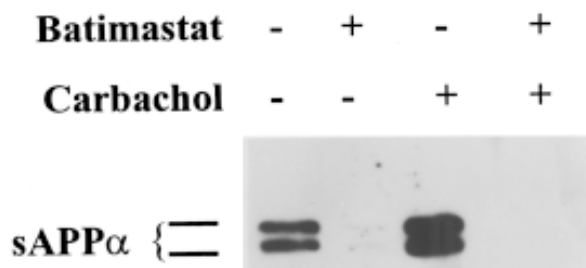


Fig. 2. Activation of  $\alpha$ -secretase by carbachol. SH-SY5Y cells were incubated in the absence or presence of carbachol ( $20 \mu\text{M}$ ) and batimastat ( $20 \mu\text{M}$ ) as indicated. After 7 h the medium was harvested, concentrated and subjected to immunoelectrophoretic blot analysis with Ab6E10 to detect sAPP $\alpha$ . Reprinted with permission from ref. 20. Copyright 1998 American Chemical Society.

3. Phosphate-buffered saline (PBS) (Gibco-BRL).
4. OptiMEM (Gibco-BRL).

### 2.3. Preparation and Concentration of Cell Medium Samples

Vivaspin 15 mL concentrators 10,000 mol wt cutoff (Vivascience, Lincoln, UK).

### 2.4. Preparation of Cell Lysate Samples

1. PBS ( $20 \text{ mM Na}_2\text{HPO}_4$ ,  $2 \text{ mM NaH}_2\text{PO}_4$ ,  $150 \text{ mM NaCl}$ , pH 7.4).
2. Lysis buffer:  $0.1 \text{ M Tris-HCl}$ ,  $5 \text{ mM EDTA}$ ,  $1\% \text{ Triton X-100}$ , pH 7.4 containing leupeptin ( $1 \mu\text{g/mL}$ ) and dichloroisocoumarin ( $10 \mu\text{M}$ ).

### 2.5. Antibodies to APP

We have used the following primary antibodies, although numerous others are available either commercially or from individual researchers:

1. Ab1–25 (SmithKline Beecham Pharmaceuticals, Harlow, UK) is a rabbit polyclonal antibody that recognizes the first 25 amino acids of the A $\beta$  peptide (*see Note 3*). Use at 1:4000 dilution.
2. Ab1A9 (SmithKline) is a mouse monoclonal antibody that recognizes the neopeptide formed at the C-terminus of the large ectodomain of APP following  $\beta$ -secretase cleavage (*see Chapter 14*) (*see Note 3*). Use at 1:3000 dilution.
3. Ab 6E10 (Senetek, Maryland Heights) is a mouse monoclonal antibody that recognizes the N-terminus of the A $\beta$  peptide (*see Note 3*). Use at 1:2000 dilution.
4. Ab 54 (SmithKline) is a rabbit polyclonal antibody that recognizes an epitope in the cytosolic C-terminus of APP (*see Note 3*). Use at 1:20,000 dilution.
- e. 22C11 (Boehringer Mannheim, Mannheim, Germany) is a mouse monoclonal antibody that recognizes an epitope towards the N-terminus of APP (*see Note 3*). Use at 1:5,000 dilution.

## 2.6. SDS-PAGE and Immunoelectrophoretic Blot Analysis

1. Dissociation buffer: 140 mM Tris-HCl, 80 mM dithiothreitol, 10% (w/v) sodium dodecyl sulfate (SDS), 20% (v/v) glycerol, 0.005% bromophenol blue, pH 6.8.
2. 10% Polyacrylamide minigel (4 cm × 3 cm). Separating gel: 10% (w/v) acrylamide in 0.37 M Tris-HCl, 0.1% SDS, pH 8.8. Stacking gel: 3% (w/v) acrylamide in 0.12 M Tris-HCl, 0.1% SDS, pH 6.8. Use an acrylamide:bis-acrylamide solution of 37.5:1.
3. High-mol-wt markers ranging from 53–212 kDa (Sigma).
4. Electrode buffer: 25 mM Tris-HCl, 190 mM glycine, 1% SDS, pH 8.6.
5. Poly(vinylidene) difluoride (PVDF) membrane with 0.45 μm pore size (Millipore, Bedford, MA).
6. Blotting buffer: 20 mM Tris, 150 mM glycine, 20% (v/v) methanol. The pH should be between 8 and 9.
7. Whatman 3MM paper (Whatman, Maidstone, UK).
8. Semidry blot apparatus (Hoefer, San Francisco, CA).
9. Blocking buffers (for Ab1–25, Aβ 6E10 and Ab54): 5% Dried milk powder in PBS, 0.1% Tween-20; (for Ab1A9) 10% dried milk powder, 2% bovine serum albumin (BSA) in PBS, 0.1% Tween-20, or 2% goat serum in PBS, 0.1% Tween-20.
10. Wash buffer: PBS, 0.1% Tween-20.
11. Antibody diluent: 2% Bovine serum albumin in PBS, 0.1% Tween-20.
12. Secondary antibody:
  - a. For Ab1–25 and Ab54: Peroxidase conjugated antirabbit antibody used at 1:6,000 dilution;
  - b. For Ab1A9, Ab6E10 and 22C11: Peroxidase conjugated antimouse antibody used at 1:3,000 dilution.
13. Tertiary antibody (for Ab1A9 only): Mouse monoclonal peroxidase antiperoxidase antibody (Sigma) used at 1:3,000 dilution.
14. Enhanced chemiluminescent detection system (Amersham, Slough, UK).
15. X-ray film.

## 3. Methods

### 3.1. Cell Culture

1. Thaw frozen vials of cells at 37°C, and transfer immediately into growth medium that has been already warmed to 37°C.
2. Centrifuge the cells at 100g for 10 min to remove the old medium containing DMSO and replace with 20 mL fresh growth medium.
3. Transfer the cells to 75 cm<sup>2</sup> flasks and incubate in sterile conditions at 37°C, 5% CO<sub>2</sub>. Once the cells become confluent, they are ready for reseeding.
4. Remove the old medium and wash the cells with PBS without Ca<sup>2+</sup> and Mg<sup>2+</sup> and incubate with 2.5 mL of trypsin/EDTA for 5 min at 37°C (see **Note 4**). Add fresh medium (8 mL) immediately, as trypsin would otherwise damage the cells.
5. Transfer the cells to 15 or 50 mL sterile tubes and centrifuge for 10 min at 100g.
6. Remove the medium and resuspend the pellet in 10 mL fresh medium.

7. Count the cells using a hemocytometer and seed at the required density (*see Note 5*). For each 75 cm<sup>2</sup> flask use 15 mL of growth medium.
8. Incubate the cells at 37°C in 5% CO<sub>2</sub> in air.

### **3.2. Incubation of Cells with Inhibitors or Carbachol**

1. When the cells are confluent and in a monolayer, remove the medium and wash the cells with PBS.
2. Replace the PBS with a serum-free medium such as OptiMEM (10 mL) (Gibco-BRL) with or without the required inhibitor or carbachol at the appropriate concentration (*see Note 6*).
3. Incubate the cells for 7 h at 37°C (*see Note 7*).
4. Remove the medium from the cells and use as a source of released soluble APP (*see Subheading 3.3.*) and prepare a cell lysate as a source of membrane-bound APP (*see Subheading 3.4.*).

### **3.3. Preparation and Concentration of Cell Medium Samples**

1. Centrifuge the medium removed from the cells (*see Subheading 3.2.*) at 100g for 10 min to remove any cells that may have become detached from the flask.
2. Remove the supernatant from this centrifugation, leaving behind 0.5 mL above the pellet in order to ensure that no cells are removed.
3. Concentrate (X50) using a Vivaspin concentrator (Vivascience) by centrifugation at 2000g for 1 h at 4°C (*see Note 8*).
4. Determine the concentration of protein in the medium sample (*see Note 9*), load equal amounts of protein (approx 40  $\mu$ g) on a 10% polyacrylamide SDS gel, and analyze the APP by immunoelectrophoretic blot analysis with the appropriate antibody (*see Subheading 3.5.*).

### **3.4. Preparation of Cell Lysate Samples**

1. Following the removal of the medium from the cells (*see Subheading 3.2.*), wash the cells twice with 10 mL PBS.
2. Using a cell scraper, harvest the cells into 10 mL PBS.
3. Centrifuge the cells at 100g for 10 min.
4. Remove the supernatant and add lysis buffer to the cell pellet (0.25 mL for each 75 cm<sup>2</sup> flask of cells).
5. Allow the cells to lyse by leaving on ice for 1 h.
6. Centrifuge the lysed cells at 8000g in a microcentrifuge at 4°C for 10 min.
7. Remove the supernatant (cell lysate) and determine the protein concentration (*see Note 9*).
8. Load equal amounts of protein (approx 100  $\mu$ g) on a 10% polyacrylamide SDS gel and analyze the APP by immunoelectrophoretic blot analysis with the appropriate antibody (*see Subheading 3.5.*).

### **3.5. SDS-PAGE and Immunoelectrophoretic Blot Analysis**

1. To samples of cell lysate (approx 100  $\mu$ g/well) and medium (approx 40  $\mu$ g/well) add dissociation buffer to a 1:1 (v/v) ratio, and boil the samples for 5 min (*see Note 10*).

2. Electrophorese the samples on a 10% polyacrylamide SDS gel alongside high-mol-wt marker proteins at 20 mA/gel in electrode buffer.
3. Cut the PVDF membrane to the size of the SDS gel (*see Note 11*). Presoak the membrane in methanol for 3 s and rinse with distilled water for 2 min, making sure that the membrane does not float, and finally immerse the PVDF membrane in blotting buffer for 10 min.
4. Cut the Whatman 3MM paper (8 sheets for each transfer) to the size of the gel and presoak in blotting buffer.
5. In the semidry blotting apparatus, make a sandwich of (from the bottom up) four sheets of Whatman 3MM paper, the PVDF membrane, the polyacrylamide gel, and four more sheets of the Whatman 3MM paper (*see Note 12*).
6. Transfer the proteins from the polyacrylamide gel onto the PVDF membrane at a current of 0.8 mA/cm<sup>2</sup> for 2 h.
7. Following the transfer, remove the PVDF membrane from the sandwich and incubate it with 50 mL of the appropriate blocking buffer (*see Subheading 2.6.*) for 3 h at room temperature.
8. Wash the membrane briefly with 20 mL wash buffer and incubate it with the appropriate primary antibody diluted in antibody diluent either overnight at 4°C or for 1 h at room temperature.
9. Remove the primary antibody and wash the membrane for 1 min with wash buffer, followed by two 15 min washes with wash buffer.
10. Incubate the PVDF membrane with the appropriate secondary antibody in antibody diluent for 1 h at room temperature.
11. Remove the secondary antibody and wash the PVDF membrane as in **step 9**.
12. Briefly wash the PVDF membrane with PBS and detect bound antibody using the enhanced chemiluminescent detection system according to the manufacturer's instructions (*see Note 13*).

#### 4. Notes

1. Any cell line either endogenously expressing APP or in which APP has been transfected can be used.
2. Numerous hydroxamic acid-based zinc metalloproteinase inhibitors are available (6) that have similar structures and that may well inhibit  $\alpha$ -secretase, although the effects of only a few have been reported.
3. Ab1–25 and A $\beta$  6E10 are used to detect sAPP $\alpha$ , as their epitopes are missing from sAPP $\beta$ . Because the neopeptide recognized by Ab1A9 is cryptic in both full-length APP and sAPP $\alpha$ , this antibody recognizes only sAPP $\beta$  (*see Chapter 14*). Ab54 is used to detect full-length APP, which retains the cytosolic C-terminus. 22C11 will react with both sAPP $\alpha$  and sAPP $\beta$  as well as full-length APP and amyloid precursorlike proteins (*see Chapter 18*).
4. If the cells do not fully detach from the flask on treatment with trypsin/EDTA, gently tap the sides of the flask to detach the cells completely.
5. The seeding density will vary depending on the cell line. We seed IMR32 cells and SH-SY5Y cells at  $4 \times 10^4$  cells/cm<sup>2</sup> and HUVECs at  $2.5 \times 10^3$  cells/cm<sup>2</sup>.

6. For hydroxamic acid-based inhibitors such as batimastat, the maximum concentration was arrived at following a cell toxicity assay (e.g., the MTT assay, detailed in Chapter 14). All the hydroxamic acid-based inhibitors were found to be nontoxic at a final concentration of 20  $\mu$ M.
7. The incubation time with inhibitors will depend on the cell line, and whether it has been transfected with APP. Shorter incubation times can be used as long as there is sufficient APP produced in the absence of inhibitors to be detected.
8. Alternative methods can be used to concentrate the cell medium, including lyophilization and precipitation of the proteins with methanol (add 5 vol methanol, incubate for 5 min at 4°C, and then centrifuge at 8000g for 5 min at 4°C).
9. Any suitable protein determination assay will suffice. We use the bicinchoninic acid (BCA) method scaled down onto a 96-well microtiter plate format with BSA (2–10  $\mu$ g as the standard) (35).
10. If you are using antibody Ab1A9, the samples should not be boiled.
11. When handling the PVDF membrane wear gloves to avoid contaminating the membrane with proteins from your fingers.
12. Make sure that there are no air bubbles trapped between each layer of the sandwich, especially between the PVDF membrane and the polyacrylamide gel, otherwise transfer of the proteins will be impaired. Gently rolling a glass rod over each layer as the sandwich is formed helps to exclude trapped air.
13. The length of time that the film has to be exposed to the blot depends on the antigen-antibody combination. For most antibodies exposure times of from 30 s up to 10 min maximum should give a good signal. However, for Ab1A9 exposure times of 15–60 min are usually required.

## Acknowledgments

The authors thank the Medical Research Council of Great Britain for their financial support of this work. They also thank Dr. E. H. Karran (SmithKline Beecham Pharmaceuticals, Harlow, UK) for providing antibodies and inhibitors.

## References

1. Esch, F. S., Keim, P. S., Beattie, E. C., Blacher, R. W., Culwell, A. R., Oltersdorf, T., et al. (1990) Cleavage of amyloid  $\beta$  peptide during constitutive processing of its precursor. *Science* **248**, 1122–1124.
2. Furukawa, K., Sopher, B. L., Rydel, R. E., Begley, J. G., Pham, D. G., Martin, G. M., et al. (1996) Increased activity-regulating and neuroprotective efficacy of  $\alpha$ -secretase-derived secreted amyloid precursor protein conferred by a C-terminal heparin-binding domain. *J. Neurochem.* **67**, 1882–1896.
3. Barger, S. W. and Harmon, A. D. (1997) Microglial activation by Alzheimer amyloid precursor protein and modulation by apolipoprotein E. *Nature* **388**, 878–881.
4. Ehlers, M. R. W. and Riordan, J. F. (1991) Membrane proteins with soluble counterparts: role of proteolysis in the release of transmembrane proteins. *Biochemistry* **30**, 10,065–10,074.
5. Rose-John, S. and Heinrich, P. C. (1994) Soluble receptors for cytokines and growth factors: generation and biological function. *Biochem. J.* **300**, 281–290.

6. Hooper, N. M., Karran, E. H., and Turner, A. J. (1997) Membrane protein secretases. *Biochem. J.* **321**, 265–279.
7. Parvathy, S., Karran, E. H., Turner, A. J., and Hooper, N. M. (1998) The secretases that cleave angiotensin converting enzyme and the amyloid precursor protein are distinct from tumour necrosis factor- $\alpha$  convertase. *FEBS Lett.* **431**, 63–65.
8. Hooper, N. M. (1991) Angiotensin converting enzyme: implications from molecular biology for its physiological functions. *Int. J. Biochem.* **23**, 641–647.
9. Williams, T. A., Soubrier, F., and Corvol, P. (1996). Biochemical, molecular and genetic aspects of angiotensin I-converting enzyme, in *Zinc Metalloproteases in Health and Disease* (Hooper, N. M., ed.), Taylor and Francis, London, pp. 83–104.
10. Oppong, S. Y. and Hooper, N. M. (1993) Characterization of a secretase activity which releases angiotensin-converting enzyme from the membrane. *Biochem. J.* **292**, 597–603.
11. Parvathy, S., Oppong, S. Y., Karran, E. H., Buckle, D. R., Turner, A. J., and Hooper, N. M. (1997) Angiotensin converting enzyme secretase is inhibited by metalloprotease inhibitors and requires its substrate to be inserted in a lipid bilayer. *Biochem. J.* **327**, 37–43.
12. Roberts, S. B., Ripellino, J. A., Ingalls, K. M., Robakis, N. K., and Felsenstein, K. M. (1994) Non-amyloidogenic cleavage of the  $\beta$ -amyloid precursor protein by an integral membrane metalloendopeptidase. *J. Biol. Chem.* **269**, 3111–3116.
13. Citron, M., Teplow, D. B., and Selkoe, D. J. (1995) Generation of amyloid b protein from its precursor is sequence specific. *Neuron* **14**, 661–670.
14. Mohler, K. M., Sleath, P. R., Fitzner, J. N., Cerretti, D. P., Alderson, M., Kerwar, S. S., et al. (1994) Protection against a lethal dose of endotoxin by an inhibitor of tumour necrosis factor processing. *Nature* **370**, 218–220.
15. Black, R. A., Rauch, C. T., Kozlosky, C. J., Peschon, J. J., Slack, J. L., Wolfson, M. F., et al. (1997) A metalloproteinase disintegrin that releases tumour-necrosis factor- $\alpha$  from cells. *Nature* **385**, 729–733.
16. Moss, M. L., Jin, S.-L. C., Milla, M. E., Burkhart, W., Carter, H. L., Chen, W.-J., et al. (1997) Cloning of a disintegrin metalloprotease that processes precursor tumour-necrosis factor- $\alpha$ . *Nature* **385**, 733–736.
17. Blobel, C. P. (1997) Metalloprotease-disintegrins: links to cell adhesion and cleavage of TNF $\alpha$  and Notch. *Cell* **90**, 589–592.
18. Wolfsberg, T. G. and White, J. M. (1996) ADAMs in fertilization and development. *Dev. Biol.* **180**, 389–401.
19. Sisodia, S. (1992)  $\beta$ -Amyloid precursor protein cleavage by a membrane-bound protease. *Proc. Natl. Acad. Sci. USA* **89**, 6075–6079.
20. Parvathy, S., Hussain, I., Karran, E. H., Turner, A. J., and Hooper, N. M. (1998) Alzheimer's amyloid precursor protein  $\alpha$ -secretase is inhibited by hydroxamic acid-based zinc metalloprotease inhibitors: similarities to the angiotensin converting enzyme secretase. *Biochemistry* **37**, 1680–1685.
21. Davies, B., Brown, P. D., East, N., Crimmin, M. J., and Balkwill, F. R. (1993) A synthetic metalloproteinase inhibitor decreases tumour burden and prolongs survival of mice bearing human ovarian carcinoma xenografts. *Cancer Res.* **53**, 2087–2091.

22. Gearing, A. J. H., Beckett, P., Christodoulou, M., Churchill, M., Clements, J., Davidson, A. H., et al. (1994) Processing of tumour necrosis factor- $\alpha$  precursor by metalloproteinases. *Nature* **370**, 555–557.
23. Botos, I., Scapozza, L., Zhang, D., Liotta, L. A., and Meyer, E. F. (1996) Batimastat, a potent matrix metalloprotease inhibitor, exhibits an unexpected mode of binding. *Proc. Natl. Acad. Sci. USA* **93**, 2749–2754.
24. Zhang, D., Botos, I., Gomis-Ruth, F. X., Doll, R., Blood, C., Njoroge, F. G., et al. (1994) Structural interaction of natural and synthetic inhibitors with the venom metalloproteinase, atrolysin C (Ht-d). *Proc. Natl. Acad. Sci. USA* **91**, 8447–8451.
25. Stams, T., Spurlino, J. C., Smith, D. L., Wahl, R. C., Ho, T. F., Qoronfle, M. W., Banks, T. M., and Rubin, B. (1994) Structure of human neutrophil collagenase reveals large S1' specificity pocket. *Nat. Struct. Biol.* **1**, 119–123.
26. Borkakoti, N., Winkler, F. K., Williams, D. H., D'Arcy, A., Broadhurst, M. J., Brown, P. A., et al. (1994) Structure of the catalytic domain of human fibroblast collagenase complexed with an inhibitor. *Nat. Struct. Biol.* **1**, 106–110.
27. LePage, R. N., Fosang, A. J., Fuller, S. J., Murphy, G., Evin, G., Beyreuther, K., et al. (1995) Gelatinase A possesses a  $\beta$ -secretase-like activity in cleaving the amyloid protein precursor of Alzheimer's disease. *FEBS Lett.* **377**, 267–270.
28. Walsh, D. M., Williams, C. H., Kennedy, H. E., Allsop, D., and Murphy, G. (1994) Gelatinase A not  $\alpha$ -secretase? *Nature* **367**, 27–28.
29. Maskos, K., Fernandez-Catalan, Huber, R., Bourenkov, G. P., Bartunik, H., Ellestad, G. A., et al. (1998) Crystal structure of the catalytic domain of human tumor necrosis factor- $\alpha$ -converting enzyme. *Proc. Natl. Acad. Sci. USA* **95**, 3408–3412.
30. Checler, F. (1995) Processing of the  $\beta$ -amyloid precursor protein and its regulation in Alzheimer's disease. *J. Neurochem.* **65**, 1431–1444.
31. Caporaso, G. L., Gandy, S. E., Buxbaum, J. D., Ramabhadran, T. V., and Greengard, P. (1992) Protein phosphorylation regulates secretion of Alzheimer  $\beta$ /A4 amyloid precursor protein. *Proc. Natl. Acad. Sci. USA* **89**, 3055–3059.
32. Buxbaum, J. D., Oishi, M., Chen, H. I., Pinkas-Kramarski, R., Jaffe, E. A., Gandy, S. E., and Greengard, P. (1992) Cholinergic agonists and interleukin 1 regulate processing and secretion of the Alzheimer  $\beta$ /A4 amyloid protein precursor. *Proc. Natl. Acad. Sci. USA* **89**, 10075–10078.
33. Dyrks, T., Monning, U., Beyreuther, K., and Turner, J. (1994) Amyloid precursor protein secretion and  $\beta$ A4 amyloid generation are not mutually exclusive. *FEBS Lett.* **349**, 210–214.
34. Petryniak, M. A., Wurtman, R. J., and Slack, B. E. (1996) Elevated intracellular calcium concentration increases secretory processing of the amyloid precursor protein by a tyrosine phosphorylation-dependent mechanism. *Biochem. J.* **320**, 957–963.
35. Hooper, N. M. (1993) Determination of mammalian membrane protein anchorage: glycosyl-phosphatidylinositol. (G-PI) or transmembrane polypeptide anchor. *Biochem. Ed.* **21**, 212–216.

## Development of Neopeptide Antibodies Against the $\beta$ -Secretase Cleavage Site in the Amyloid Precursor Protein

Carol W. Gray and Eric H. Karran

### 1. Introduction

A detailed understanding of the biochemical events leading to the proteolytic excision of the  $\beta$ -amyloid peptide ( $A\beta$ ) from the amyloid precursor protein (APP) has eluded many researchers. This is largely because the measurement of the various APP processing products is technically challenging owing to their low levels of production in in vitro and in vivo test systems. Sequence analysis of products in cell cultures, cerebrospinal fluid (CSF), and amyloid plaques has been used to predict the major cleavage sites resulting from the  $\beta$ - and  $\gamma$ -secretase proteolytic activities that release the  $A\beta$  peptide from APP (1–3). More routine identification of the secretase activities has relied on the specificity and sensitivity of antibodies raised to the predicted cleavage products and has been impeded by the difficulties associated with the generation of such reagents.

We describe here a method for the generation of antibody 1A9 that specifically detects the soluble, N-terminal fragment of APP (sAPP $\beta$ ) produced after  $\beta$ -secretase cleavage between amino acids Met<sub>596</sub> and Asp<sub>597</sub> (APP<sub>695</sub> numbering) of the holoprotein (Fig. 1) (4).

Immunodetection with this antibody was shown to be dependent on the presence of the free C-terminal Met<sub>596</sub> of sAPP $\beta$ , the neopeptide exposed after  $\beta$ -secretase cleavage. This APP cleavage product was originally detected in cell culture media and CSF using a purified polyclonal antiserum raised to amino-acids ISEVKM (APP<sub>591</sub>–APP<sub>596</sub>) that, from the known sequence of  $A\beta$  and APP, were predicted to form the C-terminus of sAPP $\beta$  (5). The specificity of the antiserum was confirmed using methods similar to those described in

*From: Methods in Molecular Medicine, Vol. 32: Alzheimer's Disease: Methods and Protocols*  
Edited by: N. M. Hooper © Humana Press Inc., Totowa, NJ

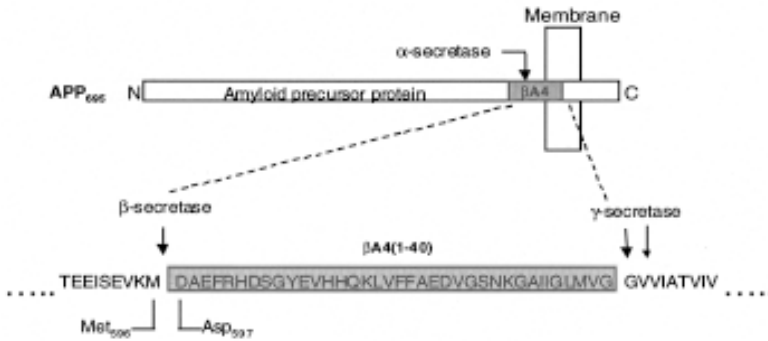


Fig. 1. Schematic representation of APP processing by  $\alpha$ -,  $\beta$ -, and  $\gamma$ -secretases.

this chapter. Radiolabeling and pulse-chase methods were used to demonstrate, in a kinetic fashion, that sAPP $\beta$  and the secreted APP product (sAPP $\alpha$ ) generated by  $\alpha$ -secretase activity were made simultaneously, thus arguing against a precursor product relationship between these two forms of secreted APP. Other groups (5–7) generated similar polyclonal antibodies to the neopeptide arising from  $\beta$ -secretase cleavage of both wild-type APP and APP carrying the Swedish double mutation K<sub>595</sub>N, M<sub>596</sub>L (APP<sup>sw</sup>) (8).

These antibodies have been useful in making some key observations:

1.  $\beta$ -Secretase is an intracellular enzyme.
2. Mutant APP<sup>sw</sup> is either processed by a different enzyme or in a different subcellular compartment to wild type APP.
3. There are cell type differences in the control or location of  $\beta$ -secretase cleavage of APP.

This latter observation is highly significant, demonstrating that sAPP $\beta$  is detected intracellularly in postmitotic neuronal cultures but not in several nonneuronal cell lines (9–11). These findings have a significant impact on the choice of cell culture model used experimentally to investigate the factors affecting  $\beta$ -secretase cleavage.

## 2. Materials

### 2.1. Antibody Generation

1. Inject maleimide-activated bovine serum albumin (BSA) and ovalbumin (Pierce, Rockville, MD, cat. nos. 77116 and 77126).
2. PD-10 desalting/buffer exchange column (Amersham Pharmacia Biotech, Amersham, UK, cat. no. 17-0851-01).
3. Freund's complete and incomplete adjuvants (Sigma, St. Louis, MO, cat. nos. F5881 and F5506).

4. ProsepA Protein A affinity matrix (Bioprocessing, Durham, UK, cat. no. 113-111-324).
5. Dulbecco's modified Eagle's medium (DMEM)/Nut Mix F-12 (DMEM/F12) media (Gibco-BRL, Paisley, Scotland, cat. no. 21331-020).
6. Fetal Bovine Serum (FBS)(Gibco-BRL, cat. no. 10106-169).
7. Conditioned media (Sigma, cat. no. H8412).
8. HAT media supplement containing hypoxanthine, aminopterin, and thymidine (Sigma, cat. no. H0262).
9. Polyethylene glycol (Sigma, cat. no. P7181)

## 2.2. ELISA

1. Antimouse alkaline phosphatase conjugate (Sigma, cat. no. A9316).
2. Fish gelatin (Amersham, cat. no. RPN 416).
3. *p*-Nitrophenylphosphate tablet set (Sigma, cat. no. N1891).
4. MaxiSorp microtiter plates (Nunc, Roskilde, Denmark, cat. no. 439454A)
5. Blocking solution: 50 mM Tris buffer, pH7.4, containing 1% (v/v) goat serum, 1% (w/v) fish gelatin, 0.5% (w/v) bovine gamma globulins, 150 mM NaCl, and 0.05% (v/v) Tween-20.

## 2.3. Western Blot and Immunoprecipitation

1. IMR-32 neuroblastoma cells (wild type and APP transfected, provided by C. Morris, MRC Neurochemical Pathology Unit, Newcastle on Tyne, UK).
2. Centriprep-10 and Centricon-10 (Amicon, Beverly, MA, cat. nos. 4304 and 4206).
3. Complete protease inhibitor cocktail (Boehringer Mannheim, Mannheim, Germany, cat. no. 1 697 498).
4. Antimouse immunoglobulin G (IgG) (Sigma, cat. no. M8645).
5. Antirabbit IgG (Sigma, cat. no. R3631).
6. Mouse peroxidase antiperoxidase (Sigma, cat. no. P2416).
7. Rabbit peroxidase antiperoxidase (Sigma, cat. no. P2026).
8. Antibody 22C11 (recognizes amino acids 66–81 of APP<sub>695</sub> [Boehringer Mannheim]).
9. Antibodies A4(1–24) and A4(1–10) (provided by David Allsop, University of Lancaster, UK [12]).
10. Antirabbit antibody-horseradish peroxidase conjugate (Pierce, cat. no. 31462).
11. Antimouse antibody-horseradish peroxidase conjugate (Pierce, cat. no. 31434).
12. Marvel (Premier Beverages, Stafford, UK) nonfat milk protein (obtained from a local retail food outlet).
13. 4–20% and 6% Tris-glycine polyacrylamide gels (Novex, San Diego, CA).
14. Enhanced chemiluminescence (ECL) reagents (Amersham, cat. no. RPN 2106).
15. Protein G Sepharose (Sigma, cat. no. P3296).
16. Reducing buffer (threefold concentrate): 0.38 M Tris-HCl pH 6.8, 6% (w/v) sodium dodecyl sulfate (SDS), 5% (v/v)  $\beta$ -mercaptoethanol, 20% (v/v) glycerol, and 0.003% bromophenol blue).

Other materials were supplied by Sigma.

### 3. Methods

#### 3.1. Monoclonal Antibody Generation

##### 3.1.1. Immunogen

The immunogen was a BSA-Cys-peptide conjugate, where the synthetic peptide was ISEVKM, corresponding to amino acids 591–596 of APP<sub>695</sub> (see **Fig. 1**). The peptide was conjugated to BSA by linkage through the cysteine residue using Inject maleimide-activated BSA (Pierce). An additional ovalbumin conjugate was made for anti-serum testing by ELISA. Both conjugates were buffer exchanged into phosphate-buffered saline (PBS) using a PD-10 column according to the manufacturer's recommendations.

##### 3.1.2. Immunization Schedule

Use three CB6/F1 mice.

1. *Day 0*: Make an emulsion of 350  $\mu$ L of peptide-BSA conjugate (500  $\mu$ g/mL PBS) and 350  $\mu$ L Freund's complete adjuvant. Inject emulsion subcutaneously into two dorsal sites per mouse, 100  $\mu$ L per site.
2. *Day 28*: Make an emulsion of 350  $\mu$ L of peptide-BSA conjugate (500  $\mu$ g/mL PBS) and 350  $\mu$ L Freund's complete adjuvant. Inject 200  $\mu$ L of emulsion intraperitoneally into each mouse.
3. *Day 29*: Take about 0.1 mL of blood from the tail veins of the mice and allow to clot at room temperature for 1 h. Separate the clot from the side of the tubes (Eppendorf, 500  $\mu$ L) and allow to contract further at 4°C for 1 h or overnight. Following this, prepare serum by centrifugation at 13,000g for 10 min at 4°C. Determine the anti-peptide immunogen titers by ELISA (**Subheading 3.2.1**). Reimmunize the mouse giving the highest titer with 2 intravenous injections of 100  $\mu$ g peptide conjugate dissolved in physiological saline and given on day 29 and on day 31, i.e., 1 and 3 d after the previous intraperitoneal on day 28.

##### 3.1.3. B-Cell Fusion

Harvest spleen cells on day 32 (1 d after the final immunization) and fuse with X68 AG8 653 myeloma cells at a ratio of 5:1 according to methods described by Zola (*13*). The myeloma cell line, which should be at a relatively low passage number, is subcultured the day before the fusion to ensure they are growing in log phase (viability typically should be 99–100%) at around 500,000 cells/mL.

##### 3.1.4. Screening and Selection

1. Disperse all the cells postfusion between 2000 microtiter wells and allow to grow in DMEM/F12 media + 10% (v/v) FBS + 10% (v/v) conditioned media (Sigma) (200  $\mu$ L of medium/well). Include HAT reagents according to the manufacturer's instructions to select for hybridoma cells. After approx 2 wk, completely replen-

**Table 1**  
**% Reduction in Absorbance  $\lambda$ 405 nm**

Peptide	ISEVKMD	ISEVKM	ISEVK	ISEV
( $\mu$ g/mL)	50 10	50 10	50 10	50 10
Antibody 1A9	0 14	76 29	10 14	5 14
Antibody 2E7	3 10	83 43	3 7	7 10

Two monoclonal antibodies, 1A9 and 2E7, were shown to recognize specifically the  $\beta$ -secretase neopeptide (C-terminal Met<sub>596</sub>) by competitive ELISA. Significant displacement of binding was obtained only with ISEVKM (APPb<sub>591-596</sub>).

ish all of the growth medium to remove antibodies that may have been produced by spleen cells prior to their removal by counter-selection. Approximately 3 d later, screen the cell culture supernatants for specific antibody production by ELISA (**Subheading 3.2.1.**). Retest positive supernatants for neopeptide specificity using a competition ELISA (**Subheading 3.2.1.**) with unconjugated peptides comprising the amino acids that overlap the required epitope (**Table 1**).

2. Select those clones with highest affinity and specificity as described in **Subheading 3.2.1.** and clone them twice by the limiting dilution method (**13**). Clones take about 2 wk to grow up after each dilution cloning.
3. Expand the resulting clones by increasing the size of the culture vessel progressively from a microtiter well, into a 24-well miniplate, then into a 25-cm<sup>2</sup> flask and finally into 1 L spinner flasks for large-scale production.

### 3.1.5. Immunoglobulin Purification from Hybridoma-Conditioned Media

1. Wash Prosep A protein A affinity column (approx 1 cm in diameter and 5 cm high) with 2 column volumes of 0.1 M citrate buffer, pH 2.5, containing 20% (v/v) glycerol.
2. Equilibrate with 5 column volumes of 1 M glycine/NaOH, pH 8.6, containing 150 mM NaCl (equilibration buffer).
3. Separate hybridoma cells from conditioned media by centrifugation at 3000g for 5 min at 4°C.
4. Dilute hybridoma-conditioned media 1:1 with equilibration buffer and filter through a 0.2- $\mu$ m or 0.45- $\mu$ m unit.
5. Load diluted hybridoma-conditioned media (approx 200 mg protein per 5 mL column) onto a Prosep A protein A affinity column at a flow rate of approx 100 column volumes per hour and wash column with 5 column volumes of equilibration buffer.
6. Elute column with approx 2 column volumes of 0.1 M citrate buffer, pH 2.5, containing 20% (v/v) glycerol.
7. Monitor the eluate at 280 nm and collect peak fractions into a beaker containing 1 M Tris-HCl, pH 7.4 plus 20% (v/v) glycerol (approx 1/10 of the collected volume) in order to neutralize the eluate. Adjust the buffer to pH 7.4 as soon as possible and store at 4°C or -20°C. Avoid repeated freeze-thawing.

## 3.2. Characterization of Antibody Specificity

### 3.2.1. ELISA

1. Coat microtiter plates overnight at 4°C with 100  $\mu$ L per well of 1  $\mu$ g/mL CISEVKM peptide-ovalbumin conjugate dissolved in PBS.
2. Aspirate coating solution and block for 1 h at 37°C with 250  $\mu$ L per well of blocking solution (**Subheading 2.2.**)
3. Wash microtiter plates four times with 400  $\mu$ L per well PBS containing 0.05% (v/v) Tween-20.
4. Incubate for 1 h at 37°C with 100  $\mu$ L per well of “test antibodies” (serum, hybridoma supernatant or purified antibody) at various concentrations, typically 1 in 500–1:100,000 dilutions. For competition ELISAs, preincubate test antibodies with approx 10-fold molar excess of the relevant peptides (**Table 1**) for 1 h at 37°C before adding to the microtiter plate.
5. Wash plates as in **step 3** and detect bound antibody by incubation for 1 h at 37°C with 100  $\mu$ L per well of antimouse antibody-alkaline phosphatase conjugate at 1 in 3000 dilution.
6. Wash plates as in **step 3** and incubate at 37°C with 100  $\mu$ L/well of *p*-nitrophenylphosphate substrate (prepared from tablets according to the manufacturer’s instructions).
7. Measure the absorbance of the microtiter plate in a plate reader ( $\lambda$  405 nm) after the color has developed sufficiently (approx 30 min).
8. The magnitude of the signal per milligram of protein is a measure of the affinity of the antibody: this is assessed most accurately at the highest dilution that elicits a readout above background. Specificity is confirmed by the absence of a significant signal when the plate is coated with an irrelevant peptide or protein such as those used in the blocking solution. The antibody epitope is explored in more detail by measuring the reduction in signal in a competition ELISA format resulting from preincubation with peptides derived from the immunogen (as described in **step 4** and **Table 1**).

### 3.2.2. Cell Culture and Preparation of Cell Conditioned Media

We have tested the utility of the 1A9 antibody to detect sAPP $\beta$  produced from IMR32 neuroblastoma cells using the following protocol.

1. Culture IMR32 cells to approx 80% confluency in DMEM/2F12 medium containing 10% FBS. Wash the cells twice with serum-free medium or PBS and incubate for 15–20 min at 37°C in serum-free medium to remove the majority of serum components. Incubate the washed cultures in serum-free medium (about 7.5 mL per T75 flask) for 16 h at 37°C and check for maintenance of cell viability by both visual inspection and 3(4,5-dimethylthiazol-2-yl)-2,5-diphenyl tetrazolium bromide (MTT) assay as described in **Subheading 3.2.2.1**.
2. Collect the cell-conditioned medium and remove cellular debris by centrifugation at a minimum of 3000g for 5 min. Proteolysis can be minimized by supplementing the medium with a concentrated cocktail of protease inhibitors (Complete, Boehringer Mannheim) and storage at 4°C.

3. Concentrate the media 50–100 fold at 4°C by ultrafiltration using a Centricon-10 or Centriprep-10 device and dilute into sample buffer for polyacrylamide gel electrophoresis.

### 3.2.2.1. MTT CELL VIABILITY ASSAY

1. Add stock solution of MTT (5 mg/mL in PBS, stored in the dark at 4°C) to cell cultures to give a final concentration of 0.5 mg/mL.
2. Incubate cells at 37°C for 4 h.
3. Dilute medium/MTT solution 1:1 with dimethyl formamide containing 20% SDS and incubate overnight at room temperature.
4. Mix and measure absorbance ( $\lambda$ 590nm).

### 3.2.3. Characterization of 1A9 Specificity by Competitive Western Blot (Fig. 2)

1. Resolve the equivalent of 2–4 mL of conditioned medium per gel lane on a Tris-glycine-buffered SDS-containing 6% polyacrylamide gel.
2. Transfer the protein to an Immobilon P membrane with a mini-Trans-Blot system (Bio-Rad, Hercules, CA) for 1 h at 100 V using a Tris-glycine transfer buffer, pH 8.3, containing 15% (v/v) methanol. Cut the membrane into strips to allow comparative immunodetection with different antibodies and conditions (*see Note 1*).
3. Block nonspecific antibody binding sites by incubating the membrane for 1 h at room temperature in PBS containing 0.1% (v/v) Tween-20 and 5% (w/v) nonfat milk proteins (Marvel).
4. Incubate the membrane overnight at 4°C in primary detection antibody diluted in PBS containing 0.1% (v/v) Tween-20 and 2% (w/v) BSA as detailed in **Table 2**.
5. Wash the membrane thoroughly in PBS containing 0.1% (v/v) Tween-20 (3 × 1 min and 2 × 5 min.).
6. Incubate membrane for 1 h at room temperature with species-specific, anti-IgG antibodies followed by further washing as described in **step 5**, and finally incubate the membrane for 1 h with peroxidase-antiperoxidase antibodies at the dilutions specified in **Table 3**. This protocol was used to achieve the results presented in **Fig. 2**. An alternative detection method is described below.
7. Wash the membrane thoroughly as described in **step 5** and detect the immunoreactive signal using ECL as described in the manufacturer's instructions.

#### 3.2.3.1. ALTERNATIVE IMMUNODETECTION PROTOCOL

The following is an alternative immunodetection protocol that is shorter but may be slightly less sensitive, depending on the affinity of the antibodies used.

1. Block, incubate in primary antibody and wash membrane as described in **Sub-heading 3.2.3.** above.
2. Incubate membrane for 1 h at room temperature in 1:5000 dilution of antimouse IgG conjugated to horseradish peroxidase or with 1:15,000 dilution of antirabbit IgG conjugated to horseradish peroxidase.

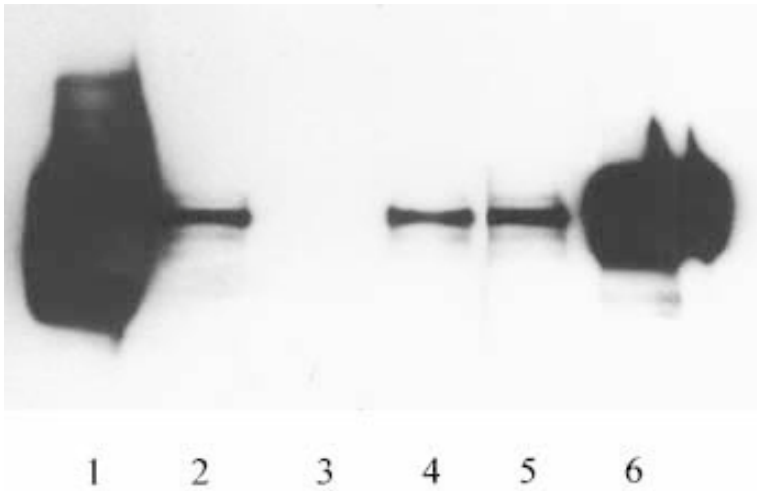


Fig. 2. Western blot of IMR-32 cell-conditioned medium (100-fold concentrate) demonstrating 1A9 epitope specificity. Immunodetection was with antibodies 22C11 (lane 1), 1A9 (lane 2), 1A9 preincubated with CISEVKM (lane 3), 1A9 preincubated with GSNKGPIIIGLM (lane 4), 1A9 preincubated with ISEVKMD (lane 5), and A4(1–10) (lane 6). 1A9 recognized a protein of approx 110 kDa that migrates with a similar molecular size to secreted APP species detected with 22C11 and to sAPP $\alpha$  detected with A4(1–10). Lower molecular weight (approx 100 kDa), less intense 1A9 immunoreactive protein bands, were visualized with longer film exposure times. The 1A9 immunoreactivity was abolished by preincubation with peptide CISEVKM, which corresponds to the amino acid sequence of the C-terminus of the C-terminus of sAPP $\beta$ , but not with peptide ISEVKMD, which has an additional C-terminal amino acid, or with peptide GSNKGPIIILM, which has a C-terminal methionine but whose amino acid sequence is unrelated to the C-terminal amino acid sequence of sAPP $\beta$ .

3. Wash and detect immunoreactive signal using the ECL reagent as described by the manufacturer.

### 3.2.3.2. GENERAL PROTEIN STAIN FOR BLOTTING MEMBRANES

This stain can be used to visualize high-abundance proteins on the membrane following immunodetection. Sensitivity can be enhanced if carried out on a membrane that has not been through the immunodetection procedure, as background staining is reduced in the absence of blocking proteins. Molecular weight markers may also be visualized with this stain, although slight shrinkage of the membrane should be taken into account if comparative molecular sizes are being estimated.

1. Wash the PVDF membrane briefly in water or PBS.

**Table 2**  
**Peptide Preincubation Conditions for Competitive Western Blot**

Primary antibody	Final Concentration
1A9 monoclonal	0.5–1 mg/mL
1A9 (1 µg/mL) preincubated for 16 h at 4°C with 60 mM CISEVKM peptide	1 µg/mL
1A9 (1 µg/mL) preincubated for 16 h at 4°C with 60 mM ISEVKMD peptide	1 µg/mL
1A9 (1 µg/mL) preincubated for 16 h at 4°C with 60 µM GSNKGPILM peptide	1 µg/mL
22C11 monoclonal	0.1 µg/mL
A4(1–10) polyclonal	1:1000 dilution

**Table 3**  
**Working Dilutions for Detection Antibodies**

Detection antibody	Working dilution
Antimouse IgG	1:3000 from stock
Antirabbit IgG	1:6000 from stock
Mouse peroxidase-antiperoxidase	1:3000 from stock
Rabbit peroxidase antiperoxidase	1:4000 from stock

2. Incubate the membrane for approx 1 min in staining solution containing 0.1% (w/v) Coomassie brilliant blue, 1% (v/v) acetic acid, and 40% (v/v) methanol in distilled H<sub>2</sub>O.
3. Destain with successive changes of 50% methanol until protein bands can be visualized above background.
4. Prevent further destaining by washing the membrane twice with water and allow the membrane to dry.
5. The staining protocol may be repeated to increase the intensity of the protein bands as necessary.

#### 3.2.4. Characterization of 1A9 Specificity by Selective Immunoprecipitation Followed by Western Blot (Fig. 3)

1. Collect the cell conditioned medium and remove cellular debris by centrifugation at a minimum of 3000g for 5 min. Add 10-fold concentrated immunoprecipitation (IP) buffer to give a final concentration of 100 mM Tris-HCl, pH 7.4, containing 150 mM NaCl, 1% Triton X-100 and a cocktail of protease inhibitors (Complete, Boehringer Mannheim).
2. Wash the stock Protein G Sepharose bead slurry gently 3 times in IP buffer. To each IP reaction containing 5–10 mL culture supernatant, add 40 µL 1:1 suspension of Protein G Sepharose and 5 µg of antibody (*see Note 2*).

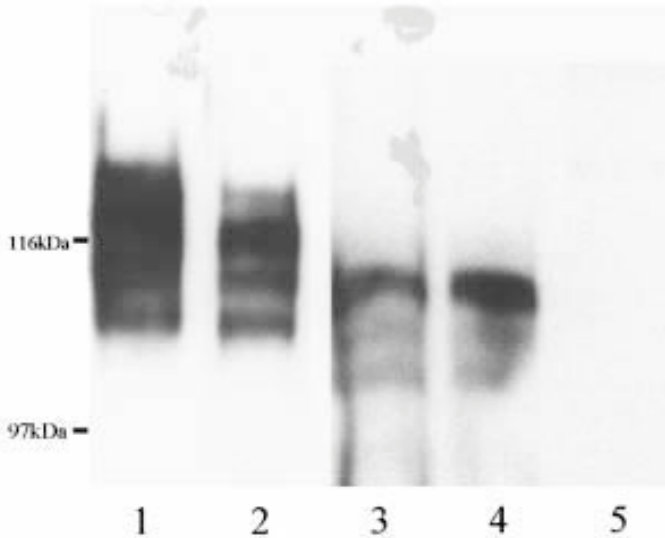


Fig. 3. Western blot demonstrating lack of cross reactivity between 1A9 monoclonal and sAPP $\alpha$ . Lanes 1, 3, and 4 contain fourfold concentrated IMR-32 (transfected with APP<sub>751</sub>) cell-conditioned medium. Lanes 2 and 5 contain sAPP $\alpha$  immunoprecipitated with A4(1–25) antibody from 7.5 mL cell-conditioned medium. Immunodetection was carried out with antibodies 22C11 for total secreted APP (lanes 1 and 2) or with 1A9 for sAPP $\beta$  (lanes 3–5). 1A9 does not detect sAPP $\alpha$  immunoprecipitated with A4(1–25).

3. Incubate antibody-Sepharose medium overnight at 4°C or 2 h at room temperature with gentle shaking/rocking.
4. Centrifuge at 1000g for 1 min or a 1-s pulse using a microfuge.
5. Wash pellet three times in IP buffer, once in IP buffer containing 500 mM NaCl and once in 10 mM Tris-HCl, pH 7.4 (transferring to fresh tubes at each stage can reduce background immunoreactivity of the final Western blot).
6. Resuspend the beads in 20  $\mu$ L threefold concentrated reducing sample buffer (described in **Subheading 2.**). Heat for 5 min at 90–100°C and centrifuge the beads at 1000g for 1 min. Fractionate the supernatant on a SDS polyacrylamide gel (typically a Tris-glycine buffered 4–20% acrylamide gradient gel).

Carry out protein transfer and immunodetection as described in the Western blot protocol in **Subheading 3.2.3.**

#### 4. Notes

1. High background staining generally can be reduced by changing, one by one, the parameters listed as follows. Nonspecific detection of proteins may be reduced by further diluting the primary antibody. Several (5–10) near-identical pieces of

membrane should be prepared that contain a track of nonspecific proteins and a track of the protein of interest in order to optimize the immunodetection steps listed below.

- a. Blocking proteins.
- b. Detection antibody batch and concentration (carried out in absence of primary antibody).
- c. Number of wash steps and volume of washes.
- d. Primary antibody concentration.
- e. Membrane type (PVDF vs nitrocellulose).

Nonspecific detection of high-abundance proteins, such as serum albumin from culture medium, can also be a problem. This is particularly the case where the immunoreactive protein and the abundant, irrelevant protein comigrate electrophoretically, as determined using a general protein stain.

2. Background immunoreactivity can be reduced by removing proteins that nonspecifically bind to Sepharose (Sigma) prior to immunoprecipitation. This may be achieved by preadsorbing the medium with Sepharose as described previously (**Subheading 3.2.4.**) omitting the antibody. Incubate for 1 h at room temperature, centrifuge at 200g, for 5 min, discard the Sepharose, and use the culture medium.

## References

1. Haass, C., Schlossmacher, M. G., Hung, A. Y., Vigo-Pelfrey, C., Mellon, A., Ostaszewski, B. L., et al. (1992) Amyloid  $\beta$ -peptide is produced by cultured cells during normal metabolism. *Nature* **359**, 322–325.
2. Seubert, P., Vigo-Pelfrey, C., Esch, F., Lee, M., Dovey, H., Davis, D., et al. (1992) Isolation and quantification of soluble Alzheimer's  $\beta$ -peptide from biological fluids. *Nature* **359**, 325–327.
3. Cheung, T. T., Ghiso, J., Shoji, M., Cai, X-D., Golde, T., Gandy, S., et al. (1994) Characterization by radiosequencing of the carboxy-terminal derivatives produced from normal and mutant amyloid  $\beta$  protein precursors. *Amyloid: Int. J. Exp. Clin. Invest.* **1**, 30–38.
4. Allsop, D., Christie, G., Gray C., Holmes, S., Markwell, R., Owen, D., et al. (1997) Studies on inhibition of  $\beta$ -amyloid formation in APP751–transfected IMR-32 cells and SPA4CT-transfected SHSY5Y cells, in *Recent Advances in Alzheimer's Disease and Related Disorders* (Iqbal, K., Mortimer, J. A., Winblad, B., and Wieniewski, H. M., eds.), Wiley, Chichester, UK, pp. 675–684.
5. Seubert, P., Oltersdorf, T., Lee, M. G., Barbour, R., Blomquist, C., Davis, D. L., et al. (1993) Secretion of  $\beta$ -amyloid precursor protein cleaved at the amino terminus of the  $\beta$ -amyloid peptides. *Nature* **361**, 260–263.
6. Howland, D. S., Savage, M. J., Huntress, F. A., Wallace, R. E., Schwartz, D. A., Loh T., et al. (1995) Mutant and native human  $\beta$ -amyloid precursor proteins in transgenic mouse brain. *Neurobiol. Aging* **16**, 685–699.
7. Siman, R., Durkin, J. T., Husten, E. J., Savage, M. J., Murthy, S., Mistretta, S., et al. (1995) Genesis and degradation of A $\beta$  protein by cultured neuroblastoma cells, in

- Recent Advances in Alzheimer's Disease and Related Disorders* (Iqbal, K., Mortimer, J. A., Winblad, B., and Wieniewski, H. M., eds.), Wiley, Chichester, UK, pp. 675–684.
8. Mullan, M., Crawford, F., Axelman, K., Houlden, H., Lilius, L., Winblad, B., and Lannfelt, L. (1992) A pathogenic mutation for probable Alzheimer's disease in the APP gene at the N-terminus of  $\beta$ -amyloid. *Nat. Genet.* **1**, 345–347.
  9. Knops, J., Suomensaaari, S., Lee, M., McConlogue, L., Seubert, P., and Sinha, S. (1995) Cell-type and amyloid precursor protein-type specific inhibition of A $\beta$  release by bafilomycin **A1**, a selective inhibitor of vacuolar ATPases. *J. Biol. Chem.* **270**, 2419–2422.
  10. Chyung, A. S. C., Greenberg, B. D., Cook D. G., Doms, R. W., and Lee, V. M.-Y. (1997) Novel  $\beta$ -secretase cleavage of  $\beta$ -amyloid precursor protein in the endoplasmic reticulum/intermediate compartment of NT2N cells. *J. Cell Biol.* **138**, 671–680.
  11. Haass, C., Lemere, C. A., Capell, A., Citron, M., Seubert, P., Schenk, D., et al. (1995) The Swedish mutation causes early-onset Alzheimer's disease by  $\beta$ -secretase cleavage within the secretory pathway. *Nat. Med.* **1**, 1291–1296.
  12. Walsh, D. M., Williams, C. H., Kennedy, H. E., and Allsop D. (1993) An investigation into proteolytic cleavage of Alzheimer amyloid precursor protein in PC-12 cells. *Biochem. Soc. Trans.* **22**, 14s.
  13. Zola, H., ed. (1987) *Monoclonal Antibodies: A Manual of Techniques*. CRC Press, Boca Raton, FL.

## $\beta$ -Secretase

### *Tissue Culture Studies of Sequence Specificity, Inhibitors, and Candidate Enzymes*

Martin Citron

#### 1. Introduction

When the amyloid precursor protein (APP) was cloned, A $\beta$  was found to be part of the large APP molecule and it became obvious that at least two endoproteolytic cleavage events are required to release A $\beta$  from its large precursor (1). More than 10 yr later nobody has published definitive identification of either of the proteases, although they are prime therapeutic targets for an anti-amyloid therapy for Alzheimer's disease.

#### **1.1. $\beta$ -Secretase Cleavage, $\beta$ -Secretase Cleavage Metabolites and the Generation of A $\beta$**

The enzymatic activity generating the N-terminus of A $\beta$  has been named  $\beta$ -secretase (Fig. 1). It is not known whether  $\beta$ -secretase is just one protease or whether several different proteases are involved in  $\beta$ -secretase cleavage. The primary  $\beta$ -secretase site is between the Met<sub>596</sub> and Asp<sub>597</sub> residues (APP<sub>695</sub> numbering), but cleavages at other positions have been described (2) and it appears likely that at least some of these cleavages are performed by different enzymes (3).  $\beta$ -Secretase cleavage of full-length APP generates two metabolites that can be tracked as markers of  $\beta$ -secretase activity: a secreted sAPP $\beta$  molecule, which ends with Met<sub>596</sub>, and a membrane-bound 12-kDa molecule, which contains the entire A $\beta$  peptide plus the C-terminal cytoplasmic tail. The 12-kDa fragment gives rise to A $\beta$  on  $\gamma$ -secretase cleavage (Fig. 1). The sAPP $\beta$  molecule can be conveniently detected with antibodies specific for the neopeptide generated by  $\beta$ -secretase cleavage (4) (see Chapter 14). If such antibodies are not available, the sAPP $\beta$  molecule can be electrophoretically

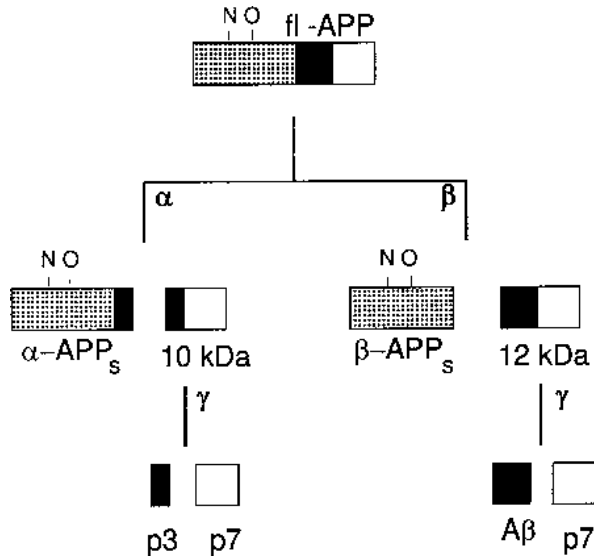


Fig. 1. The schematic shows APP695 with the large N-terminal ectodomain in black dots, the A $\beta$  region in black and the C-terminus in white (not drawn to scale). N- and O-glycosylated full-length APP can be processed by  $\alpha$ -secretase to yield secreted sAPP $\alpha$  and a membrane-bound 10 kDa fragment or by  $\beta$ -secretase to yield secreted sAPP $\beta$  and a membrane-bound 12 kDa fragment. These membrane-bound fragments can each undergo  $\gamma$ -secretase cleavage to give rise to the secreted fragments A $\beta$  and p3. The hypothetical p7 fragment has not yet been detected.

separated from the much more abundant sAPP $\alpha$  molecule based on the size difference of 17 amino acids. The 12-kDa fragment can be detected in cell extracts by immunoprecipitation with antibodies to the C-terminus of APP (5). However, these antibodies also precipitate the much more abundant 10-kDa fragment generated by  $\alpha$ -secretase cleavage. To specifically detect only the 12-kDa fragment, antibodies to the N-terminus of A $\beta$  are recommended. The 12-kDa fragment is rapidly turned over to A $\beta$ . Therefore, A $\beta$  generation can be used to monitor  $\beta$ -secretase cleavage. In studies that specifically address  $\beta$ -secretase cleavage, one of the other metabolites just described should be used as an endpoint in addition to A $\beta$  measurements, because otherwise one cannot decide whether a specific procedure has affected processes other than  $\beta$ -secretase cleavage, e. g.,  $\gamma$ -secretase cleavage or secretion of A $\beta$ .

### 1.2. Efforts to Characterize and Isolate $\beta$ -Secretase Using Synthetic Peptides Have Not Been Successful

Once the major  $\beta$ -secretase cleavage site had been defined as Met<sub>596</sub>–Asp<sub>597</sub>, the obvious approach was to generate peptide substrates as cleavage site models

and use those to screen brain fractions or test known proteases for cleavage. Using this approach, a variety of proteases have been put forward as  $\beta$ -secretase candidates, among them the proteasome, cathepsin G, cathepsin D, and various serine and metalloproteases from the human brain (for review *see* **ref. 6**). Interestingly, several of the candidates have properties that make them very unlikely, e.g., they prefer small peptides, are not found in neurons, or are located in the cytosol. Thus, the Met-Asp bond can be cleaved by various enzymes that do not play a role in  $A\beta$  generation, and screening with a small peptide cleavage site model is likely to lead to the identification of an irrelevant enzyme after a lengthy purification procedure.

### **1.3. Discovery of the Swedish Mutation and How It Influences $A\beta$ Generation**

In the early years after the cloning of APP,  $\beta$ -secretase cleavage could not be well investigated because it was generally assumed that  $A\beta$  generation occurred only under pathological conditions, i.e., in the brains of AD patients. In 1992 several groups simultaneously discovered that  $A\beta$  is generated by intact cells in tissue culture (for review *see* **ref. 7**). This finding allowed researchers to study  $\beta$ -secretase cleavage in tissue culture. Almost all our current knowledge about the secretases comes from studies on intact cells that process various APP derivatives under a variety of experimental conditions. When Mullan et al. (8) reported an AD-linked double mutation at the P1 and P2 positions of the Met-Asp  $\beta$ -secretase cleavage site, it was immediately analyzed whether this mutation would affect  $A\beta$  generation. Indeed, the Lys-Met to Asn-Leu exchange causes a massive increase in  $A\beta$  generation, and the Met $\rightarrow$ Leu exchange contributes most of that increase (9). This result suggests that  $\beta$ -secretase has some sequence specificity, so that a single mutation at the P1 position can greatly enhance  $\beta$ -secretase cleavage. Additional studies using the methods described in **Subheading 3.1.** confirmed this initial observation and demonstrated that  $\beta$ -secretase is surprisingly sequence specific.

### **1.4. Purpose and Scope**

The following paragraphs outline some of the materials and methods that have been used to generate data about the *in vivo* properties of  $\beta$ -secretase. This list is not complete and only approaches familiar to the author have been considered. However, many questions about  $\beta$ -secretase specificity could still be addressed using the tools described as follows.

## **2. Materials**

### **2.1. Cell Lines**

Any mammalian cell line that I have used seems to contain a  $\beta$ -secretase activity. Thus, the choice of a cell line should be based on the particular ques-

tion to be addressed. It may be preferable to use a cell line that is particularly easy to transfect (e.g., cos cells) or a line that can be differentiated into neurons (e.g., NT2).

## 2.2. Antibodies

Some antibodies required for the analysis are available commercially. The monoclonal antibodies 4G8 and 6E10 (Senetek, Maryland Heights, MO) are widely used to detect A $\beta$  by immunoprecipitation, ELISA, and Western blot assays. Antibody 6E10 also immunoprecipitates sAPP $\alpha$ , but not sAPP $\beta$ . Polyclonal or monoclonal antibodies to the  $\beta$ -secretase neopeptide have been described (4) (Chapter 14) and polyclonal antibodies to the APP C-terminus can easily be generated (10).

## 2.3. Transfection and Labeling

1. Lipofectin (Gibco-BRL, Gaithersburg, MD).
2. Met-free medium: Dulbecco's modified Eagle's medium (DMEM) minus methionine (Gibco-BRL), supplemented with L-glutamine and 10% dialyzed fetal calf serum (FCS) (Gibco-BRL or prepared in the lab by dialyzing regular FCS over night against DMEM minus methionine).
3. <sup>35</sup>S-Methionine (approx 10 mCi/mL, NEN DuPont [Boston, MA] or Amersham).
4. MEM Select-Amine kit (Gibco-BRL).
5. L-[2,3,4,5,6-<sup>3</sup>H] Phenylalanine (approx 1 mCi/mL, Amersham).

## 2.4. Cell Extracts

1. Phosphate-buffered saline (PBS): 140 mM NaCl, 3 mM KCl, 2 mM potassium phosphate, and 10 mM sodium phosphate, pH 7.4.
2. Sodium Tris EDTA NP40 (STEN)/lysis buffer: 50 mM Tris, pH 7.6, 150 mM NaCl, 2 mM EDTA, 1% NP-40, 0.2% bovine serum albumin (BSA), protease inhibitors of choice (e.g., AEBSF [4- $\alpha$ -aminoethyl]-benzenesulfonylfluoride], pepstatin, leupeptin, E-64).

## 2.5. Immunoprecipitation

1. Protein A Sepharose: 100 mg/mL Protein A Sepharose CL-4B (Sigma P-3391, Sigma Chemical CO., St. Louis, MO) in STEN buffer with 5 mg/mL BSA.
2. Wash buffers: 0.5 M STEN buffer (0.5 M NaCl, 50 mM Tris, pH 7.6, 150 mM NaCl, 2 mM EDTA, 0.2% NP-40), SDS-STEN buffer (0.1% SDS, 50 mM Tris, pH 7.6, 150 mM NaCl, 2 mM EDTA, 0.2% NP-40), STEN (50 mM Tris, pH 7.6, 150 mM NaCl, 2 mM EDTA, 0.2% NP-40).
3. Loading buffer: Tris-glycine SDS sample buffer or Tris-tricine SDS sample buffer (Novex, San Diego, CA).
4. 10–20% SDS Tris-tricine gels and 8% Tris-glycine gels (Novex) for analysis of A $\beta$  and sAPP $\beta$  immunoprecipitates.

## **2.6. Drugs**

All drugs were purchased from Sigma and dissolved in dimethylsulfoxide (DMSO) or ethanol.

## **3. Methods**

### **3.1. Site-Directed Mutagenesis to Study $\beta$ -secretase cleavage**

To address the sequence specificity of  $\beta$ -secretase, mutations around the  $\beta$ -secretase cleavage site were introduced using standard molecular biology techniques. The mutated APP molecule was then transiently transfected into 293 human embryonic kidney cells and the A $\beta$  peptides secreted from these cells were analyzed (*see Subheading 3.4.1.*) (11).

This method allows one to rapidly evaluate the effect a specific mutation has on A $\beta$  production, but one has to be aware of the limitations of the approach. First, immunoprecipitations from transient transfectants show a higher experiment-to-experiment variation than immunoprecipitations from stable lines that are laborious to generate (*see Note 1*). It is recommended to monitor sAPP $\alpha$  levels as a control so that the transfectant indeed overexpresses the APP construct. The second problem is that all cell lines show some endogenous A $\beta$  generation. This is not a problem when the mutant construct overproduces A $\beta$ , but if a particular mutation greatly diminishes  $\beta$ -secretase cleavage the endogenous background can be problematic. Despite these limitations the method has been successfully used to analyze various mutant constructs for their effects on  $\beta$ -secretase cleavage. Mutant constructs with substitutions around the  $\beta$ -secretase cleavage site, deletions within the A $\beta$  region and constructs with STOP codons that cause premature termination were tested for their effects on  $\beta$ -secretase cleavage (**Table 1**).

If the A $\beta$  or sAPP $\beta$  generated from the mutant construct is analyzed by an ELISA or immunoprecipitation assay, it can be clearly determined which mutations increase or decrease  $\beta$ -secretase cleavage. However, these methods do not allow one to determine whether the cleavage site has been changed by the mutation. To determine the exact  $\beta$ -secretase cleavage site, the A $\beta$  peptides can be analyzed by immunoprecipitation followed by mass spectrometry (12). Alternatively, aminoterminal radiosequencing of immunoprecipitated A $\beta$  allows one to determine the  $\beta$ -secretase cleavage site. Details of this method have been described (2).

### **3.2. Inhibitor Studies to Analyze $\beta$ -Secretase Cleavage**

Cell lines stably transfected with APP can be used in experiments to analyze the properties and subcellular localization of  $\beta$ -secretase cleavage. In this paradigm the substrate (APP) is kept constant, but the tissue culture media is

**Table 1**  
**Mutagenesis Study of  $\beta$ -Secretase Cleavage Site (11)**

Mutation	Result/interpretation
V594 $\Delta$ ,W	Substitution or deletion of P3 affects $\beta$ -secretase cleavage
K595 N,E	Substitutions at P2 also affect $\beta$ -secretase cleavage
M596 $\Delta$ ,V,A,K,E,I	These substitutions at P1 decrease $\beta$ -secretase cleavage
M596 L,Y,F	Only these large hydrophobic substitutions at P1 allow $\beta$ -secretase to cleave
D597 K,G, $\Delta$ ,I,N	These substitutions at P1' change the $\beta$ -secretase cleavage site
D597 E	Only this substitution at P1' generates normal A $\beta$
A598 $\Delta$ ,E,K	Substitutions at P2 affect $\beta$ -secretase cleavage
Deletion of A $\beta$ 5–9	Shortened A $\beta$ peptide with normal Asp1
Deletion of A $\beta$ 9–12	Shortened A $\beta$ peptide with normal Asp1
Stop after aa 51	$\beta$ -Secretase cleavage does not require cytoplasmic domain of APP
Stop after aa 40	$\beta$ -Secretase cleavage requires membrane bound substrate

manipulated and the effects of these manipulations are analyzed by immunoprecipitation, ELISA or immunocytochemistry (*see* **Notes 1** and **2**). The experiment can be performed as a pulse chase in which cells are metabolically labeled and then chased with medium containing compounds of interest. Alternatively, the labeling can be done in the presence of the compounds or cells can be incubated with compounds and the effects on A $\beta$  or sAPP $\beta$  production can be analyzed by ELISA. Effects on the cleavage site can again be analyzed by mass spectrometry or radiosequencing. A variety of compounds have been tested for effects on  $\beta$ -secretase in one of these paradigms (**Table 2**, *see also* **Note 3**).

### 3.3. Analysis of Candidate Enzymes

Using the same analysis methods employed for APP mutants or potential  $\beta$ -secretase inhibitors, candidate secretases can be analyzed (*see* **Note 1**). This has been demonstrated for cathepsin S, which was found to cause increased A $\beta$  production on transfection into 293 kidney cells. Using the methods described herein, cathepsin S was ruled out as  $\beta$ -secretase, because a potent inhibitor of this enzyme did not inhibit endogenous A $\beta$  production and radiosequencing demonstrated that in the transfected cells cathepsin S cleaved between Lys<sub>595</sub>–Met<sub>596</sub>, but not between Met<sub>596</sub>–Asp<sub>597</sub> (**13**). Any candidate  $\beta$ -secretase can be subjected to similar tests.

**Table 2**  
**Examples of β-Secretase Inhibitor Studies**

Compound	Effect	Authors' interpretation	Ref.
Leupeptin	None	β-Secretase not leupeptin sensitive	(14)
NH <sub>4</sub> Cl	Aβ decreased	β-Secretase cleavage requires acidic compartment	(14)
Bafilomycin A1	Aβ decreased	β-Secretase cleavage requires acidic compartment in primary human mixed brain cultures	(15)
AEBSF	Aβ decreased	Direct or indirect inhibition of Met <sub>596</sub> -Asp <sub>597</sub> cleavage Alternative sites cleaved by different enzymes	(3)
Brefeldin A	sAPPβ generated	Evidence for β-secretase cleavage in the endoplasmic reticulum of NT2N neurons	(16)

### 3.4. Aβ Peptide Analysis

#### 3.4.1. Transfection Experiment and Labeling

1. Transiently transfect 10 cm dishes of 293 human embryonic kidney cells with APP construct or secretase candidate of choice. Most liposome transfection methods work well, the author suggests use of lipofectin (Gibco-BRL) exactly following the manufacturer's instructions.
2. Let cells recover from transfection and label for 16 h with 600 μCi <sup>35</sup>S methionine in 4 mL methionine-free DMEM containing 10% dialyzed FBS.
3. For radioactive sequencing of Aβ, prepare phenylalanine-free medium using the MEM Select-Amine kit, supplement with 10% dialyzed FBS and label two 10 cm dishes of cells in this medium with 2.5 mCi/dish L-[2,3,4,5,6-<sup>3</sup>H] phenylalanine (Amersham, Amersham, UK). This amino acid is incorporated at positions 4, 19, and 20 of Aβ, which makes it relatively easy to determine where exactly the protein under investigation was cleaved.

#### 3.4.2. Preparation of Cell Extracts

1. Collect the medium and wash the cells once with ice-cold PBS.
2. Scrape the cells in 1 mL PBS. Transfer to a screwcapped Eppendorf tube. Centrifuge for 5 min at 3000g in a microfuge to pellet intact cells.
3. Add 800 μL STEN/lysis buffer. Resuspend the cells by vortexing (cells should lyse at this point, with insoluble cytoskeleton and nuclei visible). Incubate the cell suspension on ice for 10 min.
4. Centrifuge for 10 min at 10,000g to pellet nuclei and cytoskeleton.
5. Transfer the supernatant into a fresh screwcapped Eppendorf tube. At this point, extracts can be frozen.

### 3.4.3. Immunoprecipitation of Cell Extracts

1. Preclear samples with protein A-Sepharose to reduce background. Add 40  $\mu$ L Protein A-Sepharose and incubate with shaking at 4°C for 30 min. Then centrifuge for 5 min at 6000g. Transfer the precleared supernatant to a fresh tube.
2. Add the appropriate amount of antibody (serum: 1:100–1:300 dilution, monoclonals approx 10 mg/mL final concentration) and 25  $\mu$ L protein A-Sepharose. Incubate with shaking at 4°C for 1 h.
3. Pellet the antigen-antibody-protein A complexes by centrifuging for 5 min at 6000g in a microfuge.
4. Wash the pellet with the following buffers, each for 20 min at 4°C. Collect beads by centrifugation as before.
  - a. 1st wash — 0.5 M-STEN buffer
  - b. 2nd wash — SDS-STEN buffer
  - c. 3rd wash — STEN buffer
5. After the final centrifugation carefully remove the supernatant. Add 12–16  $\mu$ L 2X loading buffer. Boil the sample for 5 min to dissociate the complex, then centrifuge for 10 min at 14,000g in a microfuge. Transfer the supernatant to a fresh screwcapped tube. Repeat the boiling and centrifugation steps on the supernatant.
6. Load the samples onto an SDS polyacrylamide gel. Samples may be stored at –20°C prior to electrophoresis.

### 3.4.4. Immunoprecipitation of Secreted Proteins from Medium

1. Centrifuge samples for 10 min at 3000g to remove cellular debris and precipitated proteins. Depending on the size of the sample, immunoprecipitation can be done either in an Eppendorf tube or in a 15-mL conical tube. Use at least 3 mL of conditioned media for A $\beta$  immunoprecipitation. For precipitation of sAPP $\alpha$  and sAPP $\beta$  0.5 mL is sufficient.
2. Carefully transfer the supernatant to a new tube, add antibody and protein A-Sepharose, incubate with shaking at 4°C for at least 1 h, and continue as described for immunoprecipitation of cell extract (**Subheading 3.4.3.**).
3. Separate the immunoprecipitates on Tris-tricine gels and subject to fluorography or blot onto PVDF membrane for radiosequencing.

### 3.4.5. Drug Treatment Experiment

1. Grow cells stably transfected with APP to confluency.
2. Starve the cells for 45 min in methionine-free DMEM without serum.
3. Label the cells for 2 h in 4 mL methionine-free DMEM without serum in the presence of 600  $\mu$ Ci <sup>35</sup>S-methionine.
4. Discard the labeling medium, wash the cells briefly with DMEM, and incubate in DMEM containing 10% FBS, 100X methionine and the compound of choice for 2 h.
5. Prepare medium and extract and process as described in **Subheadings 3.4.2.–3.4.4.**

#### 4. Notes

1. Technical problems can arise at several steps in the protocols. Transient transfections should be carefully optimized using  $\beta$ -gal staining to establish a reproducible transient transfection procedure with high transfection efficiency in the cell line of choice. If this is not done, the results of the experiments may be difficult to interpret due to variability in transfection efficiencies between different samples and — if the expression of the transfected construct is not high enough — because of A $\beta$  production from the endogenous APP gene. In my experience it is impossible to combine transfection with a subsequent compound treatment, because cells that are still suffering from the transfection tend to die during treatment procedures in a nonreproducible manner.
2. Some compounds may not be soluble in water and require initial solubilization in organic solvents like ethanol or DMSO. It is critical that a solvent control is run in parallel to distinguish compound from solvent effects. Final DMSO concentrations below 1% have been found to be acceptable. Compounds may exert nonspecific toxic effects on the cells, which may be misinterpreted as specific inhibition of  $\beta$ -secretase. Nonspecific toxicity should be addressed by running a cell viability assay (e.g., 3-[4,5-dimethylthioxol-2-yl]-2,5-diphenyltetrazolium [MTT] (see Chapter 4) or lactate dehydrogenase [LDH] release) or by monitoring secretion of proteins other than A $\beta$ , e.g., sAPP $\alpha$ . If the labeling and the compound treatment are done in parallel, changes in  $\beta$ -secretase metabolites could be due to effects on APP protein production rather than processing. APP production effects can be excluded in a labeling-chase paradigm.
3. In the absence of a cloned or purified  $\beta$ -secretase, studies on intact living cells are the only way to extract information about this protease. The strengths of this approach are obvious: the papers referenced here have provided valuable information about the subcellular localization, properties, and sequence specificity of the elusive enzyme. The cathepsin S example demonstrates how a combination of inhibitor and transfection studies can be used to definitely exclude a candidate enzyme. By working with the natural substrate in intact cells, one can be confident that the substrate is presented in the right compartment in a membrane-bound form. However, the intrinsic limitations of this approach should not be overlooked. By working with intact cells, compounds that are not cell permeable or highly toxic cannot be tested. Compounds analyzed in intact cells can influence a variety of pathways and a given effect can often be explained by a variety of potential mechanisms. At this point, major progress in our understanding of  $\beta$ -secretase requires isolation of the enzyme.

#### References

1. Kang, J., Lemaire, H.-G., Unterbeck, A., Salbaum, J. M., Masters, C. L., Grzeschik, K.-H., et al. (1987) The precursor of Alzheimer's disease amyloid A4 protein resembles a cell-surface receptor. *Nature* **325**, 733–736.
2. Haass, C., Schlossmacher, M. G., Hung, A. Y., Vigo-Pelfrey, C., Mellon, A., Ostaszewski, B. L., et al. (1992) Amyloid  $\beta$ -peptide is produced by cultured cells during normal metabolism. *Nature* **359**, 322–325.

3. Citron, M., Diehl, T. S., Capell, A., Haass, C., Teplow, D. B., and Selkoe, D. J. (1996) Inhibition of amyloid  $\beta$ -protein production in neural cells by the serine protease inhibitor AEBSF. *Neuron* **17**, 171–179.
4. Seubert, P., Oltersdorf, T., Lee, M. G., Barbour, R., Blomquist, C., Davis, D. L., et al. (1993) Secretion of  $\beta$ -amyloid precursor protein cleaved at the amino-terminus of the  $\beta$ -amyloid peptide. *Nature* **361**, 260–263.
5. Shoji, M., Golde, T. E., Ghiso, J., Cheung, T. T., Estus, S., Shaffer, L. M., et al. (1992) Production of the Alzheimer amyloid b protein by normal proteolytic processing. *Science* **258**, 126–129.
6. Evin, G., Beyreuther, K., and Masters, C. L. (1994) Alzheimer's disease amyloid precursor protein (A $\beta$ PP): proteolytic processing, secretases and bA4 amyloid production. *Amyloid: Int. J. Exp. Clin. Invest.* **1**, 263–280.
7. Haass, C. and Selkoe, D. J. (1993) Cellular processing of  $\beta$ -amyloid precursor protein and the genesis of amyloid  $\beta$ -peptide. *Cell* **75**, 1039–1042.
8. Mullan, M., Crawford, F., Houlden, H., Axelman, K., Lilius, L., Winblad, B., and Lannfelt, L. (1992) A pathogenic mutation for probable Alzheimer's disease in the APP gene at the N-terminus of  $\beta$ -amyloid. *Nat. Genet.* **1**, 345–347.
9. Citron, M., Oltersdorf, T., Haass, C., McConlogue, L., Hung, A. Y., Seubert, P., et al. (1992) Mutation of the  $\beta$ -amyloid precursor protein in familial Alzheimer's disease increases  $\beta$ -protein production. *Nature* **360**, 672–674.
10. Podlisny, M. B., Tolan, D., and Selkoe, D. J. (1991) Homology of the amyloid  $\beta$ -protein precursor in monkey and human supports a primate model for  $\beta$ -amyloidosis in Alzheimer's disease. *Am. J. Pathol.* **138**, 1423–1435.
11. Citron, M., Teplow, D. B., and Selkoe, D. J. (1995) Generation of amyloid  $\beta$ -protein from its precursor is sequence specific. *Neuron* **14**, 661–670.
12. Wang, R., Sweeney, D., Gandy, S. E., and Sisodia, S. S. (1996) The profile of soluble amyloid b protein in cultured cell media. *J. Biol. Chem.* **271**, 31,894–31,902.
13. Munger, J. S., Haass, C., Lemere, C. A., Shi, G.-P., Wong, F., Teplow, D. B., et al. (1995) Lysosomal processing of amyloid precursor protein to A $\beta$  peptides: a distinct role for cathepsin S. *Biochem. J.* **311**, 299–305.
14. Haass, C., Hung, A. Y., Schlossmacher, M. G., Teplow, D. B., and Selkoe, D. J. (1993)  $\beta$ -amyloid peptide and a 3-kDa fragment are derived by distinct cellular mechanisms. *J. Biol. Chem.* **268**, 3021–3024.
15. Knops, J., Suomensaaari, S., Lee, M., McConlogue, L., Seubert, P., and Sinha, S. (1995) Cell-type and amyloid precursor protein-type specific inhibition of A $\beta$  release by Bafilomycin A1, a selective inhibitor of vacuolar ATPases. *J. Biol. Chem.* **270**, 2419–2422.
16. Chyung, A. S. C., Greenberg, B. D., Cook, D. G., Doms, R. W., and Lee, V. M. Y. (1997) Novel  $\beta$ -secretase cleavage of  $\beta$ -amyloid precursor protein in the endoplasmic reticulum/intermediate compartment of NT2N cells. *J. Cell. Biol.* **138**, 671–680.

## Using $\gamma$ -Secretase Inhibitors to Distinguish the Generation of the $A\beta$ Peptides Terminating at Val-40 and Ala-42

Paolo A. Paganetti and Matthias Staufenbiel

### 1. Introduction

A large body of evidence suggests a causative role of  $\beta$ -amyloid ( $A\beta$ ) in the pathogenesis of Alzheimer's disease (reviewed in refs. **1** and **2**).  $A\beta$  is neurotoxic and toxicity requires the formation of amyloid fibrils similar to those found in senile plaques (**3**). Autosomal dominant mutations linked to Alzheimer's disease were identified in three different genes (**4,5**). All mutations apparently alter amyloid precursor protein (APP) metabolism to increase the generation of  $A\beta$  peptides terminating at amino acid Ala-42. Due to the tendency of the longer  $A\beta$  peptides to more readily form fibrils (**7**), these may accelerate  $A\beta$  deposition, which ultimately leads to more aggressive, early onset forms of Alzheimer's disease (**8**). With the transgenic expression of APP in mice this was explored further (**9**). Whereas a twofold overexpression of APP did not lead to  $A\beta$  deposition, the same quantitative expression of APP with a mutation at codon 717 known to increase the formation of  $A\beta_{42}$  led to the appearance of  $A\beta$  deposits at the age of 18 mo. These data suggest that the  $A\beta$  load in the brain as well as the amyloidogenic properties of the  $A\beta$  isoforms directly regulate deposition and senile plaque formation.

A potential pharmacological site of intervention is the reduction of total  $A\beta$  generated in the brain or, specifically, that of the more fibrillogenic, longer forms of  $A\beta$ . To this end, the mechanisms underlying  $A\beta$  generation have been investigated in great detail.  $A\beta$  is produced during the normal cellular metabolism of APP, a type I transmembrane glycoprotein (**10–12**). The amino-terminus of  $A\beta$  is generated by  $\beta$ -secretase (**13**). In an alternative processing pathway, APP is cleaved by  $\alpha$ -secretase after amino acid Lys-16 of the  $A\beta$  sequence,

From: *Methods in Molecular Medicine, Vol. 32: Alzheimer's Disease: Methods and Protocols*  
Edited by: N. M. Hooper © Humana Press Inc., Totowa, NJ

precluding A $\beta$  production (14). The membrane-bound carboxy-terminal fragments (CTFs) originating from both of these cleavages are the substrates for proteolysis by  $\gamma$ -secretase, which produces the carboxy-termini of A $\beta$ , as well as that of the alternative peptide referred to as P3 following  $\alpha$ -secretase cleavage (15). This sequence of proteolytic cuts is necessary for the production of A $\beta$  and P3 (16,17). None of the secretases have yet been conclusively identified or cloned. The inhibition of  $\beta$ -secretase leads to alternative amino-terminal cleavages and thus to peptides with similar fibrillogenic properties (18,19). In addition,  $\beta$ -secretase cleavage is involved in the release of secreted APP, therefore its inhibition may result in adverse effects. From these and other considerations, it seems that  $\gamma$ -secretase is a preferred target of intervention.

To search for inhibitors of  $\gamma$ -secretase compounds may be tested on cultured cells expressing APP with A $\beta$  generation serving as a readout. A $\beta$  can be detected in the culture medium with sensitive assays such as ELISA or Western blot (*see* Chapters 5 and 6). Although this cellular “black-box” assay allows for screening of a large number of compounds, little information on the mechanism of action is obtained. Theoretically, several ways of interference exist that may impair A $\beta$  release. These include gene expression, vectorial transport along the secretory pathway, sorting to specific subcellular compartments, secretion, inhibition of  $\beta$ - and  $\gamma$ -secretase, as well as general cytotoxicity. This chapter focuses on methodologies suited to discriminate between these different mechanisms.

Treatment with leupeptin, an inhibitor of lysosomal proteases, has no effect on A $\beta$  generation although the accumulation of amyloidogenic CTFs is observed (20). These data suggest the existence of at least two metabolic pathways for the CTFs: degradation (inhibited by leupeptin) or processing to A $\beta$ . Nonlysosomal proteases that have been proposed to contribute to A $\beta$  generation include calpain and the multicatalytic proteinase complex (proteasome) (21,22). Because both can be inhibited by peptide aldehydes that easily penetrate cell membranes, these compounds were tested for their effect on A $\beta$  generation. Calpain inhibitor I (N-acetyl-Leu-Leu-norleucinal) causes a marked reduction in the release of A $\beta$  and P3 into the culture medium of cells overexpressing APP (23), whereas calpain inhibitor II (N-acetyl-Leu-Leu-methioninal) only slightly inhibited A $\beta$  and P3 secretion (23). Both calpain inhibitors caused an intracellular accumulation of CTFs with apparent molecular masses of 15 and 12 kDa, which are presumably the precursors of the A $\beta$  and P3 peptides. Testing concentrations above 10  $\mu$ M of these compounds affected cell viability during an overnight treatment. To analyze whether the effects on A $\beta$  generation were caused by cytotoxicity or by reduction of APP synthesis, and to obtain insights into the site of action of these compounds, classical pulse-chase assays were performed (23). APP was metabolically

labeled for 1 h with [<sup>35</sup>S]methionine. After a 3-h chase in the presence or absence of 50 mM calpain inhibitor I, radiolabeled A $\beta$  peptides were immunoprecipitated, separated by sodium dodecyl sulfate polyacrylamide gel electrophoresis (SDS-PAGE) and analyzed by fluorography. This method revealed again that calpain inhibitor I reduced the amounts of secreted A $\beta$  and P3, whereas the CTFs, but not A $\beta$  and P3, accumulated within the cells. The inhibition of the A $\beta$  and P3 generation and the accumulation of CTFs suggests that the peptide aldehydes interfere with the  $\gamma$ -secretase activity. To further address this point, cells transfected with a cDNA driving the expression of the 100 carboxy-terminal amino acids of APP starting at Met<sub>652</sub> of APP751 (C100) were chosen (23). C100 only requires a  $\gamma$ -secretase cleavage to produce an A $\beta$  peptide with an additional amino-terminal methionine. Pulse labeling for 1 h followed by chase in the presence of 50  $\mu$ M calpain inhibitor I resulted in the clear reduction of A $\beta$  released into the medium. These data confirm that calpain inhibitor I inhibits the  $\gamma$ -secretase, whereas an effect on  $\beta$ -secretase, which is the upstream enzymatic activity producing the CTF corresponding to C100 cannot be excluded. Meanwhile, several other peptide aldehydes have been reported to inhibit A $\beta$  generation including calpeptin (carbobenzoxy-Leu-norleucinal), MG132 (carbobenzoxy-Leu-Leu-leucinal), and MDL28170 (carbobenzoxy-Val-phenylal) (24–26).

The exact mechanisms leading to the formation of the carboxy-terminal ends of A $\beta$  at amino acid Val-40 and Ala-42 are not well understood. As mentioned earlier, the APP717 mutation leads to an alteration of APP processing to increase the ratio between A $\beta$ 42 and A $\beta$ 40. Because this missense mutation affects an amino acid residue distal to the A $\beta$  sequence, this argues against the generation of A $\beta$ 42 followed by exopeptidase trimming to produce the carboxy-terminus of A $\beta$ 40. More likely is the possibility of two distinct endoproteolytic cleavages at either amino acid Val-40 or Ala-42. It should be pointed out that the data on the peptide aldehydes were initially reported without discriminating A $\beta$ 40 and A $\beta$ 42. It is likely that these data reflect the effects on the main species A $\beta$ 40. To better clarify this aspect, the effects of calpain inhibitor I, MG132, and calpeptin (26) as well as that of MDL28170 (27) were investigated specifically on A $\beta$ 40 and A $\beta$ 42 production.

Bicine/Tris SDS-PAGE in the presence of 8 M urea and 0.25% SDS was used to resolve A $\beta$ 40 and A $\beta$ 42 (see Chapter 6). Calpain inhibitor I applied in the range of 5–50  $\mu$ M augmented A $\beta$ 42 while reducing A $\beta$ 40. The effect of MG132 on A $\beta$ 42 generation was an increase at 5  $\mu$ M and an inhibition at 50  $\mu$ M. A $\beta$ 40 was inhibited in a typical dose-dependent manner. MG132 was the more potent inhibitor of A $\beta$ - as well as P3-generation. Calpeptin did not show a differential effect on the production of A $\beta$ 40 and A $\beta$ 42 when tested on HEK-293 cells, but showed a similar effect as calpain inhibitor I and MG132

on COS cells. Together, these data indicate that the carboxy-termini of A $\beta$  at amino acid Val-40 and amino acid Ala-42 are generated by distinct  $\gamma$ -secretase activities.

As described in the previous paragraph, the effect of the peptide aldehydes on the ratio of A $\beta$ 40 vs A $\beta$ 42 is observed only at certain concentrations. It is therefore imperative to perform a complete concentration dependency for every new compound tested. It should also be noted that the identity of A $\beta$ <sub>1-40</sub> and A $\beta$ <sub>1-42</sub> is determined *bona fide* by the comigration of the cognate synthetic peptides on SDS-PAGE. The interpretation of the data should be done with particular caution, as certain cultured cells show quite heterogenous  $\beta$ -secretase cleavage at the amino-terminus of A $\beta$ , leading to an altered migration on SDS-PAGE. Moreover, this is easily perturbed by various compounds. The use of human embryo kidney (HEK)-293 or Chinese hamster ovary (CHO)-K1 cells, in which  $\beta$ -secretase generates mainly or exclusively the amino-terminus of A $\beta$  at amino acid Asp-1, is strongly recommended to study the effect of test compounds on the formation of the A $\beta$  carboxy-termini. Alternatively, cells should be transfected with APP harboring the Swedish double mutation which is an optimal substrate for  $\beta$ -secretase cleavage at amino acid Asp-1 of A $\beta$  (**18**). Antibodies reacting specifically to the free amino- and carboxy-terminal amino acids of the A $\beta$  peptides may be used to confirm the interpretation of the data.

Despite the inhibition of A $\beta$  generation with compounds referred to as calpain and proteasome inhibitors, there is little evidence to date that these proteolytic systems are involved in A $\beta$  generation. More specific inhibitors of the proteasome (lactacystin) or of calpain (calpastatin) were found to be inactive as inhibitors of A $\beta$  generation and  $\gamma$ -secretase (**25**). Finally, the effect of peptide aldehydes on A $\beta$ 40 and A $\beta$ 42 production by a modulatory effect of calpain inhibition on protein kinase C, by a modulatory effect on presenilin function, or by other indirect effects on A $\beta$ 40/A $\beta$ 42 ratio cannot be excluded completely.

## 2. Materials

### 2.1. Protease Inhibitors

1. Calpain inhibitor I and II as well as calpeptin are available from commercial sources (Boehringer Mannheim [Mannheim, Germany] and Calbiochem [San Diego, CA]).
2. MG132 was synthesized as described (**26**).
3. Prepare the 25-mM stock solutions in *N,N*-dimethyl-formamide (DMF), store at  $-20^{\circ}\text{C}$  for a maximum of 4 wk, and dilute in culture medium shortly before testing (*see* **Note 1**).

### 2.2. cDNA Constructs

The plasmids driving the expression of APP<sub>751</sub>Swedish, of APP<sub>695</sub>Swedish with the c-myc epitope Glu-Gln-Lys-Leu-Ile-Ser-Glu-Glu-Asp-Leu (**28**), and

of the 100 carboxy-terminal amino acids of APP (C100) were reported previously (23).

### 2.3. Cells and Culture Media

HEK-293 cells (American Type Culture Collection, Rockville, MD, ATCC CRL 1573) are propagated using standard cell culturing techniques in Dulbecco's modified Eagle's medium (DMEM) (Life Technologies [Gaithersburg, MD], Gibco-BRL 041-01085) containing 10% heat-inactivated fetal calf serum (FCS) (Life Technologies), on 100-mm-diameter Petri dishes (Falcon 3072, Becton Dickinson, Rutherford, NJ) in an incubator set at 37°C and 5% CO<sub>2</sub>.

### 2.4. cDNA Transfections

1. Purify the supercoiled DNA by double banding on a CsCl gradient, or by using a commercially available purification kit (Qiagen, Chatsworth, CA) (*see Note 2*).
2. 2 $\times$  BES buffered saline (BBS) (final volume 500 mL): 5.35 g N,N-bis [2-Hydroxyethyl]-l2-amino ethanesulfonic acid (BES), 8.15 g NaCl, 0.109 g Na<sub>2</sub>HPO<sub>4</sub> (anhydrous, or 133.5 mg Na<sub>2</sub>HPO<sub>4</sub>·2H<sub>2</sub>O), adjust to pH 6.95, sterile filtrate (*see Note 3*).
3. 2 M CaCl<sub>2</sub> (final volume 50 mL): 14.7 g CaCl<sub>2</sub>·2H<sub>2</sub>O, sterile filtrate.

### 2.5. Pulse Chase Assay

1. Pulse medium: 0.1 mCi/mL [<sup>35</sup>S]methionine (commercially available from several sources e.g., Amersham, NEN DuPont, Boston, MA) in methionine-free Dulbecco's modified Eagle's medium (Sigma Chemical Co., St. Louis, MO), containing 20 mM HEPES, pH 7.4 (*see Note 4*), 2% dialyzed FCS (Life Technologies) (*see Note 5*), 100 IU/mL penicillin, 100  $\mu$ g/mL streptomycin (*see Note 6*).
2. Chase medium: DMEM, containing 20 mM HEPES, pH 7.4, 10% FCS, 100 IU/mL penicillin, 100  $\mu$ g/mL streptomycin, and 1 mM methionine.

### 2.6. Immunoprecipitations

1. Lysis buffer (100 mL): 5 mL 1 M HEPES, pH 7.0 (final concentration 50 mM), 3 mL 5 M NaCl (150 mM), 2 mL 0.5 M EDTA, pH 8.0 (10 mM), 10 mL 10% NP40 (1%), 5 mL 10% sodium cholate (0.5%), 1 mL 10% sodium dodecyl sulfate (SDS) (0.1%), 1 mL 100 mg/mL bovine serum albumin (BSA) (1 mg/mL) (Sigma A7888), and 2 mL 100 mM phenylmethylsulfonyl fluoride (PMSF) dissolved in isopropanol (2 mM), this latter to be added shortly before use.
2. Antibody dilution buffer: 50 mM HEPES, pH 7.0, 150 mM NaCl, 10 mM EDTA.
3. PAS: Protein A Sepharose (Pharmacia, Uppsala, Sweden) CL4B equilibrated in WB2, 50% slurry (*see Note 7*).
4. WB1: 1 Part lysis buffer, 1 part antibody dilution buffer.
5. WB2: Antibody dilution buffer containing 0.1% BSA, 0.1% gelatin (*see Note 8*).
6. WB3: 20 mM HEPES, pH 7.0.

### 3. Methods

#### 3.1. *cDNA Transfections (29)*

1. Grow the HEK-293 cells to 60–90% confluency using a 100-mm culture Petri dish (*see Note 9*) in 10 mL of culture medium (*see Note 10*).
2. Precipitate 20  $\mu\text{g}$  DNA in a clear polystyrene or polycarbonate centrifugation tube on dry ice by adding 1/10 vol 3 M sodium acetate and 2 vol EtOH. Remove the salts by one wash with 70% EtOH, precooled at  $-20^{\circ}\text{C}$  (*see Note 11*).
3. Resuspend the sterilized DNA in 874  $\mu\text{L}$  sterile  $\text{H}_2\text{O}$ , and add 126  $\mu\text{L}$  2 M  $\text{CaCl}_2$ .
4. Slowly add 1000  $\mu\text{L}$  2 $\times$  BBS under continuous gentle shaking and incubate for 20 min at room temperature. During this time a faint haze will form in the solution (*see Note 12*).
5. Carefully add the precipitating cDNA/phosphate complex to the cells in 10 mL culture medium by gently shaking the culture dish.
6. Incubate overnight in an incubator set at  $37^{\circ}\text{C}$  and 3%  $\text{CO}_2$ .
7. Rinse the cells once with prewarmed phosphate-buffered saline (PBS) and feed with fresh culture medium. If required by the experiment, replate transfected cells in new dishes. Incubate the cells for at least a further 12–24 h at  $37^{\circ}\text{C}$  and 5%  $\text{CO}_2$  before performing the experiment (*see Note 13*).

#### 3.2. *Metabolic Radiolabeling, Pulse Chase Assay*

1. For the work with radioactive material, comply with local legislative regulations. [ $^{35}\text{S}$ ]labeled amino acids are absorbed rapidly by the body. Stock solutions usually contain volatile metabolites. Dispose of contaminated waste as required.
2. To increase the efficiency of radiolabeling, wash the cells once with PBS and starve for 30–60 min in pulse medium in the absence of radiolabeled amino acids. This will deplete most of the internal stores of amino acids that would otherwise compete with the labeled amino acids.
3. Pulse is performed for 1 h with 0.1 mCi/mL [ $^{35}\text{S}$ ]methionine in pulse medium (*see Note 6*).
4. To chase the labeled pool of protein, incubate the cells in chase medium containing excess cold methionine for the required incubation time, with or without testing compounds (*see Note 14*). This is to exclude an effect on APP synthesis (labeled pool of APP is generated in the absence of test compound) (*see Note 15*).

#### 3.3. *Immunoprecipitations (30)*

1. Collect the conditioned media containing secreted APP metabolites A $\beta$ , P3, and secreted APP and free of cell debris and insoluble material by a 5 min, 1000g centrifugation.
2. To prepare cell extracts, wash the cell layers with PBS and then lyse by adding directly to the cell layers 0.75 mL of ice-cold lysis buffer. Incubate the plates for 30 min on ice. Harvest the cell lysates using a rubber policeman, transfer by pipeting to a 1.5 mL screwcap polystyrene centrifugation tube, incubate on ice for 10 min, vigorously vortex, and free of insoluble material by a 5-min, 12,000g

centrifugation at 4°C. Collect the supernatants, i.e., cell extracts containing cell-associated APP and CTFs, in a new centrifugation tube.

3. To avoid the nonspecific immunoisolation of radiolabeled material that may bind to the solid phase carrier, preclear the conditioned media and cell extracts for 30 min at 4°C with 100  $\mu$ L sepharose CL4B (50% slurry, equilibrated in WB2) on an orbital shaker. After 5 min, 12,000g centrifugation 4°C, transfer the supernatants to a new tube.
4. Add in 1 vol antibody dilution buffer 5  $\mu$ g mouse monoclonal antibodies or 1–5  $\mu$ L crude rabbit antisera reacting to APP or metabolites thereof (*see Note 16*).
5. The binding of the antigen to its specific antibody occurs during an overnight incubation at 4°C by continuous agitation on an orbital shaker.
6. Pellet the insoluble material formed during the overnight incubation by a 5-min, 12,000g centrifugation and transfer the supernatant to new tubes.
7. Add the protein A Sepharose beads (Pharmacia) (50% slurry in WB2) and incubate for 30–60 min at 4°C on an orbital shaker.
8. Purify the protein A-bound material by washing the sepharose beads once with WB1 (this wash is only for samples originating from the cell extracts), twice with WB2, and once with WB3. Sediment the Protein A Sepharose beads between the different washes with a quick 10 s, 12,000g centrifugation.
9. After the last wash and centrifugation, recentrifuge the samples and remove all traces of the washing buffer by aspiration using a capillary.
10. Solubilize the immunoprecipitated material in an SDS-PAGE sample buffer, heat at 95°C for 5 min, and resolve by SDS-PAGE (*see Note 17*). Analysis is performed by fluorography on Kodak BioMax MR autoradiograms. Quantification of radioactive protein is done with, e.g., an InstantImager (Canberra Packard, Canberra, Australia) (*see Note 18*).

### 3.4. SDS-PAGE and Western Blots

These methods are described in Chapter 6.

## 4. Notes

1. Peptide aldehydes are labile in solution probably due to oxidation. Routinely, stock solutions in *N,N*-dimethyl-formamide that are stored at –20°C for no longer than 4 wk are prepared. Repeated thaw/freeze cycles should be avoided.
2. When performing calcium phosphate transfection, it is crucial to use high-quality DNA preparations. DNA impurities such as endotoxins greatly reduce transfection efficiency.
3. The pH of the BBS buffer is sensitive to temperature changes, and thus the pH should be adjusted when the solution is equilibrated to the temperature of the room where the precipitation is performed. Alternatively, mock precipitations can be performed with different buffers adjusted to pH values in the range 6.9–7.0. The readout for the optimal buffer is the formation of a faint haze in about 10–20 min. Sterile filtration may also affect the pH.

4. HEPES is added to stabilize the pH of the medium, as incubation times such as those used in the pulse chase assay are not sufficient to equilibrate the carbonate level in the culture medium with a 5% CO<sub>2</sub> atmosphere.
5. Dialyzed FCS is methionine and cysteine free.
6. A less expensive alternative to [<sup>35</sup>S]methionine is commercially available as a total lysate from *E. Coli* grown in [<sup>35</sup>S]sulfate (Express<sup>35</sup>S- protein labeling mix, NEN Life Science), which contains a mixture of [<sup>35</sup>S]methionine and [<sup>35</sup>S]cysteine. For the incorporation of both amino acids, use methionine- and cysteine-free DMEM (Sigma).
7. Certain monoclonal antibodies bind poorly to protein A and well to protein G.
8. To increase the stringency of the WB2 wash, the concentration of NaCl can be increased up to 500 mM. Most antibodies well tolerate the high salt concentration.
9. To improve cell adhesion, which can turn out to be a problem when several washes are required by the experimental setup, culture plates should be coated with 10 µg/mL poly-D-lysine (Sigma) for 30 min at 37°C.
10. Because the formation of the DNA precipitate is sensitive to the pH, it is recommended to change the culture medium 3–4 h before transfection.
11. To avoid cell culture contaminations, the DNA should be sterile. Large batches can be prepared in advance and resuspended in sterile water at 1 mg/mL, or stored in the presence of 1 vol chloroform.
12. Very good transfection efficiency of HEK-293 cells is obtained also with a commercially available kit (SuperFect Reagent, Qiagen). This method is greatly simplified when compared to calcium phosphate precipitation and results in good reproducibility.
13. Monitor transfection efficiency by immunostaining with specific antibodies reacting to the transgene product; do not rely on transfection markers such as β-gal or similar, as they show a tendency to lead to overestimation.
14. A 3-h chase is enough for the almost complete processing/degradation of APP, which has a short half-life.
15. Obviously, it is crucial to exclude cytotoxicity as a potential effect of test compounds. As alternative, or to complement the pulse chase assay, it is recommended to assay the APP synthesis rate, e.g., with a 10-min pulse and analysis of the radiolabeled APP pool at the end of the drug treatment time. In addition, it is possible to rely on commercially available cytotoxicity assays such as the MTS assay (Promega, Madison, WI).
16. The amount of antibody required for quantitative immunoprecipitation should be determined empirically for every antibody.
17. To avoid diffusion and loss of labeled Aβ and P3 peptides, these can be fixed in the gel with glutaraldehyde (0.25% in 0.4 M boric acid/Na<sub>2</sub>HPO<sub>4</sub>, pH 6.2).
18. To quantify the amount of metabolites generated during the chase, consider for normalization the number of methionine and cysteine residues contained in each metabolite. As an example, the APP695 isoform contains 20 methionine and 12 cysteine residues, whereas Aβ contains only 2 methionine residues.

## References

1. Yankner B. A. (1996) Mechanisms of neuronal degeneration in Alzheimer's disease. *Neuron* **16**, 921–932.
2. Selkoe, D. J. (1997) Alzheimer's disease: genotypes, phenotypes, and treatments. *Science* **275**, 630–631.
3. Lorenzo, A. and Yankner, B. A. (1994)  $\beta$ -Amyloid neurotoxicity requires fibril formation and is inhibited by congo red. *Proc. Natl. Acad. Sci. USA* **91**, 12,243–12,247.
4. Suzuki, N., Cheung, T. T., Cai, X. D., Odaka, A., Otvos, L., Eckman, C., et al. (1994) An increased percentage of long amyloid  $\beta$ -protein secreted by familial amyloid  $\beta$ -protein precursor ( $\beta$ APP<sub>717</sub>) mutants. *Science* **264**, 1336–1340.
5. Scheuner, D., Eckman, C., Jensen, M., Song, X., Citron, M., Suzuki, N., et al. (1996) Secreted amyloid  $\beta$ -protein similar to that in senile plaques of Alzheimer's disease is increased in vivo by the presenilin 1 and 2 and APP mutations linked to Alzheimer's disease. *Nat. Med.* **2**, 864–870.
6. Glenner, G. G. and Wong, C. W. (1984) Alzheimer's disease: initial report of the purification and characterization of a novel cerebrovascular amyloid protein. *Biochem. Biophys. Res. Commun.* **120**, 885–890.
7. Jarrett, J. T., Berger, E. P., and Lansbury, P. T., Jr. (1993) The carboxy-terminus of the  $\beta$ -amyloid protein is critical for the seeding of amyloid formation: implication for the pathogenesis of Alzheimer's disease. *Biochemistry* **32**, 4693–4697.
8. Iwatsubo, T., Odaka, A., Suzuki, N., Mizusawa, H., Nukina, N., and Ihara, Y. (1994) Visualization of A $\beta$ 42(43) and A $\beta$ 40 in senile plaques with end-specific monoclonals: evidence that an initially deposited species is A $\beta$ 42(43) *Neuron* **13**, 45–53.
9. Sturchler-Pierrat, C., Abramowski, D., Duke, M., Wiederhold, K.-H., Mistl, C., Rothacher, S., et al. (1997) Two amyloid precursor protein transgenic mouse models with Alzheimer's disease-like pathology. *Proc. Natl. Acad. Sci. USA* **94**, 13,287–13,292.
10. Shoji, M., Golde, T. E., Ghiso, J., Cheung, T. T., Estus, S., Shaffer, L. M., et al. (1992) Production of the Alzheimer amyloid  $\beta$ -protein by normal proteolytic processing. *Science* **258**, 126–129.
11. Haass, C., Schlossmacher, M. G., Hung, A. Y., Vigo-Pelfrey, C., Mellon, A., Ostaszewski, B. L., et al. (1992) Amyloid  $\beta$ -peptide is produced by cultured cells during normal metabolism. *Nature* **359**, 322–325.
12. Busciglio, J., Gabuzda, D. H., Matsudaira, P., and Yankner, B. A. (1993) Generation of  $\beta$ -amyloid in the secretory pathway in neuronal and nonneuronal cells. *Proc. Natl. Acad. Sci. USA* **90**, 2092–2096.
13. Golde, T. E., Estus, S., Younkin, L. H., Selkoe, D. J., and Younkin, S. G. (1992) Processing of the amyloid precursor protein to potentially amyloidogenic derivatives. *Science* **255**, 728–730.
14. Esch, F. S., Keim, P. S., Beattie, E. C., Blacher, R. W., Culwell, A. R., Oltersdorf, T., et al. (1990) Cleavage of amyloid  $\beta$ -peptide during constitutive processing of its precursor. *Science* **248**, 1122–1124.

15. Dyrks, T., Dyrks, E., Mönning, U., Urmoneit, B., Turner, J., and Beyreuther, K. (1993) Generation of  $\beta$ A4 from the amyloid protein precursor and fragments thereof. *FEBS Lett.* **335**, 89–93.
16. Citron, M., Vigo-Pelfrey, C., Teplow, D. B., Miller, C., Schenk, D., Johnston, J., et al. (1994) Excessive production of amyloid  $\beta$ -protein by peripheral cells of symptomatic and presymptomatic patients carrying the Swedish familial Alzheimer's disease mutation. *Proc. Natl. Acad. Sci. USA* **91**, 11993–11997.
17. Paganetti, P. A., Lis, M., Klafki, H.-W., and Staufenbiel, M. (1996) Amyloid precursor protein truncated at any of the  $\gamma$ -secretase sites is not cleaved to  $\beta$ -amyloid. *J. Neurosci. Res.* **46**, 283–293.
18. Haass, C., Capell, A., Citron, M., Teplow, D. B., and Selkoe D. J. (1995) The vacuolar  $H^+$ -ATPase inhibitor bafilomycin A1 differentially affects proteolytic processing of mutant and wild-type  $\beta$ -amyloid precursor protein. *J. Biol. Chem.* **270**, 6186–6192.
19. Schrader-Fischer, G. and Paganetti, P. A. (1996) Effect of alkalizing agents on the processing of the  $\beta$ -amyloid precursor protein. *Brain Res.* **716**, 91–100.
20. Haass, C., Hung, A. Y., Schlossmacher, M. G., Teplow, D. B., and Selkoe D. J. (1993)  $\beta$ -Amyloid peptide and a 3-kDa fragment are derived by distinct cellular mechanisms. *J. Biol. Chem.* **268**, 3021–3024.
21. Siman, R., Card, J. P., and Davis, L. G. (1990) Proteolytic processing of  $\beta$ -amyloid precursor by calpain I. *J. Neurosci.* **10**, 2400–2411.
22. Mundy, D. I. (1994) Identification of the multicatalytic enzyme as a possible  $\gamma$ -secretase for the amyloid precursor protein. *Biochem. Biophys. Res. Commun.* **204**, 333–341.
23. Klafki, H.-W., Paganetti, P. A., Sommer, B., and Staufenbiel, M. (1995) Calpain inhibitor I decreases  $\beta$ A4 secretion from human embryonal kidney cells expressing  $\beta$ -amyloid precursor protein carrying the APP670/671 double mutation. *Neurosci. Lett.* **201**, 29–32.
24. Higaki, J., Quon, D., Zhong, Z., and Cordell, B. (1995) Inhibition of  $\beta$ -amyloid formation identifies proteolytic precursors and subcellular site of catabolism. *Neuron* **14**, 651–659.
25. Yamazaki, T., Haass, C., Saido, T. C., Omura, S., and Ihara, Y. (1997) Specific increase in amyloid  $\beta$ -protein 42 secretion ratio by calpain inhibitors. *Biochemistry* **26**, 8377–8383.
26. Klafki, H.-W., Abramowski, D., Swoboda, R., Paganetti, P. A., and Staufenbiel, M. (1996) The carboxy-termini of  $\beta$ -amyloid peptides 1–40 and 1–42 are generated by distinct  $\gamma$ -secretase activities. *J. Biol. Chem.* **271**, 28,655–28,659.
27. Citron, M., Diehl, T. S., Gordon, G., Biere, A. L., Seubert, P., and Selkoe, D. J. (1996) Evidence that the 42- and 40-amino acid forms of amyloid  $\beta$ -protein are generated from the  $\beta$ -amyloid precursor protein by different protease activities. *Proc. Natl. Acad. Sci. USA* **93**, 13170–13175.
28. Price, K. M., Cuthbertson, A. S., Vaerndell, I. M., and Sheppard, P. W. (1990) The production of monoclonal antibodies to myc, c-erbB-2 and EFG-receptor using a synthetic peptide approach. *Dev. Biol. Stand.* **71**, 23–31.
29. Chen C. and Okayama, H. (1987) High-efficiency transformation of mammalian cells by plasmid DNA. *Mol. Cell. Biol.* **7**, 2745–2752.
30. Paganetti, P. A. and Scheller, R. H. (1994) Proteolytic processing of the *Aplysia* A peptide precursor in AfT-20 cells. *Brain Res.* **633**, 53–62.

## Designing Animal Models of Alzheimer's Disease with Amyloid Precursor Protein (APP) Transgenes

Jeanne F. Loring

### 1. Introduction

Amyloid precursor protein (APP) and Alzheimer's disease are irrevocably linked, as APP is cleaved to form the A $\beta$  peptides that are the major components of amyloid plaques. One of the most resilient hypotheses about the cause of AD centers on the A $\beta$  peptide; all genetic causes and risk factors can be fitted into a general "amyloid cascade hypothesis," which maintains that all pathology is initiated by an abnormal accumulation of A $\beta$  amyloid (1).

Unfortunately, this and other intriguing hypotheses are virtually untested. The problem lies in the fact that AD is a uniquely human disease. And, because the complex pathology of the disease cannot be properly modeled in a culture dish, the only hope for a molecular understanding of AD is the discovery of an appropriate animal model. The goal of transgenic approaches is to accurately model at least one aspect of a human disease so that the process can be examined in detail. In this regard, the transgenic model approach to understanding AD has had a successful beginning. Several transgenic *APP* mouse lines develop age-related amyloid deposits that resemble the amyloid pathology of AD. Some of these lines contain the entire human *APP* gene and are useful for studying the effects of drugs that are designed to interfere with human APP metabolism. Another kind of transgenic line has targeted changes in the mouse *APP* gene; these allow a detailed analysis of the effects of mutations on APP processing. Within the context of developing *APP* transgenic animal models for AD, this chapter discusses the rationale for using a transgenic approach, the ideas behind transgene design, the relative merits of various approaches, and in what ways a transgenic line can be analyzed for AD research.

### **1.1. Rationale for a Transgenic Approach to Modeling Human Disease**

A transgenic animal is one that harbors a deliberate change in its genome. With current technology, genes can be added, removed, or modified in situ. Genes can be added to many types of animal, but the other methods can so far only be done in the mouse. Genetic models for human disease can be “built” by combining different types of genetic modifications in the initial design of the model, or by breeding together mouse lines that contain different alterations. There is a growing trend toward combining multiple transgenes in a single animal, and the most successful human disease models of the future are likely to be made in this way.

### **1.2. History of the APP Transgenic Approach**

When researchers began thinking about making a transgenic animal model for Alzheimer’s disease, APP was the prime target. There was a strong rationale for this approach, as it was known that in Down Syndrome, there is an extra copy of the APP gene, and APP is overexpressed. Because all Down syndrome individuals acquire the brain pathology of AD, including amyloid plaques, it was logical to assume that a mouse with an extra copy of the APP gene would also develop AD pathology. The main argument against this hypothesis was that since in humans the pathology took many years to develop, the mouse might simply not live long enough to acquire AD plaques. A few laboratories began making transgenic APP mouse lines in the 1980s, but the results were disappointing because expression of the transgenic protein was very low, much less than even the endogenous mouse APP protein levels. However, improvement in transgene design and discovery of AD-causing mutations in APP greatly improved the utility of APP-transgenic mice for studying AD.

### **1.3. APP Mutations**

When the first AD-causing mutation was discovered in APP in 1991 (2) it was immediately incorporated into transgene designs. There are now three kinds of identified APP mutations that are linked to early onset AD (Fig. 1). All of the mutations affect proteolytic processing of APP. APP is a cell-surface protein that is cleaved in its extracellular domain by an enzyme termed  $\alpha$ -secretase. The identity of the enzyme is uncertain, but its characteristics are shared with a previously identified protease called tumor necrosis factor alpha converting enzyme (TACE) (2). A minor fraction of APP is not cleaved by  $\alpha$ -secretase, but is instead cut by two other unknown enzymes,  $\beta$ -secretase and  $\gamma$ -secretase, to yield the  $A\beta$  fragment (Fig. 1). Some of the  $A\beta$  produced in the brain accumulates in amyloid plaques. Most  $A\beta$  is 40 amino acids long, but about 10% is longer, the result of cleavage of APP two or three amino acids closer to

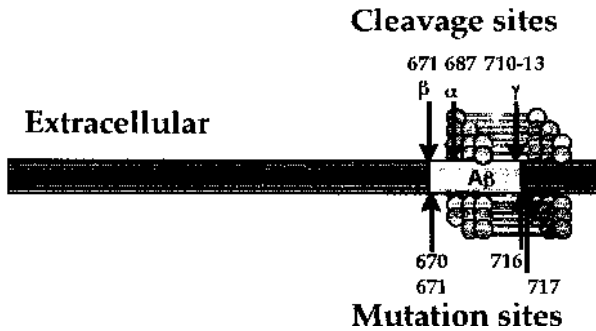


Fig. 1. Diagram of APP. The Aβ portion is shown in gray. Site numbers of cleavage sites and mutations are in reference to the 770 amino acid isoform.

**Table 1**  
**Familial Alzheimer’s Disease Mutations in APP**

Position in APP <sub>770</sub>	Site	Effect of mutation	Ref.
670 and 671 (KM–NL) (Swedish mutation)	At β-secretase site	Increase in total Aβ	4
716 (I–V) (Florida mutation)	Near γ-secretase site	Increase in Aβ <sub>42/43</sub>	7
717 (V–I, F, or G) (London mutating, Indiana mutation)	Near γ-secretase site	Increase in Aβ <sub>42/43</sub>	3,5,6

its C terminus. Aβ<sub>42/43</sub> is less soluble than Aβ<sub>40</sub> and is overrepresented in amyloid plaques. The APP mutations that cause AD all affect Aβ production. A double amino acid substitution at positions 670 and 671 leads to a fivefold increase in Aβ<sub>40</sub> (4). Three different amino acid substitutions at position 717 (3,5,6), and one at position 716 (7), all lead to an increase in the relative amount of Aβ<sub>42/43</sub> that is produced (Table 1).

**2. Transgenic Approaches to Modifying APP in Animals**

At least 25 different APP transgenic mouse lines have been reported. A representative summary of the transgenic lines is shown in Table 2 (8–24). APP is the single most popular transgene target of the last ten years, and some novel and creative transgenic approaches have been exploited in the effort to understand its role in AD. There are three fundamental methods of making a transgenic animal: (1) addition of cDNA transgenes, (2) addition of genomic transgenes, and (3) targeted modifications of the endogenous mouse gene. The methods for modifying genes in mice are evolving rapidly, and the best sources for detailed

**Table 2**  
**Transgenic Mouse Lines Expressing APP**

APP transgene	Mutations	Promoter	Transgenic protein level
A $\beta$ peptide fragment (mouse)	Wild type	Neurofilament light chain	1X
C-terminal fragment (human)	Wild type	JC-1 viral	nd
C-terminal fragment (human)	Wild type	Neurofilament light chain	1X
C-terminal fragment (human)	Wild type	N-Dystrophin	1X
751 cDNA (human)	Wild type enolase (NSE)	Neuron-specific	1X
cDNA–genomic hybrid (human)	Indiana (V717F)	Platelet-derived growth factor	4X
695 cDNA (human)	Swedish (K670N–M671L)	Hamster prion protein	5–6X
Chimeric: mouse 695 cDNA with human A $\beta$	Swedish (K670N–M671L)	Murine prion protein	2–3X
751 cDNA (human) (K670N–M671L)	Swedish	MouseThy1	7X
751 cDNA (human) London (V717I)	Swedish with	Human Thy1	2X
695 cDNA (human)	London enolase (NSE)	Neuron-specific	1X
695 cDNA (human)	Four FAD <sup>b</sup> mutations reductase (HMG)	Hydroxy-methyl-glutaryl coenzyme A	1–2X
695 cDNA (human) 751 cDNA (human)	Wild type	Neuron-specific enolase	1–3X
Genomic fragment (human) (400 kb)	Wild type	Human APP	1X
Genomic fragment (human) (400 kb)	Swedish	Human APP	6–4X
Knock-in of human sequence into mouse	Swedish (K670N–M671L)	Mouse APP	1X

<sup>a</sup>nd = Not determined.

<sup>b</sup>FAD = Familial Alzheimer's disease.

Amyloid deposits	Neurofibrillary tangle elements	Neuronal loss	Behavior	Ref.
Diffuse	Detected	Detected	nd <sup>a</sup>	<b>8</b>
Diffuse	nd	nd	nd	<b>9</b>
Rare	Detected	Detected	Spatial learning deficits	<b>10</b>
Negative	nd	Detected	nd	<b>11</b>
Diffuse	Detected	nd	Spatial learning deficits	<b>12</b>
Robust. Begin at 5–6 mo	AT8-positive	None detected	Spatial memory deficits at 2–3 mo	<b>13</b>
Robust. Begin at 12 mo	AT8-positive	None detected	Working and spatial learning deficits at 12–15 mo	<b>14</b>
Robust. Begin at 18–20 mo	Negative	nd	nd	<b>15</b>
Robust. Begin at 6 mo	AT8, PHF-1 positive	Detected	nd	<b>16,17</b>
Rare. Begin at 18 mo	Slight	None detected	nd	<b>16</b>
Negative	nd	nd	Normal	<b>18</b>
Negative	nd	nd	Normal	<b>19</b>
Negative	Negative	None detected	nd	<b>20</b>
Negative	Negative	nd	Normal	<b>21,22</b>
Robust. begin at 14–15 mo	detected	nd	nd	<b>23</b>
Negative	Negative	nd	nd	<b>24</b>

**Table 3**  
**Comparison of Methods Used to Generate Transgenic Animals**

	cDNA transgene	Genomic transgenes	Altered endogenous gene
Methods of transgene introduction	Usually microinjection	Transfection of embryonic stem cells or microinjection	Transfection of embryonic stem cells
Vector size	5–20 kb	Mb size: 650 kb for APP	10–20 kb
Vector Characteristics	Vector constructed of fragments from short sequences of different genes	Purified as an existing bacterial or yeast artificial chromosome (BAC or YAC) from a human genomic library	Vector constructed from genomic fragments of mouse sequence Selectable marker
	Strong exogenous promoter (usually neuron-specific)	All promoter and regulatory elements endogenous to the genomic structure	Mouse APP promoter and regulatory elements
	Intron to enhance expression cDNA for one APP isoform sometimes with an internal intron, may be human, mouse, or combination	All introns and coding sequence	Dependent on design, may include all mouse introns and mixed human-mouse coding sequence
	Polyadenylation site Can be easily modified to contain mutations	Endogenous upstream and downstream regulatory elements	Endogenous upstream, downstream, and intronic regulatory elements
	One isoform of the gene is expressed (inclusion of an internal intron allows limited alternative splicing)	All isoforms are made, each according to its normal tissue specificity. Alternative splicing may be determined by the species source of transgene	All isoforms are made, each according to its normal tissue specificity in the mouse

Transgene expression characteristics	Expression is controlled by specificity of the promoter, and is limited to cell types in which the promoter is active (usually neurons for APP)	Expression pattern is controlled by interaction of human (cis) and mouse (trans) regulatory elements. APP is expressed in all tissues	Expression pattern is controlled by mouse regulatory elements. APP is expressed in all tissues
	Expression level is determined by the strength of the promoter, number of functional copies, and cell-specific regulatory factors	Expression level is determined by cell-specific regulatory elements	Expression level is determined by cell-specific regulatory elements
7X	Protein expression level can reach 7 endogenous for APP	Protein expression level is 1X per copy	Protein expression remains at endogenous level
	Expression does not usually correlate with copy number, which can range from one to arrays of hundreds	Usually only one intact copy is introduced, but occasionally an array of copies is inserted	Copy number is unchanged
Endogenous (mouse) genes	Mouse APP gene remains intact	Mouse APP gene remains intact	No intact mouse APP remains

technical information are recently published laboratory manuals (25,26). There are also commercial services that can perform any or all of the transgenic techniques for a fee, and most major universities have a fee-for-service core transgenic facility. Excellent resources for current information are sites on the internet (27).

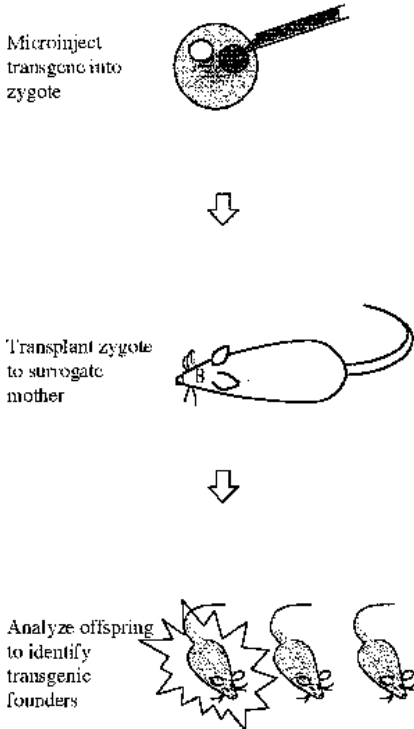
### 2.1. cDNA Transgenes

cDNA transgenes are the original and most popular vehicles for introducing exogenous genes. The general design of a cDNA transgene is a promoter, partial first intron, cDNA coding sequence, and polyadenylation site (Table 3). Such constructs are usually small, less than 20 kb, and are introduced into the animal genome by microinjection into one of the pronuclei of a fertilized egg (Fig. 2). During the first mitotic cell division, the transgene integrates randomly, usually as multicopy arrays of up to hundreds of copies, and usually at a single site in the animal genome. If the transgene is integrated during a later mitosis, the animal will be a mosaic of transgenic and nontransgenic cells. The injected zygote is transplanted to a surrogate mother, and the pup, born about 20 d later, is analyzed for the presence of the transgene. If the transgene is present, the pup is called a “founder,” and it is bred (at the age of 2 mo) to establish the transgenic line. Each line is unique, as there is almost no control over the site of integration of the transgene or the number of copies that integrate.

The details of the design of a cDNA transgene are critical to the phenotype of the transgenic animal. The promoter determines what cells will express the transgene. For APP, a neuron-specific promoter is usually used (Table 2); although APP is made by all types of cells, neurons have a higher expression level than other cell types, and it is generally assumed that the APP that generates plaque amyloid comes from neurons. The promoter also determines the amount of the transgene that will be expressed. For example, a “strong” promoter, such as the platelet-derived growth factor (PDGF) promoter, would be expected to drive more expression of the coding sequence than a weaker promoter, e.g., the NSE promoter. Increased expression has also been attributed to the presence of an intron in the transgene, and usually one is included.

The coding region of a transgene can include all or part of a cDNA, and may be modified by introduction of mutations. For APP, constructs have been made using coding sequence for the 695 and 751 amino acid isoforms. A hybrid construct, consisting of cDNA interspersed with several truncated introns, allows the expression of all three isoforms in one transgenic line (13). Although most of the transgenic lines have used the cDNA for full-length APP, several lines have been made with constructs coding for APP fragments, either the short A $\beta$  sequence or the C-terminal fragment that begins at the  $\beta$ -secretase site (Fig. 1). There is some evidence that suggests that these fragments may be more toxic than the full-length molecule (Table 2), a desirable feature for studying neurodegeneration.

**Microinjection of cDNA transgenes**



**Gene targeting and transfection of genomic transgenes**

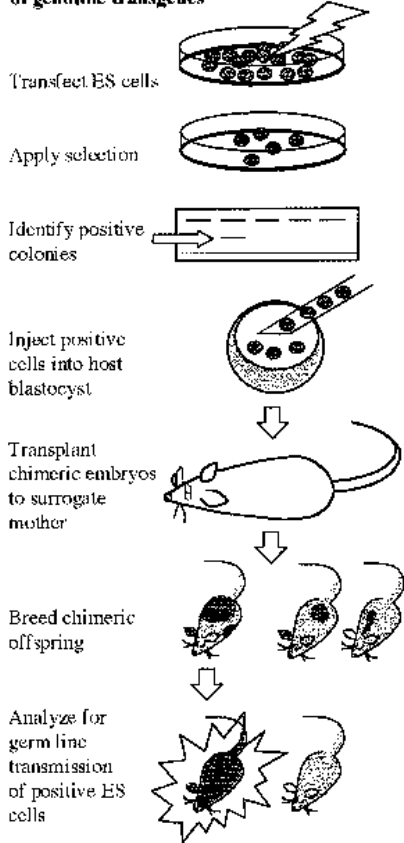


Fig. 2. Diagram of two methods for introducing transgenes into mice. **Left panel:** Microinjection: one of the pronuclei of a fertilized egg (zygote) is injected with a solution containing a transgene construct. The zygotes are transplanted to a surrogate mother, which is a female recently mated with a sterile male. When the offspring are born, founders of new transgenic lines are identified by molecular analysis. **Right panel:** Gene targeting and transfection of genomic transgenes: targeting vectors or large genomic fragments are introduced into embryonic stem (ES) cells by electroporation or lipofection, respectively. A selectable marker in the transfected DNA allows cloning of cells that have incorporated the DNA. Positive colonies are identified, usually by Southern blot analysis, and cells from these colonies are injected into a host blastocyst (three day mouse embryo). The chimeric embryos are gestated in a surrogate mother. Chimeric offspring are bred to establish transgenic lines.

The structure and design of the cDNA expression construct is not the most important factor in determining the expression level of the transgene. Because the constructs are small, they are easily influenced by the transcriptional activ-

ity of the sequences that surround the integration site. The number of copies of the transgene also determines the level of expression. There is seldom a linear relationship between copy number and expression level, but a higher number of copies usually leads to a greater expression level. Finally, since the purpose of a transgene is to produce a protein, it should be noted that there are many examples of transgenes producing respectable levels of mRNA, but no detectable protein.

### **2.3. Genomic Transgenes**

The other type of exogenous transgene is usually larger, and retains the genomic structure; this includes not only the coding sequence of the exons but all of the introns, and usually some upstream and downstream regions as well (**Table 3**). Human APP cloned in a 600-kb yeast artificial chromosome (YAC) has been introduced into the mouse (**Table 2**). This large genomic fragment contains the entire human gene, and its characteristics are different from a cDNA transgene. For example, in genomic transgenes, all of the regulatory elements are present, which results in modest but consistent expression levels, and the inclusion of alternatively spliced exons allows the normal distribution of isoforms. For introducing large genomic DNA, the microinjection method used for cDNA transgenes is usually appropriate if the genomic fragment is less than 200 kb long.

For larger genomic transgenes, often those cloned in YACs and BACs (bacterial artificial chromosomes), it is necessary to handle the DNA more carefully. For these large transgenes, the DNA is delivered by way of embryonic stem cells (ES cells), as illustrated in **Fig. 2**. ES cells are pluripotent embryonic-forming lines of cells that are usually established by culturing mouse embryos at the blastocyst stage. The ES cells are transfected with the genomic DNA and a selectable marker, usually by using liposomes ("lipofection"); the positive cells are identified and used to generate transgenic lines. The ES cells are used to make a chimeric embryo, which is transplanted to a surrogate mother. The chimeric pups that result are bred to transmit the ES cell genotype, thus establishing a stable transgenic line. In the case of APP, which is expressed in ES cells, the expression of the human gene can be confirmed in culture before the mouse is generated.

### **2.4. Gene Targeting**

The third method of transgenesis uses homologous recombination to modify genes in ES cells. This application was originally developed to inactivate, or "knock out," the endogenous mouse gene. A newer and more sophisticated application of homologous recombination can be used to introduce subtle changes in the mouse gene in situ without inactivating it. This technology, often

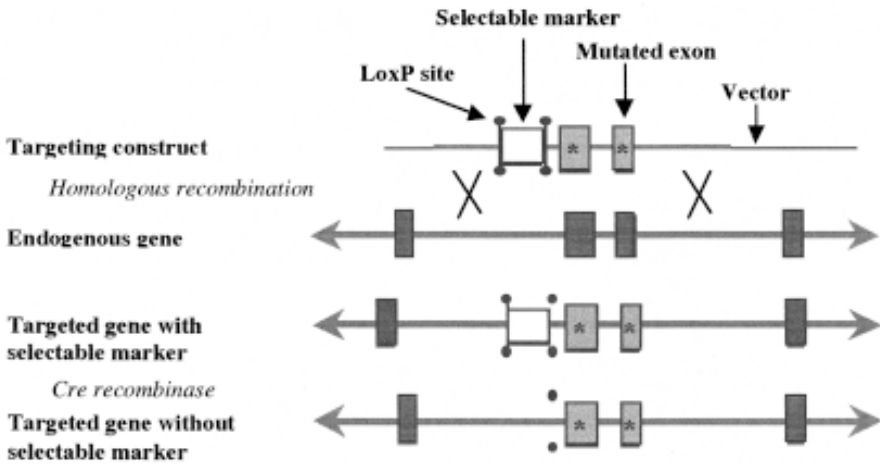


Fig 3. “Knock-in” or genetic modification of endogenous mouse genes. A targeting construct contains a sequence homology to the mouse gene, with desired mutations added and a selectable marker flanked by loxP sites. The vector is introduced into ES cells, where it is incorporated by homologous recombination. After selection for transfected cells and identification of targeted colonies, the selectable marker is removed by introducing cre recombinase into the cells.

called “knock in,” has been used to target mutations to the mouse *APP* gene (Table 2). The usual procedure for modifying mouse genes involves the use of the Cre-lox method (28). As Fig. 3 illustrates, the gene-targeting construct is composed of two elements: a sequence that is homologous to the endogenous gene and a selectable marker that is placed in a noncoding region of the gene (usually an intron). The selectable marker is flanked by loxP sites that are recognized by an enzyme (Cre recombinase); these sites enable the excision of the selectable marker after it has served its purpose in allowing selection for the insertion of the construct. The region of homology contains the sequence changes that are to be introduced into the mouse gene. The construct is introduced into ES cells, usually by electroporation (Fig. 2) and the homologous region of the construct recombines with the endogenous gene at a low frequency. Using the selectable marker, ES cells that contain insertions of the construct are isolated and assayed for gene targeting. The targeting event is confirmed by Southern blot analysis or polymerase chain reaction (PCR). Usually, before the ES cells are used to establish a transgenic line (Fig. 3), the selectable marker is excised by transfecting the ES cells with a vector containing Cre recombinase. This leaves the mouse gene virtually untouched, with only the remnants of the recombination site remaining (Fig. 3). Alternatively, the selectable marker can be removed after a mouse line is generated; if this is

desirable, the Cre recombinase is introduced by a classical microinjection technique into a fertilized egg generated by mating gene-targeted mice.

## **2.5. Comparing Transgenic Methods**

A comparison of three types of transgenic methods, addition of exogenous cDNA transgenes, addition of exogenous genomic transgenes, and targeting mouse genes, is summarized in **Table 3**.

### **2.5.1 Exogenous Transgenes**

The addition of exogenous human genes by using cDNA transgenes has the advantage of being flexible, as different promoters can be easily combined with different cDNA sequences. Probably the most important advantage of cDNA transgenes is that they can be greatly overexpressed by using powerful promoters and taking advantage of the insertion of multiple copies. Overexpression in certain cell types may be the most important factor in generating a phenotype in a mouse, and it is the most likely cause of amyloid accumulation in APP transgenic lines. As **Table 2** shows, all of the mouse lines that develop amyloid deposits express a mutant form of APP at levels that exceed the endogenous level by threefold. The expression level of the protein correlates with the time at which the deposits are detected: the more APP expressed, the earlier the deposition (**Table 2**).

The chief disadvantage of the cDNA approach is that it is virtually impossible to control the number of functional copies that integrate, and so the expression level is unpredictable. Many transgenic lines must be generated to find one with the appropriate expression level. Also, the tissue specificity of expression is controlled only by the promoter used, as the transgene lacks regulatory elements. This may result in a phenotype that is caused by the overabundance of transgene-derived protein being made in the wrong cells.

The other type of exogenous transgene, a large genomic transgene, is a gene transplant. Having the intact gene incorporated into the animal genome has the advantage that the expression is regulated in the appropriate cell types of the mouse just as it would be in a human. The disadvantage of this approach is that it is very difficult to generate animals that overexpress the transgenes. The large genomic fragments usually integrate as single copies, and the regulatory elements contained in the sequence generally preclude abnormally high or inappropriate expression. Thus, the genomic transgene is unlikely to have a dramatic phenotypic effect, unless the simple presence of the human protein, or of a mutation included in the transgene, is sufficient to create some noticeable change. Recently, genomic transgenic lines that over express mutant human APP Protein by about fivefold have been reported to develop amyloid deposits (**23;Table 2**). These genomic transgenics are proving useful for testing

potential drug therapies for AD. For drugs that are designed to interfere with production of A $\beta$  from APP, the correct expression of human APP in the mouse allows a realistic assessment of the potency of the drugs.

Whether the transgene is a cDNA or genomic fragment, one often overlooked factor bears consideration. The impact of the insertion site of a transgene is not limited to influence on the effectiveness of the transgene. There is also the very real possibility that the exogenous DNA will disrupt some unrelated gene function, either by physically disrupting and inactivating another gene, or through effects of the transgenic promoter on surrounding genes. The transgene's promoter could enhance the expression of nearby genes, or interfere by upsetting the balance of DNA binding proteins that would normally be regulating other genes in a cell.

Because of the unplanned effects of exogenous transgenes, it is essential to produce at least two independent transgenic lines in order to link transgene expression to an animal phenotype. This is especially important if animal behavior is to be an endpoint analysis. Perhaps 10% of genes can be linked in some way to behavior, including genes involved in temperature regulation, response to stress, and function of nonneuronal tissues. The best illustration of the perfidy of behavioral assays is the report that the uterine environment of a mouse has a measurable effect on learning and memory as an adult. Mice of the same strain, when gestated in surrogate mothers of different strains, showed significant differences in commonly used behavioral tests (29).

### 2.5.2. Gene Modification In Situ

The other approach to transgenesis, endogenous modification of genes by homologous recombination, avoids the problems associated with integration of exogenous transgenes, but it is not the ideal approach for every situation. One advantage is that by targeting the mouse gene, the normal mouse protein is effectively eliminated, and replaced by the modified version. This is important in situations in which the product of the endogenous mouse gene might interfere with the activity of the human transgenic protein. A disadvantage of this technique is shared with the large genomic transgene approach: the gene of interest will not be overexpressed. In addition, there may be situations in which mouse-type gene regulation differs from the human regulation of the gene, and the mouse gene regulation may be undesirable in the design of the model system.

## 3. Analysis of transgenic APP lines

The techniques used to analyze *APP* transgenic lines have been mostly centered on defining their utility as models of AD. *APP* transgenic mice have been analyzed from histological, biochemical, and behavioral perspectives. Because so many *APP* transgenic lines exist, there is much to be learned from

comparing the different lines. For example, the relationships between transgene design, expression, and phenotype have been clarified by comparing these qualities in several lines. This information, in turn, has been used to improve the strategy of new transgenic approaches.

### 3.1. Histological Analysis

Criteria for the diagnosis of definite AD are based on abundant senile plaques (SPs) and neurofibrillary tangles (NFTs) in the postmortem brain of a patient with a progressive dementia. Amyloid fibrils (formed from 40–43 amino acid A $\beta$  peptides) predominate in SPs, whereas paired helical filaments (composed of altered tau proteins) are the dominant structures in NFTs. Neuronal loss is also evident, although it is not exclusive to AD.

Because the transgenic *APP* mice that develop amyloid deposits display the most obvious similarity to AD pathology, they have been the subjects of the most detailed histological analyses. Amyloid deposits are detected by immunohistochemistry with antibodies specific to A $\beta$  (**Fig. 4**), by classical silver staining methods, and by birefringence revealed by congo red or thioflavin S staining. Of interest is the observation that several different overexpressing *APP* lines develop amyloid deposits in the same circumscribed areas of the brain, despite the fact that the promoters driving the transgenes are different. This suggests that factors other than APP expression level, such as A $\beta$  transport or A $\beta$  clearance, may have a more powerful influence on amyloid deposition. The pattern of plaque distribution is similar to that of human disease, which strengthens the argument that the mice mimic AD pathology. Amyloid deposits can be detected in animals as young as 6 mo and the time of onset of deposition appears to depend on the level of transgenic protein expressed (**Table 2**).

There are differences between the histopathology of the mice and the human AD brain, which highlight the imperfections of these animals as models of the human disease. The transgenic mice appear to accumulate a much higher amyloid burden (amount of tissue area occupied by A $\beta$  immunostaining) than has ever been seen in AD postmortem brain. Also, other histochemical markers are different. The transgenic mice analyzed so far show little or no evidence of NFT formation, although some mouse lines acquire low levels of antigenic markers for NFT. The disparity of most concern is the lack of neuronal cell death in two of the lines that have the greatest amyloid burden (**30,31**); this observation conflicts with the long-held belief that A $\beta$  amyloid is directly toxic to neurons, and is probably the most important concern of those who wish to test AD drugs in these mice. However, one transgenic line has been reported to have significant hippocampal neuronal loss (**17**). It is not clear why this animal line may differ from the others, but the neuronal loss might be linked to the more compact, plaquelike structure of the amyloid deposits in this line.

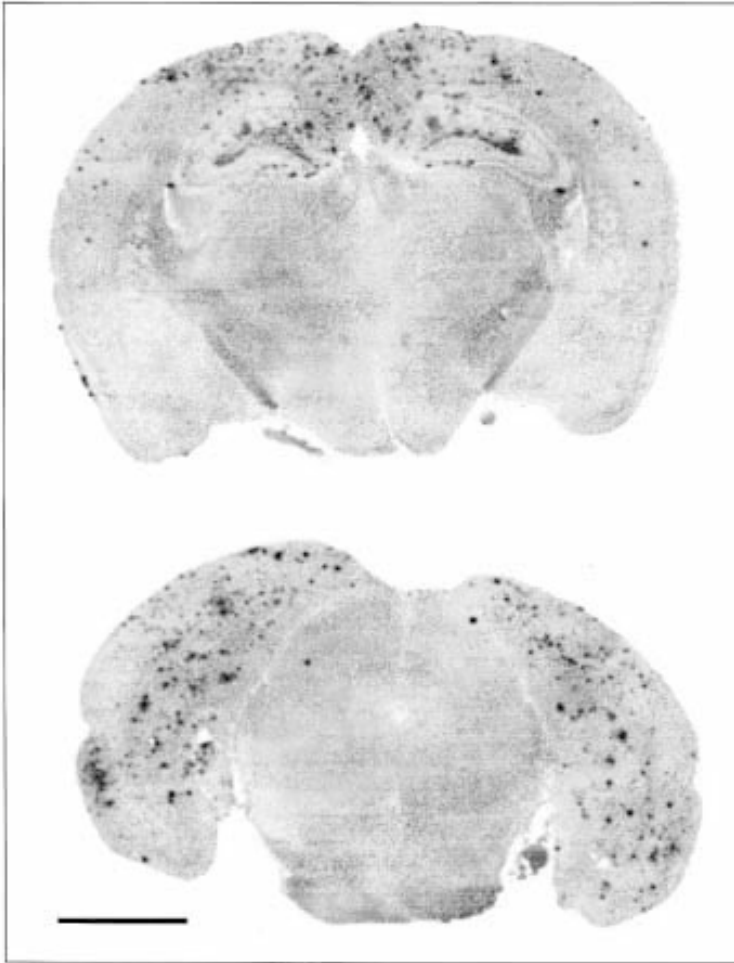


Fig 4. Brain sections from transgenic mouse overexpressing mutant human APP. Sections from a 12-mo-old PDAPP heterozygote (13), were stained with an antibody to A $\beta$  and imaged with a confocal microscanner. Dark spots are accumulations of extracellular A $\beta$ . Bar = 1 mm (modified from **ref. 40**).

### 3.2. Biochemical Analysis

Studies of transgenic APP have revealed interesting information about the synthesis and processing of this protein. The protein expression levels, measured by quantitative immunoblot or immunoprecipitation, range from undetectable to about sevenfold the endogenous level in some regions of the brain. Transgenes with neuron-specific promoters have little or no expression in the periphery, in contrast to the genomic transgenes, which follow the normal

pattern of APP expression in all tissues. A $\beta$  levels have been measured in many of the transgenic lines (**Table 4**), usually by an ELISA assay. In all of the animal lines that express human APP, human A $\beta$  has been detected in the brain; in some, plasma A $\beta$  has also been detected. The absolute levels of A $\beta$  and ratios of A $\beta$ 40 to A $\beta$ 42/43 reflect the type of familial Alzheimer's disease (FAD) mutation in the transgene. In several cases (**Table 4**), the A $\beta$  levels in the brain have been shown to increase precipitously at the time that amyloid deposition begins, indicating an exponential accumulation of the peptide.

### **3.3. Behavioral Analysis**

Transgenic *APP* mice have been subjected to modified versions of the same behavioral analysis that has been traditional for rat models. However, tests for learning and memory deficits in mice are not as straightforward as they are for the rat, and the published reports on the mice have stirred some controversy (32). Several *APP* transgenic lines have been shown to be deficient in spatial memory (**Table 2**). However, only one has reported degradation of memory with age, and several of the others appear to be less competent than the wild-type control animals even at the age of a few months. None has yet shown behavioral deficits that correlate with the development of a histological phenotype, such as amyloid deposition. These observations, combined with the many reports of behavioral deficits that are unrelated to transgene expression (i.e., insertion effects, strain differences, environmental differences), suggest that it is best to remain cautious for the present about the interpretation of behavioral analysis of APP transgenic animals.

## **4. The Future of APP Transgenic Lines**

*APP* transgenic animals have been extremely successful as experimental models. The need for an animal model of AD has driven the field, leading to innovations in transgene design, new methods of delivering transgenes, and novel techniques for phenotypic analysis. Some of the existing transgenic lines have been licensed to pharmaceutical companies, and are in use for testing drug candidates for AD that are designed to affect APP processing or amyloid deposition (41). Because several of the transgenic lines are shared with academic collaborators through material transfer agreements, they are being scrutinized by an expanded laboratory with expertise in a huge variety of technologies. New transgenic lines are being generated at an undiminished rate and there are several clear directions for further research.

### **4.1. Animals Harboring Multiple Transgenes**

AD is a complex disease, and it may require a complex transgenic animal to model it well (33). It is known that mutations in the presenilin (PS) genes cause

**Table 4**  
**A $\beta$  Levels in APP Transgenic Mouse Lines**

Transgenic mouse line	protein level <sup>a</sup>	Transgenic Age at A $\beta$ assay	A $\beta$ (pmol/g brain)			A $\beta$ increase with age	Ref.
			Total A $\beta$	A $\beta$ 40	A $\beta$ 42/43		
Human 695 cDNA, K670N–M671L	5–6X	2–5 mo 11–13 mo	nd 250	50 175	13 increased relative to A $\beta$ 40	5X (40)	<b>14</b>
Human cDNA and genomic hybrid, V717F	4X	2–4 mo 18 mo	14 (cortex) 6300 (cortex)	nd <sup>b</sup>	4.7 5600	450X (total) 1000X (42/43)	<b>13</b>
Human genomic fragment, wild type	1X	12–30 mo	4–10	nd	Detected	Small increase	<b>21,22</b>
Human genomic fragment, K670N–M671L	4–6X	3–4 mo	30	nd	15–20X higher than wild-type genomic	na <sup>c</sup>	<b>23</b>
Knock-in of human sequence into mouse, K670N–M671L	1X	3 mo	17	nd	Detected	na	<b>24</b>

<sup>a</sup>Units of transgenic protein are relative to the endogenous APP level.

<sup>b</sup>nd: not determined.

<sup>c</sup>na: not applicable.

AD, and that the PS proteins interact in some way with APP. In addition, apolipoprotein E (ApoE) is involved as a risk factor, and several other AD-related genes are known to exist but are not yet identified. Using transgenic technology to combine these human genes in an animal is a valuable way to understand their interaction. This approach has already resulted in some fundamental insights into the mechanism of AD pathology. For example, by breeding an amyloid-depositing *APP* transgenic line to a genetically engineered ApoE null mouse, it has been demonstrated that deposition (but not production) of A $\beta$  does not occur in the absence of ApoE (34). In addition, a similar *APP* transgenic lines have been to lines that carried a PS-1 mutation. The PS-1 mutation alone does not lead to amyloid deposition, but when combined with the APP overexpression it causes an acceleration of amyloid accumulation into plaques (23,35,36).

#### **4.2. Conditional Expression of Transgenes**

One shortcoming in the interpretation of phenotype of animals harboring cDNA transgenes is the fact that the transgene is expressed whenever the promoter driving it is active. This phenomenon could arguably lead to developmental defects that are misinterpreted as effects of the transgene's expression in adults. There are other uncertainties, such as identifying insertional effects, and it would be useful to be able to turn the transgene expression on and off so that direct correlation between transgene expression and phenotype could be measured. For these reasons, methods for controlling transgene expression have been developed. The most popular of these is the tetracycline-inducible system (37). The concept is relatively simple, and uses two transgenes in a single animal line. One is a cassette consisting of a tissue-specific (e.g., neuronal) promoter driving a coding sequence for a modified tet repressor (TetR). The other transgene drives the cDNA to be expressed with a compound promoter consisting of the tetracycline operator sequence, to which TetR binds, and the minimal immediate early promoter of cytomegalovirus. Two versions of the tet repressor have been engineered; one turns the transgene on in the presence of a tetracycline analog (doxycycline: Dox), and the other (reverse TetR) will turn off transgene expression when Dox is introduced. Once the doubly transgenic animal line has been established, the transgenic cDNA can be turned on or off by regulating its intake of Dox in its drinking water. One version of the "tet-on" and "tet-off" expression vectors can be obtained from commercial sources (Clontech, Palo Alto, CA).

#### **4.3. Rat Transgenic Models**

For most pharmaceutical applications, the rat has been the model system of choice. Part of the reason for this is tradition, as the rat's larger size makes it

more accessible to surgical procedures and provides more material for biochemical analysis. The long-term use of rats for drug development and toxicology testing has resulted in comprehensive databases on drug metabolism, physiology, and behavior, and comparable information does not yet exist for the mouse. Nevertheless, the advent of transgenic models of human disease has left the rat behind. The reason for this is largely technical; rat genetics has lagged behind mouse genetics, and the technology for developing rat transgenic lines is far less developed. Several cDNA transgenic rat lines have been produced, and in several instances, the transgenic rat is a more faithful model of a human disease than a mouse harboring the same transgene (38). As an AD model, the rat would be preferable to the mouse, especially for the tests of learning and memory that are more useful for the rat than for the mouse. The barrier to making the rat as genetically malleable as the mouse has been the lack of rat ES cell lines. Although deriving rat ES cell lines has proved difficult (39), efforts are underway in several laboratories and are likely to be successful in the next few years.

## References

1. Hardy, J. and Allsop, D. (1991) Amyloid deposition as the central event in the aetiology of Alzheimer's disease. *Trends Pharmacol. Sci.* **12**, 383–388.
2. Buxbaum, J. D., Liu, K. N., Luo, Y., Slack, J. L., Stocking, K. L., Peschon, J. J., et al. (1998) Evidence that tumor necrosis factor alpha converting enzyme is involved in regulated  $\alpha$ -secretase cleavage of the Alzheimer amyloid protein precursor. *J. Biol. Chem.* **273**, 27,765–27,767.
3. Goate, A., Chartier Harlin, M. C., Mullan, M., Brown, J., Crawford, F., Fidani, L., et al. (1991) Segregation of a missense mutation in the amyloid precursor protein gene with familial Alzheimer's disease. *Nature* **349**, 704–706.
4. Mullan, M., Crawford, F., Axelman, K., Houlden, H., Lilius, L., Winblad, B., and Lannfelt, L. (1992) A pathogenic mutation for probable Alzheimer's disease in the APP gene at the N-terminus of beta-amyloid. *Nat. Genet.* **1**, 345–347.
5. Murrell, J., Farlow, M., Ghetti, B., and Benson, M. D. (1991) A mutation in the amyloid precursor protein associated with hereditary Alzheimer's disease. *Science* **254**, 97–99.
6. Chartier Harlin, M. C., Crawford, F., Houlden, H., Warren, A., Hughes, D., Fidani, L., et al. (1991) Early onset Alzheimer's disease caused by mutations at codon 717 of the  $\beta$ -amyloid precursor protein gene. *Nature* **353**, 844–846.
7. Eckman, C. B., Mehta, N. D., Crook, R., Perez-tur, J., Prihar, G., Pfeiffer, E., et al. (1997) A new pathogenic mutation in the APP gene (I716V) increases the relative proportion of A beta 42(43) *Hum. Mol. Genet.* **6**, 2087–2089.
8. LaFerla, F. M., Tinkle, B. T., Bieberich, C. J., Haudenschild, C. C., and Jay, G. (1995) The Alzheimer's A beta peptide induces neurodegeneration and apoptotic cell death in transgenic mice. *Nat. Genet.* **9**, 21–30.

9. Sandhu, F. A., Salim, M., and Zain, S. B. (1991) Expression of the human beta-amyloid protein of Alzheimer's disease specifically in the brains of transgenic mice. *J. Biol. Chem.* **266**, 21,331–21,334.
10. Nalbantoglu, J., Tirado-Santiago, G., Lahsaini, A., Poirier, J., Goncalves, O., Verge, G., et al. (1997) Impaired learning and LTP in mice expressing the carboxy terminus of the Alzheimer amyloid precursor protein. *Nature* **387**, 500–505.
11. Kammesheidt, A., Boyce, F. M., Spanoyannis, A. F., Cummings, B. J., Ortegon, M., Cotman, C., et al. (1992) Deposition of beta/A4 immunoreactivity and neuronal pathology in transgenic mice expressing the carboxyl-terminal fragment of the Alzheimer amyloid precursor in the brain. *Proc. Natl. Acad. Sci. USA* **89**, 10,857–10,861.
12. Quon, D., Wang, Y., Catalano, R., Scardina, J. M., Murakami, K., and Cordell, B. (1991) Formation of beta-amyloid protein deposits in brains of transgenic mice. *Nature* **352**, 239–241.
13. Games, D., Adams, D., Alessandrini, R., Barbour, R., Berthelette, P., Blackwell, C., et al. (1995) Alzheimer-type neuropathology in transgenic mice overexpressing V717F  $\beta$ -amyloid precursor protein. *Nature* **373**, 523–527.
14. Hsiao, K., Chapman, P., Nilsen, S., Eckman, C., Harigaya, Y., Younkin, S., et al. (1996) Correlative memory deficits, A $\beta$  elevation, and amyloid plaques in transgenic mice. *Science* **274**, 99–102.
15. Borchelt, D. R., Thinakaran, G., Eckman, C. B., Lee, M. K., Davenport, F., Ratovitsky, T., et al. (1996) Familial Alzheimer's disease-linked presenilin 1 variants elevate A beta<sub>1–42</sub>/1–40 ratio in vitro and in vivo. *Neuron* **17**, 1005–1013.
16. Sturchler-Pierrat, C., Abramowski, D., Duke, M., Wiederhold, K. H., Mistl, C., Rothacher, S., et al. (1997) Two amyloid precursor protein transgenic mouse models with Alzheimer disease-like pathology. *Proc. Natl. Acad. Sci. USA* **94**, 13,287–13,292.
17. Staufenbiel, M., Sommer, B., and Jucker, M. (1998) Neuronal loss in APP transgenic mice. *Nature* **395**, 755–756.
18. Malherbe, P., Richards, J. G., Martin, J. R., Bluethmann, H., Maggio, J., and Huber, G. (1996) Lack of beta-amyloidosis in transgenic mice expressing low levels of familial Alzheimer's disease missense mutations. *Neurobiol. Aging* **17**, 205–214.
19. Czech, C., Delaere, P., Macq, A. F., Reibaud, M., Dreisler, S., Touchet, N., et al. (1997) Proteolytical processing of mutated human amyloid precursor protein in transgenic mice. *Brain Res. Mol. Brain Res.* **47**, 108–116.
20. Mucke, L., Masliah, E., Johnson, W. B., Ruppe, M. D., Alford, M., Rockenstein, E. M., et al. (1994) Synaptotrophic effects of human amyloid beta protein precursors in the cortex of transgenic mice. *Brain Res.* **666**, 151–167.
21. Buxbaum, J. D., Christensen, J. L., Ruefli, A. A., Greengard, P., and Loring, J. F. (1993) Expression of APP in brains of transgenic mice containing the entire human APP gene. *Biochem. Biophys. Res. Commun.* **197**, 639–645.
22. Lamb, B. T., Sisodia, S. S., Lawler, A. M., Slunt, H. H., Kitt, C. A., Kearns, W. G., et al. (1993) Introduction and expression of the 400 kilobase amyloid precursor protein gene in transgenic mice. *Nat. Genet.* **5**, 22–30.

23. Lamb, B. T., Bardel, K. A., Kulnane, L. S., Anderson, J. J., Holtz, G., Wagner, S. L., Sisodia, S. S., and Hoeger, E. J. (1999) Amyloid production and deposition in mutant amyloid precursor protein and presenilin-1 yeast artificial chromosome transgenic mice. *Nature Neurosci.* **3**, 695–697.
24. Reaume, A. G., Howland, D. S., Trusko, S. P., Savage, M. J., Lang, D. M., Greenberg, B. D., et al. (1996) Enhanced amyloidogenic processing of the beta-amyloid precursor protein in gene-targeted mice bearing the Swedish familial Alzheimer's disease mutations and a "humanized" A beta sequence. *J. Biol. Chem.* **271**, 23,380–23,388.
25. Hogan, B., Beddington, R., Costantini, F., and Lacey, E. (1994) *Manipulating the Mouse Embryo*, 2nd ed. Cold Spring Harbor Press, Cold Spring Harbor, NY.
26. Zambrowicz, B., Hasty, P., and Sands, A. Mouse Mutagenesis (1998) Lexicon Genetics Incorporated, The Woodlands, TX. [www.lexgen.com](http://www.lexgen.com)
27. Internet resources for transgenic research:  
TBASE (The Transgenic/Targeted Mutation Database)  
<http://www.jax.org/tbase/>  
Transgenic List  
<http://www.med.ic.ac.uk/db/dbbm/tglist.htm>  
Database of Gene Knockouts  
<http://www.bioscience.org/knockout/knocho.me.htm>  
BioMedNet Mouse Knockout Database  
<http://biomednet.com/db/mkmd>  
MGD (The Mouse Genome Database)  
<http://www.informatics.jax.org/>  
The Encyclopedia of the Mouse Genome  
<http://www.informatics.jax.org/encyclo.htm>  
Resources of the Jackson Laboratory  
<http://lena.jax.org/resources/documents/imr/>  
The Mouse and Rat Research Home Page  
[http://www.cco.caltech.edu:80/~mercer/html/rodent\\_page.html](http://www.cco.caltech.edu:80/~mercer/html/rodent_page.html)
28. Sauer, B. and Henderson, N. (1988) Site-specific DNA recombination in mammalian cells by the Cre recombinase of bacteriophage P1. *Proc. Natl. Acad. Sci. USA* **85**, 5166–5170.
29. Denenberg, V. H., Hoplight, B. J., and Mobraaten, L. E. (1998) The uterine environment enhances cognitive competence. *Neuroreport* **9**, 1667–1671.
30. Irizarry, M. C., Soriano, F., McNamara, M., Page, K. J., Schenk, D., Games, D., and Hyman, B. T. (1997) A $\beta$  deposition is associated with neuropil changes, but not with overt neuronal loss in the human amyloid precursor protein V717F (PDAPP) transgenic mouse. *J. Neurosci.* **17**, 7053–7059.
31. Irizarry, M. C., McNamara, M., Fedorchak, K., Hsiao, K., and Hyman, B. T. (1997) APPSw transgenic mice develop age-related A $\beta$  deposits and neuropil abnormalities but no neuronal loss in CA1. *J. Neuropathol. Exp. Neurol.* **56**, 965–973
32. Routtenberg, A. (1997) Measuring memory in a mouse model of Alzheimer's disease. *Science* **8**, 839–841.

33. Loring, J. F., Paszty, C., Rose, A., McIntosh, T. K., Murai, H., Pierce, J. E., et al. (1996) Rational design of an animal model for Alzheimer's disease: introduction of multiple human genomic transgenes to reproduce AD pathology in a rodent. *Neurobiol. Aging* **17**, 173–182.
34. Bales, K. R., Verina, T., Dodel, R. C., Du, Y., Altstiel, L., Bender, M., et al. (1997) Lack of apolipoprotein E dramatically reduces amyloid beta-peptide deposition. *Nat. Genet.* **17**, 263–264.
35. Duff, K., Eckman, C., Zehr, C., Yu, X., Prada, C. M., Perez-tur, J., et al. (1996) Increased amyloid-beta 42(43) in brains of mice expressing mutant presenilin 1. *Nature* **383**, 710–713.
36. Borchelt, D. R., Ratovitski, T., van Lare, J., Lee, M. K., Gonzales, V., Jenkins, N. A., et al. (1997) Accelerated amyloid deposition in the brains of transgenic mice coexpressing mutant presenilin 1 and amyloid precursor proteins. *Neuron* **19**, 939–945.
37. Baron, U., Gossen, M., and Bujard, H. (1997) Tetracycline-controlled transcription in eukaryotes: novel transactivators with graded transactivation potential. *Nucleic Acids Res.* **25**, 2723–2729.
38. Hammer, R. E., Maika, S. D., Richardson, J. A., Tang, J. P., and Taurog, J. D. (1990) Spontaneous inflammatory disease in transgenic rats expressing HLA-B27 and human beta2m: an animal model of HLA-B27-associated human disorders. *Cell* **63**, 1099–1112.
39. Brenin, D., Look, J., Bader, M., Hubner, N., Levan, G., and Iannaccone, P. (1997) Rat embryonic stem cells: a progress report. *Transplant Proc.* **29**, 1761–1765.
40. Hanzel, D. K., Trojanowski, J. Q., Johnston, R., and Loring, J. F. (1999) High throughput quantitative histological analysis of Alzheimer's disease pathology using a confocal fluorescence microscanner. *Nat. Biotechnol.* **17**, 53–57.
41. Shenk, D., Barbour, R., Dunn, W., Gordon, G., Grajeda, H., Guido, T., et al. (1999) Immunization with amyloid- $\beta$  attenuates Alzheimer-disease-like pathology in the PDAPP mouse. *Nature* **400**, 173–177.

## Phosphorylation of Amyloid Precursor Protein (APP) Family Proteins

Toshiharu Suzuki, Kanae Ando, Ko-ichi Iijima, Shinobu Oguchi, and Shizu Takeda

### 1. Introduction

It has been well established that  $\beta$ -amyloid peptide is the principal protein component of extracellular cerebral amyloid deposits in patients with Alzheimer's disease (1,2).  $\beta$ -Amyloid is derived from a large precursor protein, amyloid precursor protein (APP), which is an integral membrane protein, with a receptor-like structure (3). APP is a member of a gene family which encodes extremely well-conserved membrane proteins. APP/APP-like genes have been isolated from various species including fly (4), nematode (5), and fish (6). In mammals, two APP-like genes, amyloid precursor-like protein 1 (APLP1) and 2 (APLP2), have been isolated (7,8). The amino acid sequences of these APP family proteins are highly conserved, especially in the cytoplasmic domain, except that unlike APP, APP-like proteins lack the  $\beta$ -amyloid sequence. It has been thought that APP and APLP2 have a similar physiological function (9). In contrast, APLP1 is believed to differ functionally from APP and APLP2, although the physiological functions of these APP family proteins have not yet been well analyzed.

APP family proteins are phosphoproteins (10–12). APP and APLP2 are phosphorylated at sites located in the cytoplasmic (6,13–15) and extracellular (16,17) domains. Analysis of the phosphorylation mechanisms and identification of protein kinases that phosphorylate APP family proteins are important in understanding the physiological function of these proteins and in elucidating the underlying pathogenesis of Alzheimer's disease. Because the cytoplasmic domain contains signals responsible for the metabolism of these proteins (18–20) and, thus, is thought to be responsible for the signal transduction from

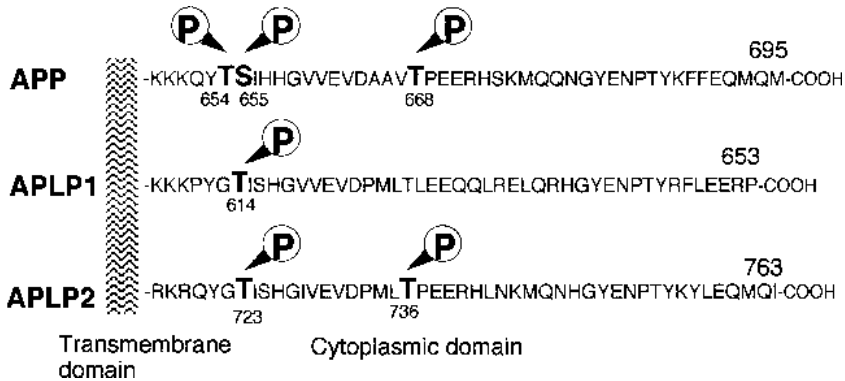


Fig. 1. Amino acid sequence and potential phosphorylation sites in the cytoplasmic domain of APP family proteins, APP, APLP1, and APLP2. Thr654 plus Ser655 of APP<sub>695</sub> are phosphorylation sites of CaMkII predicted based on amino acid sequence. Ser655 of APP<sub>695</sub>, Thr614 of APLP1<sub>653</sub>, and Thr723 of APLP2<sub>763</sub> are potential phosphorylation sites of PKC. Thr668 of APP and Thr736 of APLP2 are the sites in the consensus amino acid sequence for Cdc2 kinase. All these sites have been demonstrated as phosphorylation sites in *in vitro* studies (10,12–14). Furthermore, it has been established that Ser655 plus Thr668 of APP and Thr736 of APLP2 are phosphorylated in intact cells and tissues (6,13–15,28).

extracellular ligands (21), we have focused on the phosphorylation of the cytoplasmic domain of APP family proteins.

### 1.1. Phosphorylation of the Cytoplasmic Domain Peptide from APP Family Proteins with Purified Protein Kinases

APP family proteins possess a single short cytoplasmic domain consisting of approx 50 amino acids. Many consensus sequences recognized by protein kinases (22) are present within the amino acid sequence of the APP family proteins, APP, APLP1, and APLP2 (Fig. 1). APP, APLP1, and APLP2 contain a potential protein kinase C (PKC) phosphorylation site. APP contains two potential calcium/calmodulin-dependent protein kinase II (CaMkII) phosphorylation sites. In addition, APP and APLP2 contain a potential Cdc2 kinase phosphorylation site. We have examined whether these sites are exact phosphorylation sites by an *in vitro* phosphorylation study, using synthetic peptides and purified or recombinant protein kinases.

### 1.2. Phosphorylation of APP Family Proteins in Intact Cells and the Identification of the Phosphorylation Sites

APP and APLP2 are expressed ubiquitously in various tissues, but APLP1 is expressed only in neurons. Because it is unclear whether APLP1 is phosphory-

lated *in vivo*, only the phosphorylation of APP and APLP2 in cultured cell lines is described. It is well-known that phorbol esters such as PDBu activates PKC *in vivo* and that the synchronization of cells at the G2/M phase of the cell cycle activates Cdc2 kinase. Therefore, the phosphorylation of APP family proteins was examined with cells treated in the manner in which the corresponding protein kinase would be expected to be activated.

### **1.3. Development of the Phosphorylation State-Specific Antibodies and Detection of the Phosphorylated APP Family Proteins with Immunological Procedures**

When the phosphorylation site has already been identified, use of phosphorylation state-specific antibodies provides excellent sensitivity, selectivity, and convenience in quantifying the phosphorylation level of proteins in intact cells and tissue. The phosphorylation sites of APP and APLP2 have been identified by *in vitro* and *in vivo* studies (13–15). Cdc2 kinase phosphorylates Thr668 of APP<sub>695</sub> and Thr736 of APLP2<sub>763</sub>. To raise the phosphorylation state-specific antibody against these phosphorylated sites, a peptide containing a phosphoamino acid was designed as an antigen. A polyclonal antibody raised to the antigen shows a high specificity and does not recognize the dephosphorylated form of the protein (15). With the Western blot procedure, this antibody is useful in quantifying the level of phosphorylation of APP family proteins and, with immunocytochemical staining, in analyzing the distribution of the phosphorylated form of these proteins in cells.

## **2. Materials**

### **2.1. In Vitro Phosphorylation**

1. Synthetic peptides: Cytoplasmic domain peptide, APP<sup>645–694</sup> of APP<sub>695</sub>, APLP1<sup>608–653</sup> of APLP1<sub>653</sub> and APLP2<sup>717–763</sup> of APLP2<sub>763</sub> are synthesized and purified by a company (Quality Controlled Biochemicals, Hopkinton, MA) or a university (W. M. Keck Foundation Biotechnology Research Laboratory, Yale University, New Haven, CT) (*see Note 1*).
2. Protein kinases: PKC (23,24) and CaMkII (25) are prepared from rat brain and Cdc2 kinase is prepared from *HeLa* cells synchronized at the G2/M phase of the cell cycle (26). The purified or recombinant products of these kinases are also available from several companies (New England Bio Lab, Gibco-BRL, Calbiochem, La Jolla, CA).
3. Reaction buffers:
  - a. PKC, 50 mM HEPES (pH 7.4), 1 mM EGTA, 2 mM MgCl<sub>2</sub>, 1 mM ATP, 10 mg/mL phosphatidylserine (PS) and 1 μM phorbol-12, 13-dibutyrate (PDBu).
  - b. CaMkII, PKC buffer containing calmodulin (20 μg/mL) instead of PDBu and PS.
  - c. Cdc2 kinase, 50 mM Tris-acetate, pH 8.0, 10 mM magnesium acetate, 1 mM EDTA, 1 mM 2-mercaptoethanol.

4. [ $\gamma$ - $^{32}\text{P}$ ]ATP (3000 Ci/mmol).
5. AG-1-X8 (Bio-Rad) resin or phosphocellulose paper (Whatman P81).
6. 50 mM Tris-HCl (pH 6.8), 12.5 mM EDTA, 3.75% (w/v) sodium dodecyl sulfate (SDS), 10% (v/v) glycerol, 4 M urea, 2.5% (v/v) 2-mercaptoethanol, and 0.015% (w/v) bromophenol blue. A shorter peptide (<20 amino acids) is not suitable for SDS-PAGE analysis.

## 2.2. In Vivo Phosphorylation

1. Cultured cell lines expressing APP or APLP2 (see **Note 2**).
2. Antibodies raised against APP and APLP2 (see **Note 3**).
3. PDBu, nocodazole, and microcystin-LR. Dissolve these reagents in dimethylsulfoxide (DMSO) at 1 mM and store at  $-20^{\circ}\text{C}$ . PDBu is a specific activator of PKC. Nocodazole is an inhibitor of microtubule assembly. Microcystin-LR is a potent inhibitor of protein phosphatase 1 and 2A. These reagents are available from many chemical companies such as Calbiochem.
4. [ $^{32}\text{P}$ ] orthophosphoric acid ( $\sim 9000$  Ci/mol).
5. Cell lysis buffer: 50 mM Tris-acetate (pH 8.0), 0.27 M sucrose, 1 mM EDTA, 1 mM EGTA, 1 mM sodium vanadate, 1% (v/v) Triton X-100, 0.1% 2-mercaptoethanol, 1 mM microcystin-LR, 200  $\mu\text{g}/\text{mL}$  (w/v) pepstatin A, 200  $\mu\text{g}/\text{mL}$  (w/v) chymostatin, and 200  $\mu\text{g}/\text{mL}$  (w/v) leupeptin.
6. Protein-A sepharose (Amersham-Pharmacia).

## 2.3. Identification of Phosphorylated Form with Antibody

1. Phosphorylated antigen peptides, APP<sub>695</sub><sup>665-673</sup>[Cys][PiThr668] and APLP2<sub>763</sub><sup>732-740</sup>[Cys][PiThr736] synthesized by Quality-Controlled Biochemicals Inc. (Hopkinton, MA).
2. SulfoLink gel (Pierce, Rockford, IL).
3. *Limulus* hemocyanin (Sigma Chemical Co., St. Louis, MO).
4. SDS-lysis buffer: 50 mM Tris-HCl (pH 7.4), 1% (w/v) SDS, 2.7 M urea, 2  $\mu\text{M}$  microcystin-LR, pepstatin A (25  $\mu\text{g}/\text{mL}$ ), leupeptin (25  $\mu\text{g}/\text{mL}$ ), and chymostatin (25  $\mu\text{g}/\text{mL}$ ).

## 3. Methods

### 3.1. In Vitro Phosphorylation

1. Incubate substrate peptide (40–500  $\mu\text{M}$ ) with protein kinases (0.5–1  $\mu\text{g}$ ) in a reaction volume of 50  $\mu\text{L}$  containing the reaction buffer plus 0.1 mM [ $\gamma$ - $^{32}\text{P}$ ]ATP (4 Ci/mmol) for 30 min (see **Note 4**) at  $30^{\circ}\text{C}$ .
2. Terminate the reaction by adding 50  $\mu\text{L}$  of 30% (v/v) acetic acid containing bovine serum albumin (2 mg/mL).
3. Separate the phosphorylated peptides from free ATP by sequential chromatography using two AG1-X8 resin columns (2 mL bed vol.) equilibrated in 30% (v/v) acetic acid.

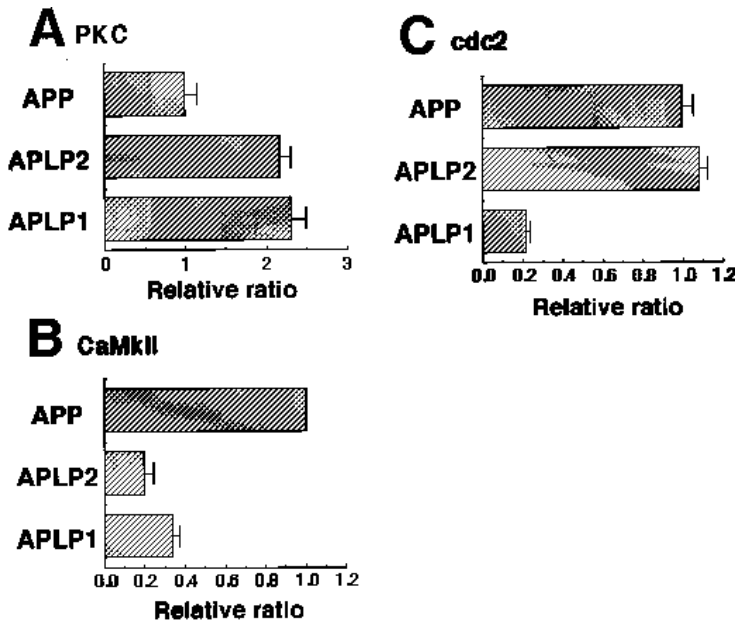


Fig. 2. Phosphorylation of cytoplasmic domain peptides from APP family proteins in vitro. Peptides were phosphorylated with (A) PKC, (B) CaMkII, or (C) Cdc2 kinase. The relative ratios of the levels of phosphorylation in APLP1<sub>653</sub><sup>608–653</sup> and APLP2<sub>763</sub><sup>717–763</sup> peptides are indicated relative to APP<sub>695</sub><sup>645–694</sup>, which was assigned a reference value of 1.0. Values are the average from duplicate studies, and error bars are indicated. (Modified from Suzuki et al. [14]. Reprinted by permission from *Biochemistry*.)

4. Dry the flow through fraction and measure the incorporation of <sup>32</sup>P into the peptide by liquid scintillation spectrometry, or dissolve the phosphorylated peptides in an SDS sample buffer, boil for 5 min, and analyze with autoradiography following SDS-PAGE (15% [w/v] polyacrylamide for the cytoplasmic peptide). Alternatively, spot an aliquot of each of the samples on a piece of P81 paper (~1.5 × 1.5 cm) after termination of the reaction, dry and wash the paper under running tap of water, then dry it again and measure the radioactivity.

This study demonstrated that APP, APLP1, and APLP2 are phosphorylated by PKC, that APP is phosphorylated by CaMkII, and that APP and APLP2 are phosphorylated by Cdc2 kinase (Fig. 2) (10,14). To identify the phosphorylation site, further classical studies such as phosphopeptide mapping and phosphoamino acid analysis are needed (12,13) (see Note 5). Because phosphorylation sites, identified by in vitro studies using purified protein kinases, have not always been subject to phosphorylation in vivo, studies to confirm the phosphorylation of APP family proteins in intact cells and/or tissues are essential.

### 3.2. In Vivo Phosphorylation

#### 3.2.1. Activation of PKC

1. Grow PC12 cells ( $2-3 \times 10^6$  cells) in Dulbecco's modified Eagle's medium (DMEM) containing 10% (v/v) fetal calf serum (FCS) and 5% (v/v) horse serum (HS).
2. Wash cells with phosphate-free DMEM and culture in phosphate-free DMEM containing dialyzed 10% (v/v) FCS, [ $^{32}\text{P}$ ] orthophosphate (1 mCi/mL) and PDBu (1  $\mu\text{M}$ ).
3. Label cells for 30–150 min and recover cells by pipetting from the plate.
4. Wash the cells with PBS and collect the cells by centrifugation at 800g for 5 min.
5. Lyse cells in lysis buffer (120  $\mu\text{L}$ ) for 30 min on ice with occasional vortexing.
6. Centrifuge (10,000g for 5 min) the samples and add 100  $\mu\text{L}$  of a solution containing 0.1 M Tris-HCl (pH 7.4), 2.2% (w/v) SDS, and 5.44 M urea to the supernatant (120  $\mu\text{L}$ ), and boil the mixture for 5 min.
7. After centrifugation (10,000g for 5 min), recover APP or APLP2 from the supernatant (200  $\mu\text{L}$ ) by immunoprecipitation using an antibody (see **Note 6**).
8. Recover the immunocomplex with protein A-Sepharose and analyze the proteins with SDS-PAGE (see **Note 7**).
9. Dry the gel and analyze the phosphorylation of protein with autoradiography.

In this study, the phosphorylated form of APP and APLP2 is not observed, which suggests that PKC does not phosphorylate APP and APLP2 in intact cells, although the kinase could phosphorylate the peptide of APP and APLP2 *in vitro*. The data suggest that the substrate that is phosphorylated *in vitro* is not always subjected to phosphorylation in intact cells, although it is now known that the site of APP phosphorylated by PKC *in vitro* is phosphorylated by an unidentified protein kinase in intact cells (15,27).

#### 3.2.2. Activation of Cdc2 Kinase

1. Culture *HeLa* cells ( $2-3 \times 10^6$  cells) in DMEM containing 10% (v/v) FCS and nocodazole (1  $\mu\text{g}/\text{mL}$ ) for 12 h (see **Note 8**).
2. Label the cells synchronized at the G2/M phase of the cell cycle for 2.5 h at 37°C with [ $^{32}\text{P}$ ] orthophosphate (1 mCi/mL) in phosphate-free DMEM containing nocodazole (1  $\mu\text{g}/\text{mL}$ ).
3. Recover and lyse the prelabeled cells, and then isolate APP and APLP2 from the resulting supernatant by immunoprecipitation as described in **Subheading 3.2.1.**, steps 4–9.

Phosphorylated APP and APLP2 are observed and the phosphorylation site is identical to that seen in studies of *in vitro* phosphorylation with purified Cdc2 kinase (13,14). This study demonstrate that APP and APLP2 are phosphorylated by Cdc2 kinase in intact cells as well as *in vitro*.

### 3.3. Identification of the Phosphorylated Form with Antibody

#### 3.3.1. Preparation of Antibody

1. Tag an extra cysteine residue on the amino-terminus of the antigen peptide.
2. Conjugate the peptide to *Limulus* hemocyanin with glutaraldehyde (see **Subheading 3.3.2.**) and inject it into a rabbit with adjuvant following standard immunization procedures.
3. In a separate study, couple the antigen peptide to SulfoLink gel, according to the manufacturer's instructions.
4. Purify the antibody by affinity chromatography using this resin (see **Subheading 3.3.3.**).

#### 3.3.2. Preparation of Peptide Conjugate

1. Dissolve 10 mg hemocyanin in 125 mM sodium phosphate buffer (pH 7.5) and add 5–10 mg of antigen peptide while stirring.
2. Add 2.5 mL of 0.2% (v/v) glutaraldehyde to sample gradually while stirring in a cold room for ~20 min and continue subsequent stirring in a cold room for 2 h.
3. Stop the coupling reaction by addition of 150  $\mu$ L of sodium borohydride (12.5 mg/mL) prepared freshly and follow additional stirring for 30 min.
4. Dialyze the sample against 2 L of 10 mM sodium phosphate (pH 7.5) for 8–12 h.
5. Change the buffer twice, recover the sample, and store as aliquots at  $-20^{\circ}\text{C}$  or  $-80^{\circ}\text{C}$ .

#### 3.3.3. Affinity Purification of Antibody

1. Apply approx 10 mL of antiserum to an antigen column (5–10 mL bed volume resin coupled with ~10 mg peptide) equilibrated with a burridge buffer consisting of 50 mM Tris-HCl (pH 7.4), 150 mM NaCl, 0.005% (w/v) sodium azide and 0.005% (v/v) Tween-20.
2. Wash column subsequently with 20 mL of the burridge and 20 mL of a BBS buffer consisting of 0.1 M boric acid-borax (pH 8.5), 1 M NaCl, and 0.1% (v/v) Tween-20.
3. Elute antibody with 4.9 M  $\text{MgCl}_2$  and add 1/10 vol. of 1 M HEPES (pH 7.6) immediately to the eluent.
4. Dialyze the eluted antibody against 4 L of a dialysis buffer consisting of 10 mM HEPES (pH 7.6) and 150 mM NaCl. Change the buffer three times every 4 h.
5. Concentrate the dialysate with Centriprep 30 (Amicon) and estimate immunoglobulin G (IgG) concentration using the value of  $\text{OD}_{280}$  (1 mg/mL IgG solution presents  $\text{OD}_{280} = 1.4$ ).

#### 3.3.4. Detection of the Phosphorylated Forms of APP and APLP2 by Western Blot Analysis

1. Synchronize cells at the G2/M phase of the cell cycle, lyse the cells in SDS-lysis buffer (see **Note 9**) and boil for 5 min.

2. Recover APP and APLP2 by immunoprecipitation with anti-APP or anti-APLP2 antibodies (*see Subheading 2.2.2.*) and protein A-Sepharose, and then separate the immunoprecipitates with SDS-PAGE (*see Note 10*).
3. Transfer the protein to a nitrocellulose membrane and probe with the phosphorylation state-specific antibodies (*see Note 11*). **Fig. 3** indicates the result of the quantification of cell cycle-dependent phosphorylation of APLP2 with this procedure.

It is very difficult to quantify the level of phosphorylated APP and APLP2 in tissues using the standard procedure with [ $^{32}\text{P}$ ] orthophosphoric acid. Using phosphorylation state-specific antibodies, we quantified the level of phosphorylated APP and APLP2 in rat tissues. Approximately identical quantities of APP or APLP2 were recovered from various rat tissues by immunoprecipitation with their respective antibodies. When recovered APP or APLP2 were separated by SDS-PAGE, transferred to a nitrocellulose membrane, probed with the phosphorylation state-specific antibody to the phosphorylated form of APP or APLP2, we found that APP and APLP2 were phosphorylated specifically in the brain and this neuron-specific phosphorylation is thought to play an important role in the process of neurite outgrowth (28, K. Iijima et al., unpublished observations). These results indicate that APP and APLP2 are phosphorylated in the brain by a fashion different from that in cultured cell lines, even when the phosphorylation site is identical.

### 3.3.5. Detection of the Phosphorylated Form of APP and APLP2 by Immunocytochemistry

The phosphorylation state-specific antibodies are useful in observing the cellular distribution of the phosphorylated APP and APLP2 using conventional immunocytochemical procedures.

1. Fix cultured cell lines and primary cultured neurons for 10 min at room temperature with 4% (w/v) paraformaldehyde in PBS (pH 7.4) containing 4% (w/v) sucrose.
2. Permeabilize the cells for 5 min at room temperature with 0.2% (v/v) Triton X-100 in PBS.
3. Wash the cells with PBS, incubate the cells with phosphorylation state-specific antibody for 12 h at 4°C.
4. Wash the cell thoroughly and then incubate the cells for 1 h at room temperature with tetraodamine isothiocyanate/fluorescein isothiocyanate-conjugated secondary antibody.

In a study using differentiated PC12 cells, the phosphorylated APP/APLP2 are detected mostly in neurites and on the plasma membrane of somata, although most dephosphorylated APP/APLP2 is found in the cell body (28, K. Iijima et al., unpublished observation). In another study using cell lines

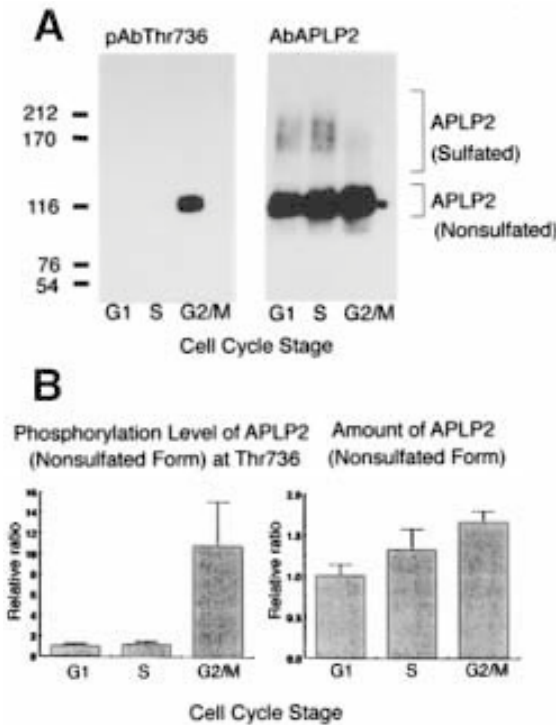


Fig. 3. Cell cycle-dependent phosphorylation and metabolism of APLP2. HeLa cells were synchronized at various cell cycle stages: G1 (synchronized by serum withdrawal), S (synchronized with aphidicolin), and G2/M (synchronized with nocodazole). APLP2 was immunoprecipitated from cell extracts using anti-APLP2 antibody, and samples were subjected to SDS-PAGE using 6% (w/v) polyacrylamide and transferred to nitrocellulose membranes. **(A)** Immunoblots were probed with anti-phosphoThr736 antibody (pAbThr736, left panel) or anti-APLP2 antibody (AbAPLP2, right panel) and [<sup>125</sup>I]protein A, and then autoradiography was performed. Numbers indicate protein molecular weight markers (kDa). **(B)** Relative levels of phosphorylation and total amounts of the nonsulfated form of APLP2 at various cell cycle stages. Immunoblots shown in **(A)** were quantitated using a Fuji BAS 2000 imaging analyzer (Fuji, Tokyo, Japan). The levels of APLP2 phosphorylated at Thr736 and nonsulfated APLP2 were standardized to the amount of protein in cell extracts, and the relative ratios of phosphorylated Thr736 at G1, S, and G2/M phases are indicated. Values are averages from duplicate studies, and error bars are indicated. (From Suzuki et al. [14]. Reprinted by permission from *Biochemistry*.)

that are synchronized at the G2/M phase of the cell cycle, the phosphorylated APP/APLP2 are detected in a specific stage of mitosis (K. Ando et al., unpublished observation). These results suggest a possibility that APP and APLP2

have a physiological function in the postmitotic neuron, which differs from that in the dividing cell.

#### 4. Notes

1. Shorter peptides containing a phosphorylation site such as APP<sup>663–676</sup> of APP<sub>695</sub> are also useful as a substrate.
2. Rat pheochromocytoma (PC12) and HeLa cells express high endogenous levels of APP and APLP2.
3. APP family protein genes have been conserved in many animals and the amino acid sequences of these proteins are high homologous, especially in the cytoplasmic domain. Therefore, affinity purification of the antibody may be necessary to prevent crossreactivity between APP and APLP2. Anti-APP antibodies are commercially available from companies such as Zymed Laboratories and Boehringer Mannheim (Mannheim, Germany).
4. When a kinetic analysis is performed, the incubation time should be 1 min.
5. Some protein kinase is autophosphorylated. Therefore, it is necessary to isolate peptide from such protein kinase with SDS-PAGE to perform exact studies of phosphoamino acid analysis and phosphopeptide mapping.
6. Control immunoprecipitation was carried out in the presence of excess antigen peptide (10  $\mu$ M).
7. 7.5% (w/v) Acrylamide gel is used for APP and APLP2, and 15% (w/v) acrylamide gel is used for analysis of the truncated cytoplasmic domain from APP and APLP2.
8. HeLa cells synchronize more readily than other adhesive cells, PC12, C6 (rat glial cell tumor), Chinese hamster ovary (CHO), and H4 (human neuroglioma). The level of synchronization was examined with fluorescence-activated cell sorter (FACS) analysis.  $1 \times 10^6$  cells were fixed with 50% methanol and DNA was stained by stain solution (50 ng/mL [w/v] propidium iodide, 100 U/mL RNase A and 0.1% [w/v] glucose in PBS). The cells were then analyzed on a Becton Dickinson FACScan Flow Cytometer (Heidelberg, Germany).
9. To examine endogenous level of phosphorylation exactly, fresh sample was lysed in a buffer containing SDS and a phosphatase inhibitor (microcystin-LR).
10. 7.5% (w/v) Polyacrylamide for intact APP or APLP2 molecule.
11. Direct Western blotting is also possible when the protein content in the cell and the phosphorylation level are relatively high.

#### References

1. Glenner, G. and Wong, C. (1984) Alzheimer's disease and Down's syndrome: sharing of a unique cerebrovascular amyloid fibril protein. *Biochem. Biophys. Res. Commun.* **122**, 885–890.
2. Master, C. L., Simms, G., Weinman, N. A., Multhaup, G., McDonald, B. L., and Beyreuther, K. (1985) Amyloid plaque core protein in Alzheimer disease and Down syndrome. *Proc. Natl. Acad. Sci. USA* **82**, 4245–4249.

3. Kang, J., Lemaire, H. G., Unterbeck, A. J., Salbaum, J. M., Masters, C. L., Grzeschik, K. H., et al. (1987) The precursor of Alzheimer's disease amyloid A4 protein resembles a cell-surface receptor. *Nature* **325**, 733–736.
4. Rosen, D. R., Martin-Morris, L., Luo, L., and White, K. (1989) A *Drosophila* gene encoding a protein resembling the human  $\beta$ -amyloid protein precursor. *Proc. Natl. Acad. Sci. USA* **86**, 2478–2482.
5. Daigle, I. and Li, C. (1993) *apl-1*, A *Caenorhabditis elegans* gene encoding a protein related to the human  $\beta$ -amyloid protein precursor. *Proc. Natl. Acad. Sci. USA* **90**, 12045–12049.
6. Iijima, K., Lee, D.-S., Okutsu, J., Tomita, S., Hirashima, N., Kirino, Y., and Suzuki, T. (1998) cDNA isolation of Alzheimer's amyloid precursor protein from cholinergic nerve terminals of the electric organ of the electric ray. *Biochem. J.* **330**, 29–33.
7. Wasco, W., Bupp, K., Magendantz, M., Gusella, J., Tanji, R. E., and Solomon, F. (1992) Identification of a mouse brain cDNA that encodes a protein related to the Alzheimer disease-associated amyloid  $\beta$  protein precursor. *Proc. Natl. Acad. Sci. USA* **89**, 10,758–10,762.
8. Wasco, W., Gurubhagavatula, S., Paradis, M. D., Romano, D. M., Sisodia, S. S., Hyman, B. T., et al. (1993) Isolation and characterization of APLP2 encoding a homologue of the Alzheimer's associated amyloid b protein precursor. *Nat. Genet.* **5**, 95–100.
9. Von Koch, C. S., Zheng, H., Chen, H., Trumbauer, M., Thinakaran, G., Van der Ploeg, L. H. T., et al. (1997) Generation of APLP2 KO mice and early postnatal lethality in APLP2/APP double KO mice. *Neurobiol. Aging* **18**, 661–669.
10. Gandy, S. E., Czernik, A. J., and Greengard, P. (1988) Phosphorylation of Alzheimer disease amyloid precursor protein peptide by protein kinase C and Ca<sup>2+</sup>/calmodulin-dependent protein kinase II. *Proc. Natl. Acad. Sci. USA* **85**, 6218–6221.
11. Oltersdorf, T., Ward, P. J., Henriksson, T., Beattie, E. C., Neve, R., Lieberburg, I., and Fritz, L. C. (1990) The Alzheimer amyloid precursor protein. Identification of a stable intermediate in the biosynthetic/degradative pathway. *J. Biol. Chem.* **265**, 4492–4497.
12. Suzuki, T., Nairn, A. C., Gandy, S. E., and Greengard, P. (1992) Phosphorylation of Alzheimer amyloid precursor protein by protein kinase C. *Neuroscience* **48**, 755–761.
13. Suzuki, T., Oishi, M., Marshak, D. M., Czernik, A. J., Nairn, A. C., and Greengard, P. (1994) Cell cycle-dependent regulation of the phosphorylation and metabolism of the Alzheimer amyloid precursor protein. *EMBO J.* **13**, 1114–1122.
14. Suzuki, T., Ando, K., Isohara, T., Oishi, M., Lim, G. S., Satoh, Y., et al. (1997) Phosphorylation of Alzheimer  $\beta$ -amyloid precursor-like proteins. *Biochemistry* **36**, 4643–4649.
15. Oishi, M., Nairn, A. C., Czernik, A. J., Lim, G. S., Isohara, T., Gandy, S. E., et al. (1997) The cytoplasmic domain of Alzheimer's amyloid precursor protein is phosphorylated at Thr654, Ser655, and Thr668 in adult rat brain and cultured cells. *Mol. Med.* **3**, 111–123.
16. Hung, A. J. and Selkoe, D. J., (1994) Selective ectodomain phosphorylation and regulated cleavage of  $\beta$ -amyloid precursor protein. *EMBO J.* **13**, 534–542.

17. Walter, J., Capell, A., Hung, A. Y., Langen, H., Schnölzer, M., Thinakaran, G., et al. (1997) Ectodomain phosphorylation of  $\beta$ -amyloid precursor protein at two distinct cellular locations. *J. Biol. Chem.* **272**, 1896–1903.
18. Norstedt, C., Caporaso, G. L., Thyberg, J., Gandy, S. E., and Greengard, P. (1993) Identification of the Alzheimer  $\beta$ /A4 amyloid precursor protein in clathrin-coated vesicles purified from PC12 cells. *J. Biol. Chem.* **268**, 608–612.
19. Lai, A., Sisodia, S. S., and Trowbridge, I. S. (1995) Characterization of sorting signals in the  $\beta$ -amyloid precursor protein cytoplasmic domain. *J. Biol. Chem.* **270**, 3565–3573.
20. Tomita, S., Kirino, Y., and Suzuki, T. (1998) A basic amino acid in the cytoplasmic domain of Alzheimer's  $\beta$ -amyloid precursor protein (APP) is essential for the cleavage of APP at the  $\alpha$ -site. *J. Biol. Chem.* **273**, 19,304–19,310.
21. Neve, R. L. (1996) Mixed signals in Alzheimer's disease. *Trends. Neurosci.* **19**, 371–372.
22. Songyang, Z., Lu, K. P., Kwon, Y., Tsai, L.-H., Filhol, O., Cochet, C., et al. (1996) A structural basis for substrate specificities of protein Ser/Thr kinases: primary sequence preference of casein kinases I and II, NIMA, phosphorylase kinase, calmodulin-dependent kinase II, CDK5, and Erk1. *Mol. Cell. Biol.* **16**, 6486–6493.
23. Woodgett, J. R. and Hunter, T. (1987) Isolation and characterization of two distinct forms of protein kinase C. *J. Biol. Chem.* **262**, 4836–4843.
24. Utida, T. and Filburn, C. R. (1984) Affinity chromatography of protein kinase C-phorbol ester receptor on polyacrylamide-immobilized phosphatidylserine. *J. Biol. Chem.* **259**, 12,311–12,314.
25. Lai, Y., Nairn, A. C. and Greengard, P. (1986) Autophosphorylation reversibly regulates the  $\text{Ca}^{2+}$ /calmodulin-dependence of  $\text{Ca}^{2+}$ /calmodulin-dependent protein kinase II. *Proc. Natl. Acad. Sci. USA* **83**, 4253–4247.
26. Brizuela, L., Draetta, G., and Beach, D. (1989) Activation of human CDC2 protein as a histone H1 kinase is associated with complex formation with the p62 subunit. *Proc. Natl. Acad. Sci. USA* **86**, 4362–4366.
27. Isohara, T., Horiuchi, A., Watanabe, T., Ando, K., Czernik, A. J., Uno, I., et al. (1999) Phosphorylation of the cytoplasmic domain of Alzheimer's  $\beta$ -amyloid precursor protein At Ser655 by a novel protein kinase. *Biochem. Biophys. Res. Commun.* **258**, 300–305.
28. Ando, K., Oishi, M., Takeda, S., Ijima, K., Isohara, T., et al. (1999) Role of phosphorylation of Alzheimer's amyloid precursor protein during neuronal differentiation. *J. Neurosci.* **19**, 4421–4427.

## Determining the Transmembrane Topology of the Presenilins

Gopal Thinakaran and Andrew Doan

### 1. Introduction

Mutations in two related genes, *PS1* (1) and *PS2* (2,3) located on chromosomes 14 and 1, respectively, account for the majority of early onset cases of familial Alzheimer's disease (FAD). *PS1* and *PS2* are predominantly localized in the endoplasmic reticulum and Golgi (4–7). *PS1* is a 467 amino acid peptide predicted to contain between seven and nine transmembrane helices based on hydrophobicity profiles (1,8). The protein topology of *PS1* and its *C. elegans* homologues, SEL-12 and HOP-1, have been examined by several investigators (7,9–13). This chapter describes two approaches we utilized to determine the topological orientation of the *PS1* N-terminal, and C-terminal domains, and a hydrophilic “loop” region encompassing amino acids 263–407. The first approach is based on the proteolytic sensitivity of amyloid precursor protein (APP) protein chimeras to endoproteolytic cleavage by  $\beta$ -secretase in the lumen of the Golgi. The second approach is based on selective permeabilization of the plasma membrane using a bacterial pore-forming toxin, streptolysin-O (SLO), and subsequent immunocytochemical probing for cytosolic epitopes using specific antibodies. Both of these methods can be easily adapted to determine the topology of other membrane proteins.

#### 1.1. Use of *PS1-APP Chimeric Proteins to Determine PS1 N-Terminus Topology*

In earlier efforts, we and others established that the APP Swedish variant (APP<sup>sw</sup>) is endoproteolytically cleaved at the lumenally exposed  $\beta$ -secretase site in the Golgi compartment, resulting in the production of a distinct ~12 kDa fragment of 99 amino acids extending from Asp + 1 of the  $\beta$ -amyloid peptide

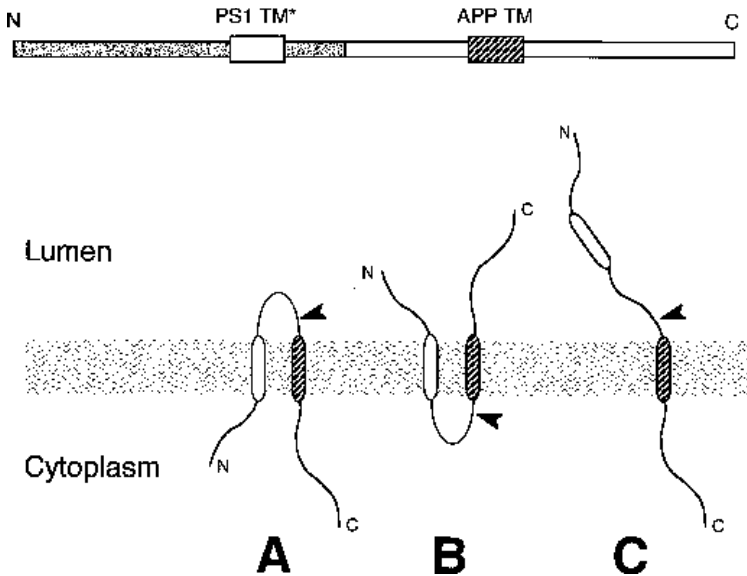


Fig. 1. Schematic representation of TM1-APP chimeric polypeptide (top) and its potential membrane topologies (bottom). Shaded bar denotes N-terminal 132 residues of human PS1; open bar denotes C-terminal 167 residues of human APP-695swe; open box marked *PS1 TM\** denotes predicted PS1 transmembrane domain 1; hatched box marked *APP TM* denotes APP transmembrane domain. Arrowhead represents  $\beta$ -secretase cleavage site.

(A $\beta$ ) to the extreme C-terminus of APP (14–16). Taking advantage of this finding, we designed a strategy aimed at testing whether potential transmembrane (TM) helices of *PS1* were sufficient to export APP sequences that included the Swedish mutations into the Golgi lumen. We generated cDNA encoding a chimeric protein (TM1-APP) consisting of a 132-amino acid region of *PS1* representing the N-terminal 80 amino acids, first predicted TM and 31 amino acids downstream fused to a 167-amino acid region of APP that includes 96 amino acids of the ectodomain harboring the Swedish double mutation, the TM, and C-terminal domains. As shown in **Fig. 1**, this chimera could adopt two configurations wherein the *PS1* N-terminal domain is resident either in the cytoplasm (model A) or in the ER/Golgi lumen (model B);  $\beta$ -secretase cleavage of the chimera would only occur if the *PS1* N-terminus is cytoplasmic. Cleavage of the chimeric polypeptide by  $\beta$ -secretase was visualized by radiolabeling transfected COS-1 cells expressing the chimeric polypeptide with [ $^{35}$ S]methionine and subsequent immunoprecipitation analysis. The cell-associated APP C-terminal fragments, and secreted A $\beta$  were immunoprecipitated from cell lysates and conditioned medium, respectively, using appropriate antibodies.

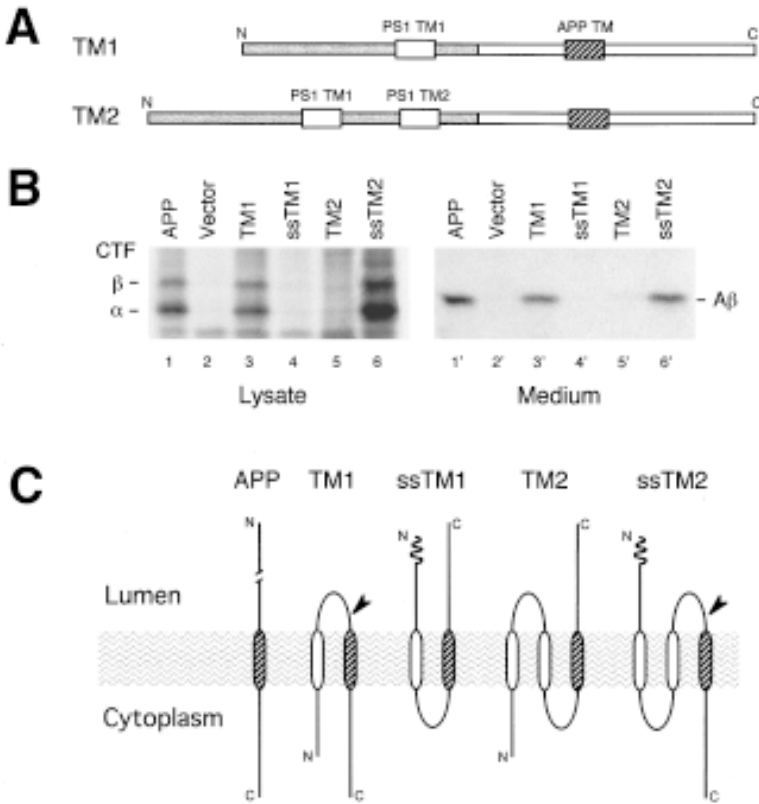


Fig. 2. Localization of PS1 N-terminus. **(A)** Schematic representation of PS1-APP chimeras. TM1-APP and TM2-APP consist of N-terminal 132 and 163 residues of human PS1, respectively, fused to C-terminal 167 residues of human APP-695swe. **(B)** Metabolism of PS1-APP chimeric polypeptides. COS-1 cells transfected with plasmids encoding chimeric polypeptides were labeled for 3 h with [<sup>35</sup>S]methionine. Lanes 1–6 represent C-terminal APP fragments ( $\alpha$  and  $\beta$  CTF) immunoprecipitated from cell lysates with Ab369 antiserum. Lanes 1'–6' represent A $\beta$  immunoprecipitated from conditioned medium using monoclonal antibody 4G8. **(C)** Schematic representation of membrane topology of chimeric PS1-APP polypeptides. Arrowhead represents  $\alpha$ - and  $\beta$ -secretase cleavage sites.

We transiently expressed TM1-APP in COS-1 cells and demonstrated the accumulation of an approx 12 kDa APP C-terminal fragment (CTF) in cell lysates (**Fig. 2B**, lane 3). This CTF comigrates with an authentic  $\beta$ -secretase-generated derivative in cells expressing native APPswe (**Fig. 2B**, lane 1). In addition, we observed intracellular accumulation of an approx 10 kDa CTF generated by  $\alpha$ -secretase (**Fig. 2B**, lane 3) and the presence of A $\beta$  in the

medium of cells expressing TM1-APP (**Fig. 2B**, lane 3'), findings similar to cells expressing APP<sup>swe</sup> (**Fig. 2B**, lane 1 and lane 1', respectively). These data support the idea that TM1-APP adopts a configuration that orients the *PSI* N-terminus towards the cytoplasm (*see Fig. 2C*, TM1).

We were aware of the possibility that cleavage at the  $\beta$ -secretase site could also occur if the *PSI* N-terminus is luminal and TM1 does not span the bilayer (**Fig. 1**, model C). In this case, only the APP TM domain would anchor the chimera in the membrane. To control for the possibility that TM1-APP might adopt an alternative configuration that orients the *PSI* N-terminus towards the ER/Golgi lumen, we examined the processing of ssTM1-APP, a chimera containing the APP signal sequence (ss) fused to the extreme N-terminus of TM1-APP. We anticipated that introduction of the APP signal sequence in ssTM1-APP would force translocation of the *PSI* region into the lumen of the ER/Golgi. Two potential topologies could be envisioned for the ssTM1-APP chimera: the entire *PSI* region (including TM1) is luminal (**Fig. 1**, model C); or, only the N-terminal 80 amino acids of *PSI* are luminal and TM1 is membrane inserted (*see Fig. 2C*, ssTM1). In the latter case, the APP  $\beta$ -secretase cleavage site would be located in the cytosolic compartment where  $\beta$ -secretase is inactive (or absent). COS-1 cells expressing ssTM1-APP neither generated CTF (**Fig. 1B**, lane 4), nor released A $\beta$  (**Fig. 2B**, lane 4'), despite the demonstration that the chimera had reached the Golgi, a site for  $\beta$ -secretase cleavage of APP<sup>swe</sup> (9) (*see Note 1*). Failure to detect APP CTF in cells expressing ssTM1-APP supports our view that both the *PSI* and APP TMs span the bilayer (as shown in **Fig. 2C**, ssTM1) and argue against the alternative model in which the entire *PSI* segment is luminal. Hence, these data are consistent with a model in which the *PSI* N-terminus is exposed to the cytoplasm.

We extended this strategy to examine TM2-APP, a chimera composed of the N-terminal 163 amino acids of *PSI* that included the first two predicted TM domains of *PSI* fused to the identical region of APP<sup>swe</sup> used in the TM1-APP chimera. If our conclusions regarding the topology of TM1-APP are correct, then TM2-APP should also adopt a configuration that orients the N-terminus towards the cytoplasm (*see Fig. 2C*, TM2). In this configuration, the protease-sensitive site is cytoplasmic, thus rendering the TM2-APP chimera incompetent for  $\beta$ -secretase cleavage. As expected, we neither detected APP CTF in cell lysates, nor A $\beta$  in the medium of COS-1 cells expressing TM2-APP (**Fig. 2B**, lane 5 and lane 5', respectively), despite transport of the chimera to the Golgi (9). On the other hand, ssTM2-APP, a chimera containing the APP signal sequence juxtaposed to the N-terminus of TM2-APP was efficiently processed by  $\beta$ -secretase to generate an approx 12 kDa C-terminal derivative (**Fig. 2B**, lane 6). Thus, the ssTM2-APP chimera must have adopted a configuration that orients the *PSI* N-terminus towards the lumen (*see Fig. 2C*, ssTM2).

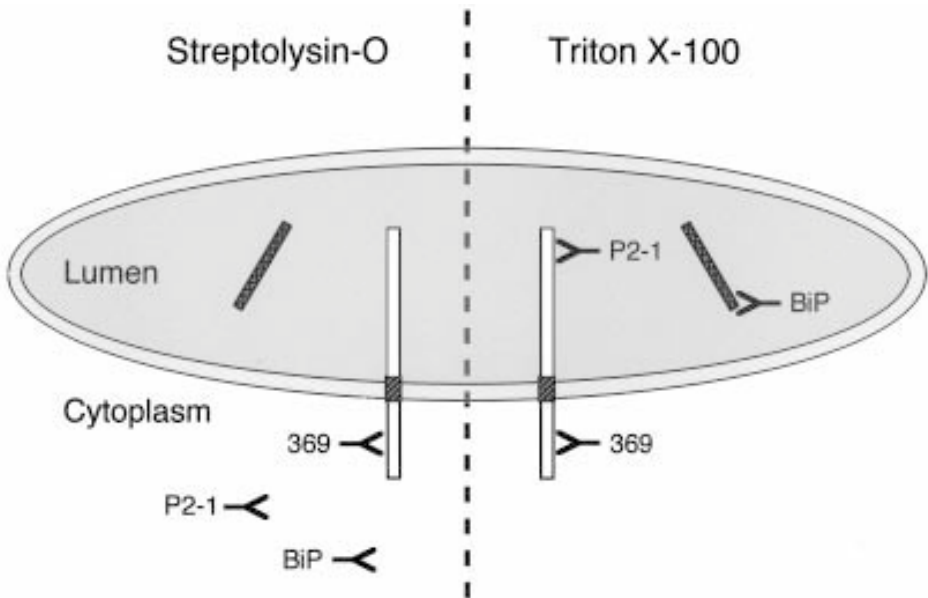


Fig. 3. Schematic representation of the SLO strategy. A schematic crosssection of ER from SLO (left) or Triton X-100 (right) permeabilized cell is shown. Treatment with Triton permeabilizes plasma membrane as well as intracellular membranes allowing antibodies to gain access to cytosol and ER lumen. Thus, in cells treated with Triton antibodies bind to epitopes oriented towards both cytosol and lumen. In contrast, treatment with SLO, selectively permeabilizes plasma membrane; because intracellular membranes are intact, antibodies P2-1 (APP N-terminal mAb) and BiP (anti-BiP) cannot gain access to the ER lumen. In the latter case, antibodies only bind epitopes oriented towards the cytosol.

These studies indicate that the predicted TM1 and TM2 helices of *PS1* span the bilayer. Moreover, efficient  $\beta$ -secretase cleavage of the ssTM2-APP chimera confirms our earlier conclusion that the N-terminus of *PS1* is oriented towards the cytoplasm.

### 1.2. Use of Selective Permeabilization to Determine Membrane Orientation of the *PS1* “Loop” Domain

The chimeric polypeptide strategy just described is easier to use for determining topology of proteins with a limited number of transmembrane domains. Because *PS1* was predicted to contain seven or more transmembrane helices, we developed an alternate strategy (Fig. 3) that examines the membrane topology of polytopic full-length proteins obviating the need to generate a number of fusion polypeptides. In this approach, the plasma membrane (PM) of cul-

tured cells was selectively permeabilized with SLO. Subsequently, we asked whether antibodies raised against specific epitopes of *PSI* could bind cognate sequences associated with intracellular membranes (IMs). SLO is a bacterial toxin that binds selectively to cholesterol (found predominantly on the PM). When applied to cells under appropriate conditions (*see below*), SLO will oligomerize, resulting in the formation of pores exceeding 30 nm, which allow passage of macromolecules (e.g., antibodies and hydrophilic drugs) across the plasma membrane (**17**). The advantage of using SLO is the high specificity of binding to cholesterol, which is mostly absent in membranes of intracellular organelles, such as the ER and Golgi. Thus, SLO permeabilization of live cells will allow antibodies to have access to cytosolic epitopes but not lumenally disposed epitopes. In contrast, incubating fixed cells with the nonionic detergent, Triton X-100, which permeabilizes all lipid bilayers (both PM and IMs) will allow antibodies to reach epitopes oriented towards both cytosol and lumen.

For our studies, we used a stable CHO line expressing human APP-695 (CHO-695) (**18**). Because the protein topology of APP is known, antibodies against APP were used as our internal control. Antibodies raised against the N-terminal domain of APP (oriented towards the lumen) will immunostain APP only in cells treated with Triton X-100, whereas antibodies raised against the C-terminal domain (oriented towards cytoplasm) will stain APP in cells treated with either SLO or Triton X-100 (**Fig. 3**).

CHO-695 cells were transiently transfected with human *PSI* cDNA and the cell monolayers were permeabilized with SLO, or Triton X-100. Cells were then fixed prior to antibody incubation. Human *PSI* “loop” domain was detected with  $\alpha$ *PSI*Loop, a polyclonal antiserum specific for amino acids 320–375 (**19**). Transfected SLO- or Triton-treated cells were coincubated with  $\alpha$ *PSI*Loop, and a monoclonal antibody (mAb), P2-1, specific for N-terminal, lumenally disposed epitopes of human APP (**20**). Bound antibodies were detected by indirect immunofluorescence (IF) microscopy. The mAb P2-1 served to control for inadvertent permeabilization of IMs by SLO. As shown in **Fig. 4A** (top),  $\alpha$ *PSI*Loop detected *PSI* loop domain epitopes in SLO-treated cells, whereas mAb P2-1 binding to APP was undetectable. The observation that mAb P2-1 failed to react with APP lumenal epitopes confirmed that IMs were resistant to permeabilization by SLO. On the other hand, cells permeabilized with Triton and incubated with antibodies  $\alpha$ *PSI*Loop and mAb P2-1 bound cognate epitopes as expected (**Fig. 4A**, bottom). Our demonstration that  $\alpha$ *PSI*Loop bound *PSI* in SLO-permeabilized cells in the absence of detectable disruption of IMs indicates that the *PSI* loop domain is oriented towards the cytoplasmic face of IMs.

We performed additional control experiments to confirm that our failure to detect APP with mAb P2-1 in SLO-permeabilized cells is not an artifact of the

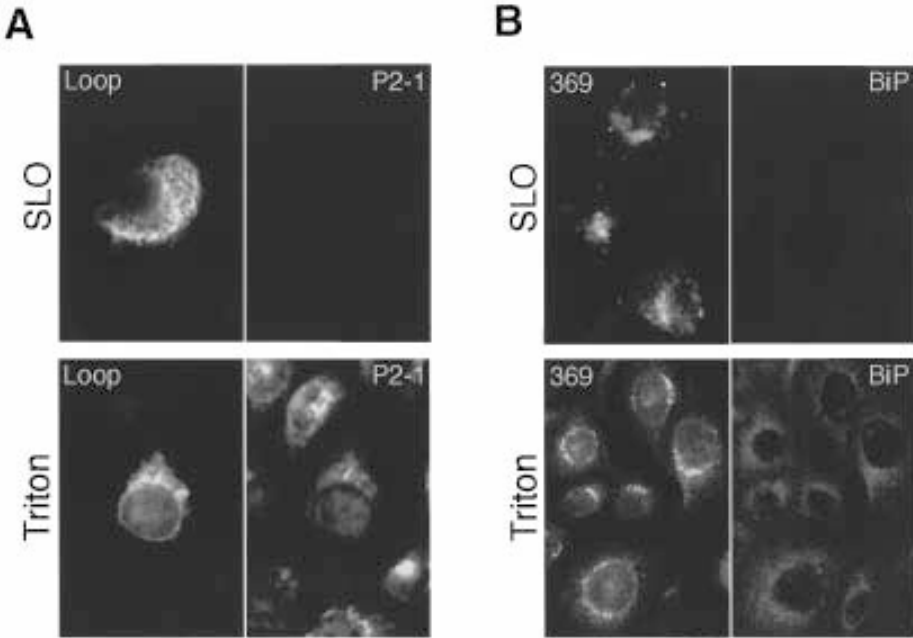


Fig. 4. Cytoplasmic localization of PS1 loop domain. CHO-695 cells stably expressing human APP were transiently transfected with human PS1 cDNA, and analyzed by indirect immunofluorescence after treatment with either SLO (top panels) or Triton X-100 (bottom panels). (A) Following permeabilization with SLO or Triton, cells were coincubated with  $\alpha$ PS1Loop (polyclonal antiserum raised against PS1 loop domain), and P2-1 (monoclonal antibody specific for APP luminal epitopes). Red and green fluorescence corresponding to  $\alpha$ PS1Loop and P2-1 staining, respectively, are shown as gray-scale images. (B) CHO-695 cells were coincubated with Ab369 (polyclonal antiserum raised against cytoplasmic domain of APP), and BiP (monoclonal antibody specific for ER luminal protein, BiP) subsequent to permeabilization with SLO or Triton. Red and green fluorescence corresponding to Ab369 and BiP staining, respectively, are shown as gray-scale images.

permeabilization procedure per se. We coincubated CHO-695 cells with a rabbit polyclonal antibody, Ab369, that recognizes epitopes in the APP cytoplasmic domain (21) and a mAb specific for a lumenally disposed epitope (KSEKDEL) of the ER chaperone Grp78 (BiP) (22). As expected, Ab369 bound APP C-terminal epitopes in both SLO and Triton-permeabilized cells; on the other hand, BiP staining was only observed in Triton-treated cells (Fig. 4B). Collectively, these results demonstrate that SLO selectively permeabilizes the PM and that this approach allows access of specific antibodies to cognate epitopes located on the cytosolic face of IMs.

## 2. Materials

### 2.1. PS-APP Chimeric Protein Studies

#### 2.1.1. Transfection

1. COS-1 cells.
2. Dulbecco's modified Eagle's medium (DMEM) (Gibco-BRL, Paisley, Scotland; cat. no. 11965-092) supplemented with L-glutamine and 10% fetal bovine serum (FBS).
3. Plasmids pCB6 (**23**) and pAPP695Swe (**24**).
4. PS-APP chimeric plasmids (**9**): pCB6TM1, pCB6TM2, pCB6ssTM1, and pCB6ssTM2.
5. 2× N-bis(2-hydroxyethyl)-2-aminoethane sulfonic acid buffered saline (BBS) (**25**): 50 mM N, N-bis(hydroxyethyl)-2-aminoethane sulfonic acid (BES), pH 6.95, 280 mM NaCl, and 1.5 mM Na<sub>2</sub>HPO<sub>4</sub>. Filter sterilized and stored at -20°C.
6. 2.5 M CaCl<sub>2</sub>. Filter sterilized and stored at -20°C.

#### 2.1.2. [<sup>35</sup>S]Methionine Labeling and Immunoprecipitation

1. Met<sup>-</sup> medium: DMEM minus methionine (Gibco-BRL; cat. no. 11970-035) supplemented with L-glutamine and 1% dialyzed fetal calf serum (Gibco-BRL; cat. no. 16440-031).
2. [<sup>35</sup>S]methionine, >1000 Ci/mmol (NEN, DuPont, Boston, MA; cat. no. NEG 009C).
3. Phenylmethylsulfonyl fluoride (PMSF) (100 mM in 100% ethanol).
4. IP buffer (**26**): 50 mM Tris-HCl, pH 7.4, 150 mM NaCl, 0.5% Nonidet P-40, 0.5% sodium deoxycholate, 5 mM EDTA, pepstatin (50 µg/mL), leupeptin (50 µg/mL), aprotinin (10 µg/mL), and PMSF (0.25 mM).
5. 20% Sodium dodecyl sulfate (SDS).
6. Protein A Agarose (Pierce, Rockford, IL; cat. no. 20333).
7. Antibodies: Ab369 (**21**); mAβ 4G8 (**27**).

### 2.2. SLO Permeabilization Studies

1. SLO was purchased from Dr. S. Bhakdi (Institute of Medical Microbiology and Hygiene, Mainz, Germany) and stock solutions prepared in 1 mg/mL bovine serum albumin (BSA) and 2 mM DTT were stored at -70°C.
2. Phosphate-buffered saline (PBS): 140 mM NaCl, 3 mM KCl, 2 mM potassium phosphate, and 10 mM sodium phosphate, pH 7.4.
3. SLO-buffer (**28**): 20 mM HEPES, pH 7.2, 125 mM K-L-glutamate, 15 mM KCl, 5 mM NaCl, 2 mM MgCl<sub>2</sub>, and 3 mM EGTA.
4. 4% Paraformaldehyde prepared in PBS.
5. Blocking buffer: 1% BSA, 50 mM NH<sub>4</sub>Cl, and 10 mM glycine in PBS.
6. Antibody dilution buffer: 1% Normal goat serum in PBS.
7. Primary antibodies: N-terminal monoclonal APP antibody, P2-1 (**20**); C-terminal polyclonal APP antiserum, Ab369 (**21**); N-terminal polyclonal *PS1* antiserum, Ab14 (**29**); polyclonal antiserum raised against the loop domain of *PS1*,

a*PSI*/Loop (**19**); monoclonal antibody raised against BiP/Grp78 (Stressgen Biotechnologies, Victoria, BC; cat. no. SPA-827).

8. Texas Red conjugated antirabbit IgG (Vector Laboratories, Burlingame, CA; cat. no. TI-1000).
9. Fluorescein isothiocyanate (FITC)-conjugated antimouse (Vector; cat. no. FI-2000).
10. 4',6-Diamidino-2-phenylindole (DAPI) 5 mg/mL stock prepared in PBS (Boehringer Mannheim, Mannheim, Germany; cat. no. 236276).
11. PermaFluor. (Immunon, cat. no. 434990).

### 3. Methods

#### 3.1. Expression Vectors

Standard molecular biology techniques were used to generate expression vectors. Sequences encoding the N-terminal 132 amino acids of human *PSI* were amplified by polymerase chain reaction (PCR) using pBSHu*PSI* (**8**) as template using the sense primer 5' CCAGATCTGGAAGGAACCTGAGC 3' (FHu*PSI*) and antisense primer, 5' GCTTGAGCTCTGAGTGCAGGGCTCTCTGG 3'. Sequences encoding the N-terminal 163 amino acids were amplified using the sense primer FHu*PSI* (above) and antisense primer, 5' GCTTGAGCTCATGGATGACCTTATAGCACC 3'. The PCR products were digested with *Bgl*III and *Sst*I, gel purified, and incubated in a ligation reaction containing a gel purified *Sst*I-*Xba*I fragment from plasmid pAPP-695swe (**24**) and pCB6 vector (**23**) with *Bgl*III and *Xba*I ends. The resulting plasmids encode chimeric proteins containing the N-terminus and predicted first TM of *PSI* (pCB6TM1), or the first two TMs of *PSI* (pCB6TM2), fused to the C-terminal 167 amino acids of APP containing the Swedish double mutation. Sequences encoding the signal peptide of huAPP were isolated as a 105-bp *Bam*HI-*Asp*718 fragment from plasmid p770 (**26**), and the ends were filled in using Klenow fragment of DNA polymerase. This fragment was ligated to plasmids pCB6TM1 and pCB6TM2 previously digested with *Asp*718 and the ends filled to generate pCB6ssTM1 or pCB6ssTM2, respectively.

#### 3.2. Transfection of COS-1 and N2a Cells

1. Seed  $0.5 \times 10^6$  cells in a 60-mm dish 24 h before transfection (*see Note 2*).
2. Prepare the transfection mixture in a sterile tube as follows: combine 10  $\mu$ g of DNA with sterile distilled water to a final volume of 225  $\mu$ L. Add 25  $\mu$ L of 2.5 M CaCl<sub>2</sub> and mix. Add 250  $\mu$ L of 2 $\times$  BBS and mix. Leave at room temperature for 20 min.
3. Add the mixture dropwise to the dish and mix gently.
4. Incubate at 37°C in 3% CO<sub>2</sub>.
5. After 14–18 h incubation, aspirate the medium and wash twice with culture medium. Add 5 mL fresh medium and return the dish to 5% CO<sub>2</sub>.
6. Label the cells with [<sup>35</sup>S]methionine the following day (*see Subheading 3.3.*).

### 3.3. Metabolism of PS1-APP Chimeric Proteins

1. Remove the culture medium and replace with 2 mL of Met<sup>-</sup> medium containing 250  $\mu$ Ci/mL [<sup>35</sup>S]methionine and incubate at 37°C for 3 h.
2. Collect the medium after labeling and add 10  $\mu$ L of 100 mM PMSF. Centrifuge at 12,000g for 5 min to remove cell debris and save the supernatant (conditioned medium).
3. Wash the monolayer of cells twice with cold PBS. Lyse the cells in 500  $\mu$ L of immunoprecipitation (IP) buffer. Immediately transfer lysate into a microfuge tube. Vortex gently and centrifuge the lysate at 12,000g for 1 min to pellet nuclei. Transfer the supernatant (detergent lysate) to a fresh tube.
4. For immunoprecipitating APP C-terminal fragments, mix 100  $\mu$ L of IP buffer and 6.25  $\mu$ L of 20% SDS with 150  $\mu$ L of detergent lysate. Heat to 100°C for 3 min.
5. Preclear the mixture by adding 40  $\mu$ L of protein A agarose and incubate with gentle mixing at 4°C for 30 min.
6. Centrifuge at 2500g for 4 min. Transfer the supernatant to a fresh tube and add 3  $\mu$ L of APP C-terminal antibody Ab369 (21) (see Note 3). Incubate overnight at 4°C with gentle mixing.
7. For A $\beta$  immunoprecipitations, add 3  $\mu$ L of mA $\beta$  4G8 (27) to 1 mL conditioned medium (see Note 3). Incubate overnight at 4°C with gentle mixing.
8. Add 40  $\mu$ L of protein A Agarose (Pierce) (see Note 4) to the immunoprecipitation mixture and continue incubation for 30 min.
9. Centrifuge the mixture at 2500g for 4 min to collect immunoprecipitates. Discard the supernatant. Wash the pellet twice with IP buffer (see Note 5).
10. Resuspend the pellet in 30  $\mu$ L of Laemmli buffer and analyze on 16% Tris-tricine gels (30) (see Note 6).

### 3.4. Streptolysin-O Permeabilization

1. Culture Chinese hamster ovary (CHO) 695 cells on glass chamber slides (or glass coverslips placed in a 60-mm dish) and transfect with *PS1* cDNA.
2. Remove the culture medium 36 h after transfection and wash the cells in cold PBS. Place slides on ice.
3. Wash once with ice-cold SLO buffer.
4. Incubate cells with 100 U SLO in 1 mL cold SLO buffer for 10 min on ice.
5. Aspirate the buffer containing SLO. Wash cells once with SLO buffer and replace with fresh SLO buffer.
6. Warm the cells to 37°C for 5 min.
7. Aspirate the buffer and wash once with cold SLO buffer.
8. Fix the cells in 4% paraformaldehyde at room temperature for 5 min and wash with PBS (see Note 7).
9. Incubate the cells in blocking buffer for 15 min at room temperature and proceed with immunofluorescence staining (see Subheading 3.6.).

### 3.5. Triton Permeabilization

1. Culture CHO 695 cells on glass chamber slides (or glass coverslips placed in a 60-mm dish) and transfect with *PS1* cDNA.

2. Remove the culture medium 36 h after transfection. Wash the cells twice with cold PBS.
3. Fix the cells in 4% paraformaldehyde at room temperature for 5 min and wash with PBS.
4. Incubate the cells in 0.5% Triton X-100 diluted in PBS for 5 min at room temperature.
5. Incubate the slides in blocking buffer for 15 min at room temperature and proceed with immunofluorescence staining (*see Subheading 3.6.*).

### 3.6. Immunofluorescence Staining

1. Incubate the blocked slides (*see Subheadings 3.4.* and *3.5.*) for 2 h at room temperature or overnight at 4°C with optimal dilution of primary antibodies. A monoclonal antibody and a polyclonal antiserum can be used simultaneously to detect independent epitopes of the same protein or epitopes on two different proteins (*see Subheading 2.*). The primary antibodies are usually used at 1:250 or 1:500 (diluted in antibody dilution buffer).
2. The following day, wash the slides several times in PBS and then incubate with both Texas Red conjugated antirabbit IgG (1:500) and FITC-conjugated antimouse IgG (1:100) (diluted in PBS) for 1 h at room temperature.
3. Wash the slides several times in PBS. Incubate the slides in 1:2000 dilution of DAPI (5 mg/mL stock) for 5 min (*see Note 8*). Remove DAPI and wash slides for 5 min in PBS.
4. Apply coverslips to the slides using an aqueous mounting medium such as PermaFluor (Immunon). Wait at least 30 min for the coverslip to set.
5. Examine the slides with a fluorescent microscope using appropriate barrier filters.

## 4. Notes

1. Transfected cells were fixed and incubated with APP C-terminal antibody 369 and visualized by indirect immunofluorescence (*see Subheading 3.*) to document the localization of the APP chimeric polypeptides in the Golgi, a compartment where  $\beta$ -secretase cleavage of APP<sup>swe</sup> polypeptides has been previously demonstrated (*14–16*).
2. Cationic lipid-based methods can be used instead of CaPO<sub>4</sub> precipitation methods for transfecting CHO and COS cells.
3. Antibodies Ab369, and 4G8 can be replaced with any monoclonal or polyclonal antibodies raised against epitopes contained within the C-terminus of APP and A $\beta$ , respectively.
4. The mA $\beta$  4G8 binds well to protein A agarose (Pierce). Because mouse IgG1 binds poorly to protein A, many researchers substitute protein G agarose in place of protein A agarose while using mouse monoclonal antibodies for immunoprecipitation.
5. When mA $\beta$  4G8 is used, wash the immunoprecipitates with 50 mM Tris-HCl, pH 7.4, 150 mM NaCl, 0.01% Nonidet P-40, 5 mM EDTA, pepstatin (50  $\mu$ g/mL), leupeptin

(50  $\mu\text{g}/\text{mL}$ ), aprotinin (10  $\mu\text{g}/\text{mL}$ ), and PMSF (0.25  $\text{mM}$ ). Presence of higher concentration of detergents in the wash buffer affects A $\beta$  binding to 4G8 antibody.

6. Commercially available 10–20% Tris-tricine gels (e.g., Novex) can be used in place of 16% Tris-tricine gels. However we find that the larger format 16% Tris-tricine gels produce the best resolution.
7. We and others (31) observed that certain cell types detach from slides during SLO permeabilization. In such cases, plasma membranes may also be selectively permeabilized by incubating cells fixed in 2% formaldehyde-PBS with digitonin (5  $\mu\text{g}/\text{mL}$  in PIPES buffer: 300  $\text{mM}$  Sucrose, 100  $\text{mM}$  KCl, 2.5  $\text{mM}$   $\text{MgCl}_2$ , 1  $\text{mM}$  EDTA, 10  $\text{mM}$  PIPES, pH 6.8) for 15 min at 4°C. This method has been used to demonstrate the cytoplasmic orientation of *PSI* N-terminal and hydrophilic “loop” domains (32).
8. A brief incubation with the nucleophilic dye DAPI will allow visualization of the nuclei of all the cells during immunofluorescence microscopy. DAPI produces a blue fluorescence with excitation at about 360 nm and emission at about 460 nm when bound to DNA. There is no emission overlap with fluorescein or Texas Red.

## Acknowledgments

The authors thank Drs. Sangram S. Sisodia, Donald L. Price, and David R. Borchelt for their discussions, encouragement, and assistance. This work was supported by the United States Public Health Service, National Institutes of Health Grant 1P01 AG14248 and by grants from Medical Scientist Training Program (A.D.) and the Adler Foundation (G.T.)

## References

1. Sherrington, R., Rogaev, E. I., Liang, Y., Rogaeva, E. A., Levesque, G., Ikeda, M., et al. (1995) Cloning of a gene bearing missense mutations in early-onset familial Alzheimer's disease. *Nature* **375**, 754–760.
2. Levy-Lahad, E., Wasco, W., Poorkaj, P., Romano, D. M., Oshima, J., Pettingell, W. H., et al. (1995) Candidate gene for the chromosome 1 familial Alzheimer's disease locus. *Science* **269**, 973–977.
3. Rogaev, E. I., Sherrington, R., Rogaeva, E. A., Levesque, G., Ikeda, M., Liang, Y., et al. (1995) Familial Alzheimer's disease in kindreds with missense mutations in a gene on chromosome 1 related to the Alzheimer's disease type 3 gene. *Nature* **376**, 775–778.
4. Cook, D. G., Sung, J. C., Golde, T. E., Felsenstein, K. M., Wojczyk, B. S., Tanzi, R. E., et al. (1996) Expression and analysis of presenilin 1 in a human neuronal system: localization in cell bodies and dendrites. *Proc. Natl. Acad. Sci. USA* **93**, 9223–9228.
5. Kovacs, D. M., Fausett, H. J., Page, K. J., Kim, T. W., Moir, R. D., Merriam, D. E., et al. (1996) Alzheimer-associated presenilins 1 and 2: neuronal expression in brain and localization to intracellular membranes in mammalian cells. *Nat. Med.* **2**, 224–229.
6. Walter, J., Capell, A., Grunberg, J., Pesold, B., Schindzielorz, A., Prior, R., et al. (1996) The Alzheimer's disease-associated presenilins are differentially phosphorylated proteins located predominantly within the endoplasmic reticulum. *Mol. Med.* **2**, 673–691.

7. De Strooper, B., Beullens, M., Contreras, B., Levesque, L., Craessaerts, K., Cordell, B., et al. (1997) Phosphorylation, subcellular localization, and membrane orientation of the Alzheimer's disease-associated presenilins. *J. Biol. Chem.* **272**, 3590–3598.
8. Slunt, H. H., Thinakaran, G., Lee, M. K., and Sisodia, S. S. (1995) Nucleotide sequence of the chromosome 14-encoded *S182* cDNA and revised secondary structure prediction. *Amyloid: Int. J. Exp. Clin. Invest.* **2**, 188–190.
9. Doan, A., Thinakaran, G., Borchelt, D. R., Slunt, H. H., Ratovitsky, T., Podlisny, M., et al. (1996) Protein topology of presenilin 1. *Neuron* **17**, 1023–1030.
10. Li, X. and Greenwald, I. (1996) Membrane topology of the *C. elegans* SEL-12 presenilin. *Neuron* **17**, 1015–1021.
11. Dewji, N. N. and Singer, S. J. (1997) The seven-transmembrane spanning topography of the Alzheimer disease-related presenilin proteins in the plasma membranes of cultured cells. *Proc. Natl. Acad. Sci. USA* **94**, 14,025–14,030.
12. Lehmann, S., Chiesa, R., and Harris, D. A. (1997) Evidence for a six-transmembrane domain structure of presenilin 1. *J. Biol. Chem.* **272**, 12,047–12,051.
13. Li, X. and Greenwald, I. (1998) Additional evidence for an eight-transmembrane-domain topology for caenorhabditis elegans and human presenilins. *Proc. Natl. Acad. Sci. USA* **95**, 7109–7114.
14. Haass, C., Lemere, C. A., Capell, A., Citron, M., Seubert, P., Schenk, D., et al. (1995) The Swedish mutation causes early-onset Alzheimer's disease by  $\beta\alpha$ -secretase cleavage within the secretory pathway. *Nat. Med.* **1**, 1291–1296.
15. Thinakaran, G., Teplow, D. B., Siman, R., Greenberg, B., and Sisodia, S. S. (1996) Metabolism of the "Swedish" amyloid precursor protein variant in neuro2a (N2a) cells. Evidence that cleavage at the "beta-secretase" site occurs in the golgi apparatus. *J. Biol. Chem.* **271**, 9390–9397.
16. Perez, R. G., Squazzo, S. L., and Koo, E. H. (1996) Enhanced release of amyloid beta-protein from codon 670/671 "Swedish" mutant beta-amyloid precursor protein occurs in both secretory and endocytic pathways. *J. Biol. Chem.* **271**, 9100–9107.
17. Bhakdi, S., Weller, U., Walev, I., Martin, E., Jonas, D., and Palmer, M. (1993) A guide to the use of pore-forming toxins for controlled permeabilization of cell membranes. *Med. Microbiol. Immunol. (Berl.)* **182**, 167–175.
18. Sisodia, S. S., Koo, E. H., Hoffman, P. N., Perry, G., and Price, D. L. (1993) Identification and transport of full-length amyloid precursor proteins in rat peripheral nervous system. *J. Neurosci.* **13**, 3136–3142.
19. Thinakaran, G., Borchelt, D. R., Lee, M. K., Slunt, H. H., Spitzer, L., Kim, G., et al. (1996) Endoproteolysis of presenilin 1 and accumulation of processed derivatives in vivo. *Neuron* **17**, 181–190.
20. Van Nostrand, W. E., Wagner, S. L., Suzuki, M., Choi, B. H., Farrow, J. S., Geddes, J. W., et al. (1989) Protease nexin-II, a potent antichymotrypsin, shows identity to amyloid beta-protein precursor. *Nature* **341**, 546–549.
21. Buxbaum, J. D., Gandy, S. E., Cicchetti, P., Ehrlich, M. E., Czernik, A. J., Fracasso, R. P., et al. (1990) Processing of Alzheimer beta/A4 amyloid precursor

- protein: modulation by agents that regulate protein phosphorylation. *Proc. Natl. Acad. Sci. USA* **87**, 6003–6006.
22. Huovila, A. P., Eder, A. M., and Fuller, S. D. (1992) Hepatitis B surface antigen assembles in a post-ER, pre-Golgi compartment. *J. Cell Biol.* **118**, 1305–1320.
  23. Brewer, C. B. (1994) Cytomegalovirus plasmid vectors for permanent lines of polarized epithelial cells. *Methods Cell. Biol.* **43 Pt A**, 233–245.
  24. Lo, A. C., Haass, C., Wagner, S. L., Teplow, D. B., and Sisodia, S. S. (1994) Metabolism of the “Swedish” amyloid precursor protein variant in Madin-Darby canine kidney cells. *J. Biol. Chem.* **269**, 30,966–30,973.
  25. Chen, C. and Okayama, H. (1987) High-efficiency transformation of mammalian cells by plasmid DNA. *Mol. Cell. Biol.* **7**, 2745–2752.
  26. Sisodia, S. S., Koo, E. H., Beyreuther, K., Unterbeck, A., and Price, D. L. (1990) Evidence that beta-amyloid protein in Alzheimer’s disease is not derived by normal processing. *Science* **248**, 492–495.
  27. Kim, K. S., Wen, G. Y., Bancher, C., Chen, C. M. J., Sapienza, V. J., Hong, H., and Wisniewski, H. M. (1990) Detection and quantitation of amyloid  $\beta$ -peptide with two monoclonal antibodies. *Neurosci. Res. Commun.* **7**, 113–122.
  28. Ahnert-Hilger, G., Bader, M. F., Bhakdi, S., and Gratzl, M. (1989) Introduction of macromolecules into bovine adrenal medullary chromaffin cells and rat pheochromocytoma cells (PC12) by permeabilization with streptolysin O: inhibitory effect of tetanus toxin on catecholamine secretion. *J. Neurochem.* **52**, 1751–1758.
  29. Seeger, M., Nordstedt, C., Petanceska, S., Kovacs, D. M., Gouras, G. K., Hahne, S., et al. (1997) Evidence for phosphorylation and oligomeric assembly of presenilin 1. *Proc. Natl. Acad. Sci. USA* **94**, 5090–5094.
  30. Schagger, H. and von Jagow, G. (1987) Tricine-sodium dodecyl sulfate-polyacrylamide gel electrophoresis for the separation of proteins in the range from 1 to 100 kDa. *Anal. Biochem.* **166**, 368–379.
  31. Otto, J. C., and Smith, W. L. (1994) The orientation of prostaglandin endoperoxide synthases-1 and -2 in the endoplasmic reticulum. *J. Biol. Chem.* **31**, 19,868–19,875.
  32. De Strooper, B., Beullens, M., Contreras, B., Levesque, L., Craessaerts, K., Cordell, B., et al. (1997) Phosphorylation, subcellular localization, and membrane orientation of the Alzheimer’s disease-associated presenilins. *J. Biol. Chem.* **272**, 3590–3598.

## Normal Proteolytic Processing of the Presenilins

Henrike Hartmann and Bruce A. Yankner

### 1. Introduction

The majority of familial Alzheimer's disease (AD) cases are linked to mutations of the presenilin 1 and 2 (*PS1*, *PS2*) genes on chromosomes 14 and 1, respectively (1–3). *PS1* and *PS2* are about 67% identical in amino acid sequence. Based on hydrophobicity analysis, the presenilins are predicted to have multiple transmembrane domains. Structural analysis (see Chapter 19) suggest that presenilins are 6–8 transmembrane proteins which are located in the endoplasmic reticulum (ER) and Golgi. The N- and C-termini and the large hydrophilic loop region are oriented to the cytoplasm (4,5). More than 40 AD-causing mutations have been identified in *PS1*, whereas only two mutations have been identified in *PS2*. The disease-causing mutations span most domains of the protein, with clusters of mutations in the second transmembrane domain and the large hydrophilic loop region (Fig. 1).

The physiological function of the presenilins is unknown, and it is also unclear how presenilin mutations cause AD. To gain a better understanding of the cellular function of presenilins, their localization, expression, and metabolism have been studied extensively. Typically, various antibodies directed against nonoverlapping epitopes of *PS1* or *PS2* are used to detect the full-length proteins and PS-related fragments in different systems.

#### 1.1. Proteolytic Processing of the Presenilins

Initially, many studies were performed by studying presenilin expression and metabolism in cell lines (COS, HEK 293 [human embryo kidney], CHO [Chinese hamster ovary], H4 human neuroglioma), which were transfected with cDNAs encoding full-length *PS1* or *PS2*. Immunoprecipitation or Western blot analysis of cell lines overexpressing *PS1* show a major species migrating at

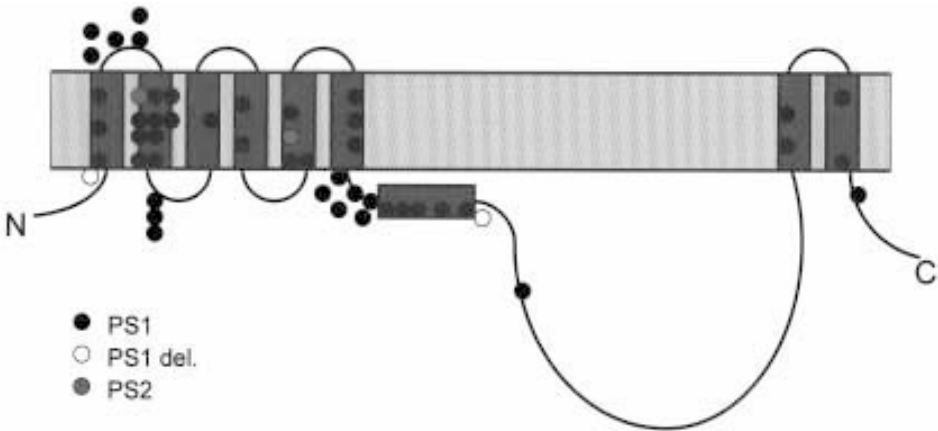


Fig. 1. Model of *PS1* as an eight-transmembrane protein localized in the ER. The circles indicate the location of the AD-causing *PS1* and *PS2* mutations. The open symbols indicate the location of the base deletions resulting in truncated forms of the protein.

45–50 kDa, corresponding to the predicted molecular weight of full-length *PS1*. This species is recognized by antibodies against the N-terminus and the large cytoplasmic loop region, and is increased by transfection. Preabsorption of the antibodies with their cognate peptides abolishes immunoreactivity, suggesting specificity for *PS1* (**Fig. 2**). In transfected cells, higher molecular weight aggregates and lower molecular weight fragments are usually also detected.

In untransfected cells, the 45–50 kDa species is expressed at extremely low levels or is barely detectable. In many cell lines, as well as in primary cultures of human fibroblasts and neurons, a major species at 25–30 kDa is detected with the N-terminal antibody, and a major species at about 20 kDa is detected with a C-terminal loop antibody. The immunoreactivity of both bands is inhibited after preabsorption of the antibodies, suggesting specificity for *PS1* (**Fig. 2**). This pattern of *PS1* fragments is also observed in mouse, rat, or human tissues. The N- and C-terminal fragments are the major endogenous species in cell lines and tissues, suggesting that full-length *PS1* undergoes endoproteolytic cleavage (6–9). This mechanism is further supported by quantitative data showing a 1:1 stoichiometry between the N- and C-terminal fragments in transgenic animals (7).

Although transfection markedly increases the level of full-length *PS1*, it only slightly increases the levels of the major N- and C-terminal fragments (**Fig. 2**). A similar mechanism was observed in transgenic mice that overexpress human *PS1*. In the brains of these animals, the N- and C-terminal *PS1* species accu-

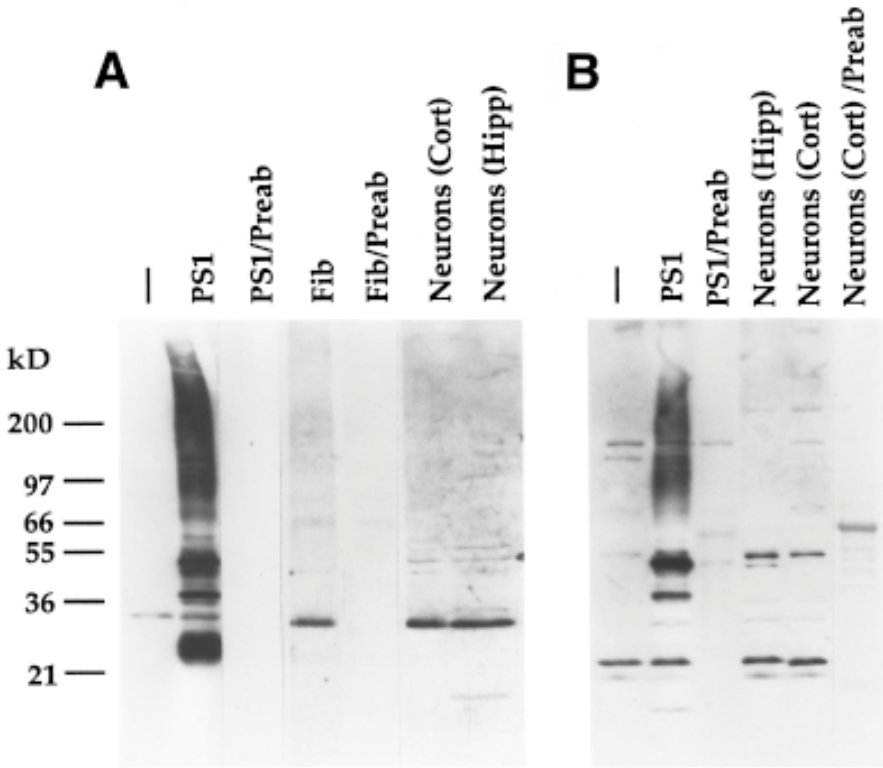


Fig. 2. Expression of *PS1* in transfected and primary cell cultures. (A) Western blot analysis of cell lysates with an antibody (6,15) directed against the N-terminus of *PS1*. (B) Western blot analysis with an antibody against the C-terminal loop region of *PS1*. Lanes: —, wild-type COS cells; *PS1*, *PS1*-transfected COS cells; *PS1*/Preab, *PS1*-transfected COS cells blotted with preabsorbed antibody; Fib, primary human fibroblasts, Fib/preab, fibroblasts blotted with the preabsorbed antibody; Neuron (Cort), cultured human cortical neurons; Neuron (Cort)/Preab, cultured human cortical neurons blotted with the preabsorbed antibody; Neuron (Hipp), cultured rat hippocampal neurons. Note the predominant 28–30 kDa N-terminal and 20–22 kDa C-terminal *PS1* fragments in nontransfected cells and primary neurons. Taken from (6).

mutate at saturable levels independent of the level of the transgene-derived mRNA (7). In transfected cell lines and transgenic animals, expression of human *PS1* is accompanied by a compensatory decrease of the endogenous mouse *PS1* (10). These findings indicate that the cellular levels of presenilin derivatives are tightly regulated. It has been suggested that the constant levels of these *PS1* and *PS2* species may be due to competition for as yet unidentified limiting cellular factors (10). Studies with various PS fragments indicate that

the levels of PS fragments can be regulated by mechanisms independent of the cleavage of full-length PS (**10,11**). Differential regulation of the full-length and cleaved forms is suggested by experiments with proteasome inhibitors, which affect the degradation of full-length *PS1* without significantly altering the levels of the fragments (**12**). The proteases involved in the constitutive cleavage of *PS1* and *PS2* have not been identified. A variety of protease inhibitors have been examined, but none have been shown to inhibit the constitutive cleavage of *PS1* and *PS2* (**9,12**).

### **1.2. Identification of the Constitutive Cleavage Site**

N-terminal sequencing of the *PS1* and *PS2* C-terminal fragments have been performed to identify the constitutive cleavage site. Podlisny et al. (**13**) demonstrated cleavage of *PS1* in transfected HEK 293 cells at amino acid 299, between methionine and alanine. Two additional minor cleavage products were identified at amino acid 292 and 293. The major cleavage site of *PS2* in transfected SHSY-5Y human neuroblastoma cells occurs at position 306/307, between lysine and leucine (**14**). Taking into account the different amino acid numbering of the two proteins the cleavage of *PS2* occurs two amino acids more C-terminal than the cleavage of *PS1*.

### **1.3. Brain- and Neuron-Specific Cleavage of *PS1***

In view of the brain-specific pathology of AD patients with PS mutations, the processing of presenilins in brain tissue and in neuronal cells is of considerable interest. In addition, the effects of AD-causing presenilin mutations on proteolytic processing is an important issue. In brain homogenates from rats at different developmental stages, similar levels of the constitutive N- and C-terminal *PS1* cleavage products are found. However, in the adult rat brain, additional longer N-terminal and shorter C-terminal *PS1* fragments are identified (**Fig. 3**). The molecular weights of these fragments add up to approximately that of full-length *PS1*, suggesting that *PS1* is cleaved at an alternative position C-terminal to the constitutive cleavage site. This alternative cleavage of *PS1* is induced by neuronal differentiation, as indicated by the generation of the alternative *PS1* fragments during the course of neuronal differentiation in primary rat hippocampal cultures. The alternative cleavage of *PS1* can also be induced in differentiated rat *PC12* cells by treatment with nerve growth factor. Consistent with the specific generation of these fragments in neurons, the alternative *PS1* fragments are barely detectable in peripheral tissues of adult animals. Furthermore, the alternative fragments are expressed at very low levels in the fetal rat brain (**15**). A similar proteolytic processing pathway for *PS2* has been demonstrated in primary hippocampal cultures. (**16**).

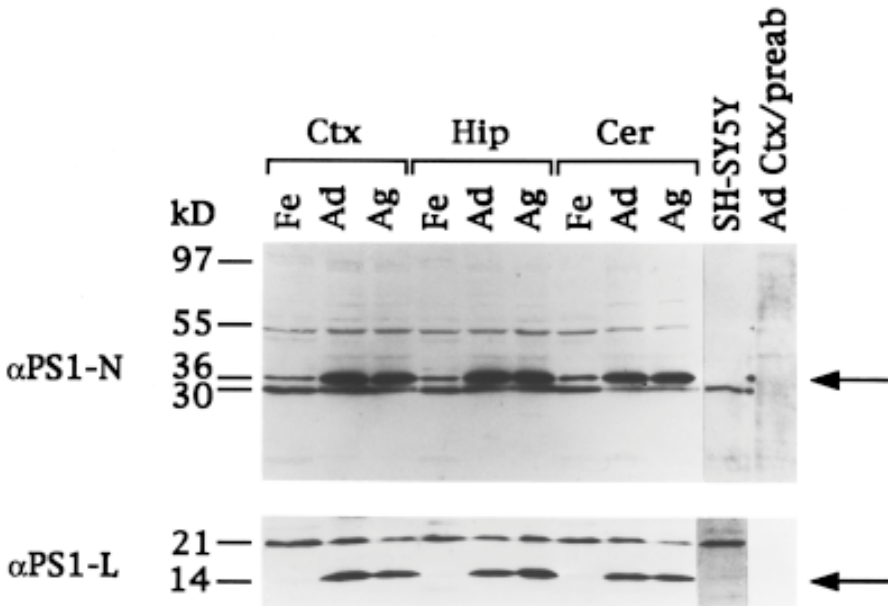


Fig. 3. Developmental regulation of *PSI* cleavage in the rat brain. Western blot analysis of rat brain homogenate with an antibody (6,15) against the N-terminal ( $\alpha$ PS1-N, top) and against the large hydrophilic loop region ( $\alpha$ PS1-L, bottom) of *PSI*. Note induction of 36 kDa N-terminal and 14 kDa C-terminal *PSI* fragments in the adult and aged rat brain (arrows). Lanes: Ctx, cortex; Hip, hippocampus; Cer, cerebellum of fetal (Fe), adult (Ad), and aged (Ag) rat brain; SH-SY5Y, undifferentiated SH-SY5Y neuroblastoma cell line; Ad Ctx/preab, adult cortex blotted with preabsorbed antibody. Taken from (15).

The neuron-specific alternative cleavage of *PSI* is species specific. In the rat, the alternative cleavage of *PSI* results in distinct N- and C-terminal bands. In the human brain, however, heterogeneous N-terminal *PSI* derivatives migrating between 30 and 40 kDa are generated (Fig. 4). Similar to the rat, these human-specific heterogeneous species are not detectable in peripheral human tissues, and are present at much lower levels in the fetal human brain. The human-specific heterogeneous *PSI* fragments can be generated in vitro by differentiation of human SHSY-5Y neuroblastoma cells with retinoic acid and tannic acid (TPA). It is also noteworthy that the levels of full-length *PSI* increase during neuronal differentiation and that high levels of full-length *PSI* appear specifically in the adult brain. Taken together, these findings suggest that presenilin levels and processing are uniquely regulated in mature neurons. The neuron-specific proteolytic cleavage of *PSI* is most likely not mediated by

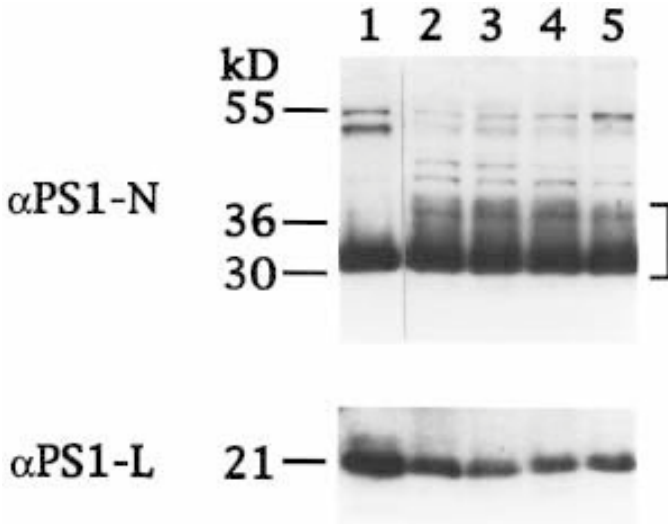


Fig. 4. Developmental regulation of *PS1* in the human brain. Western blot analysis of tissue homogenates of fetal and adult human cortex with  $\alpha$ *PS1*-N (top) and  $\alpha$ *PS1*-L (bottom). Note the ladder of alternative N-terminal *PS1* fragments in the adult human cortex (bracket). Lanes: 1, human fetal cortex, 15–17 wk of gestation; 2, adult human cortical biopsy material, 18 yr; 3, adult human cortex, 44 yr, postmortem interval (PMI) 12 h; 4, adult human cortex, 32 yr, PMI 8 h; 5, adult human cortex, 77 yr, PMI 1.5 h. Note similar levels of alternative N-terminal fragments in the biopsy sample and the autopsy samples with different PMIs, indicating that the generation of these *PS1* fragments occurs in vivo. Taken from (15).

caspases (see Chapter 21), as different caspase inhibitors do not inhibit the formation of the alternative fragments in primary rat hippocampal cultures (17).

#### 1.4. Effects of Presenilin Mutations on Proteolytic Cleavage

Constitutive cleavage of *PS1* is prevented by a splice acceptor site mutation which results in deletion of exon 9 (amino acids 290–319), which spans the major *PS1* cleavage site (7). The other disease-related *PS1* mutations have inconsistent effects on the proteolytic processing of *PS1*. Transfection with either wild-type *PS1* cDNA or cDNA constructs containing *PS1* missense mutations show no clear difference in the *PS1* cleavage pattern. In transfected PC12 cells, some *PS1* mutations were reported to inhibit *PS1* cleavage (8,18). In another study, the N141I mutation in *PS2* was found to increase the level of a 14-kDa C-terminal fragment that is generated by caspase cleavage of *PS2* (19). In transgenic animals, the A246E and M146L *PS1* mutations were found to increase the accumulation of N- and C-terminal *PS1* fragments when

normalized to the level of *PS1* transgene mRNA (20). However, in primary fibroblast cultures, where the processing of endogenous *PS1* can be assessed, levels of *PS1* N- and C-terminal fragments were similar in cells from patients with PS mutations and controls (21,22). In the human brain, no clear alteration of *PS1* cleavage related to a *PS1* mutation could be detected. However, in the frontal cortex of two cases with the G209V mutation, increased levels of a 49-kDa full-length form of the *PS1* protein was demonstrated, which was absent in controls and in cases of sporadic AD (23). Taken together, the studies to date do not provide a clear correlation between inheritance of AD and effects of *PS1* mutations on PS proteolytic processing.

### 1.5. Functional Relevance of PS Proteolytic Processing

The functional relevance of PS proteolytic cleavage to PS function is unknown. Furthermore, a central unresolved issue is which of the PS species, full-length N- or C-terminal fragments, are important for the physiological function of PS and are involved in the pathogenic mechanism. It has been shown that human *PS1* can functionally substitute for a mutated *Caenorhabditis elegans* homologue *sel12*. *PS1* with the exon 9 deletion was as effective as wild-type *PS1* in this complementation assay, indicating that proteolytic processing may not be required for *PS1* function. In contrast, the other *PS1* mutations showed loss of function in the *C. elegans* complementation assay (24,25). It has recently been shown that the N- and C-terminal *PS1* fragments are present in a heterodimeric complex, which may be required for biological function (26). In this study, the full-length *PS1* with the exon 9 deletion was able to participate in this complex in a manner similar to the *PS1* fragments, a finding that could explain why this mutant form of *PS1* is functionally active without being processed.

*PS1* and *PS2* have been shown to affect apoptosis (27,28) and APP processing to the amyloid  $\beta$  peptide (for review, see ref. 29). However, the dependence of these effects on particular presenilin species and the relationship to presenilin processing remains to be determined. Future studies should help to clarify the role of presenilin proteolytic processing in the pathogenesis of familial AD. Many experimental approaches have been used to study presenilin proteolytic processing. In **Subheading 2.**, two standard protocols are presented to examine the processing of endogenous and overexpressed *PS1*.

## 2. Materials

### 2.1. Transfection of COS-7 Cells with *PS1* cDNA

1. cDNA (here *PS1* was cloned into the pcDNA3 vector from Invitrogen).
2. Lipofectamine (Life Technologies, Gaithersburg, MD).
3. OptiMEM (Life Technologies).

4. Cell culture medium (10% fetal calf serum, glutamine, pyruvate, PenStrep [Gibco-BRL, Gaithersburg, MD] in Dulbecco's modified Eagle's medium).

## **2.2. Extraction of Proteins**

Extraction buffer: 4% SDS, 20% glycerol, in 0.1 M Tris-HCl, pH 6.8, supplemented with protease inhibitors (Complete<sup>®</sup>, Roche Biochemicals, Mannheim, Germany).

## **2.3. Sodium Dodecyl Sulfate-Polyacrylamide Gel Electrophoresis (SDS-PAGE) and Western Blotting**

1. 4–20% Tris-glycine gel.
2.  $\beta$ -Mercaptoethanol (final concentration 5%).
3. Molecular weight markers (10–250 kDa range).
4. Polyvinylidene fluoride (PVDF) membrane (e.g., Immobilon P<sup>R</sup>, Millipore, Bedford, MA).

## **2.4. Development of the Western Blot**

1. Phosphate-buffered saline/triton (PBST): 0.1% Tween-20 in PBS.
2. Blocking buffer: 5% nonfat dry milk, 3% bovine serum albumin (BSA) in PBST.
3. Primary antibodies against *PSI* (6,15).

## **3. Methods**

### **3.1. Transfection of COS-7 Cells with PS1 cDNA**

1. One day prior to transfection, plate COS cells in 60 mm dishes at a density of  $3.5 \times 10^5$  cells per plate.
2. For transfection, add 3  $\mu$ g cDNA to 500  $\mu$ L of OptiMEM (Life Technologies). In another tube, dilute 10  $\mu$ L lipofectamine in 500  $\mu$ L OptiMEM. Combine solutions, mix gently and incubate at room temperature for 30 min.
3. During this incubation, wash the cells with OptiMEM to remove serum-containing medium.
4. After the incubation, add 1 mL OptiMEM to the DNA-lipid mixture, yielding a final volume of 2 mL. Add this mixture directly to the cells.
5. Incubate the cells at 37°C in a 5% CO<sub>2</sub> incubator for 5 h.
6. Remove the transfection mixture by aspiration and replace with 4 mL of normal COS cell medium.
7. After transfecting for 36–48 h, harvest the cells for biochemical analysis (see **Note 1**).

### **3.2. Extraction of Proteins**

#### **3.2.1. Extraction of Proteins from Cells in Culture**

1. To harvest transfected cells, place the plates on ice, and remove the medium by aspiration.

2. Wash the cells once with cold PBS and lyse by adding 300  $\mu$ L extraction buffer. Tilt the plates gently and keep on ice for 10 min.
3. Use a cell scraper to collect the lysate, which is very viscous from the DNA released due to the high SDS concentration of the buffer. To reduce viscosity, shear the lysates about 10 times using a 22-gauge needle with a 1-mL syringe.
4. Clear the lysates by centrifugation at 4°C in a microfuge at 14,000g.
5. Discard the pellet and use the supernatant for further analysis (*see Note 2*).

### 3.2.2. Extraction of Proteins from Tissue

1. Extract tissues in extraction buffer (*see Subheading 2.2.*). Use a wet weight/volume ratio of 1:10.
2. If necessary, mince the tissue with a razor blade or scalpel.
3. Homogenize the tissue with a glass Dounce homogenizer.
4. Shear the samples as described in **Subheading 3.2.1.**
5. Clear the samples by centrifugation (**Subheading 3.2.1.**), and use the supernatant for protein determination. For the protein assay use a detergent-compatible protein kit, based on Lowry's method.

### 3.3. SDS-PAGE and Western Blotting

1. To prepare the samples for the SDS-PAGE under reducing conditions, add 5%  $\beta$ -mercaptoethanol and 0.05% bromophenol blue to the samples that already contain SDS (*see Notes 3 and 4*).
2. Load 20  $\mu$ g of protein per well in 12% or 4–20% acrylamide gradient Tris-glycine minigels and resolve by electrophoresis.
3. Electrotransfer the proteins to PVDF membranes using a tank or a semidry transfer system.
4. Visualize the protein transfer by staining with Ponceau S (Sigma Chemical Co., St. Louis, MO), which facilitates the marking of the molecular weight standards.

### 3.4. Development of the Western Blot

1. Incubate the membranes in blocking buffer for 1 h at room temperature or overnight at 4°C.
2. Dilute the primary antibody in blocking buffer or in 5% BSA in PBS. The appropriate dilution of the antibody needs to be titrated in each case.
3. Incubate the membranes with the primary antibody at room temperature on a rocker for 1 h.
4. Wash the membranes with three washes of PBST (each wash should be 5 min).
5. Incubate the membrane with the peroxidase-conjugated secondary antibody in blocking buffer for 1 h, followed by three washes with PBST (5 min).
6. Detect the bands by the enhanced chemiluminescence method.

## 4. Notes

1. For transfection experiments, it is recommended that an expression vector be used which results in only moderate levels of protein expression. This minimizes

the formation of aggregates (*see* **Note 3**), and the protein levels are more comparable to physiological levels. Most importantly, this will result in a higher yield of viable transfected cells, as high levels of *PS1* overexpression induce apoptosis (28).

2. Repetitive freeze thawing is problematic; samples should therefore always be aliquoted to avoid aggregation and degradation of the protein.
3. Full-length presenilins and the N-terminal fragments are very susceptible to aggregation. This results in high molecular weight aggregates in transfected cells that overexpress presenilins. Aggregation is also induced by heating of the samples. It is therefore recommended that the samples not be boiled prior to gel loading.
4. In immunoprecipitation experiments where boiling is required, adding 4 M urea to the samples prevents aggregation.

## References

1. Sherrington, R., Rogaev, E. I., Liang, Y., Rogaeva, E. A., Levesque, G., Ikeda, M., et al. (1995) Cloning of a gene bearing missense mutations in early-onset familial Alzheimer's disease. *Nature* **375**, 754–760.
2. Levy-Lahad, E., Wasco, W., Poorkaj, P., Romano, D. M., Oshima, J., Pettingell, W. H., et al. (1995) Candidate gene for the chromosome 1 familial Alzheimer's disease locus. *Science* **269**, 973–977.
3. Rogaev, E. I., Sherrington, R., Rogaeva, E. A., Levesque, G., Ikeda, M., Liang, Y., et al. (1995) Familial Alzheimer's disease in kindreds with missense mutations in a gene on chromosome 1 related to the Alzheimer's type 3 gene. *Nature* **376**, 775–778.
4. Doan, A., Thinakaran, G., Borchelt, D. R., Slunt, H. H., Ratovski, T., Podlisny, M., et al. (1996) Protein topology of presenilin 1. *Neuron* **17**, 1023–1030.
5. Li, X. and Greenwald, I. (1996) Membrane topology of the *C. elegans* SEL-12 presenilin. *Neuron* **17**, 1015–1021.
6. Busciglio, J., Hartmann, H., Lorenzo, A., Wong, C., Baumann, K.-H., Sommer, B., et al. (1997) Neuronal localization of presenilin 1 and association with amyloid plaques and neurofibrillary tangles in Alzheimer's disease. *J. Neurosci.* **17**, 5101–5107.
7. Thinakaran, G., Borchelt, D. R., Lee, M. K., Ratovski, T., Davenport, F., Nordstedt, C., et al. (1996) Endoproteolysis of presenilin 1 and accumulation of processed derivatives in vivo. *Neuron* **17**, 181–190.
8. Mercken, M., Takahashi H., Honda, T., Sato K., Murayama, M., Nakazato, Y., et al. (1996) Characterization of human presenilin using N-terminal specific monoclonal antibodies: evidence that Alzheimer mutations affect proteolytic processing. *FEBS Lett.* **389**, 297–303.
9. Kim, T.-W., Pettingell, W. H., Hallmark, O. G., Moir, R. D., Wasco, W., and Tanzi, R. E. (1997) Endoproteolytic cleavage and proteasomal degradation of presenilin 2 in transfected cells. *J. Biol. Chem.* **272**, 11,006–11,010.
10. Thinakaran, G., Harris, C. L., Ratovitski, T., Davenport, F., Slunt, H. H., Price D. L., et al. (1997) Evidence that levels of presenilins (PS1 and PS2) are coordinately

- regulated by competition for limiting cellular factors. *J. Biol. Chem.* **272**, 28,415–28,422.
11. Ratkovsi, T., Slunt, H. H., Thinakaran, G., Price, D. L., Sisodia, S. S., and Borchelt, D. R. (1997) Endoproteolytic processing and stabilization of wild-type and mutant presenilin. *J. Biol. Chem.* **272**, 11,006–11,010.
  12. Hartmann, H., Busciglio, J., and Yankner, B. A. (1998) Neuronal regulation of presenilin-1 processing, in *Presenilins and Alzheimer's Disease* (Younkin, S. G., Tanzi, R. E., and Christen, Y., eds.), Foundation Ipsen, Springer-Verlag, Heidelberg, Germany, pp. 85–91.
  13. Podlisny, M. B., Citron, M., Amarante, P., Sherrington, R. Xia, W., Zhang, J., et al. (1997) *Neurobiol. Dis.* **3**, 325–337.
  14. Shirotani, K., Takahashi, K., Ozawa, K., Kunishita, T., and Tabira, T. (1997) Determination of a cleavage site of presenilin 2 protein in stably transfected SH-SY5Y human neuroblastoma cell lines. *Biochem. Biophys. Res. Commun.* **240**, 728–731.
  15. Hartmann, H., Busciglio, J., Baumann, K.-H., Staufenbiel, M., and Yankner, B. A. (1997) Developmental regulation of presenilin-1 processing in the brain suggests a role in neuronal differentiation. *J. Biol. Chem.* **272**, 14,505–14,508.
  16. Capell, A., Saffrich, R., Olivo, J.-C., Meyn, L., Walter, J., Grünberg, J., et al. (1997) Cellular expression and proteolytic processing of presenilin proteins is developmentally regulated during neuronal differentiation. *J. Neurochem.* **69**, 2432–2440.
  17. Hartmann, H., Busciglio, B., Zhang, Z., Baumann, K.-H., Staufenbiel, M., and Yankner, B. A. (1997) Developmental regulation of presenilin-1 cleavage in the brain. *Soc. Neurosci. Abstr.* **117**, 6.
  18. Murayama, O., Honda, T., Mercken, M., Murayama, M., Yasutake, K., Nihonmatsu, N., et al. (1997) Different effects of Alzheimer-associated mutations of presenilin-1 on its processing. *Neurosci. Lett.* **229**, 61–64.
  19. Kim, T.-W., Pettingell, W. H., Jung, Y.-K., Kovacs, D., and Tanzi, R. E. (1997) Alternative cleavage of Alzheimer-associated presenilins during apoptosis by a caspase-3 family protease. *Science* **277**, 373–376.
  20. Lee, M. K., Borchelt, D. R., Kim, G., Thinakaran, G., Slunt, H. H., Ratovitski, T., et al. (1997) Hyperaccumulation of FAD-linked presenilin-1 variants in vivo. *Nat. Med.* **3**, 756–760.
  21. Hartmann, H., Busciglio, J., Wong, C., Staufenbiel, M., and Yankner, B. A. (1996) Apoptosis and the Alzheimer's disease gene presenilin-1. *Soc. Neurosci. Abstr.* 293.13.
  22. Okochi, M., Ishii, K., Usami, M., Sahara, N., Kametani, F., Tanaka, K., et al. (1997) Proteolytic processing of presenilin-1 (PS1) is not associated with Alzheimer's disease with or without PS1-mutations. *FEBS Lett.* **418**, 162–166.
  23. Levey, A. I., Heilman, C. J., Lah, J. J., Nash, N. R., Rees, H. D., Wakai, M., et al. (1997) Presenilin-1 protein expression in familial and sporadic Alzheimer's disease. *Ann. Neurol.* **41**, 7742–753.
  24. Levitan, D., Doyle, T. G., Brousseau, D., Lee, M. K., Thinakaran, G., Slunt, H. H., et al. (1996) Assessment of normal and mutant human presenilin function in *Caenorhabditis elegans*. *Proc. Natl. Acad. Sci. USA* **93**, 14,940–14,944.

25. Baumeister, R., Leimer, U., Zweckbronner, I., Jakubek, C., Grünberg, J., and Haass, C. (1997) Human presenilin-1, but not familial Alzheimer's disease (FAD) mutants, facilitate *Caenorhabditis elegans* notch signalling independently of proteolytic processing. *Genes Funct.* **1**, 149–159.
26. Capell, A., Grünberg, J., Pesold, B., Diehlmann, A., Citron, M., Nixon, R., et al. (1998) The proteolytic fragments of the Alzheimer's disease-associated presenilin-1 form heterodimers and occur as a 100–150 kD molecular mass complex. *J. Biol. Chem.* **273**, 3205–3211.
27. Vito, P., Lacana, E., and D'Adamio, L. (1996) Interfering with apoptosis: Ca<sup>2+</sup>-binding protein ALG-2 and Alzheimer's disease gene ALG-3. *Science* **271**, 521–525.
28. Wolozin, B., Iwasaki, K., Vito, P., Ganjei, J. K., Lacana, E., Sunderland, T., Zhao, B., Kusiak, J. W., Wasco, W., and D'Adamio, L. (1996) Participation of presenilin 2 in apoptosis: enhanced basal activity conferred by an Alzheimer mutation. *Science* **274**, 1710–1712.
29. Hardy, J. (1997) Amyloid, the presenilins and Alzheimer's disease. *Trends Neurosci.* **20**, 154–159.

## Apoptotic Proteolytic Cleavage of the Presenilins by Caspases

Tae-Wan Kim

### 1. Introduction

Familial Alzheimer's disease (FAD) is a genetically heterogeneous disorder that is caused by defects in at least three early onset genes (age of onset: <60 yr.): presenilin 2 (*PS2*) on chromosome 1 (**1**), presenilin 1 (*PS1*) on chromosome 14 (**2**), and amyloid protein precursor (*APP*) on chromosome 21 (**3,4**). Mutations within the *APP* gene are responsible for only a small portion (<2%) of reported cases of FAD (**5**), whereas up to half of all early onset FAD cases are caused by mutations in the *PSEN1* and *PSEN2* genes (**6,7**).

The *PSEN1* and *PSEN2* genes encode polypeptides predicted to be 463 and 448 amino acids in size, respectively (**1,2**). Both PS1 and PS2 proteins exhibit a serpentine topology and are predicted to contain six or eight transmembrane domains (**8,9**). In human neuronal cell lines transfected with presenilin genes, *PS2* appeared as a 53–54 kDa full-length holoprotein and *PS1* as a 48-kDa protein (**10–14**). In brain and native cells, little or no full presenilin species are found. Both *PS1* and *PS2* undergo endoproteolytic processing to yield saturable amounts of an N- and a C-terminal fragment (**10–14**).

Apoptosis is a form of cell death that is central for the control of cell survival during normal development and in many diseases (reviewed in **refs. 15** and **16**). Increasing evidence suggests that caspases, an evolutionarily conserved family of cysteine proteases, play critical roles in the execution of apoptosis (reviewed in **refs. 17–19**). Caspases are synthesized as inactive precursors requiring cleavage at specific Asp residues to yield two subunits that form the active enzymes (**17–19**). During apoptosis, caspases cleave multiple intracellular proteins (“death substrates”). These include poly(ADP-ribose)

polymerase (PARP), lamins, U1-70K, DNA-dependent protein kinase, and sterol regulatory element binding protein (SREBP) (reviewed in **refs. 19** and **20**).

During apoptosis, resulting from presenilin overexpression (**21**) or inhibition of proteasomal degradation (**11**), *PS1* and *PS2* are cleaved at sites distal to their normal cleavage site by apoptosis-related caspases (**21**). Alternative cleavage of the presenilins can be inhibited either by treatment with peptide inhibitors for caspases or by substitution of the Asp residue(s) at the consensus caspase cleavage sites in the substrates (**21**) (Asp329 in *PS2* and D345 in *PS1*; **22**). These findings indicate that the presenilins serve as substrates for the activated caspases and raise the possibility that the apoptosis-associated alternative presenilin fragments may harbor proapoptotic potential. Enhanced accumulation of alternative presenilin fragments was observed in the cells expressing FAD mutant forms of *PS2* and *PS1*, suggesting that the caspase-mediated cleavage event in presenilins may contribute to the pathogenesis of AD.

## 2. Materials

### 2.1. Tissue Culture

1. Dulbecco's modified Eagle medium (DMEM), liquid (high glucose).
2. Fetal bovine serum (FBS), heat inactivated.
3. Penicillin-streptomycin-glutamine mix (100 $\times$ ).
4. Tetracycline (15 mg/mL stock in ethanol); dilute to 1 mg/mL with 70% ethanol.
5. G418 (50 mg/mL) (Calbiochem, La Jolla, CA).
6. Hygromycin (50 mg/mL) (Boehringer Mannheim, Mannheim, Germany).

### 2.2. Western Blot Analysis

1. Sodium dodecyl sulfate-polyacrylamide gel electrophoresis (SDS-PAGE) apparatus.
2. Semidry electroblotting apparatus.
3. Polyvinylidene fluoride (PVDF) membrane.
4. Blotting paper.
5. Staining trays.
6. Antibodies to FLAG (DYKDDDDK) epitope and *PS2*: Antibodies against FLAG epitope tag (D8, Santa Cruz Biotech, Santa Cruz, CA; M2, Kodak IBI, Rochester, NY) or antibodies (anti-*PS1* loop and anti-*PS2* loop) raised against the large hydrophilic loop domains following predicted transmembrane domain 6 of *PS1* and *PS2*, respectively (**10**).
7. Lysis buffer (10 mM Tris-HCl, pH7.4, 150 mM NaCl, 1% Triton X-100, 0.25% NP-40, 5 mM EDTA).

### 2.3. Apoptosis

1. Staurosporine (1 mM stock in dimethylsulfoxide [DMSO]).
2. Etoposide (20 mM stock in DMSO).
3. C2-ceramide.

4. Caspase inhibitors, zVAD-fmk and zDEVD-fmk (50 mM stock in DMSO) (Enzyme System Products, Livermore, CA).
5. Antibodies to PARP (PharMingen, San Diego, CA) and caspase-3 (Transduction Laboratories, Lexington, KY).

### 3. Methods

#### 3.1. Caspase-Mediated Alternative Cleavage of Presenilins in the Inducible Cell System

##### 3.1.1. Establishment of Inducible Presenilin Cell System

###### 3.1.1.1. H4 HUMAN NEUROGLIOMA FOUNDER CELLS

We initially established founder cell lines by cotransfecting H4 human neuroglioma cells (50% confluency) in a 100-mm dish with 10  $\mu$ g of pUHD15-1 (23), a plasmid encoding a tetracycline-repressible transactivator and 1  $\mu$ g of pCMVneo (24). Individual G418-resistant colonies were isolated and characterized by transient transfection with pUHC13-3 (23), a luciferase reporter plasmid. Luciferase activity in the presence or absence of tetracycline was measured to identify cells with maximal promoter inducibility. Two cell lines with highest inducibility (clone 32neo, 340-fold; clone 15neo, 200-fold) were used to establish cells with presenilin inducible constructs (*see Note 1*).

###### 3.1.1.2. PRESENILIN CONSTRUCTS

The cDNAs for wild-type and FAD mutant forms (A246E *PS1*, N141I *PS2*, and M239V *PS2*) of presenilins were subcloned into the pUHD10-3 (23), the tetracycline-inducible expression plasmid, by polymerase chain reaction (PCR) using *Pfu* polymerase (Stratagene, La Jolla, CA). Resulting constructs were verified by DNA sequencing.

###### 3.1.1.3. INDUCIBLE PRESENILIN CELL LINES

1. Transfect the H4 founder with 10  $\mu$ g of each construct and 1  $\mu$ g of pCNH2hygro, conferring resistance to hygromycin.
2. Isolate hygromycin-resistant colonies in the presence of tetracycline, and screen for protein expression by Western blotting on withdrawal of tetracycline.
3. For each construct, select three clones demonstrating various induction levels for further study.
4. Maintain cell lines in DMEM (high glucose) supplemented with 10% heat-inactivated FBS, 2 mM L-glutamine, 100 U/mL penicillin, 100  $\mu$ g/mL streptomycin, 200  $\mu$ g/mL G418, 200  $\mu$ g/mL hygromycin, and 2-3  $\mu$ g/mL tetracycline (*see Note 2*).

##### 3.1.2. Inducible Expression of Presenilins and Detection of Alternatively Cleaved Presenilin Fragments by Western Blot Analysis

1. Wash cells five times with prewarmed PBS to remove residual tetracycline and then incubate with complete media without tetracycline for the indicated hours.

2. Lyse cells with lysis buffer containing 0.3% SDS or 1% Sarkosyl (*see Note 3*).
3. Detect full-length holoproteins and normal cleavage products (N- and C-terminal fragments) by both anti-FLAG epitope tag and anti-*PS2*loop or anti-*PS1*loop antibodies. The high molecular weight forms and smaller, alternatively cleaved C-terminal fragments can also be detected in cells either overexpressing presenilins significantly or undergoing apoptosis.

### **3.2. Apoptotic Cleavage of Endogenous Presenilins and Other Death Substrates**

1. Maintain the human H4 human neuroglioma or SK-N-SC neuroblastoma cell lines in DMEM supplemented with 10% heat-inactivated FBS, 100 U/mL penicillin, and 100  $\mu\text{g}/\text{mL}$  streptomycin in a 37°C incubator with 5%  $\text{CO}_2$ .
2. To induce apoptosis, incubate cells either alone or in the presence of apoptosis-inducing reagents: staurosporine (1  $\mu\text{M}$ ), etoposide (20  $\mu\text{M}$ ) or C2-ceramide (25  $\mu\text{M}$ ), respectively for 18 h.
3. Measure cleavage of endogenous *PS1* or *PS2* by Western blot analysis using anti-*PS1*loop and anti-*PS2*loop antibodies (**10**) as described in **Subheading 3.1.2**. In parallel, the cleavage of other known death substrates is also examined (e.g., PARP and lamin A).

### **3.3. Inhibition of Caspase-Mediated Cleavage**

#### **3.3.1 Identification of the Cleavage Sites**

The predicted consensus caspase cleavage sites for *PS2* are localized within the domain encoded by exon 11.

1. Introduce the point mutations in the potential Asp cleavage sites (D326 and D329) of *PS2* and control Asp (D308) into a *PS2* open reading frame by site-directed mutagenesis using Mutagene phagemid kit (Bio-Rad, Hercules, CA).
2. Subclone the resulting constructs into either pUHD10-1 for inducible expression or pcDNA-Zeo(-) (Invitrogen, San Diego, CA) for transient or stable transfections.
3. Transiently transfect the resulting inducible constructs (wild-type, D308A, D326A, and D329A) into tetracycline responsive founder H4 cells (**Subheading 3.1.1**).
4. Grow the cells in the absence of tetracycline for 24 h, further incubate in the presence of either 20  $\mu\text{M}$  etoposide or 1  $\mu\text{M}$  staurosporine, and analyze by Western blotting using anti-*PS2*loop antibody (**21**).

The caspase cleavage site for *PS1* has also been recently identified using a similar approach (**22**). A D345N mutation in *PS1* abolishes the caspase-mediated cleavage of *PS1* (**22**).

#### **3.3.2. Inhibition of Caspase-Mediated Cleavage Using Cell-Permeable Peptide Inhibitors**

Many caspase inhibitors have been designed on the basis of the tetrapeptide sequence comprising either the cleavage sites of caspase themselves or their death substrates. The tetrapeptide YVAD based on the cleavage site of caspase-

**Table 1**  
**Caspase Inhibitors**

Inhibitor	Suggested target caspase	Notes
Ac-WEHD-CHO (Ac-Trp-Glu-His-L-aspartic acid aldehyde)	1	R, potent and selective inhibitor for caspase- I
BD-fmk (Boc-Asp-fluoromethylketone)	—	General inhibitor
zYVAD-fmk (CBZ-Tyr-Val-Ala-Asp-fluoromethylketone)	1,4	IR
Ac-YVAD-cmk (Ac- Tyr-Val-Ala-Asp-chloromethylketone)	1,4	IR
Ac-YVAD-2,6-dimethylbenzoyloxymethylketone	1	IR
zVAD-fmk (CBZ-Val-Ala-Asp-fluoromethylketone)	1, 3, 4, 6, 7, 8, 10	Potent, irreversible general inhibitor
zIETD-fmk (CBZ-Ile-Glu-Thr-Asp-fluoromethylketone)	8,10	IR
zVDVAD-fmk (CBZ-Val-Asp-Val-Ala-Asp-fluoromethylketone)	2	IR
zVEID-fmk (CBZ-Val-Glu-Ile-Asp-fluoromethylketone)	6	IR
zDEVD-fmk (CBZ-Asp-Glu-Val-Asp-fluoromethylketone)	3,6,7,8,10	IR
Ac-ESMD-CHO (Ac-Glu-Ser-Met-L-aspartic acid aldehyde)	3	R, based on the cleavage site of the pro-caspase-3

The mode of inhibition is indicated as either reversible (R) or irreversible (IR).

1 (also known as interleukin 1 $\beta$ -converting enzyme; ICE) is a representative example. A similar approach has been applied to the PARP cleavage site (DEVD) to design a peptide to inhibit the PARP cleaving caspase (caspase-3). This method has been applied to many different caspases; examples are summarized in **Table 1**. In addition, many different chemical derivatives of these peptides are available: aldehyde CHO, chloromethyl ketone (cmk), acyloxymethyl ketone (amc), and fluoromethyl ketone (fmk).

To assess the effect of caspase inhibitors on the generation of the alternative CTF in the presenilin-overexpressing cells, incubate inducible H4 cells in the complete media without tetracycline in the presence or absence of caspase inhibitors zVAD-fmk or zDEVD-fmk (1–200  $\mu$ M) (*see Note 4*). Add inhibitors at the time of induction (removal of tetracycline). To assess the effect of the caspase inhibitors on the apoptotic cleavage of endogenous *PS1* and *PS2*, pretreat native H4 or SK-N-SC cells with indicated concentrations of inhibitors before exposure to the apoptotic stimuli (all peptide inhibitors that were used are listed in **Table 1**). Apoptotic cells were harvested by centrifugation.

#### 4. Notes

1. In addition to the tetracycline-responsive system described in this chapter, additional tetracycline-inducible gene expression systems are now commercially available, including the “Tet-on” system (Sigma, St. Louis, MO), which activates transcription of the gene of interest in the presence of tetracycline or doxycycline.
2. Tetracycline is light sensitive. Tetracycline-containing media bottles should be wrapped with aluminum foil to shield against light-induced inactivation.
3. Because alternative C-terminal fragments derived from *PS1* or *PS2* in transfected cells are insoluble in nonionic detergents such as Triton X-100 and NP-40, the lysis buffer should be supplemented with 0.3% SDS or 1% Sarkosyl.
4. DEVD-based reagents inhibit several other caspases in addition to caspase-3, including caspase-1, caspase-4, and caspase-7 (**18**).

#### References

1. Levy-Lahad, E., Wasco, W., Poorkaj, P., Romano, D. M., Oshima, J. M., Pettingell, W. H., et al. (1995) Candidate gene for the chromosome 1 familial Alzheimer’s disease locus. *Science* **269**, 973–977.
2. Sherrington, R., Rogaev, E. I., Liang, Y., Rogaeva, E. A., Levesque, G., Ikeda, M., et al. (1995) Cloning of a novel gene bearing missense mutations in early onset familial Alzheimer disease. *Nature* **375**, 754–760.
3. Tanzi, R. E., Gusella, J. F., Watkins, P. C., Bruns, G. A. P., St. George-Hyslop, P., van Keuren, M. L., et al. (1987) Amyloid  $\beta$  protein gene: cDNA, mRNA distribution and genetic linkage near the Alzheimer locus. *Science* **235**, 880–884.
4. Goate, A., Chartier-Harlin, M., Mullan, M., Brown, J., Crawford, F., Fidani, L., et al. (1991) Segregation of a missense mutation in the amyloid precursor protein gene with familial Alzheimer’s disease. *Nature* **349**, 704–706.

5. Tanzi, R. E., Vaula, G., Romano, D. M., Mortilla, M., Huang, T. L., Tupler, R. G., et al. (1992) Assessment of amyloid  $\beta$  protein precursor gene mutations in a large set of familial and sporadic Alzheimer disease cases. *Am. J. Hum. Genet.* **51**, 273–282.
6. Tanzi, R. E., Kovacs, D. M., Kim, T.-W., Moir, R. D., Guenette, S. Y., and Wasco, W. (1996) The gene defects responsible for familial Alzheimer's disease. *Neurobiol. Dis.* **3**, 159–168.
7. Tanzi, R. E., Kovacs, D. M., Kim, T.-W., Moir, R. D., Guenette, S. Y., and Wasco, W. (1996) The presenilin genes and their role in early-onset familial Alzheimer's disease. *Alzheimer's Dis. Rev.* **1**, 91–98.
8. Doan, A., Thinakaran, G., Borchelt, D. R., Slunt, H. H., Ratovitsky, T., Podlisny, M., et al. (1996) Protein topology of presenilin 1. *Neuron* **17**, 1023–1030.
9. Lehmann, S., Chiesa, R., and Harris, D. A. (1997) Evidence for a six-transmembrane domain structure of presenilin 1. *J. Biol. Chem.* **272**, 12,047–12,051.
10. Thinakaran, G., Borchelt, D., Lee, M., Slunt, H., Spitzer, L., Kim, G., et al. (1996) Endoproteolysis of presenilin 1 and accumulation of processed derivatives in vivo. *Neuron* **17**, 181–190.
11. Kim, T.-W., Pettingell, W. H., Hallmark, O. G., Moir, R. D., Wasco, W., and Tanzi, R. E. (1997a) Endoproteolytic processing and proteasomal degradation of presenilin 2 in transfected cells. *J. Biol. Chem.* **272**, 11,006–11,010.
12. Mercken, M., Takahashi, H., Honda, T., Sato, K., Murayama, M., Nakazato, Y., et al. (1996) Characterization of human presenilin 1 using N-terminal specific monoclonal antibodies: evidence that Alzheimer mutations affect proteolytic processing. *FEBS. Lett.* **389**, 297–303.
13. Podlisny, M. B., Citron, M., Amarante, P., Sherrington, R., Xia, W., Zhang, J., et al. (1997) Presenilin proteins undergo heterogeneous endoproteolysis between Thr291 and Ala299 and occur as stable N- and C-terminal fragments in normal and Alzheimer brain tissue. *Neurobiol. Dis.* **3**, 325–337.
14. Tomita, T., Maruyama, K., Saido, T. C., Kume, H., Shinozaki, K., Tokuhiro, S., et al. (1997) The presenilin 2 mutation (N141I) linked to familial Alzheimer Disease (Volga German families) increases the secretion of amyloid  $\beta$  protein ending at the 42nd (or 43rd) residue. *Proc. Natl. Acad. Sci. USA* **94**, 2025–2030.
15. Jacobson, M. D., Weil, M., and Raff, M. C. (1997) Programmed cell death in animal development. *Cell* **88**, 347–354.
16. Thompson, C. B. (1995) Apoptosis in the pathogenesis and treatment of disease. *Science* **267**, 1456–1462.
17. Cohen, G. M. (1997) Caspases: the executioners of apoptosis. *Biochem. J.* **326**, 1–16.
18. Villa, P., Kaufmann, S. H., Earnshaw, W. C. (1997) Caspases and caspase inhibitors. *TIBS* **22**, 388–393.
19. Nicholson, D. W., and Thornberry, N. A. (1997) Caspases: killer proteases. *TIBS* **22**, 299–36.
20. Tan, X. and Wang, J. Y. J. (1998) The caspase-RB connection in cell death. *Trends Cell Biol.* **8**, 116–120.
21. Kim, T.-W., Pettingell, W. H., Jung, Y.-K., Kovacs, D. M., and Tanzi, R. E. (1997b) Alternative cleavage of Alzheimer-associated presenilins during apoptosis by caspase-3 family protease. *Science* **277**, 373–376.

22. Grünberg, J., Walter, J., Loetscher, H., Deuschle, U., Jacobsen, H., and Haass, C. (1998) Alzheimer's disease associated presenilin-1 holoprotein and its 18–20 kDa C-terminal fragment are death substrates for proteases of the caspase family. *Biochemistry* **37**, 2263–2270.
23. Gossen, M. and Bujard, H. (1992) Tight control. of gene expression in mammalian cells by tetracycline-responsive promoters. *Proc. Natl. Acad. Sci. USA* **89**, 5547–5551.
24. Baker, S. J., Markowitz, S., Fearon, E. R., Wilson, J. K. V., and Vogelstein, B. (1990) Suppression of human colorectal carcinoma cell growth by wild type p53. *Science* **249**, 912–915.

## The Phosphorylation of Presenilin Proteins

Jochen Walter

### 1. Introduction

#### 1.1. Phosphorylation of Full-Length Presenilin

The phosphorylation of presenilin (PS) proteins was initially analyzed in cultured cells overexpressing the respective proteins. These studies revealed that the homologous PS proteins are differentially phosphorylated *in vivo*. Full-length *PS2* was found to be constitutively phosphorylated on serine residues (1,2). In contrast, very little if any (1) or a variable phosphorylation (2) was observed for *PS1*. The familial Alzheimer's disease (FAD) mutations tested, the A246E mutation of *PS1* and the N141I mutation (volga german) of *PS2*, apparently have no effect on the differential phosphorylation of *PS1* and *PS2* (1). Because both PS proteins appeared to reside predominantly within the endoplasmic reticulum (1–4) differential phosphorylation is not due to distinct subcellular localizations of these proteins. Instead, the differential phosphorylation seems to be determined by structural differences between *PS1* and *PS2*. The phosphorylation of full-length *PS2* was localized to its N-terminal domain preceding the first transmembrane region (1). Although both PS proteins are highly homologous (5–7), their N-terminal domains differ in the primary structure. *PS2* contains a stretch of acidic residues (amino acids 1–20), which is lacking in *PS1* (Fig. 1). This acidic domain of *PS2* contains three consensus sites for casein kinases (CK), one site for CK-1 (serine 19) and two for CK-2 (serines 7 and 9; Fig. 1). Mutagenesis analyzes demonstrated that all three serine residues (serines 7, 9, and 19) are phosphorylated in cultured cells overexpressing *PS2* (1). Moreover, *in vitro* phosphorylation demonstrated that the N-terminal domain of *PS2* can be phosphorylated by both CK-1 and CK-2 (1). Thus, it is likely that full-length *PS2* is phosphorylated by CK-1 and CK-2 *in vivo* within its N-terminal domain. The phosphorylated residues within the



acidic region of *PS2* precedes a PEST motif (8,9), which is lacking in *PS1*. PEST sequences have been shown to be implicated in the regulation of protein turnover, e.g., the degradation of proteins containing a PEST motif is enhanced (9). It will be of great interest to test whether the phosphorylation of *PS2* influences its turnover.

### 1.2. Phosphorylation of Proteolytic Fragments of *PS1*

Both *PS* proteins are cleaved by unknown protease(s) resulting in the generation of approx 30 kDa N-terminal and approx 20 kDa C-terminal fragments (NTF and CTF, respectively [10–13]). The NTFs and CTFs are the predominant species of *PS* proteins detected in vivo, whereas the levels of full-length proteins are apparently very low (11).

Analysis of the proteolytic processing products of *PS1* revealed that the 20 kDa CTF can be phosphorylated in vivo (14,15). Phosphorylation of the *PS1* CTF increases about four- to fivefold on activation of protein kinase C (PKC) with phorbol ester. Similar results were obtained on stimulation of protein kinase A (PKA) with forskolin, which elevates intracellular levels of cyclic adenosine monophosphate (cAMP) (Fig. 2). Both phorbol ester- and forskolin-induced phosphorylation of the *PS1* CTF results in a decreased electrophoretic mobility of the CTF in sodium dodecyl sulfate (SDS) gels. These data indicate that phosphorylation of the *PS1* CTF can be mediated by two different signalling pathways in vivo. One involves PKA in response to elevated intracellular cAMP levels, and the second involves PKC which can be activated by phorbol ester (Fig. 2). As shown in Fig. 1B, the large hydrophilic loop domain of *PS1* contains seven potential phosphorylation sites for PKA and/or PKC. However, the in vivo phosphorylation sites remain to be determined. Phosphorylation of the *PS1* CTF can also be stimulated by activation of muscarinic acetylcholine receptors (m1- and m3-type receptors) with the muscarinic agonist carbachol (15). Carbachol induced phosphorylation of the *PS1* CTF is suppressed by the selective PKC inhibitor GF109203x (15). Therefore, signaling via muscarinic receptors, which leads to phosphorylation of the *PS1* CTF, is mediated via PKC.

In contrast to the 20-kDa CTF, the 30-kDa NTF of *PS1* is not phosphorylated. Neither activation of PKC by phorbol ester, nor of PKA by forskolin results in phosphorylation of the 30-kDa NTF, showing that the proteolytic processing products of *PS1* were differentially modified by phosphorylation (14,15).

Interestingly, the *PS1* holoprotein is not phosphorylated by PKC or PKA, suggesting that phosphorylation of *PS1* can only occur after proteolytic processing (15). Therefore, normal proteolytic processing is a prerequisite for PKC- and PKA-mediated phosphorylation of the *PS1* CTF, whereas the full-length *PS1*

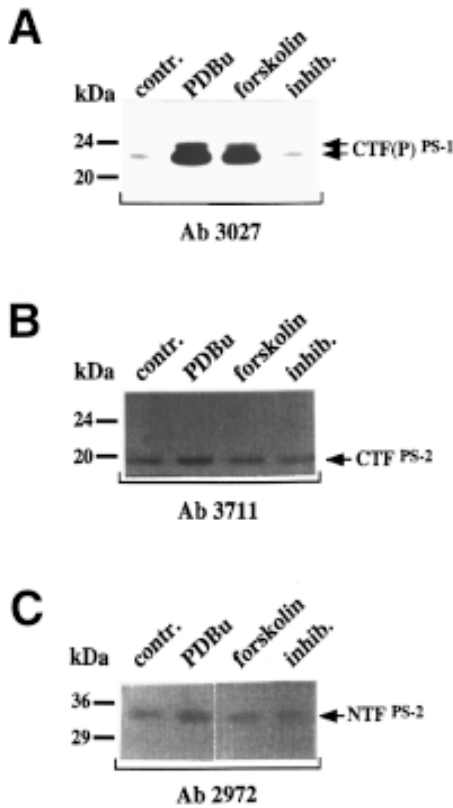


Fig. 2. Proteolytic processing products of *PS1* and *PS2* are phosphorylated by distinct protein kinases in vivo. Kidney 293 cells stably expressing *PS1* (A) or *PS2* (B,C) were incubated with  $^{32}\text{P}$ -orthophosphate in the presence or absence of PDBu ( $1\ \mu\text{M}$ ), forskolin ( $1\ \mu\text{M}$ ) or a mixture of PKC inhibitor (GF109203x;  $0.1\ \mu\text{M}$ ) and PKA inhibitor (KT5720;  $0.5\ \mu\text{M}$ ) and the CTF and NTF were immunoprecipitated with the respective antibodies as indicated.  $^{32}\text{P}$ -Labeled fragments (marked by arrows) were detected by autoradiography. Phosphorylation of the *PS1* CTF strongly increases on PDBu or forskolin treatment. In contrast, phosphorylation of the *PS2* CTF and NTF is not affected by activation or inhibition of PKC or PKA. The slightly more intensive band in lanes with PDBu is due to experimental variability.

protein is not phosphorylated by these kinases. This might indicate that the proteolytic cleavage results in structural changes to the large loop, allowing phosphorylation of amino acids that are not accessible in the holoprotein.

The functional implications of these complex phosphorylation mechanisms are unclear. Both PKA and PKC play important roles in cellular function, including the regulation of cell proliferation, differentiation, energy metabolism,

and protein sorting (for review *see* refs. 16 and 17). Notably, proteolytic processing of APP was demonstrated to be regulated by protein phosphorylation, and is dependent on both PKA and PKC activities (18). Secretion of APP increases on stimulation of PKA or PKC, and in turn generation of  $\beta$ -amyloid peptide (A $\beta$ ) decreases (19,20). Whether PKA- and PKC-mediated phosphorylation of the *PS1* CTF is directly involved in regulation of APP processing will be of great interest.

### 1.3. Phosphorylation of Proteolytic Fragments of PS2

As described in **Subheading 1.2.**, full-length *PS2* occurs as a constitutively phosphorylated protein. Like the *PS1* holoprotein, *PS2* also undergoes conventional proteolytic processing (12,13). Analysis of the phosphorylation status of the proteolytic processing products of *PS2* revealed that the conventional NTF and CTF occur as phosphorylated polypeptides *in vivo*. In contrast to the *PS1* CTF, phosphorylation of the CTF and NTF of *PS2* is not mediated by either PKA or PKC (*see* Fig. 2; [21]).

The amino acid sequence of the *PS2* loop domain contains a stretch of acidic residues including a cluster of potential phosphorylation sites for protein kinases CK-1 and CK-2 (Fig. 1). In contrast to the loop domain of *PS1*, no potential phosphorylation site is present in this domain of *PS2* (Fig. 1). *In vitro* phosphorylation assays using the recombinant loop domain of *PS2* demonstrated that CK-1 and CK-2 can readily phosphorylate this domain (Fig. 3). In contrast, PKC and PKA are not effective in phosphorylation of the *PS2* loop, which is consistent with the data from *in vivo* phosphorylation, demonstrating that activation of the respective kinases does not increase phosphorylation of the *PS2* CTF. Stoichiometric analysis of the *in vitro* *PS2* loop phosphorylation revealed three phosphorylation sites within that domain (Fig. 4). Although CK-1 can phosphorylate two distinct sites, CK-2 phosphorylates a single site within the *PS2* loop domain (Fig. 4; [21]).

Recently, the *in vivo* phosphorylation sites of the *PS2* CTF were mapped to serines 327 and 330 (7b), which are located immediately adjacent to known caspase cleavage sites of *PS2* after aspartates 326 and 329 (22,23). Phosphorylation of these sites inhibits the caspase-mediated cleavage of *PS2* during apoptosis and alters its apoptotic properties (7b).

In this chapter, methods for analyzing the phosphorylation of PS proteins are described.

## 2. Materials

### 2.1. *In Vivo* Phosphorylation of PS Proteins

1.  $\beta$ -Radiation safety equipment (plastic boxes to incubate cell culture Petri dishes, benchtop plastic protection shields).

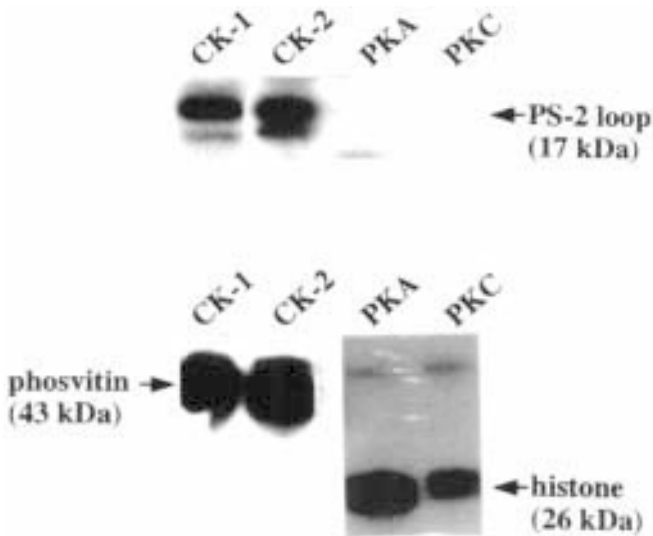


Fig. 3. In vitro phosphorylation of the *PS2* loop domain by protein kinases CK-1 and CK-2 using purified protein kinases (CK-1, CK-2, PKA and PKC). Fifty nanograms of purified *PS2* loop was incubated with 20 mM [ $\gamma$ - $^{32}\text{P}$ ]ATP in the presence of the respective kinase for 15 min at 32°C. To control for protein kinase activities, phosphovitin (as a substrate for CK-1 and CK-2) or histone (as a substrate for PKA and PKC) were phosphorylated in vitro (lower panel).  $^{32}\text{P}$ -labeled protein was detected by autoradiography. The *PS2* loop is detected as a doublet band (marked by an arrow), presumably due to proteolysis during the preparation. The recombinant loop is phosphorylated by CK-1 and CK-2, but not by PKA or PKC (21).

2. Dulbecco's minimal essential medium (DMEM) without sodium phosphate (Gibco Lifesciences, Gaithersburg, MD).
3. [ $^{32}\text{P}$ ]-Orthophosphate in aqueous solution (carrier free: 10 mCi/mL [Amersham, Amersham, UK]).
4. Specific antibodies for immunoprecipitation.
5. Buffer A: 50 mM Tris-HCl, pH 7.6, 150 mM NaCl, 2 mM EDTA, 0.2% (w/v) NP-40, 1 mM PMSF, 5  $\mu\text{g}/\text{mL}$  leupeptin.
6. Protein A Sepharose (Sigma Chemical Co., St. Louis, MO): 100 mg/mL in buffer A.
7. Inhibitors and/or activators of protein kinases (*see Note 1*).

## 2.2. Phosphoamino Acid Analysis (One-Dimensional)

1. 20  $\times$  20 cm thin-layer chromatography (TLC) cellulose plates (Merck).
2. High-voltage electrophoresis apparatus (we use the Multiphor II system from Pharmacia, Uppsala, Sweden).

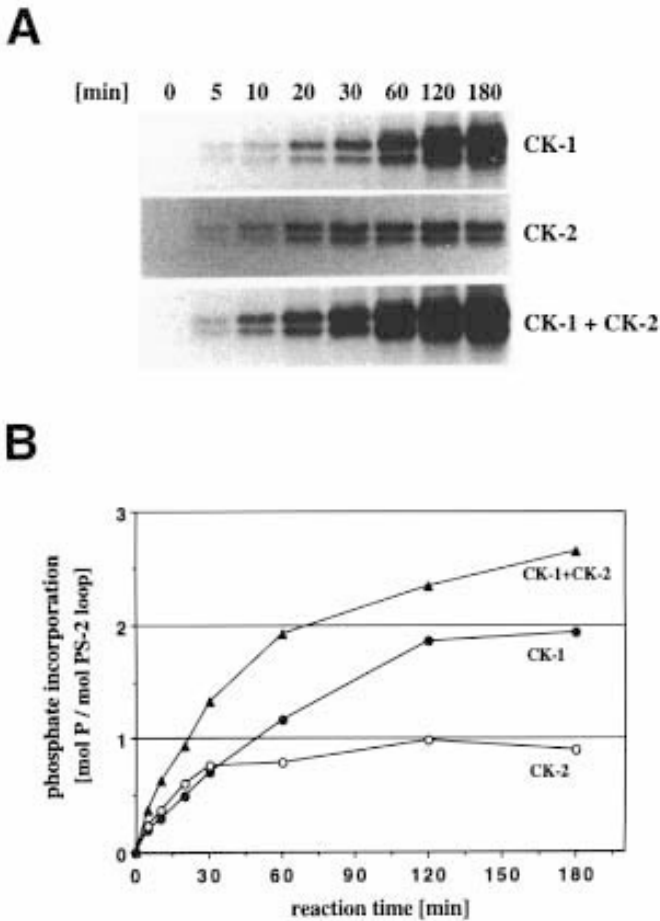


Fig. 4. The *PS2* loop contains three different *in vitro* phosphorylation sites. **(A)** 50 ng of purified *PS2* loop was incubated with 250  $\mu$ M [ $\gamma$ - $^{32}$ P]ATP in the presence of CK-1, CK-2, or a mixture of both kinases. Phosphorylation reactions were terminated at the time points indicated by the addition of SDS sample buffer. **(B)** Time course of the *PS2* loop phosphorylation. The phosphorylation reaction was carried out as described in **(A)** with CK-1 (closed circles), CK-2 (open circles) or a CK-1/CK-2 mixture (closed triangles). Quantification by phosphor imaging revealed that CK-1 incorporates 2 mol of phosphate, whereas CK-2 incorporates 1 mol of phosphate per mol of substrate. The phosphorylation of the *PS2* loop by CK-1 and CK-2 is additive, indicating that CK-1 and CK-2 phosphorylate different sites (21).

3. pH 2.5 Electrophoresis buffer: 5.9% (v/v) glacial acetic acid, 0.8% (v/v) formic acid, 0.3% (v/v) pyridine, 0.3 mM EDTA.
4. 6 M HCl.
5. Incubation oven.

6. Speed Vac concentrator (Savant Bioblock Scientific, Illkirch, France).
7. Phosphoamino acids (P-Ser, P-Thr, P-Tyr, 1  $\mu\text{g}/\mu\text{L}$  in pH 2.5 electrophoresis buffer).
8. Ninhydrin solution: 0.25% (w/v) in acetone.
9. Whatman 3MM filter paper (Whatman, Kent, UK).

### **2.3. Phosphopeptide Mapping with Trypsin (Two-Dimensional)**

1. pH 1.9 Electrophoresis buffer: 2.5% formic acid, 7.8% glacial acetic acid.
2. Digestion buffer: 50 mM  $\text{NH}_4\text{HCO}_3$ , pH 8.0.
3. Polyvinylpyrrolidone (PVP-40) 0.5% (w/v) in 100 mM acetic acid.
4. Trypsin solution, sequencing grade (1 mg/mL [Boehringer Mannheim, Mannheim, Germany]).
5. Chromatography buffer: 37.5% (v/v) *n*-butanol, 25% (v/v) pyridine, 7.5% (v/v) glacial acetic acid.
6. Performic acid: Mix nine parts of 98% formic acid and one part of 30% hydrogen peroxide and incubate 30 min at room temperature and then store in ice until used (*see Note 2*).
7. Speed Vac concentrator.
8. High-voltage electrophoresis apparatus (we use the Multiphor II system from Pharmacia).
9. Chromatography chamber for TLC plates.
10. Whatman 3MM paper.

### **2.4. In Vitro Phosphorylation of PS Proteins**

1. [ $\gamma$ - $^{32}\text{P}$ ]ATP (spec. act. 3000 Ci/mmol [Amersham], dilute with unlabeled ATP to a final concentration of 10 mM).
2. Purified protein kinases:
  - a. PKA (Boehringer Mannheim).
  - b. PKC (Biomol Research Laboratories, Plymouth Meeting, PA).
  - c. CK-1  $\delta$  (New England Biolabs, Beverly, MA).
  - d. CK-2 (Boehringer Mannheim).
3. Phosphorylation assay buffers:
  - a. Buffer B: 20 mM Tris-HCl, pH 7.5, 5 mM magnesium acetate, 5 mM dithiothreitol. This buffer is appropriate for testing PKA, CK-1, and CK-2 activities, respectively.
  - b. Buffer C: same as buffer B, supplemented with 1 mM phorbol 12,13-dibutyrate (PDBu), 0.5 mM calcium chloride, and 100  $\mu\text{g}/\text{mL}$  phosphatidylserine under mixed micellar conditions (**24**).

## **3. Methods**

Before working with  $^{32}\text{P}$ -labeled compounds, some considerations about the radiation safety should be made (*see the Notes* section in Chapter 10).

### **3.1. In Vivo Phosphorylation of PS Proteins**

1. Wash monolayer cell cultures once with prewarmed (37°C) phosphate-free medium and incubate with phosphate-free medium for 45 min. Testing the effect of

selective inhibitors of protein kinases, the respective compounds are added during this period of preincubation (*see Note 2*).

2. Aspirate the medium and add fresh phosphate-free medium together with an appropriate amount of [<sup>32</sup>P]-orthophosphate (*see Note 3*). Incubate the cell cultures at 37°C (5% CO<sub>2</sub>) for 2–4 h in the presence or absence of inhibitors/activators of protein kinases or phosphatases, respectively (*see Note 4*).
3. Aspirate the cell supernatant, wash the remaining cells once with PBS and lyse in buffer A containing 1% NP-40 for 10 min on ice. Cell lysis can be carried out within the cell culture dish. Transfer the cell lysates into microcentrifuge tubes.
4. Cell lysates are clarified by centrifugation at 14,000g for 10 min in a microcentrifuge and the supernatants are transferred to new microcentrifuge tubes. Incubate for 2–4 h together with appropriate antisera and 25 μL of the Protein A Sepharose slurry at 4°C with constant shaking (*see Note 5*).
5. Collect immunoprecipitates by centrifugation at 2000g for 5 min and wash the precipitates by three subsequent washes (for 20 min each) with buffer A containing 500 mM NaCl, buffer A containing 0.1% SDS and finally with buffer A alone. Collect immunoprecipitates by centrifugation (5 min at 2000g), add 15 μL of SDS sample buffer to the pellets and heat the samples for 5 min at 65°C (*see Note 6*).
6. Eluted proteins are separated by sodium dodecyl sulfate-polyacrylamide gel electrophoresis (SDS-PAGE) (*see Note 6*). For subsequent phosphoamino acid analysis or phosphopeptide mapping, the proteins should be transferred to PVDF or nitrocellulose membranes after SDS-PAGE (*see Note 7*). Otherwise, the gels can be dried. Radiolabeled proteins can be visualized on both dried gels or dried membranes by autoradiography or by phosphoimaging.

### 3.2. Phosphoamino Acid Analysis (One-Dimensional)

The phosphoamino acid analysis of PS proteins is essentially carried out as described for APP (*see Chapter 10, Subheading 3.3*).

### 3.3. Phosphopeptide Mapping with Trypsin (Two-Dimensional)

Two-dimensional phosphopeptide mapping of PS proteins with trypsin is essentially carried out according to a general method described by Boyle et al. (25). Digestion with other proteases can also be carried out according to this protocol.

1. Localization and tryptic digestion of the <sup>32</sup>P-radiolabeled PS proteins immobilized on nitrocellulose membranes is carried out as described for APP (*see Chapter 10, Subheading 3.4*).
2. After tryptic digestion, centrifuge the membrane/digestion mixture for 10 min at 14,000g, transfer the supernatant containing radiolabeled phosphopeptides to a new microcentrifuge tube and evaporate in a Speed Vac concentrator (Sigma) (*see Note 8*).
3. Dissolve the pellet in 50 μL ice-cold performic acid and incubate 1 h on ice (*see Note 9*). Add 500 μL H<sub>2</sub>O and evaporate. Add 300 μL H<sub>2</sub>O to the remaining pellet and vortex to dissolve the pellet. Centrifuge for 5 min at 14,000g, transfer the

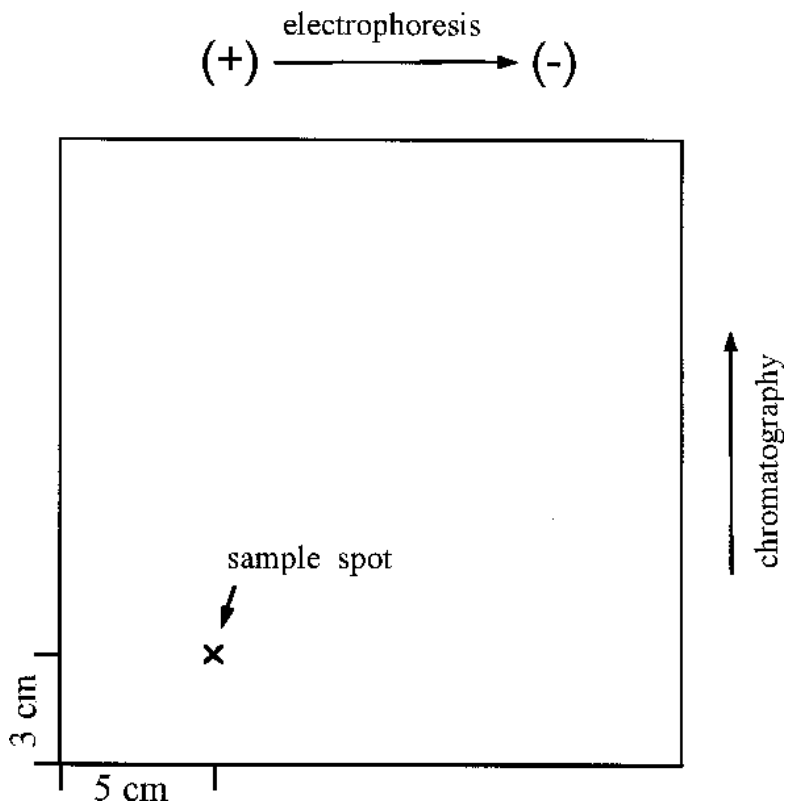


Fig. 5. Schematic representing a TLC cellulose plate used for two-dimensional phosphopeptide mapping. The sample is applied in aliquots of  $0.5 \mu\text{L}$  3 cm from the anodic edge and five cm from the bottom of the plate as indicated. After drying the sample the plate is wetted (*see Note 10*) and applied to the high-voltage electrophoresis apparatus. Most phosphopeptides migrate towards the cathode at pH 1.9. After electrophoresis the plate is dried and subjected to chromatography for separation in the second dimension.

supernatant to a new microcentrifuge tube and evaporate again in a Speed Vac concentrator.

4. Dissolve the pellet in  $300 \mu\text{L}$  of pH 1.9 buffer, vortex, and centrifuge at 14,000g for 5 min. Transfer the supernatant to a new microcentrifuge tube and evaporate. Resuspend the pellet in  $8 \mu\text{L}$  of pH 1.9 buffer and centrifuge for 5 min at 14,000g.
5. Spot the supernatant onto a TLC cellulose plate and wet the plate with a "mask" of Whatman 3MM filter paper as described in **Fig. 5** (*see Note 10*).
6. Fill both buffer tanks of the high-voltage electrophoresis apparatus with pH 1.9 buffer and place the plate in the correct orientation (*see Fig. 5*). Most phosphopeptides migrate towards the cathode at pH 1.9. The platform for holding the plates should

be precooled to 4–7°C before applying the plate. Connect the buffer tanks with the TLC cellulose plate by three prewetted (pH 1.9 electrophoresis buffer) layers of Whatman 3MM filter paper. Electrophorese for 20 min at 1.0 kV and then dry the plate in a fume hood. Do not heat the plate in an oven, as this might result in irreversible binding of peptides to the cellulose matrix.

7. Place the dried TLC cellulose plate into a chromatography tank (*see Note 11*) and chromatograph until the buffer front has reached about 2–3 cm from the top of the plate. This will take usually 8–9 h. Dry the plate again and expose to X-ray film at –80°C using an intensifying screen (*see Note 12*).

### 3.4. In Vitro Phosphorylation of PS Proteins

To analyze phosphorylation of specific domains of PS proteins both fusion proteins or purified peptides can be used as substrate (*see Note 13*).

1. Add the protein substrate to 50  $\mu\text{L}$  of the appropriate ice-cold phosphorylation buffer (e.g., buffer B for PKA, CK-1, or CK-2) and buffer C for PKC, *see Note 14*). Then add the protein kinase of interest to the reaction mixture and keep on ice until use.
2. Incubate the phosphorylation reaction mixture at 32°C for 3 min and start the phosphorylation reaction by the addition of [ $\gamma$ - $^{32}\text{P}$ ]ATP (to final concentrations of 10–100  $\mu\text{M}$ ).
3. Incubate at 32°C for the appropriate periods of time (*see Note 15*) and stop the phosphorylation reaction by the addition of SDS sample buffer.
4. Analyze phosphorylation of the respective PS protein by SDS-PAGE and autoradiography of the dried gels.

## 4. Notes

1. In studies analyzing the protein kinases that are involved in the phosphorylation of PS proteins, the following agents have been used:
  - a. Forskolin, increases the phosphorylation of the *PSI* CTF by activating PKA.
  - b. Phorbol esters, e.g., PDBu and phorbol 12-myristate 13-acetate (PMA), also increase the phosphorylation of the *PSI* CTF by activating PKC.
  - c. H-89 is a selective inhibitor of PKA (**26**) and inhibits forskolin-induced phosphorylation of *PSI* CTF.
  - d. GF109203 $\times$  is a selective inhibitor of PKC (**27**) and inhibits PDBu-induced phosphorylation of the *PSI* CTF.
  - e. Okadaic acid is a potent inhibitor of protein phosphatases 1 and 2A (**28**) and was shown to inhibit the dephosphorylation of the *PSI* CTF.

Using selective inhibitors of protein kinases in *in vivo* phosphorylation experiments, the compounds should be added during both preincubation and labeling period (*see also Note 4*). Remember to include appropriate controls with the respective solvents of these agents (e.g., ethanol, dimethyl sulfoxide).

2. The performic acid should always be prepared freshly prior to the oxidation step as described in **Subheading 2.3**.

3. The amounts of radioactivity used for *in vivo* phosphorylation may vary depending on the experimental setup. Usually, 0.25 mCi of  $^{32}\text{P}$ -orthophosphate/mL of phosphate-free medium is sufficient to label endogenous PS proteins in kidney 293 cells or COS cells.
4. Activators of PKC (e.g., PDBu) or PKA (e.g., forskolin) should be added 30 min after starting the *in vivo*  $^{32}\text{P}$ -labeling reaction. This allows radiolabeling of the intracellular ATP pool, and reduces the incorporation of phosphate from unlabeled ATP.
5. Immunoprecipitations should be carried out at 4°C to inhibit proteolysis and dephosphorylation. When immunoprecipitates appear to be “dirty” it may help to preincubate the cell lysates with 20  $\mu\text{L}$  of Protein A Sepharose slurry (Sigma) for 30 min at 4°C with constant shaking, and to remove the beads by centrifugation prior to immunoprecipitation with specific antibodies. In this case, material unspecifically binding to Protein A Sepharose will be removed from the cell lysate.
6. To avoid aggregation of PS proteins, especially of the full-length molecules, we add 4 *M* urea to both the SDS sample buffer and the polyacrylamide gels. It is also important not to boil samples, as this can also result in aggregation of PS proteins. We heat the samples for 5 min at 65°C.
7. Although there are protocols for phosphoamino acid analysis of proteins from fixed gels (40), we prefer to transfer the proteins after SDS-PAGE to PVDF membranes, as this method is faster with less working steps and the recovery of labeled phosphoamino acids appears to be higher. The use of PVDF membrane is important, because nitrocellulose membrane dissolves during acid hydrolysis in 6 *M* HCl at 110°C. Proteolytic digestions with trypsin can be carried out using either membranes, PVDF, or nitrocellulose.
8. The release of tryptic peptides from the membrane can be monitored by measuring the release of radioactivity into the digestion mixture in a scintillation counter. At the end of the digestion, 70–90% of radioactivity should be detected in the digestion supernatant. Using a Speed Vac concentrator for evaporation of acidic solutions, a NaOH trap should be connected to the system for neutralization. Alternatively, all evaporation steps in the procedures for phosphoamino acid analysis and two-dimensional phosphopeptide mapping can be substituted by lyophilization of the samples.
9. To inhibit unspecific cleavage reactions, the oxidation step of tryptic peptides of PS proteins with performic acid should be carried out on ice and the sample should be diluted after oxidation with  $\text{H}_2\text{O}$ .
10. Take care that TLC cellulose plates used for phosphoamino acid and two-dimensional peptide mapping are smooth and have an even surface. For this purpose the TLC plates can be illuminated from beneath in a lightbox. Scratches and nicks in the cellulose layer may influence the mobility of the samples and lead to smears. The sample for two-dimensional phosphopeptide mapping should be applied in aliquots of 0.5  $\mu\text{L}$  and immediately dried to keep the spots as small as possible. The TLC plate is wetted with pH 1.9 buffer using a mask of Whatman 3MM filter paper. The filter paper of 20  $\times$  20 cm with a hole at the position corresponding to

the sample spot on the TLC plate is prepared as described in Chapter 10 (**Subheading 3.3.**).

11. To prepare the chromatography chamber, fill it with chromatography buffer so that it is about 2 cm deep. Whatman 3MM filter paper prewetted with chromatography buffer is placed around the inside of the chamber. Seal the lid of the chamber using silicone grease and allow equilibration of the buffer with the gas phase of the chamber for several hours. It is recommended to prepare the chromatography chamber the day before the chromatography, which can then be carried out during the day. Take care that the chamber is tightly sealed and not moved during chromatography.
12. After autoradiography, the phosphopeptides can be recovered from the TLC plate as described by Boyle et al. (26), and then be further analyzed. The *in vivo* phosphorylation site can be determined after identification of the phosphorylated peptide by N-terminal amino acid microsequencing and/or mass spectrometry. In case more than one potential phosphorylation site is present in the identified peptide, these sites can be mutated by site directed mutagenesis. Subsequently, the phosphorylation of these mutants has to be analyzed in cultured cells and by *in vitro* phosphorylation experiments with purified protein kinases.
13. In principle, as substrates for *in vitro* phosphorylation synthetic peptides, purified PS proteins or fusion proteins can be used. We have successfully used PS protein domains (e.g., the N-terminal domain or the large hydrophilic loop domain) either fused to other proteins (maltose-binding protein, glutathione S-transferase) or after release of these domains by cleavage with factor X protease (1,21). When analyzing the phosphorylation of fusion proteins one has to control phosphorylation of the carrier protein without the PS domain.
14. To control the catalytic activity of the protein kinase used for *in vitro* phosphorylation, a control reaction with known protein substrates can be carried out in parallel (phosvitin or casein can be used as model substrates for CK-1 and CK-2, and histone for PKA and PKC; *see Fig. 3*).
15. For kinetic analysis of the phosphorylation reaction, a scaled-up volume of the reaction mixture is used and aliquots are taken from the mixture at various time points. For stoichiometric analysis, the phosphate incorporation into a known amount of protein substrate has to be determined at a time point when the phosphorylation reaction has reached the plateau phase (*see Fig. 4; [21]*).

## References

1. Walter, J., Capell, A., Grünberg, J., Pesold, B., Schindzielorz, A., Prior, R., et al. (1996) The Alzheimer's disease-associated presenilins are differentially phosphorylated proteins located predominantly within the endoplasmic reticulum. *Mol. Med.* **2**, 673–691.
2. De Strooper, B., Beullens, M., Contreras, B., Levesque, L., Craessaerts, K., Cordell, B., et al. (1997) Phosphorylation, subcellular localization and membrane orientation of the Alzheimer's disease-associated presenilins. *J. Biol. Chem.* **272**, 3590–3598.
3. Kovacs, D. M., Fausett, H. J., Page, K. J., Kim, T.-W., Moir, R. D., Merriam, D. E., et al. (1996) Alzheimer-associated presenilins 1 and 2: neuronal expression in brain and localization to intracellular membranes in mammalian cells. *Nat. Med.* **2**, 224–229.

4. Cook, D. G., Sung, J. C., Golde, T. E., Felsenstein, K. M., Wojczyk, B. S., Tanzi, R. E., et al. (1996) Expression and analysis of presenilin 1 in a human neuronal system: localization in cell bodies and dendrites. *Proc. Natl. Acad. Sci. USA* **93**, 9223–9228.
6. Sherrington, R., Rogaev, E. I., Liang, Y., Rogaeva, E. A., Levesque, G., Ikeda, M., et al. (1995) Cloning of a gene bearing missense mutations in early-onset familial Alzheimer's disease. *Nature* **375**, 754–760.
6. Rogaev, E. I., Sherrington, R., Rogaeva, E. A., Levesque, G., Ikeda, M., Liang, Y., et al. (1995) Familial Alzheimer's disease in kindreds with missense mutations in a gene on chromosome 1 related to Alzheimer's disease type 3 gene. *Nature* **376**, 775–778.
7. Levy-Lahad, E., Wasco, W., Poorkaj, P., Romano, D. M., Oshima, J., Pettingell, W. H., et al. (1995) Candidate gene for the chromosome 1 familial Alzheimer's disease locus. *Science* **269**, 973–977.
- 7a. Pearson, R. B. and Kemp, B. E. (1991) Protein kinase phosphorylation site sequences and consensus specificity motifs: tabulations. *Methods Enzymol.* **200**, 62–81.
- 7b. Walter, J., Schindzielorz, A., Grünberg, J., and Haass, C.; manuscript submitted.
8. Li, X. and Greenwald, I. (1996) Membrane topology of the *C. elegans* SEL-12 presenilin. *Neuron* **17**, 1015–1021.
9. Rechsteiner, M. and Rogers, S. W. (1996) PEST sequences and regulation by proteolysis. *Trends Biochem. Sci.* **21**, 267–271.
10. Mercken, M., Takahashi, H., Honda, T., Sato, K., Murayama, M., Nakazato, Y., et al. (1996) Characterization of human presenilin 1 using N-terminal specific monoclonal antibodies: evidence that Alzheimer mutations affect proteolytic processing. *FEBS Lett.* **389**, 297–303.
11. Thinakaran, G., Borchelt, D. R., Lee, M. K., Slunt, H. H., Spitzer, L., Kim, G., et al. (1996) Endoproteolysis of presenilin 1 and accumulation of processed derivatives in vivo. *Neuron* **17**, 181–190.
12. Kim, T.-W., Pettingell, W. H., Hallmark, O. G., Moir, R. D., Wasco, W., and Tanzi, R. E. (1997) Endoproteolytic cleavage and proteasomal degradation of presenilin 2 in transfected cells. *J. Biol. Chem.* **272**, 11006–11010.
13. Tomita, T., Maruyama, K., Takaomi, C. S., Kume, H., Shinozaki, K., Tokuhiro, S., et al. (1997) The presenilin 2 mutation (N141I) linked to familial Alzheimer disease (Volga German families) increases the secretion of amyloid  $\beta$ -protein ending at the 42nd (or 43rd) residue. *Proc. Natl. Acad. Sci. USA* **94**, 2025–2030.
14. Seeger, M., Nordstedt, C., Petanceska, S., Kovacs, D. M., Gouras, G. K., Hahne, S., et al. (1997) Evidence for phosphorylation and oligomeric assembly of presenilin 1. *Proc. Natl. Acad. Sci. USA* **94**, 5090–5094.
15. Walter, J., Grünberg, J., Capell, A., Pesold, B., Schindzielorz, A., Citron, M., et al. (1997) Proteolytic processing of the Alzheimer disease-associated presenilin-1 generates an in vivo substrate for protein kinase C. *Proc. Natl. Acad. Sci. USA* **94**, 5349–5354.
16. Asaoka, Y., Nakamura, S., Yoshida, K., and Nishizuka, Y. (1992) Protein kinase C, calcium and phospholipid degradation. *Trends. Biochem. Sci.* **17**, 414–417.
17. Walsh, D. A. and van Patten, S. M. (1994) Multiple pathway signal transduction by the cAMP-dependent protein kinase. *FASEB J.* **8**, 1227–1236.

18. Buxbaum, J. D., Gandy, S. E., Cicchetti, P., Ehrlich, M. E., Czernik, A. J., Fracasso, P. R., et al. (1990) Processing of Alzheimer  $\beta$ /A4 amyloid precursor protein: modulation by agents that regulate protein phosphorylation. *Proc. Natl. Acad. Sci. USA* **87**, 6003–6006.
19. Buxbaum, J. D., Koo, E. H., and Greengard, P. (1993) Protein phosphorylation inhibits production of Alzheimer amyloid  $\beta$ /A4 peptide. *Proc. Natl. Acad. Sci. USA* **90**, 9195–9198.
20. Hung, A. Y., Haass, C., Nitsch, R. M., Qiu, W. Q., Citron, M., Wurtman, R. J., and Selkoe, D. J. (1993) Activation of protein kinase C inhibits cellular production of the amyloid  $\beta$ -protein. *J. Biol. Chem.* **268**, 22959–22962.
21. Walter, J., Grünberg, J., Schindzielorz, A., and Haass, C. (1998) Proteolytic processing products of presenilin-1 and -2 are phosphorylated in vivo by distinct cellular mechanisms. *Biochemistry* **37**, 5961–5967
22. Loetscher, H., Deuschle, U., Brockhaus, M., Reinhardt, D., Nelboeck, P., Mous, J., et al. (1997) Presenilins are processed by caspase-type proteases. *J. Biol. Chem.* **272**, 20,655–20,659.
23. Kim, T.-W., Pettingell, W. H., Jung, Y.-K., Kovacs, D. M., and Tanzi, R. E. (1997) Alternative cleavage of Alzheimer-associated presenilins during apoptosis by a caspase-3 family member. *Science* **277**, 373–376.
24. Huang, K.-P. and Huang, F.-L. (1991) Purification and analysis of protein kinase C isoforms. *Methods Enzymol.* **200**, 241–252.
25. Boyle, W. J., van der Geer, P., and Hunter T. (1991) Phosphopeptide mapping and phosphoamino acid analysis by two-dimensional separation on thin-layer cellulose plates. *Methods Enzymol.* **201**, 110–149.
26. Chijiwa, T., Mishima, A., Hagiwara, M., Sano, M., Hayashi, K., Inoue, T., et al. (1990) Inhibition of forskolin induced neurite outgrowth and protein phosphorylation by a newly selective inhibitor of cyclic AMP-dependent protein kinase, N-[2-(p-bromocinnamylamino)ethyl]-5-isoquinolinesulfonamide (H-89), of PC-12D pheochromocytoma cells. *J. Biol. Chem.* **265**, 5267–5272.
27. Toullec, D., Pianetti, P., Coste, H., Bellevergue, P., Grand-Perret, T., Ajakane, M., et al. (1991) The bisindolylmaleimide GF109203X is a potent and selective inhibitor of protein kinase C. *J. Biol. Chem.* **266**, 15771–15781.
28. Cohen, P., Holmes, C. F., and Tsukitani, Y. (1990) Okadaic acid: a new probe for the study of cellular regulation. *Trends Biochem. Sci.* **15**, 98–102.

## Interaction of the Presenilins with the Amyloid Precursor Protein (APP)

Andreas Weidemann, Krzysztof Paliga, Ulrike Dürrwang,  
Friedrich Reinhard, Dai Zhang, Rupert Sandbrink,  
Geneviève Evin, Colin L. Masters, and Konrad Beyreuther

### 1. Introduction

The genes encoding presenilin-1 (*PS1*) and presenilin-2 (*PS2*) were identified as the genes that harbour mutations that cause more than 60% of early onset familial Alzheimer's disease cases (FAD) (*1–3*). So far, more than 40 missense mutations have been described for presenilin-1 and two have been found in the gene coding for presenilin-2 (reviewed in **refs. 4 and 5**). Carriers of mutated presenilin genes develop in their brain neuropathological changes characteristic of Alzheimer's disease including the deposition of amyloid A $\beta$  peptide. The latter is released from its cognate amyloid precursor protein (APP) by a two-step proteolytic conversion: first, proteolysis of APP by  $\beta$ -secretase, which releases the N-terminus of A $\beta$ , and second, conversion of the remaining fragment by  $\gamma$ -secretase, which cleaves within the predicted transmembrane region of APP. This releases the C-terminus of A $\beta$ , which may end either at position 40 or, to a lesser extent, at position 42 (reviewed in **ref. 6**). The latter species, A $\beta_{1-42}$ , is more prone to aggregation and deposition than A $\beta_{1-40}$  and is produced at higher levels in the brains and primary fibroblasts of FAD patients carrying PS missense mutations (*7*). The same result was obtained when cultured cells transfected with mutated *PS1* or *PS2*, or transgenic mice harboring missense *PS1* were analyzed for the production of A $\beta_{1-42}$ : in every case increased amounts of the longer A $\beta_{1-42}$  species were observed (*8–10*). The mechanisms by which mutations in the PS genes affect the proteolytic processing of APP by  $\gamma$ -secretase have not been resolved in detail. There are two possibilities by which the normal processing of APP may

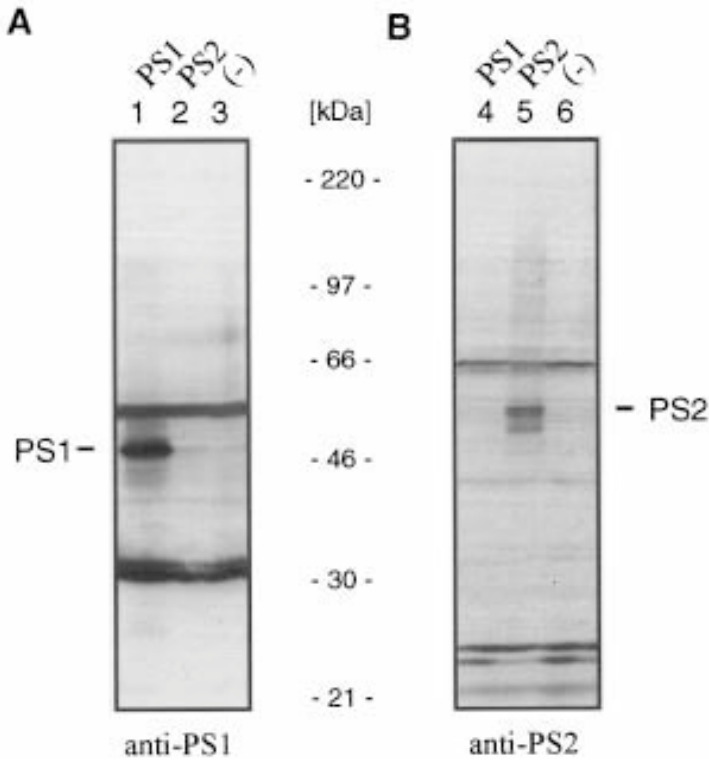


Fig. 1. Identification of *PS1* and *PS2* in transfected cells. COS7 cells were transfected with the *PS1* (lanes 1 and 4) and *PS2* (lanes 2 and 5) encoding pCEP4 plasmids and empty vector (lanes 3 and 6). Total cell homogenates were separated by SDS-PAGE and immunoblotted with polyclonal anti-*PS1* antiserum (A) or anti-*PS2* antiserum (B). Both *PS1* and *PS2* are detected as full-length species migrating in the range of 40–55 kDa.

be disturbed: either mutations in the presenilins affect APP metabolism in an indirect way by modulation of proteases or interaction with proteins involved in APP intracellular routing, or presenilins may modulate APP processing directly through physical interactions with APP. Such a direct interaction between presenilins and APP was first demonstrated by us for *PS2* (11). Later on, formation of stable complexes with APP was reported not only for *PS2* but also for *PS1* (12,13,13a).

In COS7 cells, transiently transfected with PS cDNA, presenilins were mainly detected as full-length species in the range of 40–55 kDa (Fig. 1). Compared with the amounts of full-length PS, the proteolytically processed derivatives of PS were only poorly observed in these cells, a finding that may

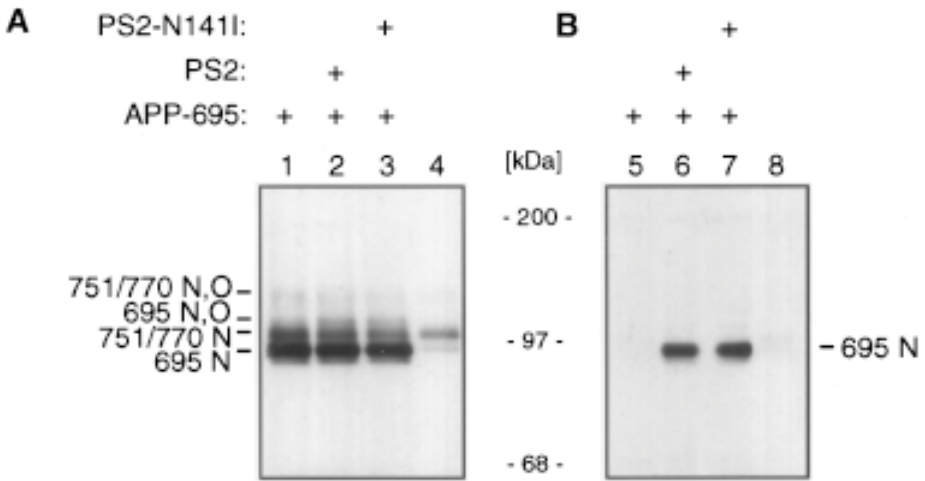


Fig. 2. Detection of APP-695 in *PS2* immunoprecipitates after Western blotting. COS7 cells were transiently transfected with pCEP encoded cDNAs for either *PS2* or *PS2-N141I* together with pCEP/APP-695 as indicated. Proteins were immunoprecipitated with anti-APP antiserum (lanes 1–4) or anti-*PS2* antiserum (lanes 5–8), followed by SDS-PAGE and immunoblotting with mAb22C11, which recognizes APP. Note that for demonstration of APP in *PS2* immunocomplexes (lanes 5–8), tenfold more cell lysate was subjected to immunoprecipitation compared to lanes 1–4. N: N-glycosylated, immature forms of APP; N,O: N- and O-glycosylated, mature forms (reproduced from **ref. 11**).

be explained by an incomplete proteolytic conversion of highly overexpressed presenilins (**14**). To prove the feasibility of a direct interaction between PS and APP, cells were cotransfected with expression plasmids encoding APP and PS. Analysis of complex formation between APP and PS was performed by two methods. (1) After immunoprecipitation of PS with polyclonal anti-PS antisera, the complexes were separated by gel electrophoresis followed by Western blotting with monoclonal anti-APP antibody (**Subheadings 3.2.1.** and **3.2.2.**; also **Fig. 2**). (2) PS immunocomplexes derived from lysates of [<sup>35</sup>S]methionine-labeled cells were first dissociated in the presence of sodium dodecyl sulfate (SDS) and urea and then subjected to a second immunoprecipitation with polyclonal anti-APP antiserum and successive gel electrophoresis (**Subheadings 3.2.1.** and **3.2.3.**; also **Fig. 3**). The species observed in the noncovalent APP-PS complexes is mainly composed of immature, ER-resident APP (**Figs. 2** and **3**), in agreement with the predominant localization of presenilins to the ER, intermediate compartment, and early Golgi of cells (**15–17**). No difference in complex formation was observed for mutant PS as compared with

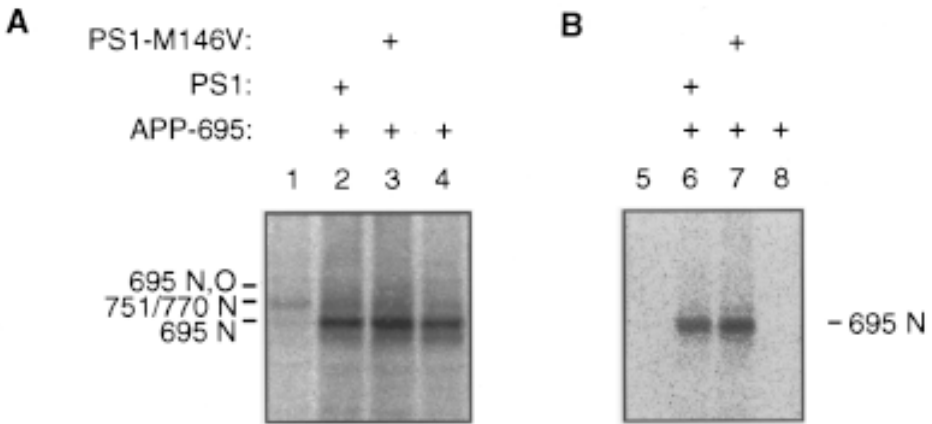


Fig. 3. Formation of stable complexes between APP-695 and *PS1*. Cells were transfected with pCEP-APP695 and plasmids encoding either wild-type *PS1* (lanes 2 and 6) or mutant *PS1*-M146V (lanes 3 and 7). After radiolabeling the cells with [<sup>35</sup>S]methionine, *PS1* complexes were immunoprecipitated with anti-*PS1* antiserum, followed by release of bound proteins by addition of SDS/urea and subjected to a second immunoprecipitation with anti-APP antiserum (**B**). APP was recovered in both wild-type *PS1* and mutant *PS1*-M146V immunocomplexes (lanes 6 and 7). The same result was obtained for *PS1*-P264L or *PS1*-L286V, indicating that the ability for complex formation was not influenced by FAD mutations (data not shown). For comparison, APP expression was monitored in parallel immunoprecipitations with anti-APP antiserum (**A**). N: N-glycosylated, immature forms of APP; N,O: N- and O-glycosylated, mature forms.

wild-type PS (**Figs. 2 and 3**) (*11–13a*). Thus, mutations in the presenilins may not directly affect their ability for complex formation with APP molecules, but instead influence the fate of the *PS2*–APP complex, e.g., by modifying its transport or its metabolism. This hypothesis is supported by the finding that the conversion of APP by  $\gamma$ -secretase(s) is largely inhibited in *PS1*-deficient mice, suggesting a role of PS as cofactors in this processing step (*18*). Additionally, mutant *PS1* fully complements the severe phenotypical aberrations observed in *PS1* knockout mice, which further validates the idea that the clinical mutations in PS result in a gain of (mis)function of mutant PS rather than a loss of function (*19,20*). Further studies on the protein domains involved in the interaction revealed that for *PS2*, the N-terminal part is sufficient for complex formation, whereas for APP, the A $\beta$  and/or transmembrane domain is implicated in the interaction (*13a*). Again, this supports the idea that PS act as cofactors in the processing of the transmembrane domain of APP by  $\gamma$ -secretases. Alternatively, based on the abundant localization of both PS

and APP-PS complexes in the ER, and based on the influence of overexpressed PS on APP transport and secretion (**11**), the function of PS could be similar to that of calnexin, which transports misfolded proteins retrogradely by recycling them between the ER, intermediate compartment, and Golgi apparatus (**21**). Alternatively, mutations in the PS genes may affect APP processing in a pathological manner similar to mutations in ERGIC-53 (ER-Golgi intermediate compartment protein-53). Here, mutations of ERGIC-53, which is localized to the intermediate compartment, cause a combined deficiency of coagulation factors V and VIII, two secretory proteins found in the blood plasma (**22**). However, although the exact function of the presenilins is not known, the demonstration of physical interactions suggests a direct participation of PS on APP processing.

## 2. Materials

### 2.1. Calcium Phosphate Coprecipitation

Buffers 2–5 should be filter-sterilized before use:

1. COS7 cells (*see Note 1*); cell culture media: Dulbecco's modified Eagle's medium (DMEM), DMEM + 10% fetal calf serum (FCS).
2. 2× HEPES-buffered saline (2× HBS): 280 mM NaCl, 1.5 mM Na<sub>2</sub>HPO<sub>4</sub>, 50 mM HEPES; adjust exactly to pH 7.13 with 1 N NaOH.
3. CaCl<sub>2</sub> solution: 2 M CaCl<sub>2</sub> in distilled H<sub>2</sub>O.
4. Tris-HCl buffer: 10 mM Tris-HCl, pH 7.5, in distilled H<sub>2</sub>O.
5. Glycerol solution: mix a 30% glycerol solution with 2× HBS in a 1:1 ratio.
6. DNA (*see Note 2*): pCEP4 (vector), pCEP-APP695, pCEP-PS1, pCEP-PS2 (and mutant derivatives of PS1 and PS2) dissolved at a concentration of 1 μg/μL in sterile TE (10 mM Tris-HCl, pH 7.5–8.0, 1 mM EDTA). The DNA should be of high quality (Qiagen, Chatsworth, CA).

### 2.2. Analysis of PS Immunocomplexes for Bound APP

1. Phosphate-buffered saline (PBS).
2. [<sup>35</sup>S]methionine (Amersham, Arlington Heights, IL), methionine-free cell culture medium (Life Technologies, Gaithersburg, MD).
3. Antibodies: Polyclonal anti-PS antiserum; polyclonal anti-APP antiserum; monoclonal anti-APP antibody (22C11, Boehringer Mannheim, Mannheim, Germany, **ref. 23**); secondary anti-mouse antibody coupled to horseradish peroxidase (Amersham).
4. Protein A-Sepharose as a 1:1 slurry in buffer A (*see step 6*) or in PBS (Pharmacia, Uppsala, Sweden).
5. Cell lysis buffer: 150 mM NaCl, 50 mM Tris-HCl, pH 7.5, 2 mM EDTA, 1% Nonidet P40 (NP40), 1% Triton X-100, supplemented with protease inhibitors (50 μg/mL aprotinin, 10 μg/mL leupeptin, 1 mM phenylmethylsulfonyl fluoride).
6. Wash buffers: Buffer A: 150 mM NaCl, 10 mM Tris-HCl, pH 7.5, 1 mM EDTA, 0.2% NP40; Buffer C: 10 mM Tris-HCl, pH 7.5.

7. Sample buffer (2×): 125 mM Tris-HCl, pH 6.8, 5% SDS, 50 mM dithiothreitol (DTT), 20% glycerol, 0.01% bromophenol blue.
8. Release buffer (2×): 125 mM Tris-HCl, pH 6.8, 1% SDS, 8 M urea, 25 mM DTT. DTT should be stored as 1 M stock solution at  $-20^{\circ}\text{C}$  and added freshly.
9. 8% SDS Tris-glycine gels, running buffer.
10. Equipment and reagents for immunoblotting; ECL solutions (Amersham).
11. HAc/MeOH solution: 30% Methanol, 10% glacial acetic acid in  $\text{H}_2\text{O}$ .

### 3. Methods

#### 3.1. Transfection of Cells with PS- and APP-Encoding Plasmids by Calcium Phosphate Coprecipitation

1. Split COS7 cells grown to confluency on a 10-cm dish (*see Note 3*) the day before transfection in a ratio of about 1:4 and seed the cells in  $12 \times 5$  cm dishes. On the day of transfection, the confluence of cells should be 70–90% (calcium phosphate coprecipitation protocol from **ref. 24**).
2. For each transfection, transfer 420  $\mu\text{L}$  Tris-HCl buffer into microtubes; add a total of 20  $\mu\text{g}$  DNA, i.e., 10  $\mu\text{g}$  pCEP-APP695 and 10  $\mu\text{g}$  pCEP-PS2 or 10  $\mu\text{g}$  pCEP-APP695 and 10  $\mu\text{g}$  pCEP-PS1. Include also control transfections with pCEP4 only, pCEP-APP695/pCEP4, and pCEP-PS/pCEP4.
3. Add 62  $\mu\text{L}$   $\text{CaCl}_2$  buffer to the DNA solution and mix the sample by pipeting up and down several times.
4. Prepare 500  $\mu\text{L}$  2× HBS in 13 mL screw-cap tubes or equivalent.
5. Place the tube with the 2× HBS solution on a vortex with moderate agitation and add dropwise the 500  $\mu\text{L}$   $\text{CaCl}_2$ /DNA solution.
6. Incubate the mixture for 20–30 min at room temperature, thus allowing the formation of calcium phosphate crystals containing DNA.
7. Without previous removal of the conditioned media, distribute dropwise the solution on the cells. After a few minutes, the crystals are detectable as a fine, uniform precipitate on the cells.
8. Incubate the cells for 3 h in the cell culture incubator.
9. Aspirate the conditioned media and add 1.5 mL glycerol solution per dish. Incubate for 2½ min. Remove the glycerol solution, wash twice with DMEM, and add fresh culture medium containing FCS (*see Note 4*).
10. Incubate the transfected cells overnight until subsequent analysis.

#### 3.2. Analysis of PS Immunocomplexes for Bound APP

The following protocols describe methods for the detection of APP<sub>695</sub> in PS immunoprecipitates. This can be achieved by analysis of PS immunocomplexes from nonlabeled cells by immunoblotting with monoclonal anti-APP antibody. However, the use of radioactive labeled proteins allows the concurrent detection of PS by phosphorimaging the blots after ECL development. This is especially useful for quantitating of the PS/APP ratio, i.e., for comparing bound APP in complexes with mutant or wild-type PS. An alternative approach can be

employed to identify APP in PS immunocomplexes: cells are radiolabeled, followed by a first immunoprecipitation with anti-PS antisera; the released immunocomplexes are analyzed by a second immunoprecipitation with anti-APP antiserum. Again, using radiolabeled cells allows the simultaneous detection of both PS and APP, and thus, quantitative studies of the corresponding ratios can be performed. The latter method of consecutive immunoprecipitations can also be used for the reverse experiments to identify PS in APP immunoprecipitates. The alternative, a direct analysis of PS in APP immunocomplexes by immunoblotting with anti-PS antisera, is not conclusive because the signal of the immunoglobulin heavy chains from the first immunoprecipitation is observed in the range of about 50 kDa, and therefore interferes with the signals obtained for full-length PS in the same molecular weight range.

### 3.2.1. Immunoprecipitation of APP and PS/APP Complexes

1. Remove media from the cells, wash three times with PBS, and add 1.5 mL methionine-free cell culture medium Petri-dish (when using nonlabeled cells, omit **steps 1–3**).
2. Add 100  $\mu\text{Ci}$  [ $^{35}\text{S}$ ]methionine per dish.
3. Incubate for 4 h in a humidified incubator at 37°C.
4. Remove the supernatant; wash once with PBS; scrape off the cells, add 0.5 mL PBS and transfer the cells into a microtube; and centrifuge for 1 min at 4000g, discard the supernatant (*see Note 5*).
5. Add 50  $\mu\text{L}$  ice-cold lysis buffer to the cell pellet, resuspend the cells in the buffer by pipeting up and down (*see Note 6*).
6. Incubate for 10 min on ice.
7. Centrifuge for 10 min at 10,000g.
8. Collect the clear supernatant in fresh tubes, discard the pellets.
9. Dilute the samples with 250  $\mu\text{L}$  buffer A, mix briefly (PS-IP); transfer 30  $\mu\text{L}$  into a tube with 270  $\mu\text{L}$  buffer A (APP-IP). Add 5  $\mu\text{L}$  anti-PS2 antiserum to the remaining 270  $\mu\text{L}$  PS-IP samples and 3  $\mu\text{L}$  anti-APP antiserum to the 300  $\mu\text{L}$  APP-IP samples (*see Note 7*). Add 30  $\mu\text{L}$  Protein A-Sepharose (Pharmacia) to all tubes.
10. Incubate for 2 h at room temperature on a head-over-head roller (*see Note 8*).
11. Wash six times with 1 mL buffer A and once with 1 mL buffer C (*see Note 9*).

### 3.2.2. Immunoblotting with Anti-APP Antibodies

The treatment of the precipitates depends on the successive experiments. For immunoblotting with anti-APP antibody, add 30  $\mu\text{L}$  sample buffer and boil the immunoprecipitates for 10 min (*see Note 10*). The samples are analyzed by gel electrophoresis on 8% polyacrylamide SDS gel followed by immunoblotting and ECL detection with monoclonal anti-APP antibody 22C11 by using standard conditions.

### 3.2.3. Analysis of Radiolabeled Immunoprecipitates for APP

1. Release bound antigens from the Protein A-Sepharose (Pharmacia) by incubation of the samples with 30  $\mu$ L release buffer for 15 min at 50°C (see **Note 10**).
2. Add 270  $\mu$ L buffer A to the samples to diminish the effective concentrations of SDS to 0.1% and the urea concentration to 0.8%, which is necessary for the subsequent immunoprecipitations.
3. Centrifuge briefly and transfer the supernatant into a fresh tube.
4. Add 5  $\mu$ L polyclonal anti-APP antiserum, and 30  $\mu$ L Protein A-Sepharose; incubate for 2 h on a head-over-head roller at room temperature.
5. Centrifuge briefly. The supernatant contains released PS (and released immunoglobulin heavy and light chains from the first immunoprecipitation), which can be analyzed separately after concentration of proteins by TCA (trichloroacetic acid) precipitation and subsequent gel electrophoresis. If this analysis is not performed, discard the supernatant, wash the Protein A-Sepharose twice with buffer A and once with buffer C.
6. Denature samples in sample buffer and apply to an 8% polyacrylamide SDS gel.
7. To immobilize the proteins, incubate the gel in HAc/MeOH solution with moderate agitation for 1 h.
8. Dry the gel and visualize proteins by phosphorimaging or autoradiography.

## 3.3. Other Methods

### 3.3.1 DNA Constructs

Cloning of *PS2* cDNA and generation of pCEP4 derivatives encoding wild-type *PS2* or mutant *PS2*-N141I (changing Asn<sub>141</sub> into Ile) has been described (**11**). *PS1* was cloned by reverse transcriptase-polymerase chain reaction using total RNA isolated from human blood lymphocytes as an alternative splice variant lacking the four residues VRSQ encoded at the 3' end of exon 3. The design of the oligonucleotide primers was based on the published sequences of *PS1* (**1,2**) and encoded an additional *Xho*I site in the 5'-sense primer and an *Cla*I site in the 3'-antisense primer. The sites were used for cloning in pBluescript SK+ (Stratagene, La Jolla, CA). Sequencing one positive clone revealed complete alignment with the cDNAs published. The *PS1* FAD mutants *PS1*-M146V, *PS1*-P264L, and *PS1*-L286V were constructed by site-directed mutagenesis of single-stranded DNA (**25**) and verified by DNA sequencing. For expression in eukaryotic cells, *PS1* and mutant *PS1* derivatives were cloned into the expression vector pCEP4 by using *Kpn*I and *Bam*HI restriction sites. Cloning and construction of eukaryotic APP expression vectors was as described before (**26**).

### 3.3.2. Cell Culture

COS7 cells were maintained in DMEM containing penicillin (50 U/mL), streptomycin (40  $\mu$ g/mL) and 10% FCS (Life Technologies).

### 3.3.3. Antisera

Preparation of rabbit polyclonal anti-APP antiserum and mouse monoclonal anti-APP antibody 22C11 has been described (23). Antisera recognizing PS2 was obtained by serial immunizations of rabbits with synthetic peptide corresponding to PS2 residues 42–58 (11). Production and characterization of polyclonal rabbit PS1 antiserum directed against a synthetic peptide encompassing residues 1–20 of PS1 has been published (17).

## 4. Notes

1. Instead of COS cells, most other cell lines that can be transfected with high efficiency should be suitable for analysis of PS-APP complex formation including Chinese hamster ovary (CHO), HeLa or human embryo kidney 293 (HEK293) cells.
2. For expression of APP and PS cDNAs, we used the commercially available pCEP4 vector (Invitrogen, San Diego, CA). Here, the gene expression is driven by the cytomegalovirus early/late promoter (CMV promoter) which belongs to one of the strongest promoters known and which is active in a wide variety of different cell lines from different species. Additionally, the pCEP4 vectors encode a marker for selection in eucaryotic cells (hygromycin B resistance gene) and an origin of replication derived from the Epstein-Barr virus. The latter allows an episomal propagation of the pCEP4 plasmids in some human and monkey cell lines, including COS7 cells or SH-SY5Y cells. Because of this episomal propagation, all transfected cells should express the cloned gene, which allows the use of pools of cells instead of screening individual colonies for establishing stable transfected cell lines. However, most other eucaryotic expression vectors should be suitable as well for transient expression of PS and APP genes in eucaryotic cells as described in this chapter.
3. Among the many different protocols, the calcium phosphate coprecipitation is still one of the common methods to transfect cells. However, most of the other transfection methods, including liposome-mediated DNA transfer or electroporation of cells, can be used for transfection of common cell lines like CHO, COS7, HeLa, or HEK293 cells. Transfection efficiency can be easily monitored by reporter plasmids encoding proteins like  $\beta$ -galactosidase, luciferase, or green-fluorescent protein.
4. Other cell lines than COS7 cells may require different conditions for high transfection efficiency. Frequently, incubation of the crystals overnight without glycerol treatment also gives high transfection rates.
5. It is recommended not to freeze cells or cell lysates because this results in decreased recoveries of APP from PS-APP complexes.
6. The use of prechilled lysis buffer is required to avoid the rupture of nuclei and the release of the chromosomal DNA, which would result in viscous solutions.
7. The direct immunoprecipitation of APP from cell lysates should be performed for the following reasons. First, to prove the expression of APP in the control experiments in which cells were only transfected with APP encoding plasmid.

Second, to control the level of APP expression because if there is no APP detected in the analysis of PS immunoprecipitates, this could be due to low transfection rates. Thus, the direct analysis of APP should be helpful to interpret negative results. Third, under the conditions described in this chapter, about 10% of total APP is found in PS immunoprecipitates. If no signal is obtained for APP by direct immunoprecipitation from the ten percent of the total cell lysates, it means that the assay/antibody used is not sensitive enough to detect APP in PS immunocomplexes.

8. Prolonged incubation (i.e., overnight) is not recommended because of some dissociation of the PS-APP complexes.
9. At this point, the immunoprecipitates may be stored at  $-20^{\circ}\text{C}$ .
10. Do not boil the samples in the case of concurrent detection of radioactive presenilins because the latter tend to aggregate heavily at high temperatures. Instead, the immunoprecipitates should be denatured at  $37\text{--}50^{\circ}\text{C}$  for 15 min in 30  $\mu\text{L}$  sample buffer containing 8 M urea.

## References

1. Sherrington, R., Rogaev, E. I., Liang, Y., Rogaeva, E. A., Levesque, G., Ikeda, M., et al. (1995) Cloning of a gene bearing missense mutations in early-onset familial Alzheimer's disease. *Nature* **375**, 754–760.
2. Levy-Lahad, E., Wasco, W., Pookaj, P., Romano, D., Oshima, J., Pettingell, P., et al. (1995) Candidate Gene for the chromosome 1 familial Alzheimer's disease locus. *Science* **269**, 973–977.
3. Rogaev, E. I., Sherrington, R., Rogaeva, E. A., Levesque, G., Ikeda, M., Liang, Y., et al. (1995) Familial Alzheimer's disease in kindreds with missense mutations in a gene on chromosome 1 related to the Alzheimer's disease type 3 gene. *Nature* **376**, 775–778.
4. Tanzi, R. E., Kovacs, D. M., Kim, T. W., Moir, R. D., Guenette, S. Y., and Wasco, W. (1996) The gene defects responsible for familial Alzheimer's disease. *Neurobiol. Dis.* **3**, 159–168.
5. Mattson, M. P., Guo, Q., Furukawa, K., and Pedersen, W. A. (1998) Presenilins, the endoplasmic reticulum, and neuronal apoptosis in Alzheimer's disease. *J. Neurochem.* **70**, 1–14.
6. Selkoe, D. J. (1997) Alzheimer's disease: genotypes, phenotypes, and treatments. *Science* **275**, 630–631.
7. Scheuner, D., Eckman, C., Jensen, M., Song, X., Citron, M., Suzuki, N., et al. (1996) Secreted amyloid  $\beta$ -protein similar to that in the senile plaque of Alzheimer's disease is increased in vivo by the presenilin 1 and 2 and APP mutations linked to familial Alzheimer's disease. *Nat. Med.* **2**, 864–870.
8. Duff, K., Eckman, C., Zehr, C., Yu, X., Prada, C. M., Perez tur, J., et al. (1996) Increased amyloid- $\beta$ 42(43) in brains of mice expressing mutant presenilin 1. *Nature* **383**, 710–713.
9. Borchelt, D. R., Thinakaran, G., Eckman, C. B., Lee, M. K., Davenport, F., Ratovitsky, T., et al. (1996) Familial Alzheimer's disease-linked presenilin 1 variants elevate A $\beta$ 1–42/1–40 ratio in vitro and in vivo. *Neuron* **17**, 1005–1013.

10. Tomita, T., Maruyama, K., Saido, T. C., Kume, H., Shinozaki, K., Tokuhiro, S., et al. (1997) The presenilin 2 mutation (N141I) linked to familial Alzheimer's disease (Volga German families) increases the secretion of amyloid  $\beta$  protein ending at the 42nd (or 43) residue. *Proc. Natl. Acad. Sci. USA* **94**, 2025–2030.
11. Weidemann, A., Paliga, K., Dürrwang, U., Czech, C., Evin, G., Masters, C. L., and Beyreuther, K. (1997) Formation of stable complexes between two Alzheimer's disease gene products: presenilin-2 and  $\beta$ -amyloid precursor protein. *Nat. Med.* **3**, 328–332.
12. Xia, W., Zhang, J., Perez, R., Koo, E. H., and Selkoe, D. J. (1997) Interaction between amyloid precursor protein and presenilins in mammalian cells: implications for the pathogenesis of Alzheimer disease. *Proc. Natl. Acad. Sci. USA* **94**, 8208–8213.
13. Wasco, W., Tanzi, R. E., Moir, R. D., Crowley, A. C., Merriam, D. E., Romano, D. M., et al. (1998) Presenilin 2 — APP interactions, in *Presenilins and Alzheimer's Disease* (Younkin, S. G., Tanzi, R. E., and Christen, Y., eds.), Springer, Heidelberg, Germany, pp. 59–70.
- 13a. Pradier, L., Carpentier, N., Delalonde, L., Clavel, N., Bock, M. D., Buee, L., Mercken, L., Tocque, B., and Czech, C. (1999) Mapping the APP/presenilin (PS) binding domains: the hydrophilic N-terminus of PS2 is sufficient for interaction with APP and can displace APP/PS1 interaction. *Neurobiol. Dis.* **6**, 43–55.
14. Thinakaran, G., Borchelt, D. R., Lee, M. K., Slunt, H. H., Spitzer, L., Kim, G., et al. (1996) Endoproteolysis of presenilin 1 and accumulation of processed derivatives in vivo. *Neuron* **17**, 181–190.
15. Kovacs, D. M., Fausett, H. J., Page, K. J., Kim, T. W., Moir, R. D., Merriam, D. E., et al. (1996) Alzheimer-associated presenilins 1 and 2: neuronal expression in brain and localization to intracellular membranes in mammalian cells. *Nat. Med.* **2**, 224–229.
16. Cook, D. B., Sung, J. C., Golde, T. E., Felsenstein, K. M., Wojczyk, B. S., Tanzi, R. E., et al. (1996) Expression and analysis of presenilin 1 in a human neuronal system: localization in cell bodies and dendrites. *Proc. Natl. Acad. Sci. USA* **93**, 9223–9228.
17. Culvenor, J. G., Maher, F., Evin, G., Malchiodi-Albedi, F., Cappai, R., Underwood, J. R., et al. (1997) Alzheimer's disease-associated presenilin 1 in neuronal cells: evidence for localization to the endoplasmic reticulum-Golgi intermediate compartment. *J. Neurosci. Res.* **49**, 719–731.
18. De Strooper, B., Saftig, P., Craessaerts, K., Vanderstichele, H., Guhde, G., Annaert, W., et al. (1998) Deficiency of presenilin-1 inhibits the normal cleavage of amyloid precursor protein. *Nature* **391**, 387–90.
19. Qian, S., Jiang, P., Guan, X. M., Singh, G., Trumbauer, M. E., Yu, H., et al. (1998) Mutant human presenilin 1 protects presenilin 1 null mouse against embryonic lethality and elevates A $\beta$ 1–42/43 expression. *Neuron* **20**, 611–617.
20. Davis, J. A., Naruse, S., Chen, H., Eckman, C., Younkin, S., Price, D. L., et al. (1998) An Alzheimer's disease-linked PS1 variant rescues the developmental abnormalities of PS1-deficient embryos. *Neuron* **20**, 603–609.

21. Hammond, C. and Helenius, A. (1994) Quality control. in the secretory pathway: retention of misfolded viral membrane glycoprotein involves cycling between the ER, intermediate compartment, and Golgi apparatus. *J. Cell Biol.* **126**, 41–52.
22. Nichols, W. C., Seligsohn, U., Zivelin, A., Terry, V. H., Hertel, C. E., Wheatley, M. A., et al. (1998) Mutations in the ER-Golgi intermediate compartment protein ERGIC-53 cause combined deficiency of coagulation factors V and VIII. *Cell* **93**, 61–70.
23. Weidemann, A., König, G., Bunke, D., Fischer, P., Salbaum, J. M., Masters, C. L., and Beyreuther, K. (1989) Identification, biogenesis, and localization of precursors of Alzheimer's disease A4 amyloid protein. *Cell* **57**, 115–126.
24. Schöler, H. R. and Gruss, P. (1984) Specific interaction between enhancer-containing molecules and cellular components. *Cell* **36**, 403–411.
25. Kunkel, T. A., Roberts, J. D., and Zakour, R. A. (1987) Rapid and efficient site specific mutagenesis without phenotypic selection. *Methods Enzymol.* **154**, 367–382.
26. Dyrks, T., Dyrks, E., Mönning, U., Urmoneit, B., Turner, J., and Beyreuther, K. (1993) Generation of  $\beta$ A4 from the amyloid protein precursor and fragments thereof. *FEBS Lett.* **335**, 89–93.

## Distribution of Presenilins and Amyloid Precursor Protein (APP) in Detergent-Insoluble Membrane Domains

Edward T. Parkin, Anthony J. Turner, and Nigel M. Hooper

### 1. Introduction

#### 1.1. Detergent-Insoluble Glycolipid-Enriched Domains

Until recently, the detergent insolubility of certain membrane-associated proteins was singularly attributed to an association with the cytoskeleton. However, in 1988 we observed that a number of glycosyl-phosphatidylinositol (GPI)-anchored proteins were resistant to solubilization by nonionic detergents such as Triton X-100 (1). This detergent insolubility is acquired as the proteins pass through the endoplasmic reticulum and on to the Golgi apparatus (2), and arises not from a direct interaction of the GPI-anchored proteins with cytoskeletal elements but as a result of the specific lipid composition of the membrane domains with which these proteins associate (3,4). Mammalian cell membranes contain hundreds of individual lipid species which can be grouped under several major headings (e.g., glycerophospholipids, sphingomyelins, ceramides, glycosphingolipids, and cholesterol) (2,5,6). Glycerophospholipids, such as phosphatidylcholine and phosphatidylethanolamine, predominate in the membrane milieu. Consequently, the bulk of the cell membrane is fluid and in a continual state of flux. However, the membrane domains with which GPI-anchored proteins associate are enriched with sphingolipids and cholesterol, making them less fluid than the membrane milieu (2,4). Such membrane domains have been referred to as “lipid rafts” (7) and there has been some controversy as to whether they exist *in vivo* or whether they form as an artefact of the procedures employed in their isolation (8). However, recent studies in both artificial lipid bilayers and living cell membranes using such techniques

From: *Methods in Molecular Medicine, Vol. 32: Alzheimer's Disease: Methods and Protocols*  
Edited by: N. M. Hooper © Humana Press Inc., Totowa, NJ

as single-particle tracking, fluorescence polarization, and protein crosslinking (9–12) have shown that GPI-anchored proteins do cluster in discrete domains. Several other names have been given to lipid rafts including DIMs (detergent-insoluble membranes), DRMs (detergent-resistant membranes), GEMs (glycosphingolipid-enriched membrane domains), and DIGs (detergent-insoluble glycolipid-enriched domains). For the purpose of this chapter the abbreviation “DIG” will be employed.

## 1.2. Caveolae and DIGs

Caveolae are 50–100 nm flask-shaped invaginations associated with, or in the vicinity of, the plasma membrane identifiable in nonneuronal tissue by a characteristically high content of the 21–24 kDa integral membrane protein caveolin (13–15). These structures have been implicated in several cellular events, including signal transduction (16–18), transcytosis (19), potocytosis (the internalization of small molecules from the extracellular medium) (20), and interaction with the actin-based cytoskeleton (21,22). Like DIGs, caveolae are insoluble in certain nonionic detergents and have a low density as a consequence of a high lipid-to-protein ratio. These similarities originally lead to the conclusion that DIGs were synonymous with caveolae (21,23,24). However, this assumption has now been disproved mainly by the pioneering work of Schnitzer and coworkers (18,25,26) who were able to separate morphologically distinguishable plasmalemmal caveolae from noninvaginated plasmalemmal DIGs. The latter of these structures was found to be highly enriched in the GPI-anchored proteins 5'-nucleotidase, carbonic anhydrase, and urokinase-plasminogen activator receptor, whereas the same proteins were effectively excluded from caveolae. These results have served to emphasise the fact that the property of detergent resistance is not confined to caveolar membranes.

Caveolae, defined morphologically as flask-shaped structures, are most abundant in simple squamous epithelia, fibroblasts, smooth muscle cells, and adipocytes (27–30). Although caveolin is highly expressed in lung and muscle tissues it is absent from other tissues such as spleen, kidney, liver, brain, and testis (22). The absence of caveolin from brain tissue and neuronal cultures initially led to the conclusion that caveolae are not abundant structures in the nervous system. However, recent reports demonstrated that detergent-insoluble membranes displaying the characteristic large size and low buoyant density of caveolae could be isolated from mouse neuroblastoma cells, mouse cerebellum, rat forebrain, and rat cortical neurons (31–35). Several proteins concentrated in caveolin-enriched membrane fractions from other tissues were also present in DIGs isolated from nervous tissue, e.g., GPI-anchored proteins, tyrosine kinases, and  $\alpha$ - and  $\beta$ -subunits of heterotrimeric G proteins (31,34). However, in all but one case (36), caveolin itself was absent from these structures.

### 1.3. DIGs and Alzheimer's Disease-Linked Proteins

Although the majority of the amyloidogenic A $\beta$  peptides (A $\beta$ 40 and A $\beta$ 42) released from the amyloid precursor protein (APP) through sequential cleavage by  $\beta$ - and  $\gamma$ -secretases is secreted from cells, A $\beta$ 40 and A $\beta$ 42 have also been detected in the *trans*-Golgi network and endoplasmic reticulum/intermediate compartment, respectively (37–40). It has also been suggested that the intracellular formation of A $\beta$  may arise through the secretase-mediated cleavage of a minor pool of the APP that resides in DIGs. An endogenous DIG-associated pool of the APP has been identified to date only in cortical (41) or hippocampal (42) neurons or rat brain cortex (43), and in our laboratory we have failed to detect the APP in DIGs isolated from mouse cerebellum and human neuroblastoma cells (35). There is strong evidence to suggest that the familial Alzheimer's disease-associated presenilins play an important role in the  $\gamma$ -secretase-mediated cleavage of the APP (44). If this process does indeed occur in DIGs, then it follows that the presenilins also should be present in these membrane structures.

Presenilin-1 (PS1) and presenilin-2 (PS2) are located predominantly within the endoplasmic reticulum and Golgi compartments (45,46). In transfected cells the C-terminal fragments of both presenilins have been identified in the detergent-resistant fraction (47,48). However, it was not clear whether this detergent-insolubility was due to an association with DIGs or with the cytoskeleton. We and others have explored this insolubility using the methods described in **Subheading 1.4.** for the isolation of DIGs.

### 1.4. Isolation and Characterization of DIGs

#### 1.4.1. Detergent-Based Isolation of DIGs

The most commonly employed method for the isolation of DIGs takes advantage of the insolubility of these membrane domains in nonionic detergents such as Triton X-100 (21,22). Cells or tissue are first solubilized in detergent and then placed at the base of a sucrose gradient. When the samples are centrifuged DIGs (because of their inherent low density), migrate up the sucrose gradient leaving the bulk of the solubilized membrane proteins at the base of the gradient (**Fig. 1**). This methodology, with various modifications, has been applied to the isolation of DIGs from both neuronal (35,49) and nonneuronal (5) tissue/cells. We routinely use the detergent-based method of DIG isolation described in **Subheading 3.2.** for the study of Alzheimer's disease-linked proteins in mouse brain. It is important to stress that these techniques should be used with caution and suitable marker proteins employed to confirm that the isolated DIGs are not contaminated with unwanted membranes (*see Note 1*).

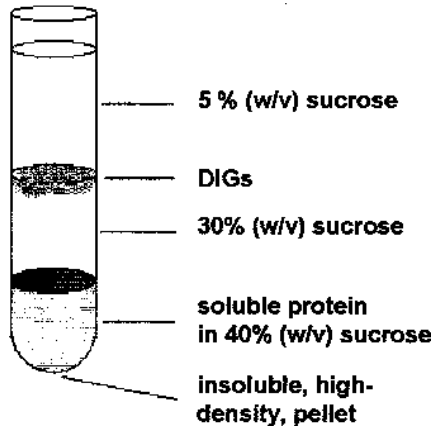
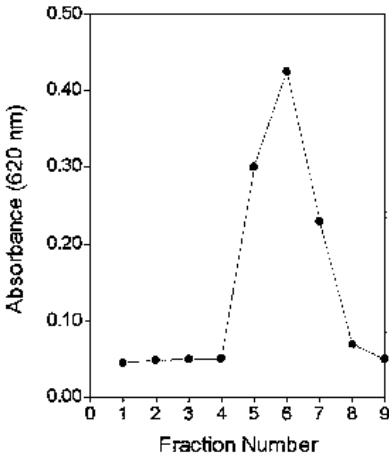


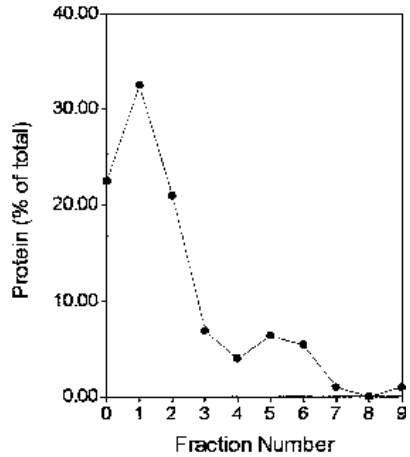
Fig. 1. Isolation of DIGs by solubilization in nonionic detergent followed by buoyant density centrifugation. Cells/tissue are solubilized in nonionic detergent (usually Triton X-100) and adjusted to 40% (w/v) sucrose by adding an equal volume of 80% (w/v) sucrose. The samples are then layered under a 5–30% (w/v) linear sucrose gradient and centrifuged overnight at 140,000g. DIGs migrate up the sucrose gradient leaving the bulk of the solubilized membrane protein in the 40% (w/v) sucrose region at the base of the gradient.

**Figure 2** shows the analysis of sucrose gradient fractions following the isolation of DIGs from mouse brain cortex by the detergent-based method described in **Subheading 3.2**. Here, the sucrose gradient has been harvested in 0.5 mL fractions from the bottom to the top, with fraction 0 representing the insoluble pellet at the base of the tube resuspended in buffer B (**Subheading 2.2**). A single light-scattering band centered on fraction 6 is observed within the 5–30% (w/v) sucrose region of the gradient (**Fig. 2A**) corresponding to the DIG fraction. The majority (approx 60%) of the cellular protein remains in the 40% (w/v) sucrose region of the gradient (**Fig. 2B**), with a further 22% of the protein located in the insoluble pellet at the bottom of the centrifuge tube (*see Note 2*). The DIG band contains approx 10% of the total protein. When the fractions are assayed for the transmembrane polypeptide-anchored protein, aminopeptidase A (**Fig. 2C**), all the activity is recovered in the 40% (w/v) sucrose region of the gradient, showing that the DIGs isolated by this method are not contaminated by incompletely solubilized regions of the plasma membrane. The GPI-anchored enzyme, alkaline phosphatase, can be used as a marker for DIGs isolated from brain cortex because of the nature of its membrane anchorage. As **Fig. 2D** shows, 80–85% of alkaline phosphatase activity is located in the DIG region of the sucrose gradient (*see Note 3*). To summarize, the method described in **Subheading 3.2** enables the isolation of

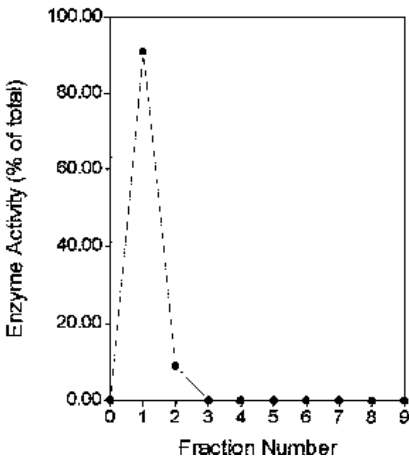
**A** Absorbance (620 nm)



**B** Protein



**C** Aminopeptidase A



**D** Alkaline phosphatase

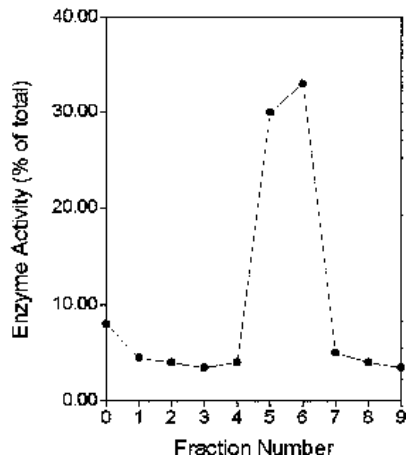


Fig. 2. Characterization of DIGs isolated from mouse brain cortex. DIGs were prepared as described in **Subheading 3.2**. The sucrose gradient was harvested in 0.5 mL fractions (fraction 0, insoluble pellet; fraction 1, base of gradient; fraction 9, top of gradient). (A) Absorbance of fractions measured at 620 nm. (B) Distribution of protein in the sucrose gradient. (C) Distribution of the transmembrane polypeptide-anchored protein aminopeptidase A in the sucrose gradient. (D) Distribution of the glycosyl-phosphatidylinositol-anchored protein alkaline phosphatase in the sucrose gradient.

DIGs, which excludes the majority of the cellular protein and many trans-membrane polypeptide-anchored proteins, but which retain most of the GPI-anchored proteins.

#### 1.4.2. Detergent-Free Isolation of DIGs

At least two different methods exist for the isolation of DIGs in the absence of detergent (**50,51**). However, whereas the detergent-based method already discussed can be applied to both whole tissues and cell cultures, detergent-free methods have not yet been successfully applied to the isolation of DIGs from tissue. The most commonly used of these methods replaces Triton X-100 with sodium carbonate and is described in **Subheading 3.3**. A recent report using this methodology (**50**) showed that DIGs isolated by detergent-free methods from nonneuronal cells contained the entire cellular complement of the APP. These results should be interpreted with caution, as the isolation procedure involved employs very harsh homogenization steps (Dounce homogenizer (VWR), Polytron tissue grinder [Kinematica GmbH, Brinkmann Instruments], sonication) and may lead to the artefactual formation of vesicles containing the APP which would otherwise not have the same density as DIGs (i.e., the method is based purely on the criteria of vesicle density and not detergent solubility) (*see Note 4*). It also remains to be shown whether the vesicles isolated are soluble or insoluble in detergent and, therefore, whether they may truly be classified as DIGs.

The aim of this chapter is to give the reader an insight into the methods employed in the isolation and characterization of DIGs by both detergent-based and detergent-free methods. The isolation of DIGs from mouse cerebral cortex is described and the results are discussed in relation to the presence of presenilins in these membrane microdomains.

## 2. Materials

### 2.1. Preparation of the Total Membrane Fraction from Mouse Brain Cortex

1. Buffer A: 150 mM NaCl, 20 mM Na<sub>2</sub>HPO<sub>4</sub>, 2 mM NaH<sub>2</sub>PO<sub>4</sub>, 1 mM EDTA, 20% (v/v) glycerol, pH 7.4.
2. Dounce homogenizer (VWR).
3. Probe sonicator, e.g., Branson Sonifier 450 (Branson Ultrasonic Corp., Middlesex, UK).

### 2.2. Detergent-Based Isolation of DIGs

1. Buffer B: MES-buffered saline; 25 mM MES, pH 6.5, and 0.15 M NaCl.
2. 1% (v/v) Triton X-100 in buffer B.
3. 80% (w/v) sucrose in buffer B.

4. 30% (w/v) sucrose in buffer B.
5. 5% (w/v) sucrose in buffer B.
6. Dounce homogenizer.
7. Ultracentrifuge with a swing-out rotor, e.g., SW50.1 (Beckman Instruments, Fullerton, CA).
8. Probe sonicator, e.g., Branson Sonifier 450 (Branson Ultrasonic Corp.).

### 2.3. Detergent-free Isolation of DIGs

1. Buffer B: MES-buffered saline; 25 mM MES, pH 6.5, and 0.15 M NaCl.
2. Buffer C: 150 mM NaCl, 20 mM Na<sub>2</sub>HPO<sub>4</sub>, 2 mM NaH<sub>2</sub>PO<sub>4</sub>, pH 7.4.
3. 500 mM Na<sub>2</sub>CO<sub>3</sub>, pH 11.
4. 90% (w/v) sucrose in buffer B.
5. Buffer D: 25 mM MES, pH 6.5, 0.15 M NaCl and 250 mM Na<sub>2</sub>CO<sub>3</sub>.
6. 35% (w/v) sucrose in buffer D.
7. 5% (w/v) sucrose in buffer D.
8. Dounce homogenizer.
9. Ultracentrifuge with a swing-out rotor, e.g., SW50.1 (Beckman Instruments).
10. Probe sonicator, e.g., Branson Sonifier 250 (Branson Ultrasonic Corp.).
11. Polytron tissue grinder (Kinematica GmbH, Brinkmann Instruments).

### 2.4. Marker Enzyme Assays

1. 10 mM *p*-Nitrophenol.
2. Buffer E: Alkaline phosphatase buffer/substrate; 50 mM glycine, 1 mM MgCl<sub>2</sub>·6H<sub>2</sub>O, 4.4 mM *p*-nitrophenyl phosphate, pH 10.5.
3. 1 mM *p*-Nitroanilide.
4. 5 mM  $\alpha$ -Glutamyl-*p*-nitroanilide.
5. Buffer F: Aminopeptidase A buffer; 0.1 M Tris-HCl, pH 7.4, and 1 mM CaCl<sub>2</sub>.

### 2.5. Protein Determination

1. Bicinchoninic acid solution (BCA) (Sigma Chemical Co., St. Louis, MO).
2. 4% (w/v) CuSO<sub>4</sub>·5H<sub>2</sub>O.
3. Bovine serum albumin (BSA) standard solution (1 mg/mL).

### 2.6. Immunodetection of Presenilin Proteins

1. Antipresenilin antibodies were obtained from the following sources; anti-PS1 (hydrophilic loop; amino acid residues 344–358) and anti-PS2 (N-terminus; amino acid residues 32–45) were from SmithKline Beecham Pharmaceuticals (Harlow, UK); anti-PS1 (N-terminus; amino acid residues 2–15) was from Dr. J. Hardy (Mayo Clinic, Jacksonville, FL).
2. Buffer C: 150 mM NaCl, 20 mM Na<sub>2</sub>HPO<sub>4</sub>, 2 mM NaH<sub>2</sub>PO<sub>4</sub>, pH 7.4.
3. Buffer G: 20 mM Tris-HCl, 150 mM glycine, 20% (v/v) methanol, pH 8–9.
4. Buffer H: 1% (v/v) Tween-20, 2% (v/v) goat serum, and 5% (w/v) dried milk powder in buffer C.

5. Buffer J: 0.1% (v/v) Tween-20, 2% (v/v) goat serum, and 5% (w/v) dried milk powder in buffer C.
6. Buffer K: 0.1% Tween-20 in buffer C.
7. Enhanced chemiluminescence detection reagents (Amersham Life Sciences, Amersham, UK).
8. Immobilon P polyvinylidene difluoride (PVDF) membrane.
9. Semi-Phor semidry transfer kit (Hoefer Scientific Instruments).

### 3. Methods

#### 3.1. Preparation of the Total Membrane Fraction from Mouse Brain Cortex

Perform all steps at 4°C.

1. Dissect one brain cortex from a 7- to 8-wk-old mouse and homogenize in 15 mL of buffer A using a Dounce homogenizer (VWR) with a glass pestle (30 passes).
2. Sonicate the homogenate on ice for ten 1-min periods (30% of maximum power for 30% of the time) with a 1-min cooling period between each round of sonication.
3. Centrifuge the homogenate at 5000g for 20 min.
4. Remove the supernatant and centrifuge it at 100,000g for 90 min.
5. Resuspend the resulting membrane pellet in approx 3 mL of buffer B.

#### 3.2. Detergent-Based Isolation of DIGs

Perform all steps at 4°C (*see Note 5*).

1. Dissect one brain cortex from a 7- to 8-wk-old mouse and homogenize in 4 mL of buffer B containing 1% (v/v) Triton X-100 using a Dounce homogenizer equipped with a glass pestle (30 passes).
2. Sonicate the homogenate on ice for five 20-s periods (30% of maximum power) with 2 minute cooling periods between each round of sonication.
3. Add an equal volume (4 mL) of buffer B containing 80% (w/v) sucrose. Mix well.
4. In a 5-mL ultracentrifuge tube, pour a 5–30% (w/v) linear sucrose gradient in buffer B to give a final volume of 4 mL.
5. Inject 1 mL of the solubilized homogenate underneath the sucrose gradient.
6. Centrifuge the sucrose gradient at 140,000g for 18–24 h in a swing-out rotor.
7. Collect 0.5 mL fractions from the base of the sucrose gradient and resuspend the insoluble pellet in 0.5 mL of buffer B (brief sonication may be required) (*see Note 6*). Measure the absorbance of each fraction (excluding the pellet) at 620 nm in order to determine the position of the DIGs in the sucrose gradient (*see Fig. 2*).

#### 3.3. Detergent-Free Isolation of DIGs

1. Wash two confluent 150-mm dishes of cells twice with ice-cold buffer C and scrape into 2 mL of 500 mM Na<sub>2</sub>CO<sub>3</sub>, pH 11.0.

2. Homogenize sequentially with a Dounce homogenizer (10 passes), a Polytron tissue grinder (three 10-s bursts), and a sonicator (three 20-s bursts).
3. Adjust the homogenate to 45% (w/v) sucrose by adding 2 mL of 90% (w/v) sucrose in buffer B.
4. In a 5-mL ultracentrifuge tube, pour 2 mL of 5% (w/v) sucrose in buffer D and inject 2 mL of 35% (w/v) sucrose in buffer D underneath the first sucrose solution.
5. Inject 1 mL of the homogenate underneath the discontinuous sucrose gradient.
6. Centrifuge the sucrose gradient at 140,000g for 18–24 h in a swing-out rotor.
7. Collect 0.5 mL fractions from the base of the sucrose gradient and resuspend the insoluble pellet in 0.5 mL of buffer B (brief sonication may be required). Measure the absorbance of each fraction (excluding the pellet) at 620 nm in order to determine the position of the DIGs in the sucrose gradient.

### 3.4. Marker Enzyme Assays

#### 3.4.1. Alkaline Phosphatase (EC 3.1.3.1)

1. Make up the standard working solution of *p*-nitrophenol by diluting 20  $\mu$ L of a 10 mM stock to 1 mL with distilled water.
2. Pipet 0 (blank), 20, 40, 60, 80, and 100  $\mu$ L aliquots of standard working solution into individual wells in a 96-well microtiter plate. Make all of these wells up to 100  $\mu$ L with distilled water.
3. Pipet a suitable volume (maximum 100  $\mu$ L) of sample into the microtiter plate wells and make up if necessary to 100  $\mu$ L with distilled water.
4. Add 100  $\mu$ L of buffer E to both the standard and sample wells and incubate at 37°C until the absorbance (405 nm) values of the samples falls within the calibration range of the standard wells (*see Note 3*).

#### 3.4.2. Aminopeptidase A (EC 3.4.11.7)

1. Pipet 0 (blank), 20, 40, 60, 80, and 100  $\mu$ L aliquots of 1 mM *p*-nitroanilide into individual wells in a 96-well microtiter plate. Make all these wells up to 100  $\mu$ L with buffer F.
2. Pipet a suitable volume (maximum 50  $\mu$ L) of sample into the microtiter plate wells and make up to 100  $\mu$ L with buffer F.
3. Add 100  $\mu$ L of 5 mM  $\alpha$ -glutamyl-*p*-nitroanilide to both the standard and sample wells and incubate at 37°C until the absorbance (405 nm) values of the samples falls within the calibration range of the standard wells (*see Note 3*).

### 3.5. Protein Determination

1. Mix the BCA and 4% (w/v)  $\text{CuSO}_4 \cdot 5\text{H}_2\text{O}$  solutions at a 50:1 ratio to give the working protein reagent.
2. Pipet 2, 4, 6, 8, and 10  $\mu$ g of BSA standards into separate wells of a 96-well microtiter plate along with 10  $\mu$ L distilled water as a blank.
3. Pipet 10  $\mu$ L of the sample into the microtiter plate wells.
4. Add 200  $\mu$ L of the working protein reagent to all of the standard, sample, and blank wells of the plate and incubate at 37°C for 30 min.
5. Read the absorbance of standards and samples at 570 nm (*see Note 3*).

### 3.6. Immunodetection of Presenilin Proteins

1. Resolve the proteins on a 7–17% polyacrylamide gel after incubation of the samples with an equal volume of reducing electrophoresis sample buffer for 30 min at room temperature (*see Note 7*).
2. Transfer the resolved proteins to an Immobilon P PVDF membrane by semidry transfer at a current density of 0.6 mA/cm<sup>2</sup> for 1 h in buffer G (*see Note 8*).
3. Remove the membrane from the transfer kit and soak it for 5 min in buffer C.
4. Block the membrane by incubation for 1 h at room temperature in buffer H with shaking.
5. Wash the membrane for 5 min in buffer C.
6. Incubate the membrane with the desired antipresenilin antibody diluted in buffer J (1:2000, anti-PS-1 hydrophilic loop; 1:5000, anti-PS-1 N-terminus; 1:1000, anti-PS-2 N-terminus) for 2 h at room temperature.
7. Wash the membrane in buffer K for 1 min, followed by two 15-min washes.
8. Incubate the membrane with peroxidase-conjugated secondary antibody diluted in buffer J (1:10,000) for 1 h at room temperature.
9. Wash the membrane in buffer C for 1 min, followed by two 15-min washes.
10. Develop the immunoblot using enhanced chemiluminescence detection reagents according to the manufacturers' instructions.

### 3.7. Presenilin Proteins in DIGs Isolated by the Detergent-Based Method

In our laboratory we have used antibodies raised against amino acid sequences in the hydrophilic loop and N-terminus regions of PS-1 to study the localization of its proteolytic fragments in DIGs (**Fig. 3**). The majority of the C-terminal fragment was effectively solubilized (i.e., the bulk of the signal was detected in fractions 1 and 2 of the sucrose gradient) (**Fig. 3A**). However, when DIGs were isolated from the sucrose gradient and concentrated by ultracentrifugation (*see Note 9*), immunoblotting revealed that the PS-1 C-terminal fragment was present in DIGs at almost the same level as in the total membrane fraction isolated from brain cortex (**Fig. 3B**). The situation was similar for the N-terminal fragment except that it was more readily detectable in unconcentrated sucrose gradient fractions than the C-terminal fragment (**Fig. 3C**). The N-terminal fragment of PS-1 was present in DIGs at a level similar to that found in the total membrane fraction (**Fig. 3D**).

We have also used several antibodies raised against amino acid sequences in the C-terminus, N-terminus, and hydrophilic loop domain of PS-2 to study the association of this protein with DIGs isolated from mouse brain cortex (**Fig. 4**). The results show that endogenous PS-2, unlike PS-1, does not appear to be proteolytically cleaved in mouse brain cortex, i.e., only the full-length protein is detected at approx 56 kDa. Results using various PS-2 expressing cell lines also showed that, although PS-1 was completely processed to C- and N-terminal

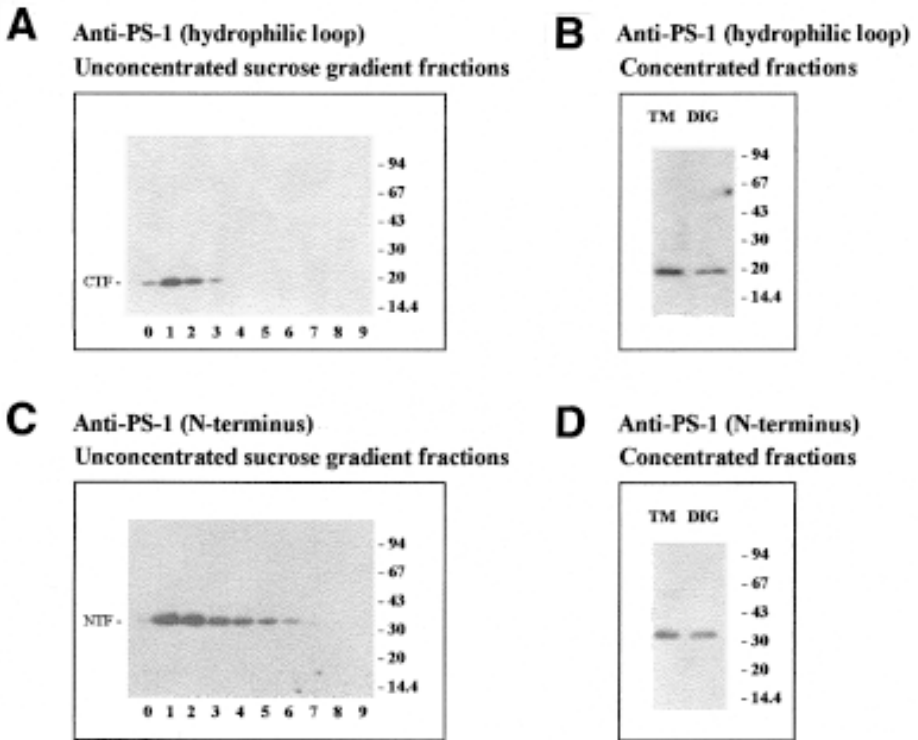


Fig. 3. PS-1 proteolytic fragments in DIGs. DIGs were prepared as described in **Subheading 3.2**. The sucrose gradient was harvested in 0.5 mL fractions (fraction 0, insoluble pellet; fraction 1, base of gradient; fraction 9, top of gradient). In the left-hand plates, protein from individual sucrose gradient fractions was resolved on acrylamide gels and transferred to PVDF membranes prior to immunodetection with either anti-PS-1 (hydrophilic loop) or anti-PS-1 (N-terminus) antibodies. In the right-hand plates, equal amounts of protein from a total membrane (TM) fraction and DIGs were resolved on acrylamide gels, transferred to PVDF membranes, and immunoblotted using the antibodies indicated.

fragments, much higher levels of PS-2 remained in the full-length form (49). The results from mouse brain cortex (Fig. 4A) show that the majority of full-length PS-2 is detergent insoluble, a significant proportion of which is associated with DIGs. Full-length PS-2 is slightly enriched in DIGs relative to the total membrane fraction (Fig. 4B).

#### 4. Notes

1. For example, if the ratio of membrane protein to detergent is too high, the membranes are incompletely solubilized and material that would otherwise be

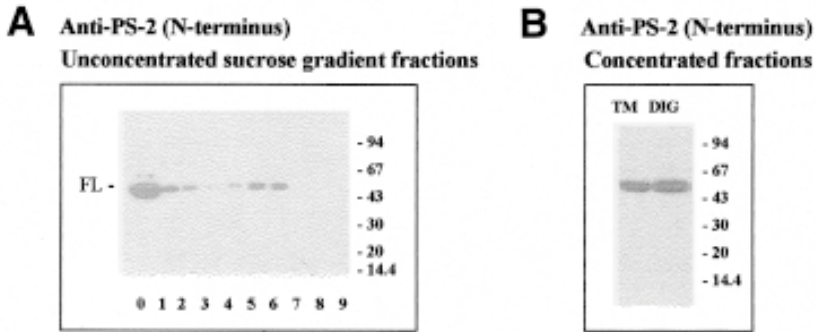


Fig. 4. PS-2 in DIGs. DIGs were prepared as described in **Subheading 3.2**. The sucrose gradient was harvested in 0.5 mL fractions (fraction 0, insoluble pellet; fraction 1, base of gradient; fraction 9, top of gradient). In the left-hand plate, protein from individual sucrose gradient fractions was resolved on an acrylamide gel and transferred to a PVDF membrane prior to immunodetection with anti-PS-2 (N-terminus) antibody. In the right-hand plate, equal amounts of protein from a TM fraction and DIGs were resolved on an acrylamide gel, transferred to a PVDF membrane, and immunoblotted using anti-PS-2 (N-terminus).

detergent-soluble migrates up the sucrose gradient along with the DIGs (E. T. Parkin, A. J. Turner, and N. M. Hooper, unpublished data).

2. With certain cell lines or tissues, it is necessary, following homogenization, to remove nuclei by centrifugation at 5000g for 10 min prior to sucrose density gradient centrifugation. Failure to do so may lead to an abnormally high level of protein in the high-density pellet at the base of the centrifuge tube.
3. Depending on the amount of cells/tissue used, the opacity of the DIGs may interfere with spectrophotometric-based enzyme assays resulting in erroneously high levels of enzyme activity in the DIG region of the sucrose gradient. This problem may be overcome by incubating samples with an equal volume of 120 mM octylglucoside prior to the addition of the reaction substrate.
4. It is possible that, if insufficient detergent is included in the homogenization buffer (especially in detergent-free methods), DIG fractions may be contaminated with membranes of a similar density to DIGs that at higher detergent concentrations would be solubilized. Although DIGs isolated by the carbonate-based method have been shown not to contain clathrin, this does not preclude contamination with coated pits, as clathrin is a peripheral protein that, most likely, is stripped from membranes by sodium carbonate treatment.
5. It is essential to maintain samples at 4°C because DIGs are solubilized by nonionic detergents at higher temperatures.
6. It is recommended that enzyme/protein assays be performed on the resuspended pellet prior to freeze-thawing, as this process leads to aggregation of the insoluble material.

7. Boiling the protein samples leads to the aggregation of PS to high molecular weight oligomers.
8. PVDF membranes must be prewetted in methanol and then soaked in distilled water for 2 min and in transfer buffer for 20 min prior to protein transfer.
9. DIGs can be concentrated/washed by dilution of the relevant sucrose gradient fractions fivefold with buffer B (see **Subheading 2.2.**) followed by ultracentrifugation at 100,000g for 90 min (4°C).

## References

1. Hooper, N. M. and Turner, A. J. (1988) Ectoenzymes of the kidney microvillar membrane. Differential solubilization by detergents can predict a glycosyl phosphatidylinositol membrane anchor. *Biochem. J.* **250**, 865–869.
2. Brown, D. A. and Rose, J. K. (1992) Sorting of GPI-anchored proteins to glycolipid enriched membrane subdomains during transport to the apical cell surface. *Cell* **68**, 533–544.
3. Schroeder, R., London, E., and Brown, D. (1994) Interactions between saturated acyl chains confer detergent resistance on lipids and glycosylphosphatidylinositol (GPI)-anchored proteins: GPI-anchored proteins in liposomes and cells show similar behaviour. *Proc. Natl. Acad. Sci. USA* **91**, 12,130–12,134.
4. Schroeder, R. J., Ahmed, S. N., Zhu, Y., London, E., and Brown, D. A. (1998) Cholesterol and sphingolipid enhance the Triton X-100 insolubility of glycosylphosphatidylinositol-anchored proteins by promoting the formation of detergent-insoluble ordered membrane domains. *J. Biol. Chem.* **273**, 1150–1157.
5. Parkin, E. T., Turner, A. J., and Hooper, N. M. (1996) Isolation and characterization of two distinct low-density, Triton-insoluble, complexes from porcine lung membranes. *Biochem. J.* **319**, 887–896.
6. Macala, L. J., Yu, R. K., and Ando, S. (1983) Analysis of brain lipids by high performance thin-layer chromatography and densitometry. *J. Lipid Res.* **24**, 1243–1250.
7. Simons, K. and Ikonen, E. (1997) Functional rafts in cell membranes. *Nature* **387**, 569–572.
8. Hooper, N. M. (1998) Do glycolipid microdomains really exist? *Curr. Biol.* **8**, R114–R116.
9. Ahmed, S. N., Brown, D. A., and London, E. (1997) On the origin of sphingolipid/cholesterol-rich detergent-insoluble cell membranes: physiological concentrations of cholesterol and sphingolipid induce formation of a detergent-insoluble, liquid-ordered lipid phase in model membranes. *Biochemistry* **36**, 10,944–10,953.
10. Sheets, E. D., Lee, G. M., Simson, R., and Jacobson, K. (1997) Transient confinement of a glycosylphosphatidylinositol-anchored protein in the plasma membrane. *Biochemistry* **36**, 12,449–12,458.
11. Varma, R. and Mayor, S. (1998) GPI-anchored proteins are organized in submicron domains at the cell surface. *Nature* **394**, 798–801.
12. Friedrichson, T. and Kurzchalia, T. V. (1998) Microdomains of GPI-anchored proteins in living cells revealed by crosslinking. *Nature* **394**, 802–805.

13. Kurzchalia, T. V., Dupree, P., Parton, R. G., Kellner, R., Virta, H., Lehnert, M., and Simons, K. (1992) VIP21, a 21 kDa membrane-protein is an integral component of trans-Golgi-network-derived transport vesicles. *J. Cell Biol.* **118**, 1003–1014.
14. Rothberg, K. G., Heuser, J. E., Donzell, W. C., Ying, Y.-S., Glenney, J. R., and Anderson, R. G. W. (1992) Caveolin, a protein-component of caveolae membrane coats. *Cell* **68**, 673–682.
15. Dupree, P., Parton, R. G., Raposo, G., Kurzchalia, T. V., and Simons, K. (1993) Caveolae and sorting in the trans-Golgi network of epithelial cells. *EMBO J.* **12**, 1597–1605.
16. Sargiacomo, M., Sudol, M., Tang, Z., and Lisanti, M. P. (1993) Signal-transducing molecules and glycosyl-phosphatidylinositol-linked proteins form a caveolin-rich insoluble complex in MDCK cells. *J. Cell Biol.* **122**, 789–807.
17. Chun, M., Liyanage, U. K., Lisanti, M. P., and Lodish, H. F. (1994) Signal-transduction of a G-protein-coupled receptor in caveolae-colocalization of endothelin and its receptor with caveolin. *Proc. Natl. Acad. Sci. USA* **91**, 11,728–11,732.
18. Schnitzer, J. E., Oh, P., Jacobson, B. S., and Dvorak, A. M. (1995) Caveolae from luminal plasmalemma of rat lung endothelium-microdomains enriched in caveolin, Ca<sup>2+</sup>-ATPase and inositol. trisphosphate receptor. *Proc. Natl. Acad. Sci. USA* **92**, 1759–1763.
19. Simionescu, N. (1983) Cellular aspects of trans-capillary exchange. *Physiol. Rev.* **63**, 1536–1560.
20. Anderson, R. G. W. (1993) Caveolae-where incoming and outgoing messengers meet. *Proc. Natl. Acad. Sci. USA* **90**, 10,909–10,913.
21. Chang, W.-J., Ying, Y. S., Rothberg, K. G., Hooper, N. M., Turner, A. J., Gambliel, H. A., et al. (1994) Purification and characterization of smooth-muscle cell caveolae. *J. Cell Biol.* **126**, 127–138.
22. Lisanti, M. P., Scherer, P. E., Vidugiriene, J., Tang, Z. L., Hermanowski-Vosatka, A., Tu, Y.-H., et al. (1994) Characterization of caveolin-rich membrane domains isolated from an endothelial-rich source implications for human disease. *J. Cell Biol.* **126**, 111–126.
23. Parpal, S., Gustavsson, J., and Stralfors, P. (1995) Isolation of phosphooligosaccharide phosphoinositol glycan from caveolae and cytosol of insulin-stimulated cells. *J. Cell Biol.* **131**, 125–135.
24. Lisanti, M. P., Tang, Z. L., Scherer, P. E., and Sargiacomo, M. (1995) Caveolae purification and glycosyl-phosphatidylinositol-linked protein sorting in polarized epithelia. *Methods Enzymol.* **250**, 655–668.
25. Schnitzer, J. E., McIntosh, D. P., Dvorak, A. M., Liu, J., and Oh, P. (1995) Separation of caveolae from associated microdomains of GPI-anchored proteins. *Science* **269**, 1435–1439.
26. Schnitzer, J. E., Liu, J., and Oh, P. (1995) Endothelial caveolae have the molecular transport machinery for vesicle budding, docking, and fusion including VAMP, NSF, SNAP, annexins, and GTPases. *J. Biol. Chem.* **270**, 14,399–14,404.
27. Bretscher, M. and Whytock, S. (1977) Membrane-associated vesicles in fibroblasts. *J. Ultrastruct. Res.* **61**, 215–217.

28. Forbes, M. S., Rennels, M., and Nelson, E. (1979) Caveolar systems and sarcoplasmic reticulum in coronary smooth muscle cells. *J. Ultrastruct. Res.* **67**, 325–339.
29. Fan, J. Y., Carpentier, J. L., Vanobberghen, E., Grunfeld, C., Gorden, P., and Orci, L. (1983) Morphological changes of the 3T3–L1 fibroblast plasma membrane upon differentiation to the adipocyte form. *J. Cell Sci.* **61**, 219–230.
30. Simionescu, N. and Simionescu, M. (1983) The cardiovascular system, in *Histology: Cell and Tissue Biology* (Weiss L., ed.), Elsevier Biomedical, New York, pp. 371–433.
31. Gorodinsky, A. and Harris, D. A. (1995) Glycolipid-anchored proteins in neuroblastoma cells form detergent-resistant complexes without caveolin. *J. Cell Biol.* **129**, 619–627.
32. Olive, S., Dubois, C., Schachner, M., and Rougon, G. (1995) The F3 neuronal glycosylphosphatidylinositol-linked molecule is localized to glycolipid-enriched membrane subdomains and interacts with L1 and Fyn kinase in cerebellum. *J. Neurochem.* **65**, 2307–2317.
33. Bouilliot, C., Prochiantz, A., Rougon, G., and Allinquant, B. (1996) Axonal amyloid precursor protein expressed by neurons *in vitro* is present in a membrane fraction with caveolae-like properties. *J. Biol. Chem.* **271**, 7640–7644.
34. Wu, C., Butz, S., Ying, Y., and Anderson, R. G. W. (1997) Tyrosine kinase receptors concentrated in caveolae-like domains from neuronal plasma membrane. *J. Biol. Chem.* **272**, 3554–3559.
35. Parkin, E. T., Hussain, I., Turner, A. J., and Hooper, N. M. (1997) The amyloid precursor protein is not enriched in caveolae-like, detergent-insoluble membrane microdomains. *J. Neurochem.* **69**, 2179–2188.
36. Henke, R. C., Hancox, K. A., and Jeffrey, P. L. (1996) Characterization of two distinct populations of detergent-resistant membrane complexes isolated from chick brain-tissues. *J. Neurosci. Res.* **45**, 617–630.
37. Wild-Bode, C., Yamazaki, T., Capell, A., Leimer, U., Steiner, H., Ihara, Y., and Haass, C. (1997) Intracellular generation and accumulation of amyloid  $\beta$ -peptide terminating at amino acid 42. *J. Biol. Chem.* **272**, 16085–16088.
38. Hartmann, T., Beiger, S. C., Bruhl, B., Tienari, P. J., Ida, N., Allsop, D., et al. (1997) Distinct sites of intracellular production for Alzheimer's disease A $\beta$  40/42 amyloid peptides. *Nat. Med.* **3**, 1016–1020.
39. Cook, D. G., Forman, M. S., Sung, J. C., Leight, S., Kolson, D. L., Iwatsubo, T., et al. (1997) Alzheimer's A $\beta$  (1–42) is generated in the endoplasmic reticulum/intermediate compartment of NT2N cells. *Nat. Med.* **3**, 1021–1023.
40. Xu, H., Sweeney, D., Wang, R., Thinakaran, G., Lo, A. C. Y., Sisodia, S. S., et al. (1997) Generation of Alzheimer  $\beta$  amyloid protein in the trans-Golgi network in the apparent absence of vesicle formation. *Proc. Natl. Acad. Sci. USA* **94**, 3748–3752.
41. Bouilliot, C., Prochiantz, A., Rougon, G., and Allinquant, B. (1996) Axonal amyloid precursor protein expressed by neurons *in vitro* is present in a membrane fraction with caveolae-like properties. *J. Biol. Chem.* **271**, 7640–7644.
42. Simons, M., Keller, P., De Strooper, B., Beyreuther, K., Dotti, C. G., and Simons, K. (1998) Cholesterol depletion inhibits the generation of  $\beta$ -amyloid in hippocampal neurons. *Proc. Natl. Acad. Sci. USA* **95**, 6460–6464.

43. Lee, S., Liyanage, U., Bickel, P. E., Xia, W., Lansbury Jr., P. T., and Kosik, K. S. (1998) A detergent-insoluble membrane compartment contains A $\beta$  *in vivo*. *Nat. Med.* **4**, 730–734.
44. De Strooper, B., Saftig, P., Craessaerts, K., Vanderstichele, H., Guhde, G., Annaert, W., et al. (1998) Deficiency of presenilin- 1 inhibits the normal cleavage of amyloid precursor protein. *Nature* **329**, 387–390.
45. Cook, D. G., Sung, J. C., Golde, T. E., Felsenstein, K. M., Wojczyk, B. S., Tanzi, R. E., et al. (1996) Expression and analysis of presenilin 1 in a human neuronal system: localization in cell bodies and dendrites. *Proc. Natl. Acad. Sci. USA* **93**, 9223–9228.
46. Takashima, A., Sato, M., Mercken, M., Tanaka, S., Kondo, S., Honda, T., et al. (1996) Localization of Alzheimer-associated presenilin 1 in transfected COS-7 cells. *Biochem. Biophys. Res. Commun.* **227**, 423–426.
47. Kim, T.-W., Pettingell, W. H., Hallmark, O. G., Moir, R. D., Wasco, W., and Tanzi, R. E. (1997) Endoproteolytic cleavage and proteasomal degradation of presenilin-2 in transfected cells. *J. Biol. Chem.* **272**, 11006–11016.
48. Tanzi, R. E., Kovacs, D. M., Kim, T.-W., Moir, R. D., Guenette, S. Y., and Wasco, W. (1996) The gene defects responsible for familial Alzheimer's disease. *Neurobiol. Dis.* **3**, 159–168.
49. Parkin, E. T., Hussain, I., Karran, E. H., Turner, A. J., and Hooper, N. M. (1998) Characterisation of detergent-insoluble complexes containing the familial Alzheimer's disease-associated presenilins. *J. Neurochem.* **72**, 1534–1543.
50. Ikezu, T., Trapp, B. D., Song, K. S., Schlegel, A., Lisanti, M. P., and Okamoto, T. (1998) Caveolae, plasma membrane microdomains for  $\alpha$ -secretase-mediated processing of the amyloid precursor protein. *J. Biol. Chem.* **273**, 10,485–10,495.
51. Smart, E. J., Ying, Y., Mineo, C., and Anderson, R. G. W. (1995) A detergent- free method for purifying caveolae membrane from tissue-culture cells. *Proc. Natl. Acad. Sci. USA* **92**, 10,104–10,108.

## Characterization and Use of Monoclonal Antibodies to Tau and Paired Helical Filament Tau

Peter Davies

### 1. Introduction

Antibodies to the microtubule-associated protein tau have been used for more than a decade, both in studies of the role of tau neuronal function, and in examination of the neurofibrillary pathology of Alzheimer's disease (AD). The vast majority of the available antibodies have been produced with preparations obtained from the brains of patients with AD, although a few antibodies have been generated with tau purified from bovine brain. This chapter restricts discussion to the production and characterization of monoclonal antibodies, although some investigators continue to use affinity-purified polyclonal antibodies. The opinions expressed in this chapter are based on the author's experience in the production of several series of monoclonal antibodies to tau and paired helical filaments (PHF-tau) over the last 10 yr. There is no doubt that modifications in the procedures described can be developed for specific purposes, but the discussion is confined to those methods that we have found to be reliable and informative.

#### 1.1. Antigen Preparation

Tau can readily be obtained in large quantities in fairly pure form either by expression of recombinant protein in bacteria (excellent detailed methodology is provided in **ref. 1**) or from animal or normal human brain using a variety of purification methods (e.g., **ref. 2**). There are also several published methods for partial purification of PHF-tau from postmortem brain tissue of AD cases (**3,4**). Purity of the preparations is not a major concern in the production of monoclonal antibodies, provided that appropriate screening methodologies are used to identify and characterize the monoclonal antibodies. However, tau or

PHF-tau should comprise at least 20% of the protein present in the immunogen.

### **1.2. Immunization**

Adjuvants have not been found to be useful in the generation of high-titer antibodies in mice (our work has used exclusively female balb/c mice, ages 6 wk to 9 mo). Depending on the purpose for which antibodies are to be produced (*see* below), crosslinking with an excess of glutaraldehyde, followed by dialysis to remove excess, can be useful. No other treatment of antigen preparations has been used in our work. Mice are immunized intraperitoneally with solutions containing 1–2 mg protein per milliliter, 0.2 mL per injection, at two weekly intervals, usually for 8 wk. One week after the last injection, blood samples are taken and serum separated out for determination of antibody titer. Immunoblotting with the preparation used for immunization (but not glutaraldehyde crosslinked) is preferred for this purpose, as the serum antibodies are very nonspecific, and the only concern here is the detection of antibodies to the protein of appropriate molecular weight. If the mice have serum titers of antibodies such that a 1:2000 dilution will stain tau bands on the blot, immunization is halted for at least a month prior to fusion. Injections of antigen every 2 wk can be continued until this titer is achieved.

### **1.3. Fusion**

Mice are injected with antigen 3 d before spleens are removed, and spleen cells are fused with myeloma cells in the presence of polyethylene glycol using a published protocol (5). Fusion products are plated in 96-well plates in selection medium (hypoxanthine-aminopterin-thymidine) and allowed to grow until cells cover about 30% of the bottom of the well. At this point, samples of culture medium are taken for initial screening.

### **1.4. Selection of Antibodies for Further Characterization**

Because a large number (500–3000) of hybrid cell lines usually result from a fusion, it is important to have a rapid and sensitive method to select the antibodies of greatest potential utility. Experience has taught that it is most efficient to screen for antibodies that will perform well in the technique for which they are intended. One of the major uses of antibodies to PHF-tau is immunocytochemical examination of the postmortem human brain, or fixed animal brain. However, screening 500–3000 cell culture medium samples by immunocytochemistry is very tedious, and the same applies to screening this number of samples by immunoblotting. If antibodies are intended for use primarily in immunocytochemistry, the crosslinking of proteins with glutaraldehyde is probably useful, as proteins in tissues are likely to be modified in the same way by

fixation in formalin, paraformaldehyde, or glutaraldehyde. Our strategy has been to adopt a rapid three-stage screening process, in which an ELISA assay is used for initial identification of antibodies reactive with the antigen preparation, followed by discarding all those hybrids that do not give robust signals (over 80% of hybrids are usually eliminated at this stage). Remaining clones are screened by immunoblotting using strips of nitrocellulose obtained by transfer of proteins from sodium dodecyl sulfate-polyacrylamide gel electrophoresis (SDS-PAGE) gels, usually run with samples of PHF-tau and/or recombinant tau (up to 50% of antibodies are eliminated at this stage). Strongly positive clones are screened by staining of formalin fixed human brain tissue. Antibodies qualifying for detailed characterization thus produce strong signals in ELISA assays, robust staining of tau and/or PHF-tau on immunoblots and strong staining of neurofibrillary pathology in tissue sections from brains of patients with AD.

It is obvious that some antibodies, e.g., those reactive with denatured proteins on immunoblots that do not stain formalin fixed tissue sections, will be discarded in such screening. However, such antibodies can be extremely difficult and time consuming to characterize and are usually better discarded. In four recent fusions, an average of 1500 clones per fusion have been screened with the above strategy, and 20–40 clones per fusion survived the selection process. About half of these antibodies have proved to be useful reagents.

## **1.5. Characterization of Antibodies**

### **1.5.1. General Considerations**

As mentioned earlier, some thought about the purpose for making tau antibodies prior to designing screening techniques is very valuable in efficient selection of antibodies, and the nature of the immunogen will also be a major factor in determining the complexity of the antibody response. Four classes of tau or PHF-tau monoclonal antibodies have been produced to date, and characterization of antibodies is facilitated by determination of which class they belong to.

### **1.5.2. Tau Sequence Antibodies**

The simplest way to identify such antibodies is by immunoblotting of bacterially expressed recombinant tau, alongside tau isolated from human or animal brain. As discussed below, this allows discrimination of antibodies to phosphoepitopes from those requiring unmodified sequences. However, it does not always distinguish antibodies dependent on conformational epitopes from those requiring a single continuous amino acid sequence. Antibodies that specifically recognize the primary amino acid sequence of tau are surprisingly rare, and only two of these have been extensively characterized in the literature.

Tau1 was raised using bovine brain tau as the immunogen and reacts with an amino acid sequence of tau in the region of amino acids 195–205 (numbering according to the longest, 441 isoform of central nervous system tau) (6). Antibody reactivity is blocked by phosphorylation of tau at serine202, and thus tau1 reactivity with PHF-tau is generally very weak, unless alkaline phosphatase treatment is used. Tau46 recognizes a sequence in the C-terminal 30 amino acids of tau, and reacts with all microtubule-associated protein-2 (MAP2) isoforms, in which the sequence is highly homologous (7). Tau46 reactivity with tau does not appear to be affected by phosphorylation, since strong reactivity with PHF-tau is obtained on immunoblots. Tau 1 and tau46 are both commercially available (Boehringer Mannheim, Mannheim, Germany), and are both useful for immunoblotting.

Once an antibody is identified as reactive with bacterially expressed recombinant tau, mapping the sequence requirements can be performed by construction of a panel of overlapping deletions of the recombinant proteins, as was done, e.g., by Carmel et al. (8). Two important points have emerged from such studies of antibodies to tau or PHF-tau.

First, antibodies have been found that require two widely separated amino acid sequences. Alz50 and MC1, two antibodies that react with all forms of tau by immunoblotting, require an N-terminal sequence *and* a sequence in the third microtubule binding domain for reactivity. The amino terminal epitope was discovered almost 10 yr ago (9,10), but the requirement for the second sequence was not defined until some 8 yr later (8,11). This emphasizes the need for a thorough examination of the tau sequence when attempting to define sequence epitopes for antibodies. Second, definition of even a single amino acid sequence as the epitope does not ensure that the antibody will be useful for immunoprecipitation. Tau1 reactivity can be masked by phosphorylation, and tau46 is only marginally useful in this application, probably because of local secondary structure at the C-terminus of tau. Alz50 and MC1 will not immunoprecipitate recombinant or animal brain tau, presumably because the two sequence epitopes are not appropriately aligned, although both antibodies are efficient at immunoprecipitation of PHF-tau, as is tau46.

Newer anti-tau monoclonal antibodies, developed for ELISA assay of tau in cerebrospinal fluid appear to be sequence-directed antibodies that recognize multiple tau isoforms. However, there is as yet no published characterization of these antibodies and they are not generally available (12,13).

### 1.5.3. Conformational Antibodies

The first antibody of this class produced was Alz50, an antibody that has been widely used in studies of tau and PHF-tau. A similar, but not identical antibody, MC1 has since been reported (11), and we have recently produced

additional monoclonals of this type. These antibodies have all been shown to require two widely separated amino acid sequences in tau for reactivity, and the assumption is that these two sequences must be brought together by protein folding to allow formation of the antibody binding site. There are several precedents for generation of conformation specific antibodies, but Alz50 and MC1 are rather unusual in that they both react with all forms of tau containing these sequences on immunoblots, after boiling the tau preparations in 2% SDS and 5%  $\beta$ -mercaptoethanol. It is generally assumed that conformation-dependent antibodies will be useless in immunoblot studies because of denaturation caused by the detergent and heat, but it appears that this treatment, followed by transfer to nitrocellulose, actually facilitates the folding of tau into the appropriate conformation for antibody reactivity (11,14). Neither recombinant tau nor tau prepared from normal animal or human brain is reactive with these two antibodies in solution assays (ELISA or immunoprecipitation) (14), indicating that under normal conditions the two epitopes are not adjacent to each other. This conclusion is supported by biophysical studies of tau, which show an essentially random coil structure (15). PHF-tau, by contrast, is bound by both Alz50 and MC1 in solution (by ELISA and immunoprecipitation), suggesting that the conformation of tau is altered in the brains of patients with AD. MC1 has been coupled to agarose beads for use as an efficient immunoaffinity purification of PHF-tau from AD brain tissue (16).

With the foregoing considerations, it is clear that conformational tau antibodies are most efficiently generated with PHF-tau as the immunogen. MC1 and three additional conformational antibodies were obtained in this way, using the screening strategy previously outlined. Distinguishing between conformational and single-sequence dependent antibodies required that initial ELISA screening be conducted with both recombinant tau (which was not reactive with conformational antibodies, but was positive with single sequence antibodies) and PHF-tau (which was positive with both), in addition to immunoblotting and tissue staining. As mentioned previously, mapping of epitopes for conformational antibodies requires a full panel of overlapping tau deletion constructs.

#### 1.5.4. Antibodies to Phosphorylated Epitopes

If tau from animal or human brain is used as an immunogen, there is a possibility of obtaining antibodies to phosphorylated sites on tau, and this appears to be quite common when PHF-tau is used. In screening, antibodies reactive on immunoblots with PHF-tau, but not with recombinant tau expressed in bacteria, are most frequently found to be dependent for binding on the presence of one or more phosphorylated amino acids. Note that such selectivity detected by ELISA or immunoprecipitation assays could result from the presence of

either conformational- or phosphorylation-dependent antibodies. However, all tau conformational antibodies discovered to date react with recombinant tau on immunoblots. Antibodies to phosphorylated epitopes usually stain neurofibrillary pathology in AD brain tissue, but show little or no staining of normal autopsy-derived human brain, and similar results are obtained with conformation-specific antibodies. Thus, care is needed in the choice of screening techniques: Alz50 was initially thought to be a phosphorylation-dependent antibody.

Initial identification of phosphorylation-dependent antibodies is usually based on a lack of reactivity with recombinant tau and reactivity with PHF-tau by immunoblotting. If alkaline phosphatase treatment of PHF-tau reduces or abolishes antibody reactivity (without significant proteolysis), it seems safe to assume that a phosphodependent antibody has been identified. However, it is virtually impossible to remove all phosphates from PHF-tau with alkaline phosphatase (17,18), thus a lack of effect of the phosphatase does not exclude the possibility that the antibody is phospho-dependent. Characterization of monoclonal antibodies thought to be dependent on phosphorylation of amino acids in tau is not a trivial exercise. More than 20 sites in tau have been reported to be phosphorylated in PHF-tau (18,19), and many of these sites also appear to be phosphorylated in both fresh animal brain tissue as well as in human tissues obtained by brain biopsy (20). Although tau is an excellent substrate for most protein kinases *in vitro* (see, e.g., ref. 16), treatment of tau with several different kinases is necessary to ensure phosphorylation at the majority of these sites. Generation of a specific phosphoepitope on recombinant tau can thus require extensive trial-and-error work with different protein kinases. Published work in this area has resorted to the use of brain extracts as a source of kinase activity (21). Once antibody reactivity can be generated using recombinant tau and a kinase preparation, panels of tau deletion constructs and/or site-directed mutagenesis can be used to attempt to precisely locate the epitope. This approach requires a great deal of work when multiple different phospho-dependent antibodies have been generated.

Synthesis of tau phosphopeptides offers a simple but costly alternative approach to characterization of antibodies of this class, and provides positive rather than negative data regarding antibody reactivity. Otvos et al. (22) mapped the phosphorylation requirements of the antibody PHF1 in this way, and showed that phosphorylation of either serine396 or serine 404 (or both) was required for reactivity (22). Jicha et al. (23) were able to confirm that both the AT180 and TG3 antibodies reacted with peptides containing phosphothreonine231 of tau, but not with the corresponding nonphosphorylated peptides (23). We have recently made a small library of tau phosphopeptides, and have used these to screen hybrid cell lines for antibodies reactive with specific phosphoepitopes.

Biotinylation of the N-terminus of the phosphopeptide allowed efficient immobilization of the peptide on avidin-coated ELISA plates. This strategy was successful in directly identifying antibodies to 11 different phosphoepitopes on tau. All the antibodies identified by this screen have been shown to react with PHF-tau by immunoblotting, and to stain tissue sections from AD brain.

Two phosphodependent antibodies have been reported to require two phosphorylations on tau for reactivity. AT100 apparently requires phosphorylation of serines 212 and 214, and MC5 requires phosphorylation at threonine 231 and serine 235 for reactivity (24, P. Davies, R. Hoffmann, and L. Otvos, Jr. unpublished work). In both cases, synthesis of the diphosphopeptide was necessary to confirm this requirement. Both antibodies show reactivity with PHF-tau on immunoblots, and stain neurofibrillary pathology in the AD brain.

### *1.5.5. Complex Antibodies*

TG3 is a mouse monoclonal antibody generated using PHF-tau as the immunogen (25). This antibody has been shown by Jicha et al. (23) to require both conformational and phosphorylated epitopes on tau. TG3 requires phosphorylation at threonine 231 of tau, but is not reactive with peptides or tau derived from normal human or animal brain if both threonine 231 and serine 235 are phosphorylated. It is, however, reactive with PHF-tau, and with the diphosphopeptide dried onto ELISA plates from trifluoroethanol, indicating that a specific conformation in the region of phosphorylation is important for antibody reactivity. TG3 is an excellent reagent for visualizing neurofibrillary pathology in the AD brain, again indicating that both conformational changes and phosphorylation of tau occurs in AD. It is worth noting that TG3 was originally thought to be a purely conformational antibody, because alkaline phosphatase treatment of PHF-tau consistently failed to remove TG3 reactivity. In this case, the studies of reactivity of this antibody with synthetic peptides and phosphopeptides proved to be critical data in characterization of this antibody.

### **1.6. Evaluation of Antibody Specificity**

Whichever class of antibody is identified by the techniques just described, there are some general points with regard to antibody specificity that need attention. Antibody specificity is rarely an absolute, and the apparent specificity of antibodies can be different depending on factors such as antibody concentration, antigen concentration, time and temperature of incubation, and the sensitivity of detection methods. Space does not permit a full discussion of all these issues, but some specificity testing is clearly essential.

The proteins most likely to crossreact with antibodies to tau are the other microtubule associated proteins, which share considerable homology. Tau46 has been cited as an example of a sequence antibody that cross reacts with all

MAP2 isoforms because of homologous sequences at the C-terminus. Heat-stable fractions from animal and human brain should be prepared for evaluation of possible crossreactivity by immunoblotting, as the molecular weights of the MAP2 isoforms are distinct from those of tau. As both single-sequence and phospho-dependent antibodies may show crossreactivity, both should be evaluated by this means. Immunoblotting of total brain homogenates is also routinely used to assess potential crossreactivity of antibodies with nonMAP proteins. Most of the antibodies recognizing phosphoserine235 of tau produced in the author's laboratory have some crossreactivity with high molecular weight neurofilament proteins, which have numerous similar epitopes (KphosphoSP). It seems likely that many phospho-dependent antibodies will show less than absolute specificity, as at least some degree of conservation of amino acid sequences is necessary to form consensus sequences for protein kinase and protein phosphatase recognition. It is somewhat surprising that this point has not been more of a problem for production of antibodies to specific phosphorylated epitopes, but this is rarely addressed in published work.

Conformation-dependent antibodies might be expected to have a very high degree of specificity, but in the case of the prototype antibody, Alz50, at least one other protein has been discovered to be reactive. FAC is a protein with no significant amino acid sequence homology to tau, and yet shows strong reactivity with Alz50 (26). A monoclonal antibody raised with recombinant FAC as the immunogen also shows strong reactivity with tau (27), arguing that, despite the lack of obvious sequence homology, these two proteins must both have a specific epitope.

## 2. Materials

### 2.1. ELISA (Direct Coating)

ELISA plates used are NUNC-Immuno plate F96 Cert.Maxisorb, obtained from Nalgene Nunc International (Roskilde, Denmark). Nonfat dried milk is Carnation brand, purchased from a local market. Peroxidase-labeled goat antimouse antibodies can be obtained from several suppliers, but we have found that consistently high-quality products are obtained from Southern Biotechnology (purchased through Fisher Scientific Suppliers, Pittsburgh, PA). 2,2'-azino-di (3-ethyl-benzthiazoline-6-sulphonic acid (ABTS) peroxidase substrate is obtained as a kit from Bio-Rad Labs.

### 2.2. ELISA (NeutrAvidin)

NeutrAvidin (Immunopure) is purchased from Pierce Chemical Co. (Rockford, IL). Bradford Protein Assay reagent is purchased from Bio-Rad Laboratories, Hercules, CA. N-hydroxysuccinimidobiotin is obtained from either Pierce or from Sigma Chemical Co. (St. Louis, MO). Use the same peroxidase-labeled goat antimouse immunoglobulin G (IgG) and substrate as in **Subheading 2.1**.

### 2.3. Immunoblotting

Use the same peroxidase-labeled goat antimouse IgG as in **Subheading 2.1.**, but use 4-chloronaphthol (Sigma) as the substrate (2 mg/mL in methanol: dilute 1:5 with Tris-buffered saline (TBS) immediately prior to use, and add 0.03% H<sub>2</sub>O<sub>2</sub>).

### 2.4. Immunocytochemistry

Use the same peroxidase-labeled goat antimouse IgG as in **Subheading 2.1.**, but use diaminobenzidine (Sigma) as the substrate (0.3 mg/mL diaminobenzidine, 0.03% H<sub>2</sub>O<sub>2</sub> in 100 mM Tris-HCl, pH 7.4, for 8 min at room temperature).

## 3. Methods

### 3.1. ELISA

All volumes in ELISA plates are 50  $\mu$ L, except for storage, where 200  $\mu$ L is added.

#### 3.1.1. Direct Coating

1. Coat ELISA plates with tau or PHF-tau in 20 mM K<sub>2</sub>HPO<sub>4</sub>/10 mM KH<sub>2</sub>PO<sub>4</sub>, 1 mM EDTA, 0.8% NaCl, 0.01% NaN<sub>3</sub>, pH 7.2, using a protein concentration (estimated with the Bradford assay) of 2  $\mu$ g/mL.
2. After coating, block plates with 10 mM Tris-HCl, 150 mM NaCl, pH 7.4 (TBS) containing 5% nonfat dry milk and store at 4°C, no longer than 48 h.

#### 3.1.2. NeutrAvidin Coating

1. Coat plates with NeutrAvidin at 5 micrograms per mL in the same buffer. Coat for 3 h at room temperature, with plates covered.
2. For NeutrAvidin plates, biotinylate tau and PHF-tau in 50 mM NaH<sub>2</sub>PO<sub>4</sub>, pH 8.0, using a 4–6 molar excess of N-hydroxysuccinimidobiotin, for 1 h at room temperature. Remove excess biotinylation reagent by dialysis, and store the protein in aliquots at –70°C. Because tau has more than 30 lysine residues, and biotinylation under these conditions is essentially random, there is little danger of destroying tau epitopes by this procedure.
3. Block and store NeutrAvidin coated plates at 4°C in coating buffer to which is added 2% bovine serum albumin (BSA); these are usable for up to 6 wk.
4. Dilute biotinylated proteins in 2% BSA in TBS to 2  $\mu$ g/mL, and apply to plates for 1 h at room temperature, immediately before use in assay (*see Note 1*). Biotinylated peptides and phosphopeptides are purified by reverse phase high-performance liquid chromatography, and used at 1  $\mu$ M to coat plates in 2% BSA in coating buffer. Peptide- and phosphopeptide-coated plates are stable for at least 48 h in the cold.

#### 3.1.3. ELISA

1. Dilute culture supernatants from hybrids in TBS containing 5% milk, generally 1:25 dilution and apply to plates, usually for 1–3 h at room temperature (*see Note 2*).

2. Detect antibody binding using goat antimouse IgG (heavy and light chain) conjugated to horseradish peroxidase (HRP) (*see Note 3*), and a suitable peroxidase substrate. Only strongly positive hybrids should be selected for subsequent analysis.

### 3.2. Immunoblotting

1. Run standard 10% SDS-PAGE gels for immunoblotting, with tau samples boiled prior to loading in 2% SDS 5%  $\beta$ -mercaptoethanol.
2. Transfer proteins to nitrocellulose, and block with TBS/5% milk for at least 1 h. Proteins appear to be stable on blocked nitrocellulose for at least 48 h. If combs with only a single large well are used, thin strips (1–2 mm wide) of nitrocellulose can be cut to allow large numbers of samples to be screened from a single gel.
3. Dilute tissue culture supernatants in milk and incubate with nitrocellulose strips for a minimum of 3 h at room temperature (or overnight at 4°C), wash, and detect antibody binding using goat antimouse IgG (heavy and light chain) conjugated to horseradish peroxidase, using 4-chloronaphthol as substrate (*see Note 4*).

### 3.3. Immunocytochemistry

1. Screen hybrids using formalin-fixed human brain tissues cut on a vibratome. The use of routine autopsy tissue is advantageous in that antibodies that stain such tissue well allow access to the archives of a typical pathology department, and hence large numbers of cases can be investigated. Antibodies that need more fixation have seldom proved to be worth keeping.
2. Cut sections at 50-micron thickness with the vibratome from human cerebral cortex (Alzheimer or normal): 2 mm square. With practice, several blocks of this size can be cut at the same time. This allows immunocytochemical screening to be performed in 48- or 96-well plates (*see Note 5*).
3. Incubate sections with TBS containing 3%  $H_2O_2$ /0.2% Triton X-100 for 30 min, and then transfer to TBS/5% milk for blocking for 1 h.
4. Transfer sections to tissue culture supernatants diluted in milk and incubate for at least 3 h at room temperature, or overnight in the cold.
5. Detect antibody binding with goat antimouse IgG (heavy and light chain) conjugated to HRP, using diaminobenzidine as substrate. With care, up to 30 sections can be mounted on a single slide for dehydration and coverslipping, and this speeds up analysis of the results considerably.

## 4. Notes

1. Milk- or serum-based blocks contain biotin, and thus should not be used with avidin-coated plates prior to coating with biotinylated proteins or peptides. Solutions containing 2% BSA provide adequate control of nonspecific binding. Once plates are coated with biotinylated peptides, solutions containing milk (e.g., diluted tissue culture supernatants) can be used without significant loss of signal.
2. The use of short incubation times and relatively high dilutions of culture supernatants favors the detection and selection of high-affinity antibodies. The same aim can be achieved by reducing concentrations of antigen. Longer

incubations and less diluted culture supernatants should be avoided unless low-affinity antibodies are particularly desired.

3. The choice of a secondary goat antimouse IgG (heavy and light chain) is to attempt to ensure that all subclasses of mouse IgG as well as IgMs are detected. Some investigators appear to have a bias against IgM antibodies, but one of the most widely used antibodies in this field, Alz50, is of this isotype. It is possible to substitute subclass-specific secondary antibodies in screening, if there is a need for an antibody of a particular isotype. Mouse IgM and IgG1 subclass antibodies bind poorly to protein A, and therefore its use will strongly bias the isotype of antibodies selected.
4. Chemiluminescent detection systems are avoided in screening antibodies, as they are much more sensitive than colorimetric methods, and the selection of robust reagents is facilitated by the use of relatively insensitive methods in screening and selection.
5. By far the most practical method we have found to screen monoclonal antibodies by immunocytochemistry is the use of formalin-fixed brain tissue cut on a vibratome. The sections are generally cut at 50-micron thickness, and are robust enough to be transferred from container to container with a disposable bacteria loop. Frontal or temporal gyrus from normal and Alzheimer cases is usually used for screening, as these structures are large enough to provide hundreds of sections, and in an advanced AD case, show an even distribution of neurofibrillary pathology. A block of a full gyrus can be cut, and the section sliced into small (2 mm square) pieces, or a block from a gyrus can be mounted on the vibratome chuck, sliced at 2 mm intervals perpendicular to the vibratome blade, and several sections are then cut with each blade stroke. Small tissue pieces are transferred to 48- or 96-well plates, and all the tissue staining can be conducted without transfer of the tissue. Blocking, washing, and staining solutions are added to the wells with multichannel pipets, and removed by careful suction, using a gel-loading pipet tip attached to a vacuum line. Some practice is advisable, to avoid sucking up the tissue section with the solution.

## Acknowledgments

The author's research is supported by National Institute of Mental Health grant 38623 and National Institute of Aging grant 06803. Many laboratory members have contributed to the development of the ideas and techniques described here, especially Ben Wolozin, Inez Vincent, and Bill Honer. Samples of the antibodies Alz50, MC1, PHF1, and TG3 are available free on the signing of an Albert Einstein College of Medicine Material Transfer Agreement. Contact the author for further information.

## References

1. Brandt, R., Kempf, M., and Lee, G. (1997) Expression and purification of tau for in vitro studies, in *Brain Microtubule-Associated Proteins: Practical*

- Approaches* (Avila, J., Brandt, R., and Kosik, K. S., eds.), Harwood Academic Publishers, pp. 245–257.
2. Vallee, R. B. (1982) A taxol-dependent procedure for the isolation of microtubules and microtubule-associated proteins (MAPs). *J. Cell Biol.* **92**, 435–442.
  3. Greenberg, S. G. and Davies, P. (1990) A preparation of Alzheimer paired helical filaments that displays distinct tau proteins by polyacrylamide gel electrophoresis. *Proc. Natl. Acad. Sci. USA* **87**, 5827–5831.
  4. Vincent, I. J. and Davies, P. (1992) A protein kinase associated with the paired helical filaments in Alzheimer's disease. *Proc. Natl. Acad. Sci. USA* **89**, 2878–2882.
  5. de St. Groth, S. F. and Scheidegger, D. (1980) Production of monoclonal antibodies: strategy and tactics. *J. Immunol. Methods* **35**, 1–21.
  6. Szendrei, G. I., Lee, V. M., and Otvos, L., Jr. (1993) Recognition of the minimal epitope of monoclonal antibody Tau-1 depends upon the presence of a phosphate group but not its location. *J. Neurosci. Res.* **34**, 243–249.
  7. Kalcheva, N., Alcala, J. S., Binder, L. I., and Shafit-Zagardo, B. (1994) Localization of specific epitopes on human microtubule-associated protein 2. *J. Neurochem.* **63**, 2336–2341.
  8. Carmel, G., Mager, E. M., Binder, L. I., and Kuret, J. (1996) The structural basis of monoclonal antibody Alz50's selectivity for Alzheimer's disease pathology. *J. Biol. Chem.* **271**, 32,789–32,795.
  9. Ksiazek-Reding, H., Chien, C. H., Lee, V. M., and Yen, S.-H. (1990) Mapping of the Alz 50 epitope in microtubule-associated proteins tau. *J. Neurosci. Res.* **25**, 412–419.
  10. Goedert, M., Spillantini, M. G., and Jakes, R. (1991) Localization of the Alz-50 epitope in recombinant human microtubule-associated protein tau. *Neurosci. Lett.* **126**, 149–154.
  11. Jicha, G. A., Bowser, R., Kazam, I. G., and Davies, P. (1997) Alz-50 and MC-1, a new monoclonal antibody raised to paired helical filaments, recognize conformational epitopes on recombinant tau. *J. Neurosci. Res.* **48**, 128–132.
  12. Vandermeeren, M., Mercken, M., Vanmechelen, E., Six, J., van de Voorde, A., Martin, J. J., and Cras, P. (1993) Detection of tau proteins in normal and Alzheimer's disease cerebrospinal fluid with a sensitive sandwich enzyme-linked immunosorbent assay. *J. Neurochem.* **61**, 1828–1834.
  13. Johnson, G. V., Seubert, P., Cox, T. M., Motter, R., Brown, J. P., and Galasko, D. (1997) The tau protein in human cerebrospinal fluid in Alzheimer's disease consists of proteolytically derived fragments. *J. Neurochem.* **68**, 430–433.
  14. Jicha, G. A., Berenfeld, B., and Davies, P. (1998) Sequence requirements for formation of conformational variants of tau similar to those found in Alzheimer's disease. *J. Neurosci. Res.* **55**, 713–723.
  15. Schweers, O., Schonbrunn-Hanebeck, E., Marx, A., and Mandelkow, E. (1994) Structural studies of tau protein and Alzheimer paired helical filaments show no evidence for beta structure. *J. Biol. Chem.* **269**, 24,290–24,297.
  16. Jicha, G. A., O'Donnell, A., Weaver, C., Angeletti, R., and Davies, P. (1998) Hierarchical phosphorylation of recombinant tau by the paired helical filament

- associated protein kinase is dependent on cAMP-dependent protein kinase. *J. Neurochem.* **72**, 214–224.
17. Ksiezak-Reding, H., Liu, W. K., and Yen, S.-H. (1992) Phosphate analysis and dephosphorylation of modified tau associated with paired helical filaments. *Brain Res.* **597**, 209–219.
  18. Greenberg, S. G., Davies, P., Schein, J. D., and Binder, L. I. (1992) Hydrofluoric acid-treated tau-PHF proteins display the same biochemical properties as normal tau. *J. Biol. Chem.* **267**, 564–569.
  19. Hasegawa, M., Morishima-Kawashima, M., Takio, K., Suzuki, M., Titani, K., and Ihara, Y. (1992) Protein sequence and mass spectrometric analyses of tau in the Alzheimer's disease brain. *J. Biol. Chem.* **267**, 17,047–17,054.
  20. Matsuo, E. S., Shin, R. W., Billingsley, M. L., Van deVoorde, A., O'Connor, M., Trojanowski, J. Q., and Lee, V. M. (1994) Biopsy-derived adult human brain tau is phosphorylated at many of the same sites as Alzheimer's disease paired helical filament tau. *Neuron* **13**, 989–1002.
  21. Goedert, M., Jakes, R., Crowther, R. A., Cohen, P., Vanmechelen, E., Vandermeeren, M., and Cras, P. (1994) Epitope mapping of monoclonal antibodies to the paired helical filaments of Alzheimer's disease: identification of phosphorylation sites in tau protein. *Biochem. J.* **301**, 871–877.
  22. Otvos, L. Jr., Feiner, L., Lang, E., Szendrei, G. I., Goedert, M., and Lee, V. M. (1994) Monoclonal antibody PHF-1 recognizes tau protein phosphorylated at serine residues 396 and 404. *J. Neurosci. Res.* **39**, 669–673.
  23. Jicha, G. A., Lane, E., Vincent, I. J., Otvos, L., Hoffmann, R., and Davies, P. (1997) A conformation and phosphorylation dependent antibody recognizing the paired helical filaments of Alzheimer's disease. *J. Neurochem.* **69**, 2087–2095.
  24. Hoffmann, R., Lee, V. M., Leight, S., Varga, I., and Otvos, L. Jr. (1997) Unique Alzheimer's disease paired helical filament specific epitopes involve double-phosphorylation at specific sites. *Biochemistry* **36**, 8114–8124.
  25. Vincent, I. J., Rosado, M., and Davies, P. (1996) Mitotic mechanisms in Alzheimer's disease? *J. Cell. Biol.* **132**, 413–425.
  26. Bowser, R., Giamboni, M. A., and Davies, P. (1995) FAC1, a novel gene identified with the monoclonal antibody Alz50, is developmentally regulated in human brain. *Devel. Neurobiol.* **17**, 20–37.
  27. Schoonover, S., Jicha, G., Kazam, I., Davies, P., and Bowser, R. (1995) A novel antibody to a primary sequence epitope of tau recognizes neuritic lesions in Alzheimer's disease. *Alzheimer's Res.* **1**, 35–40.

## Tau Phosphorylation Both In Vitro and in Cells

C. Hugh Reynolds, Graham M. Gibb, and Simon Lovestone

### 1. Introduction

Tau was originally isolated from brain microtubules and shown to be a microtubule-associated protein (MAP) that promoted tubulin polymerization (**1**). It is largely confined to axons, where it is the major MAP. It promotes microtubule nucleation, elongation, and bundling, and stabilizes microtubules by inhibiting depolymerization.

Alzheimer's disease (AD) is characterized by microscopically visible extracellular amyloid plaques, and by neurofibrillary tangles (NFT), which originate intracellularly (reviewed in **ref. 2**). Genetic studies have demonstrated that altered metabolism of amyloid precursor protein (APP) can be sufficient to increase drastically the probability of developing AD, and to reduce the age of onset of the disease (**3**). Nevertheless, loss of neurons and of synapses, and hence cognition, correlates better with the burden of NFT than that of amyloid plaques (**2,4**). NFT are tangles of filaments (mainly paired helical filaments, PHF) which consist principally of tau that is in a highly phosphorylated state, and NFT-containing cells lack microtubules and hence cannot provide proper axonal transport. Tau deposits have also been observed in rarer diseases including progressive supranuclear palsy (**5**) and Pick's disease (**6**). Recently, several different kindreds with familial frontotemporal dementia with Parkinsonism, a recognized tauopathy, have been shown to harbor mutations in the tau gene (**7–9**).

Normal brain tau is a phosphoprotein (**10,11**), and dephosphorylation increases its mobility on sodium dodecyl sulfate (SDS) polyacrylamide gels and also enhances its ability to promote microtubule assembly (**12**). Conversely, phosphorylation of tau reduces its affinity for microtubules, especially when phosphorylated at Ser262 in the microtubule-binding region (**13**). Tau from fetal and neonatal brain is more phosphorylated than tau from adult brain

**Table 1**  
**Protein Kinases that Phosphorylate Tau In Vitro**

Nonproline sites	Proline sites
CamK-II	MAP kinases
CamK-Gr	p44 ERK1
Phosphorylase kinase	p42 ERK2
Protein kinase C	SAPK (JNK)
	p38 (RK)
Protein kinase A	SAPK3
	SAPK4
Casein kinase I	
Casein kinase II	Other
	GSK3 $\alpha^a$
Tau-tubulin kinase	GSK3 $\beta$ (TPKI) <sup>a</sup>
p110 MARK1	cdc2
p110 MARK2	cdk5/p25 (TPKII)

<sup>a</sup>GSK3 also phosphorylates nonproline sites.

References: (20) reviews earlier work; see also (31–34).

(14,15). Dephosphorylation of normal tau postmortem is rapid in adult brains (16,17), whereas PHF-tau is remarkably resistant to dephosphorylation.

Hyperphosphorylation of tau appears to precede PHF formation, but it is not proven that hyperphosphorylation of tau is necessary for its aggregation into PHF. Indeed, in vitro aggregation studies suggest that aggregation per se does not require prior phosphorylation (18,19), but phosphorylation may well serve to release tau from microtubules, increasing its free concentration. The phosphorylation state of tau clearly is of relevance both to the regulation of its physiological functions and to the development of AD pathology.

The phosphorylation state of tau, as with any phosphoprotein, is determined by the relative rates of phosphorylation and dephosphorylation reactions (for review see ref. 20). Many protein kinases can phosphorylate tau in vitro (Table 1), whereas the two most active tau phosphatases appear to be PP2A, particularly PP2A<sub>1</sub> (21) and PP2B (calcineurin, which is activated by Ca<sup>2+</sup> and calmodulin) (22). In PHF-tau, over 25 phosphorylation sites have now been determined chemically (15,23), and almost half of these are on serines or threonines that are followed by prolines.

The methods described in **Subheading 2.** can be used to prepare phosphorylated tau for studies of its function in vitro, and to characterize the extent and sites of phosphorylation in vitro. Methods are also described for generating phosphorylated as well as nonphosphorylated tau in model transfected cells for study of its properties *in situ*, and their regulation by phosphorylation.

## 2. Materials

### 2.1. Preparation of Recombinant Tau

1. Clones for bacterial expression of the six human central nervous system isoforms of tau were donated by Dr. Michel Goedert (MRC Laboratory of Molecular Biology, Cambridge, UK).
2. LB broth (Life Technologies, Paisley, UK): 20 g powder per liter;  $1 \times 20$  mL +  $2 \times 500$  mL, autoclaved.
3. Ampicillin (Sigma, Gillingham, UK, cat. no. A9518), 50 mg/mL, stored frozen.
4. Isopropylthiogalactoside (Sigma, cat. no. I5502) 200 mg/mL, stored frozen.
5. 50 mM 2-(Morpholino)ethanesulfonic acid/NaOH (MES) buffer, pH 6.5.
6. 50 mM MES, pH 6.5, containing 1 mM EDTA, 10 mM Na pyrophosphate, and 10 mM NaF.
7. 50 mM MES, pH 6.5, containing 0.5 M NaCl.
8. 0.1 M Phenylmethane sulfonyl fluoride (PMSF) in isopropanol or dimethyl sulfoxide (DMSO). Always add just before use (hydrolyses rapidly in aqueous solutions). (**NB: This material is toxic**).
9. Solid NaCl (AR) and solid ammonium sulfate (AR).
10. 25 mM MES, pH 6.25, containing 50 mM NaCl and 1 mM dithiothreitol (DTT).

### 2.2. Phosphorylation of Tau In Vitro

See **Table 2**. Other materials, or those requiring further comment, are described as follows.

1. Protein kinases can be obtained from a variety of commercial sources, including Stratagene (Cambridge, UK), Upstate Biotechnology Inc. (Lake Placid, NY), Promega (Southampton, UK), and NEB (Hitchin, UK), or prepared in house (*see Note 1*).
2. Protease inhibitor cocktail: 0.1 M Benzamidine-HCl (Sigma, cat. no. B6506), 0.5 mg/mL leupeptin (Sigma, cat. no. L2884) and 0.2 mg/mL aprotinin (Boehringer Mannheim, Mannheim, Germany) (dilute  $\times 100$  when adding to buffers, i.e., add 10  $\mu$ L/0.99 mL buffer).
3. 0.1 M Sodium vanadate: Dissolve sodium orthovanadate in water, add a few drops diluted HCl until yellow, heat in a waterbath until colorless; repeat the HCl and heating until the pH is below 9. Aliquot and store frozen; check that all is redissolved before use (warm and vortex if necessary).
4. Kinase diluting buffer: 25 mM Tris-HCl (final pH 7.5), 40 mM Na<sub>2</sub> *p*-nitrophenyl phosphate, 1 mM EGTa, 1/100 protease inhibitor cocktail, 1/1000 vol of 1 mg/mL pepstatin, 1 mM DTT (1/100 vol of 0.1 M DTT), 1 mM Na vanadate (1/100 vol of 0.1 M vanadate).
5. 4 $\times$  Concentrated Laemmli sample buffer: 20% (v/v) Glycerol, 4% SDS, 125 mM Tris-HCl, pH 6.8, 0.01% bromophenol blue, 10% (v/v) 2-mercaptoethanol.
6. [ $\gamma$ <sup>32</sup>P]ATP. 9.25 MBq in 50  $\mu$ L (5  $\mu$ Ci/ $\mu$ L) (New England Nuclear, Boston, MA, cat. no. NEG002H).
7. Activated charcoal (Sigma, cat. no. C5260).

**Table 2**  
**Components of Reaction Mixture Needed for Tau Phosphorylation. To Tubes Already Containing 5  $\mu$ L Kinase or Buffer Add 10  $\mu$ L Reaction Mixture Containing the Following:**

Component	Stock Conc	Final Conc (in 15 $\mu$ L)	Vol per Reaction <sup>a</sup>
Tau	1 mg/mL	0.33 mg/mL	5 $\mu$ L
ATP	20 mM	3 mM	2.25 $\mu$ L
Tris-HCl, pH 7.5	0.5 M	50 mM	1.25 $\mu$ L <sup>b</sup>
MgCl <sub>2</sub>	1 M	10 mM	0.15 $\mu$ L
EGTA	0.1 M	1 mM	0.15 $\mu$ L
DTT	0.1 M	1 mM	0.15 $\mu$ L
Okadaic acid (in DMSO)	1 mM	5 $\mu$ M	0.075 $\mu$ L
Protease-inhibitor cocktail	<sup>c</sup>	<sup>c</sup>	0.15 $\mu$ L
Pepstatin (in DMSO or EtOH)	1 mg/mL	1 $\mu$ g/mL	0.015 $\mu$ L
Na vanadate	0.1 M	1 mM	0.15 $\mu$ L
H <sub>2</sub> O	—	—	0.63 $\mu$ L
PMSF <sup>c</sup>	0.1 M	0.2 mM	0.03 $\mu$ L

<sup>a</sup>Make up reaction mixture by scaling up these volumes according to the number of tubes in the experiment, allowing some spare. For example, if 6 incubations are to be performed, make up enough for 10 (add 10 $\times$  the above volumes). The accuracy of the volumes of protease inhibitors and okadaic acid are not critical.

<sup>b</sup>Assumes that tau does not contain Tris and that the enzyme solution contains 25 mM Tris. If otherwise, recalculate the volumes of Tris and H<sub>2</sub>O required.

<sup>c</sup>See **Subheading 2**.

8. Phosphocellulose paper (P81 from Whatman, Maidstone, UK). Cut into pieces 12.5  $\times$  15 mm.
9. Phosphoric acid 0.5% (v/v) in water (approx 75 mM).

### 2.3. Culturing Mammalian Cells, and Immunocytochemistry

1. Constructs of tau (human 1N4R and 1N3R) in pSG5, and of ERK1, ERK2, GSK3 $\alpha$  and GSK3 $\beta$  have been described (24).
2. Cells (COS-7 and Chinese hamster ovary [CHO]) are available from ECACC, Porton Down, UK.
3. Media (DMEM, MEM $\alpha$ , and Opti-MEM) and fetal calf serum (FCS) are obtainable from Life Technologies (Paisley, UK), and penicillin-streptomycin, glutamine, and trypsin from Sigma.
4. Nocodazole is obtainable from Sigma.
5. Glutaraldehyde (aqueous solution) is obtainable from Sigma.
6. Permeabilization buffer: 80 mM Piperazine N,N'-bis(2-ethanesulfonic acid) (PIPES), pH 6.8, 0.5% (w/v) Nonidet UK NP40, (Merck, Lutterworth, 5 mM EGTA, 1 mM MgCl<sub>2</sub>.

7. Blocking solution: phosphate-buffered saline (PBS) containing 1% (w/v) bovine serum albumin (BSA) and 0.2% (v/v) Tween-20.
8. Secondary reagents for immunocytochemistry: Biotinylated or fluorescein-conjugated antibodies (donkey-antirabbit immunoglobulin [Ig] and sheep-antimouse Ig), and Texas Red-conjugated streptavidin are obtained from Amersham Pharmacia (Amersham, UK).

#### **2.4. Cellular Tau Phosphorylation Studied by Western Blotting**

1. 100 mM MES, pH 6.5/1 M NaCl/50 mM NaF/0.1 mM Na vanadate.
2. 100 mM PMSF in propanol.
3. 200 mM DDT.
4. Protease inhibitor cocktail tablets (Complete, Mini, from Boehringer Mannheim, Lewes, UK).
5. Homogenizing buffer for heat-stable protein preparation (10 mL): On day of use add 100  $\mu$ L of 200 mM DDT and one tablet of protease inhibitor cocktail to 9.8 mL of MES/NaCl/NaF/Na vanadate buffer pH 6.5; just before use add 100  $\mu$ L of 100 mM PMSF.

#### **2.5. Phosphopeptide Mapping**

1. Amido Black solution: 0.1% (w/v) in methanol/acetic acid/water (30/7.5/62.5 by volume).
2. Polyvinylpyrrolidone solution: 0.04% (v/v) PVP40 (Millipore, Watford, UK) in 100 mM acetic acid.
3. pH 1.9 Electrophoresis buffer: Water/acetic acid/formic acid/EDTA: 89.9/7.8/2.2/0.1 (v/v/v/v, where the stock EDTA is itself a 0.5 M solution) (*see Note 2*).
4. Phosphopeptide chromatography solvent: *n*-Butanol/pyridine/acetic acid/water/EDTA, 37.5/25/7.5/29.9/0.1 (v/v/v/v/v, where the stock EDTA is itself a 0.5-M solution) (*see Note 2*).
5. Thin-layer cellulose chromatography (TLC) plates, 20  $\times$  20 cm (Merck, Lutterworth, UK).

#### **2.6. Metabolic Labeling of Cells with $^{32}P$**

1. [ $^{32}P$ ]Inorganic phosphate as  $H_3PO_4$  (New England Nuclear, cat. no. NEX053).
2. Phosphate-free DMEM (ICN, Thame, UK).
3. Dialyzed fetal bovine serum (FBS) (Life Technologies).
4. N-2-Hydroxyethylpiperazine-N'-2-ethanesulfonic acid (HEPES-OH). pH 7.4, 1 M solution, sterile (ICN).
5. L-Proline (Sigma, tissue culture grade) was dissolved in water at 4 mg/mL and sterilized by filtration.
6. Labeling medium: Phosphate-free DMEM containing 5% dialyzed FCS, 10 mM HEPES, pH 7.4, 2 mM L-glutamine and penicillin-streptomycin; for CHO cells 0.35 mM L-proline, i.e., 1/100 vol of 4 mg/mL stock, is also added.

### 3. Methods

#### 3.1. Preparation of Recombinant Tau

1. Pick one colony of *Escherichia coli* expressing the desired tau isoform from an ampicillin-agar plate and inoculate 20 mL LB broth/50 µg/mL ampicillin.
2. Grow overnight at 37°C, and use 10 mL to inoculate each of two 2-L flasks that contain 500 mL LB broth/ampicillin.
3. Grow with shaking at 37°C until the absorbance at 600 nm is 0.6–1 (approx 4 h), and then add 0.6 mL isopropylthiogalactoside (200 mg/mL stock in water) per 500 mL culture (final concentration 0.5 mM) to induce tau expression.
4. After 2 h, harvest the bacteria by cooling and centrifuging for 30 min at 7500 $g_{av}$  (e.g., 6000 rpm in a Sorvall RC5B centrifuge with a GSA rotor) (Sorvall Centrifuge, Newtown, CT) set at 4°C.
5. Resuspend the pellets in a total of 50 mL 50 mM MES buffer, pH 6.5, and recentrifuge in preweighed tubes at 20,000 $g_{av}$  (14,000 rpm) in a Sorvall SS34 rotor.
6. The pellets can be stored at –70°C (or –20°C overnight) if desired. All subsequent steps are performed at 0–4°C unless otherwise stated.
7. Reweigh the tubes, calculate the weights of the pellets, and suspend in 10 mL of the following buffer per gram of pellet: 50 mM MES containing 1 mM EDTA, 10 mM Na pyrophosphate, 10 mM NaF, final pH 6.5.
8. Just before sonicating, add 10 µL PMSF (0.1 M) per milliliter suspension. Sonicate the suspension using a VirSonic 475 probe sonicator (VirTis, Gardiner, NY) in 30-s bursts with cooling on ice, totalling 10 bursts per gram of pellet.
9. Centrifuge the sonicates at 40,000 $g_{av}$  for 30 min (e.g., Sorvall SS34 rotor at 18,000 rpm), and measure the volume of the clear supernatant.
10. Add 29.1 mg solid NaCl per milliliter supernatant to give 0.5 M (conveniently this can be done in a 100-mL conical flask), and dissolve while keeping the mixture cold.
11. Heat the solution in the conical flask in a boiling water-bath, with frequent swirling, for 10–15 min, cool, and centrifuge at 100,000 $g_{av}$  for 2 h.
12. Carefully remove the supernatant with a Pasteur pipet (*see Note 3*) and discard the pellet.
13. Precipitate tau by adding ammonium sulfate to 45% saturation: this requires 0.258 g solid ammonium sulfate per milliliter initial volume (*see Note 4*). Let it stand at least 1 h or overnight at 0–4°C.
14. Centrifuge the ammonium sulfate suspension at 40,000 $g_{av}$  (Sorvall SS34 rotor at 18,000 rpm for 30 min at 4°C).
15. Suspend the combined pellets in a minimum volume (1–2 mL) of 25 mM MES, pH 6.25/50 mM NaCl/1 mM DTT (*see Note 5*), and dialyze against 3 × 1 L of this buffer for a total of 18 h.
16. Centrifuge the dialysate at 12,000 $g_{av}$  for 5 min in a refrigerated microcentrifuge prior to fast protein liquid chromatography (*see Note 6*).
17. Equilibrate a 5/5 Mono S FPLC column, bed-volume 1 mL (Pharmacia) with 50 mM MES buffer, pH 6.5, and load the dialysate supernatant.

18. Elute proteins with a linear gradient of 0–500 mM NaCl in 50 mM MES, pH 6.5, total gradient volume 60 mL, at 1 mL/min. Collect 1 mL fractions and analyze the fractions using denaturing gel electrophoresis and Western blotting with a general anti-tau antibody such as TP70 (25). Combine tau-containing fractions, aliquot, and store frozen at  $-20^{\circ}\text{C}$ .

### 3.2. Phosphorylation of Tau In Vitro

#### 3.2.1. Typical Protocol

The appropriate protocol will depend on the application in view, as well as which kinase is to be used. The following protocol is suitable for producing phosphorylated but nonradioactive tau for studying phosphorylation sites either by mass spectrometry or by immunoblotting with phosphorylation-specific antibodies.

1. Pipet 5  $\mu\text{L}$  kinase, diluted if necessary in kinase diluting buffer, into a screw-capped Eppendorf tube on ice; use another tube containing 5  $\mu\text{L}$  buffer without kinase (just buffer) as a control.
2. Add 10  $\mu\text{L}$  of reaction mixture containing all the other necessary components (see **Table 2**), vortex and centrifuge the tubes, and incubate in a water bath at  $30^{\circ}\text{C}$  for 7.5 h (see **Notes 7** and **8**).
3. Stop the reactions by adding 5  $\mu\text{L}$  of 4X concentrated Laemmli sample buffer, vortex, and heat in a boiling water bath for 5 min. Samples may be stored at  $-20^{\circ}\text{C}$ .

The foregoing protocol has worked well for proline-directed kinases. The incubation conditions will need to be modified for particular kinases; for example, for  $\text{Ca}^{2+}$ -activated kinases EGTA might be omitted or used as part of a  $\text{Ca}^{2+}$  buffer.

#### 3.2.2. Preparation of Radiolabeled Phosphorylated Tau for Determination of Stoichiometry

Including [ $^{32}\text{P}$ ] in the protocol in **Table 2**, or a modification of it, is straightforward. For accurate determination of stoichiometry (the number of phosphates incorporated per molecule of tau) several requirements need to be met:

1. The chemical concentration of adenosine triphosphate (ATP) must be accurately known. Unlabeled ATP should be made up fresh, and its concentration standardized by absorbance at 260 nm (millimolar absorbance coefficient  $15.4\text{ cm}^{-1}$ ). The actual concentration of the radiolabeled ATP is usually negligible.
2. The radioactive ATP also needs to be fresh and its radiochemical purity verified, e.g., by charcoal absorption of nucleotide (see **Note 9**).
3. The chemical concentration of tau (in  $\mu\text{M}$ ) needs to be known, and this is best done by amino-acid analysis (see **Note 10**).

4. The concentrations of ATP and tau need to be such that sufficient radioactivity is incorporated into tau, per site, to be accurately measurable yet there is sufficient ATP to be capable of giving complete phosphorylation. We have found the following to be satisfactory, in an incubation volume of 20  $\mu\text{L}$ :

30  $\mu\text{M}$  tau 2N4R (11  $\mu\text{g}$ )  
1.5 mM nonradiolabeled ATP  
55 KBq (1.5  $\mu\text{Ci}$ ) [ $\gamma$ - $^{32}\text{P}$ ]ATP

Remove 5  $\mu\text{L}$  aliquots at timed intervals, e.g., 1, 3, and 6 h (**Note 7** also applies here) and pipet onto pieces of P81 phosphocellulose paper (*see Note 11*), wash six times in 75 mM phosphoric acid (10 mL per paper per wash) and count using Cerenkov radiation. This gives, per 5  $\mu\text{L}$  aliquot, approx 3500 cpm per tau site, with nonspecific binding of less than 200 cpm. Control protocols should be run without tau but with kinase, and also without kinase but with tau.

### 3.2.3. Larger-Scale Phosphorylation for Phosphopeptide Mapping

This example describes the phosphorylation of tau with GSK3 $\beta$  in the presence of heparin.

1. Incubate, in a final volume of 200  $\mu\text{L}$ , 10–50  $\mu\text{g}$  of recombinant human tau 1N4R, prepared as previously described, with 1.6–8  $\mu\text{g}$  recombinant GSK3 $\beta$  at 30°C in 20 mM HEPES buffer, pH 7.4, containing 10 mM  $\text{MgCl}_2$ , 1 mM DTT, 1 mM PMSF (added last), 10  $\mu\text{M}$  leupeptin, 10  $\mu\text{M}$  pepstatin, 1  $\mu\text{M}$  aprotinin, 5  $\mu\text{M}$  okadaic acid, 10  $\mu\text{M}$  sodium orthovanadate, and 0.1 mg/mL heparin.
2. Start the reaction by adding ATP (final concentration 3 mM, containing 0.4 MBq (10  $\mu\text{Ci}$ ) [ $\gamma$ - $^{32}\text{P}$ ]ATP).
3. After incubating overnight, terminate the reaction by adding 0.1 mL 100% (w/v) trichloroacetic acid (TCA) and leave on ice for 5 min.
4. Centrifuge at 15,800 $g_{\text{av}}$  for 5 min (in an Eppendorf microcentrifuge, maximum speed) and wash the pellet twice with ice-cold 20% (w/v) TCA and then twice with ice-cold acetone, centrifuging the sample between washes as before.
5. Resuspend the final washed material in Laemmli sample buffer for analysis by sodium dodecyl sulfate-polyacrylamide gel electrophoresis (SDS-PAGE).

## 3.3. Culturing Mammalian Cells and Immunocytochemistry

### 3.3.1. Transient Transfections of COS-7 Cells with Recombinant Plasmids Expressing Tau and Kinases

1. Culture COS-7 cells in DMEM containing 10% FBS, 2 mM glutamine, 100 IU/mL penicillin, and 100  $\mu\text{g}/\text{mL}$  streptomycin. Grow CHO cells exactly as for COS-7 cells except use MEM- $\alpha$  medium in place of DMEM.
2. Split the cells 24 h before use. Harvest 80% confluent cells with 1 mL 0.25% trypsin per T75 flask, and resuspend in Opti-MEM ( $2.5 \times 10^7$  cells/mL).
3. Electroporate 0.4 mL Opti-MEM suspension containing  $10^7$  cells and 5  $\mu\text{g}$  of each plasmid DNA in a Bio-Rad Electroporator (Bio-Rad, Hercules, CA) with a 0.4 cm path-length chamber, at settings of 220 V and 960  $\mu\text{F}$ .

4. Suspend the electroporated cells immediately in 5 mL DMEM/10% FBS (with penicillin-streptomycin and glutamine) and plate onto Petri dishes or six-well plates for harvesting 48 h later. Typically, cells from each electroporation can be plated onto three 9 cm Petri dishes.
5. For experiments involving activation of kinase signaling pathways, change the medium to serum-free medium 8 h before application of a stimulus (e.g., tumor-promoting agent or epidermal growth factor).

### 3.3.2. Immunofluorescence Microscopy of Tau in Cells

Place cells, electroporated as before, in wells containing heat-sterilized glass cover slips in six-well plates and grow for 48 h as before (without serum for the final 8 h for cell-stimulation experiments). For investigations of microtubule stability, treat the cells with 10  $\mu$ M nocodazole (Sigma) in DMEM for 30 min prior to fixation. Fixation of cells for antibody-probing requires different methods for bound proteins, including microtubule-bound tau, and for soluble proteins.

#### 3.3.2.1. FIXATION IN COLD METHANOL

Methanol-fixation permeabilizes cells and allows visualization of bound components including the cytoskeleton and also some soluble components.

1. Wash the cover slips in ice-cold PBS and drain thoroughly.
2. Add methanol that has been precooled to  $-20^{\circ}\text{C}$  and incubate for 20 min.
3. Remove and warm to  $0^{\circ}\text{C}$ , and wash once with ice-cold PBS.

#### 3.3.2.2. FIXATION OF DETERGENT-PERMEABILIZED CELLS WITH GLUTARALDEHYDE

This procedure permeabilizes cells to small molecules so that the crosslinking agent glutaraldehyde can enter the cells, whereas the soluble macromolecules remain inside. Carry out all steps at room temperature.

1. Treat the cells for 15 s with permeabilization buffer and then add 0.3% (w/v) glutaraldehyde.
2. After 10 min, wash the cover slips with PBS, and incubate with 10 mg/mL Na borohydride freshly dissolved in PBS.
3. After 7 min replace this with 0.1 M glycine in PBS for 20 min to reduce nonspecific binding to free aldehyde groups.

#### 3.3.2.3. BLOCKING AND IMMUNOLABELING

Carry out all steps at room temperature.

1. Incubate the fixed cells with blocking solution for 15 min, and then incubate with primary antibody in blocking solution for 30 min.
2. Wash  $3 \times 10$  min with PBS/0.2% Tween-20, and then incubate for 30 min with secondary antibody diluted 500 $\times$  in blocking solution and wash as above.

3. To visualize biotin-labeled proteins, incubate with streptavidin conjugated to Texas Red (diluted 3000 $\times$ ) and wash as before. Primary antibodies can include DM1A (a monoclonal antibody to  $\alpha$ -tubulin from Amersham, diluted 1/50), B19 (a polyclonal antibody recognizing all forms of tau (26), diluted 1/200) and AT8 (a monoclonal antibody recognizing tau phosphorylated at Ser202 and Thr205 from Innogenetics, diluted 1/20).

Examine the cells using normal fluorescence optics with, e.g., a Leitz (Wetzlar, Germany) Ortholux microscope, or for confocal microscopy with an Olympus BH2 microscope (Olympus Optical Co., Hamburg, Germany) and Bio-Rad MRC 600 confocal laser. An example of the effect of tau phosphorylation on microtubules in transfected COS cells is shown in **Fig. 1**.

### **3.4. Cellular Tau Phosphorylation Studied by Western Blotting**

To study expression of kinases and tau by Western blotting, prepare whole-cell lysates of COS-7 cells by rinsing the monolayers in ice-cold PBS and adding 0.5 mL hot Laemmli sample buffer per 9 cm Petri dish.

For studying the phosphorylation state of tau (*see Note 12*):

1. Wash the cells adhering to the Petri dish briefly with ice-cold PBS.
2. Scrape the cells into 1 mL of ice-cold PBS, and centrifuge the cells for 2 min in a microcentrifuge.
3. Homogenize the cells in MES/NaCl buffer containing protease and phosphatase inhibitors by rapid repeated pipeting; typically, 100  $\mu$ L of buffer is used for cells from one 9-cm Petri dish.
4. Place in a boiling water bath for 10 min, cool, and centrifuge.
5. Mix the supernatant with 1/4 volume of 5 $\times$  Laemmli sample buffer and return the sample to the boiling water-bath for 5 min.
6. Carry out SDS-PAGE and electroblotting.

Total tau levels, and electrophoretic mobilities, can be studied with a general anti-tau antibody such as TP70 (25). Several phosphorylation-specific antibodies are available commercially (*see Table 3*).

### **3.5. Phosphopeptide Mapping**

1. Separate the radiolabeled human tau (10–50  $\mu$ g in 100  $\mu$ L sample buffer) by denaturing gel electrophoresis (10% [w/v] acrylamide).
2. Transfer onto Immobilon P membrane (Millipore) at 15 V for 45 min using Bio-Rad SD semidry blotting apparatus.
3. Stain the membrane with Amido Black and identify the radiolabeled bands by autoradiography, or if available by using a Fujix Bas 1000 BioImage Analyzer or equivalent.
4. Cut out the phosphorylated tau band, count using Cerenkov radiation, and destain by incubating in 200  $\mu$ M NaOH solution twice for 30 min each at 37 $^{\circ}$ C.

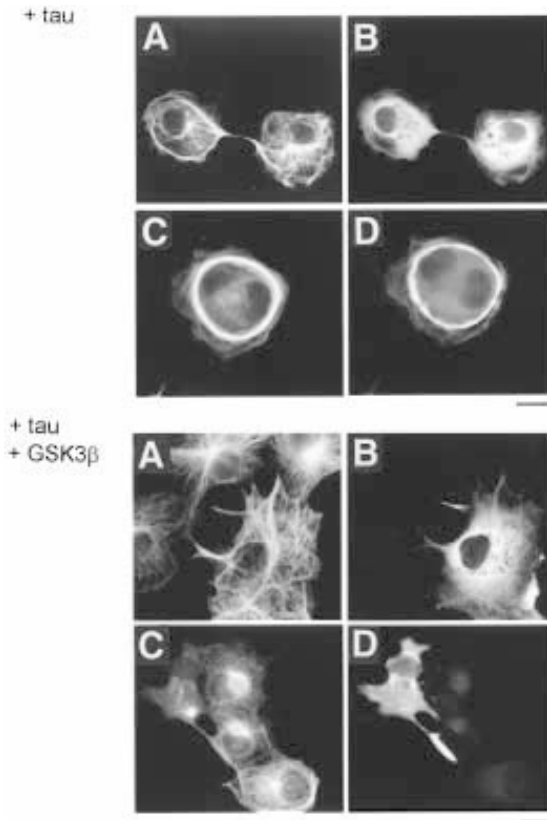


Fig. 1. Effect of GSK3 $\beta$  on the distribution of tubulin and transfected tau in COS-7 cells. COS-7 cells were transfected with tau (1N4R isoform) only (upper panel of four), or transfected with both tau and GSK3 $\beta$  (lower panel of four). In (A) and (C), tubulin was labeled with antibody DM1A (diluted 1/50), and in (B) and (D) tau was labeled with antibody B19 (diluted 1/200). The scale bars indicate 20  $\mu$ m. Tau is seen to be present in bundled microtubules (upper panels), which is abolished when GSK3 $\beta$  is cotransfected (lower panels); in contrast, cytoplasmic tau is present whether or not GSK3 $\beta$  is cotransfected.

5. Wash the destained membrane five times with 200  $\mu$ L distilled H<sub>2</sub>O per wash and then block in 200  $\mu$ L of polyvinylpyrrolidone blocking solution for 1 h at 37°C.
6. Wash the membrane again as before (5  $\times$  200  $\mu$ L H<sub>2</sub>O) and place in 200  $\mu$ L of 0.2 M ammonium bicarbonate, pH 8.0, containing trypsin (0.5–2.5  $\mu$ g, to give 1:20 (w/w) trypsin:tau) and incubate overnight at 37°C.
7. The following morning add a second identical aliquot of trypsin and continue the incubation for a further 4 h at 37°C.

**Table 3**  
**Some Widely Used Anti-Tau Monoclonal Antibodies**  
**with Phosphorylation-Dependent Epitopes**

Antibody	Site(s) of Phosphorylation	Supplier	Refs
Tau-1	Ser199 <sup>a</sup> , Ser202 <sup>a</sup>	Boehringer Mannheim (Mannheim, Germany)	(29,35)
AT8	Ser202 + Thr205	Innogenetics	(36,37)
AT100	Thr212 + Ser214 <sup>b</sup>	Innogenetics	(36,38)
AT180	Thr231	Innogenetics	(36,39)
AT270	Thr181	Innogenetics	(36,39)
SMI31 <sup>c</sup>	Ser396 + Ser404	Sternberger Monoclonals	(40)
SMI33 <sup>c</sup>	Ser235 <sup>a</sup>	Sternberger Monoclonals	(40)
SMI34 <sup>c</sup>	Conformation <sup>b</sup>	Sternberger Monoclonals	(40)
PHF-1	Ser396 + Ser404	—	(41)
12E8	Ser262 or Ser356	—	(42)
AP422	Ser422	—	(43)
8D8 <sup>c</sup>	Ser396	—	(44)

<sup>a</sup>Residues that must be nonphosphorylated for antibody to bind. (All other sites indicate need to be phosphorylated for antibody binding.)

<sup>b</sup>Antibodies that recognize particular conformational states of tau, which are induced by appropriate phosphorylations.

<sup>c</sup>These antibodies also bind to phosphorylated neurofilament proteins, which will be removed when preparing heat-stable cell extracts for Western blots.

8. Remove the Immobilon membrane from the solution of eluted peptides and dry these down using a Savant SC199 Speed Vac (Savant Bioblock Scientific, Illkirch, France) to remove all the water and ammonium bicarbonate, resuspend in 400  $\mu$ L distilled H<sub>2</sub>O and dry down.
9. Repeat this once with H<sub>2</sub>O, and then twice with 400  $\mu$ L of pH 1.9 electrophoresis buffer, each time drying the samples under reduced pressure.
10. Suspend each final dried sample in 5–10  $\mu$ L of pH 1.9 electrophoresis buffer, centrifuge at 15,800g<sub>av</sub> (14,000 rpm in an Eppendorf microcentrifuge) for 5 min (*see Note 13*), and apply the sample carefully, a small part at a time to produce a small spot, onto a thin-layer cellulose chromatography (TLC) plate (27).
11. Separate first by electrophoresis at pH 1.9 for 1.25 h using a Hunter thin-layer electrophoresis apparatus (C.B.S. Scientific, Del Mar, CA) or equivalent, air dry the plate in a fume hood, and place in an ascending chromatography tank with phosphopeptide chromatography solvent and chromatograph for 18 h.
12. Dry the plate in air in the fume hood and then visualize the phosphopeptides either by autoradiography with an enhancing screen at –70°C or imaging as described earlier.

The phosphopeptides may be further characterized by scraping off the spots and analyzing for phosphoaminoacids after acid hydrolysis. Alternatively, peptides eluted from the scraped spots can be analyzed by mass spectrometry to determine their amino-acid sequences including sites of phosphorylation (*see* (28)).

An example of a two-dimensional phosphopeptide map of tau phosphorylated by GSK3 $\beta$  is shown in **Fig. 2**. The legend indicates the identity of peptides in many of the spots obtained by mass spectrometry.

### 3.6. Metabolic Labeling of Cells with $^{32}\text{P}$

This involves incubating cells with [ $^{32}\text{P}$ ]inorganic phosphate so that the ATP becomes radiolabeled and reaches equilibrium. Kinase targets will also become labeled, the extent depending on the amount of target, its steady-state phosphorylation level, and to what extent the site itself has reached radiochemical equilibrium (*see* **Notes 14** and **15**).

1. Grow COS or CHO cells in six-well plates or 9-cm Petri dishes for metabolic labeling studies in normal growth medium (*see* above). Prepare several wells or dishes of cells for unlabeled control samples at the same time.
2. Once the cells have reached 60–80% confluency, aspirate the medium from the dishes to be labeled, rinse twice in phosphate-free labeling medium, and place in labeling medium for approx 1 h prior to adding the radioactive [ $^{32}\text{P}$ ]orthophosphoric acid (18–37 MBq, i.e., 0.5–1.0 mCi, per well or dish). One milliliter of labeling medium is added to a well in a six-well plate or 3 mL to a 9-cm Petri dish. (For safety reasons it is advisable to label only one well per multiwell plate.)
3. Incubate overnight at 37°C in a humidified incubator to achieve maximum incorporation of radioactivity.
4. The following morning, remove the medium by aspiration and wash the cell monolayers 5–10 $\times$  with ice-cold sterile PBS.
5. Scrape the cells into 1–1.5 mL PBS using a long-handled cell scraper, transfer to a screw-capped Eppendorf tube, and centrifuge at 15,800 $g_{av}$  (14,000 rpm) for 10 min in an Eppendorf microcentrifuge.
6. Remove the supernatant and repeat the PBS washing up to 5 $\times$ .
7. A heat-stable tau fraction can be prepared from this material (*see* **Subheading 3.4.**) or alternatively the cells can be scraped directly into 1 $\times$  Laemmli sample buffer for SDS-PAGE analysis.

## 4. Notes

1. Because tau can be phosphorylated by many different kinases on many different sites, it is necessary for the kinase of interest to be sufficiently pure, i.e., not contaminated by other kinases. It is often desirable where possible to add specific inhibitors of likely contaminating kinases, such as 1  $\mu\text{M}$  protein kinase A (PKA) inhibitory peptide (Sigma, cat. no. P0300). A crude brain extract has been used as a kinase source to produce highly phosphorylated tau (29).

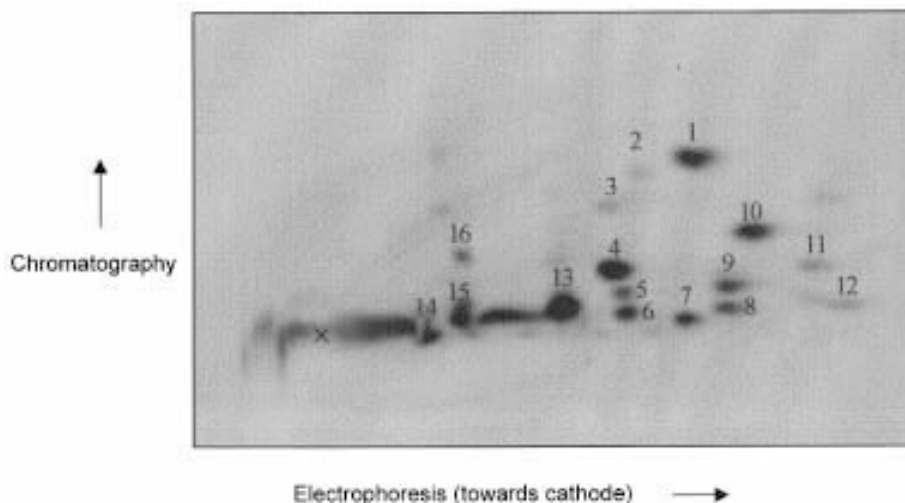


Fig. 2. Phosphopeptide map analysis of tau phosphorylated by GSK3 $\beta$ . Electrophoresis (horizontal, anode on left) was followed by ascending TLC.  $\times$  indicates the origin. Sixteen phosphopeptide spots were well resolved, individually scraped from the plate, eluted, and studied by nano-electrospray mass spectrometry. Phosphorylated residues were identified as follows: **1**, Ser356; **2**, Ser262; **3**, two peptides, one phosphorylated at Thr212 and the other at Thr217; **4**, both Thr212 and Thr217; **5**, Thr181; **6**, both Thr231 and Ser235; **9**, Thr231 and also Ser235 or Ser237 or Ser238; **10**, Thr212; **12**, Thr231; **13**, two peptides, one phosphorylated at Ser396, Ser400, and Ser404, and the other phosphorylated at Ser195 and Ser199; **15**, Ser195 and Thr205 and one of Ser198, Ser199, or Ser202; **16**, both Thr212 and Thr217.

2. EDTA is included in the electrophoresis and chromatography buffers to reduce streaking of spots.
3. The pellet is light and fragile, thus high-speed centrifugation and careful removal of the supernatant are required. However, a 2-h centrifugation at only 48,000g (Sorvall SS-34 rotor, maximum speed) has on occasion been used without serious difficulty.
4. The solution should be surrounded by ice while being magnetically stirred, and the ammonium sulfate sprinkled on, a little at a time, over approx 20–30 min, maintaining the pH at 6.5–7.0 with aqNH<sub>3</sub>. Finally, check that it has all dissolved.
5. The tau sample, if kept concentrated, can be viscous at this stage for reasons that are not clear.
6. As judged by Coomassie staining of SDS-polyacrylamide gels, tau prepared thus contains very little other protein, although some degradation products may be seen. Nonproteinaceous UV-absorbing material is present, probably nucleic acid, which may be removed by cation-exchange chromatography (e.g., FPLC using a MonoS column) (Pharmacia).

7. Condensation may accumulate on the lids of tubes; the tubes can be centrifuged, vortexed, and recentrifuged midway through long incubations and must be centrifuged before opening.
8. For long incubations (several hours or more), protease inhibitors have been found to be necessary: tau is relatively unstructured and appears to be susceptible to proteolysis. Phosphatase inhibitors limit the dephosphorylation of tau and also preserve the kinase in an active state. The ATP concentration needs to be high, presumably because of contaminating ATPases.
9. Nucleotide vs nonnucleotide radioactivity can be measured as follows. To four screw-capped Eppendorf tubes add 0.99 mL 25 mM Tris-HCl buffer, and to two tubes add a microspatula end of activated charcoal; then to each tube add 10  $\mu$ L of a solution of [ $\gamma$ <sup>32</sup>P]ATP that contains approx 20–60 kBq (approx 0.5–1.5  $\mu$ Ci); in practice, surplus reaction mixture is convenient for this, and the radioactivity in it needs to be measured anyway (make up sufficient amount). Cap, vortex, leave on ice for 10 min, revortex, centrifuge (bench microfuge for 5 min at full speed), and withdraw 10  $\mu$ L aliquots for counting.
10. Quantitative amino-acid analysis is often not readily available. UV absorbance can be used, but the tau must be free of UV-absorbing contaminants:  $E(280 \text{ nm}, 1 \text{ mM}) = 7.2$  for 4-repeat isoforms, and 7.05 for 3-repeat isoforms, calculated by Perkins's Method (30). Methods such as Lowry's and Bradford's, and the use of bicinchoninic acid only give relative values (different proteins give different color-yields) [45–47]. The Bradford color-yield of tau appears to be about half that of BSA.
11. To reduce nonspecific binding of [<sup>32</sup>P]ATP, prespot the P81 papers with 15  $\mu$ L 10 mM nonradioactive ATP and air dry.
12. Tau is heat stable, and the heat treatment removes the bulk of other cellular proteins. This decreases the crossreactive bands seen on Western blots with some of the phosphorylation-dependent antibodies.
13. Invariably some insoluble material is present that needs to be centrifuged down and that interferes with the separations.
14. The amount of label on a given site is determined, therefore, by a complex interplay of factors. However, for changes in labeling (e.g., on cell stimulation) or nonquantitative applications such as determining the locations of intracellular phosphorylation sites, it can be very useful.
15. Metabolic labeling requires relatively large amounts of label and hence should be undertaken only by well-trained personnel. Using <sup>33</sup>P instead of <sup>32</sup>P is safer, but the convenience of being able to count small samples of <sup>32</sup>P nondestructively using Cerenkov radiation will be lost.

## Acknowledgments

Work in the authors' laboratories was supported by the Wellcome Trust and the Medical Research Council. The authors thank Professor Brian Anderton and Dr. Chris Miller, with whom most of our own experiments have been carried out, and Dr. Jo Betts and Dr. Walter Blackstock (Glaxo Wellcome) for invaluable collaboration with mass spectrometry.

## References

1. Weingarten, M. D., Lockwood, A. H., Hwo, S. Y., and Kirschner, M. W. (1975) A protein factor essential for microtubule assembly. *Proc. Natl. Acad. Sci. USA* **72**, 1858–1862.
2. Smith, C. and Anderton, B. H. (1994) Dorothy Russell Memorial Lecture. The molecular pathology of Alzheimer's disease: are we any closer to understanding the neurodegenerative process? *Neuropathol. Appl. Neurobiol.* **20**, 322–338.
3. Hardy, J. (1997) Amyloid, the presenilins and Alzheimer's disease. *Trends Neurosci.* **20**, 154–159.
4. Arriagada, P. V., Growdon, J. H., Hedley Whyte, E. T., and Hyman, B. T. (1992) Neurofibrillary tangles but not senile plaques parallel duration and severity of Alzheimer's disease. *Neurology* **42**, 631–639.
5. Flament, S., Delacourte, A., Verny, M., Hauw, J. J., and Javoy Agid, F. (1991) Abnormal Tau proteins in progressive supranuclear palsy. Similarities and differences with the neurofibrillary degeneration of the Alzheimer type. *Acta Neuropathol. Berl.* **81**, 591–596.
6. Murayama, S., Mori, H., Ihara, Y., and Tomonaga, M. (1990) Immunocytochemical and ultrastructural studies of Pick's disease. *Ann. Neurol.* **27**, 394–405.
7. Hutton, M., Lendon, C. L., Rizzu, P., Baker, M., Froelich, S., Houlden, H., et al. (1998) Association of missense and 5'-splice-site mutations in *tau* with the inherited dementia FTDP-17. *Nature* **393**, 702–705.
8. Spillantini, M. G., Murrell, J. R., Goedert, M., Farlow, M. R., Klug, A., and Ghetti, B. (1998) Mutation in the tau gene in familial multiple system tauopathy with presenile dementia. *Proc. Natl. Acad. Sci. USA* **95**, 7737–7741.
9. Poorkaj, P., Bird, T. D., Wijsman, E., Nemens, E., Garruto, R. M., Anderson, L., et al. (1998) Tau is a candidate gene for chromosome 17 frontotemporal dementia. *Ann. Neurol.* **43**, 815–825.
10. Selden, S. C. and Pollard, T. D. (1983) Phosphorylation of microtubule-associated proteins regulates their interaction with actin filaments. *J. Biol. Chem.* **258**, 7064–7071.
11. Lindwall, G. and Cole, R. D. (1984) The purification of tau protein and the occurrence of two phosphorylation states of tau in brain. *J. Biol. Chem.* **259**, 12,241–12,245.
12. Lindwall, G. and Cole, R. D. (1984) Phosphorylation affects the ability of tau protein to promote microtubule assembly. *J. Biol. Chem.* **259**, 5301–5305.
13. Biernat, J., Gustke, N., Drewes, G., Mandelkow, E.-M., and Mandelkow, E. (1993) Phosphorylation of Ser<sup>262</sup> strongly reduces binding of tau to microtubules: Distinction between PHF-like immunoreactivity and microtubule binding. *Neuron* **11**, 153–163.
14. Watanabe, A., Hasegawa, M., Suzuki, M., Takio, K., Morishima-Kawashima, M., Titani, K., et al. (1993) *In vivo* phosphorylation sites in fetal and adult rat tau. *J. Biol. Chem.* **268**, 25,712–25,717.
15. Morishima-Kawashima, M., Hasegawa, M., Takio, K., Suzuki, M., Yoshida, H., Titani, K., and Ihara, Y. (1995) Proline-directed and non-proline-directed phosphorylation of PHF-tau. *J. Biol. Chem.* **270**, 823–829.

16. Garver, T. D., Harris, K. A., Lehman, R. A. W., Lee, V. M. Y., Trojanowski, J. Q., and Billingsley, M. L. (1994) Tau phosphorylation in human, primate, and rat brain: evidence that a pool of tau is highly phosphorylated in vivo and is rapidly dephosphorylated in vitro. *J. Neurochem.* **63**, 2279–2287.
17. Matsuo, E. S., Shin, R.-W., Billingsley, M. L., Van DeVoorde, A., O'Connor, M., Trojanowski, J. Q., and Lee, V. M. Y. (1994) Biopsy-derived adult human brain tau is phosphorylated at many of the same sites as Alzheimer's disease paired helical filament tau. *Neuron* **13**, 989–1002.
18. Crowther, R. A., Olesen, O. F., Smith, M. J., Jakes, R., and Goedert, M. (1994) Assembly of Alzheimer-like filaments from full-length tau protein. *FEBS Lett.* **337**, 135–138.
19. Pérez, M., Valpuesta, J. M., Medina, M., De Garcini, E. M., and Avila, J. (1996) Polymerization of  $\tau$  into filaments in the presence of heparin: the minimal sequence required for  $\tau$ - $\tau$  interaction. *J. Neurochem.* **67**, 1183–1190.
20. Lovestone, S. and Reynolds, C. H. (1997) The phosphorylation of tau: a critical stage in neurodevelopment and neurodegenerative processes. *Neuroscience* **78**, 309–324.
21. Goedert, M., Cohen, E. S., Jakes, R., and Cohen, P. (1992) p42 Map kinase phosphorylation sites in microtubule-associated protein tau are dephosphorylated by protein phosphatase 2A<sub>1</sub>: implications for Alzheimer's disease. *FEBS Lett.* **312**, 95–99.
22. Fleming, L. M. and Johnson, G. V. W. (1995) Modulation of the phosphorylation state of tau *in situ*: The roles of calcium and cyclic AMP. *Biochem. J.* **309**, 41–47.
23. Hanger, D. P., Betts, J. C., Loviny, T. L. F., Blackstock, W. P., and Anderton, B. H. (1998) New phosphorylation sites identified in hyperphosphorylated tau (paired helical filament-tau) from Alzheimer's disease brain using nanoelectrospray mass spectrometry. *J. Neurochem.* **71**, 2465–2476.
24. Lovestone, S., Reynolds, C. H., Latimer, D., Davis, D. R., Anderton, B. H., Gallo, J.-M., et al. (1994) Alzheimer's disease-like phosphorylation of the microtubule-associated protein tau by glycogen synthase kinase-3 in transfected mammalian cells. *Curr. Biol.* **4**, 1077–1086.
25. Brion, J.-P., Couck, A.-M., Robertson, J., Loviny, T. L. F., and Anderton, B. H. (1993) Neurofilament monoclonal antibodies RT97 and 8D8 recognize different modified epitopes in paired helical filament- $\tau$  in Alzheimer's disease. *J. Neurochem.* **60**, 1372–1382.
26. Brion, J. P., Hanger, D. P., Bruce, M. T., Couck, A. M., Flament-Durand, J., and Anderton, B. H. (1991) Tau in Alzheimer neurofibrillary tangles. N- and C-terminal regions are differentially associated with paired helical filaments and the location of a putative abnormal phosphorylation site. *Biochem. J.* **273**, 127–133.
27. Boyle, W. J., van der Geer, P., and Hunter, T. (1991) Phosphopeptide mapping and phosphoamino acid analysis by two-dimensional separation on thin-layer cellulose plates. *Methods Enzymol.* **201**, 110–149.
28. Betts, J. C., Blackstock, W. P., Ward, M. A., and Anderton, B. H. (1997) Identification of phosphorylation sites on neurofilament proteins by nanoelectrospray mass spectrometry. *J. Biol. Chem.* **272**, 12,922–12,927.

29. Biernat, J., Mandelkow, E.-M., Schroter, C., Lichtenberg Kraag, B., Steiner, B., Berling, B., et al. (1992) The switch of tau protein to an Alzheimer-like state includes the phosphorylation of two serine-proline motifs upstream of the microtubule binding region. *EMBO J.* **11**, 1593–1597.
30. Perkins, S. J. (1986) Protein volumes and hydration effects. The calculations of partial specific volumes, neutron scattering matchpoints and 280-nm absorption coefficients for proteins and glycoproteins from amino acid sequences. *Eur. J. Biochem.* **157**, 169–180.
31. Drewes, G., Ebneith, A., Preuss, U., Mandelkow, E.-M., and Mandelkow, E. (1997) MARK, a novel family of protein kinases that phosphorylate microtubule-associated proteins and trigger microtubule disruption. *Cell* **89**, 297–308.
32. Reynolds, C. H., Nebreda, A. R., Gibb, G. M., Utton, M. A., and Anderton, B. H. (1997) Reactivating kinase/p38 phosphorylates  $\tau$  protein in vitro. *J. Neurochem.* **69**, 191–198.
33. Reynolds, C. H., Utton, M. A., Gibb, G. M., Yates, A., and Anderton, B. H. (1997) Stress-activated protein kinase/c-Jun N-terminal kinase phosphorylates tau protein. *J. Neurochem.* **68**, 1736–1744.
34. Goedert, M., Hasegawa, M., Jakes, R., Lawler, S., Cuenda, A., and Cohen, P. (1997) Phosphorylation of microtubule-associated protein tau by stress-activated protein kinases. *FEBS Lett.* **409**, 57–62.
35. Szendrei, G. I., Lee, V. M. Y., and Otvos, L., Jr. (1993) Recognition of the minimal epitope of monoclonal antibody Tau-1 depends upon the presence of a phosphate group but not its location. *J. Neurosci. Res.* **34**, 243–249.
36. Mercken, M., Vandermeeren, M., Lubke, U., Six, J., Boons, J., Van de Voorde, A., et al. (1992) Monoclonal antibodies with selective specificity for Alzheimer tau are directed against phosphatase-sensitive epitopes. *Acta Neuropathol. Berl.* **84**, 265–272.
37. Goedert, M., Jakes, R., and Vanmechelen, E. (1995) Monoclonal antibody AT8 recognises tau protein phosphorylated at both serine 202 and threonine 205. *Neurosci. Lett.* **189**, 167–170.
38. Zheng-Fischhöfer, Q. Y., Biernat, J., Mandelkow, E.-M., Illenberger, S., Godemann, R., and Mandelkow, E. (1998) Sequential phosphorylation of Tau by glycogen synthase kinase-3 $\beta$  and protein kinase A at Thr212 and Ser214 generates the Alzheimer-specific epitope of antibody AT100 and requires a paired-helical-filament-like conformation. *Eur. J. Biochem.* **252**, 542–552.
39. Goedert, M., Jakes, R., Crowther, R. A., Cohen, P., Vanmechelen, E., Vandermeeren, M., and Cras, P. (1994) Epitope mapping of monoclonal antibodies to the paired helical filaments of Alzheimer's disease: identification of phosphorylation sites in tau protein. *Biochem. J.* **301**, 871–877.
40. Lichtenberg-Kraag, B., Mandelkow, E.-M., Biernat, J., Steiner, B., Schroter, C., Gustke, N., et al. (1992) Phosphorylation-dependent epitopes of neurofilament antibodies on tau protein and relationship with Alzheimer tau. *Proc. Natl. Acad. Sci. USA* **89**, 5384–5388.
41. Otvos, L., Jr., Feiner, L., Lang, E., Szendrei, G. I., Goedert, M., and Lee, V. M. Y. (1994) Monoclonal antibody PHF-1 recognizes tau protein phosphorylated at serine residues 396 and 404. *J. Neurosci. Res.* **39**, 669–673.

42. Seubert, P., Mawal-Dewan, M., Barbour, R., Jakes, R., Goedert, M., Johnson, G. V. W., et al. (1995) Detection of phosphorylated Ser<sup>262</sup> in fetal tau, adult tau, and paired helical filament tau. *J. Biol. Chem.* **270**, 18,917–18,922.
43. Hasegawa, M., Jakes, R., Crowther, R. A., Lee, V. M. Y., Ihara, Y., and Goedert, M. (1996) Characterization of mAb AP422, a novel phosphorylation-dependent monoclonal antibody against tau protein. *FEBS Lett.* **384**, 25–30.
44. Hanger, D. P., Hughes, K., Woodgett, J. R., Brion, J.-P., and Anderton, B. H. (1992) Glycogen synthase kinase-3 induces Alzheimer's disease-like phosphorylation of tau: generation of paired helical filament epitopes and neuronal localisation of the kinase. *Neurosci. Lett.* **147**, 58–62.
45. Lowry, D. H., Rosebrough, N.J., Farr, A. L., and Randall, R. J. (1951) Protein measurement with the Folin phenol reagent. *J. Biol. Chem.* **193**, 265–271.
46. Bradford, M. M. (1976) A rapid and sensitive method for the quantitation of microgram quantities of protein utilizing the principle of protein-dye binding. *Anal. Biochem.* **72**, 248–254.
47. Smith, P. K., Krohn, R. I., Hermanson, G. T., Mallia, A. K., Gartner, F. H., Provenzano, M. D., Fujimoto, E. K., Goeke, N. M., Olsen, B. J., and Klenk, D.C. (1985) Measurement of protein using bicinchoninic acid [published erratum appears in *Anal. Biochem.* 1987 May 15; **163**(1); 279]. *Anal. Biochem.* **150**, 76–85.

## Transglutaminase-Catalyzed Formation of Alzheimer-Like Insoluble Complexes from Recombinant Tau

Brian J. Balin and Denah M. Appelt

### 1. Introduction

Alzheimer's disease (AD) is a progressive neurodegenerative disease in which abnormal filamentous inclusions accumulate in dystrophic and dying nerve cells. These inclusions have been described as neurofibrillary tangles (NFTs) of which paired helical filaments (PHFs) are the primary constituents (1–3). The PHFs primarily are composed of the microtubule-associated protein tau, which has undergone posttranslational modification such as phosphorylation (4,5), glycation (6–9), and crosslinking by transglutaminase (TGase) (10–16). Crosslinking of proteins catalyzed by TGase results in the deposition of these proteins into insoluble matrices that are resistant to proteolytic digestion and chaotropic denaturation (for review *see* **ref. 17**). In this regard, TGase has been demonstrated to be associated with NFTs from the Alzheimer brain (13,14) and to exhibit elevated activity in the AD brain as compared with normal aged-matched control subjects (16). Here we discuss important aspects of TGase and in vitro experimental approaches that address its ability to catalyze the tau protein into insoluble complexes exhibiting biophysical and immunological properties similar to those of the Alzheimer PHFs and NFTs.

TGase-modified proteins are evident throughout the body (17) and are distributed in the plasma, tissues, and extracellular fluids. TGases catalyze the transamidation of available glutamine residues in proteins. Peptide-bound lysine residues or polyamines serve as the primary amines to form either  $\epsilon$ -( $\gamma$ -glutamic)lysine (Glu-Lys) or ( $\gamma$ -glutamic)polyamine bonds between proteins (18). The bonds formed from this catalysis are covalent, stable, and thought to be resistant to most proteolytic enzymes. TGases have been

From: *Methods in Molecular Medicine*, Vol. 32: *Alzheimer's Disease: Methods and Protocols*  
Edited by: N. M. Hooper © Humana Press Inc., Totowa, NJ

implicated in the programmed cell death and injury of several cell types, which include the human lens (19), erythrocytes (19), and hepatocytes (20). TGase activity has been demonstrated in both the central nervous system (10) and the peripheral nervous system (21), and, more recently, tissue TGase has been localized to human hippocampal neurons (13). Homogenates and synaptosomal fractions of various rat brain regions (cerebellum, brainstem, midbrain, hippocampus, cortex) have been shown to contain endogenous TGase activity (22); homogenates from the human postmortem cortex also have been shown to contain TGase activity (10,16). TGase within the nervous system may crosslink proteins critical to the normal differentiation and stabilization of neurons (17,23). In the aged and diseased brain, the regulation and expression of TGase may be altered, thereby promoting the accumulation of abnormal, insoluble protein complexes in the neuron. This accumulation could evoke a state of degeneration from which the neuron may not recover.

Previous work implicating TGase as a potential component in the pathogenesis of AD focused on TGase's ability to convert neuronal cytoskeletal proteins into insoluble structures characteristic of AD (10,11,24). In addition, bovine tau (25) and tau derived from human cDNA constructs (12,15) have been shown to be substrates for TGase. Numerous studies have presented evidence that neurons undergoing early stages of AD neurodegeneration exhibit Alz50 immunoreactivity for the tau protein (26–28). Alz50 immunoreactivity for tau also has been shown to increase in vitro following crosslinking of tau with tissue TGase (25). Recently, immunolabeling studies in our laboratory have demonstrated that TGase is present in degenerating neurons from the hippocampus of the AD brain (13). Double immunofluorescence has revealed the presence of NFTs and TGase coexisting within degenerating neurons. These results are the first to identify an association of TGase with NFTs from AD brains, and led us to evaluate the role of tissue TGase in vitro in its ability to convert the largest human recombinant form of tau (htau40) into an insoluble polymeric complex (15). The approaches outlined in the following section provide an in vitro model for studying protein insolubility as it pertains to the neurodegenerative pathology characteristic of AD.

## 2. Materials

### 2.1. Tau Purification

1. cDNA encoding the largest isoform of human tau-htau40 in the *E. coli* BL21 (DE3) expression vector. cDNA for other isoforms of human tau are available and can be used as well in an expression vector system.
2. 0.4 mM isopropyl- $\beta$ -D-thiogalactoside (IPTG).
3. Luria-Bertani (LB) broth.
4. Shaking incubator.

5. Sorvall RC 5B centrifuge (Sorvall Centrifuge, Newtown, CT), and a Beckman LM-80 (Beckman, Palo Alto, CA) ultracentrifuge with rotors.
6. Dounce homogenizer (VWR, Atlanta, GA).
7. Fisher Sonic Dismembrator (sonicator) — model 300 (Fisher Scientific, Pittsburgh, PA).
8. Reassembly buffer (RAB) (0.1 M MES [2-*N*-Morpholino]ethanesulfonic acid], 1.0 mM ethylene glycol, *bis*-( $\beta$ -aminoethyl ether) *N*, *N*, *N'*,*N'*-tetraacetic acid (EGTA), 0.75 M NaCl, 0.5 mM MgCl<sub>2</sub>, 0.5 mM phenylmethylsulfonyl fluoride (PMSF), 1% aprotinin at pH 6.9).
9. Ammonium sulfate.
10. 0.22  $\mu$ m Sterile filter and an Amicon 100,000 M<sub>r</sub> cutoff filter (Amicon, Beverly, CA).
11. UV/Vis spectrophotometer.

## 2.2. Transglutaminase Incubation

1. Purified httau40 at a final concentration of 0.2–1.0  $\mu$ g/ $\mu$ L.
2. TGase from guinea pig liver (commercially available through Sigma Chemical Co., St. Louis, MO) 0.5–1.0  $\mu$ g/ $\mu$ L.
3. 2–50 mM CaCl<sub>2</sub>.
4. 5–10 mM Ethylenediaminetetraacetic acid (EDTA).
5. 50 mM Tris-HCl buffer with 40  $\mu$ g/mL leupeptin, pH 7.5.
6. 50–100 mM MES buffer containing 0.17 M NaCl, pH 6.0.
7. 5% Sodium dodecyl sulfate (SDS)-Lammeli sample buffer containing sucrose, 0.5 M Tris-HCl, pH 6.8, 0.1 M EDTA, 0.1% bromophenol blue, 0.05% pyronine yellow, 5 mM dithiothreitol (DTT).
8. 1.6 mM Monodansylcadaverine (Sigma).
9. 1% SDS.
10. 4 M Urea.

## 2.3. SDS-PAGE and Western Blotting

1. 10% SDS-Polyacrylamide gel electrophoresis (PAGE) gels.
2. 0.22  $\mu$ m Nitrocellulose membranes.
3. 5% Phosphate-buffered saline (PBS) - nonfat milk blocking solution.
4. Water bath or heat block at 100°C.
5. Microcentrifuge and microfuge tubes (1.5 mL).
6. Antimouse and antirabbit antibodies conjugated to horseradish peroxidase.
7. Diaminobenzidine and/or 4-chloronaphthol.
8. Coomassie (Brilliant) Blue.

## 2.4. Ultrastructure — Electron and Immunoelectron Microscopy

1. Carbon-coated electron microscopy grids — 400–600 mesh.
2. 100 mM Ammonium acetate.
3. 0.25–1% Uranyl acetate.
4. 0.1% Cold-water fish gelatin diluted in PBS.

5. Secondary antibodies against rabbit and mouse conjugated to 5–10 nm colloidal gold particles 1.0 mg/mL (Amersham, Amersham, UK).
6. Antibodies to the tau protein and to TGase (*see Subheading 3.3.5.*).
7. Transmission electron microscope.

### 3. Methods

Basically, the following methods can be used for the enzymatic conversion and analysis of the tau protein following TGase-catalyzed crosslinking. We used recombinant tau proteins to address this conversion, however, tau purified from human brain and/or animal brains (e.g., bovine) could also be used. Four general methods are addressed here: (1) recombinant tau purification, (2) incubation with TGase, (3) SDS-PAGE and Western blotting of crosslinked tau, and (4) ultrastructural analysis of the crosslinked complexes.

#### 3.1. Recombinant Tau Purification

1. A cDNA clone for the largest human brain tau isoform denoted htau40 was obtained from Dr. Michel Goedert (MRC Laboratory of Molecular Biology, Cambridge, UK).
2. Express cDNA in an *E. coli* expression vector system BL21 (DE3). Incubate BL21 bacteria with 200 µg/mL final concentration of ampicillin and in 5 mL of LB Media overnight in a 37°C shaking (225 rpm) incubator.
3. Incubate the 5 mL culture in 500 mL of LB broth + 200 µg/mL final concentration of ampicillin at 37°C until reaching an optical density (OD) of 0.6–1.0 at 600 nm. Then inoculate the cultures with 0.4 mM IPTG for 2.5 h in a 37°C shaking (225 rpm) incubator (*see Notes 1–3*) followed by centrifugation at 17,000g for 20 min at 4°C.
4. Wash the resulting pellets in 0.17 M NaCl, and recentrifuge at 17,000g for 20 min at 4°C.
5. Homogenize the pellets and sonicate at 4°C in 10 mL of 1×RAB buffer per gram of pellet.
6. Centrifuge the resulting homogenate at 100,000g for 20 min at 4°C.
7. Resuspend the pellet obtained from this centrifugation in 1×RAB buffer, boil for 20 min, cool at 4°C for 20 min, and recentrifuge at 100,000g for 20 min at 4°C.
8. To the resultant supernatant, add ammonium sulfate at 50% v/v and stir overnight at 4°C, followed by centrifugation at 37,000g at 4°C.
9. Resuspend the pellet in 50 mM MES buffer, pH 7.5, containing 0.17 M NaCl, and dialyze with 4–6 vol changes overnight in the identical buffer.
10. Following dialysis, filter the suspension first through a 0.22-µm sterile filter and second centrifuge at 3000g through an Amicon 100,000 M<sub>r</sub> cutoff filter.

#### 3.2. Transglutaminase Incubation

1. a. Incubate recombinant tau (htau40) at a final concentration of 0.2–1.0 µg/µL (*see Note 7*) with guinea pig liver TGase at a final concentration of 0.5–1.0 µg/µL and 2–50 mM CaCl<sub>2</sub> or 5–10 mM EDTA for a minimum of 15 min–22 h at 37°C.

- b. The buffer for incubation can be either 50 mM Tris-HCl with 40 µg/mL leupeptin at pH 7.5, or 50–100 mM MES buffer containing 0.17 M NaCl at pH 6.0.
2. Terminate the incubation with 5% SDS Laemmli sample buffer at 100°C for 5 min.
3. As a control to demonstrate the activity of TGase and its ability to crosslink recombinant tau, one can use another incubation mixture in which 1.6 mM monodansylcadaverine is added to the incubation mixture described in **Subheading 3.2., step 1a**. Monodansylcadaverine is a lysine analog that fluoresces under UV light when crosslinked to a protein substrate in the presence of TGase.

### 3.3. SDS-PAGE and Western Blotting

1. Incubate TGase crosslinked tau samples separately in 4 M urea for 90 min at 22°C and in 1% SDS for 90 min and boil for 5 min prior to loading these samples onto the stacking gel of a 10% SDS-PAGE.
2. To examine the TGase crosslinked tau proteins, 10% SDS-PAGE minigels are used because you can run these in 1 h at constant voltage of 150 mV, and the protein bands will migrate from the top (>200 kDa) to the middle (approx 60–68 kDa) of the gel as revealed with Coomassie Blue staining.
3. A 1–2% agarose plug in the stacking gel is used and maintained at the top of the 10% separating gel in order to transfer onto nitrocellulose the high molecular weight crosslinked proteins retained at the top of the gel (*see Note 8*).
4. Western blotting is performed by electrophoresing at 1.0 A for a minimum of 1 h (max of 2 h), to transfer the proteins from the 10% SDS-PAGE minigel onto nitrocellulose in a Tris/glycine buffer containing 10% methanol followed by blocking the nitrocellulose membranes for 30 min with 5% PBS-nonfat milk to prevent nonspecific antibody binding.
5. Incubate the nitrocellulose blots overnight for 18 h at 4°C with primary antibodies diluted in the blocking solution. The primary antibodies that we used, but for which the researcher is not limited, are those to the tau protein and to TGase. The tau antibodies consisted of tau46, 1:500 dilution; PHF1, 1:100 dilution; tau1, 1:1000 dilution; tau2, 1:1000 dilution. The TGase antibodies such as anti-Factor XIIIa and antitissue TGase can be obtained commercially (Calbiochem, San Diego, CA, antifactor XIIIa) and (NeoMarkers, anti-TGase).
6. Antimouse secondary antibodies conjugated to horseradish peroxidase are used at dilutions of 1:300–1:500 diluted in the blocking solution for 2 h at room temperature.
7. The chromagen used for development of reaction product is 4-chloronaphthol for 15–30 min.

### 3.4. Ultrastructural Analysis

1. To negative stain the filaments that form on incubation of tau proteins with TGase, absorb 5–10 µL of sample onto carbon-coated copper electron microscopy grids, wash with 100 mM ammonium acetate, and stain with 0.25–1% aqueous uranyl acetate, followed by air drying.
2. For negative staining and immunoelectron microscopy, incubate 5–10 µL of sample (0.5–1.0 µg/µL of httau40 + 1.0 µg/µL of TGase + 2–50 mM CaCl<sub>2</sub> at 37°C

for >2 h) place onto carbon-coated copper electron microscope (EM) grids and wash with PBS buffer.

3. Block these grids with 0.1% cold-water fish gelatin in PBS for 10 min prior to incubating with primary antibodies for 30 min. The antibodies used are anti-TGase and anti-tau antibodies at dilutions used for Western blotting.
4. Rinse the grids in PBS and incubate for 30 min in appropriate antisecondary antibodies conjugated to 5–10 nm colloidal gold at 1.0 mg/mL.
5. Rinse these grids briefly in ddH<sub>2</sub>O, stain with 0.25–1.0% uranyl acetate, and finally examine by EM at 80 kV on a JEOL 100 CX microscope (JEOL, Peabody, MA).

### 3.5. Results Using the Previous Techniques

1. Western analysis is used to verify that recombinant tau protein is obtained following expression in our specified vector system. The tau antibodies, in particular tau2, immunolabel the recombinant tau in the molecular weight range of 45–66 kDa. In addition, following incubation of the purified recombinant tau with TGase and CaCl<sub>2</sub> for 2 h, tau2 immunolabeling reveals that the tau protein is now present on the immunoblot at a molecular weight of >200 kDa. This indicates that the tau protein has been crosslinked into a less soluble matrix. The controls for this experiment used monodansylcadaverine (*see Note 9*) to demonstrate that the complexed tau proteins at >200 kDa were indeed crosslinked by TGase to this lysine analog, thereby indicating that tau is a very good substrate for TGase and can be converted to a less soluble form by this enzyme.
2. Control incubations: Incubations of recombinant tau and TGase in the absence of CaCl<sub>2</sub> or when using EDTA (a calcium chelator) in the incubation mixture results in no crosslinking of tau into higher molecular weight complexes.
3. Tau complexes following TGase incubation: Western blotting of the TGase crosslinked tau protein will reveal that the complexed tau is retained at the interface of the 10% separating gel portion of the minigel following transfer to nitrocellulose. This retention of tau is apparent even after incubating the crosslinked tau mixture in 4 M urea and 1% SDS, thereby demonstrating that TGase catalyzed crosslinking converted soluble tau into a relatively insoluble matrix because soluble proteins are resolvable at their nominal molecular weights following incubation in either urea or SDS.
4. Morphological structures and their immunogenicity: In control experiments, neither tau nor TGase form filaments when they are incubated separately, or incubated together without calcium activation. Following activation with calcium, tau is crosslinked into high molecular weight complexes that are immunoreactive with both anti-tau and anti-TGase antibodies. Immunolabeling of paired helical filaments derived from Alzheimer brains with the anti-TGase antibodies has been demonstrated previously (*15*).

### 4. Notes

1. Induction with IPTG should be for a minimum of 2.5 h.
2. Incubation of the bacterial culture after IPTG induction should be for a minimum of 2 h.
3. Two to four 500 mL flasks of bacteria grown to an OD of 0.6–1.0 at 600 nm is recommended to obtain sufficient yields of recombinant tau proteins.

4. Recombinant tau purified with this protocol will be at a concentration of 1–10 mg/mL.
5. Although the guinea pig TGase from Sigma is not totally pure, in our hands we have found that we obtain very good crosslinking and activity of the enzyme without further purification.
6. A control for the experiments to demonstrate that the crosslinking of tau proteins in vitro results in their relative insolubility, which is comparable to that of the insoluble NFTs/PHFs from the AD brain, is to isolate the insoluble NFTs and PHFs from the AD brain. The isolation procedure to obtain these insoluble complexes is a modified protocol from Gache et al. (29). Following this isolation, the insoluble NFTs/PHFs are analyzed in a manner comparable to the analysis of the crosslinked tau complexes in vitro. This analysis provides direct comparison and confirmation of in vitro crosslinking of tau as a model for the conversion of the tau protein into insoluble complexes found in AD.
7. Tau proteins purified or enriched from brain tissues also can be used in place of recombinant tau in the aforementioned experiments.
8. Examination of the crosslinked tau proteins by SDS-PAGE may require that you use a 1–2% agarose plug in the stacking gel in order to retain the very high molecular weight proteins that are crosslinked but unable to migrate into the 10% SDS-PAGE gel. The agarose plug can be transferred to nitrocellulose for Western blotting, or it can be solubilized by heating, and the proteins trapped in this gel can be analyzed both biochemically and ultrastructurally by EM.
9. Crosslinked recombinant tau with monodansylcadaverine can be demonstrated in two ways: (1) by immunolabeling for the tau protein, and (2) by viewing under UV light because monodansylcadaverine fluoresces under UV.
10. Recombinant tau that is crosslinked by TGase in the presence of 50 mM CaCl<sub>2</sub> is much more refractory to electrophoresis than when using 2–5 mM CaCl<sub>2</sub>, and one will find that the complexed tau matrix will not migrate into the 10% separating gel.
11. TGase apparently may remain bound or incorporated to its substrate on crosslinking the tau protein in vitro. This result is to be expected and has been demonstrated previously by us (15) and by others (30).
12. The primary antibodies to recombinant tau that we found worked exceptionally well were those from the following individuals who we thank for their generous gifts: Dr. Lester Binder (Northwestern University Medical School, Department of Cell/Molecular Biology, Chicago, IL) for tau1 and tau2, Dr. Peter Davies (Department of Pathology, Albert Einstein College, Bronx, NY) for PHF1, and Dr. Virginia Lee (University of Pennsylvania, Department of Pathology, Philadelphia, PA) for tau46.

Other tau antibodies have been found to be useful for both Western blotting and immunoelectron microscopy, so one should not be limited to the antibodies used herein.

## References

1. Kidd, M. (1963) Paired helical filaments in electron microscopy of Alzheimer's disease. *Nature* **197**, 192–193.

2. Terry, R. D., Gonatas, N. K., and Weiss, M. (1964) Ultrastructural studies in Alzheimer's presenile dementia. *Am. J. Pathol.* **44**, 269–297.
3. Wisniewski, H. M., Narang, H. K., and Terry, R. D. (1976) Neurofibrillary tangles of paired helical filaments. *J. Neurol. Sci.* **27**, 173–181.
4. Greenberg, S. G. and Davies, P. (1990) A preparation of Alzheimer paired helical filaments that displays distinct tau-proteins by polyacrylamide-gel electrophoresis. *Proc. Natl. Acad. Sci. USA* **87**, 5827–5831.
5. Lee, V. M.-Y., Balin, B. J., Otvos, L., and Trojanowski, J. Q. (1991) A68 — a major subunit of paired helical filaments and derivatized forms of normal tau. *Science* **251**, 675–678.
6. Ledesma, M. D., Bonay, P., Colaco, C., and Avila, J. (1994) Analysis of microtubule-associated protein tau glycation in paired helical filaments. *J. Biol. Chem.* **269**, 21,614–21,619.
7. Yan, S.-D., Chen, X., Schmidt, A.-M., Brett, J., Godman, G., Zou, Y.-S., et al. (1994) Glycated tau protein in Alzheimer's disease: a mechanism for induction of oxidant stress. *Proc. Natl. Acad. Sci. USA* **91**, 7787–7791.
8. Smith, M. A., Sayre, L. M., Monnier, V. M., and Perry, G. (1995) Radical AGEing in Alzheimer disease. *Trends Neurosci.* **18**, 172–176.
9. Smith, M. A., Siedlak, S. L., Richey, P. L., Nagaraj, R. H., Elhammer, A., and Perry, G. (1996) Quantitative solubilization and analysis of insoluble paired helical filaments from Alzheimer disease. *Brain Res.* **717**, 99–108.
10. Selkoe, D. J., Abraham, C., and Ihara, Y. (1982a) Brain TGase: in vitro crosslinking of human neurofilament proteins into insoluble polymers. *Proc. Natl. Acad. Sci. USA* **79**, 6070–6074.
11. Selkoe, D. J., Ihara, Y., and Salazar, F. J. (1982b) Alzheimer's disease: insolubility of partially purified paired helical filaments in sodium dodecyl sulfate and urea. *Science* **215**, 1243–1245.
12. Miller, M. L. and Johnson, G. W. (1995) Transglutaminase cross-linking of the  $\tau$  protein. *J. Neurochem.* **65**, 1760–1770.
13. Appelt, D. M., Kopen, G. C., Boyne, L. J., and Balin, B. J. (1996a) Localization of transglutaminase in hippocampal neurons: implications for Alzheimer's disease. *J. Histochem. Cytochem.* **44**, 1421–1427.
14. Appelt, D. M., Howard, M. P., Loewy, A. G., and Balin, B. J. (1996b) Insoluble NFTs from Alzheimer disease contain transglutaminase-catalyzed Glu-Lys bonds as revealed by their sensitivity to a novel isopeptidase. *Soc. Neuroscience Abstr.* **22**, 559. 9.
15. Appelt, D. M. and Balin, B. J. (1997) The association of tissue transglutaminase with human recombinant tau results in the formation of insoluble filamentous structures. *Brain Res.* **745**, 21–31.
16. Johnson, G. V. W., Cox, T. C., Lockhart, J. P., Zinnerman, M. D., Miller, M. L., and Powers, R. E. (1997) Transglutaminase activity is increased in Alzheimer's disease brain. *Brain Res.* **751**, 323–329.
17. Hand, D., Perry, M. J. M., and Haynes, L. W. (1993) Cellular TGases in neural development. *Int. J. Devel. Neurosci.* **11**, 709–720.

18. Folk, J. E. and Finlayson, J. S. (1977) The  $\epsilon$ -(gamma-glutamyl)lysine cross-link and the catalytic role of Tgases. *Adv. Protein Chem.* **31**, 1–133.
19. Lorand, L. (1988) TGase-mediated cross-linking of proteins and cell aging: the erythrocyte and lens models. *Adv. Exp. Med. Biol.* **231**, 79–94.
20. Fesus, L., Thomazy, V., and Falus, A. (1987) Induction and activation of tissue TGase during programmed cell death. *FEBS Lett.* **244**, 104–108.
21. Gilad, G. M. and Kupmar, V. (1982) Absence of functional recovery after spinal hemisections in mice genetically deficient in hemolytic complement. *Exp. Neurol.* **767**, 666–669.
22. Gilad, G. M. and Varon, L. E. (1985) TGase activity in rat brain: characterization, distribution and changes with age. *J. Neurochem.* **45**, 1522–1526.
23. Byrd, J. C. and Lichti, U. (1987) Two types of TGase in the PC12 pheochromocytoma cell line. Stimulation by sodium butyrate. *J. Biol. Chem.* **262**, 11,699–11,705.
24. Miller, C. J. and Anderton, B. H. (1986) TGase and the neuronal cytoskeleton in Alzheimer's disease. *J. Neurochem.* **46**, 1912–1922.
25. Dudek, S. M. and Johnson, G. V. W. (1993) TGase catalyzes the formation of sodium dodecylsulfate-insoluble, Alz 50-reactive polymers of tau. *J. Neurochem.* **61**, 1159–1162.
26. Benzing, W. C., Ikonovic, I. M., Brady, D. R., Mufson, E. J., and Armstrong, D. M. (1993) Evidence that transmitter-containing dystrophic neurites precede paired helical filaments and Alz-50 formation within senile plaques in the amygdala of nondemented elderly and patients with Alzheimers disease. *J. Comp. Neurol.* **224**, 176–191.
27. Hyman, B. T., Van Hoesen, G. W., Wolozin, B. L., Davies, P., Kromer, J. L., and Damasio, A. R. (1988) Alz-50 antibody recognizes Alzheimer-related neuronal changes. *Ann. Neurol.* **23**, 371–379.
28. Carmel, G., Mager, E. M., Binder, L. J., and Kuret, J. (1996) The structural basis of monoclonal antibody Alz50's selectivity for Alzheimer's disease pathology. *J. Biol. Chem.* **271**, 32789–32795.
29. Gache, Y., Guilleminot, J., Ricolfi, F., Theiss, G., and Nunez, J. (1992) A tau-related protein of 130 kDa is present in Alzheimer brain. *J. Neurochem.* **58**, 2005–2010.
30. Barsigian, C, Stern, A. M., and Martinez, J. (1991) Tissue (type II) transglutaminase covalently incorporates itself, fibrinogen, or fibronectin into high molecular weight complexes on the extracellular surface of isolated hepatocytes. *J. Biol. Chem.* **266**, 22,501–22,509.